

**ISOLATION AND CHARACTERIZATION OF ANTICOAGULANT
PROTEINS FROM THE VENOM OF HEMACHATUS
HAEMACHATUS (AFRICAN RINGHALS COBRA)**

YAJNAVALKA BANERJEE (BSc., (Hons.))

**A THESIS SUBMITTED FOR THE DEGREE OF
DOCTOR OF PHILOSOPHY AT THE NATIONAL UNIVERSITY OF
SINGAPORE**



**DEPARTMENT OF BIOLOGICAL SCIENCES, FACULTY OF
SCIENCE, NATIONAL UNIVERSITY OF SINGAPORE**

April, 2007

Dedicated to the fond memories of late

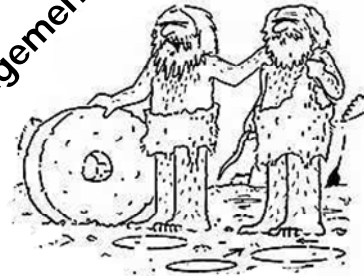
Swami Lokeshwarananda,

Secretary, the Ramakrishna Mission Institute of Culture, Calcutta

.....his life and works, have been a guiding beacon and inspiration for me, and could be best expressed in Paul Byrant's famous quote "If you believe in yourself and have dedication and pride - and never quit, you'll be a winner. The price of victory is high but so are the rewards.".....I miss him.....

I am very appreciative of the good camaraderie and academic guidance that I have enjoyed the last few years. However, the initial transition into graduate school, including moving to Singapore, was a bit bumpy. In addition to missing friends and family, I remember feeling overwhelmed by the speed of research and the amount of knowledge that seemed required to design and carry out a thesis project. Having spent a few more years here, I have developed a deep appreciation for the NUS research community.

Acknowledgements



"To be honest, I would have never invented the wheel if not for Urg's ground breaking theoretical work with the circle!"

First, I need to acknowledge those who paid the bills during my tenure as a graduate student in NUS. All the four years were supported by a Research Fellowship provided by the National University of Singapore, for which I am extremely grateful. It is probably one of the most generous fellowships available, providing not only tuition and stipend support for up to four years, but also funds for educational expenses and meeting travel. Additionally, I thank the Biomedical Research Council of Singapore, for providing a generous grant to Prof. Kini which funded my work described in this thesis.

Next, I'd like to thank the faculty who helped me along the way. First, I will like to thank my supervisor and mentor Professor RM Kini (Prof Kini as I address him). He taught me not only most of what I know about protein chemistry and coagulation biochemistry, but also about how to think and work independently...and he somehow manage to stifle his laughter every time I had to tell him that I had forgotten to sequence a peptide, which I had freeze-dried a week earlier. One of my friends once showed me a quote on scientific research by Wernher Von Braun (1912-1977), "*Research is what I'm doing when I don't know what I'm doing*"; but working with Prof. Kini I always knew what I am doing and why I am doing a particular experiment; and was that experiment going to answer the question that we asked. In science it is common for other people to pursue what others have done earlier, but I think a good scientist should come up with innovative ideas of his own to tackle a problem. In this regard I remember the famous quote of Samuel Palmer "*Wise men make proverbs, but fools repeat them*"; Prof Kini always emphasized on designing on ones own experiment(s), which in turn has helped not only me but all others in the lab to develop an analytical frame of mind (a great asset to have when one is working as or trying to become a scientist). Thanks for that!!!!!!!!!!!! In addition, I thank Prof Kini for imparting his logical and farsighted approach to scientific research, his attention to detail, and his ability to present complicated ideas with great clarity.

I thank my co-supervisor Dr. Jayaraman Sivaraman (Prof. Shiva as everybody addresses him) for his help and helpful suggestions regarding X-ray crystallography. I have benefited greatly from his scientific expertise and career advice.

I will like to thank my collaborators in Japan. Thank you Mizuguchi-san (not only for helping me in my work, but also for introducing me to the world of Japanese cuisine. I will never forget the taste of sashimi and tongkatsu, that I used to look forward to ones we were able to get the K_i for the inhibition). My hearty thanks to Professor Iwanaga-sensei at Kaketsuken, his insights into the structure-function relationship of factor VIIa were invaluable in my work. I also thank the factor VIIa group in Kaketsuken for their help and providing me with all the factor VIIa that I required to complete the studies depicted in this thesis.

My thanks to Dr Egon Persson (Egon as he has asked me to address him) of Novonordisk. First, thank you for the light chain of FVIIa that you kindly provided for my studies. Second and most importantly thank you for the excellent suggestions that you kindly provided on the part describing the structure-function of TF-FVIIa complex in the introductory chapters of the thesis. If not for Egon it would have been impossible for me write that part.

I thank Dr. Prakash Kumar for a large number of excellent suggestions during a meticulous and tireless shepherding process. Thanks to Dr Ganesh Anand, Dr Selvanayagam Nirathanan (Niru) and Dr. Sundarmurthy Kumar for useful discussions.

I thank Professor Andre Ménez (Commissariat à l’Energie Atomique, Saclay, France) for his time and helpful discussions concerning various aspects of science pertaining to my PhD project during his visits to our department in NUS.

Thanks to everyone in Prof Kini’s lab with whom I had a chance to interact. The combination of graduate students and post-docs with diverse backgrounds has made it a tremendous place to learn. In particular, I would like to thank Tse Siang for teaching me the theoretical and practical basics of protein purification and chromatography, Vivek for helping me with nuclear magnetic resonance spectroscopic studies and Gayathri for teaching me how to use the DLS machine. Thanks to Lakshmi for teaching me the basics of circular dichroism. Thanks to Bee Ling for making the lab run so smoothly. Thanks to everyone else in Prof Kini’s lab and others in protein and proteomics centre including: Joanna, Rehana, Robin, Jegan, Ahsan, Arvind, Chow Yeow, Dileep, Shi Yang, Sin Min, Kathleen, Tram, Annabelle, Shifali, Say Tin and Shashikant Joshi.

Finally and most importantly, I doubt anybody can make it through the frustrations of Ph.D. research without a social support system. I am fortunate to have two parents, who have not only supported me unconditionally in all my endeavors, but who also instilled in me the work ethic and values to be (more or less) successful at most of them. Not only that, but they never once uttered the parental phrase every grad student dreads: “So when are you gonna graduate and get a job?” I also need to specifically thank the friends who’ve listened to my bitching and moaning, chiefly Lakshmi (not only in Singapore but also after he went to US over the phone) who has endured more hours of complaints than anyone should have to; Of course, there’s no one better to commiserate with than a fellow

grad student, especially one with whom you can tour the great breweries of the world, and for that purpose Kishore and Reza have always been available.

Thanks to Srinivas Rao and Mandar for scientific discussions, beer drinking and excellent house warming parties. In this vein I also thank Naveen, Shilpa, Jaffar, Ali, Hari, Jaspreet, Akhilesh, Bobby, Deven, Vidya, Shalini, Divya and Anand.

Thanks to all the people that make the Department run so smoothly. Thanks to Joanne, Reena, Mrs Chan and Annie. Thanks to Cynthia for providing me a separate cubicle for writing my thesis without getting disturbed. Thanks to Tammy for not letting me feel bored, while I was preparing my thesis.

Thanks to my many inspirational teachers. In particular, thanks to Ajit Sengupta at Narendrapur Ramakrishna Mission for his excellent lectures at school on diversified topics in Biology and Dr. Biswanath Pyne at Presidency College Calcutta for his caring and clear instruction in biochemistry and human physiology.

And there are plenty of other friends and colleagues too numerous to mention who've helped me, hopefully if you're in this group, you know who you are and that I appreciate you!

Yajnavalka Banerjee
April, 2007

TABLE OF CONTENTS

Page		
ii		Dedication
iii		Acknowledgement
vi		Table of contents
ix		Summary
xii		Research collaborations
xiii		Acknowledgement of copyright
xix		Abbreviation
xv		List of figures
xviii		List of tables
1	Chapter One	Introduction
		<i>An overview of blood coagulation, including the anticoagulant pathways. Anticoagulants, targeting specific coagulation enzymes or steps in the coagulation pathway, with a focus on the ones targeting TF-FVIIa complex is given below. Snake venom anticoagulant proteins. Aim and scope of the thesis.</i>
60	Chapter Two	Purification of the Anticoagulant Protein
		<i>Isolation and Purification of hemextin A and hemextin B. Assessment of homogeneity of hemextin A and hemextin B. Determination of complete amino acid sequence of hemextin A and hemextin B. Anticoagulant activity of hemextin A, B and formation of hemextin AB complex. Importance of proper folding of the proteins for mediating anticoagulant activity and complex formation. Preliminary characterization of the complex using gel-filtration chromatography.</i>
87	Chapter Three	Mechanism of Anticoagulant Activity

Identification of the site of action of the anticoagulant protein and synergistic complex using “Dissection

Approach”. Serine protease specificity. Kinetics of inhibition and determination of K_i

Page

112 Chapter Four

Biophysical Characterization of Hemextin AB Complex

Conformational changes during complex formation. Changes in molecular diameters during the complex formation. Thermodynamics of hemextin AB complex formation. Effect of temperature on the complex formation. Effect of buffer ionization on the complex formation. Electrostatic interactions in hemextin AB complex formation. Hydrophobic interactions in the hemextin AB complex formation. Effect of buffer conditions on the conformation of hemextins. Model for hemextin AB complex assembly.

162 Chapter Five

Molecular Interactions with FVIIa

Binding of FVIIa to hemextin AB complex. The effect of temperature on hemextin AB-FVIIa complex formation. Conformational changes associated with hemextin AB-FVIIa complex formation. Binding of FVIIa to hemextin A. Binding of hemextin AB complex dimer to FVIIa. Effect of soluble TF on the binding of anticoagulant proteins to FVIIa. Interaction of hemextin A and hemextin AB complex with individual chains of FVIIa. Interaction of hemextin A and hemextin AB complex with active site inhibited FVIIa.

195 Chapter Six

Structural Characterization of Anticoagulant Protein Hemextin A

Crystallization of hemextin A. Data Collection. Solution of structure and refinement. Analysis of the three-dimensional structure of hemextin A.

215 Chapter Seven

Conclusion

Conclusions. Future Prospects

224

Bibliography

Journal, book and web-site references.

262

Publications

*Articles in internationally refereed journals. Patent.
Conference abstracts.*

Appendix

*Classification of venomous snakes. Classification of
snake venom anticoagulant proteins. Snake venom
protein families. Interesting facts on spitting cobra.
Publications.*

SUMMARY

During vascular injury blood coagulation is initiated by the interaction of factor VIIa (FVIIa) present in blood with freshly exposed tissue factor (TF) forming TF-FVIIa complex. As, unwanted clot formation leads to death and debilitation due to vascular occlusion; hence anticoagulants are pivotal for treating thromboembolic disorders. Snake venoms are veritable gold mines of pharmacologically active polypeptide and proteins many of which exhibit anticoagulant activity.

Two synergistically acting anticoagulant three-finger proteins, hemextin A and hemextin B were purified from the venom of the elapid *Hemachatus haemachatus* (African Ringhals cobra) using standard chromatographic procedures. Hemextin A, but not hemextin B has mild anticoagulant activity. However, hemextin B forms a complex (hemextin AB complex) with hemextin A and enhances its anticoagulant potency. Using biophysical techniques including circular dichroism, dynamic light scattering, isothermal titration calorimetry, mass spectrometry and nuclear magnetic resonance, the molecular interactions participating in complex formation were elucidated. Hemextin AB complex exists as a tetramer. Complex formation is enthalpically driven with a negative change in heat capacity, indicating the burial of hydrophobic surface area. The tetrameric complex behaves differently in buffers of higher ionic strength. It is also sensitive to the presence of glycerol in the buffer solution. Thus, a complex interplay of electrostatic and hydrophobic interactions drives the formation and stabilization of this novel anticoagulant protein complex. Based on the results of the above studies, a model was proposed for the assembly of this unique anticoagulant complex.

Coagulation and kinetic assays showed that hemextin AB complex and hemextin A inhibit clot formation by inhibiting TF-FVIIa activity. Their specificity of inhibition was demonstrated by studying their effects on 12 serine proteases; hemextin AB complex potently inhibits the amidolytic activity of FVIIa either in the presence or in the absence of soluble tissue factor (sTF). This was further confirmed with biophysical experiments. The complex inhibits FVIIa-sTF non-competitively (K_i - 25 nM) and is the first natural inhibitor of FVIIa, which unlike tissue factor pathway and nematode anticoagulant peptide c2 does not use FXa as a scaffold for its inhibitory activity.

Molecular interactions involved in the formation of hemextin AB-FVIIa complex and hemextin A-FVIIa complex were also investigated using size-exclusion chromatography and isothermal titration calorimetry. Hemextin A and hemextin AB complex bind to the heavy chain of FVIIa. Binding to FVIIa takes place with equal affinity irrespective of the presence or absence of co-factor. Binding also takes place even when the active site of FVIIa is blocked; this highlights the non-competitive nature of inhibition both for the anticoagulant protein and its complex, which is also supported by enzyme kinetic studies.

Since, hemextin A is the only known protein belonging to the three-finger toxin family that exhibits FVIIa inhibitory activity, its three-dimensional structure was determined using X-ray crystallography. Hemextin A exhibits the characteristic three-finger fold consisting of six β -strands ($\beta_2 \downarrow \beta_1 \uparrow \beta_4 \downarrow \beta_3 \uparrow \beta_6 \downarrow \beta_5 \uparrow$) which forms two β -sheets.

In conclusion, the present study provides a detailed characterization of an three-finger toxin, hemextin A and its synergistic complex with another three-finger toxin hemextin B. Hemextin AB complex is the only known heterotetrameric complex of three-finger

toxins and also the only known specific inhibitor of FVIIa. Molecular interactions of the hemextin A and hemextin AB complex with FVIIa/TF-FVIIa, provides a new paradigm in the search for anticoagulants to treat thromboembolic disorders.

RESEARCH COLLABORATIONS

No man is an island.

John Donne (1624)

The following collaborating laboratories provided help in performing some of the experiments that are discussed in this thesis. Their contribution is gratefully acknowledged.

- Professor. Sadaaki Iwanaga and Dr. Jun Mizuguchi. Blood Products Research Department, The Chemo-Sero-Therapeutic Research Institute, Kumamoto 869-1298, Japan.
 - Dr. Jayaraman Shivaraman, Dr. Sundarmurthy Kumar and Jobi Chen Chako, Structural Biology Laboratories, Department of Biological Sciences, National University of Singapore, Singapore -117543.
-

ACKNOWLEDGEMENT OF COPYRIGHT

*“For your satisfaction and for mine, please read this.....”
St. Francis of Sales(1609)¹*

- Professor. Kenneth Mann, Department of Biochemistry, University of Vermont, USA for the permission to reproduce Figure 1.2 (The current model of the blood coagulation cascade.) in Chapter 1.
- Professor. Charles T Esmon, Oklahoma Medical Research Foundation, USA for the permission to reproduce Figure 1.3 (Schematic representation of the protein C anticoagulant system) from “The Protein C Pathway”, Chest:2003 Supplement; 26S-32S in Chapter 1.
- Professor Peter Wright, Department of Molecular Biology, The Scripps Research Institute, USA for the permission to reproduce Figure 1.6C (Ribbon diagram of the minimized mean structures of NAPc2) in Chapter 1.
- Professor Carol MacKintosh, MRC Protein Phosphorylation Unit, University of Dundee for her kind permission to reproduce some part of her excellent essay titled “Chromatography: from colour writing to separation science” in the preamble of Chapter 2.
- Professor Antonio Baici, Department of Biochemistry, University of Zurich for his kind permission to reproduce some paragraphs of his excellent essay titled “Enzyme kinetics: the velocity of reactions”, in the preamble of Chapter 3.
- Professor Robert A Alberty, Department of Chemistry; Massachusetts Institute of Technology for his kind permission to reproduce some paragraphs of his excellent reflections in the Journal of Biological Chemistry titled “A Short History of the Thermodynamics of Enzyme-catalyzed Reactions” in the introductory section of Chapter 4.
- Professor Boris Turk, Department of Biochemistry and Molecular Biology, Jozef Stefan Institute, Ljubljana, Slovenia for providing me with the excellent table titled “Protease inhibitors approved for clinical use” in Chapter 5.
- Dr. Karsten W. Theis, University of Massachusetts Amherst, for allowing me to reproduce the excellent cartoon depicting the three stages of X-ray crystallography in Chapter 6.

¹ Quoted in Clinical Pharmacology by Laurence, Bennett and Brown, 8th Edition (1997)

- Professor Christian de Duve and Professor Paul D. Boyer for allowing me to reproduce some sentences from their excellent reflections published in the Journal of Biological Chemistry.
 - Dr. Wolfgang Wuster, University of Bangor, Wales, UK and Mr. Mark M Lucas, Florida, USA for the permission to reproduce some of the photographs as depicted in the Appendix of the thesis.
-

LIST OF FIGURES

Chapter One

- 1.1 When the coagulation cascade was just an idea
- 1.2 The current model of the blood coagulation cascade
- 1.3 Schematic representation of the protein C anticoagulant system.
- 1.4 Overall view of the extracellular domain of tissue factor,TF-FVIIa complex, FVIIai without TF, Inhibitory peptide A-183 (green tube) complexed with a form of zymogen FVII.
- 1.5 Schematic representation of the approaches for TF-FVIIa inhibition
- 1.6 Ribbon diagrams of the second and third kuniz domain of TFPI, Mechanism of action of TFPI, Ribbon diagram of the minimized mean structures of NAPc2, Mechanism of action of rNAPc2.
- 1.7 The predicted anticoagulant region of anticoagulant PLA₂ enzymes, Mechanism of anticoagulant activity of PLA₂
- 1.8 Overall structure of FX-bp and FXGD1-44 complex, FIX binding protein, Anticoagulant mechanism of factor IX/X-binding protein.
- 1.9 Anticoagulant mechanism of bothrojaracin

Chapter Two

- 2.1 Anticoagulant activity of the crude venom
- 2.2 Size-exclusion chromatography (SEC) of *Hemachatus haemachatus* crude venom using a Superdex 30 column
- 2.3 Cation exchange of peak 3 from SEC
- 2.4 RP-HPLC profiles of hemextin A and hemextin B
- 2.5 Rechromatography of hemextin A and B
- 2.6 ESI-MS of hemextin A and B
- 2.7 Comparison of amino acid sequence of hemextin A and hemextin B with other sequences of the three-finger toxin family.
- 2.8 CD spectra
- 2.9 Effects of hemextins A and B on prothrombin time
- 2.10 Complex formation between hemextins A and B is illustrated by their effect on prothrombin time
- 2.11 Gel filtration studies on the formation of hemextin AB complex
- 2.12 Anticoagulant activity comparison
- 2.13 Importance of fold in the formation of hemextin AB complex
- 2.14 Three-dimensional structural similarity among three-finger toxins from snake venoms

Chapter Three

- 3.1 Dissection Approach
- 3.2 Localization of the step of activity

- 3.3 Inhibition of TF-FVIIa activity
- 3.4 Complex formation demonstrated by the Inhibition of TF-FVIIa activity.
- 3.5 Effect of phospholipids on the inhibitory activity of hemextins A and B and hemextin AB complex.
- 3.6 Serine protease specificity
- 3.7 Inhibition of plasma kallikrein amidolytic activity and comparison of potency with FVIIa inhibition.
- 3.8 Nature of Inhibition

Chapter Four

- 4.1 Schematic representation of different parts of GEMMA
- 4.2 Conformational changes associated with the formation of hemextin AB complex
- 4.3 Conservation of β -sheet after complex formation
- 4.4 Measurement of molecular diameter during Hemextin AB complex formation using GEMMA.
- 4.5 Determination of hydrodynamic diameter using DLS
- 4.6 Interaction studies between hemextin A and B using ITC
- 4.7 Thermodynamics of hemextin A-hemextin B interaction
- 4.8 Enthalpy-entropy compensation
- 4.9 Effect of buffer ionization on the enthalpy for hemextin AB complex formation
- 4.10 ITC studies in buffer of high ionic strength.
- 4.11 SEC studies of Hemextin AB complex in buffer of high ionic strength
- 4.12 Determination of hydrodynamic diameter using DLS
- 4.13 Effect of buffer ionic strength on anticoagulant activity
- 4.14 ITC studies in buffer of high glycerol concentration.
- 4.15 SEC studies of Hemextin AB complex in buffer containing different concentrations of glycerol.
- 4.16 Determination of hydrodynamic diameter using DLS
- 4.17 Effect of glycerol on anticoagulant activity
- 4.18 Evaluation of solute osmotic effect on binding affinity
- 4.19 One dimensional $^1\text{H-NMR}$ studies
- 4.20 A proposed model of hemextin AB complex

Chapter Five

- 5.1 Elution profile of active site inhibited FVIIa (FFRck-FVIIa)
- 5.2 Separation of light and heavy chains derived from FVIIa
- 5.3 Binding of hemextin AB complex to FVIIa
- 5.4 Thermodynamics of FVIIa-hemextin AB complex formation
- 5.5 Conformational changes associated with the formation of hemextin AB-FVIIa complex.
- 5.6 Binding of hemextin A to FVIIa
- 5.7 Conformational changes associated with the formation of hemextin A-FVIIa complex

- 5.8 Binding of hemextin AB complex or hemextin A binding to FVIIa in 50 mM Tris buffer (pH 7.4) containing 250 mM glycerol.
- 5.9 Binding of hemextin AB complex or hemextin A binding to FVIIa in 50 mM Tris buffer (pH 7.4) containing 150 mM salt.
- 5.10 Binding of hemextin A/hemextin AB complex to sTF-FVIIa
- 5.11 Binding of hemextin A/hemextin AB complex to the heavy chain of FVIIa
- 5.12 Binding of hemextin A/hemextin AB complex to active site blocked FVIIa (FFRck-FVIIa)

Chapter Six

- 6.1 Crystal of hemextin A
 - 6.2 Electron density map
 - 6.3 Overall structure of hemextin A
 - 6.4 Surface plot of hemextin A, showing electrostatic potential
 - 6.5 Superimposition of hemextin A with three-finger proteins of highest structural similarity
-

LIST OF TABLES

Chapter Four

- 4.1 Effect of temperature on hemextin A-hemextin B interaction
- 4.2 Effect of increasing ionic-strength on hemextin A-hemextin B interaction
- 4.3 Effect of increasing glycerol concentrations on hemextin A-hemextin B interaction

Chapter Five

- 5.1 Thermodynamic analysis of FVIIa binding to hemextin AB complex at different temperatures
- 5.2 Thermodynamics of binding of hemextin AB complex/hemextin A to FVIIa in different buffer solutions
- 5.3 Thermodynamic analysis of binding to FVIIa and its derivatives to hemextin AB complex/hemextin A

Chapter Six

- 6.1 Crystallographic data and refinement statistics
-

ABBREVIATIONS

Å	Angstrom units
ACN	acetonitrile
APC	activated protein C
AT-III	anti-thrombin-III
Ca ²⁺	calcium
CD	circular dichroism spectroscopy
Da	Dalton
DLS	dynamic light scattering
EDTA	ethylenediamine tetraacetic acid
EGF	epidermal growth factor
ELISA	enzyme-linked immunosorbent assay
EM	electrophoretic mobility
ESI-MS	electrospray ionization – mass spectrometry
FIX	factor IX
FV	factor V
FVII	factor VII
FVIII	factor VIII
FX	factor X
FXI	factor XI
FXII	factor XII
FXIII	factor XIII
g	gram
GEMMA	gas-phase electrophoretic macromolecule mobility analyzer
Gla	γ-carboxyglutamic acid
HEPES	4-(2 hydroxyethyl)-1-piperazineethanesulfonic acid
HMWK	high molecular weight kininogen
IC ₅₀	concentration at half-maximal inhibition
ITC	isothermal titration calorimetry
K _{cat}	turnover number (number of moles of substrate converted to product per mole of enzyme per min)
kDa	kilo Dalton
K _m	Michaelis-Menton constant
kg	kilogram
μg	microgram
μl	microlitre
μM	micromolar
min	minutes
mM	millimolar
MW	molecular weight
<i>n</i>	number of experiments
NAP	nematode anticoagulant protein
nM	nanomolar
NMR	nuclear magnetic resonance
PBS	phosphate-buffered saline

PC	phosphatidylcholine
PDB	Protein Data Bank
PLA ₂	phospholipase A ₂
<i>p</i> NA	<i>p</i> -nitroanilide
PS	phosphatidylserine
rmsd	root mean square deviation
RP-HPLC	reversed-phase high pressure liquid chromatography
RVV	Russell's viper venom
S	seconds
S-2222	benzoyl-Ile-Glu(GluγOMe)-Gly-Arg- <i>p</i> NA·HCl
S-2238	H-D-Phe-Pip-Arg- <i>p</i> NA·2HCl
S-2251	H-D-Val-Leu-Lys- <i>p</i> NA·2HCl
S-2266	H-D-Val-Leu-Arg- <i>p</i> NA·2HCl
S-2288	H-D-Ile-Pro-Arg- <i>p</i> NA·HCl
S-2302	H-D-Pro-Phe-Arg- <i>p</i> NA·2HCl
S-2366	<i>pyro</i> -Glu-Pro-Arg- <i>p</i> NA·HCl
S-2444	<i>pyro</i> -Glu-Gly-Arg- <i>p</i> NA·HCl
S-2586	MeO-Suc-Arg-Pro-Tyr- <i>p</i> NA·HCl
S-2765	-D-Arg-Gly-Arg- <i>p</i> NA·2HCl
SDS-PAGE	sodium dodecylsulfate-polyacrylamide gel electrophoresis
sTF	soluble tissue factor
TAFI	thrombin activate-able fibrinolysis inhibitor
TAP	tick anticoagulant peptide
TF	tissue factor
TFA	trifluoroacetic acid
TFPI	tissue factor pathway inhibitor
TLE	thrombin-like enzyme
TM	thrombomodulin
t-PA	tissue plasminogen activator
V _{max}	maximal velocity

We can thank Mother Nature for providing us with some clues as to how to better our lives. Sometimes we just need to keep our eyes open...

---Using Leeches as Bait to Go Fishing for New Anticlotting Drugs: Bob Lazarus and Kevin Judice

Chapter 1

Introduction

Blood coagulation



The circulation of blood is pivotal for the survival of an organism. In vertebrates the circulation of blood occurs in a closed circulatory system i.e. the volume of blood fairly remains constant inside the body of the organism. The word

“Hemostasis” refers to the complex interaction between vessels, platelets, coagulation factors, coagulation inhibitors and fibrinolytic proteins to maintain the blood within the vascular compartment in a fluid state. The hemostatic system has evolved over millions of years from the much simpler system. In *limulus*, a 400 million-year old fossil, the entire haemostatic system is contained within a single cell (the amebocyte) that in response to endotoxin (elaborated by bacteria) engulfs the organism and forms a coagulant from the intracellular constituent. This single cell can be viewed as the progenitor of both leukocyte and platelet, serving both haemostatic and inflammatory functions. The haemostatic system that has evolved in humans features extracellular coagulation proteins. This system not only maintains blood in a fluid state under physiologic conditions, but also is primed to react to vascular injury to stem blood loss.

Following vascular injury, several steps occur to staunch the flow of blood. These steps are synergistic and simultaneous.

Vasoconstriction lessens the diameter of the vessel slowing the loss of blood.

Primary hemostasis occurs, wherein platelets bind to collagen in the exposed walls of the blood vessel to form a *hemostatic plug*.

Secondary hemostasis or coagulation occurs, where in zymogens of serine proteases circulating in the plasma are sequentially activated by limited proteolysis culminating in the formation of fibrin clot.

The coagulation cascade involves more than 20 proteases, cofactors and inhibitors. The term “cascade” was first used in 1964 by MacFarlane in describing a proposal for the mechanism of blood clotting* (MACFARLANE, 1964b) (Figure 1.1). This cascade is a sequence of enzyme reactions, each being activated by the previous one, which once initiated proceeds to the final one. The essential advantage inherent in this process is the rapid biochemical amplification of a response. In such systems, proteins operate in pairs, one acting as enzyme, the other as substrate in turn (Kerr *et al.*, 1975; Mullertz *et al.*, 1984).

The formation of blood clot is a carefully regulated process; in 1964, two similar proposals were made independently (DAVIE and RATNOFF, 1964; MACFARLANE, 1964a) which form the basis of the modern day theory of the clotting process. They suggested that the whole process of clot formation, starting from surface contact to fibrin clot formation occurred by the sequential activation of proteins (clotting factors) present in the blood. Each of the clotting factors (except fibrinogen) was proposed to exist as an inert pro-enzyme (zymogen) in the plasma milieu, which on activation activated the next member in the chain. This hypothetical system became popular under the name of the “waterfall” or the “cascade” hypothesis. Over the years

* “AFTER years of confusion, it seems that a relatively simple pattern is emerging from present theories of blood coagulation. Its recognition is assisted by the Roman numeral terminology of the International Committee on Blood Clotting Factors, which, by displacing a profusion of synonyms, allows the basis of factual agreement to be seen. Physiological clotting seems to be initiated by contact of the blood with the 'foreign' surfaces presented by many substances and tissues other than normal vascular endothelium.”

--- “*An Enzyme Cascade in the Blood Clotting Mechanism, and its Function as a Biochemical Amplifier*”
Nature 202, 498 - 499 (02 May 1964)

the waterfall or cascade hypothesis has undergone multiple amendments (Gailani and Broze, Jr., 1991; Sekiya *et al.*, 1996; Schmaier, 1997a; Schmaier, 1998).

The current model of blood coagulation involves two distinct pathways (Figure 1.2): The primary pathway commonly known as the “extrinsic or the tissue factor pathway” and the “intrinsic or the contact activation pathway”. These two pathways merge together with the formation of factor Xa (FXa), the serine protease in the prothrombinase complex responsible for the conversion of prothrombin to thrombin. Thrombin cleaves fibrinogen to fibrin, which polymerizes to form an insoluble fibrin clot. In addition, thrombin is the key activator of platelet aggregation at the site of injury (Davey and Luscher, 1967; Brass, 2003b). Platelets form a plug that stops the hemorrhage and prevents further blood loss. Also, during the activation process a multitude of proteins is released at the site of injury that initiate the process of tissue repair. These include plasma proteins such as von Willebrand factor (vWF), which plays an important role in forming a bridge between the activated platelets and the subendothelium (Girma *et al.*, 1987; de Groot, 2002). Platelet aggregation also promotes the clotting process, since activated platelets provide the phospholipid base required for the formation of the vitamin–K dependent coagulation enzyme complexes. The fibrin clot formed by the clotting cascade, complementarily strengthens the platelet plug.

The tissue factor pathway acts as a “prima ballerina” in clot initiation, and the intrinsic pathway plays a more important role in the propagation of the coagulation (Luchtman-Jones and Broze, Jr., 1995; Schmaier, 1997b). A comprehensive description of the events occurring in both these pathways is presented below.

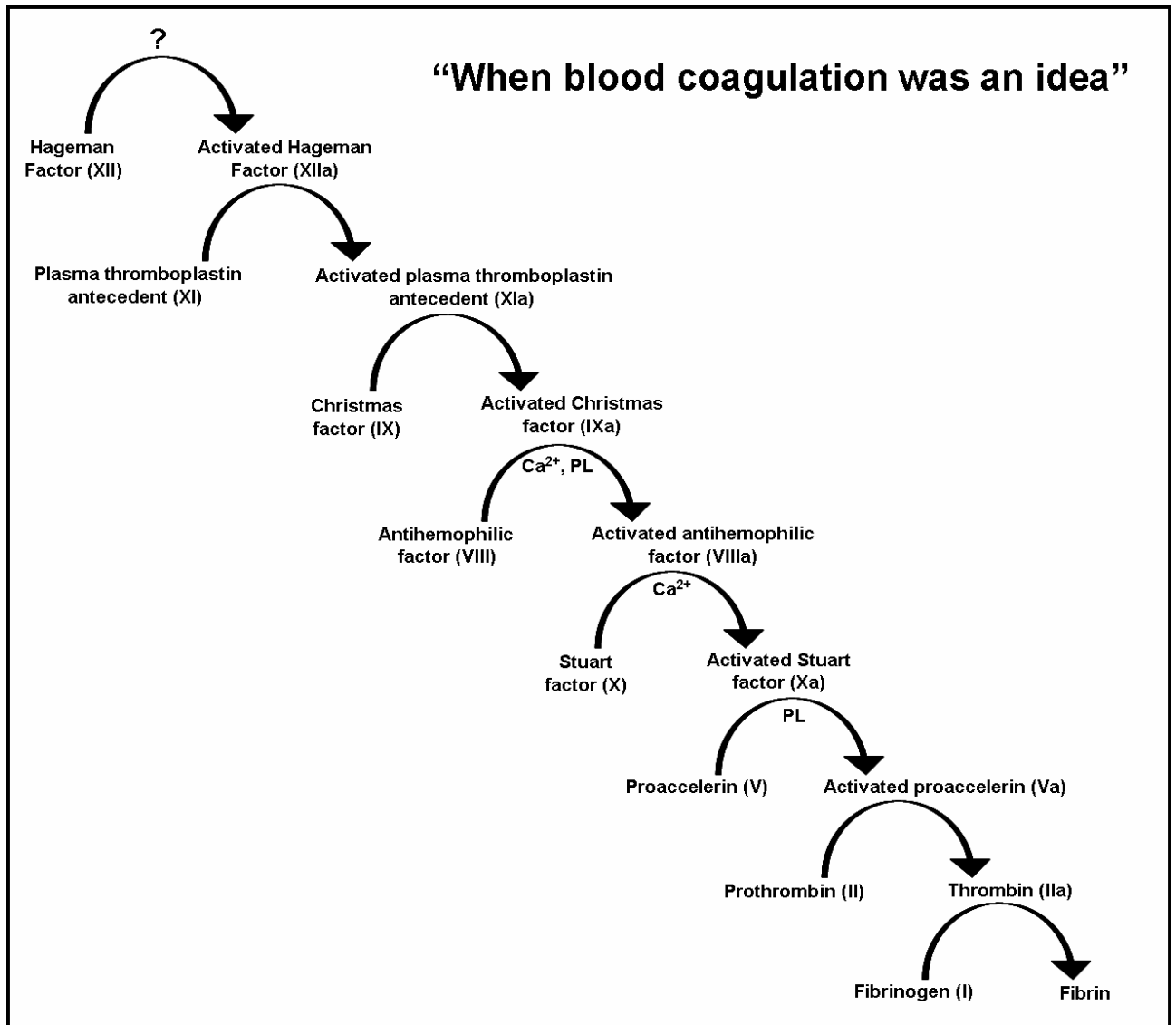


Figure 1.1 (Redrawn from MacFarlane, 1964)

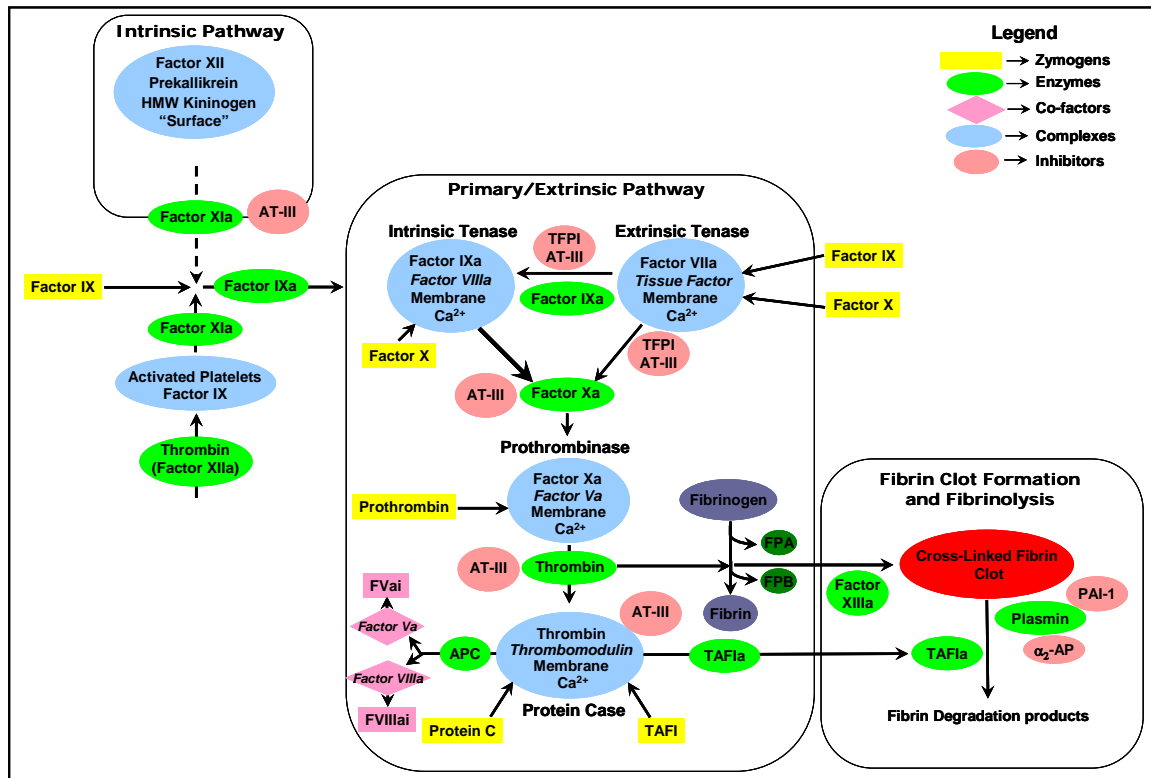


Figure 1.2 The current model of the blood coagulation cascade. There are 2 pathways, the contact activation or intrinsic pathway and the primary or extrinsic pathway. These multicomponent processes are illustrated as enzymes, inhibitors, zymogens, or complexes. The contact activation pathway has no known bleeding cause associated with it, thus this path is considered accessory to hemostasis. On injury to the vessel wall, tissue factor, the cofactor for the extrinsic tenase complex, is exposed to circulating FVIIa and forms the the extrinsic tenase. FIX and FX are converted to their serine proteases FIXa and FXa, which then form the intrinsic tenase and the prothrombinase complexes, respectively. The combined actions of the intrinsic and extrinsic tenase and the prothrombinase complexes lead to an explosive burst of the enzyme thrombin (IIa). In addition to its multiple procoagulant roles, thrombin also acts in an anticoagulant capacity when combined with the cofactor thrombomodulin in the protein Case complex. The product of the protein Case reaction, APC, inactivates the cofactors FVa and FVIIIa. The cleaved species, FVai and FVIIIai, no longer support the respective procoagulant activities. Once thrombin is generated through procoagulant mechanisms, thrombin cleaves fibrinogen (releasing fibrinopeptide A and B [FPA and FPB]) as well as activates FXIII to form a cross-linked fibrin clot. Thrombin–thrombomodulin also activates thrombin activate-able fibrinolysis inhibitor that slows fibrin degradation by plasmin. The procoagulant response is downregulated by the stoichiometric inhibitor tissue factor pathway inhibitor (TFPI) and antithrombin III (AT-III). TFPI serves to attenuate the activity of the extrinsic tenase trigger of coagulation. AT-III directly inhibits thrombin, FIXa, and FXa. The accessory pathway provides an alternate route for the generation of FIXa. Thrombin has also been shown to activate FXI. The fibrin clot is eventually degraded by plasmin yielding soluble fibrin peptides. (Redrawn with modifications from *Statins and Blood Coagulation (2005)* by Anetta Undas, K.E. Brummel-Ziedins and Kenneth G Mann)

Although it has been traditional to divide the coagulation system into intrinsic and extrinsic pathways, such a division does not occur *in vivo*, because the TF-FVIIa complex is the potent activator of both FIX and FX.

The primary pathway (The extrinsic pathway/The tissue factor pathway)

The extrinsic pathway was first formulated by Schmidt and Morawitz as early as 1892 and 1905 respectively; they proposed that thromboplastin released from the tissues, converts prothrombin to thrombin in the presence of Ca^{2+} . Thrombin then converts fibrinogen to insoluble fibrin by a proteolytic cleavage (Blomback *et al.*, 1978; Marsh, Jr. *et al.*, 1983). The classic theory remained accepted for over 50 years, till other blood coagulation factors were discovered mainly between 1940 and 1960 (Macfarlane, 1972).

The term “extrinsic” came from the observation that one of the factors (tissue factor – TF) participating in the initiation of the clotting process is extrinsic to the circulating blood. The pathway is initiated when subendothelial TF is exposed or expressed to blood flow following either damage or activation of the endothelium. This may occur due to the perforation of the vessel wall or activation of the endothelium (Geczy, 1994). Upon activation of endothelial cells (EC) by an injury, ECs immediately release vasoactive agents, such as endothelin (ET) (a potent vasoconstrictor) and nitric oxide (NO) that counteracts endothelin. In states of EC dysfunction the concentrations of bioactive NO are reduced. This leads to the relatively unopposed actions of ET which may promote the generation of pathological vasoconstriction and atherosclerosis formation leading to thrombophilia (Lopez *et al.*, 1990). Other responsive mechanisms of the activated endothelial cells are exhibited by a distinct expression of cytokines, growth factors, and their receptors, including vascular

endothelial growth factor (VEGF) and its two tyrosine kinase receptors VEGFR-1 and -2 (Matsumoto and Mugishima, 2006).

TF binds to zymogen factor VII (FVII) (Morrissey and Neuenschwander, 1996; Rao *et al.*, 1996). However, small amounts of FVII is present in already activated form in the plasma milieu (Radcliffe and Nemerson, 1975b), which also bind to TF to form a complex known as the extrinsic tenase complex. It is to be noted that, the vast majority of enzyme-cofactor complexes that are formed are TF-FVII, but only a small number is TF-FVIIa (Rao and Rapaport, 1988). A trace concentration of FXa is generated by the small number of TF-FVIIa complexes (Butenas *et al.*, 1997). The FXa so formed preferentially and rapidly activates only the FVII of TF-FVII complexes in a key amplifying step of the initiation sequence (Radcliffe and Nemerson, 1976). The activation of FVII by FXa is greatly accelerated following complex formation of FVII with TF (Nemerson and Repke, 1985). TF-FVII complex is also converted to the enzymatically active TF-FVIIa auto-catalytically by TF-FVIIa (Pedersen *et al.*, 1989; Nakagaki *et al.*, 1991; Yamamoto *et al.*, 1992). Thrombin, FIXa and FXIIa also convert FVII to FVIIa (Kisiel *et al.*, 1977; Broze, Jr. and Majerus, 1980a). Recently, a plasmatic serine protease (FVII activating protease or FSAP) has been recognized which also converts FVII to FVIIa (Miura *et al.*, 1996)

The extrinsic tenase complex catalyzes the activation of both FX (Di Scipio *et al.*, 1977a) and FIX (Di Scipio *et al.*, 1978a), the former being the more efficient substrate. Thus, the initial product formed by the activity of extrinsic tenase is FXa; formed by the cleavage of a single bond in FX (Arg52-Ile53 of the heavy chain), a 52-residue activation peptide is concomitantly released during the process (Di Scipio *et al.*, 1977b). The FIX zymogen is a competitive substrate with FX and requires two peptide bond cleavages (at Arg145 and Arg180) for activity. While both of these cleavages are being catalyzed by the extrinsic tenase complex, FXa bound to the membrane can also catalyze one (at Arg145) of the two required cleavages to generate

an intermediate. The final cleavage then occurs at Arg180, leading to the formation of FIXa. Thus, this feed back cleavage of FIX by membrane bound FXa enhances the rate of FIXa generation. (Lawson and Mann, 1991).

The initial FXa that is produced, when bound to membrane activates minute quantities of prothrombin to thrombin, albeit rather inefficiently; this initial thrombin provides the impetus to the propagation of clotting cascade by activating the platelets (Brass, 2003a), FV (Kane and DAVIE, 1988) and FVIII (Osterud *et al.*, 1971).

The intrinsic pathway/The contact activation pathway

The term “intrinsic” or “contact activation” pathway arose from the observation that coagulation occurred spontaneously when blood was placed in glass test tubes. The trigger mechanism of the intrinsic pathway has been studied in great detail on negatively charged surfaces. The main proteins participating in the contact system are – coagulation factors XII (FXII) and XI (FXI), high molecular weight kininogen (HMWK), and prekallikrein (PK).

During injury, negatively charged physiological surfaces such as sulfatides, phospholipids, urates, cholesterol and chondritin sulfates and other glycosamines are exposed. Zymogen FXII binds directly to these surfaces, promoting a conformational change in the molecule. This conformational change in FXII increases its sensitivity to proteolytic activation. Zymogens PK and FXI, circulate in the blood as complexes with HMWK, as PK-HMWK and FIX-HMWK respectively. FXI and PK attach to the negatively charged exposed membrane through their interactions with HMWK. It has been shown that HMWK binds to these surfaces through glycoproteins identical to receptor binding the globular regions of the complement C1-q component (Herwald *et al.*, 1996). Colman has shown that HMWK interacts with the receptor of the urokinase-like plasminogen activator on the surface of the endothelial cells (Ferguson, 1996). This binding brings both the zymogens to the site of injury and in direct

proximity to FXII. The membrane-bound activated form of FXII activates PK to kallikrein by cleaving the Arg371-Arg372 bond (Imamura *et al.*, 2004). Kallikrein formed activates FXII; HMWK increases the rate of the reaction (Fujikawa *et al.*, 1980). This result in the successive generation of two active forms of the factor: aFXIIa and bFXIIa. The cleavage of the Arg353-Val354 bond of FXII results in the formation of aFXIIa form of the enzyme, which consists of a heavy and a light chain (353 and 243 amino acid residues, respectively) bound by a disulfide bond. The bFXIIa form of the enzyme is generated after the hydrolysis of two more peptide bonds Arg334-Asn335 and Arg343-Leu344. These cleavages result in the formation of a 30 kDa enzyme, consisting of the light chain of the enzyme supplemented with a small fragment of the heavy chain (Cochrane *et al.*, 1973; Revak and Cochrane, 1976; Revak *et al.*, 1977; Revak *et al.*, 1978). Both the forms of FXIIa, activate FXI to FXIa by the hydrolysis of the Arg369-Ile370 bond in the presence of HMWK (Bouma and Griffin, 1977). FXIa activates FIX to FIXa by the hydrolysis of the Arg180-Ile181 bond (Di Scipio *et al.*, 1978b). FIXa forms a complex with its non-enzymatic cofactor FVIIIa (already activated by thrombin), on the activated platelet membrane to form the FVIIIa-FIXa complex also known as “intrinsic tenase complex”. This complex becomes the principal activator of FX. The FVIIIa-FIXa complex is 10^5 to 10^6 times more efficient than FIXa alone as FX activator and ~50 times more efficient than the TF-FVIIa in catalyzing FX activation (Hockin *et al.*, 2002). As a consequence most (>90%) of the FXa is produced due the catalytic activity of the intrinsic tenase complex in the TF initiated hemostatic process. Some mutations in FVIII or FIX proteins interfere in the formation of the intrinsic tenase complex

resulting in either no or poor amplification of FXa generation. This is the principal defect observed in hemophilia A and hemophilia B[†] (Palmer *et al.*, 1989).

Convergence of the pathways and fibrin clot formation

FXa formed in the above pathways complexes with FVa (already activated by thrombin) on the activated platelet membrane surface in the presence of Ca²⁺ to form FVa-FXa complex (Swords and Mann, 1993). This complex activates prothrombin to thrombin and hence known as the prothrombinase complex. This complex is 300,000 fold more active than FXa alone in catalyzing prothrombin activation (Krishnaswamy *et al.*, 1987). The principal function of thrombin formed during clotting is the conversion of fibrinogen to fibrin by limited proteolysis.

Fibrinogen is a 340 kDa protein having a symmetrical dimeric structure with two sets of three intertwined polypeptide chains, designated as A α , B β , and γ , linked together by 29 disulfide bonds (Henschen and Lottspeich, 1977; Lottspeich and Henschen, 1977; Doolittle *et al.*, 1979). The B β and γ chains also contain two pairs of carbohydrate side chains, each of molecular weight 2500 Da. Fibrinogen has three globular domains, one on each end and one in the middle where the chains are linked. Rod-like domains separate the globular domains. During the conversion of fibrinogen to fibrin, thrombin cleaves the fibrinopeptides (the short acidic NH₂-terminal sequences on the fibrinogen A α - and B β -chain that shield specific polymerisation sites), which results in a dramatic change in solubility that causes the molecules to aggregate and form fibrin fibers. Thrombin cleaves the fibrinogen between Arg16 and Gly17 and the B β chain between Arg14 and Gly15. The cleavage in the A α chain

[†] 'occasionally (in vitro) the blood of some of the haemophilic patients with a greatly prolonged clotting time...when added to other haemophilic blood possessed a coagulant action nearly as effective as normal blood'

- Pavlovsky (1947) in *Contribution to the pathogenesis of hemophilia. Blood*, 2, 185-191

leads to the formation of double-stranded twisting fibrils which are arranged in a half-staggered overlapping domain arrangement. Fibrils branch out and create structures that result in a complex network of fibers. There are likely to be two different types of branching that define the structure of the clot: In the first type, double-stranded fibrils line up side-to-side and form a tetra-molecular or bilateral branch-point. This kind of branching supports strength and rigidity in the clot. The second kind of branching is trimolecular or equilateral. This is formed by the coalescence of three fibrin molecules that conjoin three double-stranded protofibrils of equal width and probably occurs more often when the rate of fibrinopeptide release is slow. The cleavage in the B β is associated with the lateral aggregation of protofibrils. (Krakow *et al.*, 1972;Williams, 1981;Weisel *et al.*, 1981;Fowler *et al.*, 1981;Weisel *et al.*, 1985;Weisel, 1986)

During clot formation, thrombin catalyzes the conversion of factor XIII (FXIII) to factor XIIIa (FXIIIa) in the presence of Ca²⁺. FXIIIa is a transglutaminase that catalyzes the formation of intermolecular γ -glutamyl- ϵ -lysine crosslinks in the fibrin network, producing an insoluble, pliant blood clot (Ware *et al.*, 1999). Covalent crosslinks occur between opposing chains and involve γ - γ , γ - α , and α - α interactions. These covalent links lead to the formation of a very strong fibrin clot.

Lysis of fibrin clot

Once haemostasis is restored and the tissue is repaired, the clot or thrombus must be removed from the injured tissue. This is achieved by a process known as fibrinolysis. Lysis or dissolution of fibrin clots is brought about by serine protease plasmin. Plasmin circulates as inactive zymogen, plasminogen in the blood (Plow and Collen, 1981). Plasminogen contains secondary structure motifs known as kringles, which bind specifically to lysine and arginine residues in both fibrinogen and fibrin. Tissue

plasminogen activator (tPA) (released from vascular endothelial cells following injury) and, to a lesser degree, urokinase (synthesized as a zymogen prourokinase by epithelial cells lining excretory ducts and is activated by proteolytic cleavage between Leu158 and Ile159) convert plasminogen to plasmin by the cleavage of Arg28-Val29 bond (Robbins *et al.*, 1967; Summaria *et al.*, 1967). Plasmin specifically cleaves the COOH-terminal to the lysine and arginine residues producing fibrin degradation products (FDPs). FDPs compete with thrombin, and slow down the conversion of fibrinogen to fibrin (thus slowing down clot formation) (Merskey *et al.*, 1966; Marder *et al.*, 1971).

After clot lysis, plasmin is released from the clot and is inactivated by α 2-antiplasmin (a serine protease inhibitor) (Moroi and Aoki, 1976). Also, thrombin-activatable fibrinolysis inhibitor (TAFI) (a plasma carboxypeptidase B2 that is activated by a cleavage at Arg92 by the thrombin-thrombomodulin complex) (Tan and Eaton, 1995; Redlitz *et al.*, 1995) cleaves C-terminal Arg residues from fibrin rendering it less susceptible to plasmin.

Regulation of Blood coagulation

Blood coagulation is pivotal for hemostasis and unwanted clot formation can lead to death and debilitation. Therefore control is exerted at each level of the coagulation pathway through inactivation of cofactors and inhibition of enzymes. The protein C anticoagulant pathway plays a major role in the regulation of blood coagulation (For details refer to the recent review by (Mosnier and Griffin, 2006)) (Figure 1.3). Protein C (Stenflo, 1976; Esmon *et al.*, 1976), is activated by thrombin that is bound to the membrane protein thrombomodulin (TM) (Esmon, 1995) on the surface of intact endothelial cells. This complex cleaves at Arg169 to remove the activation peptide and generate activated protein C (APC). A recently described endothelial protein C receptor (EPCR) also stimulates protein C activation (Esmon *et al.*, 1999). Platelet

factor 4 (PF4), released from the platelets during activation also enhances APC generation (Slungaard *et al.*, 2003). APC proteolytically inactivates phospholipid membrane-bound cofactors FVa and FVIIIa and inhibits coagulation. Inactivation of FVa involves three cleavages at Arg306, Arg506 and Arg679 (Kalafatis *et al.*, 1994;Heeb *et al.*, 1995), whereas that of FVIIIa involves two cleavages at Arg336 and Arg562 (O'Brien *et al.*, 2000). Protein S, a vitamin K-dependent plasma protein, acts as a cofactor to APC, and further increases the degradation of FVa and FVIIIa (Walker, 1980). Protein S also exhibits anticoagulant activity individually and can bind to FXa, FVa and FVIIIa, thereby inhibiting prothrombinase and intrinsic tenase activity (Heeb *et al.*, 1993;Heeb *et al.*, 1994). Protein S also competes for procoagulant phospholipid surfaces thereby mediating anticoagulant activity(van Wijnen *et al.*, 1996).

Coagulation is also regulated by the inhibition of active proteases in the cascade. The tissue Factor Pathway Inhibitor (TFPI), a protein produced by the endothelial cells and consisting of three kunitz domains binds to and inhibits the ternary complex TF-FVIIa-FXa (Rao and Rapaport, 1987). Antithrombin (AT) is a serpin (SErine Protease INhibitor) that inhibits thrombin, FXa, FVIIa and to a lesser extent FIXa. However, thrombin bound to fibrin clot is relatively protected by AT (Weitz *et al.*, 1990). Circulating AT is a relatively inefficient, but its activity is stimulated by heparin, heparan sulphates or chondroitine sulphates that are present on the surface of endothelial cells (Weitz, 2003). The potentiation of AT efficiency by heparin is the molecular basis for the use of heparin as a therapeutic anticoagulant. FX as well as FXa is also inhibited by AT but not as potently by a serpin Z protease inhibitor (ZPI). The activity of ZPI is enhanced 1000 fold by vitamin K-dependent protein Z in the presence of phospholipids and calcium ions (Broze, Jr., 2001)

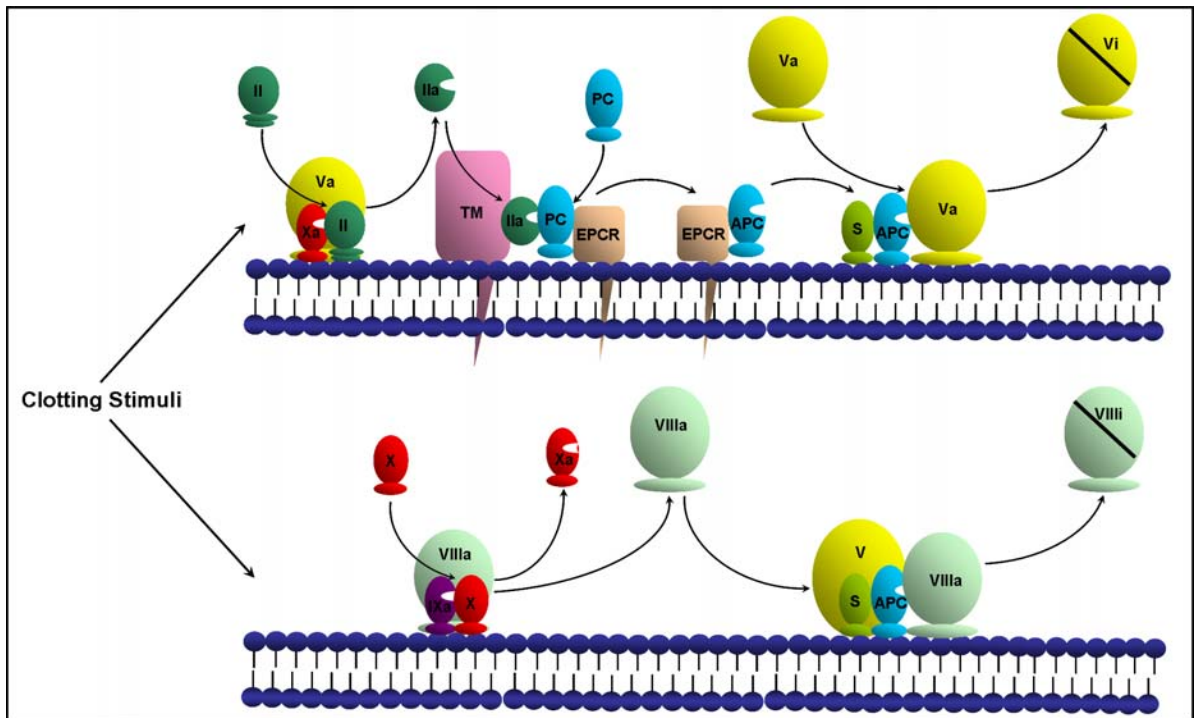


Figure 1.3 Schematic representation of the protein C anticoagulant system. (Redrawn with kind permission from "The Protein C Pathway" by Charles T Esmon, *Chest*:2003 Supplement; 26S-32S). In the presence of intact endothelium, thrombin binds to thrombomodulin and activates protein C. Endothelial protein C receptor (EPCR) stimulates the activation of protein C. Activated protein C counteracts coagulation by cleaving and inhibiting the cofactors FVa and FVIIIa. The free form of protein S in blood serves as cofactor to activated protein C. In the regulation of the tenase complex, FV plays an anticoagulant role as cofactor to activated protein C.

The “extrinsic tenase complex”: macromolecular complex initiating coagulation

As highlighted above the formation of macromolecular enzyme complexes is one of the hallmarks of the coagulation cascade. Since the focus of this thesis relates to the characterization of a protein complex that interferes at this step of the coagulation cascade, *viz.*, the extrinsic tenase complex, it will be described separately in greater detail. The extrinsic tenase complex, the principal initiator of coagulation *in vivo*, consists of TF and FVIIa.

Tissue Factor

TF also known as thromboplastin, CD142 and coagulation factor III is mainly found on the surface of the cells in which it is synthesized. It is abundant in a variety of cell types distributed through out the body, including adventitial cells surrounding all blood vessels larger than capillaries; differentiating keratinocytes in the skin and a large number of epithelial cell types, including those present in mucous membranes and many organ capsules (Drake *et al.*, 1989; Wilcox *et al.*, 1989b; Fleck *et al.*, 1990). It is a glycosylated membrane protein consisting of a single polypeptide chain of 261 to 263 amino acids (the two forms are nearly equal in abundance), with variability in length owing to the microheterogeneity at the NH₂-terminus (Spicer *et al.*, 1987; Morrissey *et al.*, 1987). The calculated molecular weight of the polypeptide is 29,447 Da and 29,593 Da, where as the mobility of the fully glycosylated protein on SDS gels suggests a molecular weight of approximately 45, 0000 Da (Broze, Jr. *et al.*, 1985). TF belongs to the class 2 cytokine receptor superfamily (Bazan, 1990). Three potential N-linked glycosylation sites are available in the extracellular domain of human TF (Paborsky and Harris, 1990), but they are dispensable for clotting activity because the recombinant form produced in bacteria is fully functional (Paborsky *et al.*, 1989). The extracellular domain consists of two fibronectin type III repeats, which

are a variation of the immunoglobulin fold. The extracellular domain has two disulfide bonds (Bach *et al.*, 1988b), at least one of which is important for activity. TF has a typical membrane-spanning domain that anchors the protein to the cell surface. Membrane anchoring of TF is essential for full procoagulant activity, although the exact nature of the membrane anchor does not appear to be important (Paborsky *et al.*, 1991b). The short cytoplasmic domain of TF (23 amino acid long) contains a cysteine residue to which a fatty acyl chain (palmitate or stearate) is attached by thioester linkage (Bach *et al.*, 1988a). In addition the cytoplasmic domain can be phosphorylated on serine (Zioncheck *et al.*, 1992). Deletion of the cytoplasmic domain has no discernible effect on procoagulant activity of TF (Paborsky *et al.*, 1991a), making its role in blood clotting unclear, but recent studies indicate that it may be involved in other non-hemostatic function such as signal transduction (Rottingen *et al.*, 1995; Nystedt *et al.*, 1996; Pendurthi *et al.*, 1997; Poulsen *et al.*, 1998).

Recent studies have shown that, much of TF remains in the 'cryptic stage' meaning that molecules are procoagulantly active. Certain stimuli such as vascular injury 'decrypt' or make them active. Protein disulfide isomerase (PDI) is a critical player which is involved in the activation process, its activity involves the breaking or forming a critical disulfide bond (Ruf *et al.*, 2006).

The crystal structure of soluble tissue factor (sTF) (only the extracellular domain) has been solved (Figure 1.4) (Harlos *et al.*, 1994; Muller *et al.*, 1994; Muller *et al.*, 1996; Muller *et al.*, 1998; Huang *et al.*, 1998b). sTF is an elongated rather rigid molecule in which the two fibronectin domains have an interdomain angle of 120 degrees (Harlos *et al.*, 1994; Muller *et al.*, 1998), which corroborates well with the structural proximity of TF with other cytokine receptors.

Factor VII/ VIIa

FVII is synthesized in the liver and secreted as a single-chain glycoprotein of 48 kDa. It consists of an NH₂-terminal γ -carboxyglutamic acid (Gla) domain, two epidermal growth factor-like domains and COOH-terminal serine protease domain (catalytic domain) (Kisiel and DAVIE, 1975; Radcliffe and Nemerson, 1975a; Broze, Jr. and Majerus, 1980b). It is activated to FVIIa by a cleavage of a peptide bond between Arg152-Ile53 (Wildgoose *et al.*, 1992; Butenas and Mann, 1996). The newly formed NH₂-terminal residue Ile153 buries its side chain in a hydrophobic environment, whilst establishing a salt bridge between its α -amino nitrogen atom and the side chain of residue Asp194. Residue Asp194 is adjacent to the catalytic Ser195, and this salt-bridge contributes to efficient catalysis. In addition, three nearby loops undergo conformational changes to form the substrate-binding cleft (Higashi *et al.*, 1994). In classical serine proteases like trypsin or chymotrypsin, these series of events produces the final active enzyme. FVIIa individually has zymogen like activity and the binding of TF is a pre-requisite for its full enzymatic activity (Higashi *et al.*, 1996). It has been observed that the α -amino nitrogen is relatively susceptible to chemical modification, until TF binds and hence the insertion of Ile153 into FVIIa core appears to be incomplete (Higashi *et al.*, 1994). TF drives the equilibrium between partially and fully active forms towards the active enzyme (Higashi *et al.*, 1996). FVIIa consists of an NH₂-derived light chain (relative molecular mass, 20,000) consisting of 152 amino acid residues and a COOH terminal-derived heavy chain (relative molecular mass, 30,000) consisting of 254 amino acid residues linked via a single disulfide bond (Cys135 to Cys262). The light chain contains the membrane-binding Gla domain (containing 10 γ -carboxyglutamic acid residues) and two EGF domains, while the heavy chain contains the catalytic protease domain (Persson, 2006).

TF-FVIIa complex – “A Classical Allosteric Pair”

Allostery involves changes in the conformation or activity of an enzyme or other protein that arise from its combination with another molecule at a point other than its “chemically active” site. FVIIa is subject to numerous allosteric influences. The ones in the light chain are associated with the binding of eight Ca²⁺ ions in the Gla and

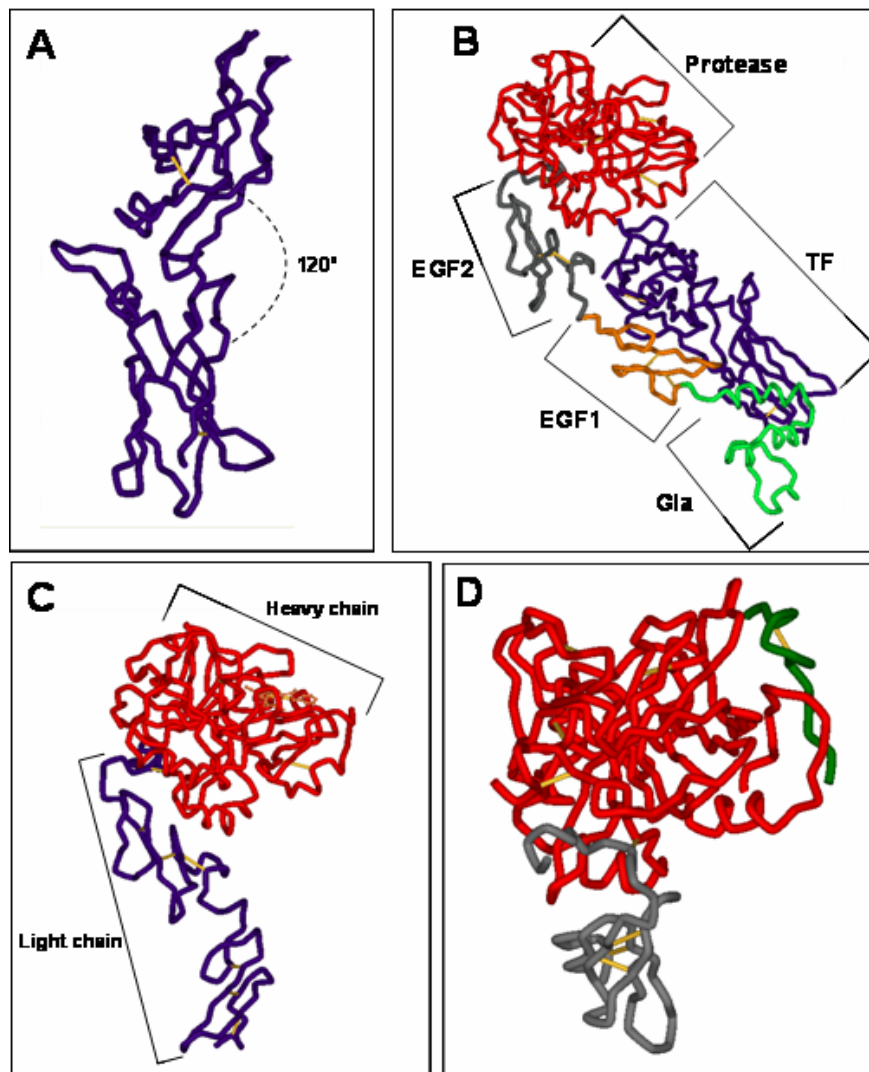


Figure 1.4 Overall view of the (A) The extracellular domain of tissue factor. Note the interdomain angle is 120 degrees. (B) TF-FVIIa complex as determined by Banner et al. (1996). The membrane is presumed to be at the bottom of this view. The three FVIIa light chain domains, Gla, EGF1, and EGF2, are shown. The FVIIa protease domain (heavy chain) is at the top. Carbohydrate moieties attached to the EGF1 and protease domains are however not depicted. (C) FVIIai without TF. (D) Inhibitory peptide A-183 (green tube) complexed with a form of zymogen FVII having only the EGF2 and protease domains

EGF1 domains. However, the exact mechanisms by which these events alter enzymatic activity at the distant active site (Persson *et al.*, 1997; Kelly *et al.*, 1997; Freskgard *et al.*, 1998; Jin *et al.*, 1999; Leonard *et al.*, 2000) still remain unclear.

The allosteric sites localized in the trypsin homology protease domain are somewhat more tractable, since these sites are localized in close proximity to each other. The protease domain contains three TF binding regions localized specifically in the active site binding cleft, and the macromolecular substrate exosite (Dickinson *et al.*, 1996). Binding events at any of these three sites induces changes at the other two. Over the years, new allosteric sites have been discovered using random peptide libraries displayed on phage (Dennis *et al.*, 2000).

TF enhances the catalytic activities of FVIIa, but there are imperative differences in the magnitudes of these changes. There is an approximate 10^5 fold enhancement of proteolytic activity when FVIIa combines with membrane bound TF (Bom and Bertina, 1990; Ruf, 1998), while sTF increases amidolytic activity by only about 50 fold (Butenas *et al.*, 1993; Neuenschwander *et al.*, 1993). The allosteric influences of TF have been brought forward by several X-ray crystal structures of FVIIai (FVIIa with a covalently attached inhibitor in the active site), sTF, and their complex. These studies are also supported by site-directed mutagenesis data.

Banner and colleagues solved the structure of sTF-FVIIa complex at 2.0 Å resolution (Banner *et al.*, 1996) (Figure 1.4). It shows the fully activated enzyme-cofactor complex with a pseudosubstrate covalently attached to active site residues, revealing details of the substrate binding subsites on the NH₂-terminal side of the scissile peptide bond. In the complex, the overall conformation of sTF remains unchanged from its un-complexed form (Harlos *et al.*, 1994). The two fibronectin domains of sTF contact all main domains of FVIIai. The first three domains of FVIIai are connected

via short linker regions and are aligned in a linear fashion, leading up and along the cofactor to place the FVIIa protease domain on top of sTF. The catalytic active site is found about 80 Å above the presumed cell membrane position (McCallum *et al.*, 1996). Recently, it has been shown that the maintenance of this specific distance of 80 Å is crucial for the enzymatic activity of FVIIa (Waters *et al.*, 2006). The NH₂-terminal Gla domain of FVIIa is fully loaded with seven Ca⁺² ions and projects three hydrophobic side chains in the presumed direction of the cell membrane. It also has significant contact with the COOH-terminal domain of TF. The first EGF domain (EGF1) has extensive contact with TF. It also contains a single Ca²⁺ ion and two glycosylation sites projecting away from TF. The EGF2 domain and the catalytic domains are connected by disulfide bonds. Both domains also contact TF, although the mutational data show the greatest contributions to TF affinity come from the Gla and EGF1 domains (Higashi *et al.*, 1996; Dickinson *et al.*, 1996). The protease domain has a high-affinity Ca⁺² binding site (Wildgoose *et al.*, 1990), localized in the loop from Glu70 to Glu80. A significant feature of this complex structure is the large distance between the protease domain NH₂-terminal Ile153 and TF, which eliminated any possibility that the connection between TF binding and NH₂-terminus insertion (detected by resistance to chemical modification of the NH₂-terminus) was allosteric in nature. The authors' speculation as to the allosteric effects of TF binding on the active site geometry was two-fold. The FVIIa loop Cys168-Cys182 (known as classically as the "methionine loop") is longer in FVII than in related proteins, and lies "between" the TF binding region on the protease domain and the substrate binding cleft. It has been suggested that without TF this loop might occlude the cleft or contact the NH₂-terminal Ile153, thus preventing its insertion and partnering with Asp194. An additional possibility, that without TF the Gla and EGF domains could

occlude the active site, has also been postulated. Recent work describing effects of mutations in the methionine loop continue to suggest some role for it in catalysis (Soejima *et al.*, 2001). Later, Zhang *et al.* reported the structure of TF-FVIIa-BPTI complex (BPTI is basic pancreatic trypsin inhibitor) at 2.1 Å resolution (Zhang *et al.*, 1999b) confirming all the highlights observed in the complex structure reported by Banner and his colleagues.

Two contemporaneous reports of nearly identical FVIIai molecules by Pike *et al.* and Kemball-Cook *et al.* showed the true nature of conformational changes in FVIIa caused by TF binding (Pike *et al.*, 1999; Kemball-Cook *et al.*, 1999) (Figure 1.4). Both structures revealed unchanged EGF2 and protease domains that were arranged in essentially the same manner as in the TF-FVIIai complex. Changes were observed in the TF binding region of the protease domain. Both the papers postulate the involvement of the methionine loop in the above change; however they are not conclusive on this point. One emanating point about these structures is the observed “allosteric cross-talk” between the substrate binding cleft and the TF binding region. The simplest interpretation is occupancy of the substrate binding cleft increases TF affinity by conditioning the TF binding region for interaction with the cofactor. However, to assess these conformational changes in FVIIa caused by TF binding and/or by occupancy of the substrate binding cleft, the lone structure of FVIIa has to be there. The recently reported FVII zymogen structure by Eigenbrot *et al.* is close to this ideal, lacking both TF and substrate mimic, but it deviates from the ideal in having an intact connection between EGF2 and the protease domain (Eigenbrot *et al.*, 2001a) (Figure 1.4).

Anticoagulants



"Oh waiter! Will you pass me the anticoagulant please?"

Anticoagulants[‡] are crucial for prevention and treatment of thromboembolic disorders and ~0.7% of the western population receives oral anticoagulant treatment. Heparin and coumarins discovered more than 60 years ago, are the most widely used anticoagulants. However, the non-specific mode of action of these anticoagulants accounts for their

therapeutic limitations in maintaining a balance between thrombosis and hemostasis. This limitation has provided the impetus for the design of new anticoagulants that target specific coagulation enzymes or steps in the coagulation pathway. These anticoagulants have been developed from proteins isolated and characterized from hematophagous organisms, using recombinant DNA technology, or by structure-based drug design. A comprehensive discussion of each of these anticoagulants with a focus on the ones targeting TF-FVIIa complex is given below.

The TF-FVIIa complex is an interesting target in thrombosis-related diseases because the inhibitors targeting TF-FVIIa might achieve anticoagulant efficacy without significantly interfering with normal hemostasis (Harker et al., 1996; Himber et al., 1997). This unusual separation of antithrombotic and antihemostatic effects in experimental models may be related to the recently discovered role of circulating TF in thrombosis (Giesen *et al.*, 1999; Rauch *et al.*, 2000; Balasubramanian *et al.*, 2002). In circulation “Blood borne” TF is associated with monocyte derived microparticles,

[‡] “An anticoagulant is a substance that prevents coagulation that is, it stops blood from clotting.”
–Definition in Wikipedia

which localize to form platelet thrombus through interaction of P-selectin glycoprotein ligand-1 (PSGL-1) with P-selectin on the surface of activate platelets (Falati *et al.*, 2003). Thus, antibody specific to P-selectin exhibits remarkable antithrombotic properties (Palabrica *et al.*, 1992). Therefore, specific inhibitors of TF-FVIIa complex may cause less bleeding because they inhibit intravascular TF at concentrations that are far below those necessary to block the high amounts of the hemostatic extravascular TF (Giesen *et al.*, 1999).

TF-FVIIa specific inhibitors are also useful for the treatment of a multitude of ailments. The complex is an important contributor to diseases pertaining to the cardiovascular system such as angina and myocardial infarction. Atherosclerotic plaque have been shown to contain TF (Wilcox *et al.*, 1989a), which on rupture lead to occlusive thrombus formation thereby triggering myocardial infarction (Badimon *et al.*, 1999). TF-FVIIa is also involved in myocardial ischemia-reperfusion injury, since specific inhibitors of the complex reduce the infarct size in experimental models (Erllich *et al.*, 2000). TF-FVIIa is also thought to participate in restenosis (Jang *et al.*, 1995), venous thrombosis (Lee *et al.*, 2001a), sepsis (Taylor, Jr. *et al.*, 1991), glomerulonephritis (Tipping *et al.*, 1995), rheumatoid arthritis (Bokarewa *et al.*, 2002), sickle cell anaemia (Belcher *et al.*, 2000) and tumor growth and metastasis (Rickles *et al.*, 2003).

Inhibitors of TF and FVIIa

A wide variety of strategic approaches have been availed for the design and synthesis of inhibitors targeting TF-FVIIa complex, as shown in Figure 1.5.

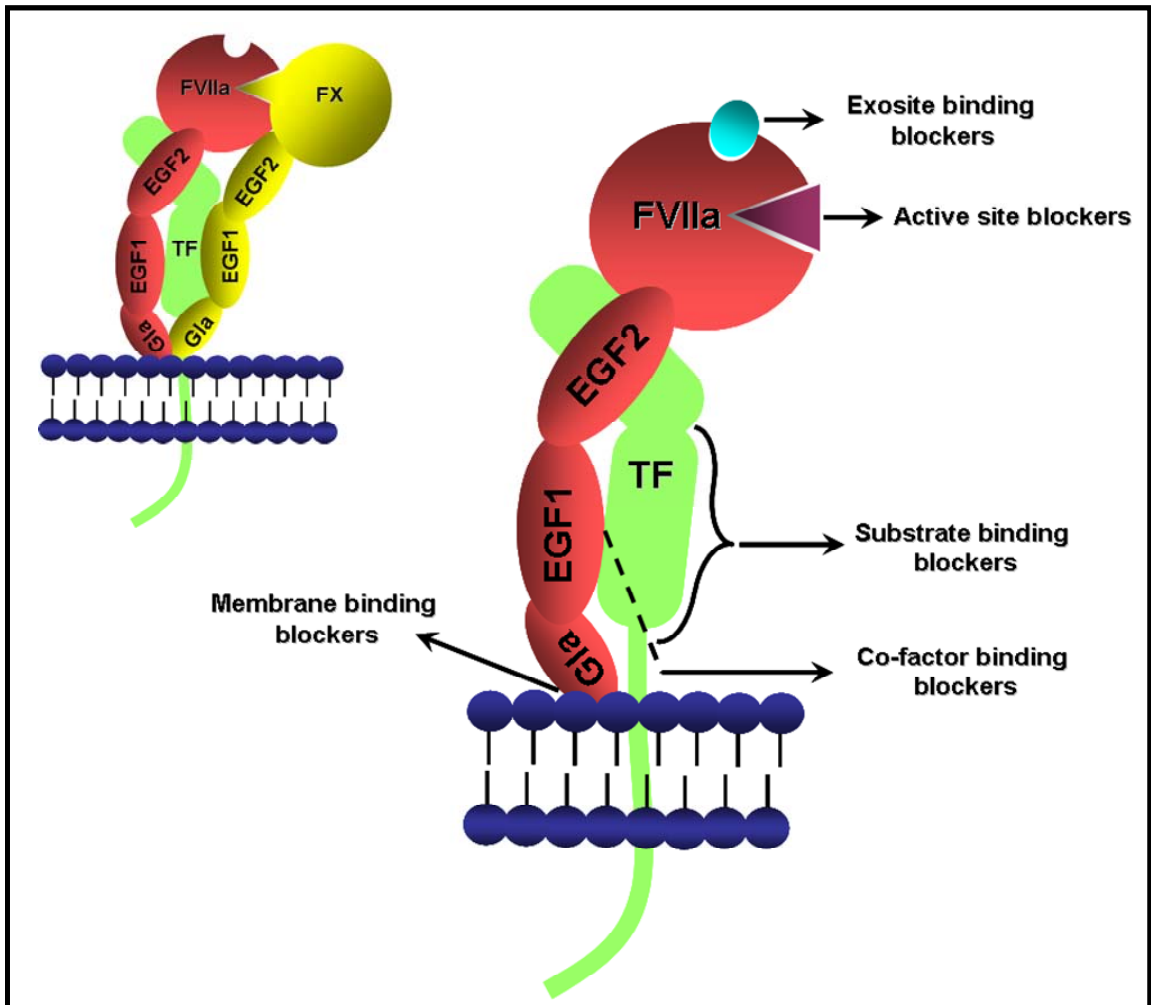


Figure 1.5 Schematic representation of the approaches for TF-FVIIa inhibition. A cartoon of the TF-FVIIa complex on a phospholipid membrane showing the FVIIa domains and the potential intervention site is depicted.

Tissue factor pathway inhibitor (TFPI)

TFPI is a 42 kDa naturally occurring endogenous plasma glycoprotein having 276 amino acid residues. It is a Kunitz-type protease inhibitor consisting of three tandem Kunitz inhibitor domains, the first and second of which inhibit TF-FVIIa complex and FXa, respectively (Bajaj *et al.*, 2001). The third domain has no inhibitory activity and contains the heparin-binding sites (Hamamoto *et al.*, 1993). Similar heparin binding site is also localized in the COOH-terminal basic region of the molecule. Interaction of the these TFPI regions with heparin enhances its anticoagulant potency (Hamamoto *et al.*, 1993). The complete structure of TFPI has not been solved, but the structures of the individual second and third kunitz domains are available (Figure 1.6) (Burgering *et al.*, 1997; Mine *et al.*, 2002).

The anticoagulant action of TFPI is a two-stage process. The second Kunitz domain first binds to a molecule of FXa and deactivates it. The first domain then rapidly binds to an adjacent TF-FVIIa complex, preventing further activation of FX (Figure 1.6) (Baugh *et al.*, 1998; Panteleev *et al.*, 2002). Interestingly, the first kunitz domain of TFPI itself inhibits TF-FVIIa with a K_i of 250 nM (Petersen *et al.*, 1996a). A chimeric protein has been designed by linking the first Kunitz domain of TFPI to the COOH-terminal of the light chain of FX. The chimera potently inhibits TF-FVIIa in the absence of FX/FXa with 14 times more potency than TFPI (Girard *et al.*, 1990).

Recombinant TFPI (tifacogin) has been compared with placebo in phase 2 (Abraham *et al.*, 2001) and phase 3 (Abraham *et al.*, 2003) clinical trials. The promising results of the phase 2 trial were not confirmed in the phase 3. Thus, further development of TFPI for anticoagulant therapy has been halted. A highly homologous protein termed TFPI-2 has also been characterized (Petersen *et al.*, 1996b), though its use as an antithrombotic is still to be tested. A truncated version of TFPI containing only the

first and second Kunitz domains has also demonstrated antithrombotic effects in animal models (Holst *et al.*, 1994).

Nematode anticoagulant protein c2 (NAPc2)

NAPc2 is an 8 kDa polypeptide originally isolated from the canine hookworm, *Ancylostoma caninum* (Cappello *et al.*, 1995). The recombinant protein, rNAPc2, is now expressed in yeast. The protein contains two antiparallel β -sheets and a short helix (Duggan *et al.*, 1999) (Figure 1.6). Both natural and recombinant NAPc2 potentially inhibit TF-FVIIa complex by a unique mechanism, which requires the initial anchoring of the protein to FX or FXa prior to the formation of a final quaternary inhibitory complex with TF-FVIIa (TF-VIIa-Xa-NAPc2). The use of FXa as an inhibitory scaffold for the inhibition of TF-FVIIa complex by NAPc2 appears similar to the mechanism of TF-FVIIa inhibition by TFPI (discussed above). However, unlike TFPI, which specifically requires an un-occupied active site on FXa to allow binding, NAPc2 interacts with FX or FXa via an extended binding site or exo-site. In addition, the unique interaction of NAPc2 with FXa allows the catalytic site of the FXa to remain unobstructed and thus enzymatically active in the quaternary inhibitory complex. However, FXa bound to NAPc2 can cleave only peptidyl substrates but not prothrombin (Lee and Vlasuk, 2003). The proposed sequential mechanism for the inhibition of TF-FVIIa by NAPc2 is schematically illustrated in Figure 1.6.

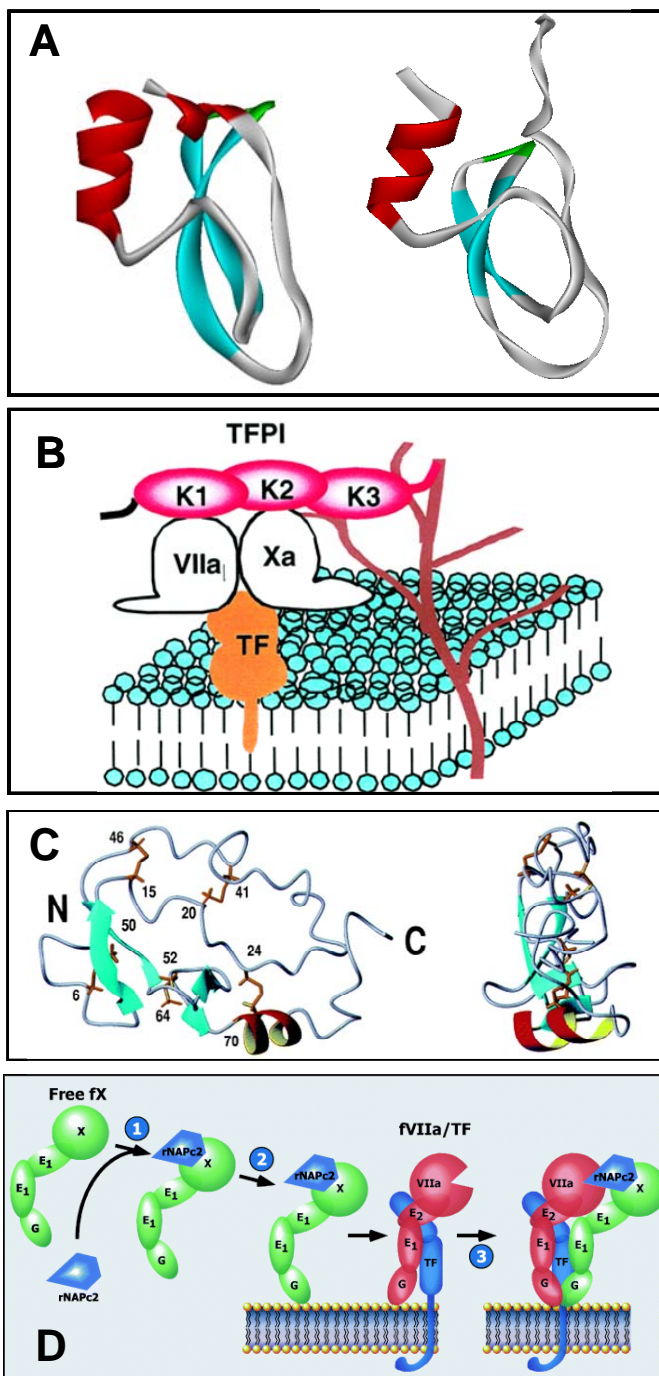


Figure 1.6 (A) Ribbon diagrams of the second and third kunitz domain of TFPI (B) Mechanism of action of TFPI: Inhibitory mechanisms of the initial reaction of blood coagulation by TFPI on cell surface. TFPI binds to factor VIIa and Xa via K1 and K2 domains and to proteoglycans via K3 and C-terminal domains (K denotes kunitz domain) (*diagram kindly provided by Dr. Jun Mizuguchi*). (C) **Ribbon diagram of the minimized mean structures of NAPc2** (*Kindly provided by Dr. Peter E Wright*).

The molecules on the right have been rotated about the vertical axis by 90°. β -strands are shown in cyan and helices in red and yellow. The cysteine side chains are shown in gold. (C) **Mechanism of action of rNAPc2** (Adapted with permission from Rezende et al., 2004). In step 1 of the scheme, rNAPc2 binds with high affinity to zymogen FX in solution (binding to FXa as an inhibitory scaffold is not shown). The resulting stable bimolecular complex between rNAPc2-FX serves as an inhibitory scaffold that facilitates docking to the membrane-bound TF-FVIIa. In this way, the inhibitory scaffold uses both a similar docking mechanism as the natural substrate (FX) and subsequent presentation to the active site of TF-FVIIa. In the last step of the mechanistic

scheme, the canonical reactive loop of rNAPc2 docks into the active site of FVIIa/TF, allowing for the formation of tightly bound quaternary inhibitory complex.

NAPc2 has a half-life of approximately 50 hours after subcutaneous injection. Its anticoagulant activity was evaluated in an open-label phase 2 dose-finding study of 293 patients undergoing elective knee arthroplasty and showed promising results. The safety of NAPc2 has also been assessed in a randomized, double-blind, placebo-controlled dose-escalation study of 154 subjects undergoing elective coronary angiography (Lee *et al.*, 2001b). The prolonged half-life of NAPc2 raised the concern of the reversibility of its anticoagulant effect. However, in a phase I trial in healthy volunteers, it was demonstrated that the use of a pro-haemostatic agent recombinant FVIIa (NovoSeven[®]; Novo Nordisk, Princeton, NJ, USA) effectively reversed the anticoagulant effects of the protein by inducing a transient procoagulant state (Moons *et al.*, 2003).

Ixolaris

This anticoagulant has been isolated from hard tick and Lyme disease vector, *Ixodes scapularis* (Francischetti *et al.*, 2002). It has been shown to inhibit TF-FVIIa induced FX activation with an inhibitory concentration of 50% (IC₅₀) in the picomolar range. At high concentration, Ixolaris attenuates the amidolytic activity of TF-FVIIa; however, in the presence of DEGR-FX or DEGR-FXa (but not des-Gla-DEGR-FXa), Ixolaris becomes a tight inhibitor of TF-FVIIa as assessed by recombinant FIX activation assays. This indicates that FX and FXa are scaffolds for Ixolaris in the inhibition of TF-FVIIa and implies that the Gla domain is necessary for TF-FVIIa-Ixolaris-FX(a) complex formation.

Active site inhibitors

Certain proteins inhibit FVIIa by directly binding to the active site. These are Kunitz type inhibitors, containing about 58 amino acid residues and three conserved disulfide bonds. They are slow tight binding, reversible inhibitors of serine proteases that bind

to the active site and inhibit according to the standard mechanism (Bode and Huber, 1992). Kunitz domain inhibitors of TF-FVIIa has also been selected from Alzheimer's amyloid beta-protein precursor inhibitor (APPI) and basic pancreatic trypsin inhibitor Kunitz domain libraries displayed on phage. An overall consensus inhibitor designated as TF7I-C, differing from APPI in four residues inhibited TF-FVIIa with an apparent K_i of 1.9 nM. But it also inhibited FXIa, plasma kallikrein and plasmin (Dennis and Lazarus, 1994). Later, the Kunitz domain of TF7I-C was utilized to develop a bifunctional inhibitor by covalently linking it to the TF mutant TFAA. The bivalent fusion protein inhibited TF-FVIIa activity specifically with 200 fold more potency than the individual components (Lee *et al.*, 1997).

A bovine pancreatic trypsin inhibitor (BPTI) variant designated as 5LI5, selected from phage display libraries and differing in 8 residues from BPTI inhibited TF-FVIIa with a K_i of 0.4 nM (Stassen *et al.*, 1995a). The crystal structure of the complex of 5LI5 with FVIIa has been solved, shading important lights on the mechanism of action (Zhang *et al.*, 1999a). Also, 5LI5 has been studied in platelet rich venous thrombosis models in hamsters yielding promising results (Stassen *et al.*, 1995b).

Active site inhibited FVIIa (Factor VIIai)

Factor VIIai (FVIIai) is inactivated FVIIa where either dansyl-L-Glu-L-Gly-L-Arg or D-Phe-L-Phe-L-Arg chloromethyl ketone have been used to alkylate the active site (Taylor, Jr., 1996). Enzyme kinetic data indicate that FVIIai behaves completely as a non-competitive inhibitor of FX activation; where the inhibition reaction proceeds through a non productive ternary TF-FVIIai-FX complex (Nemerson and Gentry, 1986). Interestingly, the affinity of TF is five-fold higher for FVIIai than FVIIa itself (Sorensen *et al.*, 1997).

Based on promising results in animal models of thrombosis (Jang *et al.*, 1995), treatment with FVIIai, in doses ranging from 50 to 400 µg/kg with or without adjunctive heparin, was compared with treatment with heparin alone in patients undergoing elective percutaneous coronary interventions. The rates of major bleeding were similar with therapy with FVIIai *plus* heparin and heparin alone. Because of these disappointing results, FVIIai has not been developed further (Lincoff AM, 2000).

Modified TF

Lysine residues at positions 165 and 166 of TF are important for substrate recognition by the TF-FVIIa complex (Roy *et al.*, 1991; Ruf *et al.*, 1992). A soluble TF mutant (TFAA; Alanine at both these positions), containing alanines at the above positions was constructed for use as a specific anticoagulant. TFAA binds to FVIIa and the resultant complex lacks FX activation activity. Moreover, in the plasma TFAA forms complex with FVII and this phenomenon further attenuates its anticoagulant function as evident from *in vitro* studies. Studies conducted in arterial thrombosis models in rabbit with TFAA have shown anti-thrombotic activity with reduced bleeding in comparison to heparin. Further, amino acid substitutions were made in TFAA, increasing its affinity for FVIIa by 20 fold.

Antibody to FVII/FVIIa (Corsevin M™)

A monoclonal antibody to FVII/FVIIa (Corsevin M™, licensed from Corvas International (San Diego, CA), is being studied by Johnson & Johnson in clinical trials. The antibody binds to the protease domain of both FVII and FVIIa in the presence or absence of TF with high affinity and shows mixed type of inhibition for FX activation. A Fab fragment of the antibody reduced circulating FVII and FVIIa

levels (Dickinson *et al.*, 1998). In a phase I study, Corsevin M™ showed immediate and dose-related anticoagulation without adverse effects (Biemond *et al.*, 1995).

Antibody to TF

Two different antibodies that specifically recognize TF at the site of thrombogenesis have been studied in experimental thrombosis models. The first type interferes with the binding of TF to FVIIa (Pawashe *et al.*, 1994; Golino *et al.*, 1996), whereas the second type interferes with substrate docking without affecting the TF binding to FVIIa (Huang *et al.*, 1998a).

Inhibitor of TF synthesis

A hairpin ribozyme has been designed that destroys TF mRNA, abrogating the induction of TF protein expression and activity in vascular smooth muscle cells (Cavusoglu *et al.*, 2002). However, the clinical applicability of this approach has not yet been examined.

Peptide exosite inhibitors

Two different classes of peptide inhibitors (A-series and E-series peptides) of FVIIa inhibitors have recently been discovered using phage display libraries. (Dennis *et al.*, 2000; Roberge *et al.*, 2001; Eigenbrot *et al.*, 2001b). A and E series of peptides have no sequence identity. Both classes of peptides bound to the protease domain of FVIIa, to two distinct exosites to inhibit extrinsic tenase activity. .

The A-series represented by the 15-mer cyclic peptide A-183 (EEWEVLCWTWETCER) is a mixed type inhibitor ($K_i \sim 200$ pM) of FX activation with an IC_{50} of 1.6 nM. (Eigenbrot *et al.*, 2001b). Structural studies showed that the binding of A-183 causes a conformational change in FVII, which disrupts the potential substrate binding sites (Eigenbrot *et al.*, 2001b).

The E-series of peptides represented by 18 residue peptide E-76 (Ac-ALCDDPRVDRWYCQFVEG-NH₂), has a K_d of 8.5 nM for FVIIa and TF-FVIIa complex (Dennis *et al.*, 2000) and inhibits both enzymatic and amidolytic activity of TF-FVIIa (IC₅₀ of ~1 nM). Structural studies with E-76 complexed with FVIIa showed the mechanism of inhibition to be a conformational change in the activation loops (the 140s loop) of FVIIa. It has also been postulated that E-76 also disrupts the hydrogen bond conformation at the oxyanion hole, which is important for stabilization of the transition state of the substrate during catalysis.

In another anticoagulant design strategy, the A and E series peptides were covalently linked together to make fusion peptides (Roberge *et al.*, 2002). The A-linker-E bifunctional peptides are potent anticoagulants that specifically inhibit of TF-FVIIa catalyzed activation of FX.

Cyclic peptide inhibitor

Another peptidic inhibitor, the cyclic pentapeptide Cys-Gln-Gln-Tyr-Cys was derived from a tripeptide motif within the second EGF domain of FVII (Orning *et al.*, 2002). This peptide is a specific and non-competitive inhibitor of TF-FVIIa complex, although in comparison to the exosite binding peptides its inhibitory potency is low.

FVa and FVIIIa inhibitors

Recombinant APC (drotrecogin alfa) mediates anticoagulant activity by inactivating FVa and FVIIIa (Bernard *et al.*, 2001). Another anticoagulant targeting FVa and FVIIIa is soluble thrombomodulin (Kearon *et al.*, 2005). Soluble thrombomodulin binds to thrombin and induces a conformational change in the active site of the enzyme that renders it a potent activator of protein C. A recombinant analog of the extracellular portion of soluble thrombomodulin, which has a half-life of 2 to 3 days has shown promising results in phase 2 clinical trials (Kearon *et al.*, 2005).

FIXa inhibitors

Antibody to FIX

Using phage display strategy, an antibody (10C12), was generated that specifically binds to the Gla domain of FIX. In addition to inhibiting platelet-dependent intrinsic tenase activity, 10C12 inhibited FIX activation by FXIa and by the extrinsic tenase complex (Refino *et al.*, 2002). *In vivo*, 10C12 exerted antithrombotic activities in guinea pig and rat models, with effects on normal hemostasis. However, its efficacy is still to be evaluated in further clinical trials.

Nitrophorin 2

Nitrophorin 2 also known as prolixin-S, is a protein isolated from the saliva of blood-sucking insect *Rhodnius prolixus* (Sun *et al.*, 1996; Isawa *et al.*, 2000). It inhibits free FIXa ($K_i \sim 12.6$ nM) and intrinsic tenase assembled FIXa ($K_i \sim 5.9$ nM).

FXa inhibitors

Pentasaccharide inhibitors

These include fondaparinux (Samama and Gerotziafas, 2003) and idraparinux (Herbert *et al.*, 1998). These inhibitors are synthetic analogs of the unique pentasaccharide sequence that mediates the interaction of heparin with antithrombin (Rezaie, 2001). Once the pentasaccharide/antithrombin complex binds FXa, the pentasaccharide dissociates from antithrombin/Xa complex and can be reutilized.

DX 9065A

DX-9065a is a nonpeptidic arginine derivative that binds to the active site of FXa. Compared to standard heparin, DX 9065A exhibited a favorable antithrombotic/bleeding ratio, therefore showing that it might be considered as a promising compound in the treatment and prevention of various thrombotic diseases

(Dyke *et al.*, 2002). Razaxaban, another synthetic active site inhibitor of FXa has shown promise as an anti-thrombotic agent (Wong *et al.*, 2007).

Inhibitors from tick

Tick anticoagulant peptide (TAP), a 60 amino acid residue polypeptide isolated from the soft tick *Ornithodoros moubata* is one of the well studied tick-derived FXa inhibitor (Waxman *et al.*, 1990). It is a slow-binding reversible inhibitor of free FXa ($K_i = 0.5$ nM) and prothrombinase assembled FXa ($K_i = 5.3$ pM) (Vlasuk, 1993). Other tick-derived FXa inhibitors include Salp14 from *Ixodes scapularis* (Narasimhan *et al.*, 2002) and factor Xa Inhibitor (fXaI) from *Ornithodoros savignyi* (Gaspar *et al.*, 1996).

Inhibitors from leech

Antistasin, a 119 amino acid residue protein isolated from the salivary glands of the Mexican leech *Haementeria officinalis* (Han *et al.*, 1989), is one of the most well studied leech derived FXa inhibitor. It is a tight-binding, reversible inhibitor of FXa ($K_i = 0.31$ - 0.62 nM) (Mao *et al.*, 1998). Other FXa inhibitors from leech include lefaxin from *Haementeria depressa* (Faria *et al.*, 1999), ghilanten from *Haementeria ghilianii* (Blankenship *et al.*, 1990; Brankamp *et al.*, 1991) and therostasin from *Theromyzon tessulatum* (Chopin *et al.*, 2000).

Nematode Anticoagulant protein 5 (NAP5)

NAP5, a 77 amino acid residue protein from canine hookworm *Ancylostoma caninum* inhibits both free FXa ($K_i \sim 43$ pM) and prothrombinase assembled FXa ($K_i \sim 144$ pM) (Stassens *et al.*, 1996). NAP6 from *Ancylostoma caninum* (Stassens *et al.*, 1996) and AceAP1 from *Ancylostoma ceylanicum* (Harrison *et al.*, 2002) are the other hookworm-derived FXa inhibitors.

Draculin

It is a 411 amino acid containing glycoprotein isolated from vampire bat *Desmodus rotundus* (Apitz-Castro *et al.*, 1995). Draculin is a tight binding non-competitive inhibitor of FXa. It also inhibits FIXa to some extent (Fernandez *et al.*, 1999).

Thrombin inhibitors

Inhibitors from leech

Hirudin is the most well studied anticoagulant belonging to this group. It is a 65 amino-acid polypeptide originally isolated from the salivary glands of medicinal leech *Hirudo medicinalis* (Scharf *et al.*, 1989; Markwardt, 1994). It is now produced using recombinant DNA technology, with the recombinant form lacking a sulfate at tyrosine-63 (Winant *et al.*, 1991). Recombinant hirudin has a high affinity for thrombin and binds to both the active center and exosite 1 on thrombin, forming a slowly reversible complex with the enzyme. Two forms of hirudin have been produced for commercial use: Repludin (leprudin, Hoechst-Marion Roussel, Kansas City, MO, USA); and Desirudin (Revasc, GCP39393, Novartis, Basle, Switzerland). Other thrombin inhibitors from leech include hirullin (bifrudin) (Connolly *et al.*, 1992) from *Hirudinaria manillensis*, thrombin (Salzet *et al.*, 2000) from *Theromyzon tessulatum* and haemadin (hemadin) (Strube *et al.*, 1993) from *Haemadipsa sylvestris*.

Hirudin derivatives

A dodecapeptide made up of residues 53 to 64 of the carboxyterminal region of hirudin designated as hirugen, is a weak inhibitor of thrombin activity (Glusa, 1994). Hirugen, by the addition of the peptide derived from the fibrinogen cleavage region of thrombin (D-Phe-Pro-Agr-Pro(Gly)₄), has been converted into a potent inhibitor of thrombin. The chimeric peptide known as hirulog (Maraganore *et al.*, 1990)

(Maraganore and Adelman, 1996), binds to both the active site and exosite I on thrombin. Hirulog was developed as bivalirudin by Biogen (Cambridge, MA, USA) (Nawarskas and Anderson, 2001). Unlike hirudin, bivalirudin can be given in weight-adjusted doses and does not require careful laboratory monitoring.

Inhibitors from tick

Numerous thrombin inhibitors have been isolated from ticks. Ornithodorin is the most well studied of the tick-thrombin inhibitors. It is a 119 amino acid residue protein from the blood sucking soft tick *Ornithodoros moubata*, which inhibits thrombin with high specificity ($K_i \sim 10^{-12}$ M). The crystal structure of the complex between ornithodorin and thrombin has been solved at 2.8 Å resolution (van de *et al.*, 1996). Other tick-derived thrombin inhibitors include madanin (two isoforms) from *Haemaphysalis longicornis* (Iwanaga *et al.*, 2003), boophilin from *Boophilus microplus* (cattle tick) (Lai *et al.*, 2004), americanin from *Amblyomma americanum* (lone star tick) (Zhu *et al.*, 1997), savignin from *Ornithodoros savignyi* (Nienaber *et al.*, 1999) and nymphal thrombin inhibitor (NTI) from *Hyalomma dromedarii* (camel tick) (Ibrahim *et al.*, 2001).

Inhibitors from other arthropods

Anophelin is the most studied protein belonging to this group. It is a cysteine less peptide containing 62 residues, isolated from the salivary glands of the mosquito *Anopheles albimanus*, which inhibits thrombin with high specificity ($K_i \sim 2$ nM) (Valenzuela *et al.*, 1999). Others include, dipetalogastin from *Dipetalogaster maximus* (Mende *et al.*, 1999), thrombostasin from *Haematobia irritans irritans* (horn fly) (Zhang *et al.*, 2002) and TTI from *Glossina morsitans morsitans* (Tsetse fly) (Cappello *et al.*, 1996).

Low molecular weight thrombin inhibitors

Several low-molecular-weight direct thrombin inhibitors have been produced. These agents bind to the active site of thrombin and are available in two classes: noncovalent and reversible covalent inhibitors. Argatroban (Novastan, Texas Biotechnology, Houston, TX, USA) (Walenga, 2002), napsagatran (Roche, Basle, Switzerland) (Roux *et al.*, 1996), inogatran (Astra Zeneca, London, UK) (Gustafsson *et al.*, 1996), and melagatran (Astra Zeneca, London, UK) (Koestenberger *et al.*, 2005) are some of the well known non covalent inhibitors. An example of a reversible covalent inhibitor of thrombin is efegatran (Eli Lilly, Indianapolis, IN) (Klootwijk *et al.*, 1999), which is currently undergoing clinical trials. Other reversible covalent inhibitors, including DNA aptamers (Macaya *et al.*, 1993), are in various stages of development.

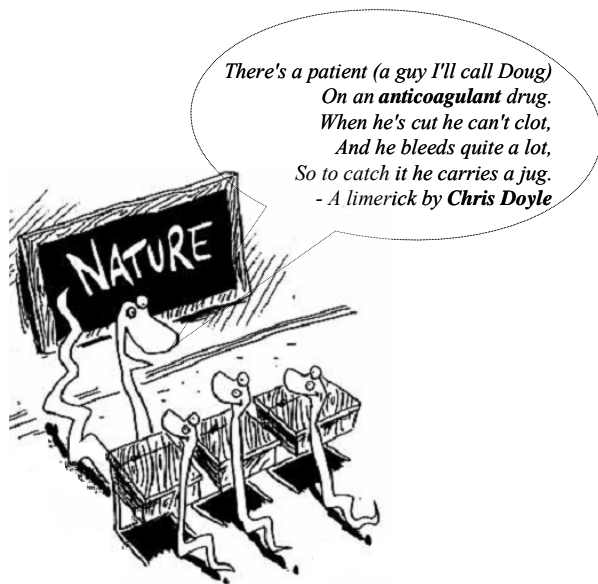
FXIIIa inhibitors

FXIIIa cross links α and λ chains of fibrinogen to fibrin to form polymers and dimers respectively, therefore of inhibition of FXIIIa has the potential to increase the susceptibility of the thrombus to lysis. Tridegin, peptide isolated from *Haementeria ghilianti* is a specific inhibitor of FXIIIa and enhances fibrinolysis *in vitro* (Finney *et al.*, 1997). Other fibrinolytic agents that have exhibited promise are destabilase from leech (Arocha-Pinango *et al.*, 1999) and desmoteplase from *Desmodus rotundus* (Stewart *et al.*, 1998).

“The search should be on” – The above discussed anticoagulants target specific steps in coagulation. Initiation of coagulation can be inhibited by agents that target the TF-FVIIa complex, whereas propagation of coagulation can be blocked by drugs that target FIXa or FXa or by inactivation of FVa or FVIIIa. Thrombin inhibitors prevent fibrin formation and block thrombin-mediated feedback activation of FV, FVIII, and FXI. However, to gain acceptance for prophylaxis and treatment of

thromboembolism, new anticoagulants must have a high benefit-to-risk ratio, which is not always the case. Therefore, the search for novel anticoagulants and anticoagulation strategies should go on to keep the pipeline of anticoagulant leads always running.

Snake Venom Anticoagulant Proteins



Snake venoms[§] are complex mixtures of proteins and peptides possessing a diverse variety of physiological activities. Proteins and peptides comprise about $90 \pm 95\%$ of the dry weight of the venom. Other components in the venom are metallic cations (Na^+ , Ca^{2+} etc.), carbohydrates (in the form of

glycoproteins), nucleosides, biogenic amines and very low levels of free amino acids and lipids (Russell, 1980). Snake venoms possess a whole host of enzymatic activities including, but not limited to, phospholipase A_2 (PLA_2), phosphodiesterase, phosphomonoesterase, L-amino acid oxidase, acetylcholinesterase, serine protease, metalloprotease, arginine esterase, 5'-nucleotidase, hyaluronidase and NAD nucleosidase (Russell, 1980). Not all these enzymes are present in all venoms. The peptides in snake venoms primarily consist of neurotoxins, cytotoxins, myotoxins, and disintegrins (Stocker, 1990).

Although, the poisonous effect of snake bite is known since antiquity, it was Macfarlane's work that first highlighted the effect of snake venoms on blood coagulation. He milked 20 assorted species of snakes and tested the crude venoms on hemophilic blood *in vitro*. The one "which stood out" was Russell's viper venom

[§] "You know, you can touch a stick of dynamite, but if you touch a venomous snake it'll turn around and bite you and kill you so fast it's not even funny" - Steve Irwin - *The Crocodile Hunter*

(RVV) (Macfarlane 1967 p. 441). Macfarlane showed that RVV reacted with FX in the presence of FV and phospholipid (Macfarlane, 1961).

Over the years, a number of snake-venom components capable of interfering in the hemostatic process have been described, which can be broadly categorized into procoagulant or anticoagulant proteins, on the basis of their ability to shorten or prolong the clotting process. Procoagulant proteins are either serine proteases or metalloproteases. Their sizes vary between 24 kDa and 300 kDa. They induce clotting either by specifically activating zymogen, of one of the blood coagulation factors, or by directly converting soluble fibrinogen into an insoluble fibrin clot. Structure-function relationship of these proteins have been studied intensively (For details refer to the review (Rosing and Tans, 1992;Kini *et al.*, 2001;Morita, 2005;Kini, 2005b).

Anticoagulant snake venom components are proteins or glycoproteins with molecular masses ranging from 6 kDa to 350 kDa. The first anticoagulant protein was purified from *Trimeresurus gramineus* snake venom by Shiau and Ouyang in 1965. This protein had an estimated molecular weight of 19.5 kDa (pI 4.5). It markedly inhibited prothrombin activation (Ouyang and Yang, 1975). Since then, numerous anticoagulant proteins have been characterized.

Based on their mechanism, snake venom anticoagulant proteins can be classified broadly into two categories; ones that impair formation of blood clot by proteolytically cleaving one or more of the components that are critical part of the coagulation machinery and others that bind to activated factors and block their coagulant activity or that bind to non-activated factors and block the formation of clotting complexes such as tenase or prothrombinase. In the former group we have enzymes such as PLA₂, serine proteases, metalloproteases and L-amino acid oxidase

(LAO). The latter group consists of non-enzymatic proteins such as C-type-lectin-related-proteins and three-finger toxins.

Anticoagulant Phospholipase A₂ (PLA₂) enzymes

PLA₂ enzymes are one of the imperative components of snake venoms. These enzymes hydrolyze glycerophospholipids at the *sn*-2 position of the glycerol backbone, liberating lysophospholipid and fatty acid. They can be divided into four distinct groups, two of which include all venom PLA₂s from snake venoms (Dennis, 1994). Most of the PLA₂s purified from Elapidae and Hydrophidae belong to group I, while those purified from Viperidae venoms belong to group II. Both group I and II PLA₂s, however share certain structural characteristics: low molecular mass (14 to 18 kDa), five to eight disulfide bridges, and Ca²⁺-dependent catalytic activity. They exhibit a typical fold, having a core of three α -helices, a distinctive backbone loop that binds catalytically important calcium ion, and a β -wing that consists of a single loop of antiparallel β -sheet. The COOH-terminal segment forms a semi-circular banister, around the Ca²⁺-binding loop (Arni and Ward, 1996;Kini, 2003;Kini, 2005a) (Figure 1.7A). Venom PLA₂s exhibit a wide array of biological activities, including neurotoxic, cardiotoxic, myotoxic, hemolytic, convulsive, anticoagulant, antiplatelet, edema inducing and tissue damaging effects (Kini, 2003).

Anticoagulant venom PLA₂s primarily mediate their effect by the hydrolysis of procoagulant phospholipids or by binding to them (Boffa and Boffa, 1976;Markland, 1998;Mounier *et al.*, 2001). Several strongly anticoagulant PLA₂s have been described, such as those isolated from *Vipera berus*, *Deboia russelli*, *Bitis caudalis*, and *Trimeresurus mucrosquamatus*. These molecules' activities are related to their capacity for binding to phospholipids, where they compete with coagulation factors (Ouyang *et al.*, 1981;Babu and Gowda, 1994), or they may hydrolyze these

phospholipids (Kini and Evans, 1989). Weakly anticoagulant PLA₂s such as superbins I and II or CM-I and CM-II from *Austrelaps supererbus* and *Naja nigricollis* respectively inhibit the extrinsic tenase complex (Stefansson *et al.*, 1989; Subburaju and Kini, 1997). The anticoagulant activities of CM-I and CM-II were shown to be dependent on the presence of phospholipids (Stefansson *et al.*, 1989). The PLA₂ from *B. lanceolatus* was shown to inhibit FX activation in a phospholipid-dependent manner (Lobo *et al.*, 2001).

Interestingly, PLA₂s also mediate anticoagulant activity by binding to coagulation factors. Stefansson *et al.* purified and characterized three isoenzymes from *Naja nigricollis* venom. The more basic PLA₂, CM-IV inhibited the prothrombinase activity independently from the presence of phospholipids, whereas the weakly anticoagulant enzymes (CM-I and CM-II) required phospholipids (Stefansson *et al.*, 1990). In addition, an enzymatically inactivated CM-IV was able to inhibit the prothrombinase complex, although it failed to inhibit the tenase complex (Stefansson *et al.*, 1990; Kini and Evans, 1995). In fact, CM-IV was shown to bind to FX ($K_d = 500$ nM, with a stoichiometry of 1.3) and compete for its interaction with FV during formation of the prothrombinase complex (Kerns *et al.*, 1999; Mounier *et al.*, 2001) (Figure 1.7B).

Notably, the anticoagulant activity of this PLA₂ is not due to its basic nature, because other basic PLA₂s such as notexin from *Notechis scutatus scutatus*, CM-III from *Naja mossambica*, and pseudexin B from *P. porphyriacus* do not exhibit this activity (Kerns *et al.*, 1999; Mounier *et al.*, 2000). Also, anticoagulant snake venom PLA₂s, such as the basic subunit CB of crotoxin, PLA₂ from *Vipera berus* and the catalytically inactive basic PLA₂ from *Bitis asper* are thought to mediate their activity by binding to FXa (Mounier *et al.*, 2000; Mounier *et al.*, 2001).

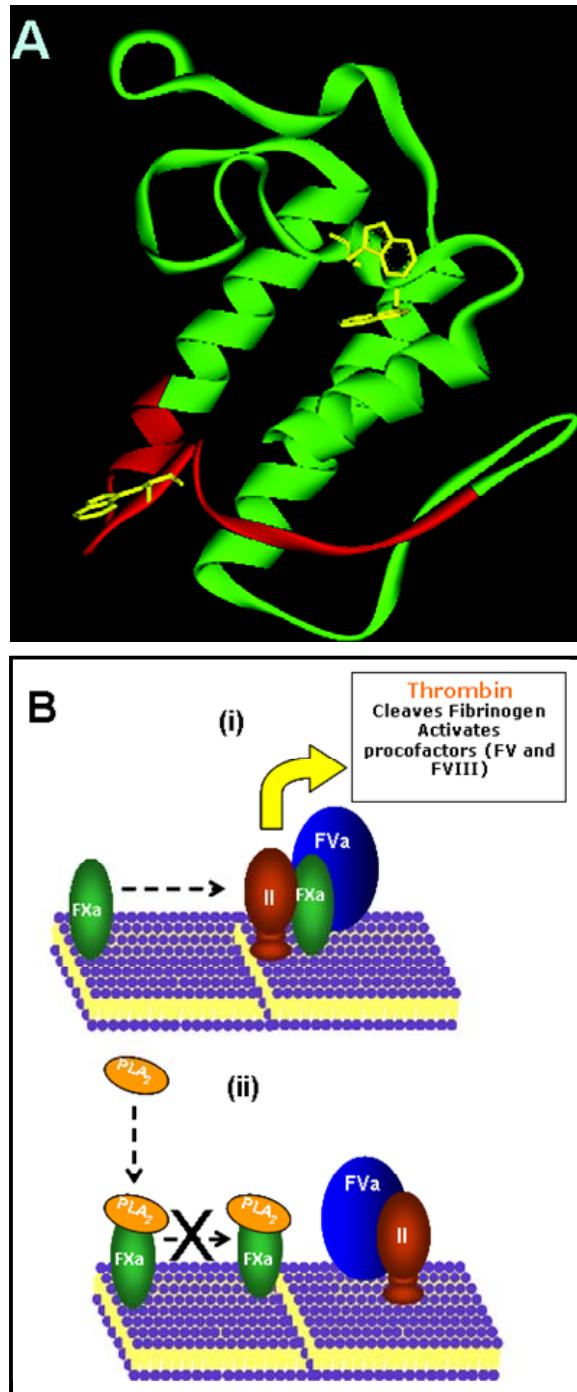


Figure 1.7 (A) The predicted anticoagulant region of anticoagulant PLA₂ enzymes. The ribbon model of *N. naja* PLA₂ was generated from the PDB file (#1POA). The predicted anticoagulant region (highlighted in red) is fully exposed on the surface and easily accessible for interaction. Tryptophan residues are shown in yellow. **(B) Mechanism of anticoagulant activity of PLA₂.** (i) Formation of regular prothrombinase complex on the negatively charged surface of a cell. (ii) The mechanism of anticoagulant action of PLA₂ is based on its interaction with factor Xa and blockage of the interaction of factor Xa with factor Va for the formation of prothrombinase complex (A). (PT, prothrombin; FVa, activated factor V; FXa, activated factor X; T, thrombin, PLA₂, anticoagulant phospholipase A₂.)

Based on a systematic comparison of the amino acid sequences of strongly, weakly, and non-anticoagulant PLA₂s, Kini and Evans (1987) proposed an anticoagulant region that lies between residues 54 and 77. This region is positively charged in strongly anticoagulant PLA₂s, where a pair of lysine residues is present at both ends, but not in weak or non- anticoagulant PLA₂s (Kini and Evans, 1987). All the chemical modification studies and site-directed mutagenesis experiments support this prediction (Kini and Evans, 1987; Inada *et al.*, 1994; Mounier *et al.*, 2000).

L-amino acid oxidase (LAO)

LAOs are hemorrhagic toxins in snake venoms, that catalyze oxidative deamination of L-amino acids with the generation of hydrogen peroxide. LAOs can alter platelet function (Sakurai *et al.*, 2001). Recently, it was shown that M-LAO i.e. LAO isolated from *Agkistrodon halys blomhoffii* venom possesses anticoagulant activity (Sakurai *et al.*, 2003). The enzyme prolongs clotting in activated partial thromboplastin time in a dose-dependent manner but does not affect prothrombin time, indicating that its principal activity is mediated via the intrinsic pathway. Later, M-LAO was found to specifically inhibit FIX in a dose-dependent manner, supporting the fact that it impairs the intrinsic clotting pathway. Interestingly, no interaction between M-LAO and FIX could be detected in surface plasmon resonance studies. On the contrary, it seems that the inhibition is dependent on the formation of hydrogen peroxide (Sakurai *et al.*, 2003); indicating that, in this case, the enzymatic activity is required for inhibition.

Serine proteases

Snake venom serine proteases affecting coagulation, like human serine proteases, belong to the trypsin like subfamily of proteases. They are abundant in *Viperidae* and *Crotalidae* venoms. They are composed of approximately 235 amino acids and

contain six conserved disulfide bridges (Markland, 1998). These enzymes are not lethal by themselves and primarily facilitate the digestion of the prey, but they also contribute to the toxic effect of the venom when associated with other proteins.

Serine proteases mediate anticoagulant effect by the activation of protein C, thereby promoting the degradation of FVa and FVIIIa. Stocker *et al.* characterized a protein C activator from southern copperhead (*Agkistrodon contortrix contortrix*) venom (Stocker *et al.*, 1987). This protein C activator is called protac and is a serine protease of molecular weight 37 kDa. The enzyme is a single chain glycoprotein possessing $16 \pm 20\%$ carbohydrate (Murakami and Arni, 2005). Similar protein C activators have been isolated from the venoms of snake species belonging to the genus *Agkistrodon* (Klein and Walker, 1986; Stocker *et al.*, 1986; Kisiel *et al.*, 1987; McMullen *et al.*, 1989; Bakker *et al.*, 1993).

Another group of anticoagulant serine proteases are designated as thrombin like enzymes (TLE). They are widely distributed within several pit viper genera (*Agkistrodon*, *Bothrops*, *Crotalus*, *Lachesis* and *Trimeresurus*), as well as some true vipers (*Bitis* and *Cerastes*) and the colubrid, *Dispholidus typus*. TLEs convert fibrinogen into fibrin by cleaving fibrinopeptides A and/or B (Aronson, 1976; Bell, Jr., 1997). As this activity resembles the most well known activity of thrombin, these venom components are generally termed 'thrombin-like' enzymes. However, the fibrin monomers generated by TLEs undergo limited polymerization, since only one fibrinopeptide is cleaved and also because these enzymes do not activate transglutaminase FXIII, to generate FXIIIa. Therefore, clot formation is hampered as cross-linking of fibrin monomers does not take place. TLEs have been isolated and characterized from numerous snake venoms. Because of their unique property they are widely used as defibrinogenating agents, ancrod [Arvin®; from *Calloselasma*

rhodostoma (the Malayan pit viper)] (Sherman, 2002) and batroxobin [Defibrase®; from *Bothrops moojeni* (the Brazilian lancehead snake)] (Huang *et al.*, 1992) are some of the well-known ones.

Snake Venom Metalloproteases (SVMP)

SVMPs belong to the M12 subfamily of metalloproteases also known as reprotins. Based on domain architecture SVMPs are classified into PI (SVMPs having only a metalloprotease domain); PII (SVMPs being synthesized with metalloprotease domain and disintegrin domain); PIII (SVMPs as being synthesized with metalloprotease domain, disintegrin-like domain and cysteine-rich domain) and PIV (SVMPs having the PIII domain structure plus lectin-like domains connected by disulfide bonds) (Bjarnason and Fox, 1995; Jia *et al.*, 1996; Fox and Serrano, 2005). Zn²⁺ ions are prerequisite for optimal catalytic activity of SVMPs. The zinc-binding site has a common amino acid sequence in the different metalloproteases, HEBXHXBGBXHZ, where H is histidine, E is glutamic acid, G is glycine, B is a bulky hydrophobic residue, X is any amino acid, and Z is different in all four subfamilies but is conserved in any given subfamily. SVMPs exhibit haemorrhagic, pro-coagulant, anticoagulant and antiplatelet effects (Fox and Serrano, 2005).

Anticoagulant SVMPs are fibrinogenases. Based on their cleavage specificity of the fibrinogen chain they are classified as either α - or β -chain fibrinogenases (Ouyang and Teng, 1976). Interestingly, no reports of a fibrinogenolytic snake venom enzyme with cleavage specificity directed solely to the γ -chain of fibrinogen are known. Specificity for the α - or β -chains is not absolute since there is substantial degradation of the alternate chain with increasing time. These enzymes differ significantly from plasmin which is a serine protease and is readily inactivated by plasma serine protease inhibitors (SERPINS). Further, plasmin cleaves peptide bonds at the COOH-terminal

side of lysine residues in the α -, β - and γ -chains of fibrinogen, sites distinctively different from the ones cleaved by the venom fibrinogenolytic enzymes (Fox and Serrano, 2005).

Anticoagulant C-type-lectin-related-proteins

Proteins belonging to this group are structurally homologous with true C-type lectins, but apparently they are unable to bind to carbohydrate (Ebner *et al.*, 2003). Anticoagulant proteins belonging to this group can be discussed broadly under FIX/FX binding proteins and thrombin and prothrombin binding proteins.

FIX/FX binding proteins

Based on their ligand recognition specificity, these proteins can be further classified into three distinct groups: FIX/FX-binding proteins, such as those purified from *T. flavoviridis* (Atoda and Morita, 1989; Atoda *et al.*, 1991), *B. jararaca* (Sekiya *et al.*, 1993), *Echis carinatus leucogaster* (Chen and Tsai, 1996), and *A. halys brevicaudus* (Koo *et al.*, 2002) snake venoms; FIX-binding proteins, purified from *T. flavoviridis* (Atoda *et al.*, 1995), *T. stejnegeri* (Xu *et al.*, 1999), and *A. halys pallas* (Zang *et al.*, 2003) venoms; and coagulation FX-binding proteins, purified from *Deinagkistrodon acutus* (Cox, 1993; Atoda *et al.*, 1998) and *A. acutus* (Xu *et al.*, 2000) venoms.

These proteins have a molecular mass of ~30 kDa and are $\alpha\beta$ -heterodimers linked by a single disulfide bridge. The only exception is halyxin, from *A.h. brevicaudus*, which contains three chains (Koo *et al.*, 2002). The structures of FIX/FX-binding protein (Mizuno *et al.*, 1997) and FIX-binding protein (Mizuno *et al.*, 1999) isolated from *T. flavoviridis* have been solved (Figure 1.8A and B). Interestingly, these two proteins possess same β subunit but different α subunits, which differ at only 19 (15%) of the total 129 amino acids. Each subunit of these molecules consists of a globular unit with an extended loop that contributes to a tight interface with the other subunit. The dimer

forms a concave interface, which is supposedly the binding site for coagulation factors' Gla-domain (Figure 1.8A and B). The amino acid residues that differ between these proteins are concentrated in part of the concave surface (Mizuno *et al.*, 1999). More recently, the structures of FX- and FIX-binding proteins complexed with the respective Gla domains of FX and FIX were solved (Mizuno *et al.*, 2001;Shikamoto *et al.*, 2003). Ca^{2+} is essential for the activity of the proteins since binding to FX is lost when Ca^{2+} is replaced by another ion such as terbium.

These proteins prolong clotting in prothrombin time assay and inhibit FXa-induced clotting. Binding studies show that they bind specifically to FX/FXa or FIX/FIXa and the stoichiometry of binding is 1:1 for both factors. However, both FIX and FX binding proteins are unable to bind with Gla-domainless factors. This shows that they bind specifically (and tightly) to the Gla domain of FIX and FX but not with the Gla-domain present in prothrombin, FVII, protein C, or protein S. However, the FIX/FX-binding protein isolated from *B. jararaca* protein is an exception since it also binds to protein S although with a lower binding affinity. Structural data obtained from X-ray crystal structures have revealed that the formation of these complexes blocks the interaction of the Gla domain (Figure 1.8C) with membrane, which is essential for augmentation of the coagulation process.

Thrombin and Prothrombin Binding Proteins

Bothrojaracin from *Bothrops jararaca* (Zingali *et al.*, 1993) and salmorin from *Agkistrodon halys brevicaudus* (Koh *et al.*, 2000) are the most well studied proteins belonging to this group. These are acidic proteins with a molecular weight of ~30 kDa (Zingali *et al.*, 1993;Koh *et al.*, 2000). They consist of two distinct but homologous chains linked together by disulfide bridges.

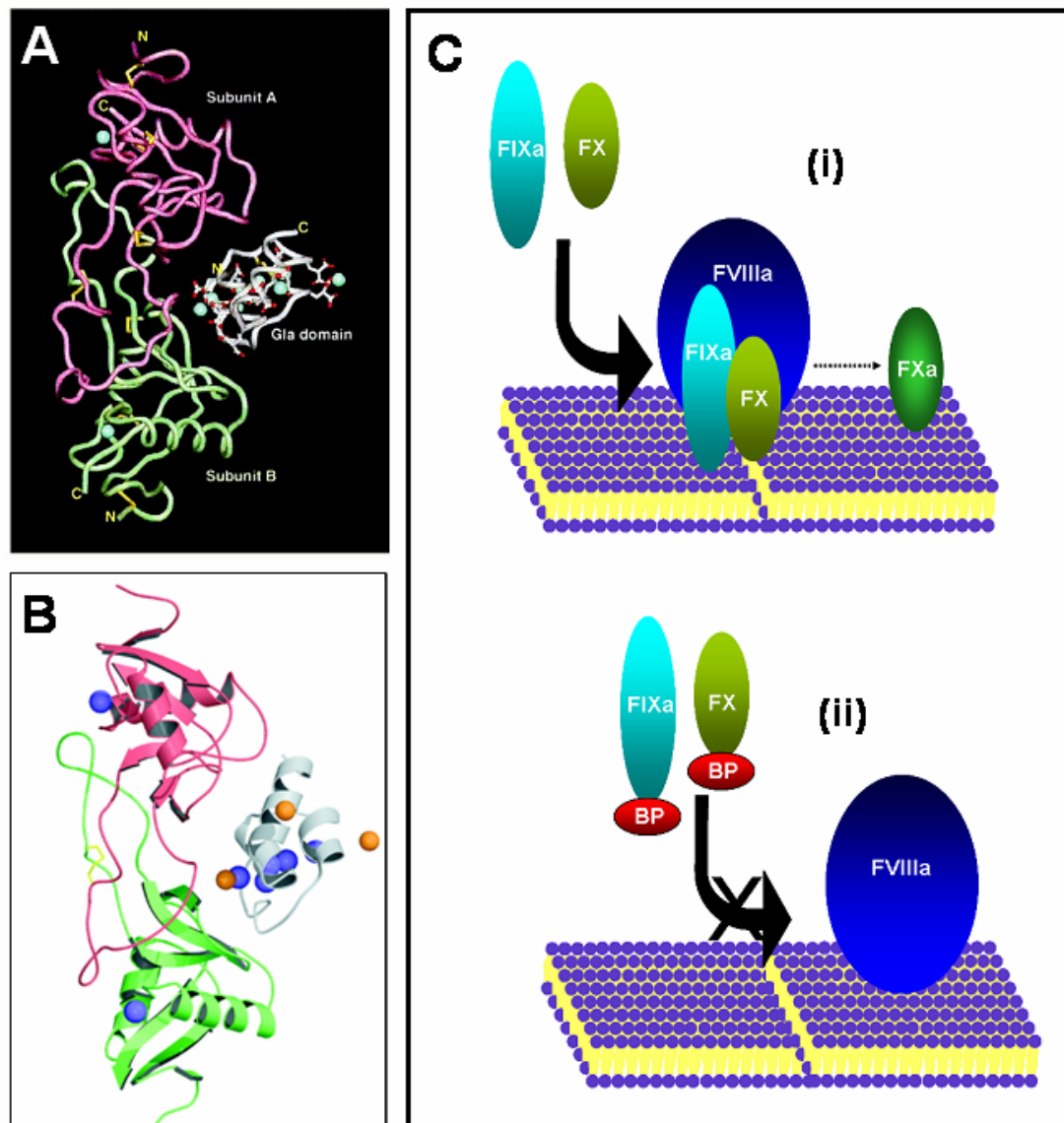


Figure 1.8 (A) Overall structure of FX-bp and FXGD1-44 complex. Stereoview of ribbon model viewed perpendicular to the pseudodyad of the molecule, showing the interface between FX-bp and FXGD1-44. The subunits A and B of FX-bp are magenta and green. FXGD1-44 is white. The side chain of Gla residues and disulfide bonds are displayed. The bound Ca²⁺ ions are denoted by blue spheres. **(B) FIX binding protein.** The subunits A and B of FIX-bp are magenta and green. FIXGD1-46 is in white, and the interchain disulfide bond is shown in yellow. The bound Mg²⁺ and Ca²⁺ ions are drawn as orange and blue spheres, respectively. (Kindly provided by Dr. Takashi Morita) **(C) Anticoagulant mechanism of factor IX/X-binding protein.** (i) Formation of regular tenase complex. (ii) Binding of factor IX/X-binding protein with the Gla domain of factor IX/IXa or X/Xa leads to blockage of the tenase complex arrangement.

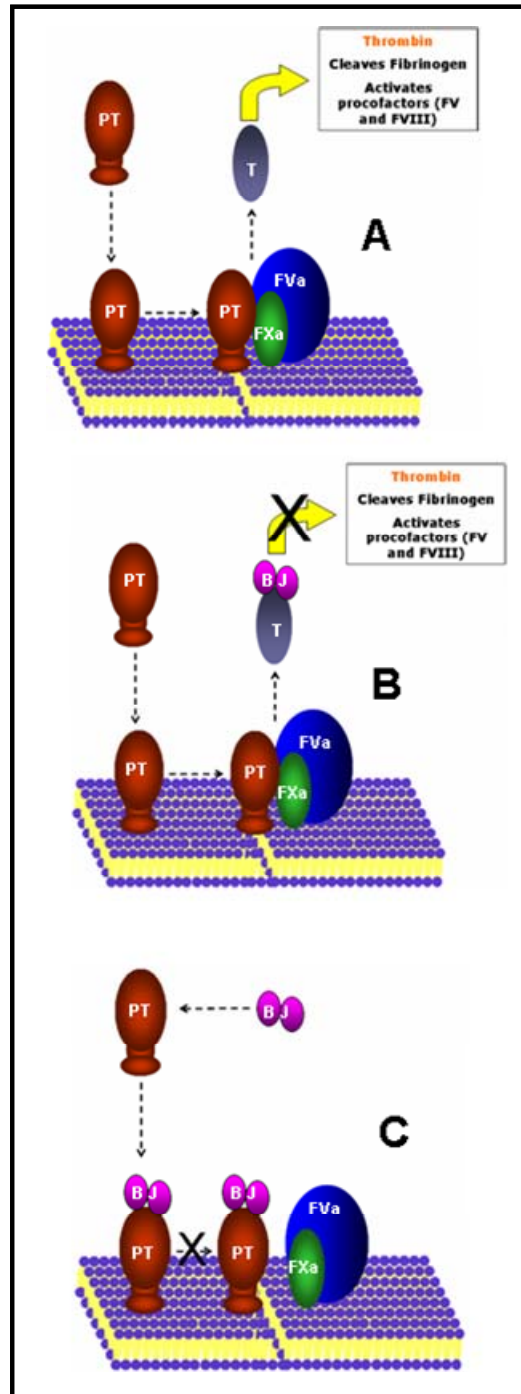


Figure 1.9 Anticoagulant mechanism of bothrojaracin. (A) Formation of regular prothrombinase complex. (B) Mechanism 1 of bothrojaracin inhibition is based on its binding to thrombin exosite I and consequent inhibition of its activities. (C) Mechanism 2 is based on the inhibition of prothrombin activation through interaction with prothrombin proexosite I. (PT, prothrombin; FVa, activated factor V; FXa, activated factor X; T, thrombin and BJ, bothrojaracin.)

Bothrojaracin has only 11 of the 13 amino acid residues that are important for the carbohydrate recognition domain (CRD) and, thus lacks the capability to bind to carbohydrates (Arocas *et al.*, 1997). Ca^{2+} is not important for its function unlike the FIX/FX binding proteins. Bothrojaracin-like proteins have been detected by biological and immunoblotting assays in other snake venoms from Brazilian snakes and purified to homogeneity (Castro *et al.*, 1999).

Bothrojaracin binds to thrombin (Figure 1.9), forming a stable 1:1 complex (Zingali *et al.*, 1993). The calculated K_d for immobilized bothrojaracin was 0.6 nM (Arocas *et al.*, 1996). Interestingly, bothrojaracin displaces all thrombin exosite I ligands, such as fibrin, hirudin, and thrombomodulin, indicating that it interacts with thrombin through exosite I. In addition, bothrojaracin inhibits the activation of FV by thrombin and is, therefore, a potent inhibitor of the feedback activation of the clotting cascade (Arocas *et al.*, 1998). It also binds to γ -thrombin, a proteolytic product of α -thrombin in which exosite I is disrupted, indicating that bothrojaracin also binds to the thrombin exosite II, although with lesser affinity (Arocas *et al.*, 1996). Bothrojaracin has also been shown to displace thrombin that is bound to the clot (Zingali *et al.*, 2001). Assays show that even when all activities of thrombin are blocked by bothrojaracin, the catalytic activity of thrombin toward chromogenic substrates is not inhibited (Zingali *et al.*, 1993). It has been observed that bothrojaracin produces two different structural changes in the thrombin catalytic site depending on whether it interacts with exosite II, as for γ -thrombin, or with exosite I, as observed for α -thrombin (Zingali *et al.*, 2005). Binding to α -thrombin increases its activity towards certain chromogenic substrates, while its binding to γ -thrombin inhibits it. This shows that bothrojaracin does not bind to the active site of thrombin. Intriguingly, bothrojaracin binds with high specificity to prothrombin (Arocas *et al.*, 1996), with a dissociation constant of

100 nM, indicating a ~100-fold lower binding affinity than that for thrombin. Although the mechanism of action of bothrojaracin is known in considerable detail, its structure-function relationship is yet to be elucidated.

Salmorin shares certain functional similarities with bothrojaracin. It inhibits hirudin interaction with thrombin, increases fibrinogen clotting time (induced by thrombin), and forms a 1:1 complex with prothrombin (Koh *et al.*, 2000). But unlike bothrojaracin, salmorin inhibits prothrombin activation by FXa independently from the presence of FV.

Anticoagulant three-finger toxins

Three-finger toxins are non-enzymatic polypeptides containing 60 to 74 amino acid residues (Kini, 2002). These proteins are abundant in elapid (cobras, kraits and mambas) and hydrophid (sea snakes) venoms. Recently, they have also been identified in colubrid venoms (Pawlak *et al.*, 2006). Although there is no report of a three-finger toxin from viper venom, but recently three-finger protein scaffolds have been noted in vipers as well (Junqueira-de-Azevedo *et al.*, 2006). These proteins contain four or five disulphide bridges. Of these four are found to be conserved in all the members. All proteins belonging to this family show an analogous pattern of folding, in which three β -stranded loops extend from a central core containing the four conserved disulphide bridges (Kini, 2002). Because of this appearance, this family of proteins is called the three-finger toxin family. Despite the overall similarity in structure they differ from each other in their biological activities. Anticoagulant effects of three-finger toxins were first identified in cardiotoxins purified from *Naja nigricollis crawshawii* (spitting cobra) venom (Kini *et al.*, 1988). Very recently our lab showed that anticoagulant activity of one of these proteins is mediated by the inhibition of the prothrombinase complex (Mahima *et al.* unpublished observations).

Protease inhibitors

Snake venoms contain serine protease inhibitors that are able to inhibit the activity of blood coagulation factors, and thus these proteins are potential anticoagulants. These proteins contain 57 to 60 amino acid residues with three disulfide bonds and belong to the Kunitz-pancreatic inhibitor family (Hollecker and Creighton, 1983).

The first report of protease inhibitors was from the venom of Russell's viper (*Vipera russelli*), in which two proteins were isolated from the venom of the snake which were able to inhibit the activity of bovine plasma kallikrein, trypsin, plasmin, and α -chymotrypsin (Takahashi *et al.*, 1974a; Takahashi *et al.*, 1974b; Iwanaga *et al.*, 1976). Presence of protease inhibitors in the venom of *Hemachatus haemachatus* and *Naja nivea* were also reported (Hokama *et al.*, 1976).

The best studied of these proteins is textilinin (txln). This protein is a 59-amino-acid polypeptide, isolated from the venom of *Pseudonaja textilis*. The protein has two distinct isoforms of molecular weights 6688 and 6692 Daltons respectively. Txln 1 and 2 are inhibitors of plasmin though the former binds very tightly with a K_i of approximately 10^{-11} mol/l while the latter bound less tightly with a K_i of approximately 10^{-9} mol/l (Masci *et al.*, 2000). Recently, the structure of txln 1 has been solved (Millers *et al.*, 2006). Txln-1 shares only 47% amino-acid identity to aprotinin; however, six cysteine residues in the two peptides are in conserved locations. The overall fold of these molecules though similar, but they have contrasting surface features. Lately, α -chymotrypsin inhibitors have also been reported from the venom of *Ophiophagus hannah* (Chang *et al.*, 2001) and *Bungarus fasciatus* (Chen *et al.*, 2001), although their anticoagulant properties are still to be investigated.

The anticoagulant proteins discussed here are potential leads for the development of antithrombotic agents. These proteins can also be used as molecular probes^{**}, to facilitate our understanding of the basic biology of hemostasis. To search for new lead molecules we and others have been focusing on isolating and characterizing pharmacologically active proteins from snake venoms that affect blood coagulation and platelet aggregation. Recently, we purified and characterized an anticoagulant protein belonging to the three-finger family^{††} from an elapid snake *Hemachatus haemachatus* (African Ringhals cobra). Individually, this protein has mild anticoagulant activity; however, its synergistic interaction with a second three-finger toxin enhances its anticoagulant potency. The anticoagulant protein and its complex inhibit clot initiation by specifically inhibiting FVIIa activity.

^{**} “But when we reach the limits of vivisection we have other means of going deeper and dealing with the elementary parts of organisms where the elementary properties of vital phenomena have their seat. We may introduce poisons into the circulation, which carry their specific action to one or another histological unit. . . Poisons are veritable reagents of life, extremely delicate instruments, which dissect vital units”. - *Claude Bernard (1813 – 1878)*

^{††} For a classification of major snake venom protein families, see Appendix.

Do, or do not. There is no 'try'.

---Yoda ('The Empire Strikes Back')

“When I first took up fishing, I always used an enormous hook... [it is] more exciting not to catch a big fish than not to catch a small one... Now I have reduced the size of my hook.”

-A. Szent Gorgyi

Aim and Scope of the Thesis



Nature's defensive molecules, the venom peptides, have long been useful as molecular probes, therapeutic agents, as well as lead molecules for drug discovery. Their usefulness, however, has centered, not only on their unique intrinsic pharmacological properties but, also, on what and how much we know about them¹. Proteins/toxins from snake venoms have inspired the design and development of a number of therapeutic agents or lead molecules, particularly for cardiovascular diseases. For example, a family of inhibitors of angiotensin converting enzyme were developed based on bradykinin potentiating peptides from South American snake venoms. Inhibitors of platelet aggregation, such as eptifibatid and tirofiban, were designed based on disintegrins, a large family of platelet aggregation inhibitors found in viperid and crotalid snake venoms. Ancrod extracted from the venom of Malayan pit viper reduces the blood fibrinogen levels and has been successfully tested in a variety of ischaemic conditions including stroke.

In this study, I have reported the purification and characterization of a three-finger toxin, hemextin A, that mediates anticoagulant activity from the venom of the elapid snake *Hemachatus haemachatus* (African Ringhals cobra). Although it has mild anticoagulant activity, its synergistic interaction with the second three-finger toxin, hemextin B, enhances its anticoagulant potency. Hemextin A and its complex, hemextin AB complex, inhibit the activation of FX by the TF-FVIIa, by binding specifically to FVIIa. Hemextin AB complex is also the only known tetrameric complex, exclusively formed between three-finger toxins. Therefore, the molecular interactions participating in the formation of the complex were studied. Further, the particular domain in FVIIa, to which the anticoagulant protein and its complex bind to mediate anticoagulant activity, was identified. Therefore, in summary, this thesis

¹ "That which we know is little, what we do not know is immense"

---- *Pierre-Simon de Laplace*

describes a unique anticoagulant protein complex from snake venom. This new anticoagulant may help us develop different strategies and therapeutic agents to inhibit the initiation step in blood coagulation.

Specifically, the objectives² of the study were:

1. To isolate the anticoagulant protein and its synergistic partner from the crude venom of *H. haemachatus* and purify them to homogeneity, followed by the determination of their complete amino acid sequence.
2. To determine the specific step in the coagulation cascade where the anticoagulant protein and the synergistic complex act to mediate the anticoagulant activity; followed by the determination of the specific coagulation serine protease to which the proteins bind to mediate their anticoagulant action.
3. To biophysically characterize the complex formation between the anticoagulant protein and its synergistic partner.
4. To identify the specific domain of the target enzyme to which the anticoagulant protein and the synergistic complex bind in order to mediate their anticoagulant function.
5. To identify the condition(s) where the anticoagulant protein hemextin A can be crystallized; and solving its structure using X-ray crystallography

² “Plan backwards as well as forward. Set objectives and trace back to see how to achieve them. You may find that no path can get you there. Plan forward to see where your steps will take you, which may not be clear or intuitive.”
---- Donald Rumsfeld (*American Secretary of Defense*)

“Every enzyme or protein requires a specific method for its purification. Our present methods of purifying both enzymes and proteins are crude and unsatisfactory for the most part. It is fairly certain that better methods will be discovered in the near future.”

- Dr. James B. Sumner; The Chemical Nature of Enzymes; Nobel Lecture; December 12, 1946



I see you in the process of conducting a protein separation and...wait, you're not adding the proper amount of solvent and the pH of the solution is not right. Now I see your supervisor turning around and slowly beginning to approach...

Chapter 2

Purification of the anticoagulant protein

Chromatography: from colour writing to separation science

“An infinite variety of complicated mixtures can be separated by chromatography, giving detailed insights into our biochemistry, our environment and even our history. Tutankhamen's wine residues, the stratosphere of Saturn's moon Titan, dyes from ancient Navarro textiles, mine drainage samples, herrings' gas bubbles, vodka and earwax are just a few substances recently analysed by chromatography. Single, active components can be isolated from mixtures; or hundreds of metabolites in a cell extract can be unscrambled in a single two-dimensional chromatography run. Primary school children can perform successful separations with coloured solutions on paper. At the other extreme, analytical chemists and molecular biologists use sophisticated, high-resolution instruments coupled with state-of-the-art detectors and databases. Chromatography underpins so much and seems so intuitive now — but it is a surprisingly recent invention.

There are 19th Century contenders, including Goppelsröder at the University of Basel, who found relationships between how high a solution rises in paper and its chemical composition¹. However, the accolade for the first chromatography run usually goes to Mikhail Semenovich Tswett, a Russian botanist, in 1903². Tswett crushed leaves in alcohol. Drops of the alcohol solutions were layered on top of tubes filled with powdered chalk. When he washed the chalk columns with petroleum-based solvents, the pigments moved down the chalk and separated into coloured bands. Immediately, the admixture of blues and yellows within every plant green was revealed. And red blossoms were found to contain hidden tints of green. These separated pigments inspired the name ‘chromatography’, literally ‘colour writing’. The name also links to the man, for Tswett in Russian means ‘colour’ or ‘a flower’.

Tswett's observations led him to conclude that pigments with an adsorptive attraction for the chalk stationary phase were being retarded, whereas those that did not interact so well were flushed through the system more rapidly. Varying the solid and liquid phases facilitated separation of different mixtures. But despite its success in his

hands, Tswett's adsorption chromatography was slow to catch on: though he worked in Switzerland and Poland he published in Russian, limiting the readership of his papers. There were also professional rivalries. Those who did attempt to repeat his experiments ran into trouble by not following his protocols precisely, particularly his warning that certain solids would “decompose the pigments adsorbed on them”. So chromatography was used only rarely until the 1930s, after L.S. Palmer in the USA had used Tswett's techniques on various natural products³. Then, Edgar Lederer and Richard Kuhn in Heidelberg obtained a translation of Tswett's paper from Kuhn's mentor, Richard Willstätter, and used chromatography to discover that lutein from egg yolk is a mixture of closely related carotenoids (published as a series of papers, including one in 1931⁴). The publicity surrounding their work gave chromatography a boost, and by the beginning of the 1940s, numerous vitamins, fatty acids, steroids and botanical compounds had been purified by adsorption chromatography, greatly accelerating the development of modern biochemistry.”

--- **Professor Carol MacKintosh, MRC Protein Phosphorylation Unit, University of Dundee, UK; *Biochem. J.* (2006)**

References:

1. Goppelsröder, F. (1862) *Memorandum on a new method for determining the nature of a mixture of dyes*. Meeting held on October 30 1861, Bull. Ind. Soc. Mulhouse **XXXII**
2. Tswett, M.S. (1906) *Berichte der Deutschen botanischen Gesellschaft* **24**, 385[translated and excerpted in Mikuláš Teich (1992), *A Documentary History of Biochemistry, 1770–1940*, Fairleigh Dickinson University Press, Rutherford,NJ]; see <http://web.lemoyne.edu/~giunta/tswett.html>
3. Palmer, L.S. (1922) *Carotinoids and related pigments: the chromolipoids*. American Chemical Society Monograph Series, Chemical Catalog Co., NY 4.
4. Kuhn, R., Winterstein, A. and Lederer, E. (1931) *The xanthophylls*. Zeit. F. Physiol. Chem. **197**, 141–16
4. Kuhn, R., Winterstein, A. and Lederer, E. (1931) *The xanthophylls*. Zeit. F.Physiol. Chem. **197**, 141–160

A single venom is a cocktail of well over a few hundred different proteins and peptides. Purification of these proteins to (relative) homogeneity¹ can, therefore, be a formidable challenge. However all these proteins (at least the more abundant ones) fall into a very small number of superfamilies. These can be translated into molecular mass ranges: for example, (in the case of several elapid venoms), >40 kDa (mainly enzymes), 12 -15 kDa (phospholipases A₂) and 6-8 kDa (three-finger toxins, proteinase inhibitors, etc.). Hence, gel-filtration or size-exclusion chromatography (SEC) also referred to as “molecular sieving”, which separates proteins solely on the basis of differences in molecular size, is an excellent initial fractionation step. Separation in (SEC) is achieved using a porous matrix to which the molecules, for steric reasons, have different degrees of access (smaller molecules have greater access and larger molecules less). The next, step is usually ion exchange chromatography that separates proteins on the basis of charge characteristics. Charged groups on the surface of a protein interact with oppositely charged groups immobilized on the ion-exchange medium, followed by their elution using a step gradient of increasing salt concentration. Reversed-phase high-pressure liquid chromatography (RP-HPLC) is usually the final step, separating the proteins on the basis of their hydrophobicity and yielding them in de-salted form. Implicit in the statement that only a few protein superfamilies exist in venom containing large numbers of different proteins, is the fact that there are numerous closely-related isoforms within each family, in the venom. Separation of these isoforms constitutes a significant challenge: parameters at the ion exchange and RP-HPLC steps, such as the choice of column, pH of buffers and the slope of the eluting gradient, need to be optimized for their

¹ **Although it may seem a paradox, all exact science is dominated by the idea of approximation.**

- Bertand Russell

efficient separation. The use of RP-HPLC often necessitates exposing the proteins to high concentrations of organic solvent (acetonitrile, ACN). This may cause protein denaturation, evidenced by a loss in activity. Fortunately, the highly disulfide-linked nature of the three-finger toxins renders them fairly resistant to denaturation and proteolysis. Nonetheless, it is prudent to perform the purification as speedily as possible, preferably at 4°C, to avoid proteolytic degradation. It is also vital to ensure that the purified protein being screened for biological activity does not contain contaminants that could mask the effects of protein. Hence, an accurate assessment of homogeneity, preferably using analytical RP-HPLC that can achieve high resolution and sensitivity to the nanomolar level is important. The primary structure of the protein is then established by the determination of its amino acid sequence and the assignment of the disulfide bonds (if any).

This chapter details the purification and NH₂-terminal sequence determination of the anticoagulant proteins. In addition, it also shows the importance of fold of the proteins for mediating anticoagulant activity. As mentioned in chapter 1, the anticoagulant protein forms a complex with another protein, and the resultant complex exhibits potent anticoagulant activity. The formation of complex between the two proteins has also been investigated using gel-filtration.

MATERIALS AND METHODS

Materials

Lyophilized *Hemachatus haemachatus* venom was obtained from African Reptiles and Venoms (Gauteng, South Africa). The pre-packed chromatography columns were purchased from the following indicated sources: Superdex 30 and Superdex 75 (1.6 × 60

cm) (GE Healthcare BioSciences AB, Uppsala, Sweden), UNO S6 column (6-ml column volume; Bio-Rad, CA, USA), Jupiter C18 columns of dimensions (1 × 25 cm) and (4.6 × 250 mm) (Phenomenex, CA, USA) and PepMap column (narrowbore; LC Packings, CA, USA) Thromboplastin with calcium (for prothrombin time assays), and 4-vinylpyridine were purchased from Sigma. The following chemicals were purchased from the sources indicated: reagents for NH₂-terminal sequencing (Applied Biosystem, Foster City, CA, USA), acetonitrile (Fisher Scientific, Fair Lawn, NJ, USA), trifluoroacetic acid (Fluka Chemika-Biochemika, Buchs Switzerland) and β-Mercaptoethanol (Nacalai Tesque, Kyoto, Japan). Human plasma was donated by healthy volunteers. All other chemicals and reagents used were of the highest purity available.

Purification of Anticoagulant Protein

Hemachatus haemachatus crude venom (100 mg in 1 ml of distilled water) was applied to a Superdex 30 gel-filtration column (1.6 × 60 cm) equilibrated with 50 mM Tris-HCl buffer (pH 7.4) and eluted with the same buffer using an ÄKTA purifier system (GE Healthcare BioSciences AB AB, Uppsala, Sweden). Individual fractions were assayed for anticoagulant activity using prothrombin time (see below). Fractions with potent anticoagulant activity were pooled and sub-fractionated on a cation-exchange column using the same chromatography system. The anticoagulant fraction was pooled and loaded onto a UNO S6 column (6-ml column volume) equilibrated with 50 mM Tris-HCl buffer (pH 7.5). Bound proteins were eluted with a linear gradient of 1 M NaCl in the same buffer. Fractions collected were assayed for anticoagulant activity. The anticoagulant peaks obtained from cation-exchange chromatography were applied to a Jupiter C18 column (1 × 25 cm) equilibrated with 0.1% trifluoroacetic acid. The bound

proteins were eluted using a linear gradient of 80% acetonitrile in 0.1% trifluoroacetic acid. Individual peaks were collected, lyophilized, examined for anticoagulant activity, and subsequently rechromatographed on a narrow bore PepMap column using a Chromeleon microliquid chromatography system.

Electrospray Ionization Mass Spectrometry

The homogeneity and mass of the anticoagulant proteins were determined by electrospray ionization (ESI) mass spectrometry using a PerkinElmer Life Sciences API-300 liquid chromatography/tandem mass spectrometry system. Typically, reverse-phase HPLC fractions were directly used for analysis. Ion spray, orifice, and ring voltages were set at 4600, 50, and 350 V, respectively. Nitrogen was used as a nebulizer and curtain gas with a flow rate of 0.6 l/min. The spectrum was recorded in the 1000-3000 mass-to-charge (m/z) range, in steps of 0.1 amu, with 2 ms dwell time. A Shimadzu LC-10AD pump was used for solvent delivery (40% acetonitrile in 0.1% trifluoroacetic acid) at a flow rate of 50 μ l/min. BioMultiview software (PerkinElmer Life Sciences, USA) was used to analyze and de-convolute raw mass spectra.

Reduction and Pyridylethylation

Purified proteins were reduced and pyridylethylated using procedures described previously. Briefly, proteins (0.5 mg) were dissolved in 500 μ l of denaturant buffer (6 M guanidine hydrochloride, 0.25 M Tris-HCl, and 1 mM EDTA (pH 8.5)). After the addition of 10 μ l of β -mercaptoethanol, the mixture was incubated under vacuum for 2 h at 37 °C. 4-Vinylpyridine (50 μ l) was added to the mixture and kept at room temperature for 2 h. Pyridylethylated proteins were purified on an analytical Jupiter C18 column (4.6

× 250 mm) using a gradient of acetonitrile in 0.1% (v/v) trifluoroacetic acid at a flow rate of 0.5 ml/min.

NH₂-terminal Sequencing

Samples were loaded onto a glass filter pre-coated with Biobrene resin (Applied Biosystem, Foster City, CA, USA) dried off under argon and introduced into sequencer. NH₂-terminal sequencing of the native and S-pyridylethylated proteins was performed by automated Edman degradation using a PerkinElmer Life Sciences Model 494 pulsed liquid-phase sequencer (Procise) with an on-line Model 785A phenylthiohydantoin-derivative analyzer.

Circular Dichroism (CD) Spectroscopy

Far-UV CD spectra (260–190 nm) were recorded using a Jasco J-810 spectropolarimeter (Jasco, MD, USA). All measurements were carried out at room temperature using 0.1-cm path length stoppered cuvettes. The instrument optics was flushed with 30 liters of nitrogen gas/min. The spectra were recorded using a scan speed of 50 nm/min, a resolution of 0.2 nm, and a bandwidth of 2 nm. A total of four scans were recorded and averaged for each spectrum, and the base line was subtracted. The CD spectra of the anticoagulant proteins and their S-pyridylethylated forms were recorded in 50 mM Tris-HCl buffer (pH 7.4).

Reconstitution of the Anticoagulant Complex

Preliminary studies indicated that the active anticoagulant protein interacted with another venom protein, forming a synergistic complex. We reconstituted the complex for various in vitro experiments immediately prior to the experiments by incubating equimolar

concentrations of the two proteins (unless mentioned otherwise) at 37 °C for 5 min in 50 mM Tris-buffer (pH 7.4).

Anticoagulant Activity using re-calcification and prothrombin time assays

Recalcification Time – The recalcification times were determined according to the method of Langdell et al. (LANGDELL *et al.*, 1953). 50 mM Tris-HCl buffer (pH 7.4; 100 µl), plasma (100 µl), and various concentrations of venom or its fraction (50 µl) were preincubated for 2 min at 37 °C. Clotting was initiated by the addition of 50 µl of 50 mM CaCl₂.

Prothrombin Time – The prothrombin times were measured according to the method of Quick (Quick, 1973). 100 µl of 50 mM Tris-HCl buffer (pH 7.4), 100 µl of plasma, and 50 µl of venom or its fractions were preincubated for 2 min at 37 °C. Clotting was initiated by the addition of 150 µl of thromboplastin with calcium reagent.

Complex Formation Studies with Size-exclusion Chromatography

The formation of a complex between anticoagulant proteins was examined by gel-filtration chromatography on a Superdex 75 gel-filtration column (1.6 x 60 cm) using an ÄKTA purifier. The column was equilibrated with 50 mM Tris-HCl buffer (pH 7.4) at a flow rate of 1 ml/min. Individual proteins and an equimolar mixture of anticoagulant proteins (native or pyridylethylated) were incubated for 30 min at 37 °C and then loaded onto the column and eluted in the same buffer. Elution was followed at 280 nm.

RESULTS

Purification of the Anticoagulant Protein – Crude venom of *H. haemachatus* exhibited potent anticoagulant activity in both recalcification and prothrombin time assays (Figure

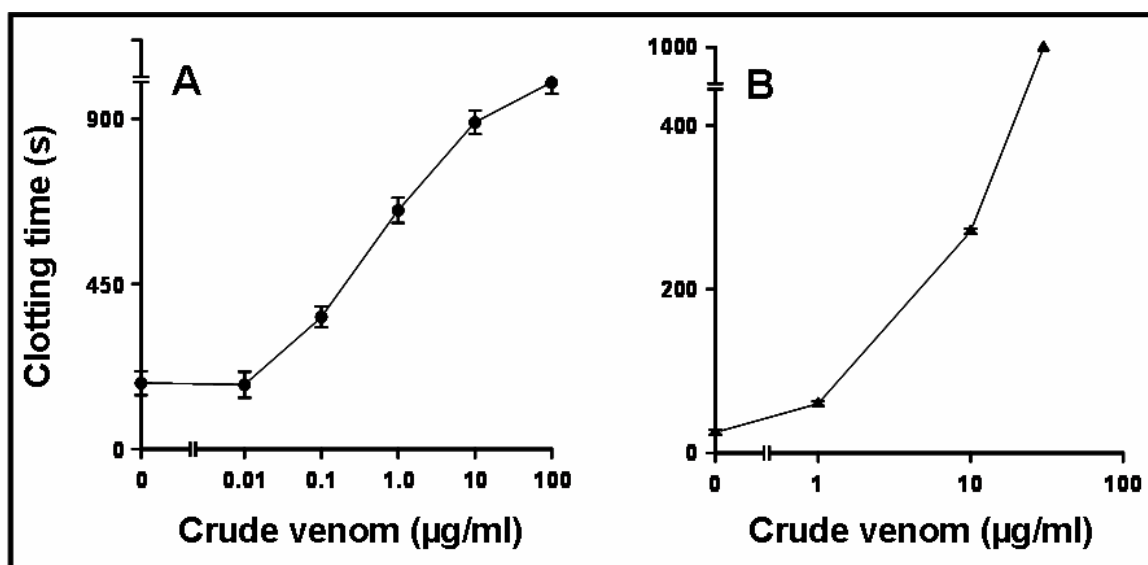


Figure 2.1. Anticoagulant activity of the crude venom. Shown are the effects of the crude venom on recalcification time (A) and prothrombin time (B). Note that the venom exhibited potent anticoagulant activity in both assays. Each data point represents the mean \pm S.D.

2.1, A and B). To purify the anticoagulant protein, the crude venom was size-fractionated by gel-filtration chromatography (Figure 2.2). Fractions corresponding to peaks 2 and 3 contained anticoagulant proteins as determined by prothrombin time assays. Peak 2 corresponded to proteins mostly containing phospholipase A2 that have been characterized previously (Condrea *et al.*, 1981). However, this peak had milder anticoagulant activity compared with peak 3 (Figure 2.2, *inset*), so we focused on isolating the anticoagulant protein from peak 3, which was fractionated further by cation-exchange chromatography on a UNO S6 column (Figure 2.3). Only peak A (labeled Hemextin A) exhibited mild anticoagulant activity. During our preliminary studies, we found that the anticoagulant activity of peak A was potentiated by peak B (labeled Hemextin B; see below). Because this anticoagulant complex specifically inhibited the extrinsic tenase complex (described in Chapter 3), we named it the hemextin AB complex (*Hemachatus extrinsic tenase inhibitor*) and the individual proteins hemextins A and B, respectively. Fractions corresponding to both hemextins A and B were pooled separately and purified by reverse-phase HPLC (Figure 2.4A and B) and capillary liquid chromatography (Figure 2.5A and B). The homogeneity and mass of the individual proteins were determined by electrospray ionization mass spectrometry. The mass spectra of hemextins A and B showed three peaks with mass/charge ratios ranging from 3 to 6 charges (data not shown) and their calculated molecular masses as 6835.00 ± 0.52 and 6792.56 ± 0.32 Da, respectively (Figure 2.6A and B).

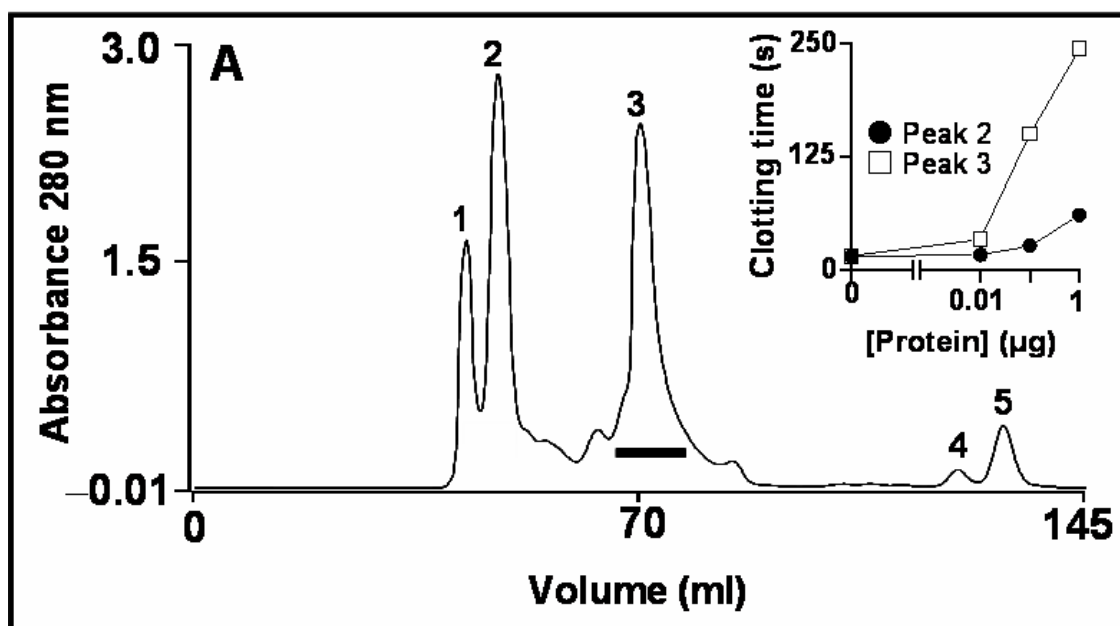


Figure 2.2 Size-exclusion chromatography (SEC) of *Hemachatus haemachatus* crude venom using a Superdex 30 column. SEC of venom on a Superdex 30 (1.6 × 60 cm) column with Tris-hydrochloride buffer (50mM; pH 7.4; flow rate 1.5 ml/min) as an eluent. Fractions constituting peak 3 (indicated by horizontal bar) were pooled and subjected to cation exchange chromatography. Elution of proteins monitored at 280 nm is shown. *Inset*, anticoagulant activity of peaks 2 and 3.

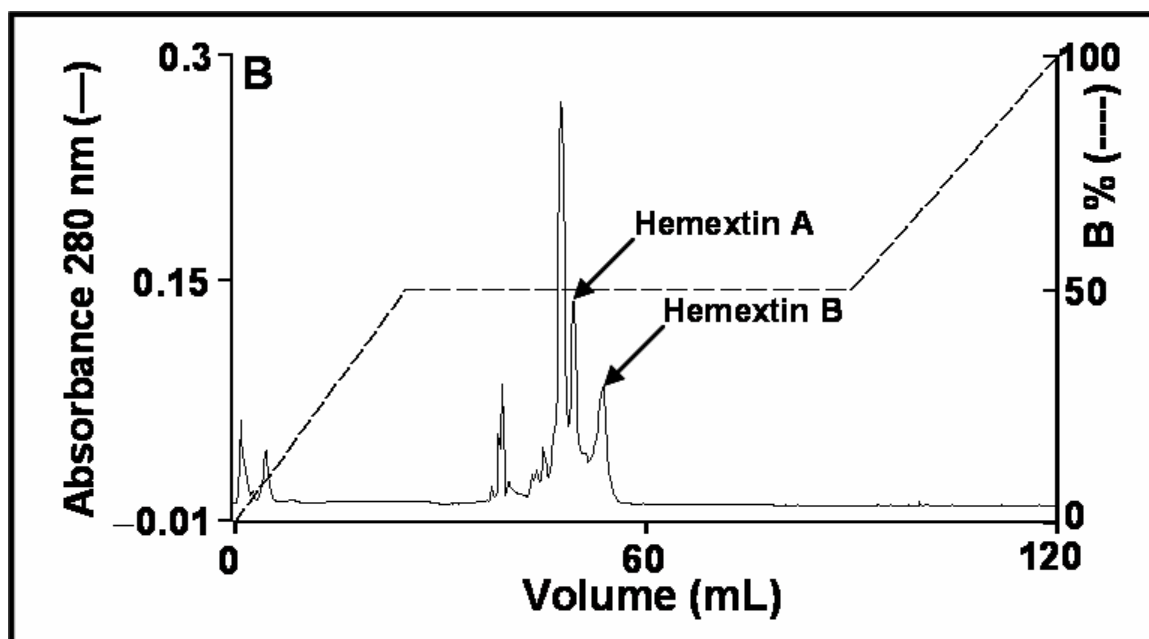


Figure 2.3 Cation exchange of peak 3 from SEC. Cation-exchange chromatography of peak 3 using a UNO S6 column (Bed volume 6 ml). Only peak A (labeled Hemextin A) exhibited mild anticoagulant activity. During our preliminary studies, we found that the anticoagulant activity of peak A was potentiated by peak B (labeled Hemextin B). Elution of proteins monitored at 280 nm is shown.

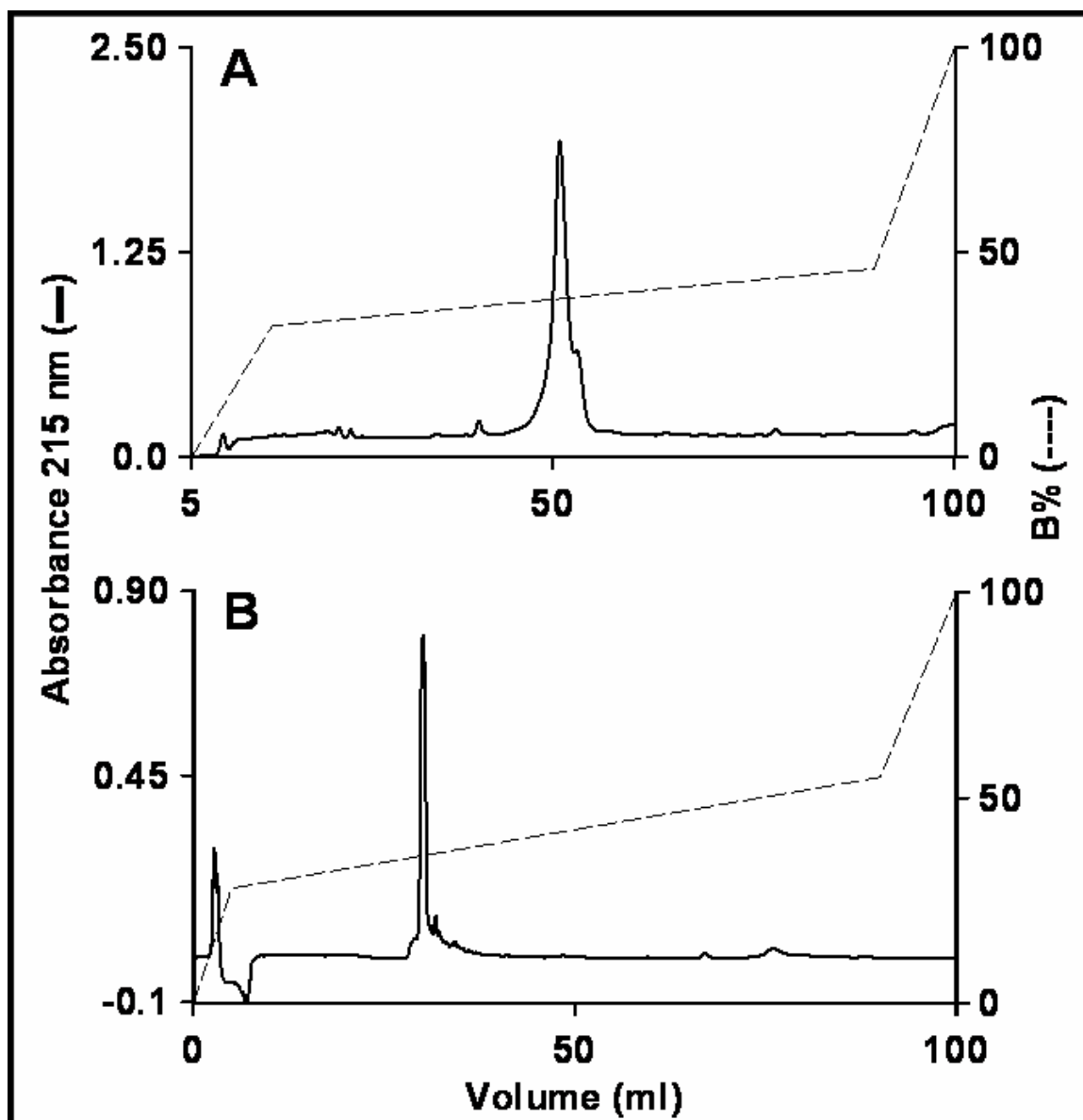


Figure 2.4 RP-HPLC profiles of hemextin A and hemextin B. A and B, Reverse-phase HPLC profiles of cation-exchange fractions containing hemextins A and B, respectively, using a Jupiter C18 semipreparative column using a linear gradient (28-55%, over 85 min for hemextin A; 28-55%, over 85 min for hemextin B) of buffer B (80% acetonitrile in 0.1% TFA) at a flow rate of 1 ml/min. Elution of proteins monitored at 215 nm is shown.

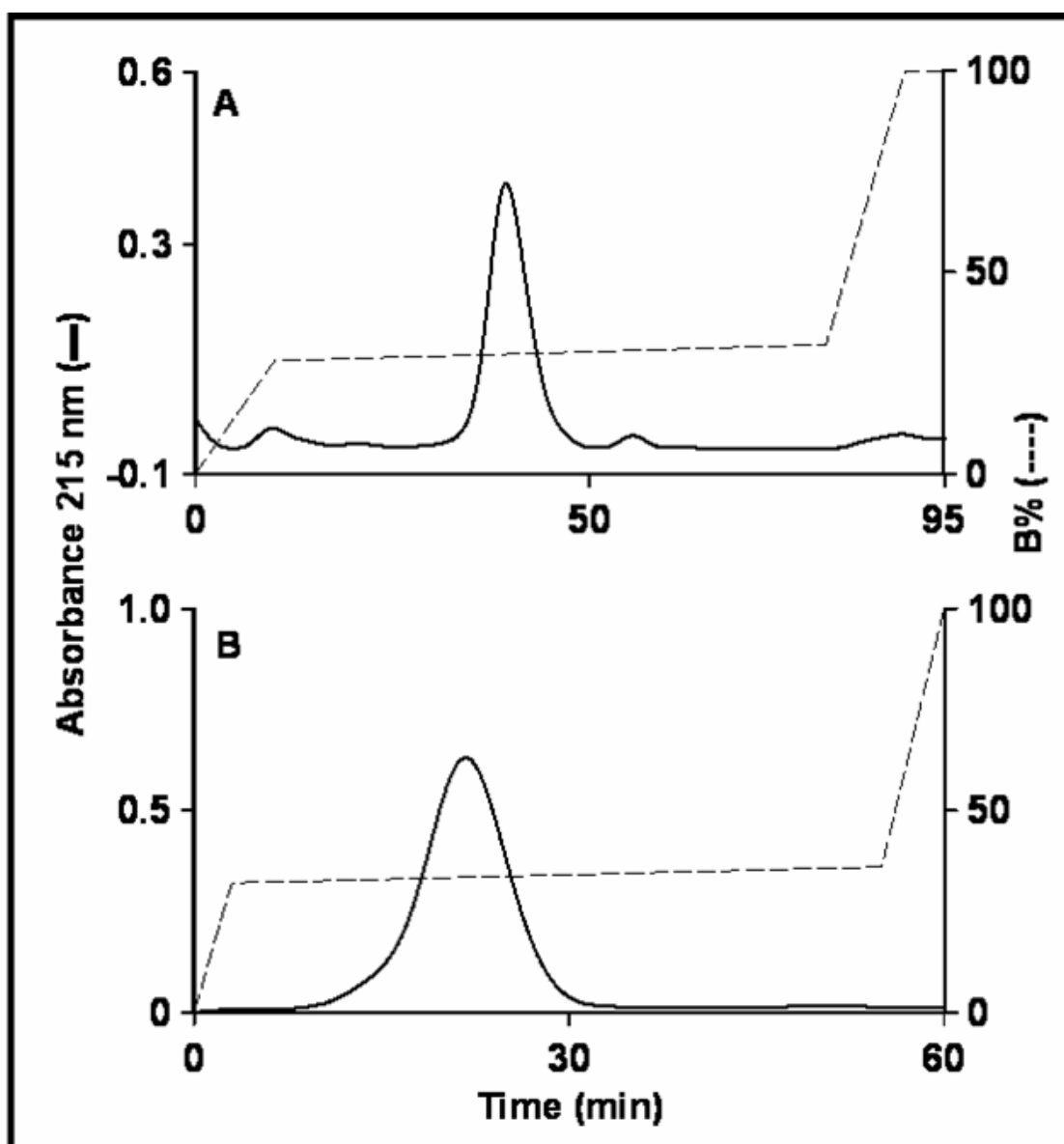


Figure 2.5 Rechromatography of hemextin A and B. A and B, Reverse-phase HPLC profiles of cation-exchange fractions containing hemextins A and B, respectively, using a Jupiter C18 semipreparative column using a linear gradient (28-55%, over 85 min for hemextin A; 28-55%, over 85 min for hemextin B) of buffer B (80% acetonitrile in 0.1% TFA) at a flow rate of 1 ml/min. Elution of proteins monitored at 215 nm is shown.

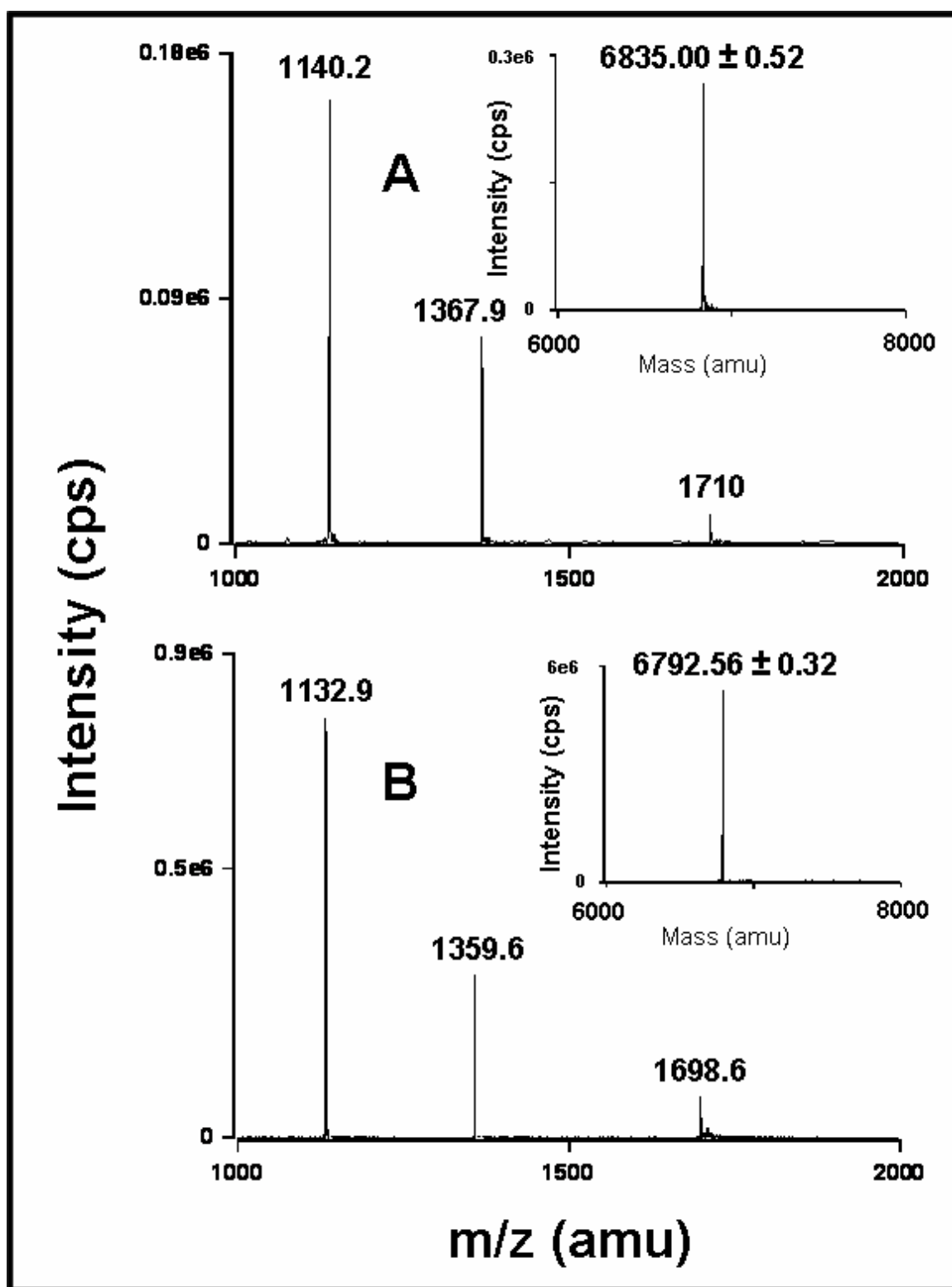


Figure 2.6 ESI-MS of hemextins A and B. ESI-MS spectra for (A) Hemextin A (B) Hemextin B. The spectra show a series of multiply charged ions. The *insets* show the determined MW.

NH2-terminal Sequence Determination - We determined the complete amino acid sequence of hemextins A and B by Edman degradation (Figure 2.7). The locations of the cysteine residues in the proteins were confirmed by sequencing the pyridylethylated proteins. Hemextin A and hemextin B have 61 and 60 amino acid residues respectively. The calculated masses of the proteins were 6835.34 Da for hemextin A and 6792.7 Da for hemextin B and coincides well with the estimated molecular masses of 6835 Da for hemextin A and 6792.56 for hemextin B.

The amino acid sequences of the proteins were subjected to a similarity search using BLAST (Altschul *et al.*, 1997). Multiple sequence alignment was carried out. The sequence data of the homologous proteins were obtained from SWISS-PROT (Swiss Institute of Bioinformatics), EMBL (European Bioinformatics Institute), PRF (Protein Research Foundation), PIR (Protein Information Resource), GENE BANK (National Center for Biotechnology Information) and PDB (Protein Data Bank) databases. The I.P.U.A.C (International Union of Pure and Applied Chemistry) one letter notation for amino acids is used throughout (1968). Both proteins show similarity to cardiotoxins, postsynaptic neurotoxins, fasciculin, and other members of the three-finger toxin family (Figure 2.7). Thus, hemextins A and B belong to three-finger toxin family

CD Spectroscopy – Both hemextins A and B exhibited negative minima at 215 nm and positive maxima at 194 nm. Thus, similar to other three-finger toxins, both hemextins A and B exhibited a predominantly β -sheet structure (Figure 2.8). However, the S-pyridylethylated forms of hemextins A and B displayed negative minima at 195 nm, i.e. a

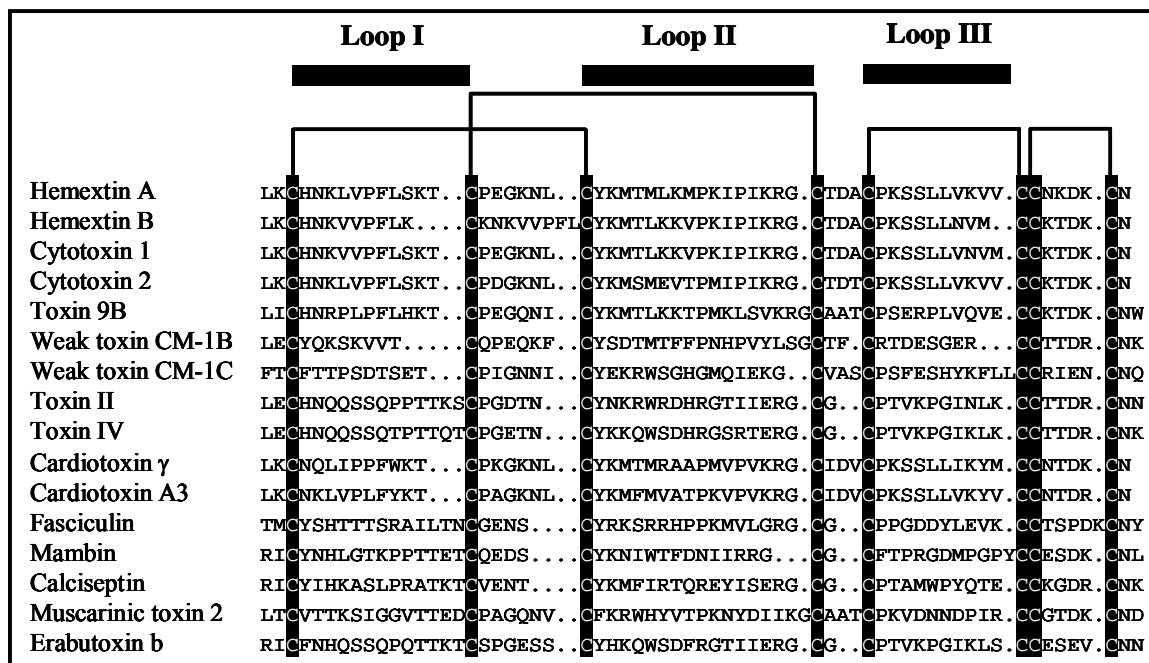


Figure 2.7 Comparison of amino acid sequence of hemexin A and hemexin B with other sequences of the three-finger toxin family. The conserved cysteine residues are indicated in black. The four conserved disulfide linkages and the segments contributing to the three loops are outlined. Comparison were made with the following sequences: cytotoxin 1, cytotoxin 2, toxin 9B, weak toxin CM-1B, weak toxin CM-1C, toxin II, toxin IV are from *Hemachatus haemachatus* (African Ringhals Cobra); cardiotoxin γ from *N. nigricollis* (Black spitting cobra); cardiotoxin A3 from *Naja atra* (Taiwan cobra); fasciculin from *Dendroaspis angusticeps*; mambin from *Dendroaspis jamesoni*; calciseptin from *Dendroaspis polylepsis*; muscarinic toxin 2 from *Dendroaspis angusticeps*; erabutoxin b from *Laticauda semifasciata*.

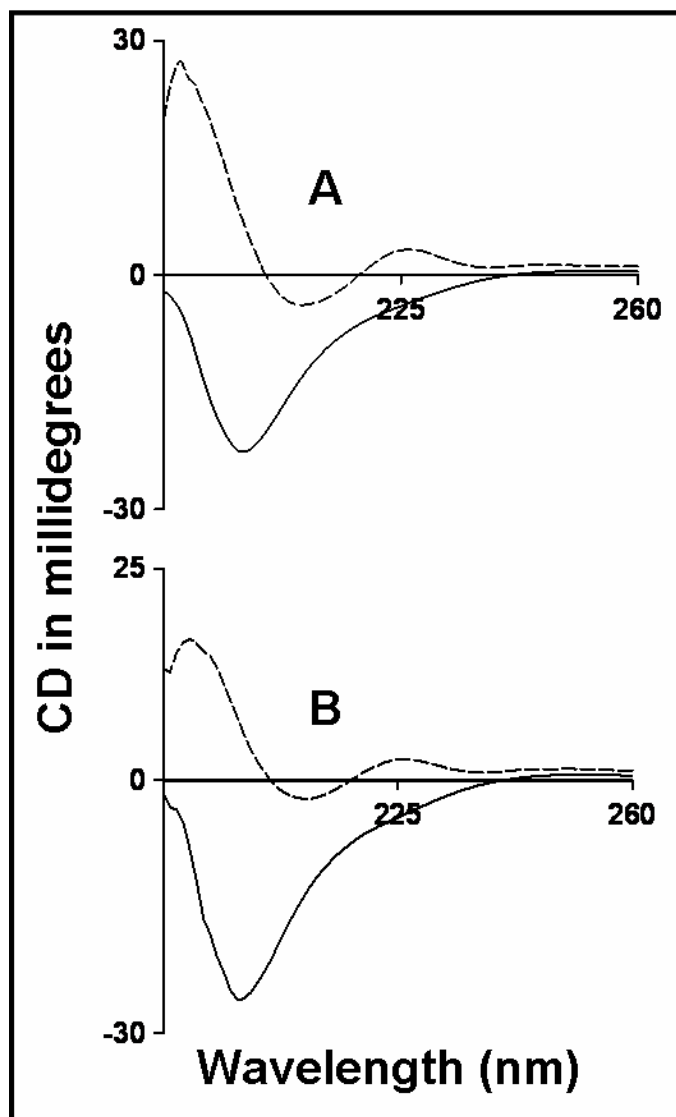


Figure 2.8 CD spectra. CD spectra of native (---) and *S*-pyridylethylated (—) (A) hemextinA and (B) hemextin B. Note, the native proteins exhibit a typical β -sheet structure, as observed in the other members of the three-finger toxin family. In the *S*-pyridylethylated the di-sulfide bonds are destroyed as a result of which the proteins loose their characteristic β -sheet fold.

predominantly random-coil structure (Figure 2.8). Thus, reduction and pyridylethylation result in the loss of folding and three-dimensional structure in hemextins A and B.

Anticoagulant Activity of Hemextins – The anticoagulant activity of hemextins A and B was determined by the prothrombin time assay (Figure 2.9). Hemextin A prolonged the clotting time and exhibited mild anticoagulant activity, whereas hemextin B did not show any significant effect on the clotting time even at higher concentrations. Interestingly, an equimolar mixture of hemextins A and B exhibited more potent anticoagulant activity, indicating synergism between these proteins (Figure 2.9). Such an increase in the anticoagulant effect could be due either to the inhibition of two separate steps in the coagulation cascade or to the formation of a complex between them. Because hemextin B by itself has no significant effect on prothrombin time, it does not inhibit a separate step; instead, it is likely that hemextins A and B form a complex.

Complex Formation between Hemextins A and B – To investigate the formation of a complex between the two proteins, we employed a titration experiment in the prothrombin time assay. In this experiment, the concentration of hemextin A was kept constant at 4.4 μM , and its anticoagulant activity was monitored with increasing hemextin B concentrations (Figure 2.10). The anticoagulant activity increased with increasing concentrations of hemextin B until the ratio reached 1:1. Further addition did not increase the anticoagulant effect. The results indicate that hemextins A and B form a 1:1 complex and that complex formation is crucial for potent anticoagulant activity. Complex formation between hemextins A and B was further confirmed by gel-filtration

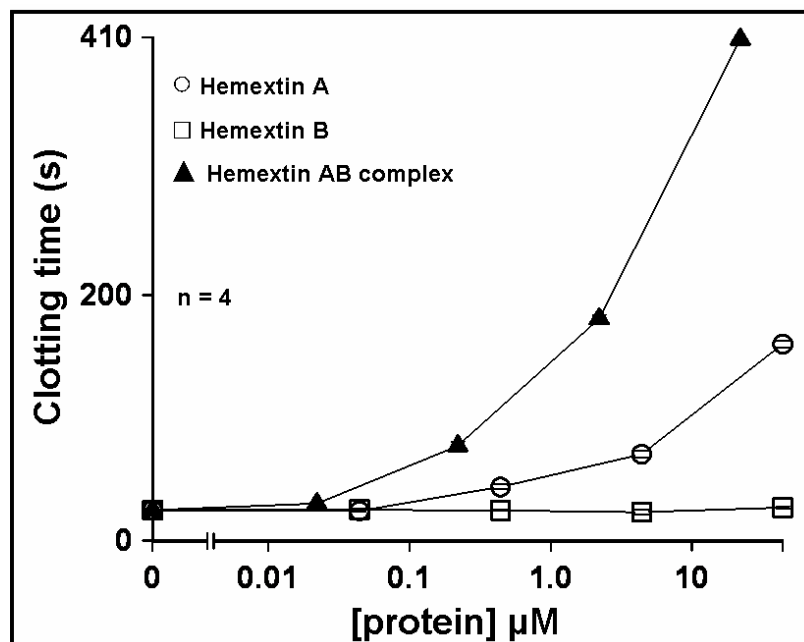


Figure 2.9 Effects of hemextins A and B on prothrombin time. A, shown are the effects of hemextin A (\circ), hemextin B (\square), and the probable hemextin AB complex (\blacktriangle) on prothrombin time. Note that the anticoagulant potency of hemextin A increased in the presence of hemextin B. Each data point represents the mean \pm S.D.

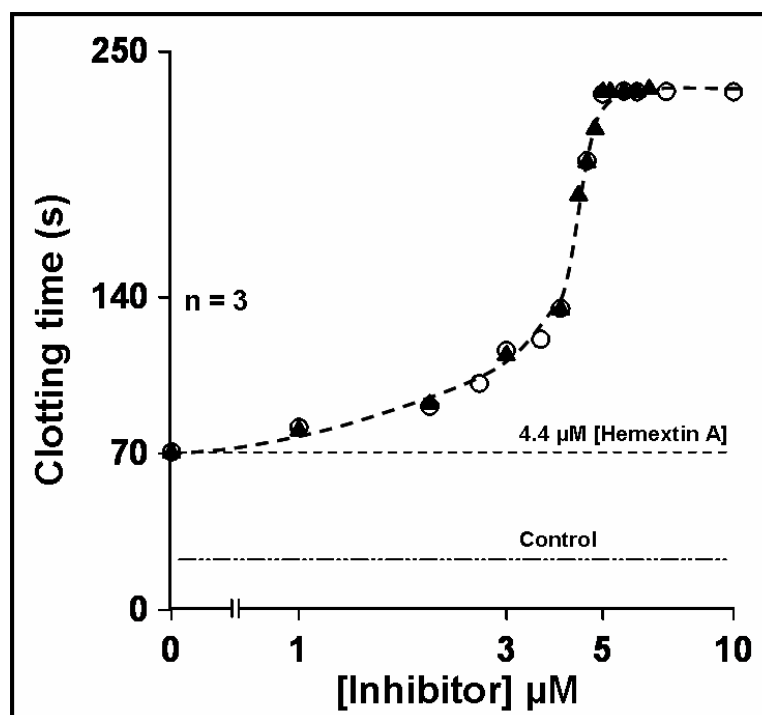


Figure 2.10 Complex formation between hemextins A and B is illustrated by their effect on prothrombin time. Note as the concentration of hemextin B increases there is an increase in anticoagulant activity; the curve plateaus out when the stoichiometric ratio of the two proteins becomes 1:1.

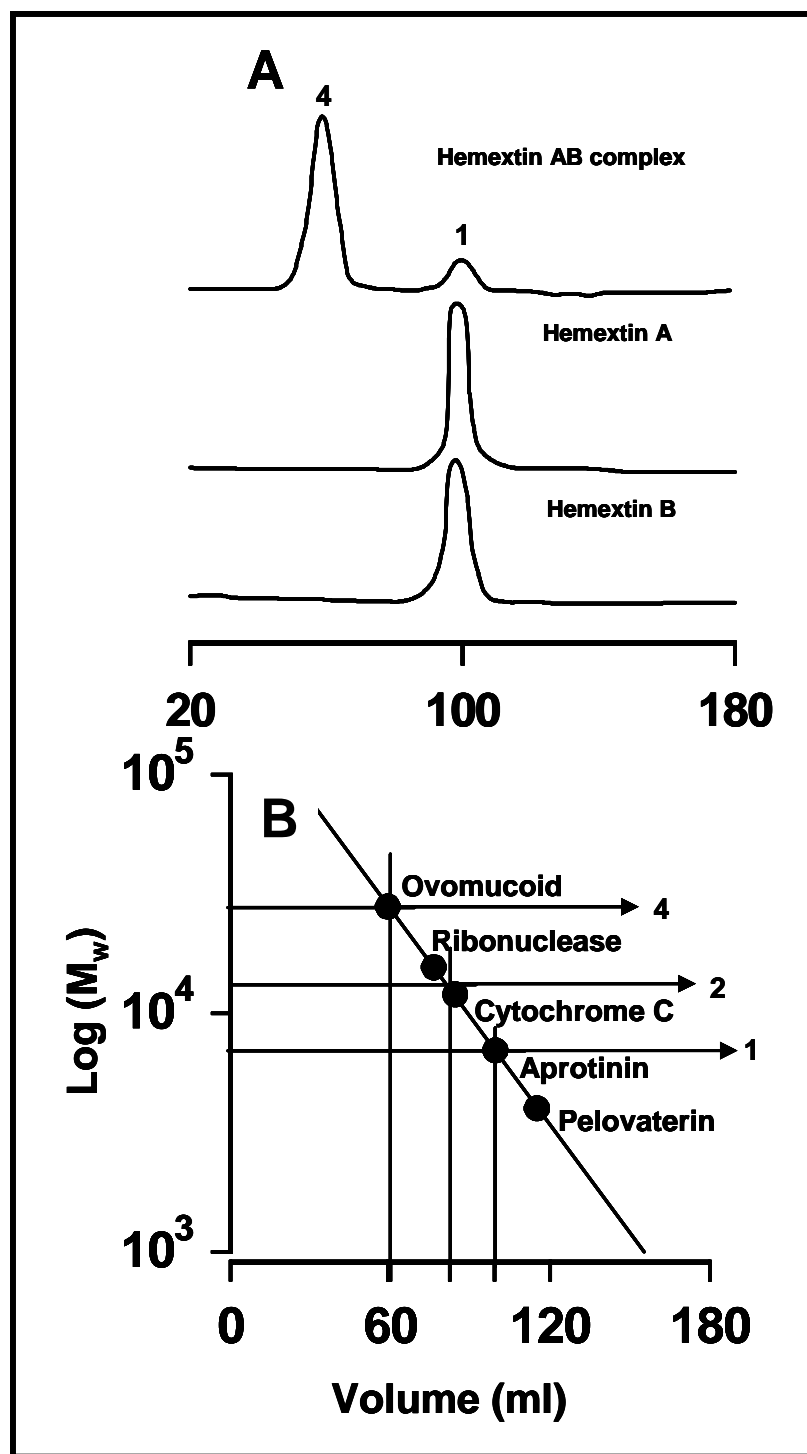


Figure 2.11 Gel filtration studies on the formation of hemexin AB complex. Note the elution time of the hemexin AB complex is reduced to ~ 40 min over that of the individual hemexins, ~ 70 min

chromatography. As shown in Fig. 2.11, the retention time of individual hemextins A and B was ~70 min. However, the reconstituted complex eluted as a major peak with a retention time of ~40 min and as a minor peak with a retention time of ~70 min. The appearance of the major peak with a reduced retention time corresponding to ~27 kDa is consistent with the formation of a tetrameric complex with two molecules each of hemextins A and B (Figure 2.11).

Importance of fold – Importance of fold for anticoagulant activity and complex formation were examined by *S*-pyridylethylated using samples. *S*-pyridylethylated hemextins did not exhibit any anticoagulant activity. An equimolar mixture of *S*-pyridylethylated hemextins A and B also failed to display any anticoagulant effect (Figure 2.12). Thus, proper folding is important for the interaction between hemextins A and B and their anticoagulant activity.

We also reconstituted the hemextin AB complex with *S*-pyridylethylated forms of the native proteins. However, no change in the retention time of the mixture was observed compared with those of the individual *S*-pyridylethylated proteins (Figure 2.13). These results indicate that proper folding is essential for the formation of the hemextin AB complex.

DISCUSSION

In this chapter the isolation and preliminary characterization of two proteins, hemextins A and B, from the venom of *H. haemachatus* was reported. These proteins synergistically induce potent anticoagulant activity. Individually, only hemextin A exhibited mild anticoagulant activity, whereas hemextin B had no anticoagulant activity (Figure 2.9). The increase in the anticoagulant potency of hemextin A in the presence of hemextin B (Figure 2.9) indicated probable complex formation between the two proteins. We have

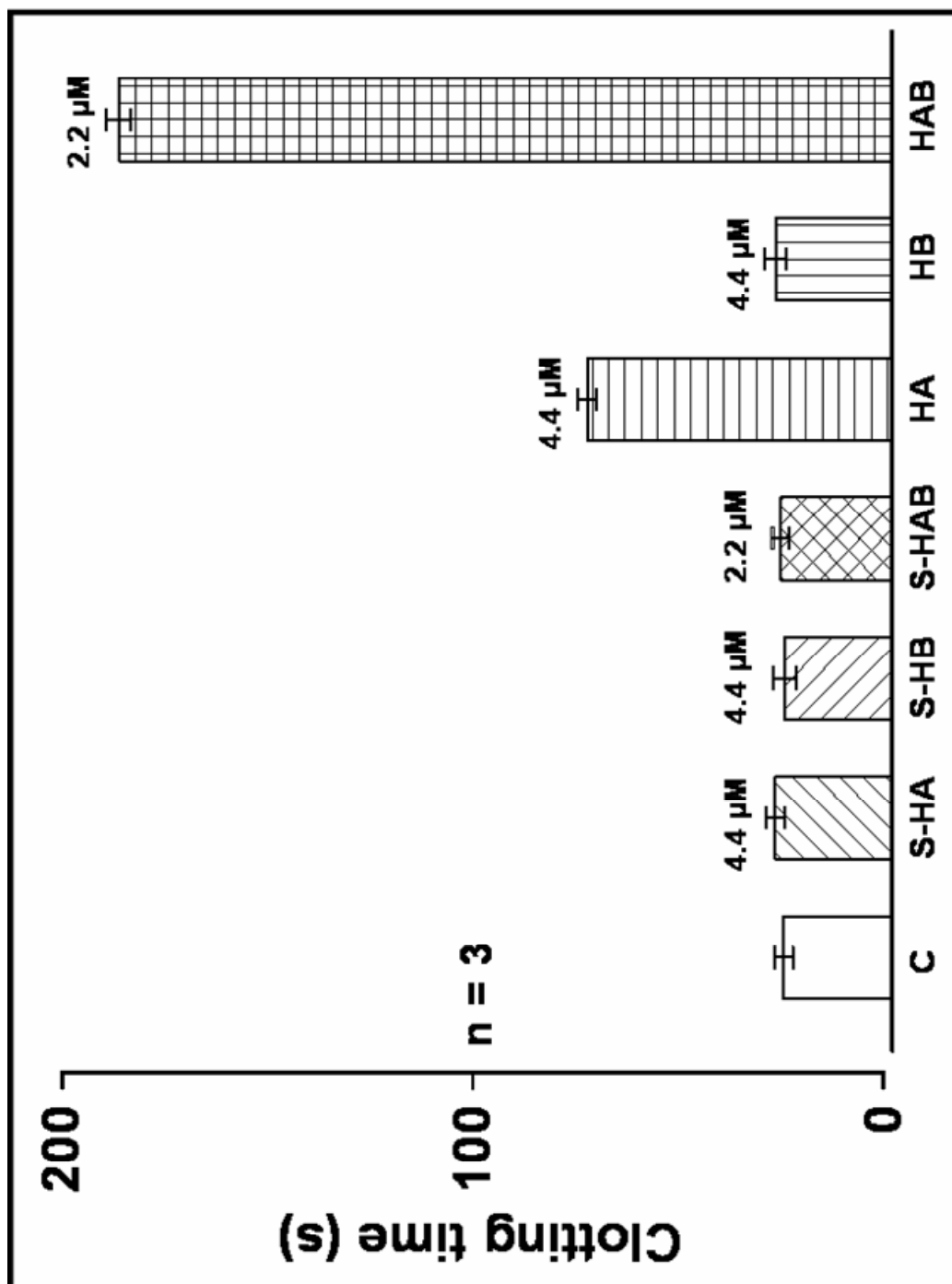


Figure 2.12 Anticoagulant activity comparison. Comparison between the anticoagulant activity of control (C) S-pyridylethylated hemexstin A (S-HA), S-pyridylethylated hemexstin B (S-HB), S-pyridylethylated mixtures of hemexstins A and B (S-HAB), hemexstin A (HA), hemexstin B (HB) and hemexstin AB complex (HAB).

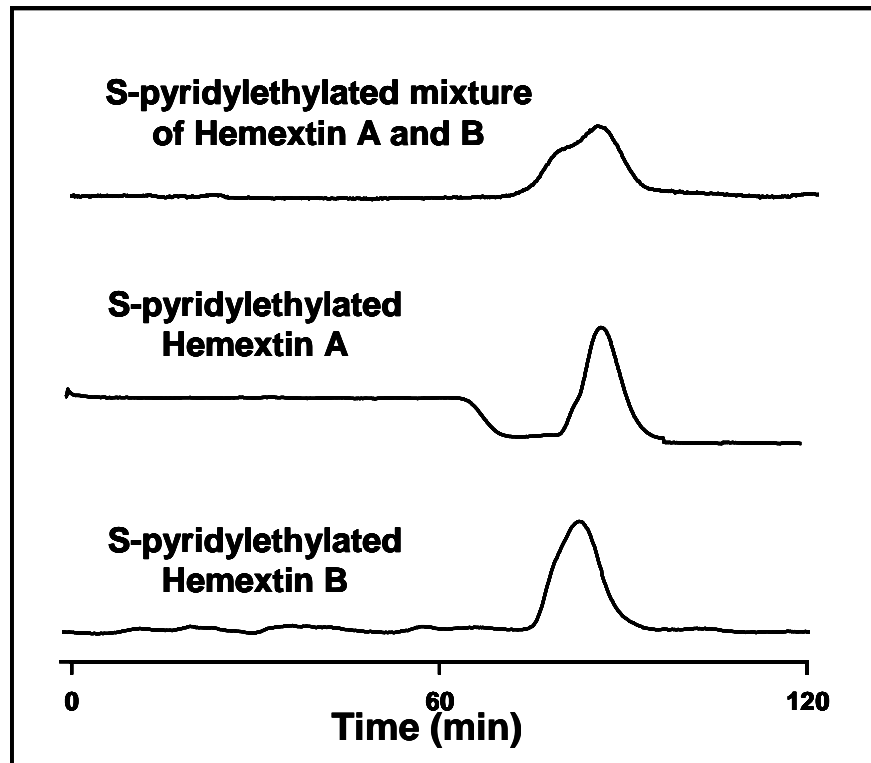


Figure 2.13 Importance of fold in the formation of hemexin AB complex. Note that the mixture of S-pyridylethylated hemexins A and B are unable to form a complex.

shown that 1:1 complex formation is important for potent anticoagulant activity using the prothrombin time assay (Figure 2.10). Complex formation was further confirmed by gel-filtration chromatography (Figure 2.11).

Both hemextins A and B belong to the three-finger family of snake venom proteins (Figure 2.7.) and not to the family of snake venom serine protease inhibitors. Proteins belonging to this group exhibit a characteristic β -sheet structure (Figure 2.14), also observed in the CD studies (Figure 2.8). It is a well known fact that disulfide bonds associated with cysteine residues are essential structural units in proteins (Debarbieux and Beckwith, 1999). To evaluate the importance of the three-finger fold in both complex formation and anticoagulant activity, we used reduced and subsequently pyridylethylated hemextins A and B. Upon pyridylethylation, they lost their native three-finger fold, as observed in the CD studies (Figure 2.8). The *S*-pyridylethylated hemextins were functionally inactive (Figure 2.12) and were unable to bind to each other to form the complex, as evident from the gel-filtration studies (Figure 2.13). This shows that proper folding of the proteins is important not only for function, but also for complex formation. Synergism² among snake venom toxins is fairly well characterized, particularly among presynaptic neurotoxins. For example, crotoxin isolated from *Crotalus durissus terrificus* venom contains two subunits; the basic subunit is a phospholipase A₂ enzyme, whereas the acidic subunit is catalytically inactive (although it is derived from a phospholipase A₂-like protein) (Habermann and Breithaupt, 1978). Individually, only the basic subunit is slightly toxic, whereas the complex exhibits potent toxicity. The acidic subunit appears to

² Synergism is the simultaneous actions of separate entities which together have greater total effect than the sum of their individual effects.

--- Buchholz and Roth

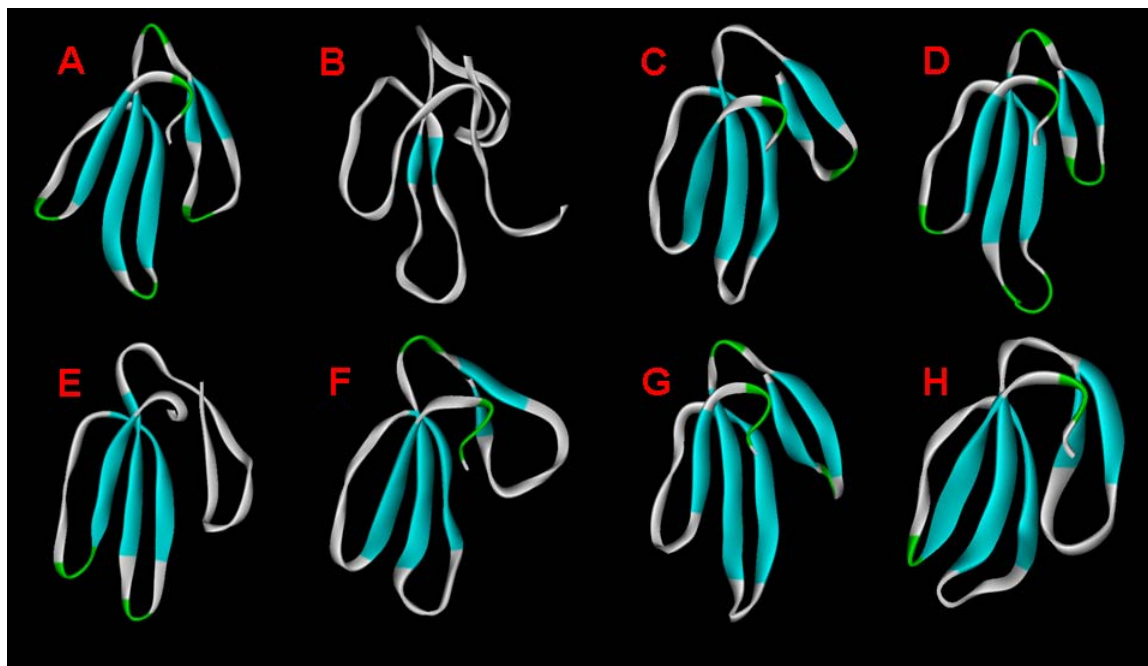


Figure 2.14 Three-dimensional structural similarity among three-finger toxins from snake venoms. (A) Erabutoxin a (1QKD); (B) α -bungarotoxin (2ABX); (C) cardiotoxin V4 (1CDT); (d) κ -bungarotoxin (1KBA); (E) candoxin (1JGK); (F) fasciculin 2 (1FAS); (G) muscarinic toxin MT-2 (1FF4; R Menez *et al.*, pers. comm., 2002); (H) FS2 toxin (1TFS). Note all these ‘sibling’ toxins share a similar structural fold; three β -sheeted ‘fingers’ start from the core. These β -sheeted loops are numbered right to left as loop I, II and III, respectively. However, these toxins differ from each other in their biological activities.

act as a chaperone and enhances the specific binding of the basic subunit to the presynaptic site. Similarly, other presynaptic neurotoxins, such as taipoxin from *Oxyuranus scutellatus* (Doorty *et al.*, 1997) and textilotoxin from *Pseudonaja textilis* (Su *et al.*, 1983) venoms, contain three and four subunits, respectively. All the subunits are structurally similar to phospholipase A₂ enzymes. The noncovalent interactions between the subunits of these toxins are important for their potent toxicity. Thus, a number of snake venom presynaptic toxins are protein complexes with phospholipase A₂ as an integral part. Taicatoxin, another protein complex isolated from *O. scutellatus* venom, blocks calcium channels and has phospholipase A₂, proteinase inhibitor, and neurotoxin (a three-finger toxin) subunits (Possani *et al.*, 1992). There are only a few noncovalent protein complexes in snake venoms that do not contain phospholipase A₂ as an integral part. For example, rhodocetin, an antiplatelet protein complex from *Calloselasma rhodostoma* venom, contains two subunits showing structural similarity to C-type lectins (Wang *et al.*, 1999). Group C prothrombin activators from Australian snakes are procoagulant protein complexes that are structurally and functionally similar to mammalian blood coagulation FXa-FVa complexes (Rao and Kini, 2002; Rao *et al.*, 2003; Rao *et al.*, 2004). Thus, hemextin AB complex is a unique snake venom protein complex formed by the interaction between two three-finger toxins, in which the anticoagulant activity of hemextin A is potentiated by its synergistic interaction with hemextin B. It should be noted that crude snake venom does not contain the hemextin AB complex.

“Keep your eyes open for the odd or unexpected and never dismiss it simply because it does not fit within your program. If chance offers you a clue, follow the trail. You may not discover what you were looking for, but what you discover may be more interesting than what you were looking for.”

- Christian de Duve (“My love affair with insulin”; J.Biol.Chem. 279, 21679-88 (2004))



*“Look- when I tell you how it works
don't keep saying 'really?'”*

Chapter 3

Mechanism of Anticoagulant Activity

Dedicated to inhibitors¹

“The effect of a competitive inhibitor on the rate of an enzyme-catalysed reaction can be appreciated using a modified form of the Michaelis–Menten equation, in which the K_m term in the denominator of v is multiplied by the factor $1 + (i/K_i)$, where i and K_i represent the concentration of inhibitor and its dissociation constant from the enzyme–inhibitor complex respectively. The resulting K_m (app) can then be used to calculate K_i , using appropriate plots at various inhibitor concentrations. A simple graphical method that simplifies this task and permits the direct calculation of K_i without the need for tedious secondary plots was published in 1953 by Malcom Dixon⁴ (yes, the same M. Dixon, co-author with M.C. Webb, of the best-seller *Enzymes*⁵). The Dixon plot for linear competitive inhibition is based on **eqn 4**.

$$\frac{1}{v} = \frac{K_m}{V_s} + \frac{1}{V} + \left(\frac{K_m}{V_s} \times \frac{i}{K_i} \right) \quad (\text{eq 4})$$

The plot of $1/v$ against i at constant s generates a straight line. Measurements at a different substrate concentration give another straight line that intersects the previous one at a point whose abscissa co-ordinate equals $-K_i$. Even though this method cannot distinguish between competitive and mixed inhibition, and does not provide the value of the dissociation constant of the EIS complex for mixed and uncompetitive inhibitors, it is highly appreciated and widely used (3926 citations until September 2005, of which 262 were between 2000 and 2005). The Dixon plot was the first graphical method specifically dedicated to enzyme inhibition and its popularity must be related to its simplicity. One can also easily get rid of the above-mentioned deficiencies by the concomitant use of a similarly conceived graphical method⁶. This is one of several kinetic inventions published

¹ The above excerpt has been taken from the excellent article titled “Enzyme kinetics: the velocity of reactions” by Prof. Antonio Baici published in the *Biochemical Journal* (2006). The article highlights the basics of enzyme kinetics, and also tells the reader about the people who have contributed to its development. I chose this particular part of the article “Dedicated to inhibitors”, since by using similar principles we were able to predict the nature of inhibition mediated by the anticoagulant hemextin AB complex and calculate the K_i of inhibition as well. As the reader will note, the author has very succinctly defined the principles based on which one identifies the mechanism of inhibition and calculates the inhibition constants, briefly touching on their merits and demerits as well.

The references cited in the excerpt are in the same order as cited in the original article and have not been modified.

in the *Biochemical Journal* by Athel Cornish-Bowden, the inexhaustible enzyme kinetic volcano, well known for his *Fundamentals of Enzyme Kinetics*⁷. When used together, the two plots complement each other and permit identification of the mechanisms of inhibition and calculation the inhibition constants.”

--- Professor Antonio Baici, Department of
Biochemistry, University of Zurich
Biochemical Journal 2006

References:

4. Dixon, M. (1953) *The determination of enzyme inhibitor constants*. *Biochem. J.* **55**, 170–171
5. Dixon, M. and Webb, E.C. (1979) In *Enzymes* 3rd edn, Longman, London
6. Cornish-Bowden, A. (1974) *A simple graphical method for determining the inhibition constants of mixed, uncompetitive and noncompetitive inhibitors*. *Biochem. J.* **137**, 143–144
7. Cornish-Bowden, A. (2004) *Fundamentals of enzyme kinetics* 3rd edn, Portland Press, London In

“Mechanism of action” refers to the specific biochemical interaction through which a substance (which in most cases is a drug or a drug lead) produces its pharmacological effect. Snake venoms form a rich source of bioactive molecules, such as peptides, proteins and enzymes with important pharmacological activities. The protein components constitute a highly evolved and organized arsenal of biomolecules that attack, often with precision and coordinated synergism, a wide variety of molecular targets vital for the physiological process. While this would well suit the despicable intentions of the snake’s venom, it also offers boundless opportunities for the study of novel biomolecules of therapeutic interest². For example, a family of inhibitors of angiotensin converting enzyme were developed based on bradykinin potentiating peptides from South American snake venoms (Higuchi *et al.*, 1999). Inhibitors of platelet aggregation, such as eptifibatid and tirofiban, were designed based on disintegrins, a large family of platelet aggregation inhibitors found in viperid and crotalid snake venoms (McClellan and Goa, 1998; O’Shea and Tchong, 2002; Kondo and Umemura, 2002; Plosker and Ibbotson, 2003; Huang and Hong, 2004; Marcinkiewicz, 2005). But prior to the use of a molecule for therapeutic purposes one has to find out the mechanism by which it acts³ and more precisely how specific it is towards its molecular target.

In the previous chapter, we have seen that hemextin A has mild anticoagulant activity, whereas hemextin B is inactive. However, the 1:1 complex of the two proteins (hemextin

² It will be an interesting paradox if it transpires that the venomous creatures that have so long been reviled by the human race turn out to provide key lessons for revolutions in medicine and science which prolong and enhance human existence.

---Mark J. Dufton, *Kill and cure: the promising future for venom research.*
Endeavour, 17:3, 138-140 (1993)

³ The most exciting phrase to hear in science, the one that heralds the most discoveries, is not "Eureka!" (I found it!) but, "That's funny..."

---Isaac Asimov

AB complex) exhibits potent anticoagulant activity. The blood coagulation cascade consists of many steps. Therefore, identification of the site of activity is important in the understanding of the mechanism of anticoagulation, mediated by hemextin A and hemextin AB complex. In this chapter we have identified the specific site in the coagulation cascade where hemextin A and hemextin AB complex act to mediate anticoagulation, followed by the identification of the specific coagulation factor which is inhibited by these anticoagulant proteins.

Several techniques, including clot based tests, chromogenic or color assays, direct chemical measurements, and ELISAs, are used for identifying the mechanism of activity of an identified anticoagulant (Breddin *et al.*, 1994; Walenga and Hoppensteadt, 2004). In order to identify the mechanism of anticoagulant activity we used clot based and chromogenic assays.

For our studies we employed three clot based assays namely, prothrombin time, stypven time and thrombin time. Using these three assays we designed a simple “Dissection Approach” (Figure 3.1) (Kini and Banerjee, 2005), to identify the specific stage in the extrinsic coagulation pathway where hemextin A and hemextin AB complex mediate their activity. In prothrombin time, thromboplastin reagent containing TF and calcium is added to citrated plasma. Formation of extrinsic tenase results in rapid fibrin formation via extrinsic and common pathways. Therefore, this clotting assay measures the effect of an anticoagulant on the extrinsic tenase and prothrombinase complexes and the conversion of fibrinogen to fibrin clot. In Stypven time, Russell's viper venom activates FX directly, and clot formation proceeds via the common pathway. Thus, Stypven time circumvents the extrinsic tenase complex and monitors the effect of an anticoagulant on

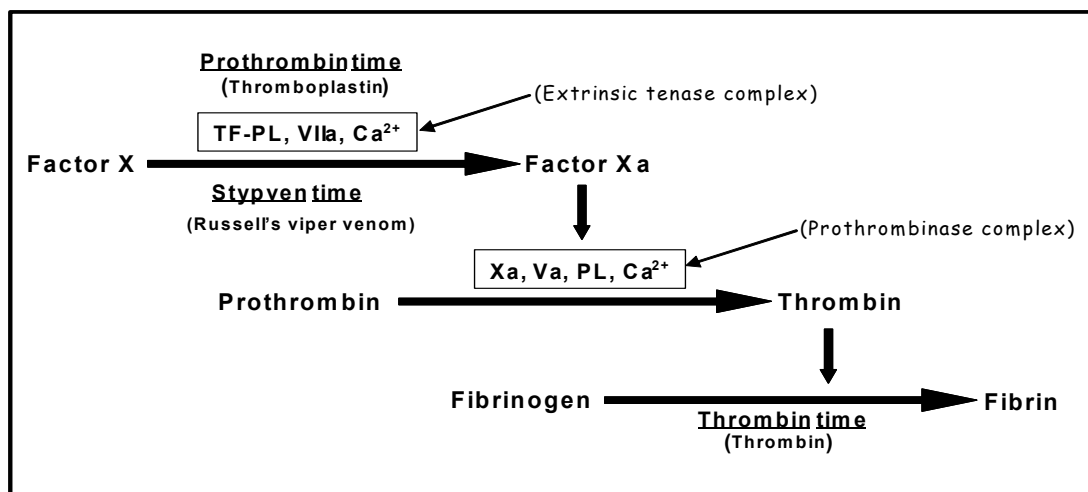


Figure 3.1 Dissection Approach. Schematic representation showing the selective activation of the extrinsic coagulation pathway by the prothrombin, Stypven and the thrombin time clotting assays. In the prothrombin time, clotting is initiated at the tenase complex by the addition of Ca²⁺ and thromboplastin, which contains tissue factor and phospholipids (TF-PL). In the Stypven time, clotting is initiated at the prothrombinase complex by the addition of dilute Russell's viper venom, which activates factor FX and factor FV by specific proteases. FXa and FVa form the prothrombinase complex on the PL surfaces with the addition of Ca²⁺. In thrombin time, clotting is initiated by the addition of thrombin, which converts soluble fibrinogen to a fibrin clot.

the prothrombinase complex and the conversion of fibrinogen to fibrin. In thrombin time, thrombin is added to citrated plasma and directly converts fibrinogen to fibrin. Thrombin time therefore, depicts the effect of an anticoagulant on the conversion of fibrinogen to fibrin only. A systematic analysis of the effect of an anticoagulant on these three clotting times would therefore help in identifying the stage of coagulation in the extrinsic coagulation cascade. Thus, the anticoagulant action of the individual proteins and their complex can be localized to certain activation step(s) in the cascade.

Chromogenic assays are based on the utilization of enzyme specific substrate onto which a chromophore has been linked. The enzyme cleaves the chromogenic substrate, releasing a colored compound that can be detected with a spectrophotometer (Walenga and Hoppensteadt, 2004). The general methodology involving such an assay, is to incubate predetermined amount of a specific coagulation enzyme with a given amount of the anticoagulant. After incubation, residual enzymatic activity is determined by the addition of a selective chromogenic substrate. These assays are therefore best suited for identifying the mechanism of inhibition, the inhibitory constants and specificity of inhibition of an anticoagulant. Therefore, by the combined use of dissection approach (which involves the clotting assays) and chromogenic assays we were able to identify the specific blood coagulation factor to which the anticoagulant protein and its synergistic complex bind to mediate anticoagulation.

MATERIALS AND METHODS

Reagents – Thromboplastin with calcium (for prothrombin time assays), Russell's viper venom (RVV) (for Stypven time assays) and thrombin reagent (for thrombin time assays) were purchased from Sigma (St. Louis, MO, USA). The chromogenic substrates H-D-Ile-

Pro-Arg-*p*-nitroanilide (*p*NA) dihydrochloride (2HCl), (S-2288), *pyro*-Glu-Pro-Arg-*p*NA·HCl (S-2366), H-D-Phe-Pip-Arg-*p*NA·2HCl (S-2238), H-D-Pro-Phe-Arg-*p*NA·2HCl (S-2302), Z-D-Arg-Gly-Arg-*p*NA·2HCl (S-2765), *pyro*-Glu-Gly-Arg-*p*NA·HCl (S-2444), benzoyl-Ile-Glu(GluγOMe)-Gly-Arg-*p*NA·HCl (S-2222), H-D-Val-Leu-Lys-*p*NA·2HCl (S-2251), H-D-Val-Leu-Arg-*p*NA·2HCl (S-2266) and MeO-Suc-Arg-Pro-Tyr-*p*NA·HCl (S-2586) were from Chromogenix AB, Stockholm, Sweden. Spectrozyme[®] FIXa (H-D-Leu-Ph'Gly-Arg-*p*NA·2AcOH) was obtained from American Diagnostica Inc., Stamford, CT, USA. All substrates were reconstituted in deionized water prior to use. Recombinant human tissue factor (Innovin) was purchased from Dade Behring, Marburg, Germany. Human plasma was donated by healthy volunteers. All other chemicals and reagents used were of highest purity available.

Proteins - Human plasma derived FVIIa and FX and FXa was a gift from factor VII's group (Kazuhiko Tomokiyo, Yasushi Nakatomi, Teruhisa Nakashima and Soutatou Gokudan) of Kaketsuken, which were purified as described earlier (Wildgoose and Kisiel, 1989; Nakagaki *et al.*, 1991). Recombinant human soluble TF (residues 1-218; sTF) was a gift from Dr. Toshiyuki Miyata, National Cardiovascular Center, Suita, Japan and it was prepared as described earlier (Stone *et al.*, 1995). Human plasma-derived thrombin, activated protein C, and factor IXa were gifts from Hiroshi Kaetsu, Shinji Nakahira, and Takayoshi Hamamoto, from Kaketsuken, respectively as described (Okajima *et al.*, 1990; Nakagaki *et al.*, 1991; Kaetsu *et al.*, 1998). We also thank Dr. Mitsuhiro Ohta, Kobe Pharmaceutical University for providing three cardiotoxins (CM-14, CM-17, CM-18 *Naja Naja Atra*). Plasma kallikrein and plasmin were purchased from Enzyme Research Laboratories Inc, South Bend, IN, USA. Factor XIa and factor

XIIa were purchased from Haemtech, Essex junction, VT, USA. Proteins t-PA and u-PA were purchased from American Diagnostica Inc., Stamford, CT, USA. α – chymotrypsin and trypsin were obtained from Worthington Biochemical Corporation, Lakewood, NJ, USA.

Reconstitution of the anticoagulant complex – Studies described in the previous chapter indicated that the hemexin A interacted with hemexin B forming a synergistic complex. We reconstituted the complex for various *in vitro* experiments immediately prior to the experiment by incubating equimolar concentration of the two proteins (unless mentioned otherwise) at 37° C for a period of 5 min in 50 mM Tris-buffer (pH 7.4).

Anticoagulant activity – For our studies we used four coagulation tests which were conducted using a BBL fibrometer:

1. *Recalcification time*: The recalcification times were determined according to the method of Langdell et al. (LANGDELL *et al.*, 1953). 50 mM Tris-HCl buffer (pH 7.4) (100 μ L), plasma (100 μ L) and various concentrations of venom or its fraction (50 μ L) were preincubated for 2 min at 37°C. Clotting was initiated by the addition of 50 μ L of 50 mM CaCl₂.
2. *Prothrombin time*: The prothrombin times were measured according to the method of Quick (Quick, 1973). 100 μ L of 50 mM Tris-HCl buffer (pH 7.4), 100 μ L of plasma and 50 μ L of venom or its fractions were preincubated for 2 min at 37°C. Clotting was initiated by the addition of thromboplastin with calcium reagent (150 μ L).
3. *Stypven time*: Stypven time measurements were determined according to the method of Hougie (Hougie, 1956). Plasma (100 μ L), 50 mM Tris-HCl buffer

(pH 7.4) (100 μ L) and RVV (0.01 μ g in 100 μ L) and individual proteins or the reconstituted complex (50 μ L) were preincubated for 2 min at 37°C. Clotting was initiated by the addition of 50 mM CaCl₂ (50 μ L).

4. *Thrombin time*: Thrombin time was determined according to the method of Jim (JIM, 1957). Individual proteins or the reconstituted complex were incubated with 100 μ L of plasma and 100 μ L of 50 mM Tris-HCl buffer (pH 7.4) for 2 min at 37°C in a total volume 250 μ L. Clotting was initiated by the addition of standard thrombin reagent (0.01 NIH units in 50 μ L).

Reconstitution of the extrinsic tenase complex – TF-FVIIa complex was reconstituted by incubating 10 pM FVIIa with 70 nM of recombinant human TF (Innovin) in Buffer A (20 mM HEPES, 150 mM NaCl, 10 mM CaCl₂ and 1% BSA, pH 7.4) for 10 min at 37° C. Then FX was added to the mixture to obtain a final concentration of 30 nM. The activation was stopped by the addition 50 μ L of stop buffer (20 mM HEPES, 150 mM NaCl, 50 mM EDTA and 1% BSA, pH 7.4) to 50 μ L aliquots of the reaction mixture after 15 min incubation. FXa formed was measured by the hydrolysis 1 mM of S-2222 in Buffer A in a microtiter plate reader at 405 nm. The inhibitory effect on extrinsic tenase activity was determined by adding the individual proteins or the anticoagulant complex 15 min prior to FX addition.

Serine protease specificity – The selectivity profile of anticoagulant proteins and their complex was examined against 12 serine proteases - procoagulant serine proteases (FIXa, FXa, FXIa, FXIIa, plasma kallikrein and thrombin), anticoagulant serine protease activated protein C (APC), fibrinolytic serine proteases (urokinase, t-PA and plasmin) and classical serine proteases (trypsin and chymotrypsin). Various concentrations of the

purified individual proteins or the reconstituted anticoagulant complex were preincubated with each of the enzymes for a period of five minutes at a temperature of 37°C, followed by the addition of appropriate chromogenic substrate.

In a total volume of 200 μ l in the individual wells of the microtiter plate, final concentrations of FVIIa (300 nM)/S-2288, FVIIa-sTF (30 nM)/S-2288, FXa (0.75 nM)/S-2765, α -thrombin (0.66 nM)/S-2238, plasmin (2 nM)/S-2251, FIXa (3 μ M)/spectrozyme® fIXa, FXIa (0.34 nM)/S-2366, FXIIa (0.4 nM)/S-2302, recombinant tissue plasminogen activator (80 nM)/S-2288, APC (0.34 nM)/S-2366, urokinase /S-2444, plasma kallikrein (0.4 nM)/S-2302, trypsin (2.17 nM)/S-2222 and chymotrypsin (0.4 nM)/S-2586. The kinetic rate of substrate hydrolysis (mOD/min) was measured over 5 min.

Kinetics of inhibition – All studies were performed in assay buffer containing 50 mM Tris-HCl, pH 7.4, containing 150 mM NaCl, 10 mM CaCl₂, and 1% BSA at 37°C. The kinetics of hydrolysis of the chromogenic substrate S-2288 by FVIIa-sTF was measured prior to examining the inhibitory effects of the individual proteins and the reconstituted anticoagulant complex. Reactions were initiated by the addition of S-2288 (0 – 5 mM) to the individual wells of a 96-well plate containing FVIIa (30 nM) in complex with sTF (100 nM) in a final volume of 180 μ l. Initial reaction velocities were measured as a linear increase in the absorbance at 405 nm ($A_{405 \text{ nm}}$) over 5 min, with a SPECTRAMax plus® temperature-controlled microplate spectrophotometer (Molecular Devices, Sunnyvale, CA, USA).

The inhibitory potency of anticoagulant complex was measured over a range of substrate concentrations. Reactions were initiated by the addition of S-2288 to premixed enzyme-

cofactor and inhibitor in the wells of a microtiter plate. Reactions with FVIIa-sTF contained 0.025 to 0.1 μ M of inhibitor complex and 0 to 3 mM of S-2288. The initial velocities were measured over 5 min under steady-state conditions and were fit by reiterative nonlinear regression to Equation 1, describing a classical non-competitive inhibitor, to derive the K_i value.

$$\frac{1}{V} = \frac{K_m}{V_{\max}} \left(1 + \frac{[I]}{K_i} \right) \times \frac{1}{[S]} + \frac{1}{V_{\max}} \left(1 + \frac{[I]}{K_i} \right) \dots\dots\dots \text{(Eq.1)}$$

RESULTS

Site of anticoagulant activity – As observed in the studies depicted in the previous chapter, hemextin A and hemextin AB complex prolong clotting in prothrombin time clotting assays. To identify the specific stage in the extrinsic coagulation pathway, we used a simple "dissection approach" (Figure 3.1) (see above for details).

Hemextin A exhibited a mild anticoagulant activity by prolonging the clotting time in the prothrombin time assay, but did not prolong Stypven time and thrombin time (Figure 3.2A). As expected, hemextin B did not prolong clotting times in prothrombin time, Stypven time and thrombin time assays (Figure 3.2B). The hemextin AB complex exhibited a potent anticoagulant activity by prolonging the clotting time in prothrombin time assay. However, the clotting times in the other two assays were not affected (Figure 3.2C). These results indicate that hemextin A and hemextin AB complex affect only the extrinsic tenase complex, but not the prothrombinase complex or conversion of fibrinogen to fibrin clot.

To confirm the site of inhibition, we examined the effects of hemextins A and B and their complex on the reconstituted TF-FVIIa complex (Figure 3.3). Hemextin A exhibited mild inhibitory activity at higher concentrations. Hemextin B, on the other hand, did not mediate any inhibitory activity on the enzymatic action of the extrinsic tenase complex. However, hemextin AB complex completely inhibited extrinsic tenase activity (Figure 3.3) with an IC_{50} value (concentration of the inhibitor which inhibits 50% of the activity) of 100 nM. Neither the individual proteins nor the complex mediated any inhibitory effect on FXa amidolytic activity (described below). The effect of the individual hemextins and the hemextin AB complex was also assessed on the intrinsic pathway

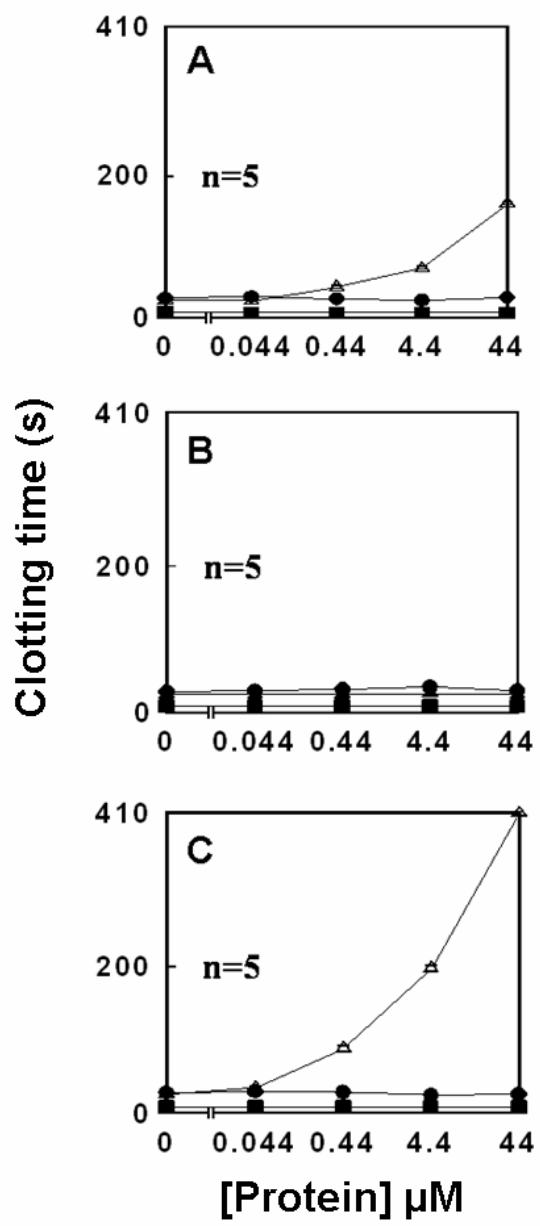


Figure 3.2 Localization of the step of activity. Effect of hemexin A (A) hemexin B (B) and hemexin AB complex complex (C) on the prothrombin time (Δ); Stypven time (\bullet) and thrombin time (\blacksquare) clotting assays(see text for details). Each data point represents the average \pm SD.

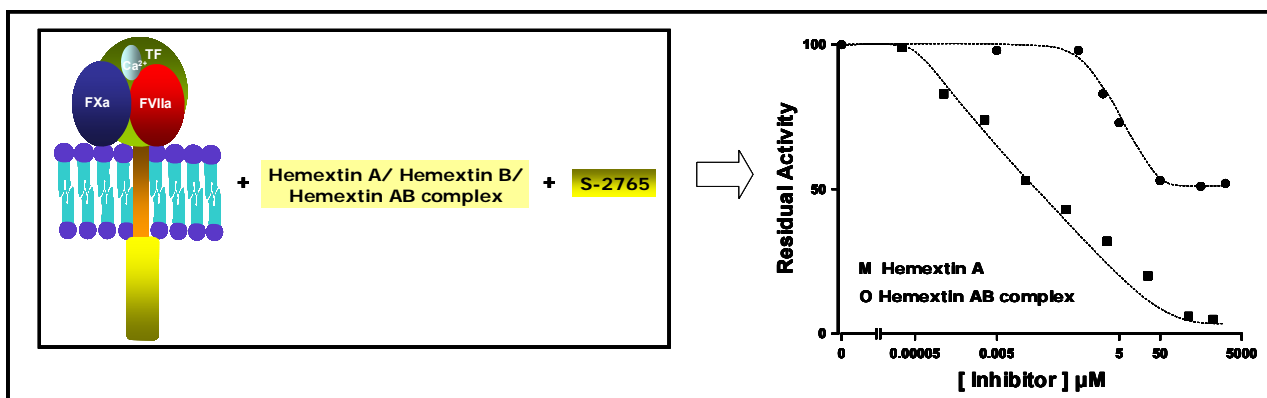


Figure 3.3 Inhibition of TF-FVIIa activity. The inhibitory potency of hemexin A and hemexin AB complex for the inhibition of TF-FVIIa. Hemexin B did not exhibit any inhibitory effect.

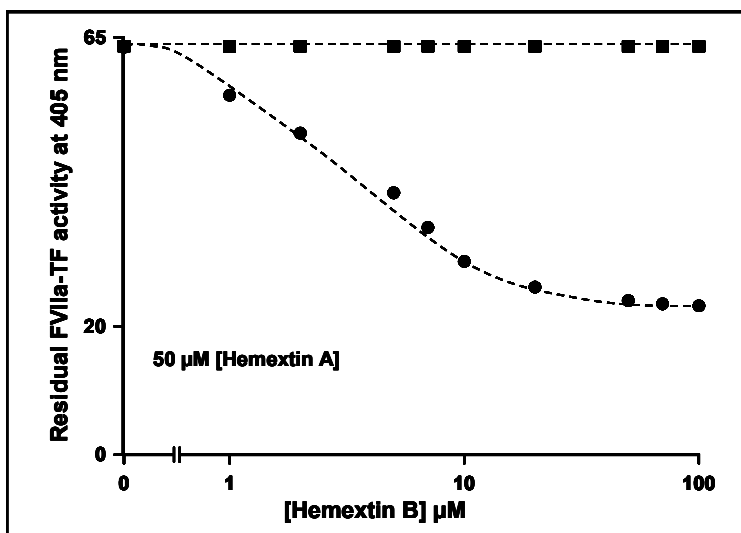


Figure 3.4 Complex formation demonstrated by the Inhibition of TF-FVIIa activity. Formation of hemexin AB complex (●) between hemexin A (■) and hemexin B is illustrated by their effect on TF-FVIIa enzymatic activity. To determine the stoichiometry of complex formation, the concentration of hemexin A was kept low so that 100% TF-FVIIa activity is not inhibited upon complex formation. (The experiment was carried out on two separate days)

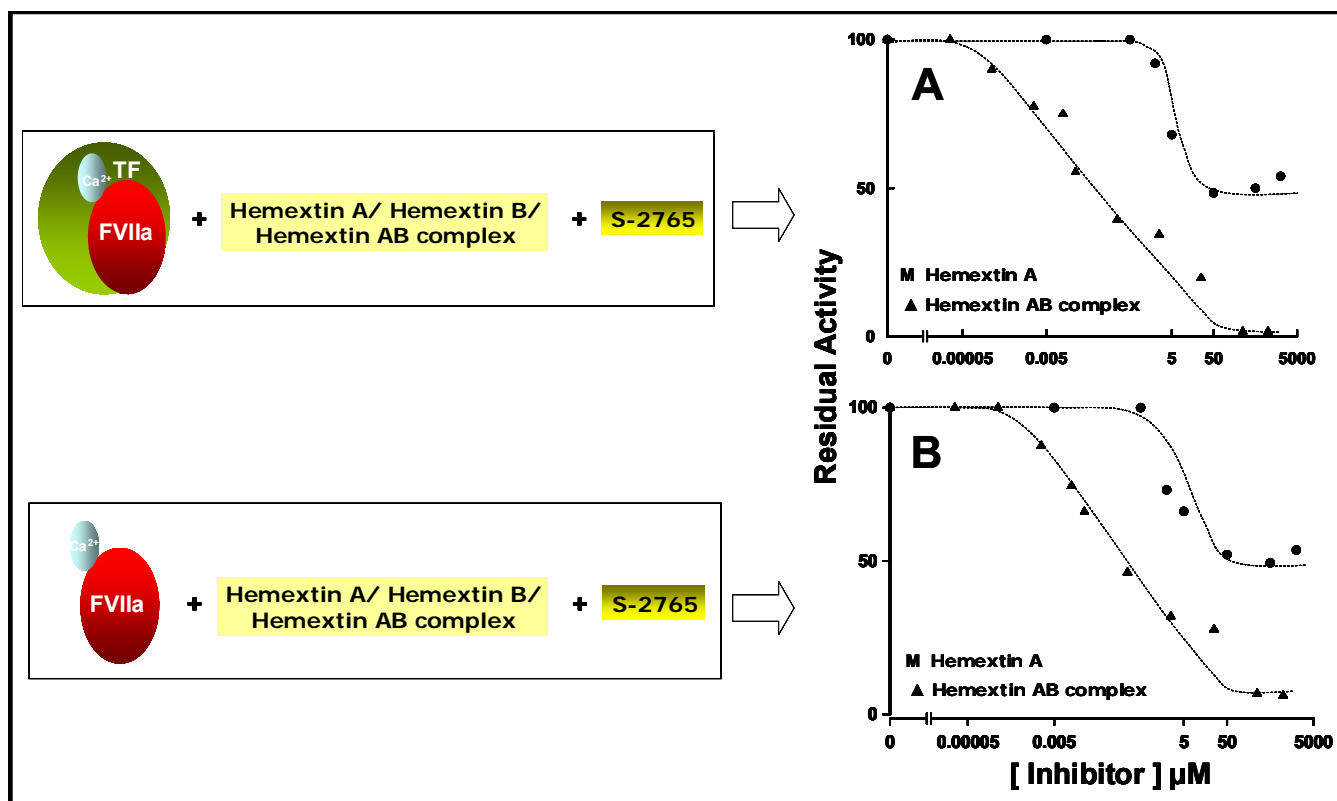


Figure 3.5 Effect of phospholipids on the inhibitory activity of hemexstins A and B and hemexstin AB complex. The inhibitory potency of hemexstin A and hemexstin AB complex for the inhibition of (A) FVIIa and (B) FVIIa-sTF amidolytic activity. (Note the absence of phospholipids do not affect the inhibitory potency of the protein(s) and the reconstituted complex; hemexstin B did not exhibit any inhibitory activity in these assays). (The experiment was carried out on two separate days)

using recalcification time assays. No anticoagulant activity was observed on the intrinsic pathway (data not shown).

Further the effects of other three-finger toxins, particularly cardiotoxins/cytotoxins, which are structurally similar to hemextin A and B was also monitored on the TF-FVIIa proteolytic activity. CM - 14, CM – 17 and CM - 18 from *Naja naja atra* did not inhibit FXa formation by TF-FVIIa complex (data not shown). To determine the importance of hemextin AB complex formation for the inhibition of TF-FVIIa complex, we performed a similar titration experiment. The concentration of hemextin A was kept constant at 50 μ M so that only 70% activity of TF-FVIIa complex is inhibited, and its inhibitory activity on extrinsic tenase activity was evaluated in the presence of increasing concentrations of hemextin B. Higher concentrations of hemextin A was not used since it would not have been possible to monitor the stoichiometry of complex formation. As shown in (Figure 3.4), the inhibitory activity of hemextin A increases with the increasing concentrations of hemextin B until the ratio reached 1:1. Further addition did not increase the anticoagulant effect. The results indicated that hemextins A and B form a 1:1 complex and the complex formation is crucial for the potent anticoagulant activity. No further increase in the inhibitory activity was observed after equimolar ratios of hemextins A and B. These observations further confirmed the importance of complex formation between hemextins A and B.

To understand the effect of phospholipids, the inhibitory activity of hemextin A and hemextin AB complex was monitored on FVIIa amidolytic activity either in the presence or absence of sTF. In both the cases we observed potent inhibitory activity (Figure 3.5A and B) in a dose-dependant manner.

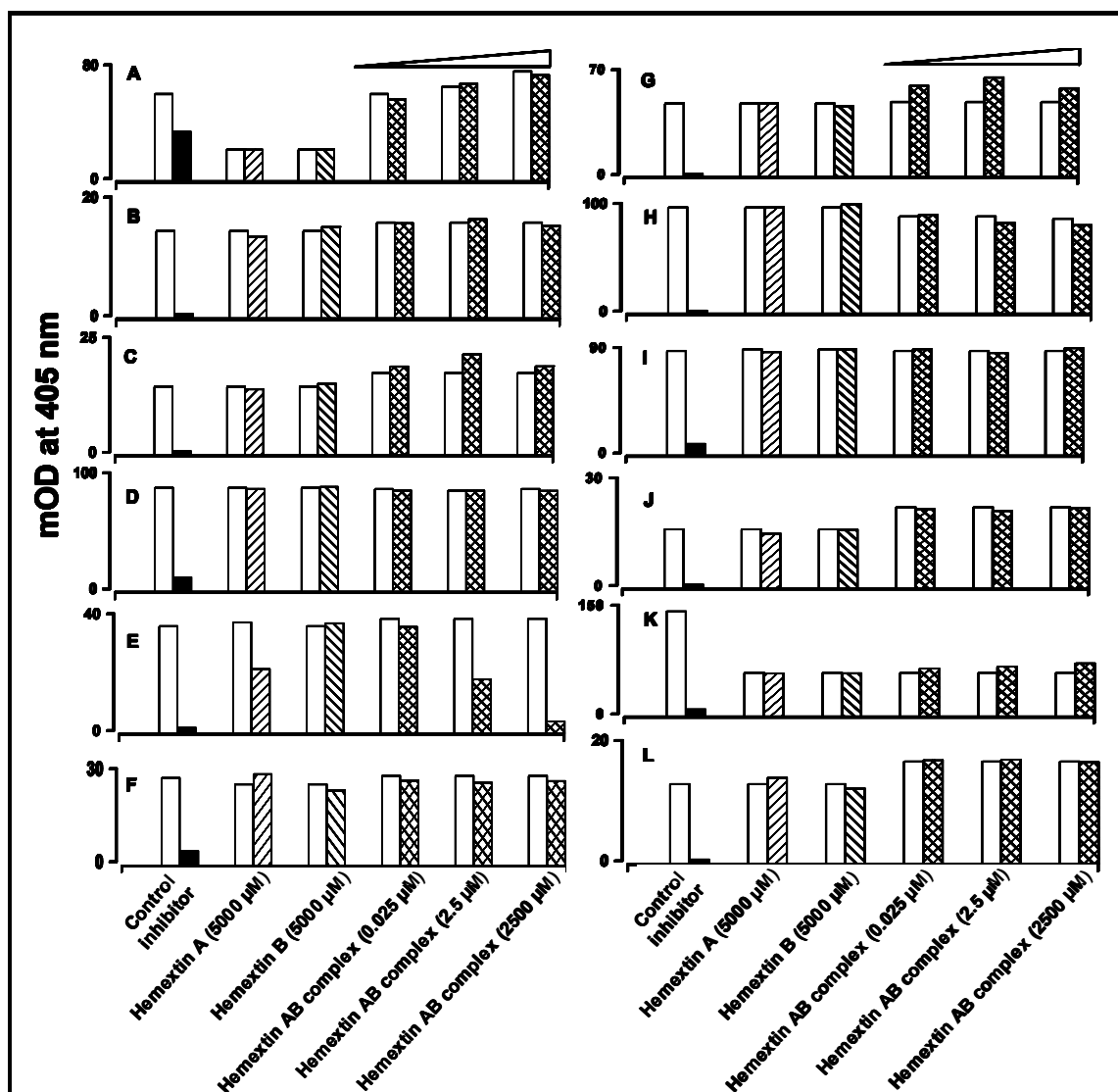


Figure 3.6 Serine protease specificity. Effect of hemexetin A, hemexetin B and the hemexetin complex on the amidolytic activity of (A) FIXa, (B) FXa, (C) FXIa, (D) FXIIa, (E) plasma kallikrein, (F) thrombin, (G) trypsin, (H) chymotrypsin, (I) urokinase, (J) plasmin, (K) APC and (L) tPA. Benzamidine (■) was used as a positive control in all the experiments except in case of plasmin and chymotrypsin where aprotinin was used. The inhibitory potency of the proteins and the reconstituted complex was measure with respect to the blank (□), assay mixture containing assay buffer in place of the proteins. Note both hemexetin A and hemexetin complex, but not hemexetin B inhibit the amidolytic activity of plasma kallikrein.

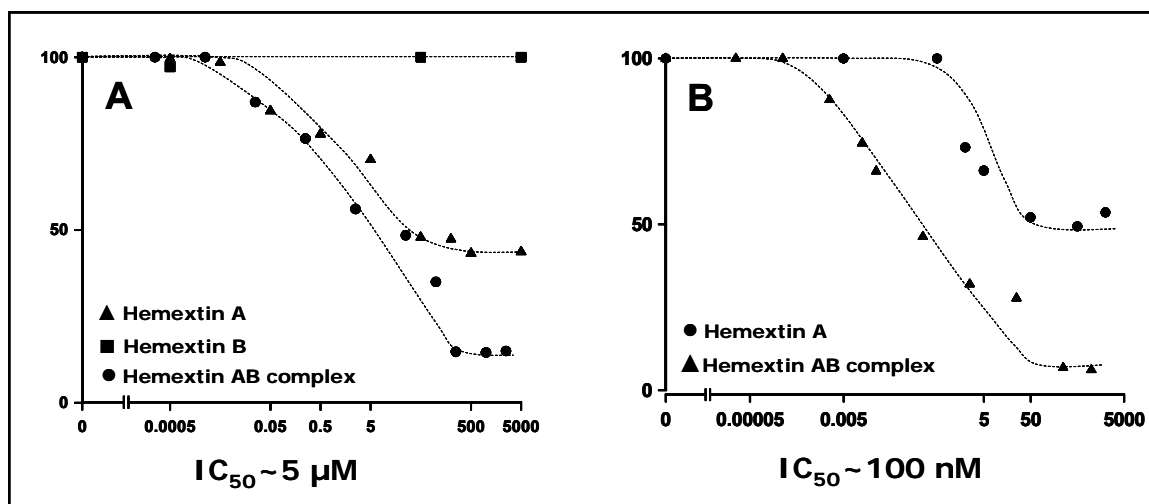


Figure 3.7 Inhibition of plasma kallikrein amidolytic activity and comparison of potency with FVIIa inhibition. (A) The inhibitory potency of hemexstin A, hemexstin B and hemexstin AB complex for the inhibition of plasma kallikrein amidolytic activity. (B) The inhibitory potency of hemexstin A and hemexstin AB complex for coagulation FVIIa. (Note that the IC_{50} is $\sim 5 \mu M$ for the inhibition of plasma kallikrein activity in comparison to 100 nM as observed in the case of FVIIa, indicating that both the protein and its complex are potent inhibitors of FVIIa) (The experiment was carried out on two separate days).

Specificity of inhibition – To determine the specificity of inhibition, hemextins A and B and their complex were screened against 12 serine proteases (Figure 3.6). No inhibitory activity was observed against any of the serine protease with the exception of FVIIa and plasma kallikrein. As with FVIIa, hemextins A and hemextin AB complex inhibit plasma kallikrein in a dose-dependant manner (Figure 3.7). Hemextin B did not inhibit kallikrein's protease activity. However, the inhibitory potency towards FVIIa (either in the absence or presence of sTF) was at least 50 times higher than towards plasma kallikrein (Figure 3.7).

Kinetics of inhibition – To determine the mechanism of inhibition, we examined the inhibitory kinetics of hemextin AB complex on amidolytic activity of sTF-FVIIa complex on S-2288. Kinetic studies revealed that hemextin inhibited FVIIa-sTF activity non-competitively. Lineweaver-Burk plots showed that K_m remained unaltered where as V_{max} decreased with increasing concentrations of inhibitor (Figure 3.8A) a characteristic of a non-competitive inhibitor. The K_i value for inhibition was determined to be 25 nM (Figure 3.8B). We also calculated the turnover number (K_{cat}) (number of moles of substrate converted to product per mole of enzyme per min) at different concentrations of the inhibitor. As observed in the case of classical non-competitive inhibitors K_{cat} decreased with increasing concentrations of hemextin AB complex (data not shown). Since the amidolytic activity of FVIIa alone is very weak (Maun *et al.*, 2005), we did not study the kinetics for the inhibition of FVIIa amidolytic activity of alone by hemextin AB complex.

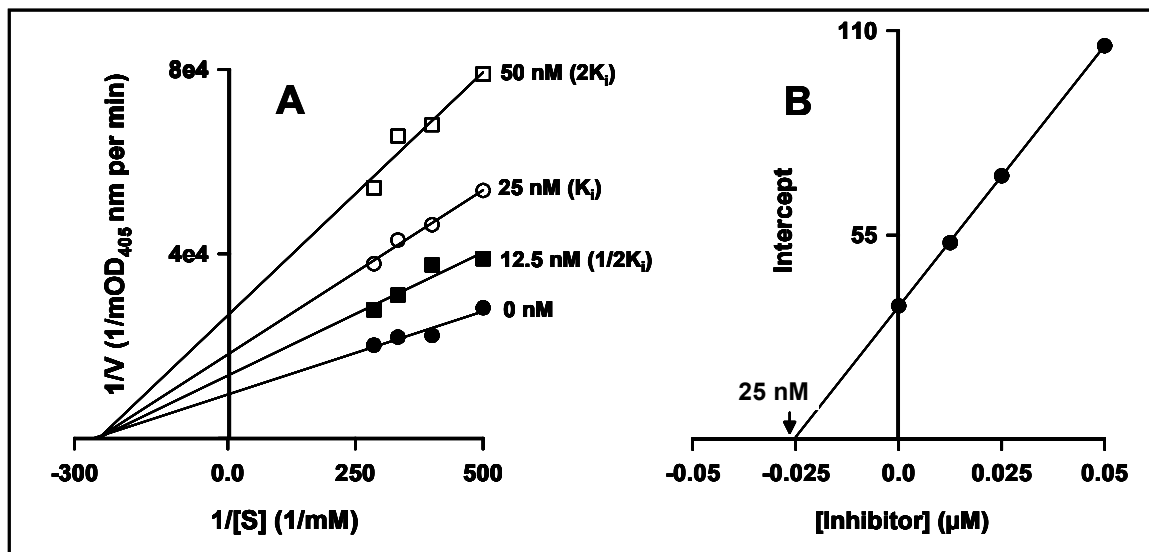


Figure 3.8 Nature of Inhibition. (A) Double reciprocal (Lineweaver-Burk) plots for the kinetic activity of FVIIa-sTF in the presence of 50 nM (\square) ($2K_i$), 25 nM (\circ) (K_i), 12.5 nM (\blacksquare) ($1/2 K_i$) of reconstituted hemexin AB complex. (\bullet) represents the kinetic activity FVIIa-sTF in the absence of hemexin AB complex. Note that the V_{\max} decreases with increase in the inhibitor concentration whereas the K_m remains unchanged, a classical phenomenon observed in non-competitive inhibitors. (B) Corresponding secondary plot depicting the K_i for the inhibition. (The experiment was carried out on two separate days)

DISCUSSION

It is a well known fact that formation of unwanted clots has detrimental or debilitating effects and hence the need for anticoagulant therapies. Current anticoagulants used for treating these disorders, are non-specific and have a narrow therapeutic range necessitating careful laboratory monitoring to achieve optimal efficacy and minimize bleeding (Goolsby, 2002). This is further complicated by other factors such as dietary intake. Therefore, novel anticoagulant and antiplatelet agents are being sought after. Since the FVIIa is the key initiator of blood coagulation and is present in the plasma milieu at very low concentrations, it beckons to be an attractive drug target for the design and development of anticoagulants. So far, only two proteins are known that specifically inhibit the TF-FVIIa complex have been well characterized, namely, tissue factor pathway inhibitor (TFPI) and nematode anticoagulant peptide c2 (NAPc2). TFPI is an endogenous inhibitor of this complex, whereas NAPc2 is an exogenous inhibitor isolated from canine hookworm, *Ancylostoma caninum* and now expressed in yeast. The anticoagulation mechanism of each of these anticoagulants has been dealt in detail in the introductory chapters of the thesis. But most importantly, both the anticoagulants use FXa and TF as scaffold to bind to FVIIa. In other words they inhibit both coagulation serine proteases FVIIa and FXa. This limitation has prompted the design of specific inhibitors targeting FVIIa (the details of which are provided in the introductory chapter). However, this presents a formidable challenge since the domain architecture of FVIIa is very similar to the other coagulation serine proteases. To suffice to this necessity, we and others have been focusing on isolating and characterizing pharmacologically active proteins from snake venoms that affect blood coagulation and platelet aggregation.

Hemextin A and its synergistic complex with hemextin B prolong clotting in prothrombin time assays. Using the “dissection approach” we identified the site of anticoagulant action of hemextin A and its synergistic complex. Both hemextin A and hemextin AB complex inhibit the extrinsic tenase complex but not other steps in the extrinsic pathway. These results were further confirmed by studying the effect of hemextin A and its complex on the reconstituted TF-FVIIa complex. Both hemextin A and hemextin AB complex inhibit the FXa formation by the reconstituted extrinsic tenase complex (Figure 3.3). Further, hemextin A and hemextin AB complex inhibit the amidolytic activity of FVIIa both in the presence and in the absence of sTF (Figure 3.5). Hemextin AB complex inhibits with IC_{50} values of ~ 100 nM and ~ 105 nM respectively. Similar IC_{50} values may be indicative of the fact that hemextin A and hemextin AB complex do not bind to the cofactor binding site of FVIIa. The inhibitory activity of hemextin A and hemextin AB complex may not be due to nonspecific interaction of hemextin A or its complex with the phospholipids in the extrinsic tenase complex, as indicated by their inability to prolong the Stypven time, since they failed to inhibit the prothrombinase complex, which is also formed on the phospholipid surfaces. This was further confirmed by determining the inhibitory activity of hemextin A and hemextin AB complex on the amidolytic of reconstituted extrinsic tenase complex using sTF and FVIIa. Further, hemextin A and hemextin AB complex inhibited amidolytic activity of FVIIa. Hemextin B, however, did not exhibit any inhibitory activity in the absence of hemextin A. To further characterize the inhibitory properties and determine the specificity of inhibition, we screened hemextins A and B and hemextin AB complex against 12 serine proteases. In addition to FVIIa and its complexes, hemextin A and hemextin AB complex inhibited the amidolytic

activity of only kallikrein in a dose-dependant manner (Figure 3.7). However, the IC_{50} for the inhibition of kallikrein was $\sim 5 \mu\text{M}$, in contrast to that of FVIIa/TF-FVIIa/sTF-FVIIa which was $\sim 100 \text{ nM}$.

Kinetic studies revealed that hemextin AB complex is a non-competitive inhibitor of FVIIa-sTF complex with a K_i of 25 nM . Thus these data strongly indicate that hemextin AB complex is a highly specific inhibitor of FVIIa.

Some other anticoagulants from snake venoms also inhibit extrinsic tenase complex. However, they are not as specific. For example, CM IV, a strongly anticoagulant phospholipase A_2 (PLA_2) from *Naja nigricollis* venom prolongs coagulation by inhibiting two successive steps in the coagulation cascade. It inhibits the TF-FVIIa complex by both enzymatic and nonenzymatic mechanisms, whereas it inhibits the prothrombinase complex by only nonenzymatic mechanism (Stefansson *et al.*, 1990; Kerns *et al.*, 1999). Hemextin A and its synergistic complex are the first reported specific inhibitors of FVIIa isolated from snake venom.

Similar dose-dependent inhibition of TF-FVIIa complex and FVIIa indicates that hemextin AB complex neither requires TF for its inhibitory activity nor interferes in the binding of TF to FVIIa. Unlike TFPI and NAPC2, it also does not use FXa as a scaffold to bind to FVIIa and thus does not require FX or FXa to inhibit FVIIa. Further, TFPI and NAPC2 bind to the active site of FVIIa. In contrast, as shown by the kinetic studies (Figure 3.8) hemextin AB complex is a noncompetitive inhibitor, unlike competitive inhibitors which bind to the active site. Therefore, hemextin A and hemextin AB complex are novel inhibitors of FVIIa and TF-FVIIa complex.

These inhibitors will help us develop different strategies and therapeutic agents to inhibit the initiation step in blood coagulation⁴, providing a new paradigm in the search for anticoagulant drugs.

⁴ If it was so, it might be; and if it were so, it would be; but as it isn't, it ain't. That's logic. -- Lewis Carroll

“The invention of deliberately oversimplified theories is one of the major techniques of science, particularly of the ‘exact’ sciences, which make extensive use of mathematical analysis. If a biophysicist can usefully employ simplified models of the cell and the cosmologist simplified models of the universe then we can reasonably expect that simplified games may prove to be useful models for more complicated conflicts.”

"A Beautiful Mind, The Life of Mathematical Genius and Nobel Laureate John Nash"



Chapter 4

Biophysical Characterization of Hemextin AB Complex

A Short History of the Thermodynamics of Enzyme-catalyzed Reactions¹

“The first and second laws of thermodynamics were known before Gibbs wrote his great paper "Equilibrium of Heterogeneous Substances" that was published in the *Transactions of the Connecticut Academy* in 1876 (1), but he completely changed the character of thermodynamics by showing it obeyed all the rules of calculus and introducing the chemical potential μ and what we now call the Gibbs energy, G . Obeying the rules of calculus means that there are many relationships between various thermodynamic properties. The introduction of the chemical potential made it possible to treat chemical reactions. The first law introduces the internal energy U that provides the criterion for spontaneous change and equilibrium at constant volume V and entropy S . The enthalpy H is defined by:

$$H = U + PV \dots \dots \dots (\text{Eq.1})$$

and it provides the criterion for spontaneous change and equilibrium at constant pressure and entropy. The Helmholtz energy A is defined by:

$$A = U - TS \dots \dots \dots (\text{Eq.2})$$

and it provides the criterion for spontaneous change and equilibrium at constant volume and temperature. This is beginning to look useful in the laboratory except that chemistry is usually carried out at constant pressure and temperature. Gibbs defined the property G , which we now call the Gibbs energy, as follows:

$$G = H - TS \dots \dots \dots (\text{Eq.3})$$

The Gibbs energy provides the criterion for spontaneous change and equilibrium at constant temperature and pressure. These three definitions are what we now refer to as

¹ I have taken this excerpt from Professor Robert A Alberty's reflections published in the journal of biological chemistry. The above excerpt is the introductory section of the excellent article and comprehensively pin points the key concepts in thermodynamics that form the basis for any chemical reaction, protein-protein interaction included. In this chapter, I have used isothermal titration calorimetry to study the thermodynamics of hemextin AB assembly, and the first three equations form the basis of the study. I hope the reader will feel the same.

Legendre transforms. Legendre transforms are the most significant concept in this short history. Note that Equations 1, 2, 3 each involve a product of conjugate variables that yields energy. Everybody knows that the variables in an equation can be changed by simply substituting an equation for one of the variables in terms of a new variable. Not everybody knows that a derivative can be introduced as a new variable, but Gibbs did. I wrote a review on Legendre transforms in 1994 (2), and later I chaired an IUPAC Committee that wrote a Technical Report on Legendre transforms (3). Two more Legendre transforms will be used in these Reflections.

Before going further, we must be clear about what thermodynamics can tell us about a reaction system. Callen (4) has written: "Prediction of the new equilibrium state is the central problem of thermodynamics." Thermodynamic measurements on systems at equilibrium can be used to calculate properties that can be used to predict whether reactions in a system will go to the right or the left under a given set of conditions in addition to making it possible to calculate the equilibrium composition. It is not necessary to have measurements on the actual reactions in the system to do this because other pathways can be used to calculate the equilibrium composition. Rather than tabulating equilibrium constants of chemical reactions, chemists recognized a long time ago that the most efficient way to store thermodynamic information on chemical reactions was to make tables of the standard Gibbs energies of formation, $\Delta_f G^0$, standard enthalpies of formation, $\Delta_f H^0$, and standard molar entropies, S_m , of species (5)."

--- Professor Robert A. Alberty,
Department of Chemistry; Massachusetts
Institute of Technology. Reflections, *J. Biol.
Chem.*, Vol. 279, Issue 27, 27831-27836, July 2,
2004

References:

1. Gibbs, J. W. (1948) *The Collected Works of J. Willard Gibbs*, Vol. 1, Yale University Press, New Haven, CT
2. Alberty, R. A. (1994) *Chem. Rev.* 94, 1457–1482
3. Alberty, R. A., Barthel, J. M. G., Cohen, E. R., Ewing, M. B., Goldberg, R. N., and Wilhelm, E. (2001) *Pure Appl. Chem.* 73, 1349–1380
4. Callen, H. B. (1985) *Thermodynamics and an Introduction to Thermostatistics*, p. 26, John Wiley & Sons, Inc., New York
5. Wagman, D. D., Evans, W. H., Parker, V. B., Schumm, R. H., Halow, I., Bailey, S. M., Churney, K. L., and Nutall, R. L. (1982) *J. Phys. Chem. Ref. Data* 11, Suppl. 2, 1–392

Proteins play a wide variety of functional roles in biological systems, including catalysis, transport, regulation, defense, and maintenance of cell architecture. All of these functions depend on specific interactions between proteins and other molecules. These interactions must be characterized in structural and energetic terms to understand the functions of proteins in a cellular context. An initial goal might be merely to demonstrate that a particular protein interacts with a particular ligand and perhaps explore the specificity of this interaction by surveying a range of other potential ligands. If an interaction is demonstrated, the high-resolution structural methods of X-ray crystallography or nuclear magnetic resonance (NMR) could be used to provide atomic-level structural information about the interaction. However, a second, and perhaps more important, goal is to explore the energetics of the interaction, in both thermodynamic and kinetic terms, and for this, a range of other methods can be employed.

A principal challenge involved in studying non-covalent protein-protein interactions, is their rapid detection. In recent years, mass spectrometry (MS) is an important tool used in the detection of formation of protein-protein complexes. Detection of protein-protein complexes in physiological buffer solutions is also done using dynamic light scattering (DLS). Various biophysical techniques are available to characterize binding and assembly of macromolecules in solution, including calorimetry, fluorescence spectroscopy, UV spectroscopy, stopped-flow kinetics, circular dichroism, mass spectrometry and NMR.

Calorimetry specifically isothermal titration calorimetry (ITC) permits the study of macromolecular interactions in solution, and is the only technique that can resolve the enthalpic (ΔH) and entropic components (ΔS) of binding affinity and hence the difference in the Gibbs free energy (ΔG) between the initial and final states.

CD in the far ultraviolet region (178–260 nm) arises from the amides of the protein backbone and is sensitive to the conformation of the protein. Thus CD can determine whether there are changes in the conformation of proteins when they interact. CD bands in the near ultraviolet (350–260 nm) and visible regions arise from aromatic and prosthetic groups. There are also changes in these regions when proteins bind to each other. Because CD is a quantitative technique, changes in CD spectra are directly proportional to the amount of the protein–protein complexes formed, and these changes can be used to estimate binding constants. Changes in the stability of the protein complexes as a function of temperature or added denaturants, compared to the isolated proteins, can also be used to determine binding constants.

NMR gives information about the dynamic structural changes that take place in the macromolecules upon interaction. Thus, a combination of these methods can provide the accurate quantitative information about the binding affinity between the interacting partners in a protein complex. They also allow us to explore the interaction on the molecular level and obtain parameters such as the order of the binding kinetics, the kinetic rate constants and the thermodynamics of the interactions (including independent measurements of ΔG , ΔS and ΔH).

Hemextin AB complex specifically and non-competitively inhibits the TF-FVIIa complex with a K_i of 25 nM. Further, it inhibits FVIIa in the absence of TF and FX (Banerjee *et al.*, 2005c; Banerjee *et al.*, 2005d). Thus, unlike TFPI and NAPc2, this unique complex neither requires FX scaffold nor does it bind to the active site of FVIIa. Also, it is the only known snake venom hetero-tetrameric protein complex formed by the interaction between two three-finger toxins. Thus, hemextin AB complex is both structurally and functionally unique. In this chapter, we have investigated the molecular interactions involved in the assembly of this unique

anticoagulant complex. In particular, the role of electrostatic and hydrophobic interactions in complex formation has been examined. The anticoagulant complex has identical molecular diameter in both gas and solution phases. ITC studies reveal that complex formation is entropically unfavored, which indicates the reduced structural flexibility of the complex. Hemextin AB assembly is an enthalpically driven process, with some conformational changes accompanying the complex formation. The tetrameric complex behaves differently in buffers of higher ionic strength. It is also sensitive to the presence of glycerol in the buffer solution. Thus, a complex interplay of electrostatic and hydrophobic interactions drives the formation and stabilization of this novel anticoagulant protein complex. Based on our observations, we propose a model for the assembly of hemextin AB complex.

MATERIALS AND METHODS

CD spectroscopic studies – Far UV CD spectra (260-190 nm) were recorded using a Jasco J-810 spectropolarimeter (Jasco Corporation, Tokyo, Japan). All measurements were carried out at room temperature using 0.1 cm path-length stoppered cuvettes. The instrument optics was flushed with 30 l/min of nitrogen gas. The spectra were recorded using a scan speed of 50 nm /min, resolution 0.2 nm, and band width 2 nm. For each spectrum, a total of six scans were recorded, averaged and baseline subtracted. Conformation of hemextin A and hemextin B at different concentrations were monitored in 50 mM Tris-HCl buffer (pH 7.4). *To study the complex formation*, titration experiments were carried out by keeping the concentration of the hemextin A constant at 0.5 mM, and varying the concentrations of hemextin B.

Determination of molecular diameters – The apparent molecular diameters of the hemextin AB complex and the individual hemextins were determined in both the gas and solution phases.

(A) *Gas Phase Electrophoretic Mobility Macromolecule Analyzer (GEMMA)* – The molecular diameters in the gas phase were determined with GEMMA (Loo *et al.*, 2005) using a nano-differential mobility analyzer, model 3980 (TSI, St Paul, MN, USA), and a standard condensation particle counter type 3025 (TSI, St Paul, MN, USA). Since GEMMA is a considerably new technique for studying protein-protein interaction, a comprehensive sketch on the technique is provided below.

GEMMA works on the principles of aerosol physics of nanometer-sized particles (Knutson EO and Whitby KT, 1973a; Knutson EO and Whitby KT, 1973b). In this technique, protein molecules are treated as nearly spherical particles and their electrophoretic mobility (EM) in air is measured. Using the Millikan's equation, which establishes a correlation between the analyte diameters to the singly charged particle mobility in air (Tammet H., 1995), a spectrum of particle concentration versus an equivalent EM diameter is plotted. In order to measure the EMs in a laminar stream of air, protein molecules are first transferred into the gas phase at atmospheric pressure. Charged droplets are produced by an electrospray process from an aqueous buffer containing the sample. The electrospray conditions are selected in such a way that the mean number of protein molecules per generated charged aerosol droplet is below unity. The mono disperse droplets are 'dried' and charge-reduced to produce singly charged positive or negative molecular ions. These ions are separated according to their electrophoretic mobilities (EMs), by a differential mobility analyzer (DMA). (Kousaka Y *et al.*, 1985) Depending on the applied air flow rate and voltage, ions with certain mobility leave the DMA and are detected by a condensation particle counter (CPC). Finally, the number of detected ions is plotted against the inverse EM of ions. A schematic representation of the system is depicted in Figure 4.1.

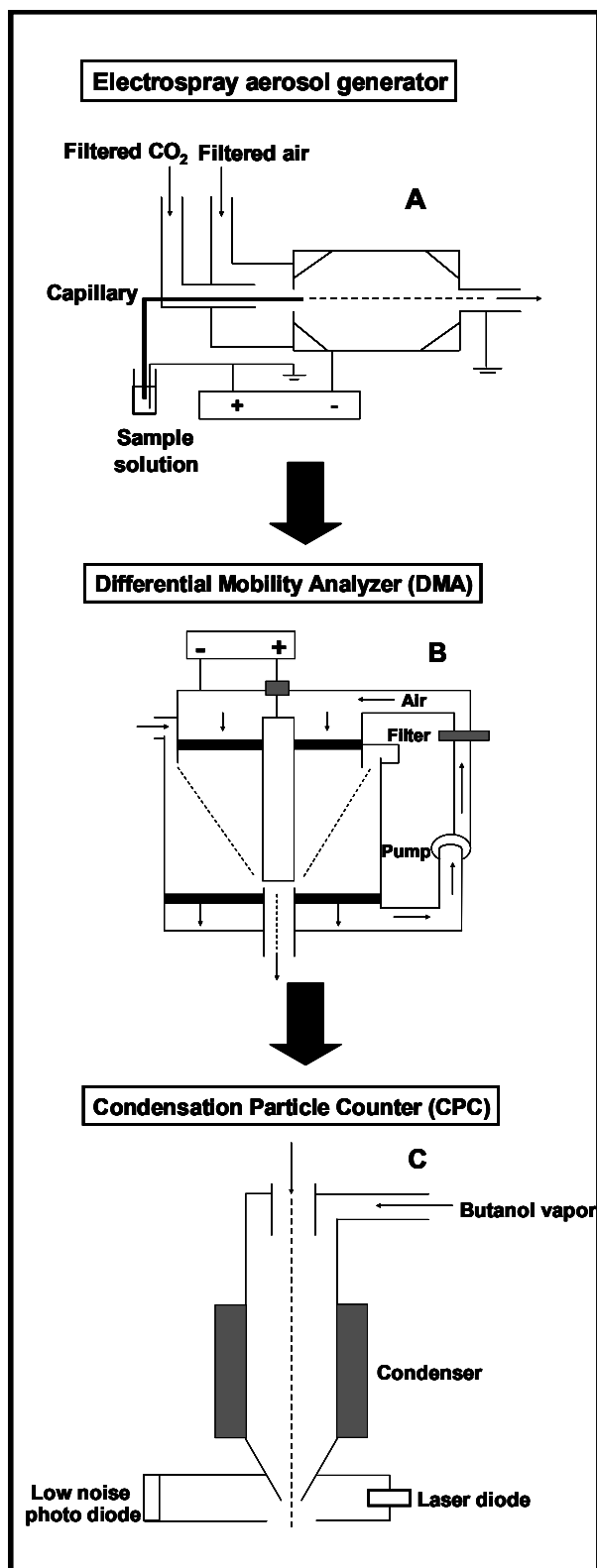


Figure 4.1 Schematic representation of different parts of GEMMA

In this study the instrument was operated in the ‘cone jet’ mode with an operating voltage between 2.5 and 3.0 kV, resulting in currents from 200 to 300 nA. Filtered ambient air at 2 l/min and a concentric sheath gas flow of filtered CO₂ at 0.1 l/min was used to stabilize the electrospray against corona discharge. Sample solutions of hemectin A (4 ng/ml) and hemectin B (4 ng/ml) were prepared in 20 mM ammonium acetate (pH 7.4) immediately prior to the experiment. Hemectin AB complex (4.5 ng/ml) was reconstituted in the above buffer and was incubated at 37°C for 10 min. Another three-finger protein, toxin C isolated and purified from the same venom was used as a control in the GEMMA experiments. The samples were infused into the electrospray chamber with an inlet flow rate of 100 nl/min. Twenty scans over the whole EM diameter range (0 to 25 nm) were recorded and averaged to obtain a GEMMA spectrum. No smoothing algorithm was applied for the data presentation.

(B) *DLS* – Complex formation studies with DLS were carried out at 25 °C using a BI200SM instrument (Brookhaven Instruments Corporation, Holstville, NY, USA). A vertically polarized argon ion laser (514.2 nm, 75 mW; NEC model GLG-3112) was used as the light source. Sample solutions of hemectin A (4 mM), hemectin B (4.1 mM) and hemectin AB complex (4.6 mM) in 50 mM Tris-HCl buffer (pH 7.4), were prepared immediately prior to the experiment. The hydrodynamic diameter for the hemectin AB complex and the individual hemectins were recorded at 25 °C in solutions of different ionic strengths and at different glycerol concentrations. The ionic strengths were varied by the addition of NaCl. From the measured translational diffusion coefficient (D_T), the hydrodynamic radius (R_H) can be calculated using the Stokes-Einstein relation:

$$D_T = k_B T / 6\pi\eta R_H \dots \dots \dots (Eq. 1),$$

where, k_B is the Boltzmann constant, T is the temperature in Kelvin and η being the viscosity of the solvent. The intensity-intensity time correlation functions were obtained with a BI-9000 digital correlator equipped with the instrument. The particle size and size distribution were obtained by analyzing the field correlation function $|g^{(1)}(\tau)|$ using constrained regularized CONTIN method (Provencher, 1976).

Thermodynamics of hemextin AB complex formation – ITC experiments were performed using a Microcal VP-ITC calorimeter (Microcal LLC, Northampton, MA) to study the thermodynamics of the formation of hemextin AB complex. Unless otherwise noted, all experiments were performed in 50 mM Tris-HCl buffer (pH 7.4). Both the proteins were dissolved in the same buffers, filtered and degassed prior to titration. Hemextin A (0.1 mM) was kept in the sample cell and hemextin B (1 mM) was loaded into the syringe. The syringe stirring speed was set to 300 rpm. Data were collected in high feedback mode, with a filter period of 3 s. For each experiment, a control titration was performed by injecting hemextin B into the appropriate buffer. Finally, the control data were subtracted from the raw data to obtain an isotherm corrected for heats of dilution. The first injections presented defects in the baseline and these data points were not included in the fitting process. The calorimetric data were processed and fitted to the single set of identical sites model using Microcal Origin (Version 7.0) data analysis software supplied with the instrument. The expression for the heat released per injection, $\Delta Q_{(i)}$, is given by

$$\Delta Q_{(i)} = Q_{(i)} + dV_i / 2V_0 [Q(i) + Q(i-1)] - Q(i-1) \dots \dots \dots (Eq. 2),$$

where $Q_{(i)}$ is the total heat content, dV_i is the volume injected at the i^{th} injection, and V_0 is the cell volume. The total heat content Q of the solution (determined relative to zero for the un-liganded species) contained in the V_0 , was calculated according to

Equation 3, where K_A is the binding affinity constant, n is the number of sites, ΔH is the enthalpy of ligand binding, M_t and X_t is the bulk concentration of macromolecule and ligand, respectively, for the binding $X + M \leftrightarrow XM$

$$Q = \frac{nM_t \Delta H V_0}{2} \left[1 + \frac{X_t}{nM_t} + \frac{1}{nK_a M_t} - \sqrt{\left(1 + \frac{X_t}{nM_t} + \frac{1}{nK_a M_t} \right)^2 - \frac{4X_t}{nM_t}} \right] \dots\dots\dots (Eq. 3)$$

The change in heat (ΔQ) measured between the completions of two consecutive injections is corrected for dilution of the protein and ligand in the cell according to standard Marquardt method (Levenberg, 1944; Marquardt, 1963). The free energy change (ΔG) during the interaction was calculated using the relationship: ($\Delta G = \Delta H - T\Delta S = -RT \ln K_d$). All the experiments were performed at 37 °C unless otherwise indicated.

The role of *electrostatic interactions* in the complex formation was evaluated by performing ITC experiments in 50 mM Tris-HCl buffer of various ionic strengths. The ionic strengths of the buffers were altered by adding sodium chloride (NaCl) (35 mM to 150 mM). To study the role of *hydrophobic interactions* in the complex formation, experiments were performed in 50 mM Tris-HCl buffer (pH 7.4) containing various concentrations of glycerol (125 mM to 250 mM). Glycerol has been shown to form hydration layer around proteins, nullifying the hydrophobic interactions (Liu *et al.*, 2004b). To study *the effects of protonation* on complex formation; additional calorimetric experiments were performed in PBS (pH 7.4) or in 10 mM MOPS (pH 7.4).

Size-exclusion chromatography (SEC) studies – All SEC experiments were carried out at room temperature on a pre-packed Superdex 75 gel filtration column (1.6 × 60 cm) using a ÄKTA Purifier system (Amersham Biosciences, Uppsala, Sweden). The

column was eluted with 50 mM Tris-HCl buffer (pH 7.4) or the specified elution buffer, at a flow rate of 1 ml/min. The sample volume applied to the column was 4 ml. The column was calibrated using ovomucoid (28 kDa) ribonuclease (15.6 kDa), cytochrome C (12 kDa), apoprotinin (7 kDa) and pelovaterin (4 kDa) (Lakshminarayanan et al., 2005) as molecular weight markers. The void volume was determined by running Blue Dextran. The column was equilibrated with at least two bed volumes of the elution buffer prior to each run. *Electrostatic contributions* in the hemextin AB complex formation were studied by monitoring its elution in 50 mM Tris-HCl buffer (pH 7.4) with different concentrations of NaCl (75 mM and 150 mM). *Hydrophobic contributions* for the complex formation were determined by recording the elution of hemextin AB complex in 50 mM Tris-HCl buffer (pH 7.4) with different concentrations of glycerol (125 mM and 250 mM). In both the studies, the column was first equilibrated with the desired buffer prior to the application of the reconstituted hemextin AB complex in the respective buffer to the column. The protein elution was monitored by recording absorbance at 280 nm.

Anticoagulant activity – The anticoagulant activity of individual hemextins and hemextin AB complex were determined using prothrombin time clotting assay (Quick AJ., 1935). The anticoagulant activity of a specific concentration of hemextin A (4.4 μ M), hemextin B (4.4 μ M) and hemextin AB complex (0.22 μ M) was monitored in 50 mM Tris-HCl (pH 7.4) containing different concentrations of NaCl (35 mM to 150 mM for studying the role of *electrostatic interactions*) and glycerol (125 mM to 250 mM for studying the role of *hydrophobic interactions*). The concentrations of hemextin A and hemextin AB complex were chosen in a way such that in the absence of salt/glycerol the recorded clotting times are similar. Control experiments were

performed without the addition of the anticoagulant proteins to evaluate the effect of salt and glycerol on clotting.

1D-NMR spectroscopy – One-dimensional proton NMR experiments were carried out using Bruker 700 MHz spectrometer, equipped with a modern cryo-probe, and electronic variable temperature unit. The spectra were acquired using Topspin software (Bruker) interfaced to the spectrometer. Hemextin A (0.5 mM) and hemextin B (0.5 mM) were prepared in 50 mM Tris-HCl buffer (pH 7) and transferred to a 5 mm diameter Willmad NMR tube. All deuterated solvents were purchased from Aldrich Laboratories with 99.9% isotopic purity. The spectral width was set to 11,202 Hz for all NMR experiments. The huge resonance due to the water protons was suppressed by the WATERGATE pulse sequence (Piotto et al., 1992). Typically, 512 scans were averaged for each FID before apodization and then performing the Fourier transformation. ¹H chemical shifts were referenced to a sodium 2,2-dimethyl-2-silapentane-5-sulfonate solution (DSS).

RESULTS AND DISCUSSION

Conformational changes during complex formation – In chapter 3, it was shown using clotting and kinetic assays that, hemextin A and hemextin B interact with each other and form a 1:1 heterotetrameric complex and this complex formation is important for its ability to inhibit FVIIa and clot initiation.

To study the conformational changes associated with the hemextin AB complex formation we used far UV-CD. First, we recorded the CD spectra of individual hemextins A and B (Figure 4.2, A and B). Their CD spectra display negative minima at 217 nm and positive maxima at 196 nm, which are due to the n to π^* transition and the π to π^* transition of the amide chromophore, respectively, typical of a β -sheet structure (Figure 4.2, A and B).

Next, a titration CD experiment was performed in order to study the complex formation between the two proteins. In this experiment, the concentration of hemextin A was kept constant at 0.5 mM and the conformational changes in hemextin A in the presence of various concentrations of hemextin B were recorded. The shape of the CD spectrum upon addition of hemextin B to hemextin A did not change significantly (Figure 4.2C). However, the CD intensity at 217 nm increases with the incremental addition of hemextin B and reaches maximum at the 1:1 molar ratio suggesting stoichiometric binding of hemextin B to hemextin A (Figure 4.2D). The difference spectrum obtained by subtracting the CD spectrum of 1:1 complex from the sum of the CD spectra of hemextin A and hemextin B indicates the formation of additional β -sheet structure or the stabilization of β -sheet structure during the complex formation (Figure 4.3).

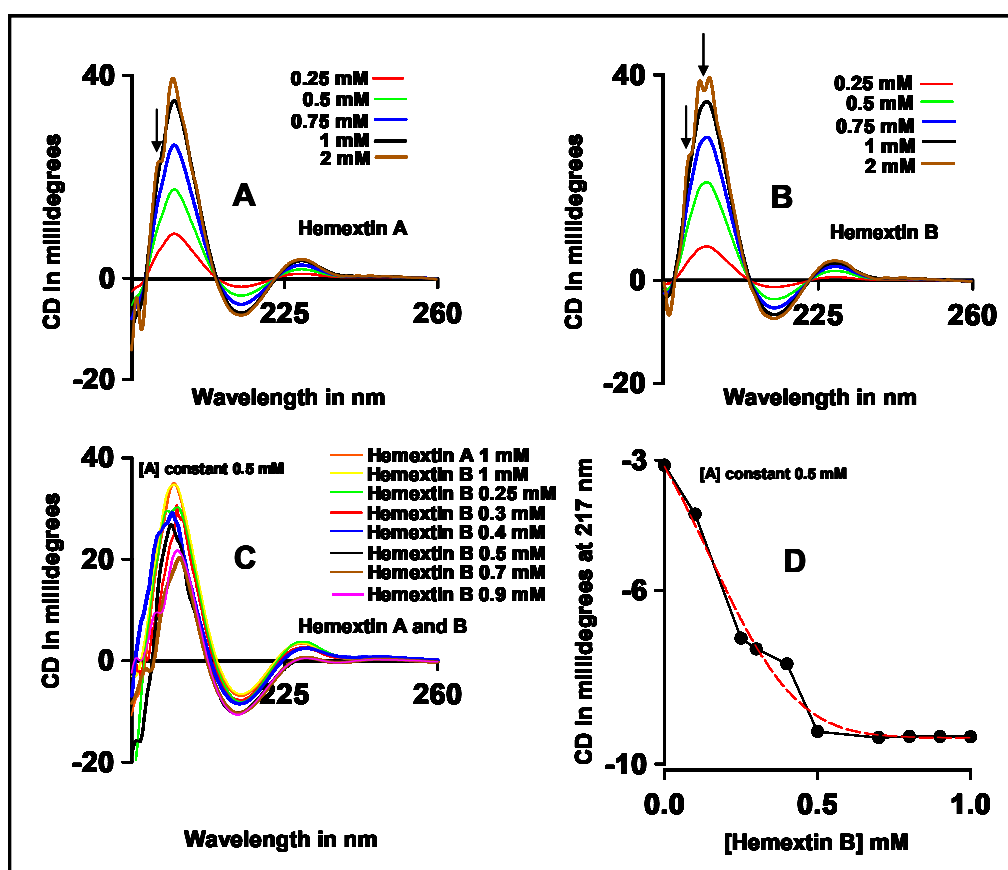


Figure 4.2 Conformational changes associated with the formation of hemextin AB complex. CD spectra of (A) hemextin A and (B) hemextin B at various protein concentrations are shown. The conformational changes due to the aggregation at higher concentrations are marked with arrows. (C) Conformational changes in hemextin A with increasing concentrations of hemextin B. (D) CD change in hemextin A at 217 nm with increasing concentrations of hemextin B. No significant changes in CD spectra were observed with further addition of hemextin A after the ratio of hemextin A to hemextin B reached 1:1 (C and D).

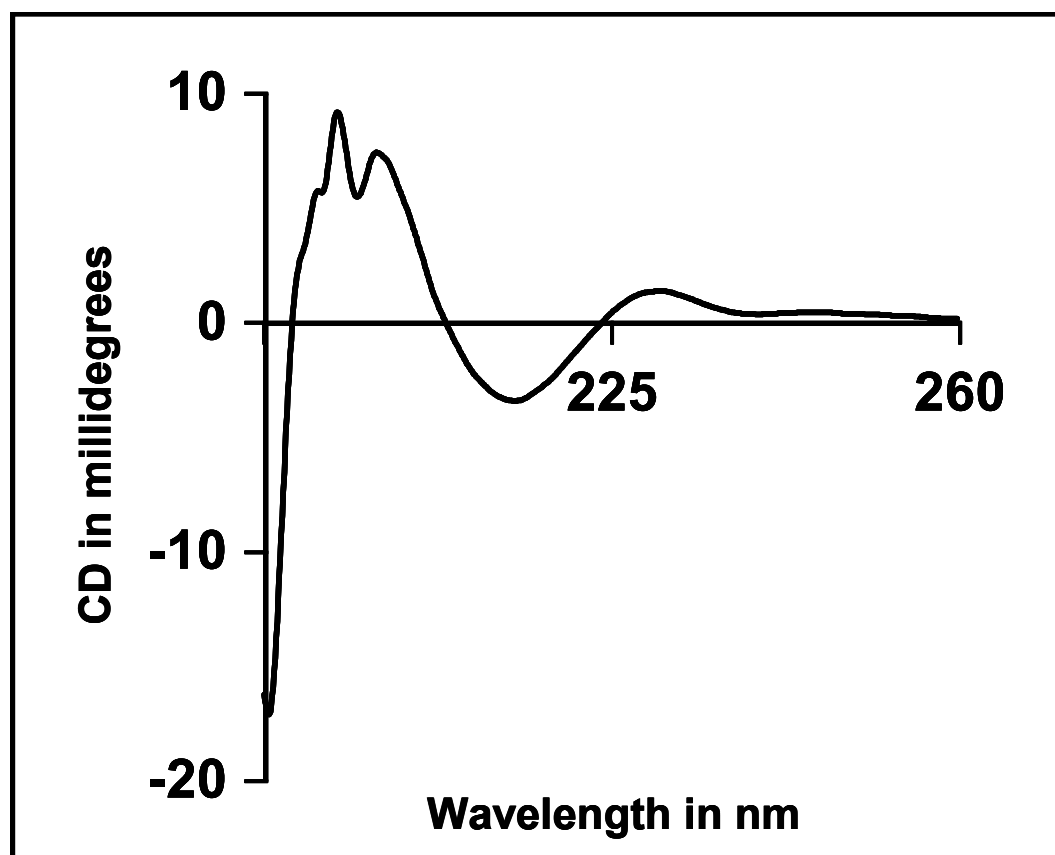


Figure 4.3 Conservation of β -sheet after complex formation. The difference spectrum obtained by subtracting the CD spectrum of 1:1 complex from the sum of the CD spectrum of hemextin A and hemextin B. (Note the conservation of β -sheet structure in the complex, suggesting possible folding upon complex formation.)

Changes in molecular diameters during the complex formation – The diameter of the individual hemextins and hemextin AB complex were determined in both gas and solution phases.

In the gas phase analysis using GEMMA, hemextin A and hemextin B showed the apparent molecular diameters of 10.20 ± 0.38 nm and 8.82 ± 0.42 nm, respectively (Figure 4.4). Hemextin AB complex exhibited a larger diameter of 16.30 ± 0.43 nm. To further confirm on the GEMMA results, we examined the effect of toxin C, another three-finger toxin isolated from the venom of *H. haemachatus*, on the molecular diameters of hemextins A and B, to determine the specificity of interaction. Toxin C did not affect the anticoagulant activity of hemextin A in prothrombin time clotting assay (data not shown) and did not form a complex with hemextin A. At equimolar concentration of toxin C, the molecular diameter of hemextin A or hemextin B remains unaffected (Figure 4.3).

The solution phase studies with DLS also confirmed the increase in molecular diameter associated with the complex formation. Single scattering populations (unimodal distribution) for hemextin A, hemextin B and hemextin AB complex were observed in DLS suggesting the homogeneity of the sample preparations with hydrodynamic diameters of 10.3 nm, 9.9 nm and 16.8 nm, respectively (Figure 4.5). The narrow size distribution of a single monodisperse species for 1:1 mixture of hemextin A and hemextin B suggests the formation of a well-defined complex. It is important to note that the tetrameric hemextin AB complex and individual hemextins exhibited comparable molecular diameters in both gas and solution phases. The apparent molecular dimensions are significantly larger than the theoretical diameter estimated for a native protein and much smaller than the estimated length of the proteins in completely “extended conformation” (Lu *et al.*, 1998; Wilkins *et al.*, 1999).

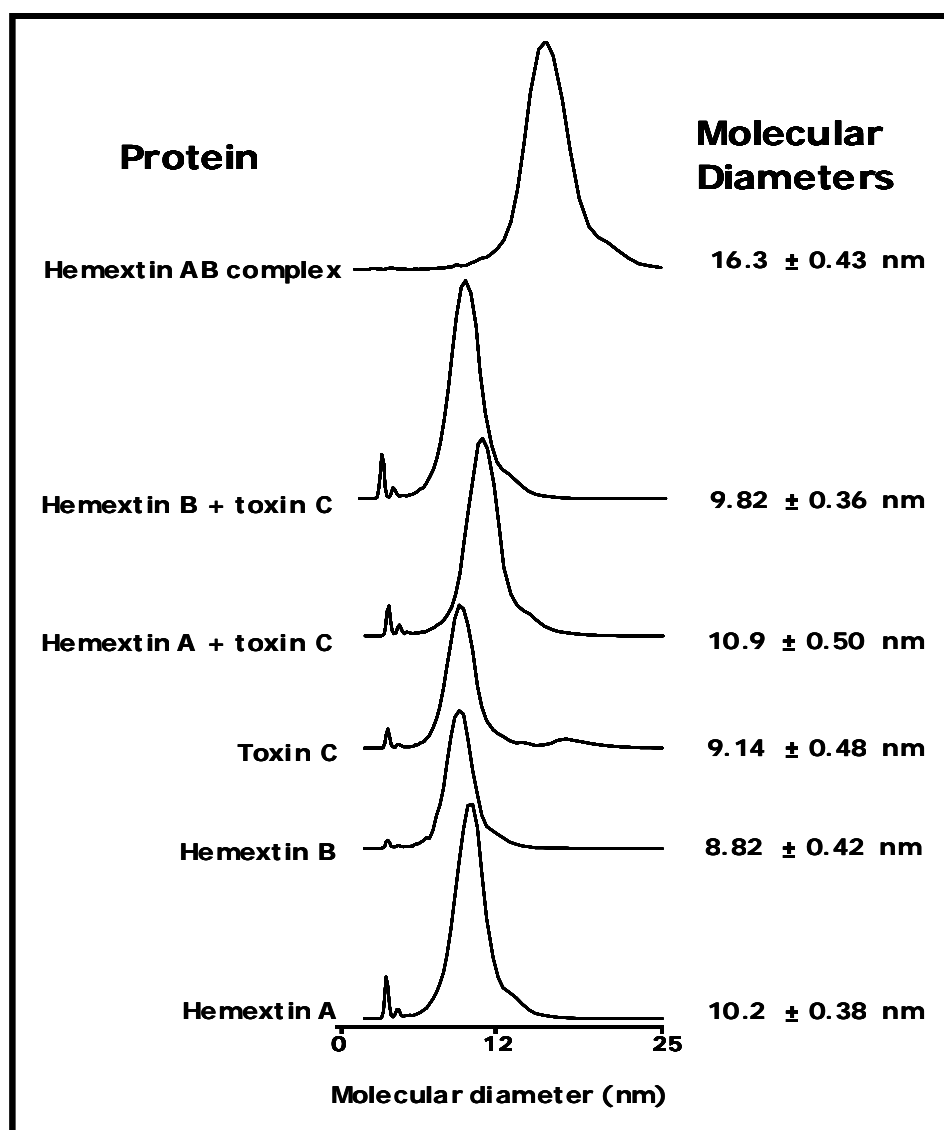


Figure 4.4 Measurement of molecular diameter during Hemextin AB complex formation using GEMMA. The molecular diameters of the individual hemextins and the hemextin AB complex are calculated based on their electrophoretic mobility. The formation of hemextin AB complex leads to an increase in the molecular diameter. Addition of equimolar toxin C does not show any significant increase in the molecular diameters of hemextin A and hemextin B validating the obtained data.

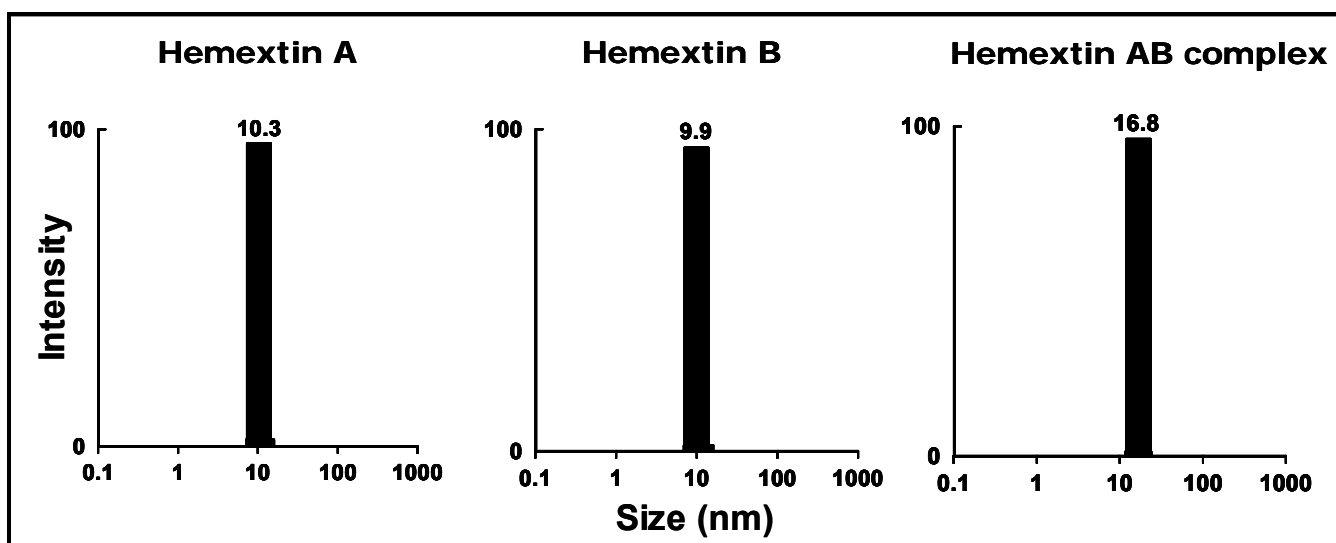


Figure 4.5 Determination of hydrodynamic diameter using DLS. A. CONTIN analysis hemextin A, hemextin B and hemextin AB complex in 50 mM Tris-HCl buffer. Note the formation of the hemextin AB complex leads to an increase in the hydrodynamic diameter.

Such an anomaly could be due to the non-globular conformation of the proteins (Longhi *et al.*, 2003). The molecular diameter of hemextin AB complex is, however, much smaller compared to the estimated size of a tetramer indicating that the four monomers are compactly packed.

Thermodynamics of hemextin AB complex formation — ITC was used to study the thermodynamics of hemextin AB complex formation. Each injection gave rise to negative (exothermic) heat of reaction (Figure 4.6). The binding isotherm fits to a single set of binding sites model, suggesting an equimolar binding between hemextin A and hemextin B. The interaction between them is thermodynamically allowed (as indicated by negative ΔG) (Table 4.1). A favorable negative ΔH but unfavorable negative ΔS changes indicate that the complex formation is enthalpically driven and, van der Waals interactions and hydrogen bonds may play an important role in the complex formation. Also, the formation of a less dynamic complex is entropically disfavored, as has been observed in the studies pertaining to the dimerization of insulin (Tidor and Karplus, 1994). Thus the recorded negative entropic change (ΔS) indicates the formation of a less flexible or less disordered hemextin AB complex. The binding constant (K_A) for the formation of hemextin AB complex was $2.23 \times 10^6 \text{ M}^{-1}$ and it falls within the K_A values for protein-protein interactions in biologically relevant processes that range from 10^4 to 10^{16} M^{-1} (Stites, 1997b).

The effect of temperature on the complex formation — To further understand energetics of the complex formation, complete temperature profile of the thermodynamic parameters associated with the binding of hemextin A to hemextin B was studied over the temperature range of 25-45 °C. The temperature dependence of

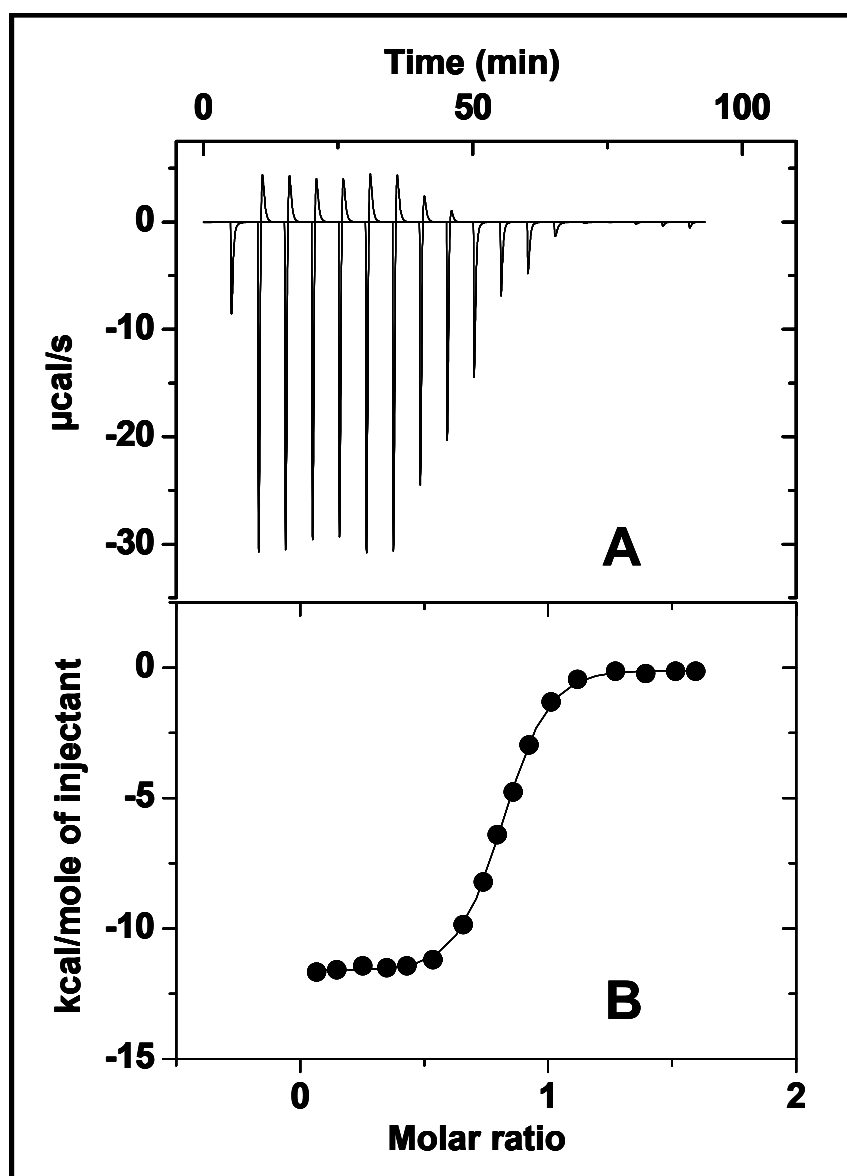


Figure 4.6 Interaction studies between hemextin A and B using ITC. (A) Raw ITC data showing heat release upon injections of 1 M hemextin B into a 1.4-ml cell containing 0.1 mM of hemextin A; (B) Integration of the raw ITC data yields the heat/mol *versus* molar ratio. The best values of the fitting parameters are 1.04 for N , $2.23 \times 10^6 \text{ M}^{-1}$ for K_a and $-11.68 \text{ kcal.M}^{-1}$ for ΔH (Table 4.1).

Table 4.1

Effect of temperature on hemextin A-hemextin B interaction

ITC experiments	$K_A \times 10^6$ (M⁻¹)	ΔH (kcal/mole)	ΔS (cal/deg.mole)	ΔG (kcal/mole)
At different temperatures (°C)				
25	2.07	-9.928	-4.435	-8.606
37	2.23	-11.68	-8.645	-9.225
45	1.97	-13.127	-12.49	-9.001

ΔH is shown in Figure 4.7A and Table 4.1. The temperature dependence of ΔH over a narrow temperature range is given by the equation:

$$\Delta H = \Delta H_0 + \Delta C_p(T-T_0) \dots \dots \dots (Eq. 4)$$

where, ΔH_0 is the binding enthalpy at an arbitrary reference temperature and ΔC_p is the heat capacity change of binding. The ΔC_p obtained from the slope ($\Delta C_p = \delta\Delta H / \delta T$) (Figure 4.7A), is $-163 \text{ cal/K}^{-1}\text{mol}^{-1}$. Negative ΔC_p indicates a reduction in the nonpolar solvent-accessible surface area, as explained by the following equation (Murphy and Freire, 1992),

$$\Delta C_p = 0.45(\Delta ASA_{nonpol}) - 0.26 (\Delta ASA_{pol}) \text{ cal /molK} \dots \dots \dots (Eq. 5)$$

where, ΔASA_{pol} and ΔASA_{nonpol} are the change in the polar- and non-polar-accessible surface areas, respectively. Thus, hemextin AB complex formation is associated with the burial of hydrophobic surface area.

Figure 4.7B, shows the plot of ΔG and ΔH as a function of $T\Delta S$. It is clear that the ΔG of binding remained temperature independent and is a result of linear dependence of ΔH on $T\Delta S$. This strongly suggests the enthalpy-entropy compensation for the binding of hemextin A to hemextin B. This phenomenon is a universal feature for protein-peptide interactions, where weak molecular interactions undergo constant rearrangements to realize a lower free energy of binding (Schwarz *et al.*, 1995; Sharma *et al.*, 2002; Perozzo *et al.*, 2004; Prabhu and Sharp, 2005). The co-relation between entropy and enthalpy for a range of interacting protein-protein systems was determined ($r^2 = 0.956$). The data for hemextin AB complex falls well along this correlation line (Figure 4.8).

The negative ΔC_p indicates the net thermodynamic driving force for the association to shift from entropic to enthalpic with increasing temperature. At the intersection point of both lines $\Delta G = \Delta H = -8.4 \text{ kCal.mol}^{-1}$ (Figure 4.7B), which corresponds to a

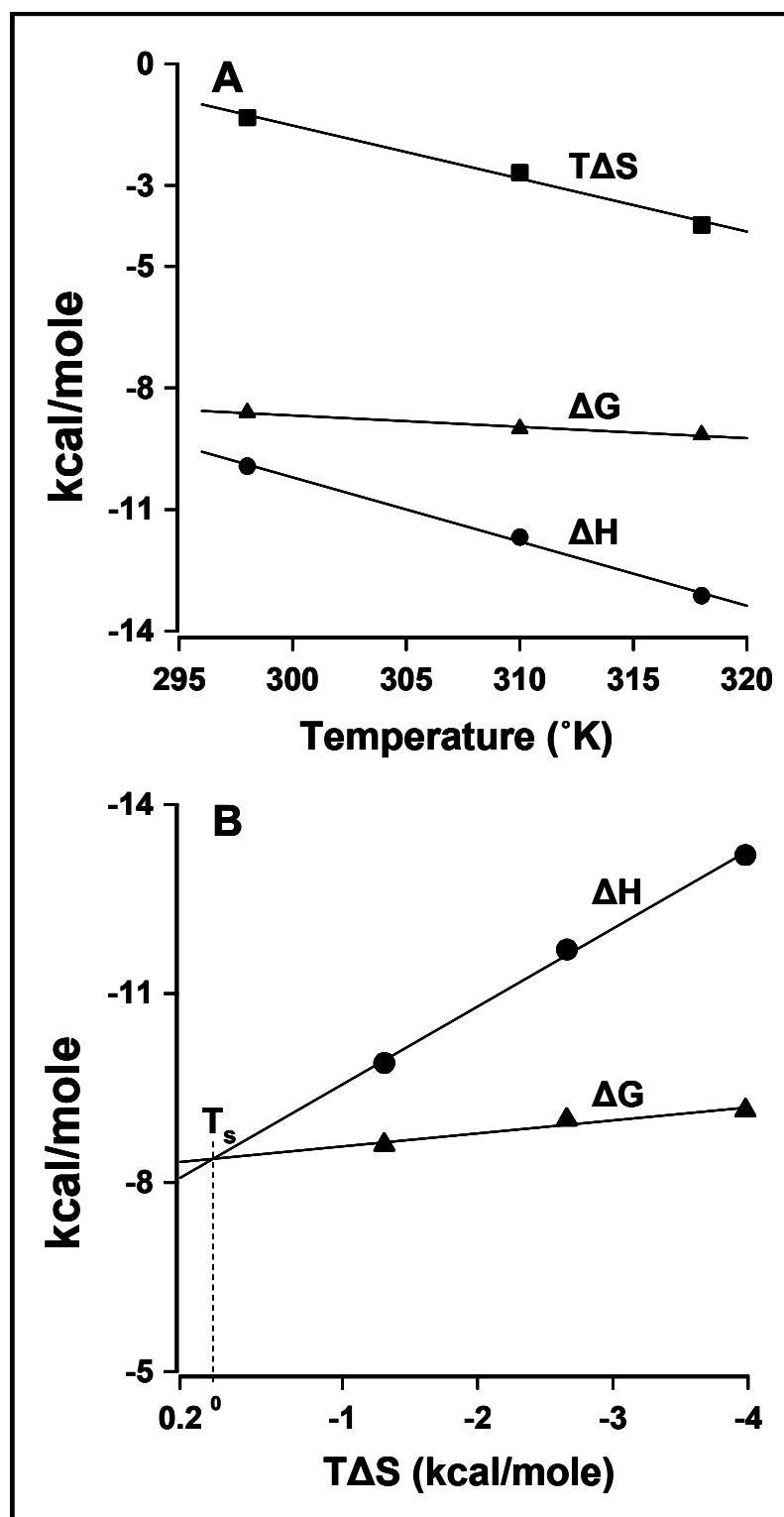


Figure 4.7 Thermodynamics of hemextin A-hemextin B interaction. (A) Effect of temperature on the energetics of hemextin A-hemextin B interaction: enthalpy change (ΔH), change in entropy term ($T\Delta S$) and free energy change (ΔG). (B) Enthalpy-entropy compensation in complex formation. (Note: Point of intersection of lines corresponding to ΔH and ΔG corresponds to T_s)

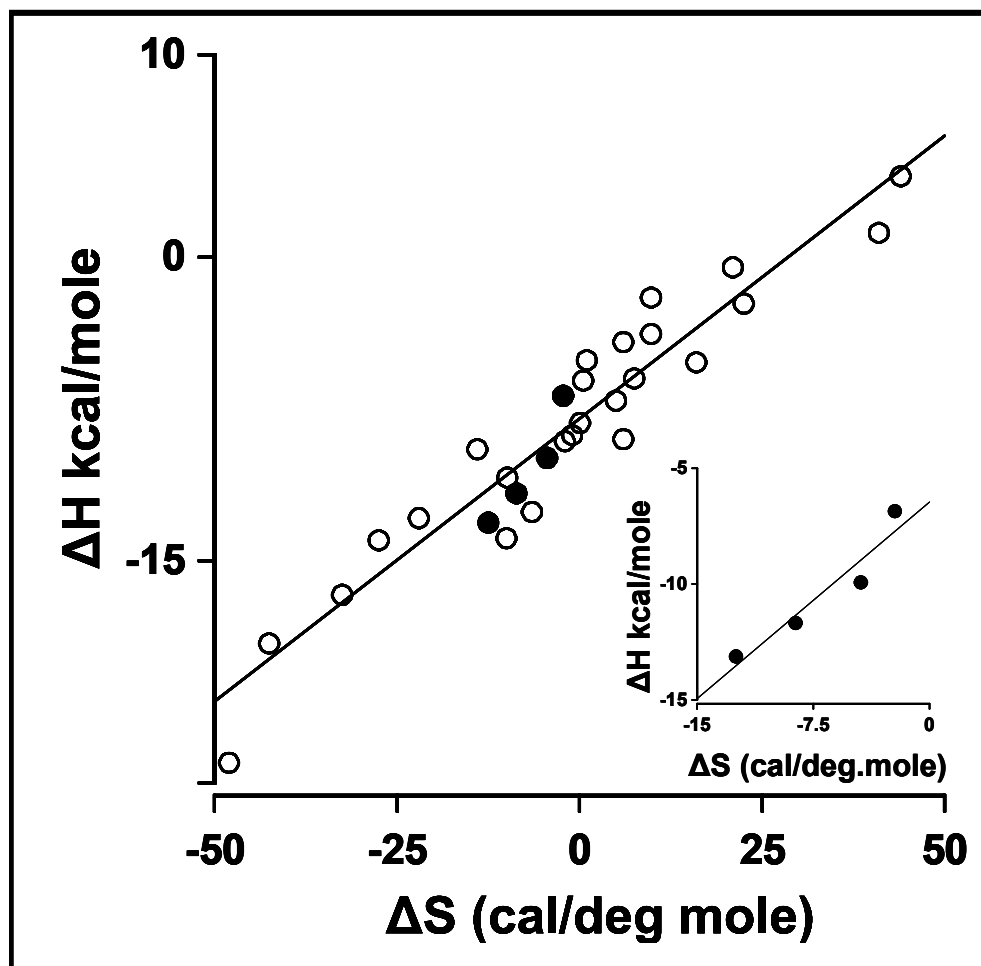


Figure 4.8 Enthalpy-entropy compensation. Enthalpy-entropy compensation in various protein-protein interactions described in the literature (O) (Data were taken from Ye and Wu (Ye and Wu, 2000), McNemar et al. (McNemar et al., 1997) and references cited in the review by Stites (Stites, 1997a) and hemextin A-hemextin B (●) interactions (this chapter) are shown. *Inset* shows the enthalpy-entropy compensation in hemextin A-hemextin B interaction.

temperature T_s (Temperature at which the contribution from entropy is zero (von Hippel, 1994; Spolar and Record, Jr., 1994). At T_s the contribution from entropy changes from favorable to unfavorable. From Figure 5A, $\Delta H = -8.4 \text{ kcal.mol}^{-1}$ is connected with a T_s of $16 \text{ }^\circ\text{C}$ ($289 \text{ }^\circ\text{K}$).

The negative ΔC_p for the hemextin AB complex formation further suggests that the observed entropy change upon binding must include significant contribution from the hydrophobic effect in the physiological temperature range. Therefore, for protein-protein/ligand interaction(s) the net entropy of association is given by the equation:

$$\Delta S_{assoc} = \Delta S_{HE} + \Delta S_{rt} + \Delta S_{other} \dots\dots\dots (Eq. 6)$$

where, ΔS_{HE} , ΔS_{rt} , and ΔS_{other} are the entropy changes due to hydrophobic effect, reduction of rotational and translational degree of freedom, and from other sources, respectively.

At T_s , the overall entropy of association is zero and the above equation becomes:

$$\Delta S_{assoc} = \Delta S_{HE}(T_s) + \Delta S_{rt} + \Delta S_{other} = 0 \dots\dots\dots (Eq. 7)$$

In the absence of crystallographic data, the $\Delta S_{HE}(T_s)$ was estimated from the equation,

$$\Delta S_{HE}(T_s) = 1.35 \Delta C_p \ln(T_s/386) \dots\dots\dots (Eq. 8)$$

and found to be $64 \text{ cal deg}^{-1} \text{ mol}^{-1}$. It has been shown that protein-protein interaction ΔS_{rt} is nearly equal to $-50 \text{ cal deg}^{-1} \text{ mol}^{-1}$ (Janin and Chothia, 1978; Finkelstein and Janin, 1989). Thus the ΔS_{other} is calculated to be $-14 \text{ cal deg}^{-1} \text{ mol}^{-1}$. The non-zero value of ΔS_{other} suggests that the hemextin AB complex formation is not a rigid-body-association but formed through local unfolding and refolding during binding interaction. Again, $\Psi = \Delta S_{other} / -5.6 \text{ cal deg}^{-1} \text{ mol}^{-1}$, where Ψ designates the number amino acid residues involved in the folding transition (Hilpert et al., 2003). Therefore, approximately three residues are involved in the folding transition. Also, From Figure

4.7B, the enthalpic counterpart of T_S , namely T_H , the temperature at which the enthalpic contribution to the Gibbs free energy of binding changes from favorable to unfavorable is calculated to be 244 °K. Therefore, below -29 °C the binding process is entropically driven and only in the interval between T_S and T_H (i.e., between -29 °C and 16°C), both the entropic and enthalpic part of the Gibbs free energy of binding are favorable.

The effect of buffer ionization on the complex formation — The observed calorimetric enthalpy is a result of the binding event in addition to all the associated events (water a(di)ssociation, ionization of the components, heats of dilution, heats of mixing, etc). To facilitate binding, residues at the interface may be protonated or deprotonated, resulting in the exchange of protons with the buffer. Under such circumstances, as calorimetric enthalpy is dependent on the buffer ionization enthalpy, calorimetric titrations were also performed in phosphate and MOPS buffers at pH 7.4. An increase in the enthalpy change (ΔH_{obs}) was observed with an increase in the change of buffer ionization enthalpy (ΔH_{ion}) on the complex formation. A plot of calorimetric enthalpy against ionization enthalpy yielded the number of protons (n_H^+) involved in the interaction, and the binding enthalpy was corrected for protonation effects (ΔH_{bin}) according to the following relationship:

$$\Delta H_{obs} = \Delta H_{bin} + n_H^+ \cdot \Delta H_{ion} \dots\dots\dots(Eq. 9)$$

A positive slope indicates propensity for the uptake of protons from the buffer, whereas a negative value indicates propensity for the release of protons into the buffer. The plot (Figure 6A) yielded an n_H^+ value of -0.57 and a binding enthalpy (ΔH_{bin}) of -3.638 kcal/mole for the complex formation. Thus, hemextin AB complex formation is associated with a net release of protons into the buffer.

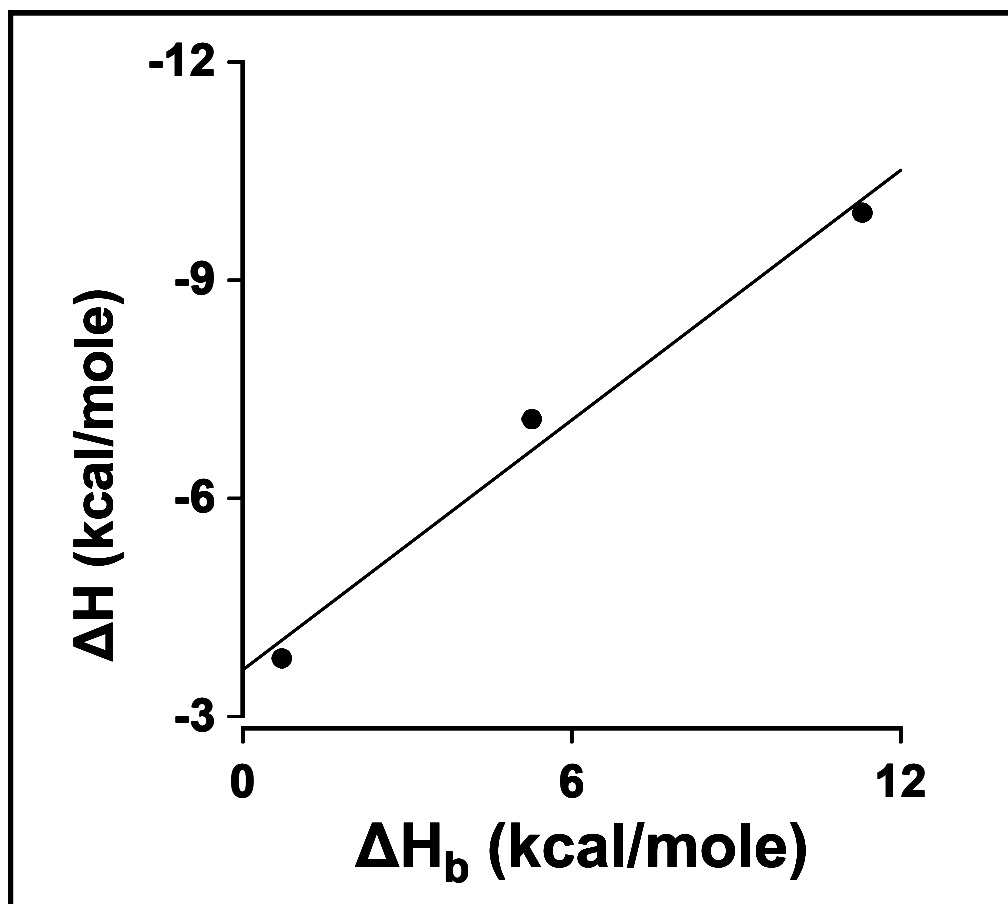


Figure 4.9 Effect of buffer ionization on the enthalpy for hemextin AB complex formation. All experiments were performed at pH 7.4. Ionization enthalpy changes used for buffers were 0.71 kcal/mol for phosphate, 5.27 kcal/mol for MOPS, and 11.3 kcal/mol for Tris (Katragadda *et al.*, 2004)

Oligomerization states of the anticoagulant complex and individual hemextins – As highlighted in Chapters 2 and 3, hemextin AB complex exists as a tetramer and the complex formation is pivotal for its potent anticoagulant activity (Banerjee *et al.*, 2005a). Therefore, we evaluated the role of both electrostatic and hydrophobic interactions in complex formation.

(A) Electrostatic interactions in hemextin AB complex formation – Firstly, the binding constant for hemextin AB complex formation was determined by ITC in buffers of increasing ionic strength. The $\log K_A$ values for the complex formation decreased linearly with the increasing NaCl concentration (Figure 4.10B, Table 4.2), illustrating the participation of electrostatic interactions in complex formation. Secondly, the effect of buffer ionic strength on the assembly of hemextin AB complex was examined with the help of SEC. In the absence of salt, the complex eluted as a tetramer and the individual hemextins as monomers (Figure 4.11A). In the presence of 75 mM NaCl the tetramer started dissociating into dimer (Figure 4.11B). With further increase in ionic strength of the buffer (NaCl 150 mM) the complex eluted mostly as a dimer and monomer(s). ESI-MS and HPLC analyses of the dimer peak indicated that it contains both hemextins A and B (data not shown). This observation again reconfirms the importance of electrostatic interactions in hemextin AB assembly. Interestingly, an additional protein peak eluted slower than the monomers indicating hemextin A and/or hemextin B was undergoing a conformational change in buffers of high ionic strength. Therefore, we monitored the elution profiles of individual hemextins in buffers of high ionic strength. Hemextin A at 75 mM NaCl concentration showed two peaks; a second protein peak eluted slower than the monomer (Figure 4.11B). With further increase in the ionic strength (NaCl 150 mM)

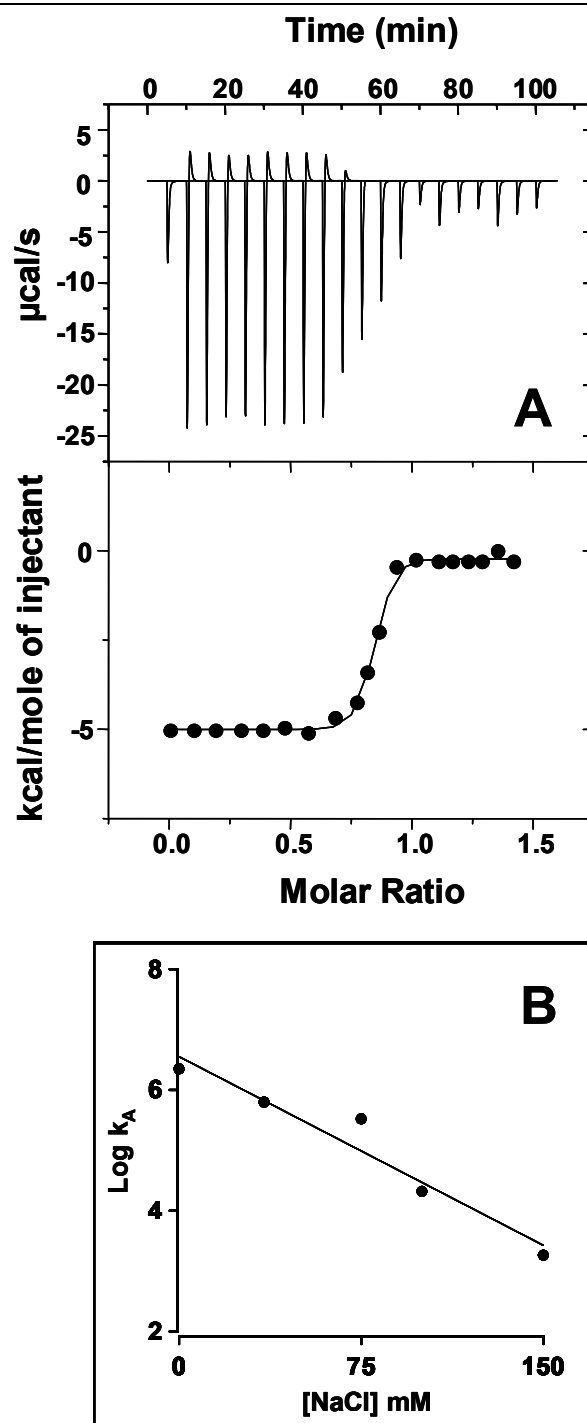


Figure 4.10 ITC studies in buffer of high ionic strength. (A) Representative thermogram of hemextin A – hemextin B interaction with corresponding binding isotherm in 50 mM Tris-HCl buffer (pH 7.4) containing 150 mM NaCl. (B) Dependence of K_A on the ionic strength of the buffer. The binding affinity decreases with the increase in buffer ionic strength indicating the importance of electrostatic interactions.

Table 4.2

Effect of increasing ionic-strength on hemextin A-hemextin B interaction

ITC experiments	$K_A \times 10^6 (M^{-1})$	ΔH (kcal/mole)	ΔS (cal/deg.mole)	ΔG (kcal/mole)
At different salt concentrations (mM)				
0.00	2.23	-11.7	-8.645	-9.0
35	0.63	-10.5	-7.2	-8.2
75	0.33	-9.32	-4.8	-7.8
100	0.02	-7.31	-3.82	-6.12
150	0.002	-5.01	-1.2	-4.6

Note: All experiments were conducted at 37 °C

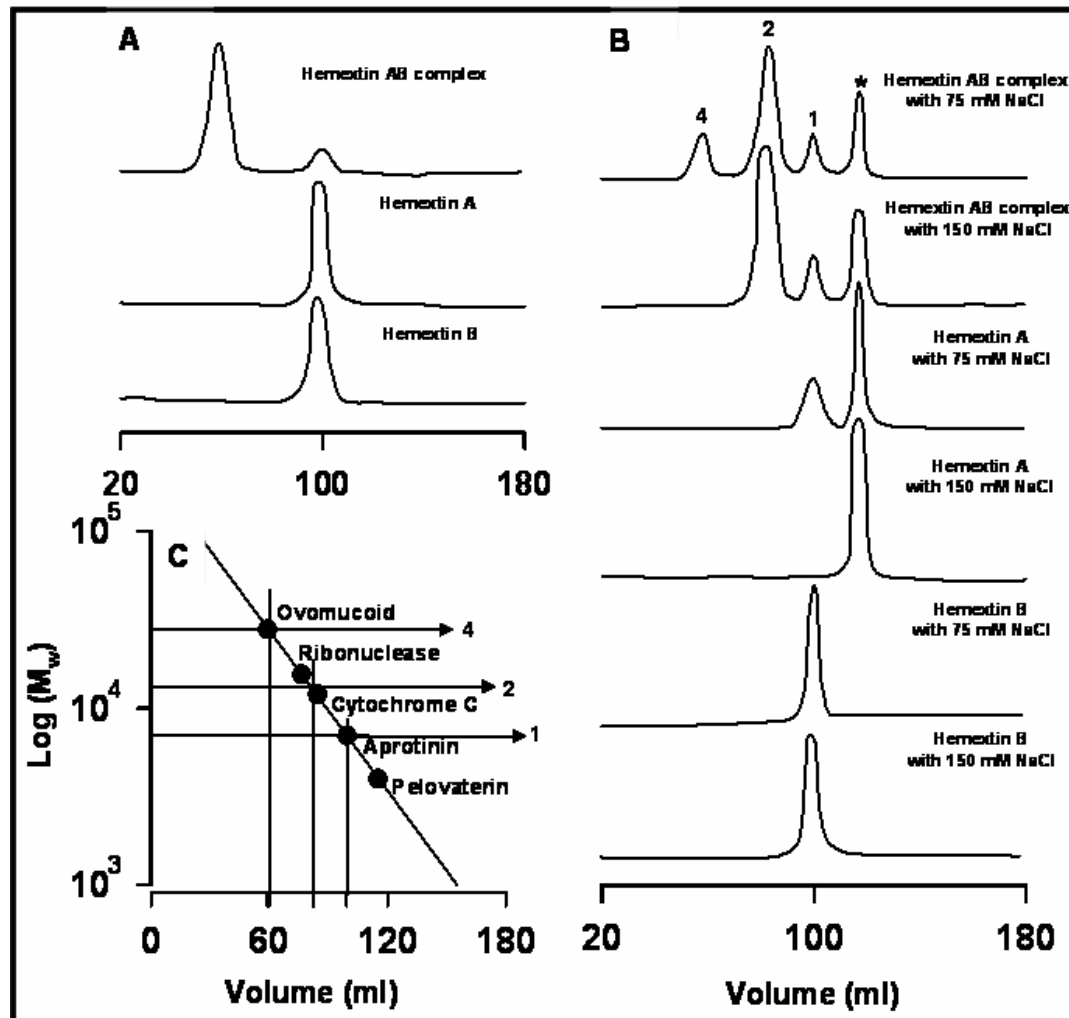


Figure 4.11 SEC studies of Hemextin AB complex in buffer of high ionic strength. A. Elution profiles of hemextin AB complex in Tris-HCl buffer. Effect various concentrations of NaCl (B) on hemextin AB complex. The tetrameric complex (peak denoted by 4) dissociates into dimer and monomer (peaks denoted by 2 and 1, respectively) with the increase in salt. *Asterisk* denotes the peak containing conformationally altered hemextin A. (C) Calibration of the column using the following proteins as molecular weight markers – ovomucoid (28 kDa), ribonuclease (15.6 kDa), cytochrome C (12 kDa), apoprotinin (7 kDa) and pelovaterin (4 kDa). The molecular weights of the tetramer, dimer and monomers were calculated from the calibration curve.

hemextin A eluted mostly in the second peak. ESI-MS and HPLC analyses of this second peak show that it is structurally intact hemextin A (data not shown). Thus, the change in the elution profile of hemextin A in buffers of higher ionic strength hinted a conformational change in the protein, which was further confirmed by 1D NMR studies (see below). Increased ionic strength of buffer did not have any effect on the elution of hemextin B (Figure 4.11A and B).

We also determined the hydrodynamic diameters of hemextin AB complex and individual hemextins in buffer solutions of high ionic strength using DLS (Figure 4.12). (As GEMMA works on the principle of nano-ESI, we did not determine the molecular diameters in buffers containing high salt using this technique.). At high salt concentrations, the hemextin AB complex exhibits a high polydispersity indicating the presence of different species. At 75 mM NaCl, there are three different populations. In addition to the monomer(s) and the tetramer, there is an additional population with an apparent molecular diameter of 12.4 nm. Based on our SEC results (Figure 4.11B), we suggest that the 12.4 nm species could be the dimeric hemextin AB complex. As expected, the population of 12.4 nm species increases when the concentration of NaCl is increased to 150 mM (Figure 4.12). Thus DLS data also suggests the dissociation of the tetrameric complex to a dimer. As expected, polydispersity was also observed with hemextin A in buffers of high ionic strength (Figure 4.12). An additional population of 11.57 nm sized particle, in addition to its native size of 10.4 nm is observed. Based on the SEC (Figure 11B) and 1D-NMR (see below), we suggest that the 11.57 nm species represents the conformationally altered form of hemextin A. No change in the hydrodynamic diameter of hemextin B was observed with the increase in buffer ionic strength (Figure 4.12).

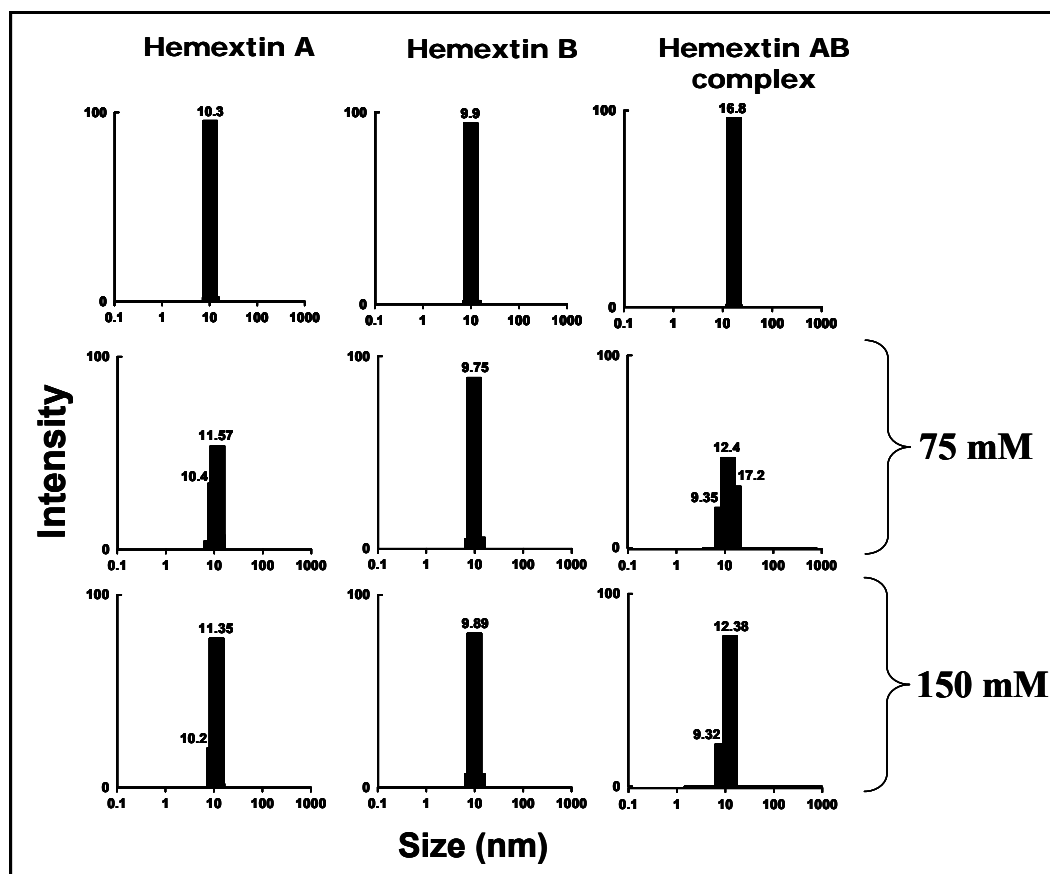


Figure 4.12 Determination of hydrodynamic diameter using DLS. CONTIN analysis hemexin A, hemexin B and hemexin AB complex in 50 mM Tris-HCl buffer and at different NaCl concentrations. The calculated hydrodynamic diameters for each molecular species are shown.

To understand the implications of the change in conformation of hemextin A and the breakdown of tetrameric complex, we monitored the anticoagulant activity of the complex and individual hemextins in buffers of high ionic strengths. Higher concentration of NaCl did not affect the anticoagulant activity of hemextin A (Figure 4.13). Thus despite the change(s) in conformation (see below), hemextin A retains its anticoagulant activity. The anticoagulant activity of hemextin AB complex, in contrast, decreased with the increase in ionic strength up to 100 mM NaCl (Figure 4.13). However, further increase in the salt concentration did not significantly affect the anticoagulant activity. At 150 mM NaCl the complex exists as a mixture of a dimer, monomer(s) and conformationally altered hemextin A as is evident from the SEC experiments (Figure 4.11B). Therefore, the remaining anticoagulant activity observed at 150 mM or higher NaCl concentration is due to the presence of monomeric hemextin A and not due to dimeric hemextin AB complex. Hence, it can be concluded that the dimer formed at high salt concentrations does not have any significant anticoagulant activity.

Thus, these studies in buffers of high ionic strength strongly suggest that electrostatic interactions play crucial role in the assembly of hemextin AB complex. As hemextin A undergoes conformational change(s) in the presence of salt (see below), the dissociation of tetramer in a buffer of high ionic strength may not only be due to the disruption of electrostatic interaction but also due to conformational change(s) in hemextin A. Further, high salt concentration leads to the formation of a dimer which is functionally inert (in terms of lack of synergic increase in anticoagulant activity). Based on the obtained results, we hypothesize that the dimer assembled at 150 mM NaCl concentration is probably formed by the interplay of predominantly

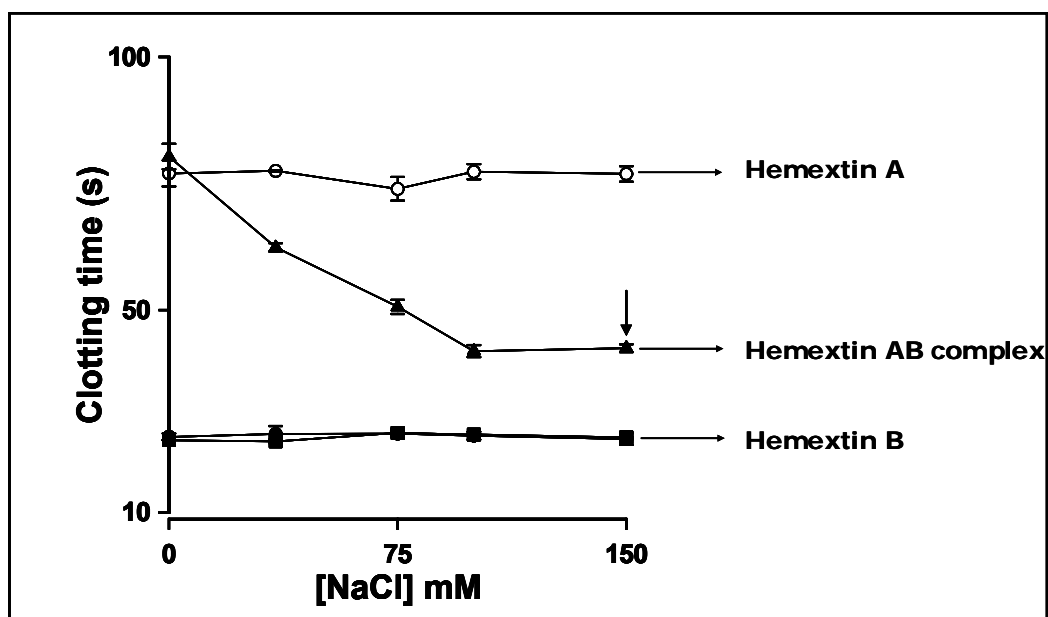


Figure 4.13 Effect of buffer ionic strength on anticoagulant activity. Effect various concentrations of NaCl on the anticoagulant activity of hemextin A (O), hemextin B (●), hemextin AB complex (▲). The anticoagulant activity of hemextin AB complex decreases with the increase in concentrations of NaCl and glycerol. The arrow inside the plot indicates the concentrations of NaCl where the anticoagulant complex exists mostly as a mixture of dimer and monomers (see text for details). (■) denotes the anticoagulant activity recorded in the absence of the proteins.

hydrophobic interactions. Therefore, successive experiments were carried out to evaluate the importance of hydrophobic interactions in the complex formation.

(B) Hydrophobic interactions in the hemextin AB complex formation – We carried out ITC experiments in buffers containing increasing concentrations of glycerol. Glycerol has been shown to form a ‘hydration’ layer around the proteins, thereby inhibiting hydrophobic interactions (Liu *et al.*, 2004c). This behavior of glycerol is evident because of the fact that it increases the osmotic second virial co-efficient

(B_{22}). B_{22} , formally defined by:
$$B_{22} = \frac{-1}{16\pi^2 MW^2} \int (\exp(-\Delta G_{inter}/kT) - 1) d\Omega$$
, where

ΔG_{inter} represents the interaction energy (potential of mean force) acting between two protein molecules in solution, MW is the molecular weight of the protein(s), and the $d\Omega$ indicates that the integral is carried out over all possible relative orientations of the two. A positive or an increase in B_{22} reflects overall repulsive forces between protein molecules, where protein solutions are stable; a negative or a decrease B_{22} , on the other hand indicates overall interprotein attraction that favors fluid-fluid phase separation. These observations have been made in case of the studies depicting the effect of monohydric and polyhydric alcohols including glycerol on the self interaction of hen-egg lysozyme (Liu *et al.*, 2004a).

A decrease in the association constant was observed with the increase in glycerol concentration (Figure 4.14 and Table 4.3), showing the importance of hydrophobic interactions in the complex formation. We monitored the elution of hemextin AB complex in buffers containing glycerol on a Superdex 75 column (Figure 4.15B). In buffers containing high glycerol concentration the tetramer dissociates into dimer and monomers. ESI-MS and HPLC analyses of the dimer peak indicate that it contains both hemextins A and B (data not shown). However, no additional peak

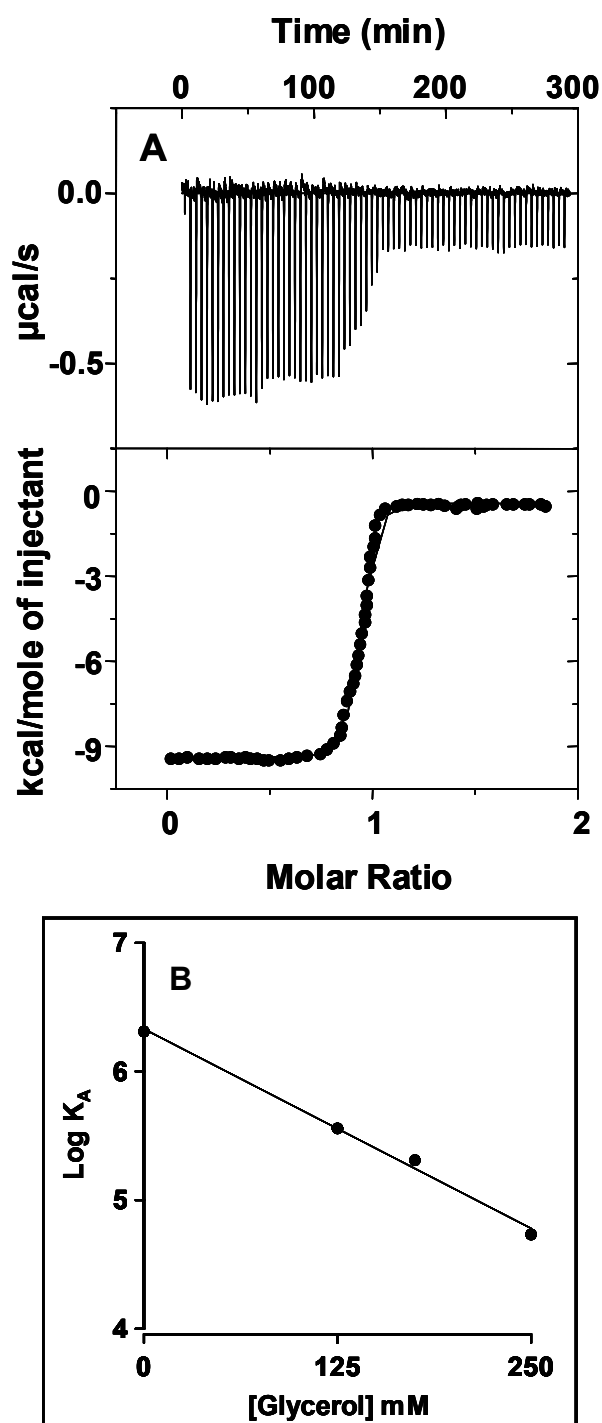


Figure 4.14 ITC studies in buffer of high glycerol concentration. (A) Representative thermogram of hemextin A – hemextin B interaction with corresponding binding isotherm in 50 mM Tris-HCl buffer (pH 7.4) containing 250 mM glycerol. (B) Dependence of K_a on the glycerol concentration. The binding affinity decreases with the increase in glycerol concentration indicating the importance of hydrophobic interactions

Table 4.2

Effect of increasing glycerol concentrations on hemextin A-hemextin B interaction

ITC experiments	$K_A \times 10^6 (M^{-1})$	ΔH (kcal/mole)	ΔS (cal/deg.mole)	ΔG (kcal/mole)
At different glycerol concentrations (mM)				
0.00	2.23	-11.7	-8.645	-9.0
125	0.32	-10.8	-11.01	-7.6
175	0.2	-10.5	-10.6	-7.2
250	0.05	-9.4	-10.0	-6.4

Note: All experiments were conducted at 37 °C

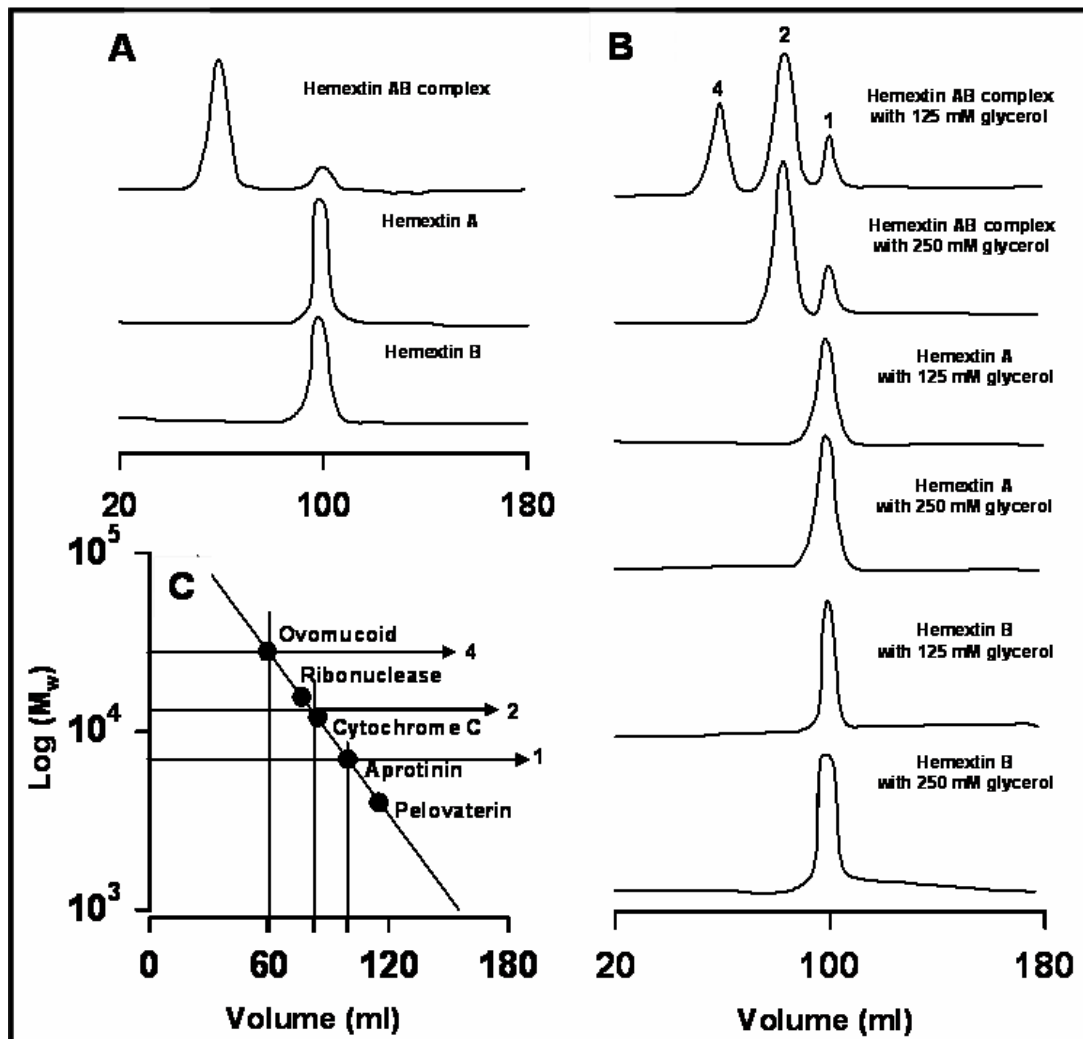


Figure 4.15 SEC studies of Hemextin AB complex in buffer containing different concentrations of glycerol. A. Elution profiles of hemextin AB complex in Tris-HCl buffer. Effect various concentrations of glycerol (B) on hemextin AB complex. The tetrameric complex (peak denoted by 4) dissociates into dimer and monomer (peaks denoted by 2 and 1, respectively) with the increase in glycerol. (C) Calibration of the column using the following proteins as molecular weight markers – ovomucoid (28 kDa), ribonuclease (15.6 kDa), cytochrome C (12 kDa), apoprotinin (7 kDa) and pelovaterin (4 kDa). The molecular weights of the tetramer, dimer and monomers were calculated from the calibration curve

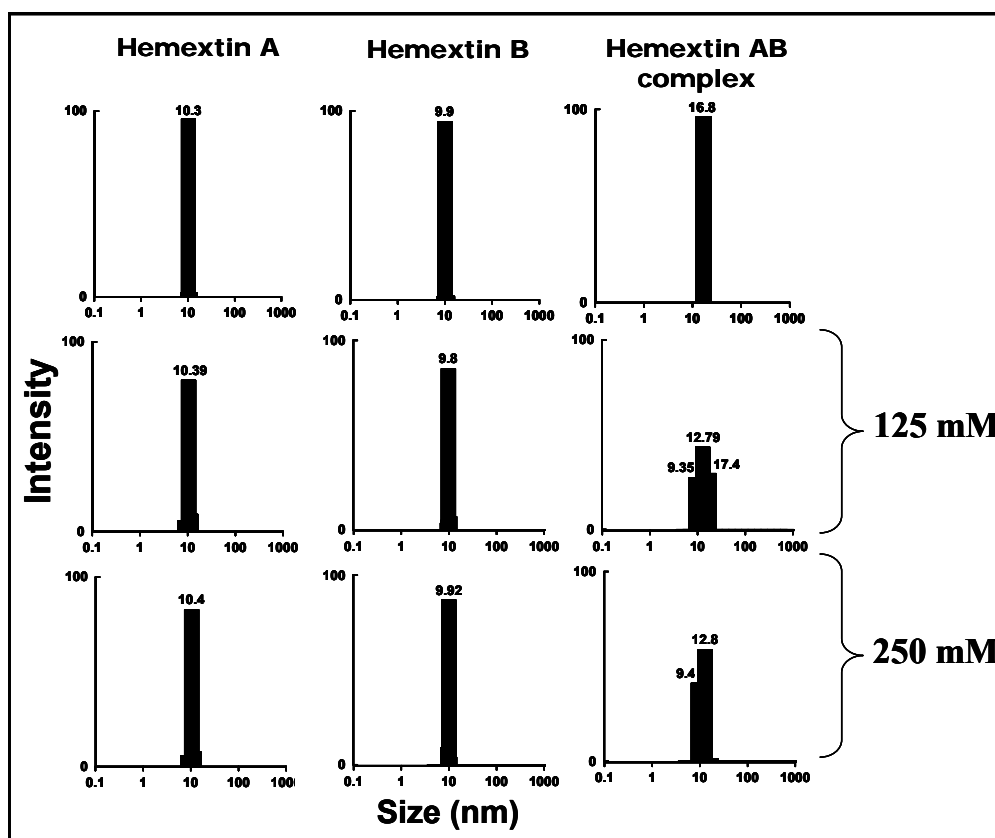


Figure 4.16 Determination of hydrodynamic diameter using DLS. CONTIN analysis hemextin A, hemextin B and hemextin AB complex in 50 mM Tris-HCl buffer and at different glycerol concentrations. The calculated hydrodynamic diameters for each molecular species are shown.

corresponding to altered conformation of hemextin A was observed. The elution of individual hemextins remained unaltered in the presence of glycerol (Figure 4.15B). The breakdown of hemextin AB complex in the presence of glycerol was also observed in the DLS studies (Figure 4.16). At 125 mM glycerol concentration, an additional population of 12.8 nm-sized species was observed in addition to the monomers and the tetrameric complex. Based on SEC studies, we propose that the 12.8 nm species is a dimer. The 12.8 nm species increases with the increase in glycerol concentration (Figure 4.16). It is important to note that the apparent molecular diameter of this dimer is different from the dimer formed in buffers of high ionic strength (12.8 nm versus 12.4 nm; Figure 4.16 and 4.12). (As GEMMA works on the principle of nano-ESI, we did not determine the molecular diameters in buffers containing glycerol using this technique.). No polydispersity was observed in the case of individual hemextins in the presence of glycerol (Figure 4.16).

To further understand the implication of the breakdown of hemextin AB complex in glycerol, we monitored its anticoagulant activity and that of the individual hemextins in buffers containing different concentrations of glycerol. The anticoagulant activity of hemextin AB complex decreased with the increase in glycerol concentration (Figure 4.17). At 125 mM glycerol concentration there is no decrease in the anticoagulant activity. However, at 250 mM glycerol concentration (at which hemextin AB complex exists as a mixture of dimer and monomers; Figure 4.15B) there is a decrease in the anticoagulant activity. But this activity is higher than that of the anticoagulant effect of hemextin A alone. Therefore, we conclude that the dimer observed at 250 mM glycerol concentration exhibits the anticoagulant activity higher than hemextin A alone but lower than that of the tetramer. In other words, dimer formed in the presence of glycerol is different from the dimer formed in salt; the

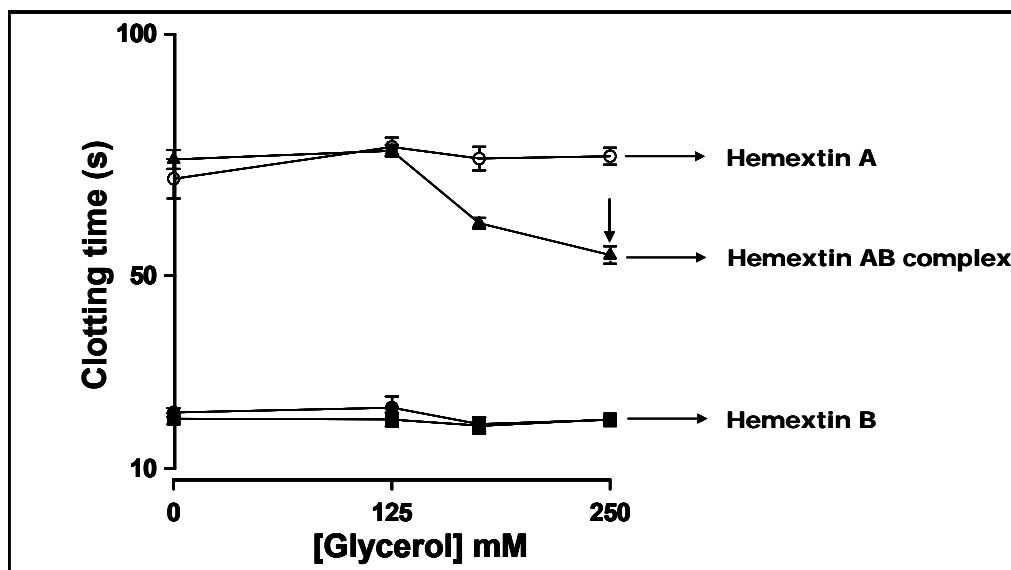


Figure 4.17 Effect of glycerol on anticoagulant activity. Effect various concentrations of glycerol on the anticoagulant activity of hemextin A (O), hemextin B (●), hemextin AB complex (▲). The anticoagulant activity of hemextin AB complex decreases with the increase in the glycerol concentration. The arrows indicate the concentrations of glycerol where the anticoagulant complex exists mostly as a mixture of dimer and monomers (see text for details). (■) denotes the anticoagulant activity recorded in the absence of the proteins

former dimer exhibiting an increased anticoagulant activity compared to hemextin A alone, whereas the latter not doing so. Glycerol, however, did not affect the anticoagulant activity of individual hemextins (Figure 4.17). The dissociation of the tetramer into dimer and monomers in the presence of glycerol indicates the importance of hydrophobic interactions in the tetrameric complex formation. This is further supported by the negative ΔC_p change observed during the formation of hemextin AB complex.

Our data strongly suggests that both electrostatic and hydrophobic interactions are important for the formation of tetrameric hemextin AB complex. To confirm that decrease in binding affinity between the monomers observed in salt and glycerol is not a solute osmotic effect, the K_A recorded in salt and glycerol was plotted against osmotic pressure (Figure 4.18). At similar osmolality of salt and glycerol decrease in binding affinity was more pronounced in salt than glycerol. This indicates that fall binding affinity is due to disruption of either electrostatic (for salt) or hydrophobic (for glycerol) interactions.

The effect of buffer conditions on the conformation of hemextins – Earlier studies using SEC (Figure 4.11B) and DLS (Figure 4.12) indicated that hemextin A undergoes conformational changes in the presence of salt. We conducted 1D-NMR analysis to study the conformation of hemextins A and B under different buffer conditions (Figure 4.19). In the presence of NaCl, there is a decrease in the number of $H\alpha$ resonance peaks between 4.8 ppm and 6 ppm in the case of hemextin A (Figure 19A). These chemical shifts contribute to the inter-residue NOE cross peaks between $H\alpha$ of different amino acid residues forming anti-parallel β -sheet structure typically observed in all three-finger toxins. Thus a decrease in the β -sheet content of hemextin A is observed in the presence of NaCl. In addition, there are several changes in the

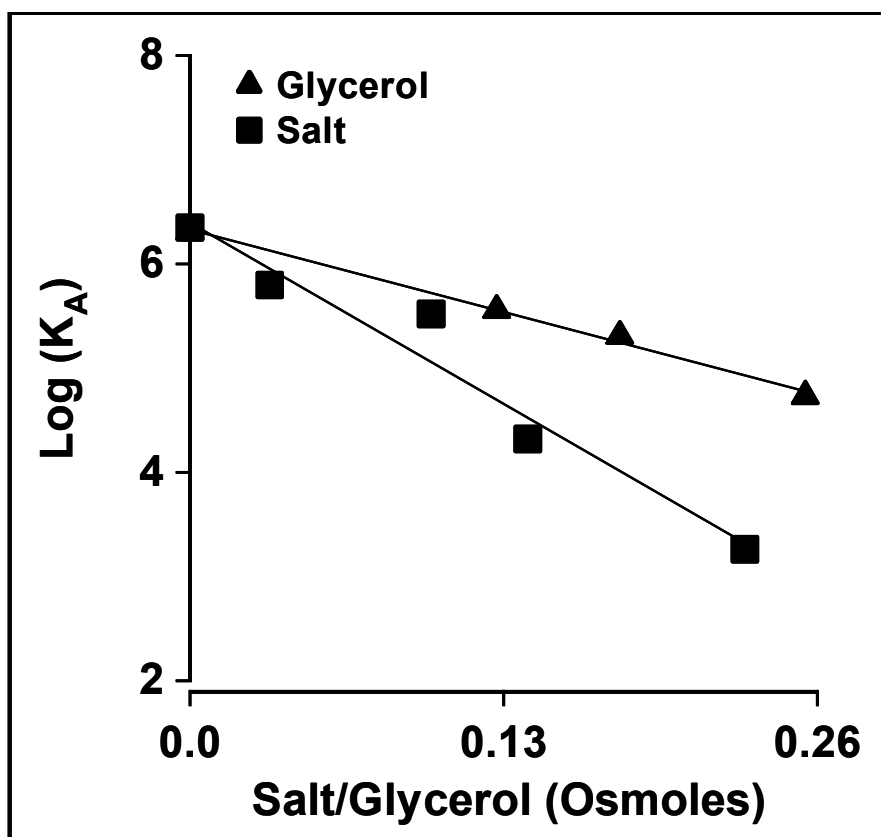


Figure 4.18 Evaluation of solute osmotic effect on binding affinity. The effect of solute osmolality (for NaCl and glycerol) on the binding affinity between the hemextin A and hemextin B was evaluated. Note that at similar osmolality of NaCl and glycerol, effect on binding affinity decreases more in the presence of NaCl than glycerol. This indicates that the decrease in binding affinity is not an osmotic effect.

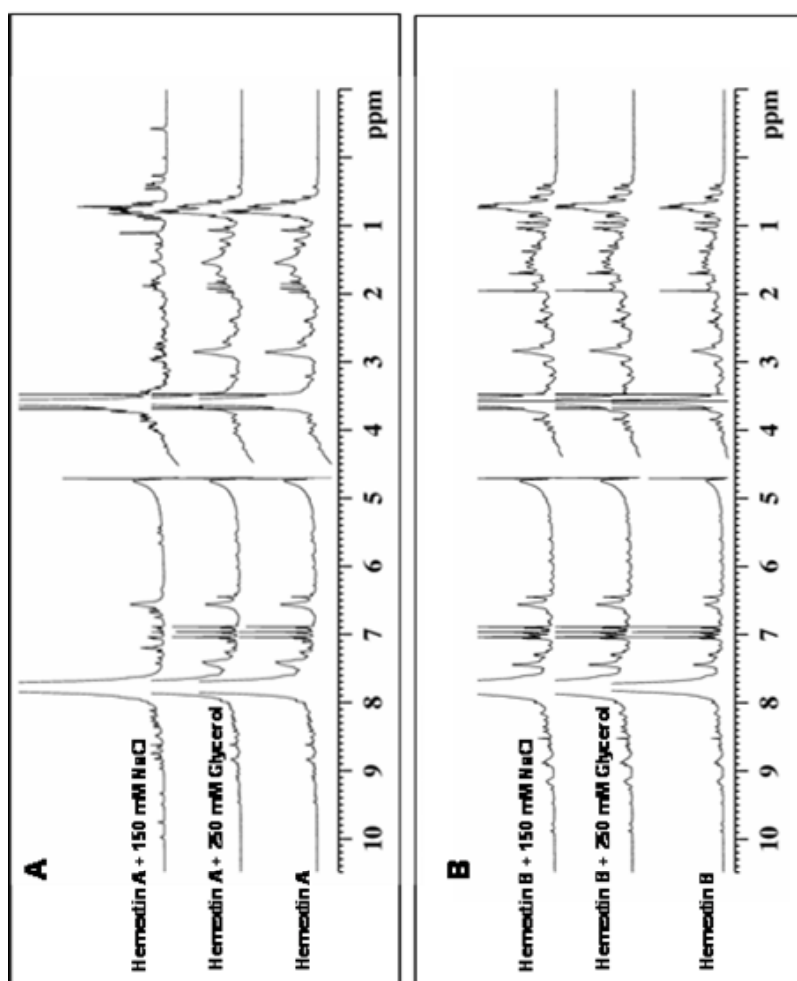


Figure 4.19 One-dimensional ^1H NMR studies. Spectrum of (A) hemextin A and hemextin B under different buffer conditions. *Note*, in the presence of salt hemextin A undergoes a conformational change. Also, the peaks are sharp throughout the spectrum. In addition, all 1D ^1H NMR spectra also exhibited a wide range of chemical shift dispersions (amide region 7 to 10 ppm, $\text{H}\alpha$ region 3.8 to 6 ppm and methyl region -0.4 to 1.5 ppm) which is a characteristic of well folded proteins. Therefore, the observed structural change is not due to resonance broadening or aggregation (as no aggregation state was observed as mentioned) but it is only due to addition of NaCl to hemextin A

chemical shifts of side chains. A notable change is a highly shielded methyl peak which appears at the negative chemical shift value (-0.38 ppm) in the presence of salt. These observations strongly support conformational changes in hemextin A in the presence of NaCl. The overall dispersion of 1D proton NMR spectra of hemextin A in the presence of glycerol (deuterated) remains the same with the subtle changes in the amide region (Figure 4.19A). Thus, hemextin A did not undergo any significant conformational change upon the addition of glycerol. Similar studies with hemextin B show that it did not undergo any significant conformational changes in the presence of NaCl or glycerol (Figure 4.19B) since there is almost one to one match for the spectral frequencies.

Model for hemextin AB complex – Based on our studies we propose a model for the assembly of hemextin AB complex (Figure 4.20). Two molecules each of hemextin A and B form the tetrameric complex in Tris-HCl buffer (Figure 4.20A). The formation of this compact, synergistic complex is important for its anticoagulant activity. As illustrated earlier, hemextin AB dimer in high salt is different from the dimer formed in the presence of glycerol (Figure 4.20C). The former dimer has an apparent molecular diameter of 12.4 nm and lacks anticoagulant activity, whereas the latter has an apparent molecular diameter of 12.8 nm and exhibits slightly higher anticoagulant effects (Figure 4.20C). Thus, the breakdown of tetramer to dimer probably occurs in two different interfaces of interaction between hemextin A and B. One interface is sensitive to the ionic strength of its surroundings while the other is sensitive to glycerol (Figure 4.20C). Further, in the presence of salt, hemextin A undergoes conformational changes (Figure 4.20B) which may interfere in the tetramer formation. The dimer formed under high ionic conditions lacks the complete synergistic anticoagulant site (marked by a dotted semicircle in Figure 4.20C). In contrast,

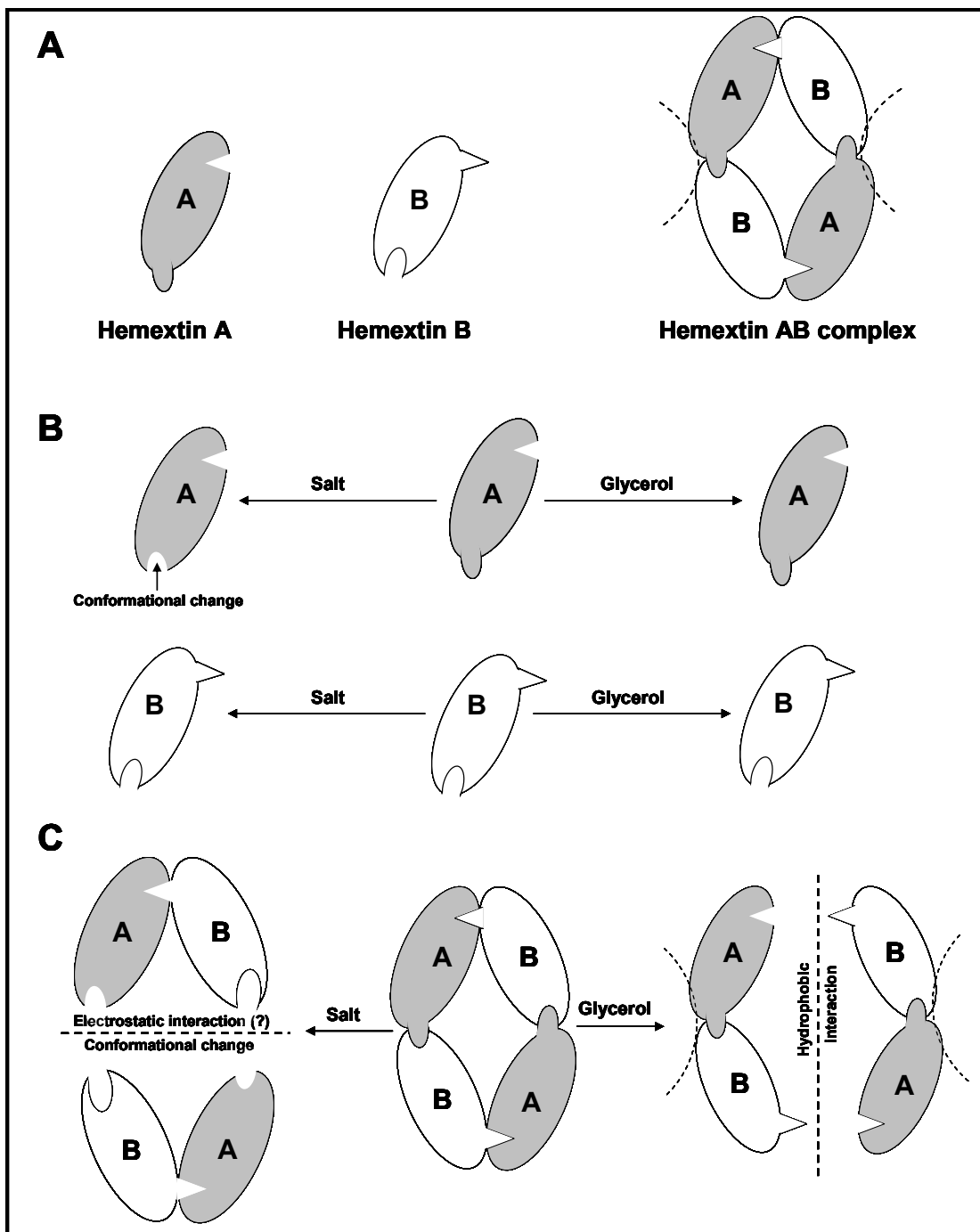


Figure 4.20 A proposed model of hemextin AB complex. A. Schematic diagram depicting the formation of hemextin AB complex. Hemextins A and B, two structurally similar three-finger toxins, form a compact and rigid tetrameric complex with 1:1 stoichiometry. B (Banerjee *et al.*, 2005b; Banerjee *et al.*, 2005d). Schematic diagram showing the effect of salt and glycerol on conformations of hemextins A and B. Hemextin A undergoes a conformational change in the presence of salt. C. Dissociation of the tetrameric hemextin AB complex in the presence of salt and glycerol. The dissociation probably occurs in two different planes. Thus the hemextin AB dimer in high salt is different from the dimer formed in the presence of glycerol. Two putative anticoagulant sites are shown with dotted semicircles (See text for details).

hydrophobic interactions are predominant in the second interface. Therefore, glycerol dissociates the tetramer into dimers. However, in this case only minor changes occur in the synergistic anticoagulant site of the complex (as shown in Figure 4.20C) and hence the resultant dimer is active. We propose that the tetramer formation most likely stabilizes the anticoagulant site of hemextin A. The binding between hemextin AB complex/ hemextin A and FVIIa has been characterized to validate the proposed model, the details of which are provided in Chapter 5.

CONCLUDING REMARKS

Hemextin AB complex is the first synergistic anticoagulant complex isolated from snake venom comprising solely of two three-finger toxins – hemextin A and hemextin B. The complex formation is a pre-requisite for the synergistic inhibition of FVIIa. The complex exists as a tetramer; where as individual hemextins are monomers. The complex formation is an enthalpically driven process. Unfavorable entropic change associated with the complex formation, and identical apparent molecular diameters recorded in the gas and solution phases indicate that the complex has lesser structural flexibility in comparison to the monomers. The complex formation is associated with protein unfolding and refolding. Both electrostatic and hydrophobic interactions are important for the assembly of the tetramer. Based on our results we proposed that the tetramer formation takes place by the participation of two interfaces. One of the interfaces is sensitive to the buffer ionic strength, indicating that electrostatic interactions are predominantly active in that interface. The other being sensitive to B_{22} of the solution indicates the participation of mostly hydrophobic interactions. The proposed model may help in a better understanding of the structure-function relationship of this novel anticoagulant complex.

Thank you note,

The work described in this chapter is currently under consideration in the Biophysical Journal. During revision of the paper, the reviewers wanted me to show, that dissociation of the tetramer into dimer in salt/glycerol is not due to solute osmotic effect, but due to disruption of electrostatic (for salt) or hydrophobic (for glycerol) interactions. For the calculation of osmotic pressure, for a given concentration of salt or glycerol, the reviewers kindly proposed a website which was supposed to have the conversion tables. Unfortunately, the site was experiencing technical problems. Since the revised version of a manuscript is to be submitted within a stipulated period, I had no other means², but to write to some of the scientists who are studying the effect of solute osmolality on biological molecules, for the conversion tables. Before I proceed to the next chapter, I will like to thank Dr. Jörg Rösger (University of Texas Medical Branch), and Dr. Nina Sidorova and Dr. Donald Rau (NIH/NICHD/LPSB) for kindly providing me with the conversion tables, and also for helpful discussions on how the data should be analyzed. Because of their help, I was able to submit the revised version of the manuscript and also include the data on osmotic effect in this chapter.

-- Yajnavalka Banerjee

² “The end does not justify the means, but justifiable means that bring about a fair and necessary conclusion are not to be dismissed”.

--- *Joel Converse in Robert Ludlum's The Aquitaine Progression (Pg 185)*

“The scientific accomplishment of the Twentieth Century that I admire most is the revealing of the multifaceted capabilities of proteins and of their structures that make these capabilities possible.”

--- Paul D. Boyer (“A Research Journey with ATP Synthase” J. Biol. Chem., Vol. 277, Issue 42, 39045-39061, October 18, 2002



“Let's find out where it takes us”

Chapter 5

Molecular Interactions with FVIIa

Targeting proteases: successes, failures and future prospects¹

Protease inhibitors approved for clinical use

Indication	Compound	Company	Target	Protease class
Hypertension, myocardial infarction	Captopril	Bristol-Myers Squibb	ACE	Metallo
	Enalapril	Merck		
	Lisinopril	AstraZeneca		
	Trandolapril	Abbott		
	Zofenopril	Menarini group		
	Ramipril	Aventis		
	Moexipril	Boehringer Mannheim		
	Imidapril	Trinity Pharmaceuticals		
	Perindopril	Daiichi Pharmaceutical, Servier/Solvay		
	Qinapril	Pfizer		
	Fosinopril	Bristol-Myers Squibb		
	Benazepril	Novartis		
	Cilazapril	Roche		
Periodontitis	Periostat	CollaGenex	MMP1, MMP2	
AIDS	Ritonavir	Abbott	HIV protease	Aspartic
	Amprenavir	Vertex Pharmaceuticals, GlaxoSmithKline		
	Fosamprenavir	GlaxoSmithKline		
	Atazanavir	Bristol-Myers Squibb		
	Lopinavir	Abbott		
	Indinavir	Merck		
	Saquinavir	Hoffmann-La Roche		
	Nelfinavir mesylate	Pfizer		
Thrombosis	Ximelagatran*	AstraZeneca	Thrombin	Serine
	Argatroban	Mitsubishi Pharma		
	Lepirudin	Aventis (Hoechst Marion Roussel)		
	Desirudin	Novartis		
	Fondaparinux sodium (indirect)	Sanofi Synthelabo	Factor X	
Thrombosis, unstable angina	Bivalirudin	The Medicines Company		
Respiratory disease	Sivelestat	Ono	Human neutrophil elastase	
Pancreatitis	Camostat mesilate	Ono	Trypsin-like	
Pancreatitis, inflammation	Nafamostat mesilate	Japan Tobacco	Broad-spectrum	
Cancer	Bortezomib	Millennium	Proteasome	Threonine

*Withdrawn from production because of liver toxicity. ACE, angiotensin-converting enzyme; MMP, matrix metalloproteinase.

--- Professor Boris Turk, *Department of Biochemistry and Molecular Biology at Jozef Stefan Institute, Ljubljana, Slovenia. Nature Reviews Drug Discovery* 5, 785–799 (September 2006)

¹ The above table is taken from the excellent review article “*Targeting proteases: successes, failures and future prospects*” by Professor Boris Turk published in *Nature Reviews Drug Discovery*, in September 2006. The table shows the current protease inhibitory drugs approved for clinical use, anticoagulants included (under the section of thrombosis). I will like to highlight to the reader that the current anticoagulants approved for clinical use, target FX and thrombin, which are downstream proteases in the clotting cascade. Therefore, hemexin AB complex which is a specific inhibitor of FVIIa, provides a new paradigm in our search for anticoagulants targeting clot initiation (in spite of its large size), though there is a long way to go before its clinical viability can be evaluated.

Understanding the molecular interaction between the inhibitor and its target enzyme is the key to drug design. As illustrated in the introductory section of the thesis FVIIa is the key to initiation of the coagulation cascade. In Chapter 3, we have seen that hemexin A hemexin AB complex specifically inhibit FVIIa activity to mediate anticoagulation. In this chapter we investigate the molecular interactions involved in the formation of hemexin AB-FVIIa complex and hemexin A-FVIIa complex. Effect of the presence of co-factor on the binding between FVIIa and the anticoagulant proteins has also been studied. Since, the anticoagulant protein and its complex inhibit FVIIa non-competitively (as illustrated in Chapter 3), their binding to active site occupied FVIIa was also studied. Lastly, binding site of hemexin AB complex and hemexin A on the FVIIa molecule was identified. For these studies, we primarily use isothermal titration calorimetry (ITC) and size-exclusion chromatography (SEC).

MATERIALS AND METHODS

Materials –The chromogenic substrate H-D-Ile-Pro-Arg-p-nitroanilide (pNA) dihydrochloride (2HCl), (S-2288) was from Chromogenix AB, Stockholm, Sweden and was reconstituted in deionized water prior to D-Phe-L-Phe-L-Arg chloromethyl ketone (FFR-ck) was purchased from Bachem (King of Prussia, PA, USA). All other chemicals and reagents used were of highest purity available.

Proteins – Hemexin A and hemexin B was purified similarly as described in Chapter 2. Human plasma-derived FVIIa was kindly provided by Factor VII Group (Kazuhiko Tomokiyo, Yasushi Nakatomi, Teruhisa Nakashima, and Soutatou Gokudan) of KAKETSUKEN and were purified as described (Nakagaki *et al.*, 1991). Recombinant

human soluble TF (sTF; residues 1–218) was a gift from Dr. Toshiyuki Miyata (National Cardiovascular Center, Suita, Japan), and it was prepared as described (Stone *et al.*, 1995).

Reconstitution of the anticoagulant complex – We reconstituted the complex for various *in vitro* experiments immediately prior to the experiment by incubating equimolar concentration of hemexin A with hemexin B (unless mentioned otherwise) at 37° C for a period of 5 min in 50 mM Tris-buffer (pH 7.4).

Reconstitution of the sTF-FVIIa complex – sTF-FVIIa complex was reconstituted by incubating 30 nM FVIIa with 100 nM of sTF in 50 mM Tris-HCl buffer (pH 7.4), containing 10 mM CaCl₂, and 1% BSA for 10 min at 37° C. The kinetics of hydrolysis of the chromogenic substrate S-2288 by sTF-FVIIa was measured prior to the binding studies to ensure proper complex formation.

Preparation of active site inhibited FVIIa – Active site inhibitor FFR-ck was used for the studies. For the preparation, FVIIa was treated with 2-fold molar excess of FFR-ck. Unreacted FFR-ck was separated from active site blocked FVIIa by size-exclusion chromatography on a Superdex 200 gel filtration column (1.0 × 30 cm) using an ÄKTA Purifier system (Figure 5.1). The residual FVIIa activity, of active site inhibited FVIIa was measured in an FVIIa-specific amidolytic assay using S-2288 as the substrate.

FVIIa-specific amidolytic assay – The assay was performed in assay buffer containing 50 mM Tris-HCl, pH 7.4, containing 10 mM CaCl₂, and 1% BSA at 37°C. In a total volume of 200 µl in the individual wells of the microtiter plate, final concentrations of FVIIa/active site inhibited FVIIa was 300 nM. Reactions were initiated by the addition of S-2288 (1 mM). Initial reaction velocities were measured as a linear increase in the

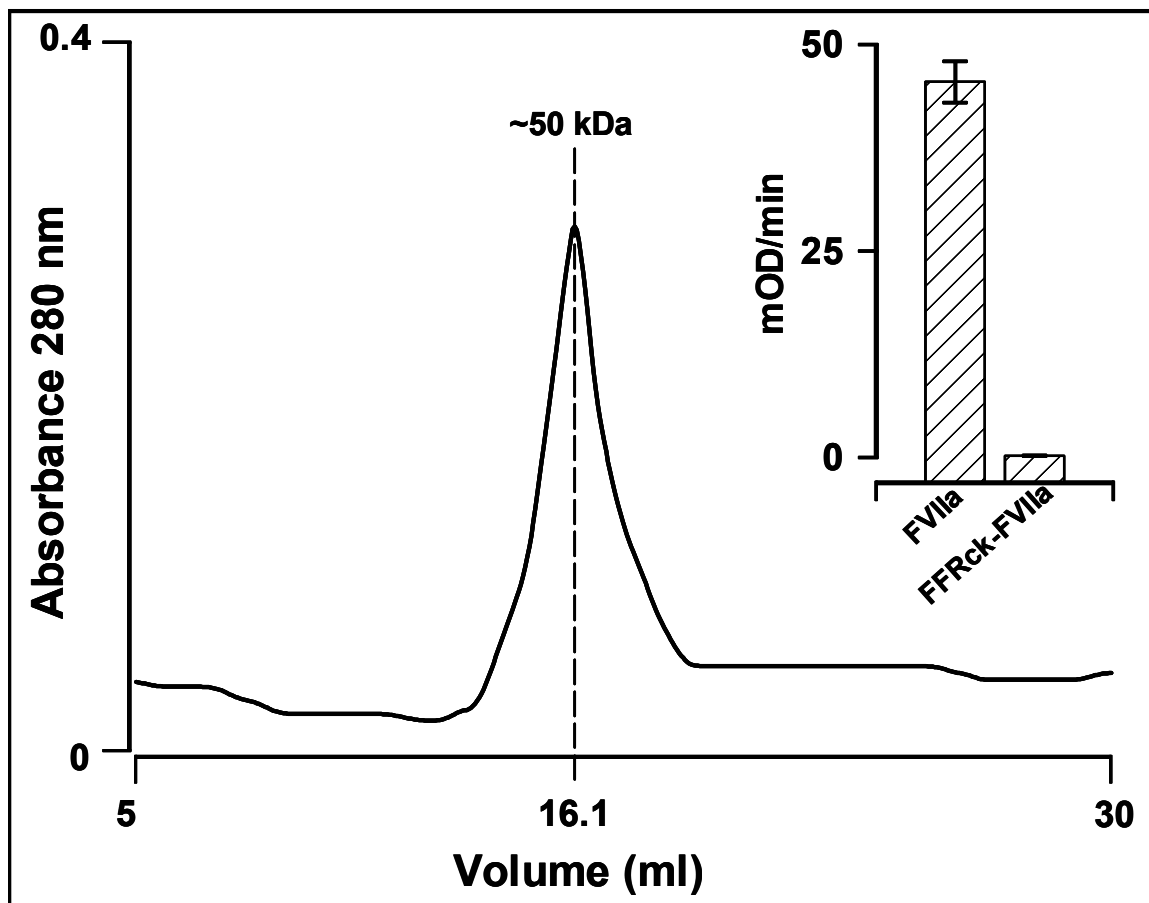


Figure 5.1 Elution profile of active site inhibited FVIIa (FFRck-FVIIa). Note the eluted peak had a retention volume of 16.1 ml corresponding to a mass of ~50 kDa. Fractions corresponding to the peak were pooled and checked for FVIIa activity. The pooled fractions had less <XX% residual activity.

absorbance at 405 nm over 5 min, with a SPECTRAmax plus® temperature-controlled microplate spectrophotometer (Molecular Devices, Sunnyvale, CA, USA). FFRck-FVIIa had 5% residual activity (Figure 5.1, *inset*) as measured in the assay.

Separation of light and heavy chains of FVIIa – Partially reduced FVIIa was separated under the conditions described in the legend (Figure 5.2A). Both the chains were treated with 10 mM iodoacetamide for 20 min in ice water, in the dark. Homogeneity and molecular weight of the chains were determined by eluting each of them in TBS on a pre-packed Superdex 200 gel filtration column (1.0 × 30 cm) using the same chromatography system (Figure 5.2B to C) and also on SDS-PAGE (Figure 5.2A *inset*).

Preparation of light chain of FVIIa under non-reduced conditions – The FVIIa light chain (residues 1-144 plus 248-266) was isolated as described in (Persson and Petersen, 1995).

Circular dichroism (CD) spectroscopy – Conformational changes in FVIIa, associated with binding to hemextin AB complex were monitored using CD. Far UV CD spectra (260-190 nm) were recorded using a Jasco J-810 spectropolarimeter (Jasco Corporation, Tokyo, Japan). All measurements were carried out at room temperature using 0.1 cm path length stoppered cuvettes. The instrument optics was flushed with 40 l/min of nitrogen gas. The spectra were recorded using a scan speed of 50 nm /min, resolution 0.2 nm, and band width 2 nm. For each spectrum, a total of 4 scans were recorded, averaged and baseline subtracted.

Isothermal Titration Calorimetric (ITC) studies – The thermodynamics of binding of individual hemextins and the reconstituted anticoagulant complex with FVIIa and its different derivatives were monitored using a VP-ITC titration calorimetric system

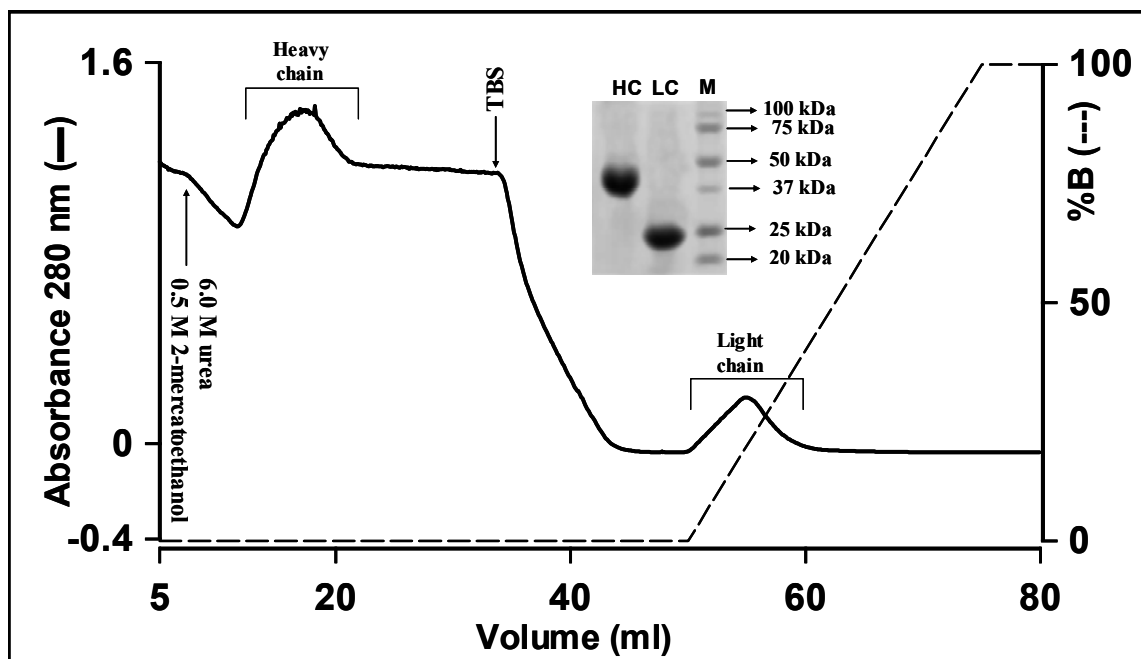


Figure 5.2 Separation of light and heavy chains derived from FVIIa. Human FVIIa (3.5 mg) was incubated with 0.5 M 2-mercaptoethanol in 1.1 ml of TBS at 20 °C for 30 min. The sample was applied to a column (6 ml) of DEAE-Sepharose CL-6B column, equilibrated with TBS containing 0.5 M 2-mercaptoethanol. The flow rate was 2 ml/min. After washing the column with 20 ml of the equilibration buffer, the heavy chain of FVIIa was eluted with 35 ml of TBS containing 6.0 M urea and 0.5 M 2-mercaptorthanol. Then the column was washed with 20 ml of TBS and a linear gradient from 0.1 to 0.6 M NaCl in 50 mM Tris-HCl, pH 8.0 was performed to elute the light chain of FVIIa. The separated heavy and light chains were rerun in TBS on a pre-packed Superdex 200 gel filtration column (1.0 × 30 cm) (data not shown). The patterns of the isolated light and heavy chains on SDS-PAGE are shown in the *inset*: HC, heavy chain of FVIIa; LC light chain of FVIIa; M, molecular mass of standard proteins used.

(MicroCal, LLC, Northampton, MA). FVIIa or its derivatives were taken in 50 mM Tris-HCl buffer (pH 7.4) in the calorimetric cell and were titrated with individual hemexins or the reconstituted anticoagulant complex dissolved in the same buffer in a 250- μ l injection syringe with continual stirring at 300 rpm at 37 °C. All protein solutions were filtered and degassed prior to titration. The first injections presented defects in the base line, and these data were not included in the fitting process. Additional experiments were performed with FVIIa in 50 mM Tris-HCl buffer (pH 7.4) containing 150 mM NaCl or 250 mM glycerol at 37 °C. The calorimetric data were processed and fitted to the *single set of identical sites* in the same way as described in Chapter 4.

Size-exclusion chromatographic (SEC) studies – Binding studies with FVIIa and its derivatives were also carried out using SEC. All SEC experiments were carried out at room temperature on a pre-packed Superdex 200 gel filtration column (1.0 \times 30 cm) using the ÄKTA Purifier system. The column was equilibrated with 50 mM Tris-HCl buffer (pH 7.4) or the specified elution buffer, at a flow rate of 0.5 ml/min. The sample volume applied to the column was 0.4 ml. The column was calibrated using catalase (232-kDa), lactate dehydrogenase (140-kDa), bovine serum albumin (67-kDa), ovalbumin (43-kDa), chymotrypsinogen A (25-kDa) and ribonuclease A (13.7-kDa) as molecular weight markers. The void volume was determined by running Blue Dextran. The column was equilibrated with at least three bed volumes of the elution buffer prior to each run. Protein elution was monitored by recording absorbance at 280 nm.

RESULTS AND DISCUSSION

Binding of FVIIa to hemextin AB complex – The binding between hemextin AB complex and FVIIa was studied in Tris buffer (pH 7.4) using ITC (Figure 5.3A, Table 5.1), as under these conditions the complex exists as a heterotetramer (Chapter 4). Interestingly, two kinetic phases were associated with each injection. Immediately following injection, an initial exothermic phase (negative numbers) which was followed by a smaller and slower endothermic phase (positive numbers), suggesting that a slow conformational rearrangement takes place after binding. Similar kind of thermogram has also been observed in the binding of FXa with human secretory phospholipase A2, where a conformational rearrangement takes place on binding (Mounier *et al.*, 1998). The binding is enthalpically driven with 1:1 stoichiometry (Table 5.1). SEC studies show that the estimated molecular weight of the tetrameric hemextin AB complex-FVIIa complex is ~88,000 Da (Figure 5.3B). Both these studies indicate that only one FVIIa binds to tetrameric hemextin AB complex. In the proposed model for hemextin AB complex assembly (Chapter 4), the tetramer possesses two identical anticoagulant sites and therefore could bind two molecules of FVIIa. However, both ITC and SEC studies show that hemextin AB complex binds to only one molecule of FVIIa (Figures 5.3). This could be due to either steric hindrance or negative cooperativity. The two FVIIa binding sites on the tetramer juxtaposed very closely, as a result the binding of the first FVIIa molecule precludes the binding of the second FVIIa molecule. Such steric interference in protein-protein interactions is well documented (Lewicki and Gallagher, 2002; Pflieger and Eidne, 2006). Alternatively, the binding of the first FVIIa rapidly induces structural changes in the other binding site destroying the adjacent binding site resulting in negative

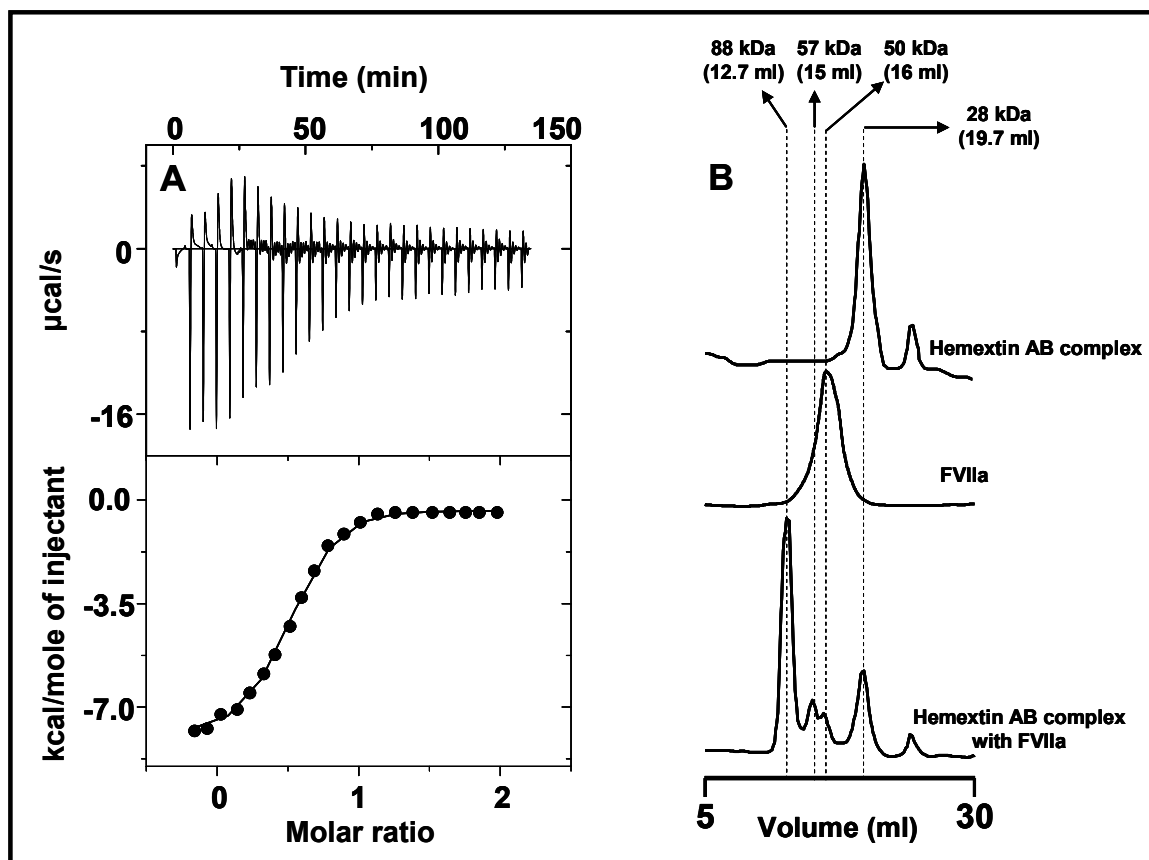


Figure 5.3 Binding of hemextin AB complex to FVIIa. (A) ITC studies. Thermogram with the corresponding binding isotherm for the binding of hemextin AB complex to FVIIa in 50 mM Tris buffer (pH 7.4). (B) SEC studies Elution profiles of the complex of FVIIa with hemextin AB complex in 50 mM Tris buffer (pH 7.4); *Note* on complex formation there is a reduction in retention time.

cooperativity (Kim *et al.*, 2001). The larger size of FVIIa and fairly stable conformation of hemextin AB complex supports the steric hindrance.

The effect of temperature on hemextin AB-FVIIa complex formation — Since, hemextin AB complex is the only known natural and specific inhibitor of FVIIa, the energetics of complex formation between the two molecules was investigated in detail. Complete temperature profile of the thermodynamic parameters associated with the binding of hemextin AB complex to FVIIa was studied over the temperature range of 25-45 °C (298-318 °K). The temperature dependence of ΔH is shown in Figure 5.4A and Table 5.1. The temperature dependence of ΔH over a narrow temperature range is given by the equation:

$$\Delta H = \Delta H_0 + \Delta C_p(T-T_0) \dots \dots \dots (Eq. 1)$$

where, ΔH_0 is the binding enthalpy at an arbitrary reference temperature and ΔC_p is the heat capacity change of binding. The ΔC_p obtained from the slope ($\Delta C_p = \delta \Delta H / \delta T$) (Figure XA), is -121.43 cal/K⁻¹mol⁻¹. Negative ΔC_p indicate a reduction in the nonpolar solvent-accessible surface area, as explained by the following equation (Murphy and Freire, 1992),

$$\Delta C_p = 0.45(\Delta ASA_{nonpol}) - 0.26 (\Delta ASA_{pol}) \text{ cal /molK} \dots \dots \dots (Eq. 2)$$

where, ΔASA_{pol} and ΔASA_{nonpol} are the change in the polar- and non-polar-accessible surface areas respectively.

Figure 5.4B, shows the plot of ΔG and ΔH as a function of $T\Delta S$. It is clear that the ΔG of binding remained temperature independent and is a result of linear dependence of ΔH on $T\Delta S$. This strongly suggests the enthalpy-entropy compensation for the binding of hemextin A to hemextin B. This phenomenon is a universal feature for protein-peptide

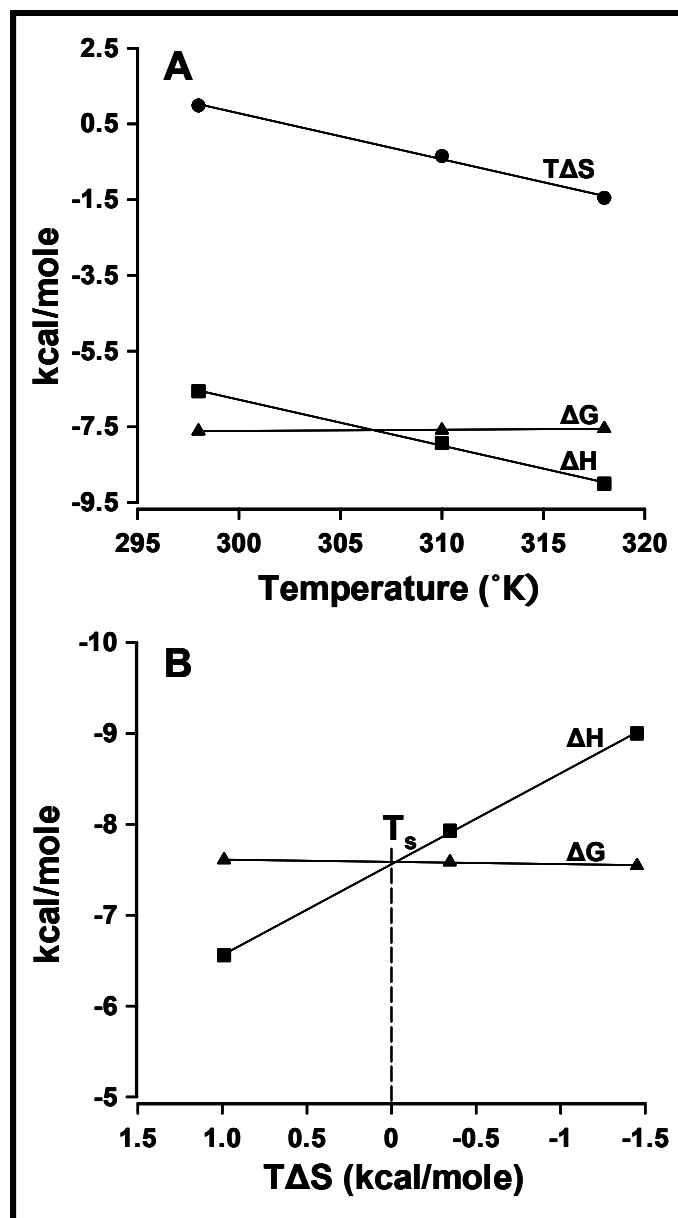


Figure 5.4 Thermodynamics of FVIIa-hemexin AB complex formation. (A) Effect of temperature on the energetics of FVIIa-hemexin AB complex interaction: enthalpy change (ΔH), change in entropy term ($T\Delta S$) and free energy change (ΔG). (B) Enthalpy-entropy compensation in complex formation. (Note: Point of intersection of lines corresponding to ΔH and ΔG corresponds to T_s)

Table 5.1

Thermodynamic analysis of FVIIa binding to hemexin AB complex at different temperatures

Binding to FVIIa	$K_A \times 10^5$ (M ⁻¹)	ΔH (kcal/mole)	ΔS (cal/deg.mole)	ΔG (kcal/mole)	Number of binding sites (N)
At different temperatures (°C)					
25	3.84	-6.56	3.322	-7.61	0.97
37	4.11	-7.931	-1.112	-7.586	1.01
45	1.55	-9.0010	-4.55	-7.548	1.08

interactions, where weak molecular interactions undergo constant rearrangements to realize a lower free energy of binding.

The negative ΔC_p also indicates the net thermodynamic driving force for the association to shift from entropic to enthalpic with increasing temperature. At the intersection point of both lines $\Delta G = \Delta H = -7.5 \text{ kcal.mol}^{-1}$ (Figure 5.4B), which corresponds to a temperature T_s (Temperature at which the contribution from entropy is zero. At T_s the contribution from entropy changes from favorable to unfavorable. From Figure 5.4A, $\Delta H = -7.5 \text{ kcal.mol}^{-1}$ is connected with a T_s of $33.3 \text{ }^\circ\text{C}$ ($306.3 \text{ }^\circ\text{K}$). A positive entropy change observed at 25°C (298 K) that is lower than T_s , further confirms this finding.

The negative ΔC_p for the hemextin AB complex formation further suggests that the observed entropy change upon binding must include significant contribution from the hydrophobic effect in the physiological temperature range. Therefore, for protein-protein/ligand interaction(s) the net entropy of association is given by the equation:

$$\Delta S_{assoc} = \Delta S_{HE} + \Delta S_{rt} + \Delta S_{other} \dots\dots\dots(Eq. 3)$$

where, ΔS_{HE} , ΔS_{rt} , and ΔS_{other} are the entropy changes due to hydrophobic effect, reduction of rotational and translational degree of freedom, and from other sources, respectively.

At T_s , the overall entropy of association is zero and the above equation becomes:

$$\Delta S_{assoc} = \Delta S_{HE}(T_s) + \Delta S_{rt} + \Delta S_{other} = 0 \dots\dots\dots(Eq. 4)$$

In the absence of crystallographic data, the $\Delta S_{HE}(T_s)$ was estimated from the equation,

$$\Delta S_{HE}(T_s) = 1.35 \Delta C_p \ln(T_s/386) \dots\dots\dots(Eq. 5)$$

and found to be $37.86 \text{ cal deg}^{-1} \text{ mol}^{-1}$. It has been shown that protein-protein interaction ΔS_{rt} is nearly equal to $-50 \text{ cal deg}^{-1} \text{ mol}^{-1}$

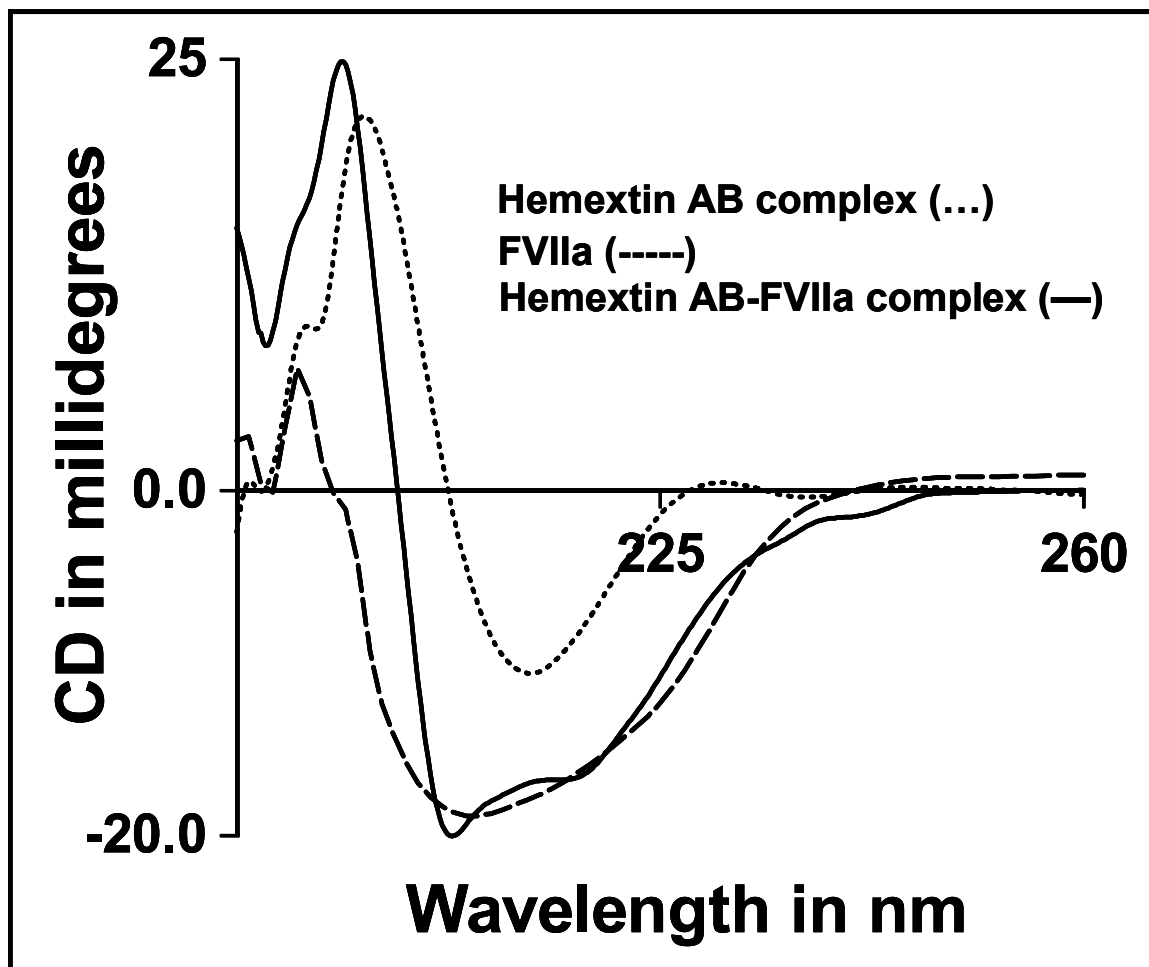


Figure 5.5 Conformational changes associated with the formation of hemextin AB-FVIIa complex. Individual spectra of hemextin AB complex, FVIIa are also shown for comparison. As shown in the figure complex formation leads to an increase in the 3_{10} -helix structure.

(Janin and Chothia, 1978; Finkelstein and Janin, 1989). Thus the ΔS_{other} is calculated to be $-12.14 \text{ cal deg}^{-1} \text{ mol}^{-1}$. The non-zero value of ΔS_{other} suggests that the FVIIa-hemexin AB complex formation, is not a rigid-body-association but formed through local unfolding and refolding during binding interaction.

Conformational changes associated with hemexin AB-FVIIa complex formation – The above analysis of the thermodynamic parameters indicated a plausible conformational change associated with complex formation between FVIIa and hemexin AB complex. Circular dichroism is a useful technique to monitor the conformational changes for a moderately weak to strong protein-protein interactions ($K_d \sim 1 \text{ mM}$ to $1 \text{ }\mu\text{M}$). Figure 5.5 shows the CD spectra of hemexin AB complex, FVIIa, and hemexin AB-FVIIa complex. The CD spectra of hemexin AB complex exhibits dominant presence of β -sheet structure (Figure 5.5). The CD of FVII exhibits a strong double minimum at 207 nm and 222 nm, and a weak positive maxima around 195 nm indicating the presence of a right-handed helical structure. However, the ratio of $[\theta_{222}]/[\theta_{207}]$ is 0.7 indicates the interconverting populations of the presence of both 3_{10} - and α -helical structure (Millhauser, 1995). The hemexin AB-FVIIa complex exhibited a slight increase in θ_{222} indicating an increase in 3_{10} -helix structure upon complexation. The result suggests considerable unfolding upon complex formation. Since CD was recorded at room temperature much below T_s , the complex formation is driven by favourable entropy changes. Thus, CD difference spectra of hemexin-FVIIa complex studies support the thermodynamic data obtained from ITC.

Binding of FVIIa to hemexin A – The binding between hemexin A and FVIIa was also investigated. ITC studies revealed that the binding is predominantly exothermic with 1:1

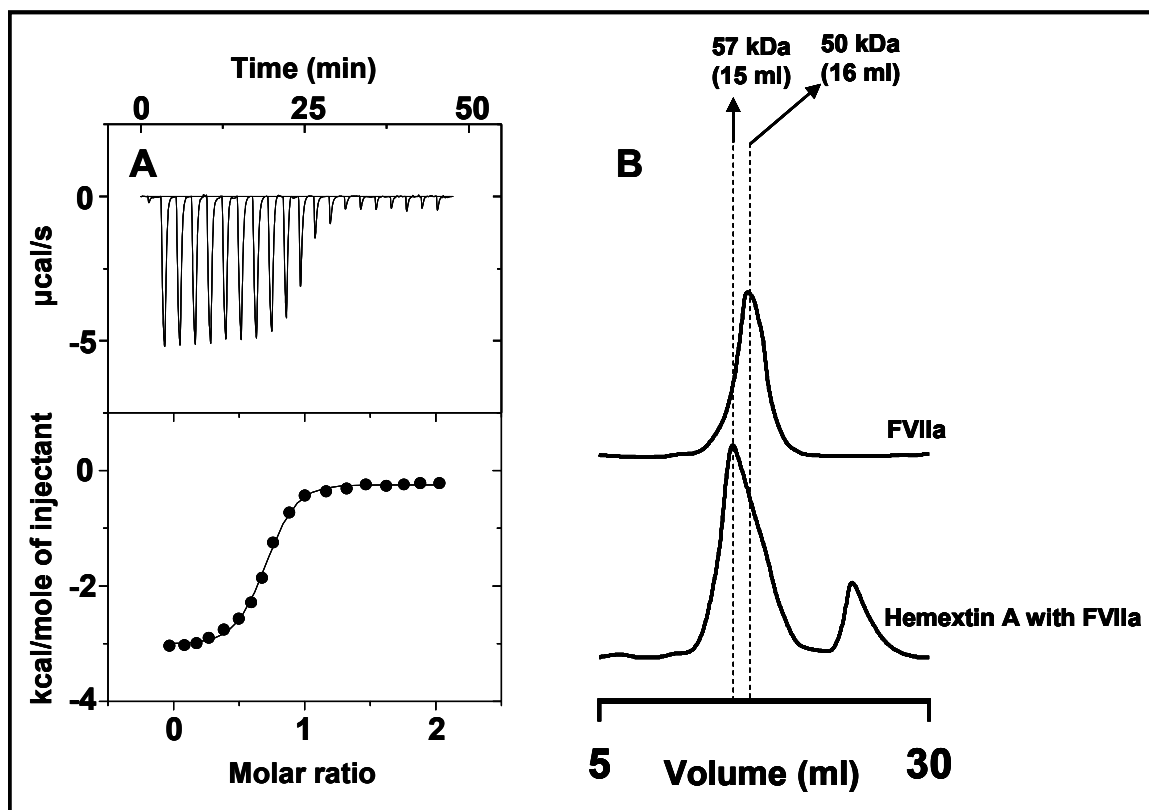


Figure 5.6 Binding of hemextin A to FVIIa. (A) ITC studies. Thermogram with the corresponding binding isotherm for the binding of hemextin A complex to FVIIa in 50 mM Tris buffer (pH 7.4); Note the presence of only one kinetic phase, unlike two as observed in the case of hemextin AB-FVIIa formation (B) SEC studies. Elution profiles of the complex of FVIIa with hemextin AB complex in 50 mM Tris buffer (pH 7.4); Note on complex formation there is a reduction in retention time.

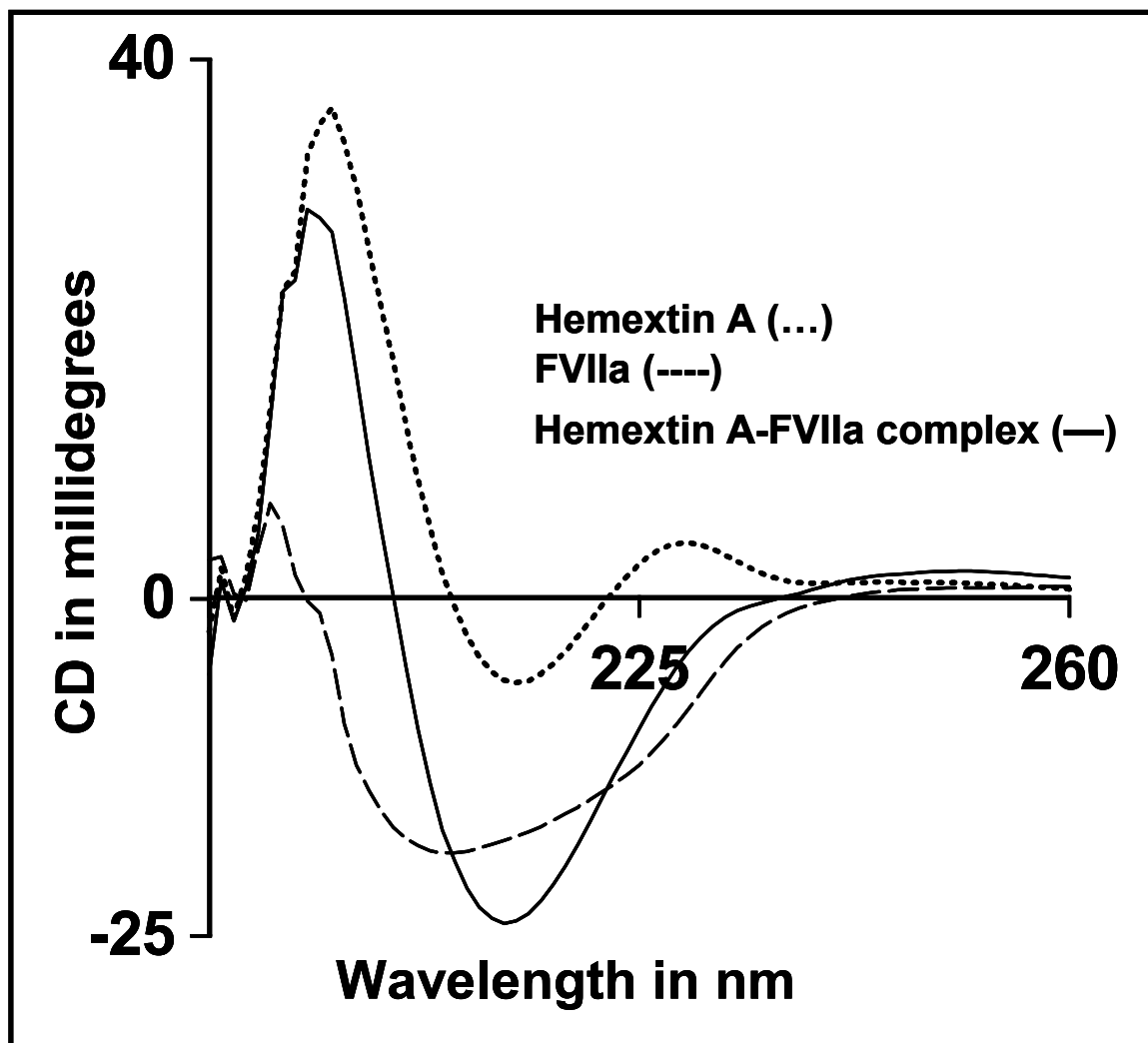


Figure 5.7 Conformational changes associated with the formation of hemextin A-FVIIa complex. Individual spectra of hemextin A, FVIIa are also shown for comparison.

stoichiometry (Figure 5.6A). Unlike, the thermogram of hemextin AB-FVIIa complex formation (Figure 5.3A) which has two kinetic phases, hemextin A-FVIIa complex had only one kinetic phase. The binding affinity (80 μ M) was also lower than that observed for the binding between tetrameric hemextin AB complex and FVIIa (Table 5.1), explaining the lower anticoagulant potency of hemextin A. The estimated molecular weight of the hemextin A- FVIIa complex from SEC studies was \sim 57000 Daltons (Figure 5.6B) validating 1:1 stoichiometry of complex formation. Since hemextin AB complex on binding to FVIIa, induces a conformational change in the FVIIa molecule, a similar study was conducted with hemextin A (Figure 5.7). CD studies with hemextin A and FVIIa showed that, hemextin A-FVIIa complex has a predominantly β -sheeted structure.

Binding of hemextin AB complex dimer to FVIIa – In chapter 4, we have seen that the anticoagulant complex exists as a tetramer. However, in the presence of glycerol (250 mM) and NaCl (150 mM), it dissociates and predominantly exists as a dimer. Prothrombin time assay indicate that the dimer in glycerol is active where as that in NaCl has no anticoagulant activity. We studied the binding between hemextin AB complex dimer (formed in both salt and glycerol) and FVIIa using ITC and SEC and compared it to the binding between FVIIa and hemextin A.

To determine whether the dimer formed in glycerol binds to FVIIa, we studied the interaction of hemextin AB complex with FVIIa in the presence of glycerol (250 mM). ITC experiments show that the interaction of dimeric hemextin AB complex with FVIIa is predominantly exothermic with 1:1 stoichiometry (Figure 5.8A). This was further confirmed using SEC, where the estimated molecular weight of the complex between dimeric hemextin AB complex and FVIIa complex was \sim 64000 Daltons. However, the

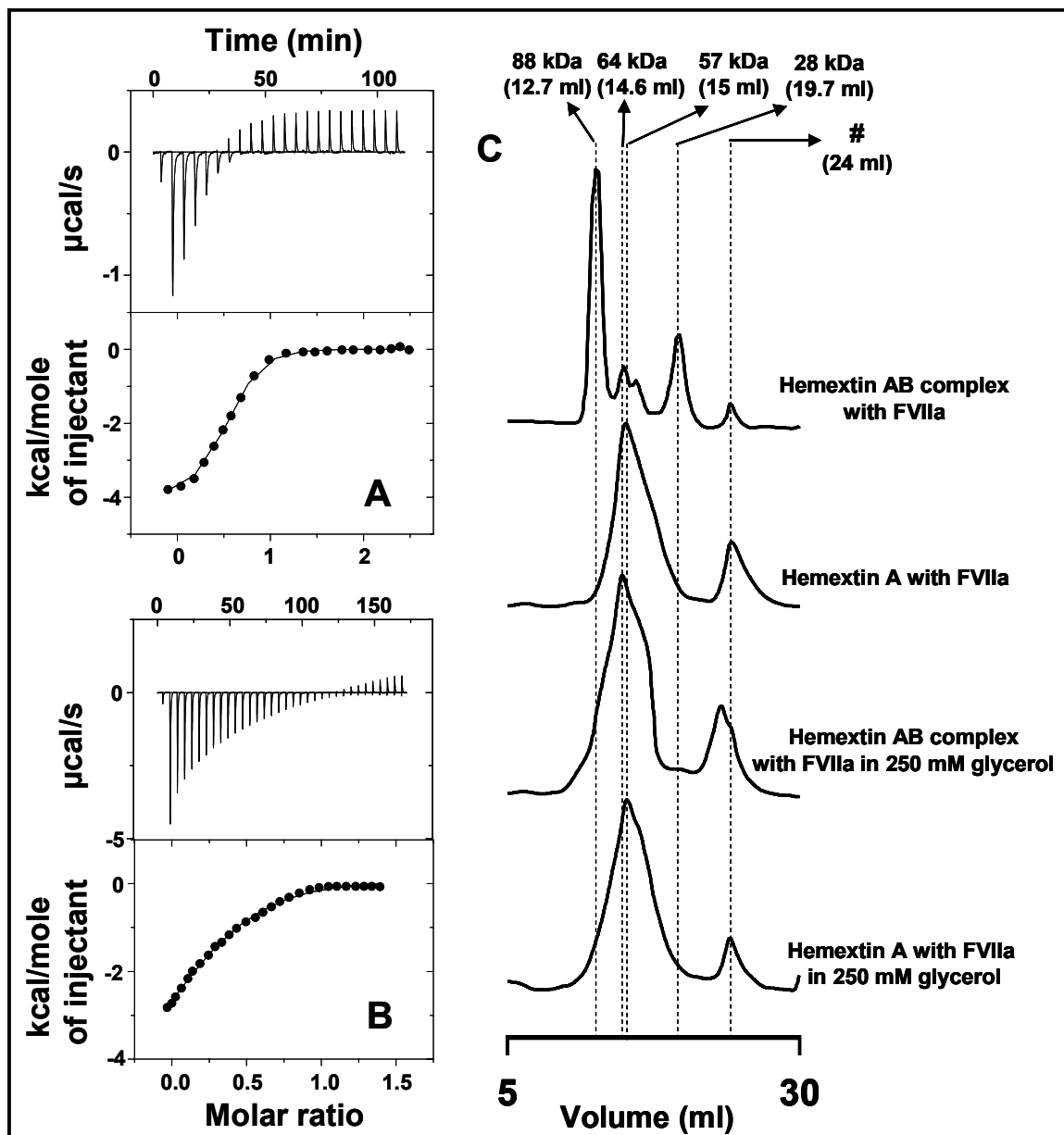


Figure 5.8 Binding of hemextin AB complex or hemextin A binding to FVIIa in 50 mM Tris buffer (pH 7.4) containing 250 mM glycerol. Thermograms with the corresponding binding isotherm for the binding of (A) hemextin AB complex (B) hemextin A to FVIIa. in Tris buffer containing 250 mM glycerol; (C) Elution profiles of hemextin AB complex or hemextin A with FVIIa in Tris-HCl buffer containing 250 mM glycerol.

Table 5.2

Thermodynamics of binding of hemextin AB complex/hemextin A to FVIIa in different buffer solutions

Binding to FVIIa	$K_A \times 10^5$ (M ⁻¹)	ΔH (kcal/mole)	ΔS (cal/deg.mole)	ΔG (kcal/mole)	Number of Binding Sites (<i>N</i>)
<i>Hemextin AB complex</i>					
Tetramer in Tris-HCl Buffer	4.11	-7.931	-1.112	-7.586	1.01
Dimer in glycerol	1.77	-3.933	-1.1	-3.62	1.05
Dimer in salt	0.119	-2.994	-1.66	-2.54	0.89
<i>Hemextin A</i>					
In Tris-HCl buffer	0.125	-3.005	-1.7	-2.5	1.00
In glycerol	0.118	-2.821	-1.74	-2.3	0.97
In salt	0.121	-3.042	-1.56	-2.6	1.03

Note: All experiments were carried at 37 °C

binding affinity for FVIIa was lower than that of the tetrameric hemextin AB complex but higher than that of hemextin A, alone (Table 5.2).

Binding between hemextin A and FVIIa in the presence of glycerol was predominantly exothermic (Figure 5.8B). The 1:1 stoichiometry of complex formation was confirmed by ITC (Figure 5.8B) and SEC (Figure 5.8C). The estimated molecular weight of hemextin A–FVIIa complex in glycerol was ~57000 Daltons (Figure 5.8C). No significant difference in the binding affinity of hemextin A for FVIIa was observed in the presence or absence of glycerol (Table 5.2). However, binding affinity of hemextin A for FVIIa was lower than that of the tetramer and dimeric hemextin AB complex in the presence of glycerol (Table 5.2).

Hemextin AB complex predominantly exists as a dimer in the presence of 150 mM NaCl. The dimer in salt has lower anticoagulant potency than that in glycerol and the anticoagulant potency of the dimer is same as that of hemextin A. To determine if the dimer in salt binds to FVIIa, ITC studies were conducted in 150 mM NaCl. Figure 5.9A and Table 5.2; show that the binding is predominantly exothermic with 1:1 stoichiometry. The estimated molecular weight of the dimeric hemextin AB- FVIIa complex from the SEC experiments was ~57000 Daltons (Figure 5.9C). Interestingly, the binding affinity of the dimer in salt for FVIIa was lower than that of the tetramer and the dimer in glycerol, but was almost identical that observed for hemextin A (in all the three conditions) (Table 5.2).

We also studied the binding of hemextin A to FVIIa in the presence of salt and glycerol. In salt hemextin A complexed with FVIIa with a 1:1 stoichiometry (Figure 5.9B) and the binding was predominantly exothermic. The estimated molecular weight of

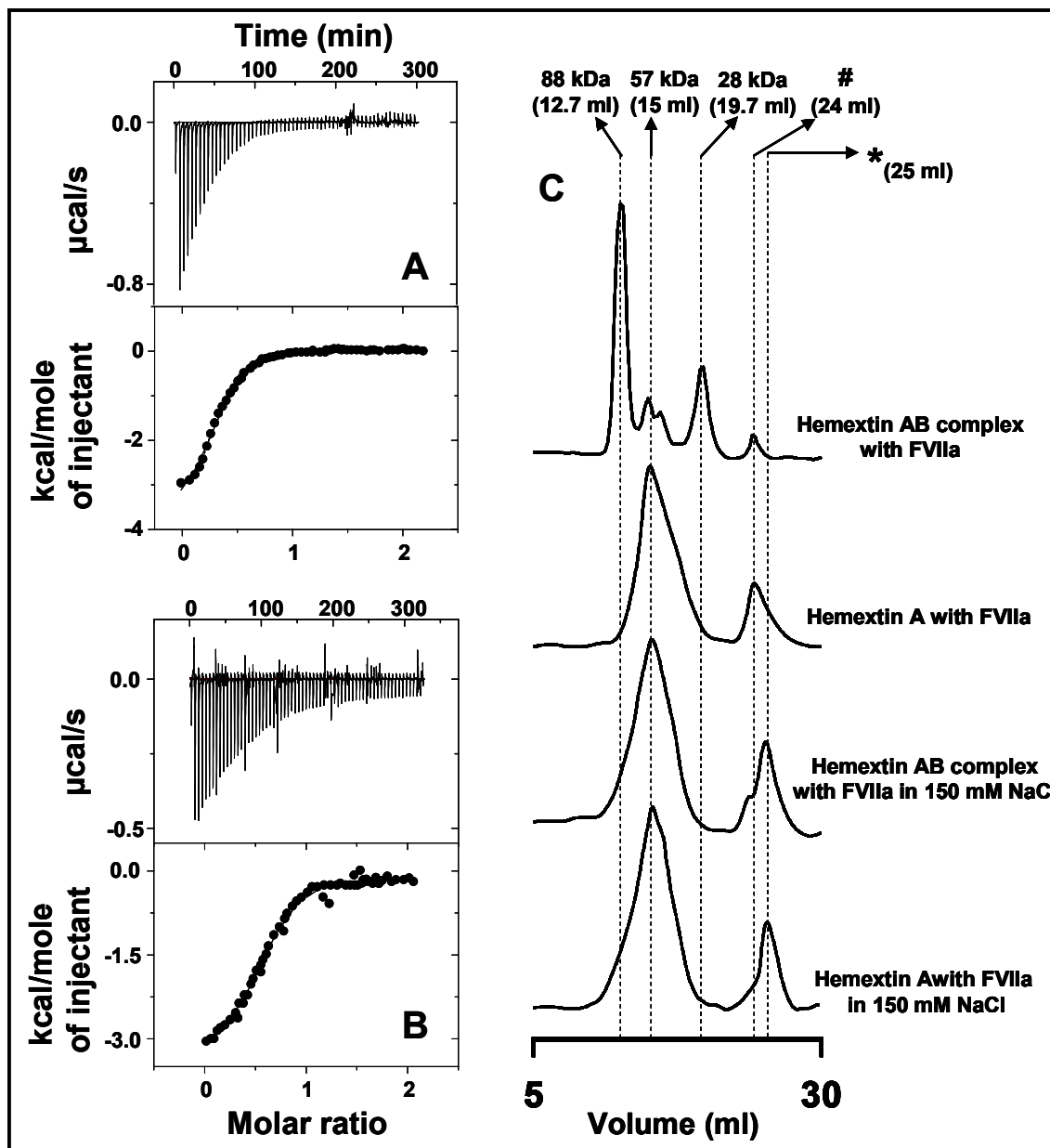


Figure 5.9 Binding of hemextin AB complex or hemextin A binding to FVIIa in 50 mM Tris buffer (pH 7.4) containing 150 mM salt. Thermograms with the corresponding binding isotherm for the binding of (A) hemextin AB complex (B) hemextin A to FVIIa. in Tris buffer containing 150 mM NaCl; (C) Elution profiles of hemextin AB complex or hemextin A with FVIIa in Tris-HCl buffer containing 150 mM NaCl.

the hemextin A- FVIIa complex in salt was ~57000 Daltons (Figure 5.9C), confirming the stoichiometry of complex formation. The binding affinity of hemextin A for FVIIa in the presence of salt was almost identical to that observed in the other two conditions (Table 5.2). This shows that the conformational change occurring in hemextin A in the presence of salt does not alter its affinity for FVIIa. However, the observed binding affinity of hemextin A for FVIIa was lower than that observed for tetrameric hemextin AB complex and dimeric hemextin AB complex (formed in glycerol) (Table 5.2). Interestingly, the observed binding affinity of hemextin A for FVIIa was nearly the same as that of dimeric hemextin AB complex (formed in the presence of salt).

The dimeric hemextin AB complex formed in the presence of glycerol binds to FVIIa with a higher affinity than hemextin A and hemextin AB complex dimer formed in salt. Again, the dimer formed in salt has the same binding affinity for FVIIa as that of hemextin A (Table 5.2). From these observations it can be concluded that the dimer formed in glycerol is different from the dimer formed in salt and dissociation of the tetramer into a dimer can take place in two different planes depending on buffer condition (which validates the proposed model). The reason for the higher anticoagulant potency of the dimer formed in glycerol is probably because one of the anticoagulant sites of the tetramer is conserved in this type of dimer. This observation also corroborates well with the proposed model. However, the lower anticoagulant potency of dimer formed in glycerol over that of the tetramer may be because of the fact that dimer formation destabilizes the anticoagulant site. Thus, although the stoichiometry remains the same, the binding affinity for FVIIa is diminished. The dimer in salt has similar binding affinity as hemextin A in the presence of salt (Table 5.2), albeit slightly lower. Under these

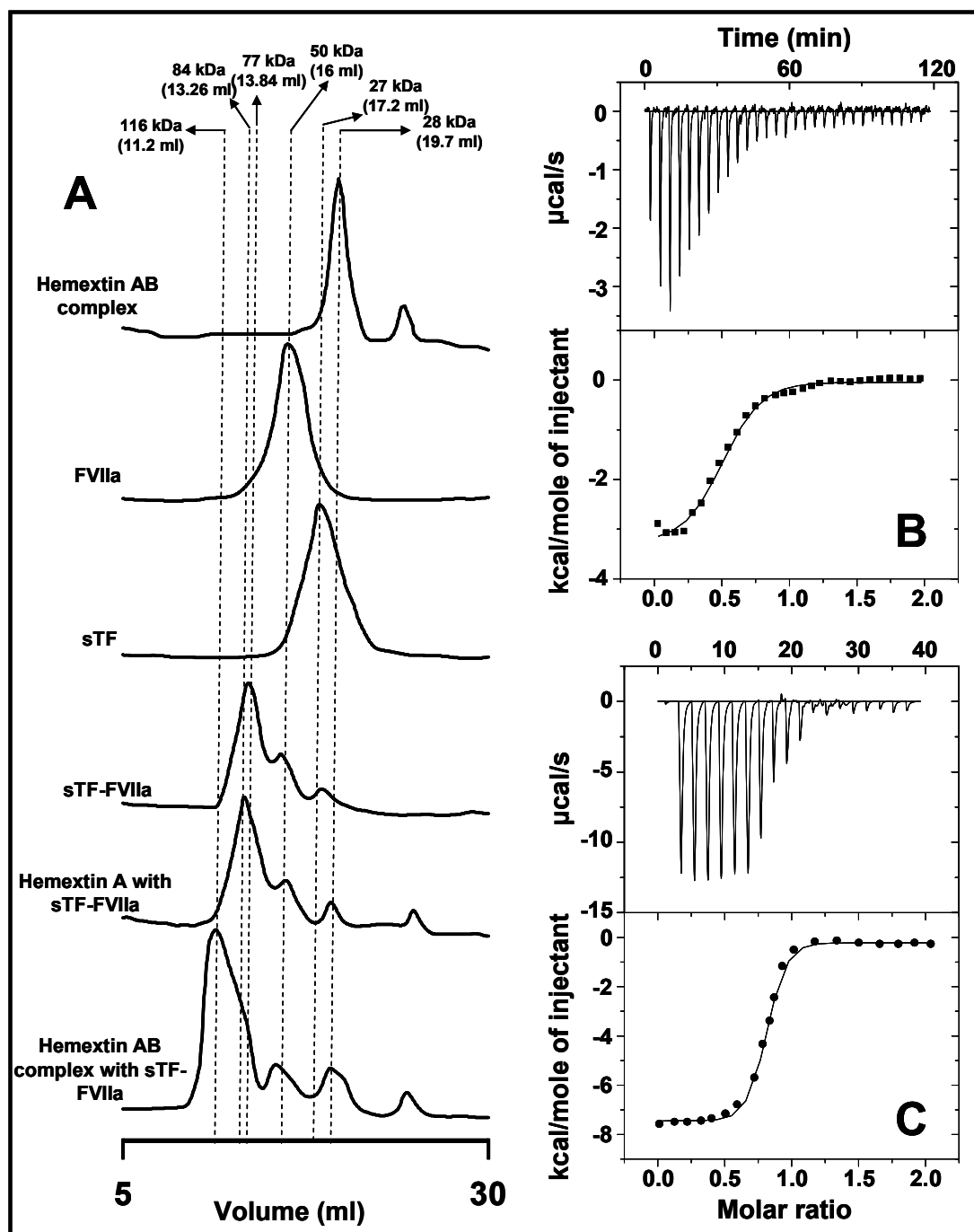


Figure 5.10 Binding of hemexin A/hemexin AB complex to sTF-FVIIa. (A) Elution profiles of the complex of sTF-FVIIa with hemexin AB complex/hemexin A. Thermograms with the corresponding binding isotherm for the binding of (B) hemexin A and (C) hemexin AB complex to sTF-FVIIa. (Note, the presence of sTF does not affect the binding between FVIIa and the anticoagulant protein or its complex.).

Table 5.3.

Thermodynamic analysis of binding to FVIIa and its derivatives to hemextin AB complex/hemextin A

Binding to FVIIa and its derivatives	$K_A \times 10^5 (M^{-1})$	ΔH (kcal/mole)	ΔS (cal/deg.mole)	ΔG (kcal/mole)	Number of binding site (N)
<i>Hemextin AB complex</i>					
FVIIa	4.11	-7.931	-1.112	-7.586	1.01
sTF-FVIIa	4.06	-7.84	-1.13	-7.49	1.16
FVIIa-Heavy chain	5.2	-7.82	-0.5	-7.67	0.921
FFRck-FVIIa	0.33	-5.01	-3.7	-4.74	1.08
<i>Hemextin A</i>					
FVIIa	0.125	-3.005	-1.7	-2.5	1.00
sTF-FVIIa	0.127	-3.1	-1.5	-2.69	1.07
FVIIa-Heavy chain	0.798	-4.1	-1.2	-3.7	0.96
FFRck-FVIIa	0.065	-2.3	-1.2	-1.3	0.94

Note: All experiments were carried at 37 °C

conditions only hemexin A forms a complex with FVIIa and the molecular weight is ~57000 Daltons.

Effect of sTF on the binding of anticoagulant proteins to FVIIa – In Chapter 3, we have seen that hemexin AB complex exhibits similar IC₅₀ values (~100 nM) for inhibition of both FVIIa and sTF-FVIIa. Therefore, we investigated the binding of the anticoagulant protein and its synergistic complex with sTF-FVIIa, and compared it to the binding to FVIIa alone. Hemexin A binds to sTF-FVIIa with 1:1 stoichiometry (Figure 5.10B), the estimated molecular weight of the sTF-FVIIa-hemexin A complex being 77,000 Da (Figure 5.10A). Hemexin AB complex also binds to sTF-FVIIa in 1:1 stoichiometry, though its binding affinity towards the procoagulant complex is higher than hemexin A (Figure 5.10C) (Table 5.3). The estimated molecular weight of the FVIIa-sTF-hemexin AB complex was estimated to be 116,000 Da (Figure 5.10A).

Interestingly, no significant change was observed in the recorded binding affinity between FVIIa and the anticoagulant proteins, in the presence of sTF (Table 5.3). According to the X-ray crystallographic structure of sTF-FVIIa solved by Banner *et al.* at 2.0 Å resolution (PDB code 1DAN) (Banner *et al.*, 1996), the two fibronectin domains of sTF have extensive contact with the γ -carboxyglutamic acid (Gla) and the first epidermal growth factor (EGF1) like domains of FVIIa. This observation is also supported by mutational data. However, minor contact regions do exist between sTF and the second EGF and protease domains of FVIIa. Since, sTF does not affect the binding affinity between FVIIa and hemexin A/hemexin AB complex, the regions of FVIIa participating in complex formation with sTF are not involved in binding with the anticoagulant protein or its complex.

Interaction with individual FVIIa chains – FVIIa consists of an NH₂-derived light chain (relative molecular mass, 20,000) consisting of 152 amino acid residues and a COOH terminal-derived heavy chain (relative molecular mass, 30,000) consisting of 254 amino acid residues linked via a single disulfide bond (Cys135 to Cys262). The light chain contains the membrane-binding Gla domain and two EGF domains (EGF1 and EGF2), while the heavy chain contains the catalytic protease domain (Kranjc *et al.*, 2005). Above studies with sTF showed that the binding site of the anticoagulant protein and its complex can not be localized in the Gla and EGF1 domains of FVIIa light chain. Therefore, we studied the interaction of the individual separated chains of FVIIa with hemextin A and hemextin AB complex.

Light chain of FVIIa showed no binding to either hemextin A or hemextin AB complex. This may not be due to the conformational change(s) in the light chain isolated under reducing conditions since light chain produced under non-reducing conditions did not exhibit any binding as well. This observation ruled out EGF2 domain of FVIIa as a binding site for the anticoagulant protein and its complex. The separated heavy chain of FVIIa exhibited binding to both hemextin A and hemextin AB complex (Figure 5.11). Interestingly, the recorded binding affinity of the anticoagulant protein and its complex for the heavy chain was slightly higher than that recorded for FVIIa (Table 3). This may be due to better exposure of the anticoagulant binding site in the absence of the light chain. Thus, the binding site of hemextin A and hemextin AB complex is localized in the heavy chain of FVIIa.

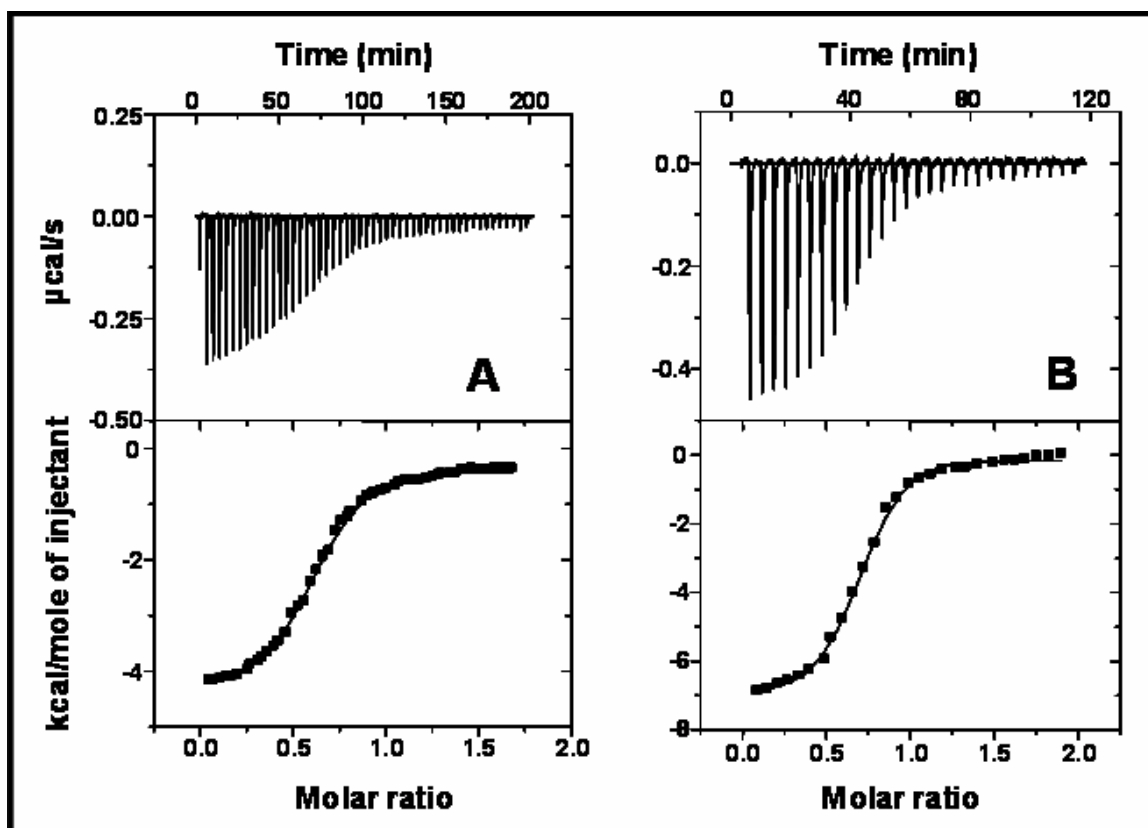


Figure 5.11 Binding of hemextin A/hemextin AB complex to the heavy chain of FVIIa. Thermograms with the corresponding binding isotherm for the binding of (A) hemextin A and (B) hemextin AB complex to the heavy chain of FVIIa.

Interaction with active site inhibited FVIIa – Previous studies show that hemexin AB complex is a non-competitive inhibitor of sTF-FVIIa ($K_i = 25$ nM). Therefore, occupation of the active site of FVIIa will not inhibit complex formation between FVIIa and anticoagulant protein/complex. We investigated the complex formation of FFRck-FVIIa with hemexin A and hemexin AB complex. SEC studies showed that FFRck-FVIIa retains complex formation ability with hemexin A and hemexin AB complex (Figure 5.12). The estimated molecular weight of FFRck-FVIIa-hemexin A complex and FFRck-FVIIa-hemexin AB complex was 57,000 Da and 88,000 Da respectively. No, significant change in the molecular weight was observed over that of the corresponding complexes of the anticoagulant proteins with FVIIa. This may be because; the molecular weight of FFRck is negligible and therefore adds little to the molecular weight of FVIIa. Binding was further confirmed using ITC. The binding is exothermic and takes in 1:1 stoichiometry (Figure 5.12B and C). However, the recorded binding affinity showed that the anticoagulant protein and its complex bind with lower affinity to FFRck-FVIIa than FVIIa (Table 3). This may be because of the conformational changes involved at the S2 sub-site (According to the nomenclature of Schechter and Berger (Schechter and Berger, 1967)) originating from the active site; taking place on the binding of FFRck to FVIIa (Kemball-Cook *et al.*, 1999). This observation again highlights the binding site of the anticoagulant protein and its complex to be localized in the heavy chain of FVIIa, but away from the active site.

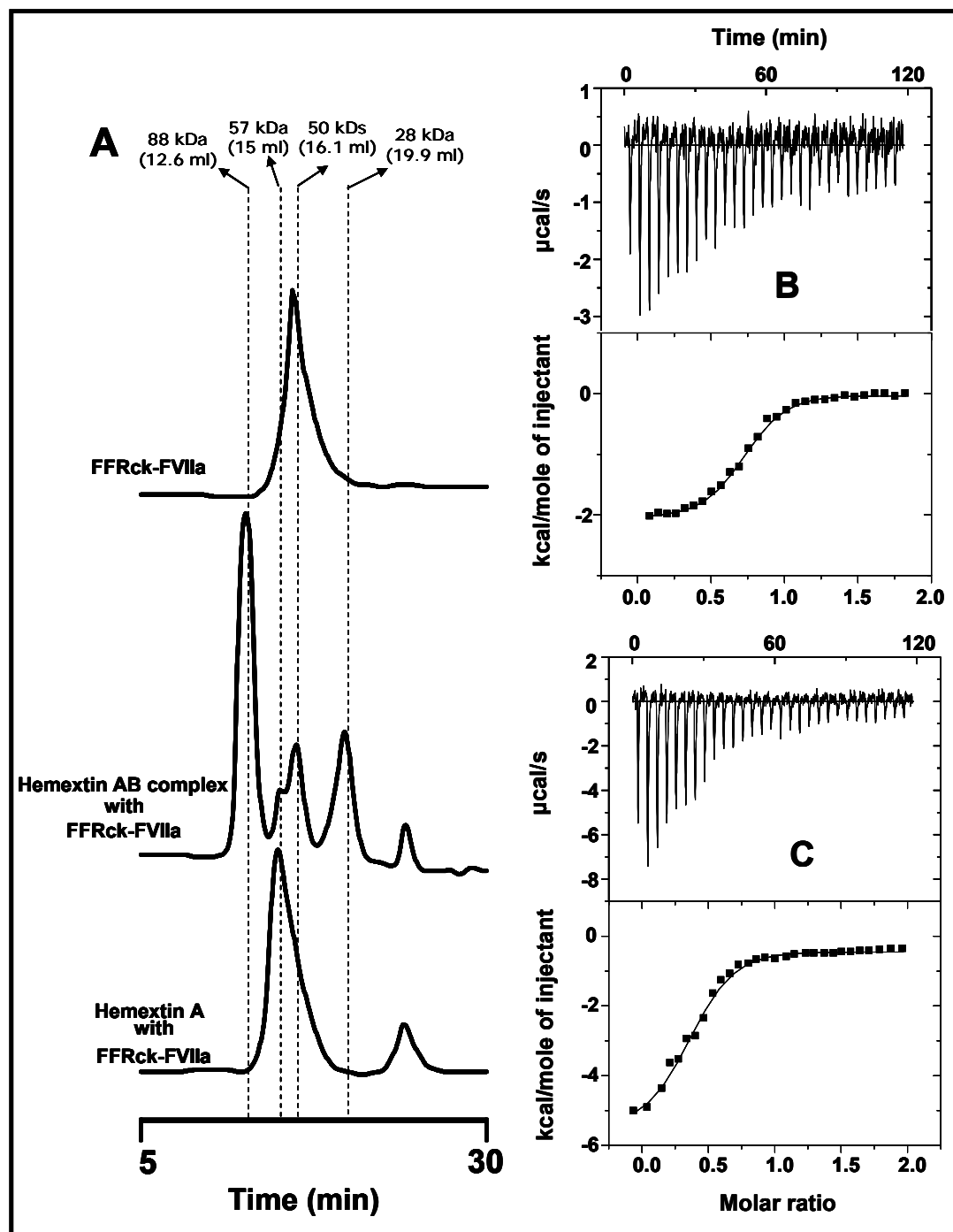


Figure 5.13 Binding of hemexin A/hemexin AB complex to active site blocked FVIIa (FFRck-FVIIa). (A) Elution profiles of the complex of FFRck-FVIIa with hemexin AB complex/hemexin A. Thermograms with the corresponding binding isotherm for the binding of (B) hemexin A and (C) hemexin AB complex to FFRck-FVIIa.

CONCLUDING REMARKS

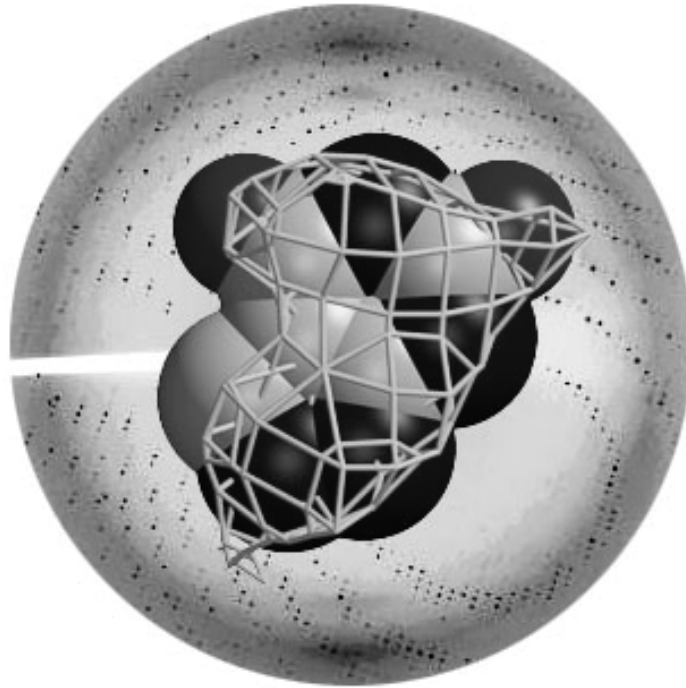
Hemextin A and hemextin AB complex bind to the heavy chain of FVIIa. Binding to FVIIa takes place with equal affinity irrespective of the presence or absence of co-factor. However, further studies with exosite binding peptides will help us to identify the particular region of the FVIIa heavy chain that participates in the binding process. Binding also takes place even when the active site of FVIIa is blocked; this highlights the non-competitive nature of inhibition both for the anticoagulant protein and its complex, which is also supported by enzyme kinetic studies (Chapter 3). This study therefore facilitates our understanding of the inhibitory mechanism of the hemextin A and hemextin AB complex, and therefore will help in devising novel anticoagulation strategies targeting the heavy chain of FVIIa.

Thank you note,

The work narrated in chapter 5 is currently under consideration in the Journal of Biological Chemistry. After, finding out that hemextin AB complex/hemextin A specifically binds to FVIIa, I was intrigued to find out the exact chain of FVIIa to which the anticoagulant proteins bind. For these studies, I needed an in depth knowledge of the structure & function of FVIIa, and many a times I had to write to the stalwarts in the field of FVIIa biochemistry for their suggestions. Two of them had always answered my questions and without their help I would not have been able to complete some of the experiments detailed in the chapter. Before I proceed to the next chapter, I will like to thank Dr James H. Morrissey (Department of Biochemistry, University of Illinois College of Medicine, Urbana-Champaign) and Dr Robert A. Lazarus (Department of Protein Engineering, Genentech, Inc.) for helpful discussions.

-- Yajnavalka Banerjee

“When I am working on a problem I never think about beauty. I only think about how to solve the problem. But when I have finished, if the solution is not beautiful, I know it is wrong.” - Buckminster Fuller (1895-1983)



Chapter 6¹

Structural Characterization of Anticoagulant Protein Hemexin A

¹This picture shows three stages in solving a biological structure by X-ray crystallography. The background is a diffraction image, which we can observe on a X-ray sensitive detector when illuminating a crystal with X-rays. The spots of varying intensity carry the structural information we are interested in. The foreground is electron density and the interpretation of it, the atomic model (shown as space-filling model). (Adapted with kind permission from the lab page of Dr. Karsten W. Theis, University of Massachusetts Amherst)

The Future of X-Ray Analysis

The number of papers on crystal structure rose rapidly until 1933, then fluctuated about a mean. This date may be taken as the end of the heroic age of X-ray analysis. It was then realized that the new structures would be essentially like the old ones, and interest was directed towards new and more complex phenomena... Beyond the ordinary compounds of organic chemistry there lies the wide range of complicated biological molecules of which the proteins are the best known but by no means the only type...The structure of the proteins, fundamental to the understanding of living processes, will not yield to X-ray analysis alone; the attack must be combined with biochemical, electrophoretic, electron microscope and other methods, but there is no doubt that X-rays will play a crucial part in verifying all hypothetical structures put forward on any other basis.

--- Prof. J.D. Bernal, FRS, Birkbeck College, London; Nature, June 1945.

Much of our understanding of protein function at the atomic level originates from studying protein structures. Several technologies are employed to study the three-dimensional structures of proteins. The two techniques that have been widely used to elucidate protein structure are: single-crystal X-ray diffraction and nuclear magnetic resonance (NMR) spectroscopy².

For the proteins that form suitable crystals, X-ray crystallography represents a mature and rapid approach. Since, this technique was used for determining the structure of hemextin A, the methodology will be discussed in a greater detail (see below).

Soluble proteins that do not crystallize readily can only be studied by solution state NMR spectroscopy. For proteins larger than around 15 kDa, however, this method is relatively slow compared to crystallography, and isotope labeling is required. But, NMR has a number of important uses that are complementary to crystallography. It is particularly good at studying relatively small proteins or domains, which are often difficult to crystallize. It can also be used to help with the "phase" problem, by providing structural information about domains within a larger protein. It can also identify flexible regions in a protein that may be causing problems with crystallization or difficulties with chain tracing. NMR has a unique ability to study unfolded proteins at the atomic level and it can play a significant role as an analytical tool - defining the purity and stability of

²“If biology were a car, structural biologists would be looking under the bonnet to find out how the engine works. Put more prosaically, structural biology aims to understand how biology works at the molecular level. Much information is gleaned by studying at atomic resolution the three-dimensional structures of molecules that make up living organisms, and the interactions of these molecules with one another. But, just as a photograph of a car engine doesn’t tell us how that engine actually works, static biological structures alone may not suffice for us to work out the functional mechanisms of biomolecules. Instead, a video of the structural dynamics — analogous to observations of a running car engine made from inside and out — would be much more revealing.”

– Ad Bax and Dennis A. Torchia, “Molecular Machinery in Action” *Nature* (2007), 445, 609

protein preparations. It can also be used to identify the relative flexibility of domains in a multi-domain protein (Ulmer *et al.*, 2002).

Electron microscopy (EM) can be utilized in protein structural analyses. However, EM is not extensively utilized for the determination of three-dimensional structure of proteins, but for solving the structures of large supramolecular assemblies. Although mainly aiming at molecular resolution (10-30 Å), electron microscopy can provide near-atomic resolution e.g., tubulin (Nogales *et al.*, 1998), aquaporin (Murata *et al.*, 2000), light-harvesting complex (Kuhlbrandt *et al.*, 1994), and bacteriorhodopsin (Henderson *et al.*, 1990). Time-resolved techniques offer the possibility of studying conformations that are inaccessible to X-ray crystallography. For example, the activated state of the nicotinic acetylcholine receptor, which has a lifetime of 10 ms, was studied at 4.6-9 Å resolution, using three-dimensional helical reconstruction of tubular membrane crystals (Unwin, 1995; Miyazawa *et al.*, 1999). Another means of imaging biological samples with molecular resolution is by atomic force microscopy (AFM). In addition to providing topographical images of surfaces with nanometer- to angstrom-scale resolution, forces between single molecules and mechanical properties of biological samples can be investigated. Other lesser used approaches for studying protein structure include correlative microscopy, multi-color labeling/cluster analysis and electron tomography.

X-ray crystallography

X-ray diffraction analysis of crystal structures is quite analogous to using a very high-power microscope that can see molecular shapes. The wavelength of the light used is usually in the vicinity of 1.5 Å, about the length of a single carbon-carbon bond, and the use of X-rays with this wavelength permits, in theory, resolution of individual atoms.

In this technique, the intensities of the diffracted X-rays from the single crystal together with some additional data described below, allows one to compute the three dimensional structure of the protein (present in the crystal). The crystal acts as a three-dimensional diffraction grating and scatters the incident beam of X-rays only in certain directions. But all the molecules in the crystal scatter together in these directions, and since there are $>10^{15}$ molecules, at least in most crystals, this enables the scattered signal to be recorded before the specimen is destroyed by radiation damage.

It can be demonstrated that this diffraction is the vector sum of the diffraction by the individual atoms of the unit cell, each having amplitude that is related to the number of electrons and the size of the atom as well as a phase that is derived from the position of the atom within the unit cell. The sum of these individual contributions is a vector with an amplitude $|F(\underline{h})|$ and a phase $\alpha(\underline{h})$ where \underline{h} is equal to (hkl) and h , k , and l are the Miller indices that define the diffraction maxima.

$F(\underline{h})$, designated as the structure factor (because it depends only on the structure of the scatterer), can be expressed in terms of the f_j , the individual scattering factors for the j atoms in the unit cell, and the atomic coordinates x_j .

$$F(\underline{h}) = \sum_j f_j \exp 2\pi i (h \cdot x_j) = |F(\underline{h})| \exp i \alpha(\underline{h}) \dots\dots\dots (Eq.1)$$

By rotating the crystal relative to the X-ray beam, it is possible to record and measure the complete diffraction pattern of the crystal. $|F(\underline{h})|$ can directly be measured since it is related to the intensities of the diffraction maxima, but the phase angle $\alpha(\underline{h})$, cannot be measured experimentally. These lost phases are recovered by mainly using three methods, two of which (multiple isomorphous replacement (Green *et al.*, 1964) and

anomalous scattering (Yang *et al.*, 1990)) involve heavy atoms, while the third uses a procedure called molecular replacement. When both the amplitudes and the phases of the scattered X rays are known, they can be combined to produce an electron-density map of the contents of the unit cell, the repeating unit of the crystal. The electron density (ρ) at any position xyz in the unit cell of the crystal is represented by the following equation (with i equal to the square root of -1).

$$\rho(x, y, z) = \sum_{hkl} |F(h, k, l)| \exp i\alpha(hkl) \exp -2\pi i(hx + ky + lz) \dots\dots\dots \text{(Eq.2)}$$

The resolution of the electron density map depends on the angular extent to which the intensity data have been measured. This is related to the spacing, d , of lattice planes within the unit cell according to Bragg's Law:

$$\lambda = 2d \sin \theta \dots\dots\dots \text{(Eq.3)}$$

where, λ is the wavelength of the diffracted X rays and θ is the diffraction angle. Resolution in a protein structure is usually defined as the value of the d_{\min} corresponding to the θ_{\max} of the data set. For highly ordered small-molecule crystals that can diffract to the limit allowed by the wavelength of the X rays used i.e., to $\theta_{\max} = 90^\circ$, the resolution would be $1/2 \text{ \AA}$. Proteins have not yet been observed to attain this resolution.

After an electron density of good resolution is obtained, the polypeptide sequence of the protein is fitted to this map to generate the initial model of the protein. The initial model of the protein will contain significant errors resulting from the imperfect phasing of the experimental electron-density map. This model is therefore improved, a procedure called refinement. The aim of refinement is to minimize differences between the calculated and experimental structure factors while at the same time optimizing the stereochemistry.

There are a variety of software packages available for refinement, listed in Westhof and Dumas (Westhof and Dumas, 1996). The progress of the refinement can be indicated partly by the value of the so-called *R* factor, given by:

$$R = \frac{\sum \|F_o(\underline{h}) - |F_c(\underline{h})|\|}{\sum |F_o(\underline{h})|} \dots\dots\dots \text{(Eq.4)}$$

R factor can vary from 0.4 to 0.5 (or from 40% to 50%, if expressed as a percentage) for an essentially correct but unrefined structure, to values as low as 0.12 (12%) for an exceptionally well-refined structure. Most well-refined structures produce *R* values <0.2 (20%).

After the initial structure of the protein is obtained, it is assessed for errors using the Ramachandran plot (RAMACHANDRAN *et al.*, 1963). The Ramachandran plot is used by structural biologist to verify the stereochemistry of the determined structure. Recently, Brunger (Sutton *et al.*, 1998) has proposed a cross-validation procedure that involves omitting a certain percentage (approximately 10%) of the reflections in the refinement but using them to calculate an *R*_{free}, which will then provide an independent check of the validity of the structure.

Structure of hemexin A

As discussed in the previous chapters, hemexin AB complex is the only known heterotetrameric complex of three-finger toxins. It is also the only known natural inhibitor of FVIIa, which unlike the other known natural inhibitors (TFPI and NAPc2) does not use FX or TF to bind to FVIIa. Of the two proteins that participate in the formation of hemexin AB complex, hemexin A individually exhibits mild anticoagulant activity where as hemexin B is inactive. Using X-ray crystallography, we have solved

the three-dimensional structure of hemextin A. In this chapter, we discuss the crystallization, data collection and structure determination of hemextin A, the active component participating in the formation of hemextin AB complex.

MATERIALS AND METHODS

Proteins and Reagents – Hemextin A, was isolated from the crude venom of *H. haemachatus* in the same way as detailed in Chapter 2. Crystallization Screens (I & II), crystallization trays and grease were purchased from Hampton Research 34 Journey, Aliso Viejo, CA, USA. All other reagents were of the highest analytical grade.

Crystallization of hemextin A – Two of the most commonly used methods for protein crystallization³ fall under the category of vapor diffusion. These are known as the hanging drop and sitting drop methods. Both entail a droplet containing purified protein, buffer, and precipitant being allowed to equilibrate with a larger reservoir containing similar buffers and precipitants in higher concentrations. Initially, the droplet of protein solution contains an insufficient concentration of precipitant for crystallization, but as water vaporizes from the drop and transfers to the reservoir, the precipitant concentration increases to a level optimal for crystallization. Since the system is in equilibrium, these optimum conditions are maintained until the crystallization is complete (McPherson, 1990).

³ The protein crystallization process is still empiric and a biggest part of the success is hidid (hidden) in the hand and experience of the scientist who performed the protein crystallization and pure luck.

- Rhodes, Gale. "Crystallography Made Crystal Clear". San Diego: Academic Press, 1993

The hanging drop method differs from the sitting drop method in the vertical orientation of the protein solution drop within the system. It is important to mention that both methods require a closed system, that is, the system must be sealed off from the outside using an airtight container or high-vacuum grease between glass surfaces.

Crystallization trials for hemextin A were conducted using the hanging drop vapor diffusion method and a wide range of conditions were tested using the Hampton Research Screens (I & II). In either case, the protein concentration was kept approximately 30 mg/ml and the drops were prepared by mixing equal volumes (1 μ l) of protein solution and the crystallizing solution. The initial screening identified the crystallization conditions for hemextin A with polyethyleneglycol (PEG) 4000 as a precipitating agent. By systematic optimization around the preliminary condition, we obtained diffraction quality crystals for hemextin A. The crystals of hemextin A were obtained from 0.2 M ammonium acetate, 0.1 M sodium acetate trihydrate, 30% (w/v) PEG 4000 (pH 4.6) and appeared 12 to 15 days after they were set up. The crystals were rod-shaped and belonged to the orthorhombic crystal system (Figure. 6.1).

Data Collection – One complete native data set for hemextin A was collected. Prior to data collection, crystals of the protein were briefly soaked in a cryo-protectant solution consisting of mother liquor supplemented with 25% (w/v) glycerol. Crystals were picked by a nylon cryo-loop, and frozen at 100 K in nitrogen (gas) cold stream (Cryostream cooler; Oxford Cryosystems, Oxford, England). A complete data set was then measured both at R-Axis IV++ area detector mounted on a rotating anode X-ray generator (CuK α radiation) and at synchrotron beamline using Quantum 4-CCD detector, Brookhaven National Laboratory.

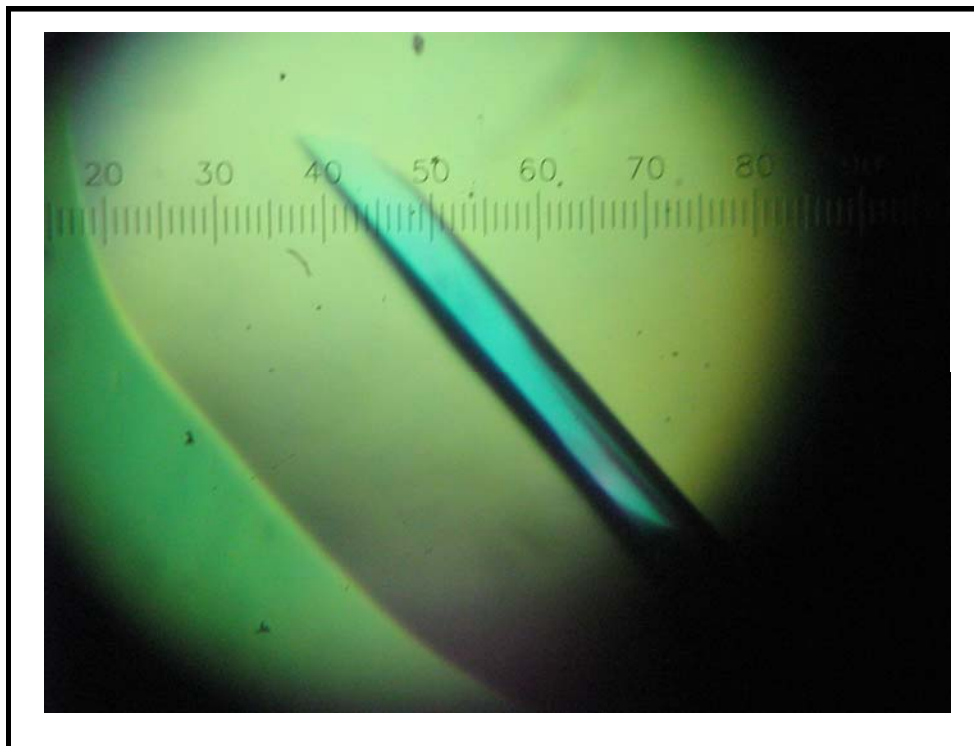


Figure 6.1 Crystal of hemextin A. Diffraction quality crystals for hemextin A. were obtained from 0.2 M ammonium acetate, 0.1 M sodium acetate trihydrate, 30% (w/v) PEG 4000 (pH 4.6) and appeared 12 to 15 days after they were set up. The crystals were rod-shaped and belonged to the orthorhombic crystal system

The data were indexed, integrated, and scaled using *HKL2000* (Yeates, 1997). Hemextin A crystal belonged to the orthorhombic system, and diffracted up to 1.5 Å resolution. The space group was established as $P2_12_12_1$, with $a = 49.27$, $b = 49.51$ and $c = 57.87\text{Å}$, $V_m = 2.92 \text{ Å}^3 \text{ Da}^{-1}$, two molecules per asymmetric unit and corresponded to a solvent content of 57.9%.

Solution of structure and refinement – The structure of the hemextin A was determined by molecular replacement method using MolReP program. The coordinates of *Naja nigricollis* toxin- γ monomer structure (PDB code 1tgx) were used as a search model. Two hemextin A molecules were located in the asymmetric unit after rotation and translation function searches. The rigid body refinement after determining the translation components gave a correlation coefficient of 0.63 and $R = 0.51$. The resultant electron-density map obtained for hemextin A was of good quality. Several cycles of map fitting with the using O v7.0 (Jones *et al.*, 1991), and refinement using the program CNS v.1.1. (Brunger *et al.*, 1998) led to convergence. During the initial stage of refinement Non Crystallographic Symmetry (NCS) restraints were used. The crystallographic and refinement statistics were given in Table 6.1.

Table 6.1 Crystallographic data and refinement statistics*

Data set	Hemextin A
Crystal	
Space Group	P2 ₁ 2 ₁ 2 ₁
Unit Cell Parameters (Å)	a= 49.27 b= 49.51 c= 57.87
Data collection	
Resolution range (Å)	50-1.50
Wavelength (Å)	0.9795
Observed reflections	287505
Unique reflections	23374
Completeness (%)	99.9
Overall ($I/\sigma I$)	10.5
Redundancy	12
R_{sym}^a (%)	7.1
Refinement and Quality	
Resolution range (Å) $I > \sigma(I)$	20-1.50
R_{work}^b	0.2276
R_{free}^c	0.2577
RMSD bond lengths (Å)	0.01
RMSD bond angles(°)	1.9
Average B-factors (Å²)	
Protein atoms (928 atoms)	14.41
Water molecules (361 atoms)	36.88
Ramachandran plot	
Most favored regions (%)	86.5
Additional allowed regions (%)	11.6
Generously allowed regions (%)	1.9
Disallowed regions (%)	0

* Statistics from the current model. ^a $R_{\text{sym}} = \sum |I_i - \langle I \rangle| / \sum I_i$ where I_i is the intensity of the i^{th} measurement, and $\langle I \rangle$ is the mean intensity for that reflection.

^b $R_{\text{work}} = \sum |F_{\text{obs}} - F_{\text{calc}}| / \sum F_{\text{obs}}$ where F_{calc} and F_{obs} are the calculated and observed structure factor amplitudes, respectively.

^c R_{free} = as for R_{work} , but for 8.0% of the total reflections chosen at random and omitted from refinement.

Model Validation – The correctness of stereo-chemistry of the model was verified using *PROCHECK*. The calculations of r.m.s. deviations from ideality for bonds, angles, and dihedral and improper angles performed in *CNS* showed satisfactory stereochemistry. Ramachandran plot, showed approximately 87% of all residues within the most favored regions and no residues in the disallowed regions. An example of the electron density from a simulated annealing omit map in the conserved region is presented in Figure 6.2.

RESULTS AND DISCUSSION

Structure of hemextin A – The three-dimensional structure of hemextin A was determined at 1.5Å resolution. The crystal structure of hemextin A shows the general three-fingered folding and consists of six β -strands ($\beta 2 \downarrow \beta 1 \uparrow \beta 4 \downarrow \beta 3 \uparrow \beta 6 \downarrow \beta 5 \uparrow$) which forms two β -sheets (Figure 6.3). The first β -sheet consists of two antiparallel β -strands $\beta 1$ (Lys2-Lys6) and $\beta 2$ (Phe10-Thr14), while the second contains four antiparallel strands $\beta 3$ (Leu21-Thr26), $\beta 4$ (Ile35-Thr40), $\beta 5$ (Ala42-Ser47) and $\beta 6$ (Lys51-Asn56). The overall structure of the protein is conserved with other members of the three-finger family. The fold of hemextin A is maintained by four disulfide bonds.

As mentioned above, there are two molecules in the asymmetric unit. The overall dimensions of the dimeric hemextin A is approximately $36 \times 22 \times 22 \text{Å}$, with that of the monomer being $29 \times 13 \times 22 \text{Å}$. The two molecules of the asymmetric unit are held together by the hydrophobic interactions mediated by the side chains of Leu7, Tyr23, Met25, Leu27, Ile35, Pro44, Leu48, Leu49 and Val50 from both monomers.

A search for topologically similar proteins within the PDB was performed with the program DALI (Holm and Sander, 1993). Significant structural similarity was found between the hemextin A and several three finger toxins. The highest structural similarity is observed between hemextin A and toxin- γ (Bilwes *et al.*, 1994), a carditoxin from *Naja nigricollis* (PDB code 1tgx) yielding an RMSD of 1.7Å for 60 C α atoms, with a Z score 10.7. This is followed by bucandin (Torres *et al.*, 2001), a presynaptic neurotoxin from *Bungarus candidus* (PDB code 1f94; RMSD of 2.3Å for 56 C α atoms with a Z score 8.6 and erabutoxin b (REF), a neurotoxic protein binding to acetylcholine receptor from the

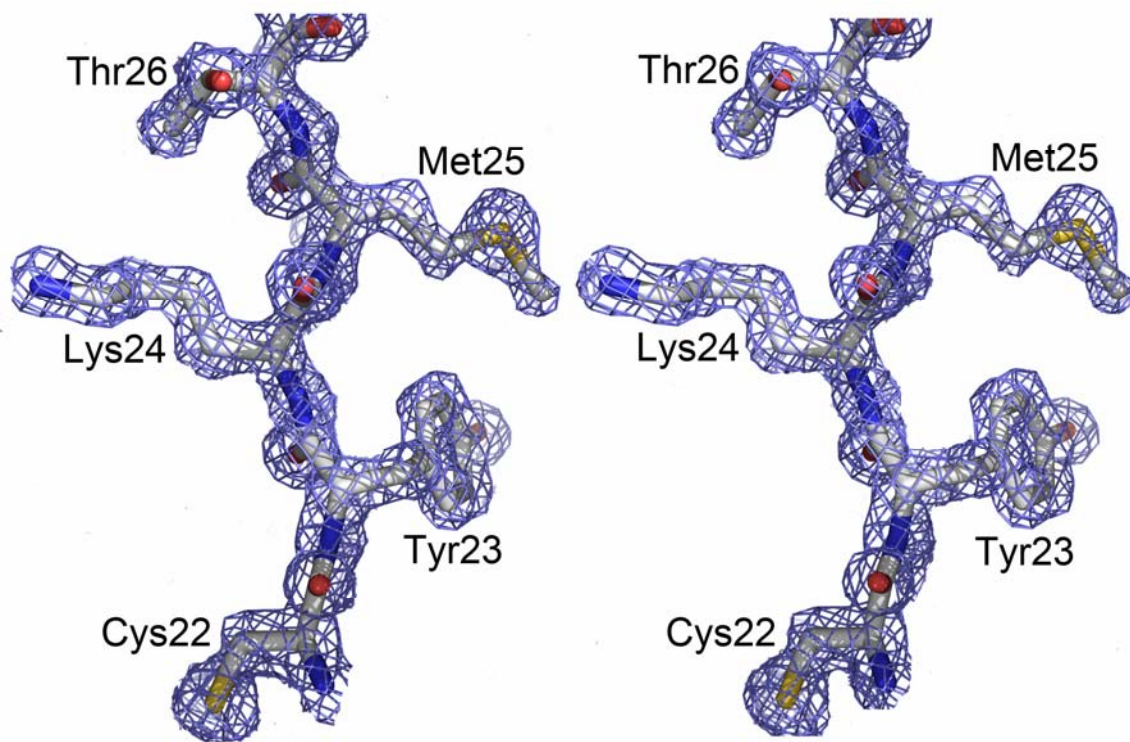


Figure 6.2 Electron density map. An example of the electron density from a simulated annealing omit map in the conserved region (stereo view)

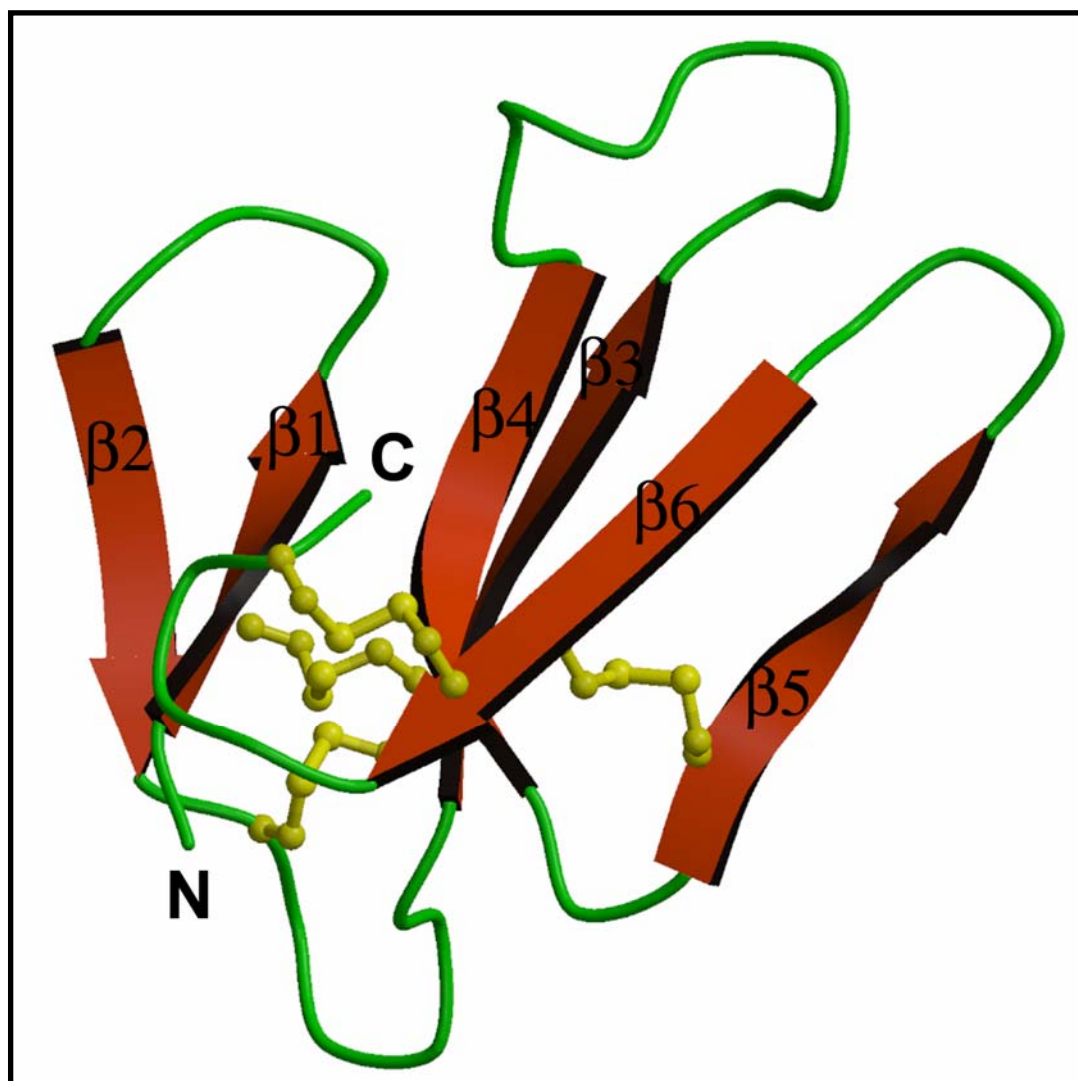


Figure 6.3 Overall structure of hemextin A. Note, the three-fingered folding consisting of six β -strands ($\beta 2 \downarrow \beta 1 \uparrow \beta 4 \downarrow \beta 3 \uparrow \beta 6 \downarrow \beta 5 \uparrow$). Cysteine bonds are shown in *yellow*

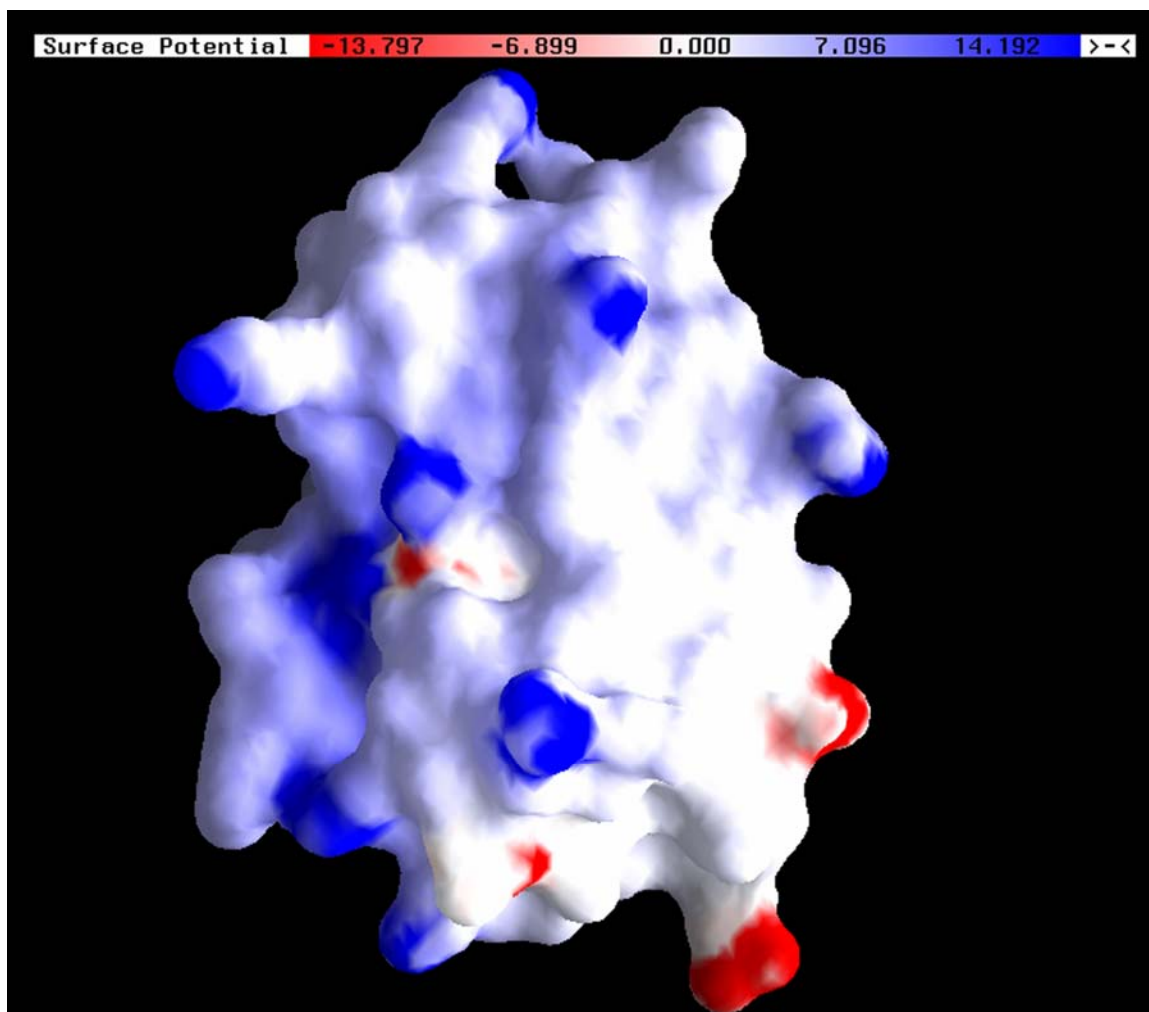


Figure 6.4 Surface plot of hemextin A, showing electrostatic potential. The localization of negative charges are indicated in *red*, whereas that of positive charges are indicated in *blue*.

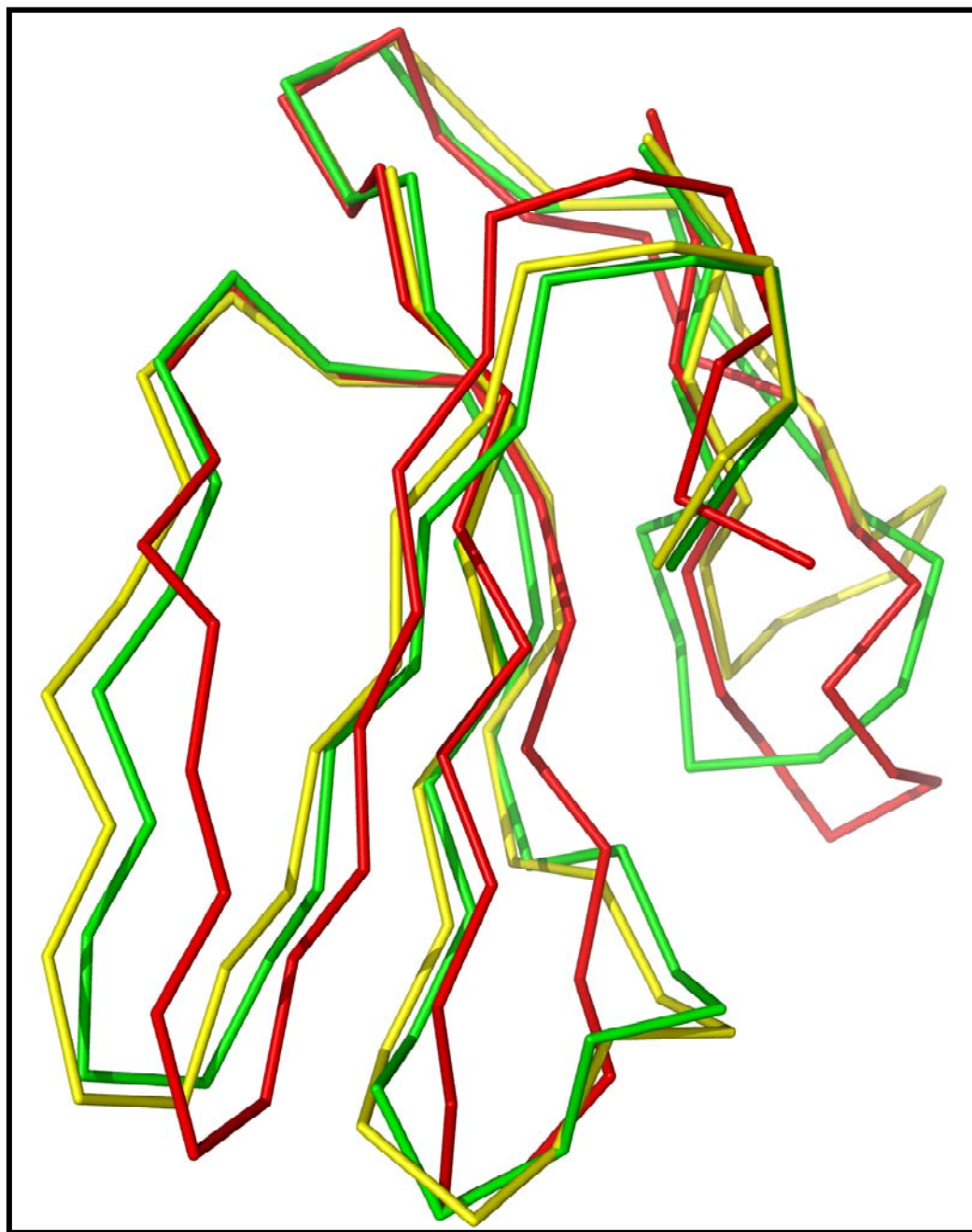


Figure 6.5 Superimposition of hemextin A with three-finger proteins of highest structural similarity. Hemextin A (*green*) with toxin γ (PDB code 1tgx; *yellow*) and erabutoxin-b (PDB code 3ebx; *green*).

venom of the sea snake *Laticauda semifasciata* (PDB code 3ebx; RMSD of 2.5Å for 55 Cα atoms; Z score = 7.2)(Low *et al.*, 1976). These observations are consistent with an evolutionarily conserved structure for the three finger toxins. Figure 6.5 shows the superposition of hemextin A with topologically similar three-finger toxins.

Concluding remarks

In conclusion, the structure of hemextin A shows that it belongs to the three-finger family of snake venom proteins. Proteins belonging to this family differ from each other in their biological activities (Kini, 2002). However, hemextin A is the only known three-finger protein that exhibits FVIIa inhibitory activity. Therefore, even a cautious guess⁴ about the critical residues required for the anticoagulant activity can not be made, and can only be identified either by site directed mutagenesis studies or by solving the FVIIa-hemextin A complex structure. The structure of hemextin A will help us in identifying the position of the active site residues and the conformation of the active site. This will in turn facilitate the design of anticoagulant peptides for the treatment of thromboembolic disorders.

As evident from the other chapters in the thesis, hemextin A forms a complex with another three-finger toxin hemextin B. Currently, we have optimized the crystallization condition for hemextin AB complex and the structure of the complex will be solved using X-ray crystallography. Though the present structure of hemextin A does not shade light on the residues important for complex formation, it is pivotal in the understanding of the conformational changes which the protein undergoes upon complex formation. These

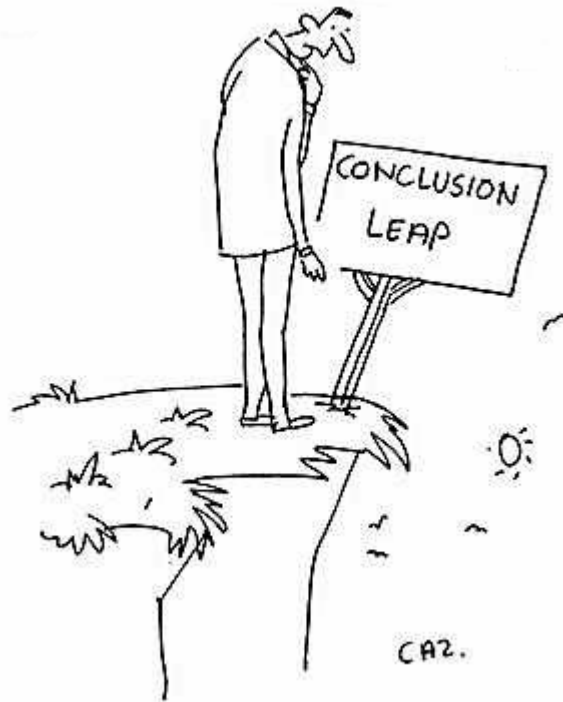
⁴ First you guess. Don't laugh, this is the most important step. Then you compute the consequences. Compare the consequences to experience. If it disagrees with experience, the guess is wrong. In that simple statement is the key to science. It doesn't matter how beautiful your guess is or how smart you are or what your name is. If it disagrees with experience, it's wrong. That's all there is to it. ---- *Richard P. Feynman (US theoretical physicist)*

conformational restrains can be introduced into the molecule, which will help in improving the potency of anticoagulant activity of hemextin A.

In, summary the structure of hemextin A is the first stepping stone in the path of understanding the structure-function relationship of the hemextin AB complex⁵.

⁵ **Just because something doesn't do what you planned it to do doesn't mean it's useless.**

--- Thomas Alva Edison



Chapter 7

Conclusions

A conclusion is the place where you got tired of thinking.

- Martin H. Fischer

A dissertation is never finished. It is abandoned at the least damaging point.

- Phil Race, How to get a good degree (1999)

This thesis reports the isolation and characterization of two proteins – hemextin A and hemextin B from the venom of *H. haemachatus* that synergistically induce potent anticoagulant activity. Individually, only hemextin A exhibited mild anticoagulant activity, whereas hemextin B has no anticoagulant activity. Hemextin A has 61 amino acid residues with a molecular weight of 6835 Da where as hemextin B consists of 60 amino acid residues with a molecular weight of 6792 Da. The primary structure of both proteins show that the cysteine bonding pattern is conserved with the important members of the three-finger family of snake venom proteins, which shows that both the proteins are members of this family.

The increase in the anticoagulant potency of hemextin A in the presence of hemextin B indicated probable complex formation between the two proteins. 1:1 complex formation was detected between hemextins A and B. This complex was designated as hemextin AB complex. Complex formation between the two proteins is pivotal for the potent anticoagulant activity.

It is a well known fact that disulfide bonds (SS) associated with cysteine residues are essential structural units in proteins. Hemextins A and B consist of eight cysteine residues associated with four disulfide bonds. Proper folding of the proteins is a pre-requisite not only for the anticoagulant function but also for proper formation of hemextin AB complex.

Using “dissection approach”, it was revealed that both hemextin A and hemextin AB complex inhibit the extrinsic tenase complex but not other steps in the extrinsic pathway. Further studies showed that hemextin A and hemextin AB complex inhibit the amidolytic activity of FVIIa both in the presence and in the absence of sTF, the inhibitory potency of

the synergistic complex being higher than hemextin A, the IC_{50} of inhibition being ~ 100 nM in both the assays. Similar IC_{50} values may be indicative of the fact that hemextin A and hemextin AB complex do not bind to the cofactor binding site of FVIIa. Specificity of hemextin A and the hemextin AB complex were screened against 12 serine proteases, which revealed that both hemextin A and the complex are specific and potent inhibitors of FVIIa. However, both hemextin A and hemextin AB complex also inhibited plasma kallikrein activity with lesser potency. Kinetic data showed that hemextin AB complex is a noncompetitive inhibitor of FVIIa-sTF complex with a K_i of 25 nM.

Hemextin AB complex is only known heterotetrameric complex formed by two three-finger toxins, and therefore molecular interactions participating in complex formation were characterized biophysically. Complex formation is enthalpically driven and indicates burial of hydrophobic surface area. Hemextin AB complex has a relatively larger molecular diameter than the individual hemextins in both gas and solution phases. Its formation is not a rigid-body-association, but the assembly takes place through local unfolding and refolding. Both electrostatic and hydrophobic interactions are important for the assembly of the tetramer. Based on our results we have proposed a model for the formation of the tetramer. This model predicts that complex formation takes place by the participation of two interfaces. One of the interfaces is sensitive to the buffer ionic strength, indicating that electrostatic interactions are predominantly active in that interface. The other being sensitive to the glycerol concentration of the solution indicates the participation of mostly hydrophobic interactions.

The proposed model was further validated, in the studies where the particular binding site in the FVIIa for the anticoagulant protein and its complex was identified. Hemextin A

and hemextin AB complex bind specifically to the heavy chain of FVIIa. Interestingly, the binding affinity of both the anticoagulant protein and the complex for FVIIa is not affected by soluble tissue-factor (the co-factor for FVIIa). This highlights the fact that the anticoagulant binding site is distinct from the co-factor binding site. Since, hemextin AB complex is a non-competitive inhibitor of FVIIa, we also tested the binding of the anticoagulant for active site blocked FVIIa. Binding was detected, though there was fall in the binding affinity which can be attributed to the conformational change in the heavy chain that takes place when the active site of FVIIa is occupied. But the finding clearly highlights the fact that the anticoagulant site is distinct from the active site of FVIIa.

Since hemextin A is the only known three-finger protein that exhibits FVIIa inhibitory activity, its structure was solved using X-ray crystallography at 1.5 Å resolution. Hemextin A, like all three-finger proteins has the characteristic three-finger fold and consists of six β -strands. Currently, the condition for crystallizing the tetrameric hemextin AB complex is being optimized and in the near future its structure will be solved.

Thus, in summary this thesis details the isolation, purification and characterization of an anticoagulant three-finger protein and its synergistic complex with another protein belonging to the same family, that specifically inhibit clot initiation by inhibiting the activity of coagulation FVIIa. This study therefore provides a new paradigm in the search for anticoagulants inhibiting the initiation of blood coagulation.

FUTURE PROSPECTS

A PhD is about finding more and more about less and less, until one eventually knows everything about nothing
Anon

While the work ascribed to this thesis has addressed some fundamental issues pertaining to the structure and function of hemextin AB complex (a synergistic anticoagulant complex between two three-finger toxins hemextins A and B, from Ringhals venom), it has also given rise to some pertinent questions¹ that could open up new and interesting avenues of research.

1. Why does hemextin A undergo conformational change in salt, and hemextin B does not?

Both the proteins belong to the three-finger toxin family and share 84% sequence identity. But it is hemextin A that is sensitive to the ionic strength of its surroundings and not hemextin B. Therefore, it will be interesting to study the molecular dynamics of both the proteins, especially hemextin A in solutions of different ionic strength(s) using NMR spectroscopy. This study also has great potential in a broader sense, since it may shade light on the effect of electrostatics on protein folding.

2. How will the 3D-structure of tetrameric hemextin AB complex look like?

Hemextin AB complex is the only known tetrameric complex between two three-finger toxins. This thesis describes the crystallization and structure of hemextin A. The next step would be to solve the structure of the synergistic complex. The individual structure of hemextin B can then be solved using MR. A comparison of the

¹ “Science is wonderfully equipped to answer the question "How?" but it gets terribly confused when you ask the question "Why?"”

--- Erwin Chargaff (1905–2002)

structures will show the conformational changes that both proteins undergo on complex formation. More importantly, it will tell how hemexin B potentiates the anticoagulant activity of hemexin A, and the key residues in the proteins involved in complex formation.

3. Which part(s) of the heavy chain of FVIIa is involved in binding to the anticoagulant complex?

In this thesis it has been shown that hemexin AB complex binds to the heavy chain of FVIIa. However, the specific part of the heavy chain involved in interaction still remains to be elucidated. The heavy chain of FVIIa has two distinct exosites (Banner *et al.*, 1996). Peptides have been identified that bind to these exosites (Dennis *et al.*, 2000). Competition binding experiments can be conducted with these peptides to confirm if these exosites of the heavy chain are involved the binding process.

Further, H-D exchange studies, between isolated FVIIa heavy chain and hemexin AB complex can be carried out to identify the particular segment of heavy chain that is involved in the binding process.

4. How will the 3D-structure of FVIIa-hemexin AB complex /sTF-FVIIa-hemexin AB complex look like?

Hemexin AB complex can be co-crystallized with coagulation FVIIa or reconstituted sTF-FVIIa complex, followed by the determination of 3D-structure using MR, since the individual structures of both sTF-FVIIa (Banner *et al.*, 1996) and FVIIa (Kemball-Cook *et al.*, 1999) are known. If solved, this structure will provide valuable information regarding the residues that are involved in the binding between enzyme

and inhibitor. The principal challenge however, will be to optimize the conditions for the proper growth of enzyme-inhibitor complex.

5. How to design² an anticoagulant?

Hemextin A and its synergistic complex with hemextin B, inhibit clot initiation by binding specifically to coagulation FVIIa. Hemextin A is the active protein. Before designing an anticoagulant one needs to identify the specific residues that are important for anticoagulant activity. Site directed mutagenesis can achieve that aim. A point to keep note of in this step is the correct fold of the mutants, since the work in this thesis shows that β -sheet fold of hemextin A is important for its anticoagulant activity.

After the residues important for anticoagulant activity have been identified, we can mimic this activity in a protein scaffold that has a three-finger fold, but is itself inert and has lesser amino acid residues compared to hemextin A. Following the successful identification of the protein scaffold, using the combinatorial search algorithm (Looger *et al.*, 2003) one will be able to identify the particular region of the scaffold that satisfies the constraints, where the active residues (identified from mutagenesis studies) can be inserted. Since the anticoagulant activity of hemextin A is potentiated by hemextin B, it can be concluded that a particular conformation of the protein has potent anticoagulant activity, and the protein attains this conformation upon binding to hemextin B. Biophysical studies have shown that on complex formation there is stabilization of β -sheet in hemextin A. Therefore, various conformers of the scaffold

² “A common mistake that people make when trying to design something completely foolproof is to underestimate the ingenuity of complete fools.”

--- Douglas Adams(1952-2001)

with the active residues (S_{AR}) can be synthesized using iterative higherarchial approach algorithm (Hellinga and Richards, 1991). The S_{AR} conformer with the highest anticoagulant activity is to be selected. Further optimization of the anticoagulant site in S_{AR} can be done using the RD algorithm (Dwyer *et al.*, 2004). The binding affinity of this binding site optimized S_{AR} for FVIIa is to be determined. Next, by using PARE (Predicting Association Rate Enhancement) algorithm (Schreiber and Fersht, 1996), further increase in the k_{on} between FVIIa and S_{AR} can be made, and can be experimentally evaluated using Biacore. The final version of S_{AR} then can be directed for evolution by random mutagenesis (Dwyer *et al.*, 2004). The final version of the rationally designed S_{AR} can then be evaluated for anticoagulant activity *in vivo* models.

Thank you note,

The part on future prospect depicts some of my ideas that can be pursued to answer some of the questions which I feel pertinent regarding the project. Out of all the questions the final one of designing an anticoagulant, came to my mind while reading an excellent paper published in Science titled “Computational design of a biologically active enzyme” by Professor Hellinga and his colleagues. However, I got some help in the understanding of the algorithms, since this aspect of science was completely new to me. For this I will like to thank Prof. Gideon Schreiber (Department of Biological Chemistry, Weizmann Institute of Science), who not only answered my questions but also sent me all the material on PARE algorithm (which is designed by him), including a complete book chapter. If the reader however, finds any flaw in the sequence of experimental design(s), it is I who is to be blamed solely.

-- Yajnavalka Banerjee

“The point is that you can and should find many more examples by reading the literature yourself. If you read things at face value and don’t wise up to the hidden meanings in paper-speak, you might miss an opportunity to extend your own research. Worse, you might even get a left behind if your field is one that moves on rapidly. Use every opportunity to consult experienced and trusted colleagues on what they think the authors mean, when they use a particular word or phrase. This way you’ll also learn another great lesson: different people interpret the same passage in different ways. So much for scientific papers being unambiguous and crystal clear!”

--- Phil Dee (Building a Successful Career in Scientific Research)



Bibliography

IUPAC-IUB Commission on Biochemical Nomenclature. A one-letter notation for amino acid sequences. Tentative rules. (1968). *J.Biol.Chem.* 243, 3557-3559.

Abraham,E., Reinhart,K., Opal,S., Demeyer,I., Doig,C., Rodriguez,A.L., Beale,R., Svoboda,P., Laterre,P.F., Simon,S., Light,B., Spapen,H., Stone,J., Seibert,A., Peckelsen,C., De Deyne,C., Postier,R., Pettila,V., Artigas,A., Percell,S.R., Shu,V., Zwingelstein,C., Tobias,J., Poole,L., Stolzenbach,J.C., Creasey,A.A. (2003). Efficacy and safety of tifacogin (recombinant tissue factor pathway inhibitor) in severe sepsis: a randomized controlled trial. *JAMA* 290, 238-247.

Abraham,E., Reinhart,K., Svoboda,P., Seibert,A., Olthoff,D., Dal Nogare,A., Postier,R., Hempelmann,G., Butler,T., Martin,E., Zwingelstein,C., Percell,S., Shu,V., Leighton,A., Creasey,A.A. (2001). Assessment of the safety of recombinant tissue factor pathway inhibitor in patients with severe sepsis: a multicenter, randomized, placebo-controlled, single-blind, dose escalation study. *Crit Care Med.* 29, 2081-2089.

Altschul,S.F., Madden,T.L., Schaffer,A.A., Zhang,J., Zhang,Z., Miller,W., Lipman,D.J. (1997). Gapped BLAST and PSI-BLAST: a new generation of protein database search programs. *Nucleic Acids Res.* 25, 3389-3402.

Apitz-Castro,R., Beguin,S., Tablante,A., Bartoli,F., Holt,J.C., Hemker,H.C. (1995). Purification and partial characterization of draculin, the anticoagulant factor present in the saliva of vampire bats (*Desmodus rotundus*). *Thromb.Haemost.* 73, 94-100.

Arni,R.K., Ward,R.J. (1996). Phospholipase A2--a structural review. *Toxicon* 34, 827-841.

Arocas,V., Castro,H.C., Zingali,R.B., Guillin,M.C., Jandrot-Perrus,M., Bon,C., Wisner,A. (1997). Molecular cloning and expression of bothrojaracin, a potent thrombin inhibitor from snake venom. *Eur.J.Biochem.* 248, 550-557.

Arocas,V., Lemaire,C., Bouton,M.C., Bezeaud,A., Bon,C., Guillin,M.C., Jandrot-Perrus,M. (1998). Inhibition of thrombin-catalyzed factor V activation by bothrojaracin. *Thromb.Haemost.* 79, 1157-1161.

Arocas,V., Zingali,R.B., Guillin,M.C., Bon,C., Jandrot-Perrus,M. (1996). Bothrojaracin: a potent two-site-directed thrombin inhibitor. *Biochemistry* 35, 9083-9089.

Arocha-Pinango,C.L., Marchi,R., Carvajal,Z., Guerrero,B. (1999). Invertebrate compounds acting on the hemostatic mechanism. *Blood Coagul.Fibrinolysis* 10, 43-68.

Aronson,D.L. (1976). Comparison of the actions of thrombin and the thrombin-like venom enzymes ancrod and batroxobin. *Thromb.Haemost.* 36, 9-13.

Atoda,H., Hyuga,M., Morita,T. (1991). The primary structure of coagulation factor IX/factor X-binding protein isolated from the venom of *Trimeresurus flavoviridis*. Homology with asialoglycoprotein receptors, proteoglycan core protein, tetranectin, and lymphocyte Fc epsilon receptor for immunoglobulin E. *J.Biol.Chem.* 266, 14903-14911.

Atoda,H., Ishikawa,M., Mizuno,H., Morita,T. (1998). Coagulation factor X-binding protein from *Deinagkistrodon acutus* venom is a Gla domain-binding protein. *Biochemistry* 37, 17361-17370.

Atoda,H., Ishikawa,M., Yoshihara,E., Sekiya,F., Morita,T. (1995). Blood coagulation factor IX-binding protein from the venom of *Trimeresurus flavoviridis*: purification and characterization. *J.Biochem.(Tokyo)* 118, 965-973.

Atoda,H., Morita,T. (1989). A novel blood coagulation factor IX/factor X-binding protein with anticoagulant activity from the venom of *Trimeresurus flavoviridis* (Habu snake): isolation and characterization. *J.Biochem.(Tokyo)* 106, 808-813.

Babu,A.S., Gowda,T.V. (1994). Dissociation of enzymatic activity from toxic properties of the most basic phospholipase A2 from *Vipera russelli* snake venom by guanidination of lysine residues. *Toxicon* 32, 749-752.

Bach,R., Konigsberg,W.H., Nemerson,Y. (1988b). Human tissue factor contains thioester-linked palmitate and stearate on the cytoplasmic half-cystine. *Biochemistry* 27, 4227-4231.

Badimon,J.J., Lettino,M., Toschi,V., Fuster,V., Berrozpe,M., Chesebro,J.H., Badimon,L. (1999). Local inhibition of tissue factor reduces the thrombogenicity of disrupted human atherosclerotic plaques: effects of tissue factor pathway inhibitor on plaque thrombogenicity under flow conditions. *Circulation* 99, 1780-1787.

Bajaj,M.S., Birktoft,J.J., Steer,S.A., Bajaj,S.P. (2001). Structure and biology of tissue factor pathway inhibitor. *Thromb.Haemost.* 86, 959-972.

Bakker,H.M., Tans,G., Yukelson,L.Y., Janssen-Claessen,T.W., Bertina,R.M., Hemker,H.C., Rosing,J. (1993). Protein C activation by an activator purified from the venom of *Agkistrodon halys halys*. *Blood Coagul.Fibrinolysis* 4, 605-614.

Balasubramanian,V., Grabowski,E., Bini,A., Nemerson,Y. (2002). Platelets, circulating tissue factor, and fibrin colocalize in ex vivo thrombi: real-time fluorescence images of

thrombus formation and propagation under defined flow conditions. *Blood* 100, 2787-2792.

Banerjee,Y., Mizuguchi,J., Iwanaga,S., Kini,R.M. (2005a). Hemextin AB complex, a unique anticoagulant protein complex from *Hemachatus haemachatus* (African Ringhals cobra) venom that inhibits clot initiation and factor VIIa activity. *J Biol.Chem* 280, 42601-42611.

Banerjee,Y., Mizuguchi,J., Iwanaga,S., Kini,R.M. (2005b). Hemextin AB complex--a snake venom anticoagulant protein complex that inhibits factor VIIa activity. *Pathophysiol.Haemost.Thromb.* 34, 184-187.

Banner,D.W., D'Arcy,A., Chene,C., Winkler,F.K., Guha,A., Konigsberg,W.H., Nemerson,Y., Kirchhofer,D. (1996). The crystal structure of the complex of blood coagulation factor VIIa with soluble tissue factor. *Nature* 380, 41-46.

Baugh,R.J., Broze,G.J., Jr., Krishnaswamy,S. (1998). Regulation of extrinsic pathway factor Xa formation by tissue factor pathway inhibitor. *J Biol.Chem* 273, 4378-4386.

Bazan,J.F. (1990). Structural design and molecular evolution of a cytokine receptor superfamily. *Proc.Natl.Acad.Sci.U.S.A* 87, 6934-6938.

Belcher,J.D., Marker,P.H., Weber,J.P., Hebbel,R.P., Vercellotti,G.M. (2000). Activated monocytes in sickle cell disease: potential role in the activation of vascular endothelium and vaso-occlusion. *Blood* 96, 2451-2459.

Bell,W.R., Jr. (1997). Defibrinogenating enzymes. *Drugs* 54 Suppl 3, 18-30.

Bernard,G.R., Vincent,J.L., Laterre,P.F., LaRosa,S.P., Dhainaut,J.F., Lopez-Rodriguez,A., Steingrub,J.S., Garber,G.E., Helderbrand,J.D., Ely,E.W., Fisher,C.J., Jr. (2001). Efficacy and safety of recombinant human activated protein C for severe sepsis. *N.Engl.J.Med.* 344, 699-709.

Biamond,B.J., Levi,M., ten Cate,H., Soule,H.R., Morris,L.D., Foster,D.L., Bogowitz,C.A., van der,P.T., Buller,H.R., ten Cate,J.W. (1995). Complete inhibition of endotoxin-induced coagulation activation in chimpanzees with a monoclonal Fab fragment against factor VII/VIIa. *Thromb.Haemost.* 73, 223-230.

Bilwes,A., Rees,B., Moras,D., Menez,R., Menez,A. (1994). X-ray structure at 1.55 Å of toxin gamma, a cardiotoxin from *Naja nigricollis* venom. Crystal packing reveals a model for insertion into membranes. *J.Mol.Biol.* 239, 122-136.

Bjarnason, J.B., Fox, J.W. (1995). Snake venom metalloendopeptidases: reprolysins. *Methods Enzymol.* 248, 345-368.

Blankenship, D.T., Brankamp, R.G., Manley, G.D., Cardin, A.D. (1990). Amino acid sequence of ghilanten: anticoagulant-antimetastatic principle of the South American leech, *Haementeria ghilianii*. *Biochem. Biophys. Res. Commun.* 166, 1384-1389.

Blomback, B., Hessel, B., Hogg, D., Therkildsen, L. (1978). A two-step fibrinogen--fibrin transition in blood coagulation. *Nature* 275, 501-505.

Bode, W., Huber, R. (1992). Natural protein proteinase inhibitors and their interaction with proteinases. *Eur. J. Biochem.* 204, 433-451.

Boffa, M.C., Boffa, G.A. (1976). A phospholipase A2 with anticoagulant activity. II. Inhibition of the phospholipid activity in coagulation. *Biochim. Biophys. Acta* 429, 839-852.

Bokarewa, M.I., Morrissey, J.H., Tarkowski, A. (2002). Tissue factor as a proinflammatory agent. *Arthritis Res.* 4, 190-195.

Bom, V.J., Bertina, R.M. (1990). The contributions of Ca²⁺, phospholipids and tissue-factor apoprotein to the activation of human blood-coagulation factor X by activated factor VII. *Biochem. J.* 265, 327-336.

Bouma, B.N., Griffin, J.H. (1977). Human blood coagulation factor XI. Purification, properties, and mechanism of activation by activated factor XII. *J. Biol. Chem.* 252, 6432-6437.

Brankamp, R.G., Manley, G.G., Blankenship, D.T., Bowlin, T.L., Cardin, A.D. (1991). Studies on the anticoagulant, antimetastatic and heparin-binding properties of ghilanten-related inhibitors. *Blood Coagul. Fibrinolysis* 2, 161-166.

Brass, L.F. (2003). Thrombin and platelet activation. *Chest* 124, 18S-25S.

Breddin, H.K., Radziwon, P., Boczkowska-Radziwon, B. (1994). Laboratory monitoring of new antithrombotic drugs. *Clin. Lab Med.* 14, 825-846.

Broze, G.J., Jr. (2001). Protein Z-dependent regulation of coagulation. *Thromb. Haemost.* 86, 8-13.

Broze, G.J., Jr., Leykam, J.E., Schwartz, B.D., Miletich, J.P. (1985). Purification of human brain tissue factor. *J. Biol. Chem.* 260, 10917-10920.

Broze,G.J., Jr., Majerus,P.W. (1980). Purification and properties of human coagulation factor VII. *J.Biol.Chem.* 255, 1242-1247.

Brunger,A.T., Adams,P.D., Clore,G.M., DeLano,W.L., Gros,P., Grosse-Kunstleve,R.W., Jiang,J.S., Kuszewski,J., Nilges,M., Pannu,N.S., Read,R.J., Rice,L.M., Simonson,T., Warren,G.L. (1998). Crystallography & NMR system: A new software suite for macromolecular structure determination. *Acta Crystallogr.D.Biol.Crystallogr.* 54, 905-921.

Burgering,M.J., Orbons,L.P., van der,D.A., Mulders,J., Theunissen,H.J., Grootenhuys,P.D., Bode,W., Huber,R., Stubbs,M.T. (1997). The second Kunitz domain of human tissue factor pathway inhibitor: cloning, structure determination and interaction with factor Xa. *J Mol.Biol.* 269, 395-407.

Butenas,S., Mann,K.G. (1996). Kinetics of human factor VII activation. *Biochemistry* 35, 1904-1910.

Butenas,S., Ribarik,N., Mann,K.G. (1993). Synthetic substrates for human factor VIIa and factor VIIa-tissue factor. *Biochemistry* 32, 6531-6538.

Butenas,S., van', V, Mann,K.G. (1997). Evaluation of the initiation phase of blood coagulation using ultrasensitive assays for serine proteases. *J.Biol.Chem.* 272, 21527-21533.

Cappello,M., Bergum,P.W., Vlasuk,G.P., Furmidge,B.A., Pritchard,D.I., Aksoy,S. (1996). Isolation and characterization of the tsetse thrombin inhibitor: a potent antithrombotic peptide from the saliva of *Glossina morsitans morsitans*. *Am.J.Trop.Med.Hyg.* 54, 475-480.

Cappello,M., Vlasuk,G.P., Bergum,P.W., Huang,S., Hotez,P.J. (1995). *Ancylostoma caninum* anticoagulant peptide: a hookworm-derived inhibitor of human coagulation factor Xa. *Proc.Natl.Acad.Sci.U.S.A* 92, 6152-6156.

Castro,H.C., Fernandes,M., Zingali,R.B. (1999). Identification of bothrojaracin-like proteins in snake venoms from Bothrops species and *Lachesis muta*. *Toxicon* 37, 1403-1416.

Cavusoglu,E., Chen,I., Rappaport,J., Marmur,J.D. (2002). Inhibition of tissue factor gene induction and activity using a hairpin ribozyme. *Circulation* 105, 2282-2287.

Chang,L., Chung,C., Huang,H.B., Lin,S. (2001). Purification and characterization of a chymotrypsin inhibitor from the venom of *Ophiophagus hannah* (King Cobra). *Biochem.Biophys.Res.Commun.* 283, 862-867.

Chen,C., Hsu,C.H., Su,N.Y., Lin,Y.C., Chiou,S.H., Wu,S.H. (2001). Solution structure of a Kunitz-type chymotrypsin inhibitor isolated from the elapid snake *Bungarus fasciatus*. *J.Biol.Chem.* 276, 45079-45087.

Chen,Y.L., Tsai,I.H. (1996). Functional and sequence characterization of coagulation factor IX/factor X-binding protein from the venom of *Echis carinatus leucogaster*. *Biochemistry* 35, 5264-5271.

Chopin,V., Salzet,M., Baert,J., Vandenbulcke,F., Sautiere,P.E., Kerckaert,J.P., Malecha,J. (2000). Therostasin, a novel clotting factor Xa inhibitor from the rhynchobdellid leech, *Theromyzon tessulatum*. *J.Biol.Chem.* 275, 32701-32707.

Cochrane,C.G., Revak,S.D., Wuepper,K.D. (1973). Activation of Hageman factor in solid and fluid phases. A critical role of kallikrein. *J.Exp.Med.* 138, 1564-1583.

Condrea,E., Fletcher,J.E., Rapuano,B.E., Yang,C.C., Rosenberg,P. (1981). Effect of modification of one histidine residue on the enzymatic and pharmacological properties of a toxic phospholipase A2 from *Naja nigricollis* snake venom and less toxic phospholipases A2 from *Hemachatus haemachatus* and *Naja atra* snake venoms. *Toxicon* 19, 61-71.

Connolly,T.M., Jacobs,J.W., Condra,C. (1992). An inhibitor of collagen-stimulated platelet activation from the salivary glands of the *Haementeria officinalis* leech. I. Identification, isolation, and characterization. *J.Biol.Chem.* 267, 6893-6898.

Cox,A.C. (1993). Coagulation factor X inhibitor from hundred-pace snake (*Deinagkistrodon acutus*) venom. *Toxicon* 31, 1445-1457.

Davey,M.G., Luscher,E.F. (1967). Actions of thrombin and other coagulant and proteolytic enzymes on blood platelets. *Nature* 216, 857-858.

Davie,E.W., Ratnoff,O.D. (1964). Waterfall sequence for intrinsic blood clotting. *Science* 145, 1310-1312.

de Groot,P.G. (2002). The role of von Willebrand factor in platelet function. *Semin.Thromb.Hemost.* 28, 133-138.

Debarbieux,L., Beckwith,J. (1999). Electron avenue: pathways of disulfide bond formation and isomerization. *Cell* 99, 117-119.

Dennis,E.A. (1994). Diversity of group types, regulation, and function of phospholipase A2. *J.Biol.Chem.* 269, 13057-13060.

Dennis,M.S., Eigenbrot,C., Skelton,N.J., Ultsch,M.H., Santell,L., Dwyer,M.A., O'Connell,M.P., Lazarus,R.A. (2000). Peptide exosite inhibitors of factor VIIa as anticoagulants. *Nature* 404, 465-470.

Dennis,M.S., Lazarus,R.A. (1994). Kunitz domain inhibitors of tissue factor-factor VIIa. I. Potent inhibitors selected from libraries by phage display. *J.Biol.Chem.* 269, 22129-22136.

Di Scipio,R.G., Hermodson,M.A., DAVIE,E.W. (1977). Activation of human factor X (Stuart factor) by a protease from Russell's viper venom. *Biochemistry* 16, 5253-5260.

Di Scipio,R.G., Kurachi,K., DAVIE,E.W. (1978). Activation of human factor IX (Christmas factor). *J.Clin.Invest* 61, 1528-1538.

Dickinson,C.D., Kelly,C.R., Ruf,W. (1996). Identification of surface residues mediating tissue factor binding and catalytic function of the serine protease factor VIIa. *Proc.Natl.Acad.Sci.U.S.A* 93, 14379-14384.

Dickinson,C.D., Shobe,J., Ruf,W. (1998). Influence of cofactor binding and active site occupancy on the conformation of the macromolecular substrate exosite of factor VIIa. *J Mol.Biol.* 277, 959-971.

Doolittle,R.F., Watt,K.W., Cottrell,B.A., Strong,D.D., Riley,M. (1979). The amino acid sequence of the alpha-chain of human fibrinogen. *Nature* 280, 464-468.

Doorty,K.B., Bevan,S., Wadsworth,J.D., Strong,P.N. (1997). A novel small conductance Ca^{2+} -activated K^{+} channel blocker from *Oxyuranus scutellatus* taipan venom. Re-evaluation of taicatoxin as a selective Ca^{2+} channel probe. *J.Biol.Chem.* 272, 19925-19930.

Drake,T.A., Morrissey,J.H., Edgington,T.S. (1989). Selective cellular expression of tissue factor in human tissues. Implications for disorders of hemostasis and thrombosis. *Am.J.Pathol.* 134, 1087-1097.

Duggan,B.M., Dyson,H.J., Wright,P.E. (1999). Inherent flexibility in a potent inhibitor of blood coagulation, recombinant nematode anticoagulant protein c2. *Eur.J.Biochem.* 265, 539-548.

Dwyer,M.A., Looger,L.L., Hellinga,H.W. (2004). Computational design of a biologically active enzyme. *Science* 304, 1967-1971.

Dyke,C.K., Becker,R.C., Kleiman,N.S., Hochman,J.S., Bovill,E.G., Lincoff,A.M., Gerstenblith,G., Dzavik,V., Gardner,L.H., Hasselblad,V., Zillman,L.A., Shimoto,Y.,

Robertson,T.L., Kunitada,S., Armstrong,P.W., Harrington,R.A. (2002). First experience with direct factor Xa inhibition in patients with stable coronary disease: a pharmacokinetic and pharmacodynamic evaluation. *Circulation* 105, 2385-2391.

Ebner,S., Sharon,N., Ben Tal,N. (2003). Evolutionary analysis reveals collective properties and specificity in the C-type lectin and lectin-like domain superfamily. *Proteins* 53, 44-55.

Eigenbrot,C., Kirchhofer,D., Dennis,M.S., Santell,L., Lazarus,R.A., Stamos,J., Ultsch,M.H. (2001). The factor VII zymogen structure reveals reregistration of beta strands during activation. *Structure*. 9, 627-636.

Erlich,J.H., Boyle,E.M., Labriola,J., Kovacich,J.C., Santucci,R.A., Fearn,C., Morgan,E.N., Yun,W., Luther,T., Kojikawa,O., Martin,T.R., Pohlman,T.H., Verrier,E.D., Mackman,N. (2000). Inhibition of the tissue factor-thrombin pathway limits infarct size after myocardial ischemia-reperfusion injury by reducing inflammation. *Am.J Pathol.* 157, 1849-1862.

Esmon,C.T. (1995). Thrombomodulin as a model of molecular mechanisms that modulate protease specificity and function at the vessel surface. *FASEB J.* 9, 946-955.

Esmon,C.T., Stenflo,J., Suttie,J.W. (1976). A new vitamin K-dependent protein. A phospholipid-binding zymogen of a serine esterase. *J.Biol.Chem.* 251, 3052-3056.

Esmon,C.T., Xu,J., Gu,J.M., Qu,D., Laszik,Z., Ferrell,G., Stearns-Kurosawa,D.J., Kurosawa,S., Taylor,F.B., Jr., Esmon,N.L. (1999). Endothelial protein C receptor. *Thromb.Haemost.* 82, 251-258.

Falati,S., Liu,Q., Gross,P., Merrill-Skoloff,G., Chou,J., Vandendries,E., Celi,A., Croce,K., Furie,B.C., Furie,B. (2003). Accumulation of tissue factor into developing thrombi in vivo is dependent upon microparticle P-selectin glycoprotein ligand 1 and platelet P-selectin. *J Exp.Med.* 197, 1585-1598.

Faria,F., Kelen,E.M., Sampaio,C.A., Bon,C., Duval,N., Chudzinski-Tavassi,A.M. (1999). A new factor Xa inhibitor (lefaxin) from the *Haementeria depressa* leech. *Thromb.Haemost.* 82, 1469-1473.

Ferguson,J.J. (1996). American College of Cardiology 45th Annual Scientific Session, Orlando, Florida, March 24 to 27, 1996. *Circulation* 94, 1-5.

Fernandez,A.Z., Tablante,A., Beguin,S., Hemker,H.C., Apitz-Castro,R. (1999). Draculin, the anticoagulant factor in vampire bat saliva, is a tight-binding, noncompetitive inhibitor of activated factor X. *Biochim.Biophys.Acta* 1434, 135-142.

Finkelstein,A.V., Janin,J. (1989). The price of lost freedom: entropy of bimolecular complex formation. *Protein Eng* 3, 1-3.

Finney,S., Seale,L., Sawyer,R.T., Wallis,R.B. (1997). Tridegin, a new peptidic inhibitor of factor XIIIa, from the blood-sucking leech *Haementeria ghilianii*. *Biochem.J.* 324 (Pt 3), 797-805.

Fleck,R.A., Rao,L.V., Rapaport,S.I., Varki,N. (1990). Localization of human tissue factor antigen by immunostaining with monospecific, polyclonal anti-human tissue factor antibody. *Thromb.Res.* 59, 421-437.

Fowler,W.E., Hantgan,R.R., Hermans,J., Erickson,H.P. (1981). Structure of the fibrin protofibril. *Proc.Natl.Acad.Sci.U.S.A* 78, 4872-4876.

Fox,J.W., Serrano,S.M. (2005). Structural considerations of the snake venom metalloproteinases, key members of the M12 reprotolysin family of metalloproteinases. *Toxicon* 45, 969-985.

Francischetti,I.M., Valenzuela,J.G., Andersen,J.F., Mather,T.N., Ribeiro,J.M. (2002). Ixolaris, a novel recombinant tissue factor pathway inhibitor (TFPI) from the salivary gland of the tick, *Ixodes scapularis*: identification of factor X and factor Xa as scaffolds for the inhibition of factor VIIa/tissue factor complex. *Blood* 99, 3602-3612.

Freskgard,P.O., Petersen,L.C., Gabriel,D.A., Li,X., Persson,E. (1998). Conformational stability of factor VIIa: biophysical studies of thermal and guanidine hydrochloride-induced denaturation. *Biochemistry* 37, 7203-7212.

Fujikawa,K., Heimark,R.L., Kurachi,K., Davie,E.W. (1980). Activation of bovine factor XII (Hageman factor) by plasma kallikrein. *Biochemistry* 19, 1322-1330.

Gailani,D., Broze,G.J., Jr. (1991). Factor XI activation in a revised model of blood coagulation. *Science* 253, 909-912.

Gaspar,A.R., Joubert,A.M., Crause,J.C., Neitz,A.W. (1996). Isolation and characterization of an anticoagulant from the salivary glands of the tick, *Ornithodoros savignyi* (Acari: Argasidae). *Exp.Appl.Acarol.* 20, 583-598.

Geczy,C.L. (1994). Cellular mechanisms for the activation of blood coagulation. *Int.Rev.Cytol.* 152, 49-108.

Giesen,P.L., Rauch,U., Bohrmann,B., Kling,D., Roque,M., Fallon,J.T., Badimon,J.J., Himber,J., Riederer,M.A., Nemerson,Y. (1999). Blood-borne tissue factor: another view of thrombosis. *Proc.Natl.Acad.Sci U.S.A* 96, 2311-2315.

Girard,T.J., MacPhail,L.A., Likert,K.M., Novotny,W.F., Miletich,J.P., Broze,G.J., Jr. (1990). Inhibition of factor VIIa-tissue factor coagulation activity by a hybrid protein. *Science* 248, 1421-1424.

Girma,J.P., Meyer,D., Verweij,C.L., Pannekoek,H., Sixma,J.J. (1987). Structure-function relationship of human von Willebrand factor. *Blood* 70, 605-611.

Glusa,E. (1994). Desulfated hirugen (hirudin 54-65) induces endothelium-dependent relaxation of porcine pulmonary arteries. *Thromb.Haemost.* 72, 318-321.

Golino,P., Ragni,M., Cirillo,P., Avvedimento,V.E., Feliciello,A., Esposito,N., Scognamiglio,A., Trimarco,B., Iaccarino,G., Condorelli,M., Chiariello,M., Ambrosio,G. (1996). Effects of tissue factor induced by oxygen free radicals on coronary flow during reperfusion. *Nat.Med.* 2, 35-40.

Goolsby,M.J. (2002). Clinical practice guidelines. Managing oral anticoagulant therapy. *J.Am.Acad.Nurse Pract.* 14, 16-18.

Green,D.W., Ingram,V.M., Perutz,M.F. (1964). The structure determination of haemoglobin. IV. Sign determination by the isomorphous replacement method. *Proc.R.Soc.Lond.* A225, 287-307.

Gustafsson,D., Elg,M., Lenfors,S., Borjesson,I., Teger-Nilsson,A.C. (1996). Effects of inogatran, a new low-molecular-weight thrombin inhibitor, in rat models of venous and arterial thrombosis, thrombolysis and bleeding time. *Blood Coagul.Fibrinolysis* 7, 69-79.

Habermann,E., Breithaupt,H. (1978). Mini-review. The crotoxin complex--an example of biochemical and pharmacological protein complementation. *Toxicon* 16, 19-30.

Hamamoto,T., Yamamoto,M., Nordfang,O., Petersen,J.G., Foster,D.C., Kiesel,W. (1993). Inhibitory properties of full-length and truncated recombinant tissue factor pathway inhibitor (TFPI). Evidence that the third Kunitz-type domain of TFPI is not essential for the inhibition of factor VIIa-tissue factor complexes on cell surfaces. *J Biol.Chem* 268, 8704-8710.

Han,J.H., Law,S.W., Keller,P.M., Kniskern,P.J., Silberklang,M., Tung,J.S., Gasic,T.B., Gasic,G.J., Friedman,P.A., Ellis,R.W. (1989). Cloning and expression of cDNA encoding antistasin, a leech-derived protein having anti-coagulant and anti-metastatic properties. *Gene* 75, 47-57.

Harker,L.A., Hanson,S.R., Wilcox,J.N., Kelly,A.B. (1996). Antithrombotic and antilesion benefits without hemorrhagic risks by inhibiting tissue factor pathway. *Haemostasis* 26 Suppl 1, 76-82.

Harlos,K., Martin,D.M., O'Brien,D.P., Jones,E.Y., Stuart,D.I., Polikarpov,I., Miller,A., Tuddenham,E.G., Boys,C.W. (1994). Crystal structure of the extracellular region of human tissue factor. *Nature* 370, 662-666.

Harrison,L.M., Nerlinger,A., Bungiro,R.D., Cordova,J.L., Kuzmic,P., Cappello,M. (2002). Molecular characterization of Ancylostoma inhibitors of coagulation factor Xa. Hookworm anticoagulant activity in vitro predicts parasite bloodfeeding in vivo. *J.Biol.Chem.* 277, 6223-6229.

Heeb,M.J., Kojima,Y., Greengard,J.S., Griffin,J.H. (1995). Activated protein C resistance: molecular mechanisms based on studies using purified Gln506-factor V. *Blood* 85, 3405-3411.

Heeb,M.J., Mesters,R.M., Tans,G., Rosing,J., Griffin,J.H. (1993). Binding of protein S to factor Va associated with inhibition of prothrombinase that is independent of activated protein C. *J.Biol.Chem.* 268, 2872-2877.

Heeb,M.J., Rosing,J., Bakker,H.M., Fernandez,J.A., Tans,G., Griffin,J.H. (1994). Protein S binds to and inhibits factor Xa. *Proc.Natl.Acad.Sci.U.S.A* 91, 2728-2732.

Hellinga,H.W., Richards,F.M. (1991). Construction of new ligand binding sites in proteins of known structure. I. Computer-aided modeling of sites with pre-defined geometry. *J.Mol.Biol.* 222, 763-785.

Henderson,R., Baldwin,J.M., Ceska,T.A., Zemlin,F., Beckmann,E., Downing,K.H. (1990). An atomic model for the structure of bacteriorhodopsin. *Biochem.Soc.Trans.* 18, 844.

Henschen,A., Lottspeich,F. (1977). Amino acid sequence of human fibrin. Preliminary note on the completion of the beta-chain sequence. *Hoppe Seylers.Z.Physiol Chem.* 358, 1643-1646.

Herbert,J.M., Herault,J.P., Bernat,A., van Amsterdam,R.G., Lormeau,J.C., Petitou,M., van Boeckel,C., Hoffmann,P., Meuleman,D.G. (1998). Biochemical and pharmacological properties of SANORG 34006, a potent and long-acting synthetic pentasaccharide. *Blood* 91, 4197-4205.

Herwald,H., Dedio,J., Kellner,R., Loos,M., Muller-Esterl,W. (1996). Isolation and characterization of the kininogen-binding protein p33 from endothelial cells. Identity with the gC1q receptor. *J.Biol.Chem.* 271, 13040-13047.

Higashi,S., Matsumoto,N., Iwanaga,S. (1996). Molecular mechanism of tissue factor-mediated acceleration of factor VIIa activity. *J.Biol.Chem.* 271, 26569-26574.

Higashi,S., Nishimura,H., Aita,K., Iwanaga,S. (1994). Identification of regions of bovine factor VII essential for binding to tissue factor. *J.Biol.Chem.* 269, 18891-18898.

Higuchi,S., Murayama,N., Saguchi,K., Ohi,H., Fujita,Y., Camargo,A.C., Ogawa,T., Deshimaru,M., Ohno,M. (1999). Bradykinin-potentiating peptides and C-type natriuretic peptides from snake venom. *Immunopharmacology* 44, 129-135.

Hilpert,K., Wessner,H., Schneider-Mergener,J., Welfle,K., Misselwitz,R., Welfle,H., Hocke,A.C., Hippenstiel,S., Hohne,W. (2003). Design and characterization of a hybrid miniprotein that specifically inhibits porcine pancreatic elastase. *J Biol.Chem* 278, 24986-24993.

Himber,J., Kirchhofer,D., Riederer,M., Tschopp,T.B., Steiner,B., Roux,S.P. (1997). Dissociation of antithrombotic effect and bleeding time prolongation in rabbits by inhibiting tissue factor function. *Thromb.Haemost.* 78, 1142-1149.

Hockin,M.F., Jones,K.C., Everse,S.J., Mann,K.G. (2002). A model for the stoichiometric regulation of blood coagulation. *J.Biol.Chem.* 277, 18322-18333.

Hokama,Y., Iwanaga,S., Tatsuki,T., Suzuki,T. (1976). Snake venom proteinase inhibitors. III. Isolation of five polypeptide inhibitors from the venoms of *Hemachatus haemachatus* (Ringhal's cobra) and *Naja nivea* (Cape cobra) and the complete amino acid sequences of two of them. *J.Biochem.(Tokyo)* 79, 559-578.

Hollecker,M., Creighton,T.E. (1983). Evolutionary conservation and variation of protein folding pathways. Two protease inhibitor homologues from black mamba venom. *J.Mol.Biol.* 168, 409-437.

Holst,J., Lindblad,B., Bergqvist,D., Nordfang,O., Ostergaard,P.B., Petersen,J.G., Nielsen,G., Hedner,U. (1994). Antithrombotic effect of recombinant truncated tissue factor pathway inhibitor (TFPI1-161) in experimental venous thrombosis--a comparison with low molecular weight heparin. *Thromb.Haemost.* 71, 214-219.

Hougie (1956). Effect of Russell's viper venom (stypven) on Stuart clotting defect. *Proc.Soc.Exp.Biol.Med.* 98, 570-573.

Huang,D.X., Gai,L.Y., Wang,S.R., Li,T.D., Yang,T.S., Zhi,G., Du,L.S., Li,L.H. (1992). Defibrase, a purified fibrinolytic protease from snake venom in acute myocardial infarction. *Acta Cardiol.* 47, 445-458.

Huang,F., Hong,E. (2004). Platelet glycoprotein IIb/IIIa inhibition and its clinical use. *Curr.Med.Chem.Cardiovasc.Hematol.Agents* 2, 187-196.

Huang,M., Syed,R., Stura,E.A., Stone,M.J., Stefanko,R.S., Ruf,W., Edgington,T.S., Wilson,I.A. (1998b). The mechanism of an inhibitory antibody on TF-initiated blood coagulation revealed by the crystal structures of human tissue factor, Fab 5G9 and TF.G9 complex. *J.Mol.Biol.* 275, 873-894.

Huang,M., Syed,R., Stura,E.A., Stone,M.J., Stefanko,R.S., Ruf,W., Edgington,T.S., Wilson,I.A. (1998a). The mechanism of an inhibitory antibody on TF-initiated blood coagulation revealed by the crystal structures of human tissue factor, Fab 5G9 and TF.G9 complex. *J.Mol.Biol.* 275, 873-894.

Ibrahim,M.A., Ghazy,A.H., Maharem,T., Khalil,M. (2001). Isolation and properties of two forms of thrombin inhibitor from the nymphs of the camel tick *Hyalomma dromedarii* (Acari: Ixodidae). *Exp.Appl.Acarol.* 25, 675-698.

Imamura,T., Potempa,J., Travis,J. (2004). Activation of the kallikrein-kinin system and release of new kinins through alternative cleavage of kininogens by microbial and human cell proteinases. *Biol.Chem.* 385, 989-996.

Inada,M., Crowl,R.M., Bekkers,A.C., Verheij,H., Weiss,J. (1994). Determinants of the inhibitory action of purified 14-kDa phospholipases A2 on cell-free prothrombinase complex. *J.Biol.Chem.* 269, 26338-26343.

Isawa,H., Yuda,M., Yoneda,K., Chinzei,Y. (2000). The insect salivary protein, prolixin-S, inhibits factor IXa generation and Xase complex formation in the blood coagulation pathway. *J.Biol.Chem.* 275, 6636-6641.

Iwanaga,S., Okada,M., Isawa,H., Morita,A., Yuda,M., Chinzei,Y. (2003). Identification and characterization of novel salivary thrombin inhibitors from the ixodidae tick, *Haemaphysalis longicornis*. *Eur.J.Biochem.* 270, 1926-1934.

Iwanaga,S., Takahashi,H., Suzuki,T. (1976). Proteinase inhibitors from the venom of Russell's viper. *Methods Enzymol.* 45, 874-881.

Jang,Y., Guzman,L.A., Lincoff,A.M., Gottsauner-Wolf,M., Forudi,F., Hart,C.E., Courtman,D.W., Ezban,M., Ellis,S.G., Topol,E.J. (1995). Influence of blockade at specific levels of the coagulation cascade on restenosis in a rabbit atherosclerotic femoral artery injury model. *Circulation* 92, 3041-3050.

Janin,J., Chothia,C. (1978). Role of hydrophobicity in the binding of coenzymes. Appendix. Translational and rotational contribution to the free energy of dissociation. *Biochemistry* 17, 2943-2948.

- Jia,L.G., Shimokawa,K., Bjarnason,J.B., Fox,J.W. (1996). Snake venom metalloproteinases: structure, function and relationship to the ADAMs family of proteins. *Toxicon* 34, 1269-1276.
- Jim, R.T. (1957). A study of the plasma thrombin time. *J.Lab Clin.Med.* 50, 45-60.
- Jin,J., Chang,J., Chang,J.Y., Kelley,R.F., Stafford,D.W., Straight,D.L. (1999). Factor VIIa's first epidermal growth factor-like domain's role in catalytic activity. *Biochemistry* 38, 1185-1192.
- Jones,T.A., Zou,J.Y., Cowan,S.W., Kjeldgaard,M. (1991). Improved methods for building protein models in electron density maps and the location of errors in these models. *Acta Crystallogr.A* 47 (Pt 2), 110-119.
- Junqueira-de-Azevedo,I.L., Ching,A.T., Carvalho,E., Faria,F., Nishiyama,M.Y., Jr., Ho,P.L., Diniz,M.R. (2006). *Lachesis muta* (Viperidae) cDNAs reveal diverging pit viper molecules and scaffolds typical of cobra (Elapidae) venoms: implications for snake toxin repertoire evolution. *Genetics* 173, 877-889.
- Kaetsu,H., Mizuguchi,J., Hamamoto,T., Kamimura,K., Yoshida,Y., Nakagaki,T., Ogata,Y., Miyamoto,S., Funatsu,A. (1998). Large-scale preparation of human thrombin: polyethylene glycol potentiates the factor Xa-mediated activation of prothrombin. *Thromb.Res.* 90, 101-109.
- Kalafatis,M., Rand,M.D., Mann,K.G. (1994). The mechanism of inactivation of human factor V and human factor Va by activated protein C. *J.Biol.Chem.* 269, 31869-31880.
- Kane,W.H., DAVIE,E.W. (1988). Blood coagulation factors V and VIII: structural and functional similarities and their relationship to hemorrhagic and thrombotic disorders. *Blood* 71, 539-555.
- Katragadda,M., Morikis,D., Lambris,J.D. (2004). Thermodynamic studies on the interaction of the third complement component and its inhibitor, compstatin. *J Biol.Chem* 279, 54987-54995.
- Kearon,C., Comp,P., Douketis,J., Royds,R., Yamada,K., Gent,M. (2005). Dose-response study of recombinant human soluble thrombomodulin (ART-123) in the prevention of venous thromboembolism after total hip replacement. *J.Thromb.Haemost.* 3, 962-968.
- Kelly,C.R., Dickinson,C.D., Ruf,W. (1997). Ca²⁺ binding to the first epidermal growth factor module of coagulation factor VIIa is important for cofactor interaction and proteolytic function. *J.Biol.Chem.* 272, 17467-17472.

Kemball-Cook,G., Johnson,D.J., Tuddenham,E.G., Harlos,K. (1999). Crystal structure of active site-inhibited human coagulation factor VIIa (des-Gla). *J.Struct.Biol.* 127, 213-223.

Kerns,R.T., Kini,R.M., Stefansson,S., Evans,H.J. (1999). Targeting of venom phospholipases: the strongly anticoagulant phospholipase A(2) from *Naja nigricollis* venom binds to coagulation factor Xa to inhibit the prothrombinase complex. *Arch.Biochem.Biophys.* 369, 107-113.

Kerr,M.A., Walsh,K.A., Neurath,H. (1975). Catalysis by serine proteases and their zymogens. A study of acyl intermediates by circular dichroism. *Biochemistry* 14, 5088-5094.

Kim,M., Chen,B., Hussey,R.E., Chishti,Y., Montefiori,D., Hoxie,J.A., Byron,O., Campbell,G., Harrison,S.C., Reinherz,E.L. (2001). The stoichiometry of trimeric SIV glycoprotein interaction with CD4 differs from that of anti-envelope antibody Fab fragments. *J.Biol.Chem.* 276, 42667-42676.

Kini,R.M. (2002). Molecular moulds with multiple missions: functional sites in three-finger toxins. *Clin.Exp.Pharmacol.Physiol* 29, 815-822.

Kini,R.M. (2003). Excitement ahead: structure, function and mechanism of snake venom phospholipase A2 enzymes. *Toxicon* 42, 827-840.

Kini,R.M. (2005a). Structure-function relationships and mechanism of anticoagulant phospholipase A2 enzymes from snake venoms. *Toxicon* 45, 1147-1161.

Kini,R.M. (2005b). The intriguing world of prothrombin activators from snake venom. *Toxicon* 45, 1133-1145.

Kini,R.M., Banerjee,Y. (2005). Dissection approach: a simple strategy for the identification of the step of action of anticoagulant agents in the blood coagulation cascade. *J.Thromb.Haemost.* 3, 170-171.

Kini,R.M., Evans,H.J. (1987). Structure-function relationships of phospholipases. The anticoagulant region of phospholipases A2. *J.Biol.Chem.* 262, 14402-14407.

Kini,R.M., Evans,H.J. (1989). A model to explain the pharmacological effects of snake venom phospholipases A2. *Toxicon* 27, 613-635.

Kini,R.M., Evans,H.J. (1995). The role of enzymatic activity in inhibition of the extrinsic tenase complex by phospholipase A2 isoenzymes from *Naja nigricollis* venom. *Toxicon* 33, 1585-1590.

Kini,R.M., Haar,N.C., Evans,H.J. (1988). Non-enzymatic inhibitors of coagulation and platelet aggregation from *Naja nigricollis* venom are cardiotoxins. *Biochem.Biophys.Res.Commun.* 150, 1012-1016.

Kini,R.M., Rao,V.S., Joseph,J.S. (2001). Procoagulant proteins from snake venoms. *Haemostasis* 31, 218-224.

Kisiel,W., Davie,E.W. (1975). Isolation and characterization of bovine factor VII. *Biochemistry* 14, 4928-4934.

Kisiel,W., Fujikawa,K., DAVIE,E.W. (1977). Activation of bovine factor VII (proconvertin) by factor XIIa (activated Hageman factor). *Biochemistry* 16, 4189-4194.

Kisiel,W., Kondo,S., Smith,K.J., McMullen,B.A., Smith,L.F. (1987). Characterization of a protein C activator from *Agkistrodon contortrix contortrix* venom. *J.Biol.Chem.* 262, 12607-12613.

Klein,J.D., Walker,F.J. (1986). Purification of a protein C activator from the venom of the southern copperhead snake (*Agkistrodon contortrix contortrix*). *Biochemistry* 25, 4175-4179.

Klootwijk,P., Lenderink,T., Meij,S., Boersma,H., Melkert,R., Umans,V.A., Stibbe,J., Muller,E.J., Poortermans,K.J., Deckers,J.W., Simoons,M.L. (1999). Anticoagulant properties, clinical efficacy and safety of efegatran, a direct thrombin inhibitor, in patients with unstable angina. *Eur.Heart J.* 20, 1101-1111.

Knutson EO, Whitby KT (1973b). *J.Aerosol Sci.* 6, 443.

Knutson EO, Whitby KT (1973a). *J.Aerosol Sci.* 6, 453.

Koestenberger,M., Gallistl,S., Cvirn,G., Baier,K., Leschnik,B., Muntean,W. (2005). Anticoagulant action of melagatran, the active form of the oral direct thrombin inhibitor ximelagatran, in umbilical cord and adult plasma: an in vitro examination. *Thromb.Res.* 115, 135-142.

Koh,Y., Chung,K., Kim,D. (2000). Purification and cDNA cloning of salmorin that inhibits fibrinogen clotting. *Thromb.Res.* 99, 389-398.

Kondo,K., Umemura,K. (2002). Clinical pharmacokinetics of tirofiban, a nonpeptide glycoprotein IIb/IIIa receptor antagonist: comparison with the monoclonal antibody abciximab. *Clin.Pharmacokinet.* 41, 187-195.

Koo,B.H., Sohn,Y.D., Hwang,K.C., Jang,Y., Kim,D.S., Chung,K.H. (2002). Characterization and cDNA cloning of halyxin, a heterogeneous three-chain anticoagulant protein from the venom of *Agkistrodon halys brevicaudus*. *Toxicon* 40, 947-957.

Kousaka Y, Okuyama K, Adachi M. (1985). Determination of particle size distribution of ultra-fine aerosols using a differential mobility analyzer. *Aerosol.Sci.technol.* 4, 225.

Krakow,W., Endres,G.F., Siegel,B.M., Scheraga,H.A. (1972). An electron microscopic investigation of the polymerization of bovine fibrin monomer. *J.Mol.Biol.* 71, 95-103.

Kranjc,A., Kikelj,D., Peterlin-Masic,L. (2005). Recent advances in the discovery of tissue factor/factor VIIa inhibitors and dual inhibitors of factor VIIa/factor Xa. *Curr.Pharm.Des* 11, 4207-4227.

Krishnaswamy,S., Church,W.R., Nesheim,M.E., Mann,K.G. (1987). Activation of human prothrombin by human prothrombinase. Influence of factor Va on the reaction mechanism. *J.Biol.Chem.* 262, 3291-3299.

Kuhlbrandt,W., Wang,D.N., Fujiyoshi,Y. (1994). Atomic model of plant light-harvesting complex by electron crystallography. *Nature* 367, 614-621.

Lai,R., Takeuchi,H., Jonczy,J., Rees,H.H., Turner,P.C. (2004). A thrombin inhibitor from the ixodid tick, *Amblyomma hebraeum*. *Gene* 342, 243-249.

Lakshminarayanan,R., Chi-Jin,E.O., Loh,X.J., Kini,R.M., Valiyaveetil,S. (2005). Purification and characterization of a vaterite-inducing peptide, pelovaterin, from the eggshells of *Pelodiscus sinensis* (Chinese soft-shelled turtle). *Biomacromolecules.* 6, 1429-1437.

Langdell,R.D., Wagner,R.H., Brinkhous,K.M. (1953). Effect of antihemophilic factor on one-stage clotting tests; a presumptive test for hemophilia and a simple one-stage antihemophilic factor assay procedure. *J.Lab Clin.Med.* 41, 637-647.

Lawson,J.H., Mann,K.G. (1991). Cooperative activation of human factor IX by the human extrinsic pathway of blood coagulation. *J.Biol.Chem.* 266, 11317-11327.

Lee,A., Agnelli,G., Buller,H., Ginsberg,J., Heit,J., Rote,W., Vlasuk,G., Costantini,L., Julian,J., Comp,P., van Der,M.J., Piovello,F., Raskob,G., Gent,M. (2001). Dose-response study of recombinant factor VIIa/tissue factor inhibitor recombinant nematode anticoagulant protein c2 in prevention of postoperative venous thromboembolism in patients undergoing total knee replacement. *Circulation* 104, 74-78.

Lee,A.Y., Vlasuk,G.P. (2003). Recombinant nematode anticoagulant protein c2 and other inhibitors targeting blood coagulation factor VIIa/tissue factor. *J.Intern.Med.* 254, 313-321.

Lee,G.F., Lazarus,R.A., Kelley,R.F. (1997). Potent bifunctional anticoagulants: Kunitz domain-tissue factor fusion proteins. *Biochemistry* 36, 5607-5611.

Leonard,B.J., Clarke,B.J., Sridhara,S., Kelley,R., Ofosu,F.A., Blajchman,M.A. (2000). Activation and active site occupation alter conformation in the region of the first epidermal growth factor-like domain of human factor VII. *J.Biol.Chem.* 275, 34894-34900.

Levenberg,K. (1944). A Method for the Solution of Certain Problems in Least Squares. *Quart.Appl.Math.* 2, 164-168.

Lewicki,D.N., Gallagher,T.M. (2002). Quaternary structure of coronavirus spikes in complex with carcinoembryonic antigen-related cell adhesion molecule cellular receptors. *J.Biol.Chem.* 277, 19727-19734.

Lincoff AM (2000). First clinical investigation of a tissue-factor inhibitor administered during percutaneous coronary revascularization: a randomized, double-blinded, dose-escalation trial assessing safety and efficacy of FFR-FVIIa in percutaneous transluminal coronary angioplasty (ASIS) trial. *J Am Coll Cardiol.* 36, 312.

Liu,W., Bratko,D., Prausnitz,J.M., Blanch,H.W. (2004). Effect of alcohols on aqueous lysozyme-lysozyme interactions from static light-scattering measurements. *Biophys.Chem* 107, 289-298.

Lobo,d.A., Kamiguti,A., Bon,C. (2001). Coagulant and anticoagulant activities of *Bothrops lanceolatus* (Fer de lance) venom. *Toxicon* 39, 371-375.

Longhi,S., Receveur-Brechot,V., Karlin,D., Johansson,K., Darbon,H., Bhella,D., Yeo,R., Finet,S., Canard,B. (2003). The C-terminal domain of the measles virus nucleoprotein is intrinsically disordered and folds upon binding to the C-terminal moiety of the phosphoprotein. *J Biol.Chem* 278, 18638-18648.

Loo,J.A., Berhane,B., Kaddis,C.S., Wooding,K.M., Xie,Y., Kaufman,S.L., Chernushevich,I.V. (2005). Electrospray ionization mass spectrometry and ion mobility analysis of the 20S proteasome complex. *J Am.Soc.Mass Spectrom* 16, 998-1008.

Looger,L.L., Dwyer,M.A., Smith,J.J., Hellinga,H.W. (2003). Computational design of receptor and sensor proteins with novel functions. *Nature* 423, 185-190.

Lopez,J.A., Armstrong,M.L., Piegors,D.J., Heistad,D.D. (1990). Vascular responses to endothelin-1 in atherosclerotic primates. *Arteriosclerosis* 10, 1113-1118.

Lottspeich,F., Henschen,A. (1977). Amino acid sequence of human fibrin. Preliminary note on the completion of the gamma-chain sequence. *Hoppe Seylers.Z.Physiol Chem.* 358, 935-938.

Low,B.W., Preston,H.S., Sato,A., Rosen,L.S., Searl,J.E., Rudko,A.D., Richardson,J.S. (1976). Three dimensional structure of erabutoxin b neurotoxic protein: inhibitor of acetylcholine receptor. *Proc.Natl.Acad.Sci.U.S.A* 73, 2991-2994.

Lu,H., Isralewitz,B., Krammer,A., Vogel,V., Schulten,K. (1998). Unfolding of titin immunoglobulin domains by steered molecular dynamics simulation. *Biophys.J* 75, 662-671.

Luchtman-Jones,L., Broze,G.J., Jr. (1995). The current status of coagulation. *Ann.Med.* 27, 47-52.

Macaya, R.F., Schultze,P., Smith,F.W., Roe,J.A., Feigon,J. (1993). Thrombin-binding DNA aptamer forms a unimolecular quadruplex structure in solution. *Proc.Natl.Acad.Sci.U.S.A* 90, 3745-3749.

Macfarlane,R.G. (1964). An enzyme cascade in the blood clotting mechanism, and its function as a biochemical amplifier. *Nature* 202, 498-499.

Mao,S.S., Przysiecki,C.T., Krueger,J.A., Cooper,C.M., Lewis,S.D., Joyce,J., Lellis,C., Garsky,V.M., Sardana,M., Shafer,J.A. (1998). Selective inhibition of factor Xa in the prothrombinase complex by the carboxyl-terminal domain of antistasin. *J.Biol.Chem.* 273, 30086-30091.

Maraganore,J.M., Adelman,B.A. (1996). Hirulog: a direct thrombin inhibitor for management of acute coronary syndromes. *Coron.Artery Dis.* 7, 438-448.

Maraganore,J.M., Bourdon,P., Jablonski,J., Ramachandran,K.L., Fenton,J.W. (1990). Design and characterization of hirulogs: a novel class of bivalent peptide inhibitors of thrombin. *Biochemistry* 29, 7095-7101.

Marcinkiewicz,C. (2005). Functional characteristic of snake venom disintegrins: potential therapeutic implication. *Curr.Pharm.Des* 11, 815-827.

Marder,V.J., Matchett,M.O., Sherry,S. (1971). Detection of serum fibrinogen and fibrin degradation products. Comparison of six technics using purified products and application in clinical studies. *Am.J.Med.* 51, 71-82.

- Markland,F.S. (1998). Snake venoms and the hemostatic system. *Toxicon* 36, 1749-1800.
- Markwardt,F. (1994). The development of hirudin as an antithrombotic drug. *Thromb.Res.* 74, 1-23.
- Marquardt,D. (1963). An Algorithm for Least-Squares Estimation of Nonlinear Parameters. *SIAM J.Appl.Math.* 11, 431-441.
- Marsh,H.C., Jr., Meinwald,Y.C., Thannhauser,T.W., Scheraga,H.A. (1983). Mechanism of action of thrombin on fibrinogen. Kinetic evidence for involvement of aspartic acid at position P10. *Biochemistry* 22, 4170-4174.
- Masci,P.P., Whitaker,A.N., Sparrow,L.G., de Jersey,J., Winzor,D.J., Watters,D.J., Lavin,M.F., Gaffney,P.J. (2000). Textilins from *Pseudonaja textilis textilis*. Characterization of two plasmin inhibitors that reduce bleeding in an animal model. *Blood Coagul.Fibrinolysis* 11, 385-393.
- Matsumoto,T., Mugishima,H. (2006). Signal transduction via vascular endothelial growth factor (VEGF) receptors and their roles in atherogenesis. *J.Atheroscler.Thromb.* 13, 130-135.
- Maun,H.R., Eigenbrot,C., Raab,H., Arnott,D., Phu,L., Bullens,S., Lazarus,R.A. (2005). Disulfide locked variants of factor VIIa with a restricted beta-strand conformation have enhanced enzymatic activity. *Protein Sci.* 14, 1171-1180.
- McCallum,C.D., Hapak,R.C., Neuenschwander,P.F., Morrissey,J.H., Johnson,A.E. (1996). The location of the active site of blood coagulation factor VIIa above the membrane surface and its reorientation upon association with tissue factor. A fluorescence energy transfer study. *J.Biol.Chem.* 271, 28168-28175.
- McClellan,K.J., Goa,K.L. (1998). Tirofiban. A review of its use in acute coronary syndromes. *Drugs* 56, 1067-1080.
- McMullen,B.A., Fujikawa,K., Kisiel,W. (1989). Primary structure of a protein C activator from *Agkistrodon contortrix contortrix* venom. *Biochemistry* 28, 674-679.
- McNemar,C., Snow,M.E., Windsor,W.T., Prongay,A., Mui,P., Zhang,R., Durkin,J., Le,H.V., Weber,P.C. (1997). Thermodynamic and structural analysis of phosphotyrosine polypeptide binding to Grb2-SH2. *Biochemistry* 36, 10006-10014.
- McPherson,A. (1990). Current approaches to macromolecular crystallization. *Eur.J.Biochem.* 189, 1-23.

Mende,K., Petoukhova,O., Koulitchkova,V., Schaub,G.A., Lange,U., Kaufmann,R., Nowak,G. (1999). Dipetalogastin, a potent thrombin inhibitor from the blood-sucking insect. *Dipetalogaster maximus* cDNA cloning, expression and characterization. *Eur.J.Biochem.* 266, 583-590.

Merskey,C., Kleiner,G.J., Johnson,A.J. (1966). Quantitative estimation of split products of fibrinogen in human serum, relation to diagnosis and treatment. *Blood* 28, 1-18.

Millers,E.K., Masci,P.P., Lavin,M.F., de Jersey,J., Guddat,L.W. (2006). Crystallization and preliminary X-ray analysis of a Kunitz-type inhibitor, textilinin-1 from *Pseudonaja textilis textilis*. *Acta Crystallograph.Sect.F.Struct.Biol.Cryst.Commun.* 62, 642-645.

Millhauser,G.L. (1995). Views of helical peptides: a proposal for the position of 3(10)-helix along the thermodynamic folding pathway. *Biochemistry* 34, 3873-3877.

Mine,S., Yamazaki,T., Miyata,T., Hara,S., Kato,H. (2002). Structural mechanism for heparin-binding of the third Kunitz domain of human tissue factor pathway inhibitor. *Biochemistry* 41, 78-85.

Miyazawa,A., Fujiyoshi,Y., Stowell,M., Unwin,N. (1999). Nicotinic acetylcholine receptor at 4.6 Å resolution: transverse tunnels in the channel wall. *J.Mol.Biol.* 288, 765-786.

Mizuno,H., Fujimoto,Z., Atoda,H., Morita,T. (2001). Crystal structure of an anticoagulant protein in complex with the Gla domain of factor X. *Proc.Natl.Acad.Sci.U.S.A* 98, 7230-7234.

Mizuno,H., Fujimoto,Z., Koizumi,M., Kano,H., Atoda,H., Morita,T. (1997). Structure of coagulation factors IX/X-binding protein, a heterodimer of C-type lectin domains. *Nat.Struct.Biol.* 4, 438-441.

Mizuno,H., Fujimoto,Z., Koizumi,M., Kano,H., Atoda,H., Morita,T. (1999). Crystal structure of coagulation factor IX-binding protein from habu snake venom at 2.6 Å: implication of central loop swapping based on deletion in the linker region. *J.Mol.Biol.* 289, 103-112.

Moons,A.H., Peters,R.J., Bijsterveld,N.R., Piek,J.J., Prins,M.H., Vlasuk,G.P., Rote,W.E., Buller,H.R. (2003). Recombinant nematode anticoagulant protein c2, an inhibitor of the tissue factor/factor VIIa complex, in patients undergoing elective coronary angioplasty. *J.Am.Coll.Cardiol.* 41, 2147-2153.

Morita,T. (2005). Structures and functions of snake venom CLPs (C-type lectin-like proteins) with anticoagulant-, procoagulant-, and platelet-modulating activities. *Toxicon* 45, 1099-1114.

Moroi,M., Aoki,N. (1976). Isolation and characterization of alpha2-plasmin inhibitor from human plasma. A novel proteinase inhibitor which inhibits activator-induced clot lysis. *J.Biol.Chem.* 251, 5956-5965.

Morrissey,J.H., Fakhrai,H., Edgington,T.S. (1987). Molecular cloning of the cDNA for tissue factor, the cellular receptor for the initiation of the coagulation protease cascade. *Cell* 50, 129-135.

Morrissey,J.H., Neuenschwander,P.F. (1996). The ability of tissue factor to promote factor VII activation. *Blood* 88, 3664-3666.

Mosnier,L.O., Griffin,J.H. (2006). Protein C anticoagulant activity in relation to anti-inflammatory and anti-apoptotic activities. *Front Biosci.* 11, 2381-2399.

Mounier,C.M., Bon,C., Kini,R.M. (2001). Anticoagulant venom and mammalian secreted phospholipases A(2): protein- versus phospholipid-dependent mechanism of action. *Haemostasis* 31, 279-287.

Mounier,C.M., Hackeng,T.M., Schaeffer,F., Faure,G., Bon,C., Griffin,J.H. (1998). Inhibition of prothrombinase by human secretory phospholipase A2 involves binding to factor Xa. *J.Biol.Chem.* 273, 23764-23772.

Mounier,C.M., Luchetta,P., Lecut,C., Koduri,R.S., Faure,G., Lambeau,G., Valentin,E., Singer,A., Ghomashchi,F., Beguin,S., Gelb,M.H., Bon,C. (2000). Basic residues of human group IIA phospholipase A2 are important for binding to factor Xa and prothrombinase inhibition comparison with other mammalian secreted phospholipases A2. *Eur.J.Biochem.* 267, 4960-4969.

Muller,Y.A., Kelley,R.F., de Vos,A.M. (1998). Hinge bending within the cytokine receptor superfamily revealed by the 2.4 Å crystal structure of the extracellular domain of rabbit tissue factor. *Protein Sci.* 7, 1106-1115.

Muller,Y.A., Ultsch,M.H., de Vos,A.M. (1996). The crystal structure of the extracellular domain of human tissue factor refined to 1.7 Å resolution. *J.Mol.Biol.* 256, 144-159.

Muller,Y.A., Ultsch,M.H., Kelley,R.F., de Vos,A.M. (1994). Structure of the extracellular domain of human tissue factor: location of the factor VIIa binding site. *Biochemistry* 33, 10864-10870.

- Mullertz,S., Thorsen,S., Sottrup-Jensen,L. (1984). Identification of molecular forms of plasminogen and plasmin-inhibitor complexes in urokinase-activated human plasma. *Biochem.J.* 223, 169-177.
- Murakami,M.T., Arni,R.K. (2005). Crystallization and preliminary X-ray crystallographic studies of Protac, a commercial protein C activator isolated from *Agkistrodon contortrix contortrix* venom. *Biochim.Biophys.Acta* 1752, 202-204.
- Murata,K., Mitsuoka,K., Hirai,T., Walz,T., Agre,P., Heymann,J.B., Engel,A., Fujiyoshi,Y. (2000). Structural determinants of water permeation through aquaporin-1. *Nature* 407, 599-605.
- Murphy,K.P., Freire,E. (1992). Thermodynamics of structural stability and cooperative folding behavior in proteins. *Adv.Protein Chem* 43, 313-361.
- Nakagaki,T., Foster,D.C., Berkner,K.L., Kisiel,W. (1991). Initiation of the extrinsic pathway of blood coagulation: evidence for the tissue factor dependent autoactivation of human coagulation factor VII. *Biochemistry* 30, 10819-10824.
- Narasimhan,S., Koski,R.A., Beaulieu,B., Anderson,J.F., Ramamoorthi,N., Kantor,F., Cappello,M., Fikrig,E. (2002). A novel family of anticoagulants from the saliva of *Ixodes scapularis*. *Insect Mol.Biol.* 11, 641-650.
- Nawarskas,J.J., Anderson,J.R. (2001). Bivalirudin: a new approach to anticoagulation. *Heart Dis.* 3, 131-137.
- Nemerson,Y., Gentry,R. (1986). An ordered addition, essential activation model of the tissue factor pathway of coagulation: evidence for a conformational cage. *Biochemistry* 25, 4020-4033.
- Nemerson,Y., Repke,D. (1985). Tissue factor accelerates the activation of coagulation factor VII: the role of a bifunctional coagulation cofactor. *Thromb.Res.* 40, 351-358.
- Neuenschwander,P.F., Branam,D.E., Morrissey,J.H. (1993). Importance of substrate composition, pH and other variables on tissue factor enhancement of factor VIIa activity. *Thromb.Haemost.* 70, 970-977.
- Nienaber,J., Gaspar,A.R., Neitz,A.W. (1999). Savignin, a potent thrombin inhibitor isolated from the salivary glands of the tick *Ornithodoros savignyi* (Acari: Argasidae). *Exp.Parasitol.* 93, 82-91.
- Nogales,E., Wolf,S.G., Downing,K.H. (1998). Structure of the alpha beta tubulin dimer by electron crystallography. *Nature* 391, 199-203.

Nystedt,S., Ramakrishnan,V., Sundelin,J. (1996). The proteinase-activated receptor 2 is induced by inflammatory mediators in human endothelial cells. Comparison with the thrombin receptor. *J.Biol.Chem.* 271, 14910-14915.

O'Brien,L.M., Mastri,M., Fay,P.J. (2000). Regulation of factor VIIIa by human activated protein C and protein S: inactivation of cofactor in the intrinsic factor Xase. *Blood* 95, 1714-1720.

O'Shea,J.C., Tcheng,J.E. (2002). Eptifibatide: a potent inhibitor of the platelet receptor integrin glycoprotein IIb/IIIa. *Expert.Opin.Pharmacother.* 3, 1199-1210.

Okajima,K., Koga,S., Kaji,M., Inoue,M., Nakagaki,T., Funatsu,A., Okabe,H., Takatsuki,K., Aoki,N. (1990). Effect of protein C and activated protein C on coagulation and fibrinolysis in normal human subjects. *Thromb.Haemost.* 63, 48-53.

Orning,L., Fischer,P.M., Hu,C.K., Agner,E., Engebretsen,M., Husbyn,M., Petersen,L.B., Orvim,U., Llinas,M., Sakariassen,K.S. (2002). A cyclic pentapeptide derived from the second EGF-like domain of Factor VII is an inhibitor of tissue factor dependent coagulation and thrombus formation. *Thromb.Haemost.* 87, 13-21.

Osterud,B., Rapaport,S.I., Schiffman,S., Chong,M.M. (1971). Formation of intrinsic factor-X activator activity, with special reference to the role of thrombin. *Br.J.Haematol.* 21, 643-660.

Ouyang,C., Jy,W., Zan,Y.P., Teng,C.M. (1981). Mechanism of the anticoagulant action of phospholipase A purified from *Trimeresurus mucrosquamatus* (Formosan habu) snake venom. *Toxicon* 19, 113-120.

Ouyang,C., Teng,C.M. (1976). Fibrinogenolytic enzymes of *Trimeresurus mucrosquamatus* venom. *Biochim.Biophys.Acta* 420, 298-308.

Ouyang,C., Yang,F.Y. (1975). Purification and properties of the anticoagulant principle of *Trimeresurus gramineus* venom. *Biochim.Biophys.Acta* 386, 479-492.

Paborsky,L.R., Caras,I.W., Fisher,K.L., Gorman,C.M. (1991b). Lipid association, but not the transmembrane domain, is required for tissue factor activity. Substitution of the transmembrane domain with a phosphatidylinositol anchor. *J.Biol.Chem.* 266, 21911-21916.

Paborsky,L.R., Caras,I.W., Fisher,K.L., Gorman,C.M. (1991a). Lipid association, but not the transmembrane domain, is required for tissue factor activity. Substitution of the transmembrane domain with a phosphatidylinositol anchor. *J.Biol.Chem.* 266, 21911-21916.

Paborsky,L.R., Harris,R.J. (1990). Post-translational modifications of recombinant human tissue factor. *Thromb.Res.* 60, 367-376.

Paborsky,L.R., Tate,K.M., Harris,R.J., Yansura,D.G., Band,L., McCray,G., Gorman,C.M., O'Brien,D.P., Chang,J.Y., Swartz,J.R., . (1989). Purification of recombinant human tissue factor. *Biochemistry* 28, 8072-8077.

Palabrica,T., Lobb,R., Furie,B.C., Aronovitz,M., Benjamin,C., Hsu,Y.M., Sajer,S.A., Furie,B. (1992). Leukocyte accumulation promoting fibrin deposition is mediated in vivo by P-selectin on adherent platelets. *Nature* 359, 848-851.

Palmer,T.D., Thompson,A.R., Miller,A.D. (1989). Production of human factor IX in animals by genetically modified skin fibroblasts: potential therapy for hemophilia B. *Blood* 73, 438-445.

Panteleev,M.A., Zarnitsina,V.I., Ataulkhanov,F.I. (2002). Tissue factor pathway inhibitor: a possible mechanism of action. *Eur.J Biochem.* 269, 2016-2031.

Pawashe,A.B., Golino,P., Ambrosio,G., Migliaccio,F., Ragni,M., Pascucci,I., Chiariello,M., Bach,R., Garen,A., Konigsberg,W.K., . (1994). A monoclonal antibody against rabbit tissue factor inhibits thrombus formation in stenotic injured rabbit carotid arteries. *Circ.Res.* 74, 56-63.

Pawlak,J., Mackessy,S.P., Fry,B.G., Bhatia,M., Mourier,G., Fruchart-Gaillard,C., Servent,D., Menez,R., Stura,E., Menez,A., Kini,R.M. (2006). Denmotoxin, a three-finger toxin from the colubrid snake *Boiga dendrophila* (Mangrove Catsnake) with bird-specific activity. *J.Biol.Chem.* 281, 29030-29041.

Pedersen,A.H., Lund-Hansen,T., Bisgaard-Frantzen,H., Olsen,F., Petersen,L.C. (1989). Autoactivation of human recombinant coagulation factor VII. *Biochemistry* 28, 9331-9336.

Pendurthi,U.R., Alok,D., Rao,L.V. (1997). Binding of factor VIIa to tissue factor induces alterations in gene expression in human fibroblast cells: up-regulation of poly(A) polymerase. *Proc.Natl.Acad.Sci.U.S.A* 94, 12598-12603.

Perozzo,R., Folkers,G., Scapozza,L. (2004). Thermodynamics of protein-ligand interactions: history, presence, and future aspects. *J Recept.Signal.Transduct.Res.* 24, 1-52.

Persson,E. (2006). Macromolecular substrate affinity for free factor VIIa is independent of a buried protease domain N-terminus. *Biochem.Biophys.Res.Commun.* 341, 28-32.

- Persson,E., Olsen,O.H., Ostergaard,A., Nielsen,L.S. (1997). Ca²⁺ binding to the first epidermal growth factor-like domain of factor VIIa increases amidolytic activity and tissue factor affinity. *J.Biol.Chem.* 272, 19919-19924.
- Persson,E., Petersen,L.C. (1995). Structurally and functionally distinct Ca²⁺ binding sites in the gamma-carboxyglutamic acid-containing domain of factor VIIa. *Eur.J.Biochem.* 234, 293-300.
- Petersen,L.C., Bjorn,S.E., Olsen,O.H., Nordfang,O., Norris,F., Norris,K. (1996a). Inhibitory properties of separate recombinant Kunitz-type-protease-inhibitor domains from tissue-factor-pathway inhibitor. *Eur.J.Biochem.* 235, 310-316.
- Petersen,L.C., Sprecher,C.A., Foster,D.C., Blumberg,H., Hamamoto,T., Kisiel,W. (1996b). Inhibitory properties of a novel human Kunitz-type protease inhibitor homologous to tissue factor pathway inhibitor. *Biochemistry* 35, 266-272.
- Pfleger,K.D., Eidne,K.A. (2006). Illuminating insights into protein-protein interactions using bioluminescence resonance energy transfer (BRET). *Nat.Methods* 3, 165-174.
- Pike,A.C., Brzozowski,A.M., Roberts,S.M., Olsen,O.H., Persson,E. (1999). Structure of human factor VIIa and its implications for the triggering of blood coagulation. *Proc.Natl.Acad.Sci.U.S.A* 96, 8925-8930.
- Piotto,M., Saudek,V., Sklenar,V. (1992). Gradient-tailored excitation for single-quantum NMR spectroscopy of aqueous solutions. *J Biomol.NMR* 2, 661-665.
- Plosker,G.L., Ibbotson,T. (2003). Eptifibatide: a pharmacoeconomic review of its use in percutaneous coronary intervention and acute coronary syndromes. *Pharmacoeconomics.* 21, 885-912.
- Plow,E.F., Collen,D. (1981). The presence and release of alpha 2-antiplasmin from human platelets. *Blood* 58, 1069-1074.
- Possani,L.D., Martin,B.M., Yatani,A., Mochca-Morales,J., Zamudio,F.Z., Gurrola,G.B., Brown,A.M. (1992). Isolation and physiological characterization of taicatoxin, a complex toxin with specific effects on calcium channels. *Toxicon* 30, 1343-1364.
- Poulsen,L.K., Jacobsen,N., Sorensen,B.B., Bergenhem,N.C., Kelly,J.D., Foster,D.C., Thastrup,O., Ezban,M., Petersen,L.C. (1998). Signal transduction via the mitogen-activated protein kinase pathway induced by binding of coagulation factor VIIa to tissue factor. *J.Biol.Chem.* 273, 6228-6232.

Prabhu,N.V., Sharp,K.A. (2005). Heat capacity in proteins. *Annu.Rev Phys.Chem* 56, 521-548.

Provencher,S.W. (1976). A Fourier method for the analysis of exponential decay curves. *Biophys.J* 16, 27-41.

Quick AJ. (1935). The prothrombin time in haemophilia and in obstructive jaundice. *J.Biol.Chem.* 109, 73-74.

Quick,A.J. (1973). Quick on Quick's test. *N.Engl.J.Med.* 288, 1079.

Radcliffe,R., Nemerson,Y. (1975). Activation and control of factor VII by activated factor X and thrombin. Isolation and characterization of a single chain form of factor VII. *J.Biol.Chem.* 250, 388-395.

Radcliffe,R., Nemerson,Y. (1976). Mechanism of activation of bovine factor VII. Products of cleavage by factor Xa. *J.Biol.Chem.* 251, 4749-4802.

Ramachandran,G.N., Ramakrishnan,C., Sasisekharan,V. (1963). Stereochemistry of polypeptide chain configurations. *J.Mol.Biol.* 7, 95-99.

Rao,L.V., Rapaport,S.I. (1987). Studies of a mechanism inhibiting the initiation of the extrinsic pathway of coagulation. *Blood* 69, 645-651.

Rao,L.V., Rapaport,S.I. (1988). Activation of factor VII bound to tissue factor: a key early step in the tissue factor pathway of blood coagulation. *Proc.Natl.Acad.Sci.U.S.A* 85, 6687-6691.

Rao,L.V., Williams,T., Rapaport,S.I. (1996). Studies of the activation of factor VII bound to tissue factor. *Blood* 87, 3738-3748.

Rao,V.S., Kini,R.M. (2002). Pseutarin C, a prothrombin activator from *Pseudonaja textilis* venom: its structural and functional similarity to mammalian coagulation factor Xa-Va complex. *Thromb.Haemost.* 88, 611-619.

Rao,V.S., Swarup,S., Kini,R.M. (2003). The nonenzymatic subunit of pseutarin C, a prothrombin activator from eastern brown snake (*Pseudonaja textilis*) venom, shows structural similarity to mammalian coagulation factor V. *Blood* 102, 1347-1354.

Rao,V.S., Swarup,S., Manjunatha,K.R. (2004). The catalytic subunit of pseutarin C, a group C prothrombin activator from the venom of *Pseudonaja textilis*, is structurally similar to mammalian blood coagulation factor Xa. *Thromb.Haemost.* 92, 509-521.

Rauch,U., Bonderman,D., Bohrmann,B., Badimon,J.J., Himber,J., Riederer,M.A., Nemerson,Y. (2000). Transfer of tissue factor from leukocytes to platelets is mediated by CD15 and tissue factor. *Blood* 96, 170-175.

Redlitz,A., Tan,A.K., Eaton,D.L., Plow,E.F. (1995). Plasma carboxypeptidases as regulators of the plasminogen system. *J.Clin.Invest* 96, 2534-2538.

Refino,C.J., Jeet,S., DeGuzman,L., Bunting,S., Kirchhofer,D. (2002). A human antibody that inhibits factor IX/IXa function potently inhibits arterial thrombosis without increasing bleeding. *Arterioscler.Thromb.Vasc.Biol.* 22, 517-522.

Revak,S.D., Cochrane,C.G. (1976). The relationship of structure and function in human Hageman factor. The association of enzymatic and binding activities with separate regions of the molecule. *J.Clin.Invest* 57, 852-860.

Revak,S.D., Cochrane,C.G., Bouma,B.N., Griffin,J.H. (1978). Surface and fluid phase activities of two forms of activated Hageman factor produced during contact activation of plasma. *J.Exp.Med.* 147, 719-729.

Revak,S.D., Cochrane,C.G., Griffin,J.H. (1977). The binding and cleavage characteristics of human Hageman factor during contact activation. A comparison of normal plasma with plasmas deficient in factor XI, prekallikrein, or high molecular weight kininogen. *J.Clin.Invest* 59, 1167-1175.

Rezaie,A.R. (2001). Prothrombin protects factor Xa in the prothrombinase complex from inhibition by the heparin-antithrombin complex. *Blood* 97, 2308-2313.

Rickles,F.R., Patierno,S., Fernandez,P.M. (2003). Tissue factor, thrombin, and cancer. *Chest* 124, 58S-68S.

Robbins,K.C., Summaria,L., Hsieh,B., Shah,R.J. (1967). The peptide chains of human plasmin. Mechanism of activation of human plasminogen to plasmin. *J.Biol.Chem.* 242, 2333-2342.

Roberge,M., Peek,M., Kirchhofer,D., Dennis,M.S., Lazarus,R.A. (2002). Fusion of two distinct peptide exosite inhibitors of Factor VIIa. *Biochem.J* 363, 387-393.

Roberge,M., Santell,L., Dennis,M.S., Eigenbrot,C., Dwyer,M.A., Lazarus,R.A. (2001). A novel exosite on coagulation factor VIIa and its molecular interactions with a new class of peptide inhibitors. *Biochemistry* 40, 9522-9531.

Rosing,J., Tans,G. (1992). Structural and functional properties of snake venom prothrombin activators. *Toxicon* 30, 1515-1527.

Rottingen,J.A., Enden,T., Camerer,E., Iversen,J.G., Prydz,H. (1995). Binding of human factor VIIa to tissue factor induces cytosolic Ca²⁺ signals in J82 cells, transfected COS-1 cells, Madin-Darby canine kidney cells and in human endothelial cells induced to synthesize tissue factor. *J.Biol.Chem.* 270, 4650-4660.

Roux,S., Tschopp,T., Baumgartner,H.R. (1996). Effects of napsagatran (Ro 46-6240), a new synthetic thrombin inhibitor and of heparin in a canine model of coronary artery thrombosis: comparison with an ex vivo annular perfusion chamber model. *J.Pharmacol.Exp.Ther.* 277, 71-78.

Roy,S., Hass,P.E., Bourell,J.H., Henzel,W.J., Vehar,G.A. (1991). Lysine residues 165 and 166 are essential for the cofactor function of tissue factor. *J Biol.Chem* 266, 22063-22066.

Ruf,W. (1998). The interaction of activated factor VII with tissue factor: insight into the mechanism of cofactor-mediated activation of activated factor VII. *Blood Coagul.Fibrinolysis* 9 Suppl 1, S73-S78.

Ruf,W., Miles,D.J., Rehemtulla,A., Edgington,T.S. (1992). Cofactor residues lysine 165 and 166 are critical for protein substrate recognition by the tissue factor-factor VIIa protease complex. *J Biol.Chem* 267, 6375-6381.

Russell,F.E. (1980). Snake Venom Poisoning. Lippincott, Philadelphia.

Sakurai,Y., Shima,M., Matsumoto,T., Takatsuka,H., Nishiya,K., Kasuda,S., Fujimura,Y., Yoshioka,A. (2003). Anticoagulant activity of M-LAO, L-amino acid oxidase purified from *Agkistrodon halys blomhoffii*, through selective inhibition of factor IX. *Biochim.Biophys.Acta* 1649, 51-57.

Sakurai,Y., Takatsuka,H., Yoshioka,A., Matsui,T., Suzuki,M., Titani,K., Fujimura,Y. (2001). Inhibition of human platelet aggregation by L-amino acid oxidase purified from *Naja naja kaouthia* venom. *Toxicon* 39, 1827-1833.

Salzet,M., Chopin,V., Baert,J., Matias,I., Malecha,J. (2000). Theromin, a novel leech thrombin inhibitor. *J.Biol.Chem.* 275, 30774-30780.

Samama,M.M., Gerotziafas,G.T. (2003). Evaluation of the pharmacological properties and clinical results of the synthetic pentasaccharide (fondaparinux). *Thromb.Res.* 109, 1-11.

Scharf,M., Engels,J., Tripier,D. (1989). Primary structures of new 'iso-hirudins'. *FEBS Lett.* 255, 105-110.

Schechter,I., Berger,A. (1967). On the size of the active site in proteases. I. Papain. *Biochem.Biophys.Res.Comm.* 27, 157-162.

Schmaier,A.H. (1997). Contact activation: a revision. *Thromb.Haemost.* 78, 101-107.

Schmaier,A.H. (1998). Plasma contact activation: a revised hypothesis. *Biol.Res.* 31, 251-262.

Schreiber,G., Fersht,A.R. (1996). Rapid, electrostatically assisted association of proteins. *Nat.Struct.Biol.* 3, 427-431.

Schwarz,F.P., Tello,D., Goldbaum,F.A., Mariuzza,R.A., Poljak,R.J. (1995). Thermodynamics of antigen-antibody binding using specific anti-lysozyme antibodies. *Eur.J Biochem.* 228, 388-394.

Sekiya,F., Atoda,H., Morita,T. (1993). Isolation and characterization of an anticoagulant protein homologous to botrocetin from the venom of *Bothrops jararaca*. *Biochemistry* 32, 6892-6897.

Sekiya,F., Yoshida,M., Yamashita,T., Morita,T. (1996). Magnesium(II) is a crucial constituent of the blood coagulation cascade. Potentiation of coagulant activities of factor IX by Mg²⁺ ions. *J.Biol.Chem.* 271, 8541-8544.

Sharma,S.K., Ramsey,T.M., Bair,K.W. (2002). Protein-protein interactions: lessons learned. *Curr.Med.Chem Anti.-Canc.Agents* 2, 311-330.

Sherman,D.G. (2002). Ancrod. *Curr.Med.Res.Opin.* 18 Suppl 2, s48-s52.

Shikamoto,Y., Morita,T., Fujimoto,Z., Mizuno,H. (2003). Crystal structure of Mg²⁺- and Ca²⁺-bound Gla domain of factor IX complexed with binding protein. *J.Biol.Chem.* 278, 24090-24094.

Slungaard,A., Fernandez,J.A., Griffin,J.H., Key,N.S., Long,J.R., Piegors,D.J., Lentz,S.R. (2003). Platelet factor 4 enhances generation of activated protein C in vitro and in vivo. *Blood* 102, 146-151.

Soejima,K., Mizuguchi,J., Yuguchi,M., Nakagaki,T., Higashi,S., Iwanaga,S. (2001). Factor VIIa modified in the 170 loop shows enhanced catalytic activity but does not change the zymogen-like property. *J.Biol.Chem.* 276, 17229-17235.

Sorensen,B.B., Persson,E., Freskgard,P.O., Kjalke,M., Ezban,M., Williams,T., Rao,L.V. (1997). Incorporation of an active site inhibitor in factor VIIa alters the affinity for tissue factor. *J Biol.Chem* 272, 11863-11868.

Spicer,E.K., Horton,R., Bloem,L., Bach,R., Williams,K.R., Guha,A., Kraus,J., Lin,T.C., Nemerson,Y., Konigsberg,W.H. (1987). Isolation of cDNA clones coding for human tissue factor: primary structure of the protein and cDNA. *Proc.Natl.Acad.Sci.U.S.A* 84, 5148-5152.

Spolar,R.S., Record,M.T., Jr. (1994). Coupling of local folding to site-specific binding of proteins to DNA. *Science* 263, 777-784.

Stassen,J.M., Lambeir,A.M., Matthyssens,G., Ripka,W.C., Nystrom,A., Sixma,J.J., Vermynen,J. (1995a). Characterisation of a novel series of aprotinin-derived anticoagulants. I. In vitro and pharmacological properties. *Thromb.Haemost.* 74, 646-654.

Stassen,J.M., Lambeir,A.M., Vreys,I., Deckmyn,H., Matthyssens,G., Nystrom,A., Vermynen,J. (1995b). Characterisation of a novel series of aprotinin-derived anticoagulants. II. Comparative antithrombotic effects on primary thrombus formation in vivo. *Thromb.Haemost.* 74, 655-659.

Stassens,P., Bergum,P.W., Gansemans,Y., Jespers,L., Laroche,Y., Huang,S., Maki,S., Messens,J., Lauwereys,M., Cappello,M., Hotez,P.J., Lasters,I., Vlasuk,G.P. (1996). Anticoagulant repertoire of the hookworm *Ancylostoma caninum*. *Proc.Natl.Acad.Sci.U.S.A* 93, 2149-2154.

Stefansson,S., Kini,R.M., Evans,H.J. (1989). The inhibition of clotting complexes of the extrinsic coagulation cascade by the phospholipase A2 isoenzymes from *Naja nigricollis* venom. *Thromb.Res.* 55, 481-491.

Stefansson,S., Kini,R.M., Evans,H.J. (1990a). The basic phospholipase A2 from *Naja nigricollis* venom inhibits the prothrombinase complex by a novel nonenzymatic mechanism. *Biochemistry* 29, 7742-7746.

Stefansson,S., Kini,R.M., Evans,H.J. (1990b). The basic phospholipase A2 from *Naja nigricollis* venom inhibits the prothrombinase complex by a novel nonenzymatic mechanism. *Biochemistry* 29, 7742-7746.

Stenflo,J. (1976). A new vitamin K-dependent protein. Purification from bovine plasma and preliminary characterization. *J.Biol.Chem.* 251, 355-363.

Stewart,R.J., Fredenburgh,J.C., Weitz,J.I. (1998). Characterization of the interactions of plasminogen and tissue and vampire bat plasminogen activators with fibrinogen, fibrin,

and the complex of D-dimer noncovalently linked to fragment E. *J.Biol.Chem.* 273, 18292-18299.

Stites,W.E. (1997). Protein-Protein Interactions: Interface Structure, Binding Thermodynamics, and Mutational Analysis. *Chem Rev* 97, 1233-1250.

Stocker,K. (1990). Snake Venom Protein Affecting Hemostasis and Fibrinolysis. In *Medical Use of Snake Venom Proteins*. CRC Press, Boca Raton.

Stocker,K., Fischer,H., Meier,J., Brogli,M., Svendsen,L. (1986). Protein C activators in snake venoms. *Behring Inst.Mitt.* 37-47.

Stocker,K., Fischer,H., Meier,J., Brogli,M., Svendsen,L. (1987). Characterization of the protein C activator Protac from the venom of the southern copperhead (*Agkistrodon contortrix*) snake. *Toxicon* 25, 239-252.

Stone,M.J., Ruf,W., Miles,D.J., Edgington,T.S., Wright,P.E. (1995). Recombinant soluble human tissue factor secreted by *Saccharomyces cerevisiae* and refolded from *Escherichia coli* inclusion bodies: glycosylation of mutants, activity and physical characterization. *Biochem.J.* 310 (Pt 2), 605-614.

Strube,K.H., Kroger,B., Bialojan,S., Otte,M., Dodt,J. (1993). Isolation, sequence analysis, and cloning of haemadin. An anticoagulant peptide from the Indian leech. *J.Biol.Chem.* 268, 8590-8595.

Su,M.J., Coulter,A.R., Sutherland,S.K., Chang,C.C. (1983). The presynaptic neuromuscular blocking effect and phospholipase A2 activity of textilotoxin, a potent toxin isolated from the venom of the Australian brown snake, *Pseudonaja textilis*. *Toxicon* 21, 143-151.

Subburaju,S., Kini,R.M. (1997). Isolation and purification of superbins I and II from *Austrelaps superbis* (copperhead) snake venom and their anticoagulant and antiplatelet effects. *Toxicon* 35, 1239-1250.

Summaria,L., Hsieh,B., Robbins,K.C. (1967). The specific mechanism of activation of human plasminogen to plasmin. *J.Biol.Chem.* 242, 4279-4283.

Sun,J., Yamaguchi,M., Yuda,M., Miura,K., Takeya,H., Hirai,M., Matsuoka,H., Ando,K., Watanabe,T., Suzuki,K., Chinzei,Y. (1996). Purification, characterization and cDNA cloning of a novel anticoagulant of the intrinsic pathway, (prolixin-S) from salivary glands of the blood sucking bug, *Rhodnius prolixus*. *Thromb.Haemost.* 75, 573-577.

Sutton,R.B., Fasshauer,D., Jahn,R., Brunger,A.T. (1998). Crystal structure of a SNARE complex involved in synaptic exocytosis at 2.4 Å resolution. *Nature* 395, 347-353.

Swords,N.A., Mann,K.G. (1993). The assembly of the prothrombinase complex on adherent platelets. *Arterioscler.Thromb.* 13, 1602-1612.

Takahashi,H., Iwanaga,S., Kitagawa,T., Hokama,Y., Suzuki,T. (1974a). Snake venom proteinase inhibitors. II. Chemical structure of inhibitor II isolated from the venom of Russell's viper (*Vipera russelli*). *J.Biochem.(Tokyo)* 76, 721-733.

Takahashi,H., Iwanaga,S., Suzuki,T. (1974b). Snake venom proteinase inhibitors. I. Isolation and properties of two inhibitors of kallikrein, trypsin, plasmin, and alpha-chymotrypsin from the venom of Russell's viper (*Vipera russelli*). *J.Biochem.(Tokyo)* 76, 709-719.

Tammet H. (1995). Size and mobility of nanometer particles, clusters, and ions. *J.Aerosol.Sci.* 26, 459.

Tan,A.K., Eaton,D.L. (1995). Activation and characterization of procarboxypeptidase B from human plasma. *Biochemistry* 34, 5811-5816.

Taylor,F.B., Jr. (1996). Role of tissue factor and factor VIIa in the coagulant and inflammatory response to LD100 Escherichia coli in the baboon. *Haemostasis* 26 Suppl 1, 83-91.

Taylor,F.B., Jr., Chang,A., Ruf,W., Morrissey,J.H., Hinshaw,L., Catlett,R., Blick,K., Edgington,T.S. (1991). Lethal E. coli septic shock is prevented by blocking tissue factor with monoclonal antibody. *Circ.Shock* 33, 127-134.

Tidor,B., Karplus,M. (1994). The contribution of vibrational entropy to molecular association. The dimerization of insulin. *J Mol.Biol.* 238, 405-414.

Tipping,P.G., Erlich,J.H., Apostolopoulos,J., Mackman,N., Loskutoff,D., Holdsworth,S.R. (1995). Glomerular tissue factor expression in crescentic glomerulonephritis. Correlations between antigen, activity, and mRNA. *Am.J Pathol.* 147, 1736-1748.

Torres,A.M., Kini,R.M., Selvanayagam,N., Kuchel,P.W. (2001). NMR structure of buccandin, a neurotoxin from the venom of the Malayan krait (*Bungarus candidus*). *Biochem.J.* 360, 539-548.

Ulmer,T.S., Werner,J.M., Campbell,I.D. (2002). SH3-SH2 domain orientation in Src kinases: NMR studies of Fyn. *Structure.* 10, 901-911.

- Unwin,N. (1995). Acetylcholine receptor channel imaged in the open state. *Nature* 373, 37-43.
- Valenzuela,J.G., Francischetti,I.M., Ribeiro,J.M. (1999). Purification, cloning, and synthesis of a novel salivary anti-thrombin from the mosquito *Anopheles albimanus*. *Biochemistry* 38, 11209-11215.
- van de,L.A., Stubbs,M.T., Bode,W., Friedrich,T., Bollschweiler,C., Hoffken,W., Huber,R. (1996). The ornithodorin-thrombin crystal structure, a key to the TAP enigma? *EMBO J.* 15, 6011-6017.
- van Wijnen,M., Stam,J.G., van't Veer,C., Meijers,J.C., Reitsma,P.H., Bertina,R.M., Bouma,B.N. (1996). The interaction of protein S with the phospholipid surface is essential for the activated protein C-independent activity of protein S. *Thromb.Haemost.* 76, 397-403.
- Vlasuk,G.P. (1993). Structural and functional characterization of tick anticoagulant peptide (TAP): a potent and selective inhibitor of blood coagulation factor Xa. *Thromb.Haemost.* 70, 212-216.
- von Hippel,P.H. (1994). Protein-DNA recognition: new perspectives and underlying themes. *Science* 263, 769-770.
- Walenga,J.M. (2002). An overview of the direct thrombin inhibitor argatroban. *Pathophysiol.Haemost.Thromb.* 32 Suppl 3, 9-14.
- Walenga,J.M., Hoppensteadt,D.A. (2004). Monitoring the new antithrombotic drugs. *Semin.Thromb.Hemost.* 30, 683-695.
- Walker,F.J. (1980). Regulation of activated protein C by a new protein. A possible function for bovine protein S. *J.Biol.Chem.* 255, 5521-5524.
- Wang,R., Kini,R.M., Chung,M.C. (1999). Rhodocetin, a novel platelet aggregation inhibitor from the venom of *Calloselasma rhodostoma* (Malayan pit viper): synergistic and noncovalent interaction between its subunits. *Biochemistry* 38, 7584-7593.
- Ware,S., Donahue,J.P., Hawiger,J., Anderson,W.F. (1999). Structure of the fibrinogen gamma-chain integrin binding and factor XIIIa cross-linking sites obtained through carrier protein driven crystallization. *Protein Sci.* 8, 2663-2671.
- Waters,E.K., Yegneswaran,S., Morrissey,J.H. (2006). Raising the active site of factor VIIa above the membrane surface reduces its procoagulant activity but not factor VII autoactivation. *J.Biol.Chem.* 281, 26062-26068.

Waxman,L., Smith,D.E., Arcuri,K.E., Vlasuk,G.P. (1990). Tick anticoagulant peptide (TAP) is a novel inhibitor of blood coagulation factor Xa. *Science* 248, 593-596.

Weisel,J.W. (1986). Fibrin assembly. Lateral aggregation and the role of the two pairs of fibrinopeptides. *Biophys.J.* 50, 1079-1093.

Weisel,J.W., Phillips,G.N., Jr., Cohen,C. (1981). A model from electron microscopy for the molecular structure of fibrinogen and fibrin. *Nature* 289, 263-267.

Weisel,J.W., Stauffacher,C.V., Bullitt,E., Cohen,C. (1985). A model for fibrinogen: domains and sequence. *Science* 230, 1388-1391.

Weitz,J.I. (2003). Heparan sulfate: antithrombotic or not? *J Clin.Invest* 111, 952-954.

Weitz,J.I., Hudoba,M., Massel,D., Maraganore,J., Hirsh,J. (1990). Clot-bound thrombin is protected from inhibition by heparin-antithrombin III but is susceptible to inactivation by antithrombin III-independent inhibitors. *J Clin.Invest* 86, 385-391.

Westhof,E., Dumas,P. (1996). Refinement of protein and nucleic acid structures. *Methods Mol.Biol.* 56, 227-244.

Wilcox,J.N., Smith,K.M., Schwartz,S.M., Gordon,D. (1989). Localization of tissue factor in the normal vessel wall and in the atherosclerotic plaque. *Proc.Natl.Acad.Sci.U.S.A* 86, 2839-2843.

Wildgoose,P., Kazim,A.L., Kisiel,W. (1990). The importance of residues 195-206 of human blood clotting factor VII in the interaction of factor VII with tissue factor. *Proc.Natl.Acad.Sci.U.S.A* 87, 7290-7294.

Wildgoose,P., Kisiel,W. (1989). Activation of human factor VII by factors IXa and Xa on human bladder carcinoma cells. *Blood* 73, 1888-1895.

Wildgoose,P., Nemerson,Y., Hansen,L.L., Nielsen,F.E., Glazer,S., Hedner,U. (1992). Measurement of basal levels of factor VIIa in hemophilia A and B patients. *Blood* 80, 25-28.

Wilkins,D.K., Grimshaw,S.B., Receveur,V., Dobson,C.M., Jones,J.A., Smith,L.J. (1999). Hydrodynamic radii of native and denatured proteins measured by pulse field gradient NMR techniques. *Biochemistry* 38, 16424-16431.

Williams,R.C. (1981). Morphology of bovine fibrinogen monomers and fibrin oligomers. *J.Mol.Biol.* 150, 399-408.

- Winant,R.C., Lazar,J.B., Johnson,P.H. (1991). Chemical modifications and amino acid substitutions in recombinant hirudin that increase hirudin-thrombin affinity. *Biochemistry* 30, 1271-1277.
- Wong,P.C., Crain,E.J., Watson,C.A., Wexler,R.R., Lam,P.Y., Quan,M.L., Knabb,R.M. (2007). Razaxaban, a direct factor Xa inhibitor, in combination with aspirin and/or clopidogrel improves low-dose antithrombotic activity without enhancing bleeding liability in rabbits. *J.Thromb.Thrombolysis*.
- Xu,Q., Wu,X.F., Xia,Q.C., Wang,K.Y. (1999). Cloning of a galactose-binding lectin from the venom of *Trimeresurus stejnegeri*. *Biochem.J.* 341 (Pt 3), 733-737.
- Xu,X., Liu,Q., Xie,Y., Wu,S. (2000). Purification and characterization of anticoagulation factors from the venom of *Agkistrodon acutus*. *Toxicon* 38, 1517-1528.
- Yamamoto,M., Nakagaki,T., Kisiel,W. (1992). Tissue factor-dependent autoactivation of human blood coagulation factor VII. *J.Biol.Chem.* 267, 19089-19094.
- Yang,W., Hendrickson,W.A., Crouch,R.J., Satow,Y. (1990). Structure of ribonuclease H phased at 2 Å resolution by MAD analysis of the selenomethionyl protein. *Science* 249, 1398-1405.
- Ye,H., Wu,H. (2000). Thermodynamic characterization of the interaction between TRAF2 and tumor necrosis factor receptor peptides by isothermal titration calorimetry. *Proc.Natl.Acad.Sci U.S.A* 97, 8961-8966.
- Yeates,T.O. (1997). Detecting and overcoming crystal twinning. *Methods Enzymol.* 276, 344-358.
- Zang,J., Teng,M., Niu,L. (2003). Purification, crystallization and preliminary crystallographic analysis of AHP IX-bp, a zinc ion and pH-dependent coagulation factor IX binding protein from *Agkistrodon halys Pallas* venom. *Acta Crystallogr.D.Biol.Crystallogr.* 59, 730-733.
- Zhang,D., Cupp,M.S., Cupp,E.W. (2002). Thrombostasin: purification, molecular cloning and expression of a novel anti-thrombin protein from horn fly saliva. *Insect Biochem.Mol.Biol.* 32, 321-330.
- Zhang,E., St Charles,R., Tulinsky,A. (1999). Structure of extracellular tissue factor complexed with factor VIIa inhibited with a BPTI mutant. *J.Mol.Biol.* 285, 2089-2104.
- Zhu,K., Bowman,A.S., Brigham,D.L., Essenberg,R.C., Dillwith,J.W., Sauer,J.R. (1997). Isolation and characterization of americanin, a specific inhibitor of thrombin, from the

salivary glands of the lone star tick *Amblyomma americanum* (L.). *Exp.Parasitol.* 87, 30-38.

Zingali,R.B., Bianconi,M.L., Monteiro,R.Q. (2001). Interaction of bothrojaracin with prothrombin. *Haemostasis* 31, 273-278.

Zingali,R.B., Ferreira,M.S., Assafim,M., Frattani,F.S., Monteiro,R.Q. (2005). Bothrojaracin, a *Bothrops jararaca* snake venom-derived (pro)thrombin inhibitor, as an anti-thrombotic molecule. *Pathophysiol.Haemost.Thromb.* 34, 160-163.

Zingali,R.B., Jandrot-Perrus,M., Guillin,M.C., Bon,C. (1993). Bothrojaracin, a new thrombin inhibitor isolated from *Bothrops jararaca* venom: characterization and mechanism of thrombin inhibition. *Biochemistry* 32, 10794-10802.

Zioncheck,T.F., Roy,S., Vehar,G.A. (1992). The cytoplasmic domain of tissue factor is phosphorylated by a protein kinase C-dependent mechanism. *J.Biol.Chem.* 267, 3561-3564.



"Surely you were aware when you accepted the position, Professor, that it was publish or perish."

Publications

"Publishing is the currency in which researchers deal"
---- *Celeste M. Simon, The Scientist (2001)*

Full papers in internationally referred journals

1. **Banerjee, Y.**, Mizuguchi, J., Iwanaga, S., Kini, R.M. (2005a). Hemextin AB complex, a unique anticoagulant protein complex from *Hemachatus haemachatus* (African Ringhals cobra) venom that inhibits clot initiation and factor VIIa activity. *J.Biol.Chem.* 280, 42601-42611.
2. **Banerjee, Y.**, Mizuguchi, J., Iwanaga, S., Kini, R.M. (2005b). Hemextin AB complex--a snake venom anticoagulant protein complex that inhibits factor VIIa activity. *Pathophysiol.Haemost.Thromb.* 34, 184-187.
3. Kini, R.M., **Banerjee, Y.** (2005). Dissection approach: a simple strategy for the identification of the step of action of anticoagulant agents in the blood coagulation cascade. *J.Thromb.Haemost.* 3, 170-171.
4. Kuruppu, S., Reeve, S., **Banerjee, Y.**, Kini, R.M., Smith, A.I., Hodgson, W.C. (2005). Isolation and pharmacological characterization of cannitoxin, a presynaptic neurotoxin from the venom of the Papuan Taipan (*Oxyuranus scutellatus canni*). *J.Pharmacol.Exp.Ther.* 315, 1196-1202.
5. Lakshminarayanan, R., Loh, X.J., Gayathri, S., Sindhu, S., **Banerjee, Y.**, Kini, R.M., Valiyaveetil, S. (2006). Formation of transient amorphous calcium carbonate precursor in quail eggshell mineralization: an in vitro study. *Biomacromolecules.* 7, 3202-3209.
6. Lumsden, N.G., **Banerjee, Y.**, Kini, R.M., Kuruppu, S., Hodgson, W.C. (2007). Isolation and characterization of rufoxin, a novel protein exhibiting neurotoxicity from venom of the psammophiine, *Rhamphiophis oxyrhynchus* (Rufous beaked snake). *Neuropharmacology* 52, 1065-1070.

Manuscripts in preparation

7. **Banerjee, Y.**, Lakshminarayanan, R., Vivekanandan, S., Anand, G., Valiyaveetil, S. and Kini R.M.; Biophysical Characterization of Anticoagulant Hemextin AB Complex from the Venom of Snake *Hemachatus haemachatus*
8. **Banerjee, Y.**, Persson, E., Lakshminarayanan, R, Mizuguchi, J., Doley, R., Iwanaga, S. and Kini R.M.; Molecular Interactions in the Binding of Anticoagulant Hemextin AB Complex from *Hemachatus haemachatus* (African Ringhals Cobra) to Blood Coagulation Factor VIIa.
9. **Banerjee, Y.**, Kumar, S., Chacko, J., Kini R.M and Sivaraman, J.; Crystallization and Preliminary X-ray Diffraction Analysis of Hemextin A: A Unique Anticoagulant Protein from *Hemachatus haemachatus* venom.

10. Lakshminarayanan,R., Vivekanandan,S., Samy, P.R., **Banerjee,Y.**, Emma,O.C.J., Teo,K.W., Jois,D.S., Kini,R.M. and Valiyaveetil,S.; Structure, Function and Self-assembly of Pelovaterin: A Novel β -defensin Like Protein from the Chinese Soft-shelled Turtle Eggshell, (*Pelodiscus sinensis*).

Patent

Kini, R. M. and **Banerjee, Y.**: Novel anticoagulant polypeptides and complex. US Patent Application No. 60/706,250.

Selected Conference Abstracts

1. **Banerjee, Y.**, Kini, R.M.; Isolation and characterization of anticoagulant proteins from the venom of *Hemachatus haemachatus*; INTERNATIONAL CONFERENCE ON PLANT, ANIMAL AND MICROBIAL TOXINS, Adelaide (Australia), **2003**
2. **Banerjee, Y.**, Kini, R.M.; Purification and amino acid sequence determination of anticoagulant proteins, (Oral Presentation) 8TH BIOLOGICAL SCIENCES GRADUATE CONGRESS, Singapore, **2003**.
3. Vijeydasa,L., **Banerjee, Y.**, Kini, R.M.; Isolation and Purification of procoagulant protein form the venom of African Night Adder. 4th SINO-SINGAPORE SYMPOSIUM, **2003**.
4. **Banerjee,Y.**, Mizuguchi,J., Iwanaga,S., Kini,R.M; Hemextin AB complex – a Snake Venom Protein Complex that inhibits the Tissue Factor-Factor VIIa Activity. CONFERENCE ON EXOGENOUS FACTORS AFFECTING THROMBOSIS AND HAEMOSTASIS, Australia, **2005**
5. **Banerjee,Y.**, Mizuguchi,J., Iwanaga,S., Kini,R.M; Proteins affecting clot initiation. INTERNATIONAL SOCIETY FOR THROMBOSIS AND HAEMOSTASIS CONFERENCE, Australia, **2005**
6. **Banerjee,Y.**, Mizuguchi,J., Iwanaga,S., Kini,R.M; Hemextin AB complex – A unique anticoagulant. SCIENCE CONGRESS, Singapore, **2005 (Poster presentation; Recipient of the best poster award)**

7. **Banerjee, Y.**, Mizuguchi, J., Iwanaga, S., Kini, R.M.; Hemextin AB complex as a FVIIa inhibitor. BIOLOGICAL SCIENCE CONGRESS, Singapore **2005. (Poster presentation; Recipient of the best poster award)**

 8. **Banerjee, Y.**, Lakshminarayanan, R., Vivekanandan, S., Valiyaveetil, S. and Kini R.M.; Hemextin AB Complex from *Hemachatus haemachatus* Venom: Molecular Interactions in the Formation of the Anticoagulant Protein Complex. A*STAR NUS-UCSD BILATERAL MEETING, San Diego (USA), **2006.**

 9. **Banerjee, Y.**, Lakshminarayanan, R., Mizuguchi, J., Vivekanandan, S., Iwanaga, S., Valiyaveetil, S. and Kini R.M.; Hemextin AB complex – a Snake Venom Protein Complex that Inhibits Clot Initiation. APSTH-JSTH JOINT SYMPOSIUM IN JSTH CONFERENCE, Utsunomiya (Japan), **2006. (Oral presentation; Recipient of the best presenter award and Young Investigator Award; Recipient of the International Travel Award)**

 10. **Banerjee, Y.**, Lakshminarayanan, R., Mizuguchi, J., Vivekanandan, S., Iwanaga, S., Valiyaveetil, S. and Kini R.M.; Hemextin AB Complex - a Unique Anticoagulant Protein Complex Inhibiting Clot Initiation from Snake Venom. JSPS CONFERENCE, Bangkok (Thailand), **2006. (Oral presentation; Recipient of the JSPS Travel Award)**
-

Appendix

*What the caterpillar calls the end of the world, the master calls a butterfly
----Richard Bach (American writer)*

Snakes, particularly the venomous ones, have always been creatures of the myth. For example in Egyptian history, the snake plays an important role, with the Nile cobra adorning the crown of the pharaoh in ancient times. Similarly, in Greek mythology snakes are often associated with deadly and dangerous antagonists. The nine headed Hydra Hercules defeated and the three Gorgon sisters are literary examples. Interestingly, two medical symbols involving snakes are still used today - "Bowl of Hygieia", symbolizing pharmacy, and the "Caduceus and Rod of Asclepius", which are symbols denoting medicine in general. Present day Hollywood movie captions like "It will take your breath away" (on the poster of the movie *Anaconda*) and "Sit back. Relax. Enjoy the fright" (on the poster of the movie *Snakes on a Plane*), still heighten our fear and curiosity about these wonderful creatures. But some of us rather than giving snakes of all descriptions a wide berth, seek them out. They are as you might have rightly guessed, snake charmers and snake venom researchers. While charming of snakes is outside the scopes of this thesis, the study of venom is its substance. But in order to maintain the flow of the thesis, it was not possible for me to elucidate on the different varieties of venomous snakes, different families of snake venom proteins and also on the different types of spitting cobras (one of which have made this study possible by generously providing me with its venom), in the actual chapters. In the following pages, brief overviews of the above mentioned topics are given, to provide the reader with preliminary information about snake venoms in general and spitting cobras in particular.

Table 1. Classification of venomous snakes

Family	Number of Species	Examples	Distribution	Characteristics
Elapidae (Front Fanged)	150	Kraits, Cobras, Mambas	Americas, Africa, Asia, Australasia	Small head, short and fixed fangs.
Viperidae (Folding fang)	40	Puff adder, pit viper	Europe, Africa, Asia	Large, flattened triangular head, large grooved fangs on the maxillary bone.
Crotalidae (Folding fang)	40	Pit vipers	Americas, Parts of Southeast Asia, Southeast Europe	Similar to the family Viperidae, but they possess heat-sensitive pits on head
Boigaenae (Rear Fanged)	1000	Boomslang	In all parts of the world, except Australasia	Short grooved fangs at rear of upper jaws.
Hydrophidae (Front Fanged)	50	Sea snakes	Asia and Australasia	Nostrils dorsally on head, flattened tail.

From: Harris J.B. (1991) In: Snake toxins (Ed Harvey, A.L.)

There are about 3200 species of snakes. Approximately 1300 species are venomous. Avoid them all!







Venomous snakes are usually defined as those which possess venom glands and specialized venom-conducting fangs, which enable them to inflict serious bites upon their victims. In general there are five families of venomous snakes recognized: the Colubridae, which possess small rear fangs; the front-fanged Elapidae and Hydrophidae; and the viper group, which consists of the Viperidae and Crotalidae. Venomous snakes are widespread throughout the world. However they do not occur in several islands, New Zealand, Ireland, Iceland, the Azores and Canaries.



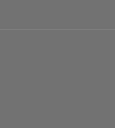


Table 2. Anticoagulant proteins from snake venom

Protein		Mechanism of action	Remarks
Enzymatic anticoagulant proteins			
Phospholipase A₂ enzymes		Inhibits activation of FX to FXa by extrinsic tenase complex	By both enzymatic and nonenzymatic mechanisms; target protein not known
	Strongly anticoagulant	Inhibits activation of prothrombin to thrombin by prothrombinase complex	By nonenzymatic mechanism; binds to FXa and interferes in the prothrombinase complex formation
	Weakly anticoagulant	Inhibits activation of FX to FXa by extrinsic tenase complex	By nonenzymatic mechanism through hydrolysis of phospholipids
Metalloproteinases (α-fibrinogenase)		Weaker soft clot formation due to physical destruction of fibrinogen	By cleaving A α -chain of fibrinogen
Serine	Protein C activators	Inactivation of cofactors FVa and FVIIIa degradation	Directly activate protein C

proteinases	Thrombin like enzymes	Deplete fibrinogen in the plasma	Releases either fibrinopeptide A or B; fibrin clots are removed leading to depletion of fibrinogen content
	Fibrinogenases	Physical destruction of fibrinogen	Mechanism not known
L-Amino acid oxidase		Inhibits FIX activity	Mechanism not known
Non-enzymatic anticoagulant proteins			
C-type lectin related proteins	FX and FIX binding proteins	Inhibit the formation of coagulation complexes	Bind to the Gla domain of FIX and FX, and interfere in their binding to phospholipids
	Bothrojaracin, bothroalteinin	Inhibit activity of thrombin	Bind to α -thrombin at both exosite-1 and exosite-2
Three-finger toxin	Cardiotoxins from <i>Naja nigricollis</i> <i>crawshawii</i> venom	Act on the extrinsic pathway of the clotting cascade	Mechanism not known
	Hemextin A and hemextin AB complex from <i>Hemachatus haemachatus</i> venom	Prevents clot initiation by inhibiting extrinsic tenase activity	Specifically binds to FVIIa

Table 3. Snake venom protein families

Family	Fold	Features	Pharmacological Effects	Examples
Phospholipase A ₂ enzymes		118 - 130 residues; 7 disulfide bonds; His is the active site residue; Ca ²⁺ -dependent activity	Pre- and post-synaptic neurotoxicity, myotoxicity, cardiotoxicity, convulsant effect, hypotensive effect, platelet aggregation induction and inhibition, hemolysis, edema, tissue damage, anticoagulant effect	Taipoxin, notexin, β-bungarotoxin
Serine proteases		~235 residues; 6 disulfide bonds; His, Ser, Asp form catalytic triad; various protein substrates	Procoagulant activity, fibrinolytic activity, anticoagulant activity, edema	APC activators, TLEs, trocarnin
Metalloproteases		~200 residues; 3 - 4 disulfides; 4 -domains (Domain A - metalloprotease-disintegrin- Cys-rich); various protein substrates	Hemorrhage, anti -platelet effect, anticoagulant effect, procoagulant effect	Atrolysin, ecarin
Acetylcholinesterases		~545 residues; monomers, dimers or tetramers; 3 disulfide bonds; His, Ser, Glu form active site triad	Not Known	Acetylcholinesterase in ringhals cobra venom
L-Amino acid Oxidases		80 - 140 Kd; two subunits; flavoproteins	Platelet aggregation, anticoagulant activity, edema, apoptosis	M-LAO
Three-finger toxins		58 - 75 residues; 4 - 5 disulfide bonds; typical three finger-like loops with disulfide-rich core	Post-synaptic neurotoxicity, cardiotoxicity, cytotoxicity, platelet aggregation inhibition, analgesic effect, ion channel blocking activity, inhibition of acetylcholinesterase	Hemextin A, hemextin B, fasciculins

Serine protease inhibitors		58 - 65 residues; 3 disulfide bonds; bovine pancreatic trypsin inhibitor family	Proteinase inhibition; potassium channel blocking activity	Dendrotoxin
Disintegrins		Long, medium or short chain; 48 - 85 residues; 4-7 disulfides; precursor contains metalloproteinase domain	Inhibition of platelet aggregation	Echistatin, eristostatin
Helveprins		19 - 24 kDa; Cys-rich C-terminal; homology with helothermine and Cys rich secretory proteins from testes	Blocking of cyclic nucleotide-gated ion channels	Pseudechitoxin, Cysteine-rich venom protein, bucarin, opharin, asurin
Wapriins		~50 residues, 5 disulfide bonds, similar domain architecture like Whey Acidic Proteins	Antimicrobial activity	Nawaprin, Omwaprin
C-type lectin - related proteins		Dimers, trimers or tetramers; Similar or different subunits held by disulfide bonds; ~130 residues; 3 intrachain and 1 interchain disulfide bond	Induction or inhibition of platelet aggregation, platelet agglutination; anticoagulant effect	Bothrojaracin, rhodocetin, salmorin

Spitting Cobras

This group of snakes refers to any one of several species of cobras that have the ability to spit or eject venom from their mouth when defending



themselves against predators. The spit venom is far diluted than the one that is secreted and is harmless to intact skin. However it can cause permanent blindness if introduced to the eye causing chemosis and corneal swelling.

The venom is not actually spitted but sprayed. Spraying is carried out using muscular contractions upon the venom glands. The muscles squeeze the glands and force the venom out the forward

facing holes at the tip of the fang. Upon leaving the fang tip a large gust of air is expelled from the lung. The venom is propelled forward, mist-like, in the form of droplets. Four out of seven species of cobras found in Africa and seven out of nine species found in Asia can spit to varying degrees. While spitting is typically their primary form of defense, all spitting cobras are also capable of delivering venom through a bite as well. A brief description of some of the spitting cobras including the one, the venom of which has been used in this study is given below.

Photograph kindly provided by Dr. Wolfgang Wuster

Hemachatus haemachatus (African Ringhals Cobra)

Ringhals cobras are generally dull grey, grey brown or black and have white bars on the neck. The number of bars varies between one and 3 but is usually



2. They have keeled scales and are ovoviviparous, which make them unique among elapids. Unlike cobras, they have light bars on dark ventral scales, whereas the cobras have dark bars on lighter scales. The ventral scales of this species are normally dark grey to light grey, but white in juveniles.

They are found in Southern Africa. However, isolated populations also exist in Zimbabwe and Mozambique. In South Africa ringhals are primarily distributed in the south cape through Swaziland, Orange free state, Natal, Transkei, Lesotho and southern Transvaal.

Ringhals cobra is only a small snake, adults have a average length of 100 cm but large ones may grow up to 150 cm. Their preferred habitat is grassland and moist savanna. But they also live in rocky areas as well. They are also known to live close to permanent water holes and scrub. In the wild ringhals mostly eat toads but also small rodents, birds, lizards and even snakes. As mentioned above ringhals is ovoviviparous. In the wild the females give birth to 20-35 young, but as many as 65 babies have been recorded. The babies have an average length of 17 cm.

Ringhals' bites are not common but can be potentially lethal. The average yield of venom per milking is around 80-120 mg and approximately 30-40mg is fatal. Antivenin is extremely effective in treatment.

Photograph reproduced with kind permission from Mr. Mark M Lucas

***Naja Pallida* (Red Spitting Cobra)**

Red spitting cobra ranges in length between 70 to 120 cm, with a maximum of 150 cm. It has a long tail which can be (15-19) % of the total body length. It is a relatively small cobra that is quite slender in body proportions. It has a small head (some specimens however, can have big

heads with huge swollen venom glands clearly seen at the side of the head) with large eyes, with a round pupil. The tail is long and the body is cylindrical in shape.

The colour of this cobra can be variable depending on the origin of the snake. The specimens from southern Kenya and northern Tanzania have an orange red colour, with a broad steel blue or black throat band. In some specimens from East Africa two or three throat bands has also been observed. The ventral side of the snake is also reddish in colour with sometimes a crèmes white throat. Specimens from other areas can be yellow, pinkish, pink-grey, pale red or steel grey which can be mistaken for dark green, most of them will have the throat band, but this throat band will fade or even sometimes disappear in larger adults. The true red specimens will become red-brown with increase in their size.

These cobras prefer grassland semi desserts and savannah. They are often found near water holes where they hunt on frogs and other amphibians which is their main food. They are also known to be cannibalistic, this could be the reason that the juveniles and smaller specimens are day active while adult are preferred nocturnal.

The venom spat by red spitting cobras has been analyzed to document variations in protein composition occurring over short temporal periods (less than 5 min). These cobras exhibited distinct control of venom flow with spits averaging 1.7% of the volume of the venom gland, thus enabling the cobras to

rapidly expel over 40 consecutive spits. Variations in the low and high molecular weight proteins were observed when comparing the 1st, 20th and 40th spits produced by the same specimens. The first few spits were characterized by a distinctive 9 kDa protein which was never observed beyond the 7th spit; but was present in milked venom and was present when the spitting behavior was preceded by a 5 min period of induced defensive behaviors.

Photograph reproduced with kind permission from Mr. Mark M Lucas

***Naja nigricollis nigricollis* (Black-necked Spitting Cobra)**

This species is recognized in three subspecies black-necked spitting cobra (*Naja nigricollis nigricollis*), black Spitting cobra (*Naja nigricollis woodi*),



western barred spitting cobra (*Naja nigricollis nigricincta*). Adults

snake reach an average length of 1 m (maximum 1.5 m).

It is a long, slender, pitch black snake. It is more agile and thinner than a black mole snake and when threatened, it will spread the characteristic cobra

hood.

This is an arid-adapted snake found in some of the harshest areas of the Northern and Western Cape provinces in Africa. It is a generalist and will eat most reptiles, amphibians and rodents. It is alert and agile and can normally evade danger by spreading a hood in an attempt to get an attacker to back off and then by rapidly retreating to a place of safety under a rock or down a hole. If escape is hindered, it will spit venom profusely at its attacker and take advantage of any hesitation this may cause to affect its escape. It is a good spitter and can spit venom several meters. If molested further, it will bite. The venom is neurotoxic and a bite from this species may cause death if not treated. If venom is sprayed in the eyes of a mammal, it may cause blindness if not washed out immediately with a neutral solvent such as water.

Photograph reproduced with kind permission from Mr. Mark M Lucas

Naja Siamensis (Golden Spitting Cobra)

Also known as Isan spitting cobra; *Naja (naja) isanensis*. However, it is often mislabeled as *Naja sputatrix*. The latter does not have a black and white pattern.



The identification pattern of this species is highly variable. Specimens from northern and eastern Thailand tend to be uniformly light brown, olive, sometimes distinctly greenish, often with a somewhat

faded appearance. Specimens from central Thailand are highly variable. Some have a very contrasting black-and-white pattern, with or without speckling and cross-banding, and a light venter with or without broad dark cross-bands, others are some shade of brown or greyish brown, with or without lighter cross-bands on dorsum, often with several broad dark bands across belly, others, especially from the west, are uniformly black. Hood mark in northern, eastern and southeastern Thailand V, U, or, most commonly, spectacle-shaped, but often very indistinct or absent altogether; in central Thailand, H-shaped hood marks are also common, but hood marks are often absent altogether.

This species have 25-31 scale rows around hood, 19-21 just ahead of midbody; 153-174 ventrals, 45-54 subcaudals, basal pairs sometimes undivided. They are usually 90-120 cm in length with a maximum of 160 cm. This species is widely distributed in Thailand (except on Malayan Peninsula), western Laos, Cambodia, southern Vietnam.

Photograph reproduced with kind permission from Mr. Mark M Lucas

***Naja Sputatrix* (Javan Spitting Cobra)**



This species is also known as south Indonesian spitting cobra or Malayan spitting cobra.

Specimens from Java are usually uniform yellowish, brown or blackish; juveniles often have throat band and lateral throat spots, sometimes a hood mark, which is most often chevron-shaped, rarely mask-

spectacle-, horseshoe- or O-shaped; specimens from the Lesser Sunda Islands usually medium or light brown, with lighter scale bases; throat band and heart-shaped hood mark persist into adulthood. This species possess 19-28 scale rows around hood, 18-21 just ahead of midbody; Javan specimens have more scale rows than Lesser Sunda specimens; 162-183 ventrals, 42-54 subcaudals, normally all divided. An adult snake is up to 150 cm, rarely more.

The species is widely distributed in Southern Indonesia: Java, Bali, Lombok, Sumbawa, Komodo, Flores, Lomblen, Alor, possibly other islands in the group. However, the occurrence of this species on Timor and Sulawesi requires confirmation.

Photograph reproduced with kind permission from Mr. Mark M Lucas

Naja Nubiae

This is a new species of spitting cobra described from north-eastern Africa. The distinctiveness of the new species has been confirmed by multivariate



analysis of pattern and scalation data. Phylogenetic analysis of mitochondrial DNA sequences reveals the new species to be the sister taxon of *N. pallida*, but with considerable levels of sequence divergence relative to that species.

The populations concerned had previously been assigned to *N. pallida*. The new species differs from *N. pallida* principally in having more than one dark band across the neck and under the throat, as well as a pair of spots under the throat. It occupies a disjunct range across Egypt, the Sudan, Chad, Niger and Eritrea, where it seems to occupy primarily relatively mesic habitats. *Naja mossambica* is more closely related to *N. nigricollis* than to *N. pallida* and the new species (REF).

Photograph kindly provided by Dr. Wolfgang Wuster



**Manuscripts submitted in
Internationally refereed journals**

LETTERS TO THE EDITOR

Dissection approach: a simple strategy for the identification of the step of action of anticoagulant agents in the blood coagulation cascade

R. M. KINI† and Y. BANERJEE*

*Protein Science Laboratory, Department of Biological Sciences, Faculty of Science, National University of Singapore, Singapore 117 543, Singapore; and †Department of Biochemistry and Molecular Biophysics, Medical College of Virginia, Virginia Commonwealth University, Richmond, VA 13298, USA

To cite this article: Kini RM, Banerjee Y. Dissection approach: a simple strategy for the identification of the step of action of anticoagulant agents in the blood coagulation cascade. *J Thromb Haemost* 2005; 3: 170–1.

Thromboembolic disorders, such as phlebitis, phlebothrombosis, deep vein thrombosis and pulmonary embolism, are important problems in the aging population worldwide. Anticoagulant agents are used for the effective prophylaxis and treatment of thrombosis. Identifying the site at which the anticoagulants affect the blood coagulation cascade and understanding the mechanism are essential steps in the characterization of novel and efficacious anticoagulants. We designed a simple approach [1] to determine the particular step at which an anticoagulant interferes in the extrinsic pathway. This 'dissection approach' is rapid, cost effective and employs three commonly used clotting assays, namely prothrombin time [2], Stypven time [3] and thrombin time [4]. It is based on the simple principle that initiating the cascade 'upstream' from the inhibited step will result in elevated clotting times, while initiating the cascade 'downstream' from the inhibited step will not affect the clotting time [1] (Fig. 1A).

Prothrombin time [2] measures the effect of an anticoagulant on the extrinsic tenase and prothrombinase complexes and the conversion of fibrinogen to fibrin clot. Stypven time [3] circumvents the extrinsic tenase complex and monitors its effect on the prothrombinase complex and the conversion of fibrinogen to fibrin. Thrombin time [4] depicts its effect on the conversion of fibrinogen to fibrin only. A systematic analysis of the effect of an anticoagulant on these three clotting times would help in identifying the stage of coagulation in the extrinsic coagulation cascade.

We successfully used this approach to localize the site of action of three anticoagulant proteins in the extrinsic pathway:

Correspondence: R. Manjunatha Kini, Department of Biological Sciences, Faculty of Science, 14 Science Drive 4, National University of Singapore, Singapore 117 453.

Tel.: +65 6874 5235; fax: +65 6779 2486; e-mail: dbskinim@nus.edu.sg

Received 2 August 2004, accepted 17 August 2004

a weak anticoagulant (CM-I), a strong anticoagulant (CM-IV) phospholipase A₂ enzyme purified from the venom of *Naja nigricollis* [1,5], and a three finger toxin (protein A) purified from the venom of *Hemachatus haemachatus*. All three proteins delay prothrombin time showing that they interfere in the extrinsic pathway (Fig. 1B–D). CM-I and protein A did not prolong clotting in Stypven and thrombin time assays (Fig. 1B,C), showing that they inhibit only the extrinsic tenase

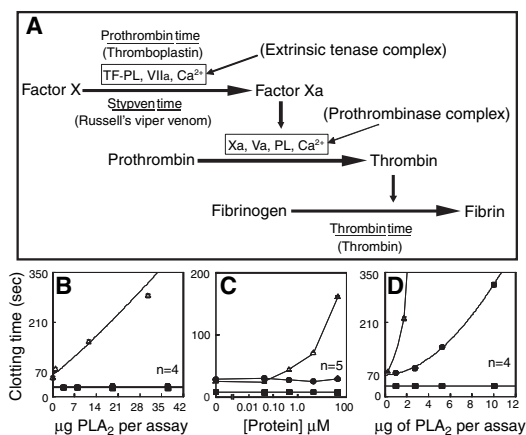


Fig. 1. (A) Schematic representation showing the selective activation of the extrinsic coagulation pathway by the prothrombin, Stypven and the thrombin time clotting assays. In the prothrombin time, clotting is initiated at the tenase complex by the addition of Ca²⁺ and thromboplastin, which contains tissue factor and phospholipids (TF-PL). In the Stypven time, clotting is initiated at the prothrombinase complex by the addition of dilute Russell's viper venom, which activates factor (F)X and factor (F)V by specific proteases. FXa and FVa form the prothrombinase complex on the PL surfaces with the addition of Ca²⁺. In thrombin time, clotting is initiated by the addition of thrombin, which converts soluble fibrinogen to a fibrin clot. Effect of weakly anticoagulant phospholipase A₂ (CM-I) (B), a three finger toxin, protein A (C) and strongly anticoagulant phospholipase A₂ (CM-IV) (D) on the prothrombin time (Δ), Stypven time (●) and thrombin time (■) clotting assays. Each point represents the average ± SD.

complex. On the other hand, CM-IV prolonged the Stypven time, but did not prolong the thrombin time (Fig. 1D). Thus, CM-IV has no effect on the conversion of fibrinogen to fibrin, but it may affect either the prothrombinase complex alone or both the extrinsic tenase and prothrombinase complexes. Subsequent studies using reconstituted complexes have confirmed these conclusions. CM-I [6] and protein B (Y. Banerjee and R. M. Kini, unpublished observations) inhibit only the extrinsic tenase complex, whereas CM-IV inhibits both the extrinsic tenase and prothrombinase complexes [5,7,8].

Currently, to identify the steps, the anticoagulant is screened serially with either the coagulation factors involved in the extrinsic pathway or those that are plasma deficient in specific coagulation factors, making the procedure cumbersome and costly. The dissection approach allows us to identify the specific site of anticoagulant activity in the extrinsic pathway rapidly and in a cost-effective manner. Therefore, this simple approach will be useful in characterizing the potential anticoagulants and in developing lead compounds for the prevention/treatment of thromboembolic disorders.

References

- 1 Stefansson S, Kini RM, Evans HJ. The inhibition of clotting complexes of the extrinsic coagulation cascade by the phospholipase A₂ isoenzymes from *Naja nigricollis* venom. *Thromb Res* 1989; **55**: 481–91.
- 2 Quick AJ. The prothrombin time in haemophilia and in obstructive jaundice. *J Biol Chem* 1935; **109**: 73–4.
- 3 Hougie C. Effect of Russell's viper venom (Stypven) on Stuart clotting defect. *Proc Soc Exp Biol Med* 1956; **98**: 570–3.
- 4 Jim RT. A study of the plasma thrombin time. *J Lab Clin Med* 1957; **50**: 45–60.
- 5 Stefansson S, Kini RM, Evans HJ. The basic phospholipase A₂ from *Naja nigricollis* venom inhibits the prothrombinase complex by a novel nonenzymatic mechanism. *Biochemistry* 1990; **29**: 7742–6.
- 6 Kini RM, Evans HJ. The role of enzymatic activity in inhibition of the extrinsic tenase complex by phospholipase A₂ isoenzymes from *Naja nigricollis* venom. *Toxicon*. 1995; **33**: 1585–90.
- 7 Kini RM, Evans HJ. Structure–function relationships of phospholipases. The anticoagulant region of phospholipases A₂. *J Biol Chem* 1987; **262**: 14402–7.
- 8 Kerns RT, Kini RM, Stefansson S, Evans HJ. Targeting of venom phospholipases: the strongly anticoagulant phospholipase A₂ from *Naja nigricollis* venom binds to coagulation factor Xa to inhibit the prothrombinase complex. *Arch Biochem Biophys* 1999; **369**: 107–13.

Factor XIII—circulating levels and Val34Leu polymorphism in relatives of South Asian patients with ischemic stroke

K. KAIN, J. BAMFORD, J. BAVINGTON, J. YOUNG and A. J. CATTO

Academic Unit of Molecular Vascular Medicine, University of Leeds, Leeds, UK

To cite this article: Kain K, Bamford J, Bavington J, Young J, Catto AJ. Factor XIII—circulating levels and Val34Leu polymorphism in relatives of South Asian patients with ischemic stroke. *J Thromb Haemost* 2005; **3**: 171–3.

Epidemiological studies demonstrate an association of coagulation factors with a family history of stroke. The aim of this study was to investigate whether there was an association of factor (F)XIII measures and FXIIIVal34Leu genotype with a family history of stroke in South Asians. One hundred and forty-three South Asian first-degree relatives of confirmed stroke patients were compared with 146 control subjects [1]. All the subjects gave written informed consent according to a protocol approved by Local Research Ethics Committee. Blood samples were taken under optimum conditions and the biochemical, coagulation and fibrinolytic assays were performed by standard techniques. FXIII activity was determined by biotin incorporation microtiter plate-based assay using

fibrinogen and 5-(biotinamido) pentylamine as substrates, based on a modified method described by Song *et al.* [2]. FXIII B-subunit antigen levels were determined by sandwich-ELISA and A2B2 was measured by ELISA based on an anti-B/anti-A sandwich.

The Val34Leu polymorphism was determined by polymerase chain reaction using forward 5'-ACC CAG AGT GGT GGG GAA G-3' and reverse 5'-GAC CTT GTA AAG TCA AAA ATG TC-3' primers. Statistical analyses were performed with SPSS for Windows Version 8.0 (SPSS Inc., Chicago, IL, USA). Trendlines were calculated with linear regression analysis.

The general and metabolic characteristics of South Asian relatives and controls are given in Table 1. FXIII B-subunit antigen significantly correlated positively with triglycerides ($r = 0.20/0.25$) in both groups and negatively with HDL-cholesterol in controls ($r = -0.14$). FXIII B-subunit antigen correlated with fibrinogen ($r = 0.31/0.44$), factor (F)VII antigen ($r = 0.20/0.30$) in both groups, plasminogen activator inhibitor (PAI)-1 antigen ($r = 0.20$) and von Willebrand factor (VWF) ($r = 0.21$) in relatives only. FXIII B had no correlation with FXIII cross-linking activity.

Correspondence: K. Kain, Leeds University, Academic Unit of Molecular Vascular Medicine, Leeds, West Yorkshire, UK.

Tel.: +44 113 343 7721; fax: +44 113 343 7738; e-mail: k.kain@leeds.ac.uk

Received 13 August 2004, accepted 30 August 2004

VOLUME 280 (2005) 42601–42611

Hemextin AB complex, a unique anticoagulant protein complex from *Hemachatus haemachatus* (African Ringhals cobra) venom that inhibits clot initiation and factor VIIa activity.

Yajnavalka Banerjee, Jun Mizuguchi, Sadaaki Iwanaga, and R. Manjunatha Kini

We inadvertently reported wrong concentrations of hemextin AB complex in the experiments examining the anticoagulant activity; factor VIIa-TF, factor VIIa, and factor VIIa-sTF inhibitory activity; kinetics of inhibition; and isothermal titration calorimetric studies. Because the complex formed had a ratio of 1:1 between hemextin A and hemextin B, it was assumed that the complex exists as a dimer. The gel filtration data that were included during the revision of the manuscript showed that the complex is a tetramer. However, we did not recalculate the molar concentrations of the hemextin AB complex to reflect the tetramer situation instead of the original assumption of a dimer. Therefore, the concentrations of the hemextin AB complex should be half that depicted in the article. This error, however, does not affect our main conclusions as depicted in the paper.

The following corrected statements should be incorporated.

PAGE 42603:

The second sentence in the second paragraph under the subheading “Kinetics of Inhibition” should read: “contained 0.0125–0.05 μM inhibitor complex . . .”

The second sentence in the first paragraph under the subheading “Isothermal Titration Calorimetry (ITC)” should read: “reconstituted anticoagulant complex (0.2 mM) . . .”

PAGE 42607:

In the first full paragraph in the left column, line 8, the IC_{50} for inhibition should appear as “100 nM” instead of 200 nM.

PAGE 42608:

In the left column, the last line of the figure legend for Fig. 8, the IC_{50} for inhibition should appear as “5 μM ” instead of 10 μM .

In the first full paragraph in the right-hand column, the last two sentences should read: “The binding was exothermic, with $\Delta H = -7.931 \text{ kcal}\cdot\text{M}^{-1}$, $\Delta G = -7.543 \text{ kcal}\cdot\text{M}^{-1}$, and $\Delta S = -1.25 \text{ cal}\cdot\text{M}^{-1}$. The calculated K for the binding was $4.11 \times 10^5 \text{ M}^{-1}$.” The calculated concentration affects the molar ratio in Fig. 10; the modified Fig. 10 and its corresponding legend are shown following.

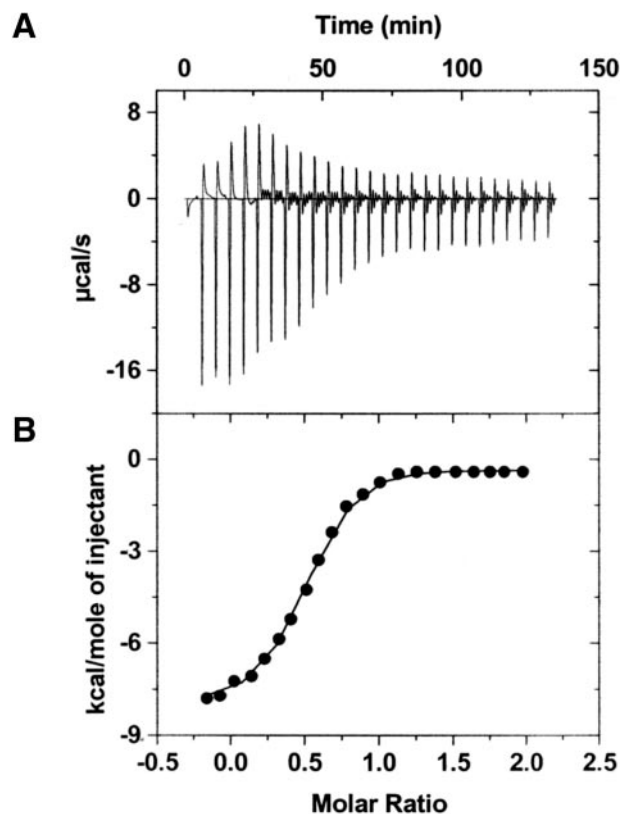


FIGURE 10. ITC studies on the formation of a complex between the hemextin AB complex and FVIIa. *A*, raw data in $\mu\text{cal/s}$ versus time showing heat release upon injections of 0.2 mM reconstituted hemextin AB complex into a 1.4-ml cell containing 10 μM FVIIa. *B*, integration of the raw data yielding the heat/mol versus molar ratio. The best values of the fitting parameters were $4.11 \times 10^5 \text{ M}^{-1}$ for K , $-7.931 \text{ kcal}\cdot\text{M}^{-1}$ for ΔH , and $-1.25 \text{ cal}\cdot\text{M}^{-1}$ for ΔS .

PAGE 42609:

In the first paragraph in the right-hand column, the sentence beginning in line 4 should read: “The hemextin AB complex inhibited with IC_{50} values of ~ 100 and $\sim 105 \text{ nM}$, respectively.”

Also, in the same paragraph, lines 24–27 should read: “However, the IC_{50} for the inhibition of kallikrein was $\sim 5 \mu\text{M}$, in contrast to that of FVIIa/TF-FVIIa/sTF-FVIIa, which was $\sim 100 \text{ nM}$. Kinetic studies revealed that the hemextin AB complex is a noncompetitive inhibitor of the sTF-FVIIa complex, with a K_i of 25 nM.”

We suggest that subscribers photocopy these corrections and insert the photocopies in the original publication at the location of the original article. Authors are urged to introduce these corrections into any reprints they distribute. Secondary (abstract) services are urged to carry notice of these corrections as prominently as they carried the original abstracts.

A single aromatic amino acid at the carboxyl terminus of *Helicobacter pylori* α 1,3/4 fucosyltransferase determines substrate specificity.

Bing Ma, Leon H. Lau, Monica M. Palcic, Bart Hazes, and Diane E. Taylor

PAGE 36848:

In the Abstract, lines 19–21, this sentence should read: “These mutations did not decrease α 1,3 activity but reduced the α 1,4 activity to 66.9, 55.6, and 3.1% of wild type level, respectively.”

PAGE 36850:

In the right-hand column, lines 11–13, this sentence should read: “However, the α 1,4 activities were reduced to 66.9, 55.6, and 3.1% of the WT level, and their α 1,4/ α 1,3 ratios were at 55.6, 65.2, and 1.8% of the WT level, respectively (Fig. 1).”



Hemextin AB Complex, a Unique Anticoagulant Protein Complex from *Hemachatus haemachatus* (African Ringhals Cobra) Venom That Inhibits Clot Initiation and Factor VIIa Activity*

Received for publication, August 15, 2005, and in revised form, September 28, 2005. Published, JBC Papers in Press, October 4, 2005, DOI 10.1074/jbc.M508987200

Jaynavalka Banerjee^{†1}, Jun Mizuguchi[§], Sadaaki Iwanaga[§], and R. Manjunatha Kini^{‡¶12}

From the [‡]Protein Science Laboratory, Department of Biological Sciences, Faculty of Science, National University of Singapore, Singapore 117543, the [§]Blood Products Research Department, The Chemo-Sero-Therapeutic Research Institute, Kumamoto 869-1298, Japan, and the [¶]Department of Biochemistry, Virginia Commonwealth University Medical Center, Medical College of Virginia, Virginia Commonwealth University, Richmond, Virginia 23298

During injury or trauma, blood coagulation is initiated by the interaction of factor VIIa (FVIIa) in the blood with freshly exposed tissue factor (TF) to form the TF·FVIIa complex. However, unwanted clot formation can lead to death and debilitation due to vascular occlusion, and hence, anticoagulants are important for the treatment of thromboembolic disorders. Here, we report the isolation and characterization of two synergistically acting anticoagulant proteins, hemextins A and B, from the venom of *Hemachatus haemachatus* (African Ringhals cobra). N-terminal sequences and CD spectra of the native proteins indicate that these proteins belong to the three-finger toxin family. Hemextin A (but not hemextin B) exhibits mild anticoagulant activity. However, hemextin B forms a complex (hemextin AB complex) with hemextin A and synergistically enhances its anticoagulant potency. Prothrombin time assay showed that these two proteins form a 1:1 complex. Complex formation was supported by size-exclusion chromatography. Using a “dissection approach,” we determined that hemextin A and the hemextin AB complex prolong clotting by inhibiting TF·FVIIa activity. The site of anticoagulant effects was supported by their inhibitory effect on the reconstituted TF·FVIIa complex. Furthermore, we demonstrated their specificity of inhibition by studying their effects on 12 serine proteases; the hemextin AB complex potentially inhibited the amidolytic activity of FVIIa in the presence and absence of soluble TF. Kinetic studies showed that the hemextin AB complex is a noncompetitive inhibitor of soluble TF·FVIIa amidolytic activity, with a K_i of 50 nM. Isothermal titration calorimetric studies showed that the hemextin AB complex binds directly to FVIIa with a binding constant of $1.62 \times 10^5 \text{ M}^{-1}$. The hemextin AB complex is the first reported natural inhibitor of FVIIa that does not require a scaffold to mediate its inhibitory activity. Molecular interactions of the hemextin AB complex with FVIIa/TF·FVIIa will provide a new paradigm in the search for anticoagulants that inhibit the initiation of blood coagulation.

Blood coagulation is an innate response to vascular injury that results from a series of amplified reactions in which zymogens of serine pro-

teases circulating in the plasma are sequentially activated by limited proteolysis, leading to the formation of blood clot, thereby preventing the loss of blood (1–3). It is initiated through the extrinsic pathway (4). Membrane-bound tissue factor (TF),³ exposed during vascular injury, interacts with factor VIIa (FVIIa), which preexists in the plasma (at 1–2% of total factor VII) (5, 6), and forms the extrinsic tenase complex. This complex activates FX to FXa. In association with its cofactor FVa, FXa performs a proteolytic cleavage of prothrombin to thrombin. Thrombin cleaves fibrinogen to fibrin, promoting the formation of a fibrin clot, and activates platelets for inclusion in the clot. The TF·FVIIa complex can also activate FIX to FIXa, thus helping in the propagation of the coagulation cascade through the intrinsic pathway. The coagulation cascade is under tight regulation. Any imbalance in its regulation could lead to either unclottable blood, resulting in excessive bleeding during injuries, or unwanted clot formation, resulting in death and debilitation due to vascular occlusion with the consequence of myocardial infarction, stroke, pulmonary embolism, or venous thrombosis (3). Therefore, there is an urgent need for the prophylaxis and treatment of thromboembolic disorders.

Anticoagulants are pivotal for the prevention and treatment of thromboembolic disorders, and ~0.7% of the western population receives oral anticoagulant treatment (7). Coumarins and heparin are the most well known clinically used anticoagulants. Coumarins inhibit the activity of all vitamin K-dependent proteins, including procoagulants (thrombin, FXa, FIXa, and FVIIa) and anticoagulants (activated protein C and protein S), whereas heparin mediates its anticoagulant activity by enhancing the inhibition of thrombin and FXa by antithrombin III (8, 9). The nonspecific mode of action of these anticoagulants accounts for their therapeutic limitations in maintaining a balance between thrombosis and hemostasis (10). These limitations have provided the impetus for the development of new anticoagulants that target specific coagulation enzymes or a particular step in the clotting process (11, 12). Because of its relatively low concentrations in blood (10 nM) and its pivotal role in the initiation of the coagulation cascade (13), FVII/FVIIa is an attractive drug target for the development of novel and specific anticoagulant agents.

Proteins/toxins from snake venoms have inspired the design and development of a number of therapeutic agents or lead molecules, particularly for cardiovascular diseases (14). For example, a family of inhib-

* This work was supported in part by the Biomedical Research Council, Agency for Science and Technology, Singapore. The costs of publication of this article were defrayed in part by the payment of page charges. This article must therefore be hereby marked “advertisement” in accordance with 18 U.S.C. Section 1734 solely to indicate this fact.

¹ Recipient of a National University of Singapore research scholarship.

² To whom correspondence should be addressed. Tel.: 65-6874-5235; Fax: 65-6779-2486; E-mail: dbskinim@nus.edu.sg.

³ The abbreviations used are: TF, tissue factor; FVIIa, factor VIIa; pNA, p-nitroanilide; 2HCl, dihydrochloride; <Glu, pyroglutamic acid; sTF, soluble tissue factor; HPLC, high pressure liquid chromatography; ITC, isothermal titration calorimetry; TFPI, tissue factor pathway inhibitor; NAPc2, nematode anticoagulant peptide c2.

Factor VIIa Inhibitor from Snake Venom

itors of angiotensin-converting enzyme was developed based on bradykinin-potentiating peptides from South American snake venoms (15). Inhibitors of platelet aggregation, such as eptifibatid and tirofiban, were designed based on disintegrins, a large family of platelet aggregation inhibitors found in viperid and crotalid snake venoms (16–21). Ancrod (extracted from the venom of the Malayan pit viper) reduces blood fibrinogen levels and has been successfully tested in a variety of ischemic conditions, including stroke (22). To search for new lead molecules, we and others have been focusing on isolating and characterizing pharmacologically active proteins from snake venoms that affect blood coagulation and platelet aggregation. In this study, we report the purification and characterization of a three-finger toxin that mediates anticoagulant activity from the venom of the elapid snake *Hemachatus haemachatus* (African Ringhals cobra). Although it has mild anticoagulant activity, its synergistic interaction with the second three-finger toxin enhances its anticoagulant potency. The anticoagulant protein and its complex specifically inhibit the activation of FX by the TF-FVIIa complex by noncompetitively inhibiting the enzymatic activity of FVIIa. This is the first report of a naturally occurring FVIIa inhibitor that does not require a scaffold to mediate its inhibitory activity.

EXPERIMENTAL PROCEDURES

Materials

Lyophilized *H. haemachatus* venom was obtained from African Reptiles and Venoms (Gauteng, South Africa). Thromboplastin with calcium (for prothrombin time assays), Russell's viper venom (for Stypven time assays), thrombin reagent (for thrombin time assays), benzamidine hydrochloride, and 4-vinylpyridine were purchased from Sigma. β -Mercaptoethanol was purchased from Nacalai Tesque (Kyoto, Japan). The chromogenic substrates *H*-D-Ile-Pro-Arg-*p*-nitroanilide (*p*NA) dihydrochloride (2HCl) (S-2288), <Glu-Pro-Arg-*p*NA·HCl (S-2366), *H*-D-Phe-pipecolyl-Arg-*p*NA·2HCl (S-2238), *H*-D-Pro-Phe-Arg-*p*NA·2HCl (S-2302), *Z*-D-Arg-Gly-Arg-*p*NA·2HCl (S-2765), <Glu-Gly-Arg-*p*NA·HCl (S-2444), benzoyl-Ile-Glu(Glu- γ -methoxy)-Gly-Arg-*p*NA·HCl (S-2222), *H*-D-Val-Leu-Lys-*p*NA·2HCl (S-2251), *H*-D-Val-Leu-Arg-*p*NA·2HCl (S-2266), and methoxysuccinyl-Arg-Pro-Tyr-*p*NA·HCl (S-2586) were from Chromogen AB (Stockholm, Sweden). Spectrozyme® FIXa (*H*-D-Leu-phenylalanyl-Gly-Arg-*p*NA·2-AcOH) was obtained from American Diagnostica Inc. (Stamford, CT). All substrates were reconstituted in deionized water prior to use. Recombinant human TF (Innovin) was purchased from Dade Behring (Marburg, Germany). Human plasma was donated by healthy volunteers. All other chemicals and reagents used were of the highest purity available.

Proteins

Human plasma-derived FVIIa, FX, and FXa were a gift from the Factor VII Group (Kazuhiko Tomokiyo, Yasushi Nakatomi, Teruhisa Nakashima, and Soutatou Gokudan) of KAKETSUKEN and were purified as described (23, 24). Recombinant human soluble TF (sTF; residues 1–218) was a gift from Dr. Toshiyuki Miyata (National Cardiovascular Center, Suita, Japan), and it was prepared as described (25). Human plasma-derived thrombin, activated protein C, and FIXa were gifts from Hiroshi Kaetsu, Shinji Nakahira, and Takayoshi Hamamoto (KAKETSUKEN), respectively, and prepared as described (23, 26, 27). Three cardiotoxins (CM-14, CM-17, and CM-18 from *Naja naja atra*) were obtained from Dr. Mitsuhiro Ohta (Kobe Pharmaceutical University). Plasma kallikrein and plasmin were purchased from Enzyme Research Laboratories (South Bend, IN). FXIa and FXIIa were purchased from Haemtech (Essex Junction, VT). Tissue plasminogen acti-

vator and urokinase-type plasminogen activator were purchased from American Diagnostica Inc. α -Chymotrypsin and trypsin were obtained from Worthington.

Purification of Anticoagulant Protein

H. haemachatus crude venom (100 mg in 1 ml of distilled water) was applied to a Superdex 30 gel-filtration column (1.6 \times 60 cm) equilibrated with 50 mM Tris-HCl buffer (pH 7.4) and eluted with the same buffer using an Δ KTA purifier system (Amersham Biosciences AB, Uppsala, Sweden). Individual fractions were assayed for anticoagulant activity using prothrombin time (see below). Fractions with potent anticoagulant activity were pooled and subfractionated on a cation-exchange column using the same chromatography system. The anticoagulant fraction was pooled and loaded onto a UNO S6 column (6-ml column volume; Bio-Rad) equilibrated with 50 mM Tris-HCl buffer (pH 7.5). Bound proteins were eluted with a linear gradient of 1 M NaCl in the same buffer. Fractions collected were assayed for anticoagulant activity. The anticoagulant peaks obtained from cation-exchange chromatography were applied to a Jupiter C₁₈ column (1 \times 25 cm) equilibrated with 0.1% trifluoroacetic acid. The bound proteins were eluted using a linear gradient of 80% acetonitrile in 0.1% trifluoroacetic acid. Individual peaks were collected, lyophilized, examined for anticoagulant activity, and subsequently rechromatographed on a narrow bore PepMap column using a Chromeleon microliquid chromatography system (LC Packings, San Francisco, CA).

Electrospray Ionization Mass Spectrometry

The homogeneity and mass of the anticoagulant proteins were determined by electrospray ionization mass spectrometry using a PerkinElmer Life Sciences API-300 liquid chromatography/tandem mass spectrometry system. Typically, reverse-phase HPLC fractions were directly used for analysis. Ion spray, orifice, and ring voltages were set at 4600, 50, and 350 V, respectively. Nitrogen was used as a nebulizer and curtain gas. A Shimadzu LC-10AD pump was used for solvent delivery (40% acetonitrile in 0.1% trifluoroacetic acid) at a flow rate of 50 μ l/min. BioMultiview software (PerkinElmer Life Sciences) was used to analyze and deconvolute raw mass spectra.

Reduction and Pyridylethylation

Purified proteins were reduced and pyridylethylated using procedures described previously (28). Briefly, proteins (0.5 mg) were dissolved in 500 μ l of denaturant buffer (6 M guanidine hydrochloride, 0.25 M Tris-HCl, and 1 mM EDTA (pH 8.5)). After the addition of 10 μ l of β -mercaptoethanol, the mixture was incubated under vacuum for 2 h at 37 °C. 4-Vinylpyridine (50 μ l) was added to the mixture and kept at room temperature for 2 h. Pyridylethylated proteins were purified on an analytical Jupiter C₁₈ column (4.6 \times 250 mm) using a gradient of acetonitrile in 0.1% (v/v) trifluoroacetic acid at a flow rate of 0.5 ml/min.

N-terminal Sequencing

N-terminal sequencing of the native and S-pyridylethylated proteins was performed by automated Edman degradation using a PerkinElmer Life Sciences Model 494 pulsed liquid-phase sequencer (Procise) with an on-line Model 785A phenylthiohydantoin-derivative analyzer.

CD Spectroscopy

Far-UV CD spectra (260–190 nm) were recorded using a Jasco J-810 spectropolarimeter. All measurements were carried out at room temperature using 0.1-cm path length stoppered cuvettes. The instrument optics was flushed with 30 liters of nitrogen gas/min. The spectra were

recorded using a scan speed of 50 nm/min, a resolution of 0.2 nm, and a bandwidth of 2 nm. A total of four scans were recorded and averaged for each spectrum, and the base line was subtracted. The CD spectra of the anticoagulant proteins and their *S*-pyridylethylated forms were recorded in 50 mM Tris-HCl buffer (pH 7.4).

Reconstitution of the Anticoagulant Complex

Preliminary studies indicated that the active anticoagulant protein interacted with another venom protein, forming a synergistic complex. We reconstituted the complex for various *in vitro* experiments immediately prior to the experiments by incubating equimolar concentrations of the two proteins (unless mentioned otherwise) at 37 °C for 5 min in 50 mM Tris-buffer (pH 7.4).

Anticoagulant Activity

The anticoagulant activities of *H. haemachatus* venom and its fractions were determined by four coagulation tests using a BBL Fibrometer.

Recalcification Time—The recalcification times were determined according to the method of Langdell *et al.* (29). 50 mM Tris-HCl buffer (pH 7.4; 100 μ l), plasma (100 μ l), and various concentrations of venom or its fraction (50 μ l) were preincubated for 2 min at 37 °C. Clotting was initiated by the addition of 50 μ l of 50 mM CaCl₂.

Prothrombin Time—The prothrombin times were measured according to the method of Quick (30). 100 μ l of 50 mM Tris-HCl buffer (pH 7.4), 100 μ l of plasma, and 50 μ l of venom or its fractions were preincubated for 2 min at 37 °C. Clotting was initiated by the addition of 150 μ l of thromboplastin with calcium reagent.

Stypven Time—The Stypven times were measured according to the method of Hougie (31). Plasma (100 μ l), 50 mM Tris-HCl buffer (pH 7.4; 100 μ l), Russell's viper venom (0.01 μ g in 100 μ l), and individual proteins or the reconstituted complex (50 μ l) were preincubated for 2 min at 37 °C. Clotting was initiated by the addition of 50 μ l of 50 mM CaCl₂.

Thrombin Time—The thrombin times were determined according to the method of Jim (32). Individual proteins or the reconstituted complex was incubated with 100 μ l of plasma and 100 μ l of 50 mM Tris-HCl buffer (pH 7.4) for 2 min at 37 °C in a total volume of 250 μ l. Clotting was initiated by the addition of standard thrombin reagent (0.01 NIH unit in 50 μ l).

Complex Formation Studies with Size-exclusion Chromatography

The formation of a complex between anticoagulant proteins was examined by gel-filtration chromatography on a Superdex 30 gel-filtration column (1.6 \times 60 cm) using an Δ KTA purifier. The column was equilibrated with 50 mM Tris-HCl buffer (pH 7.4) at a flow rate of 1 ml/min. Individual proteins and an equimolar mixture of anticoagulant proteins (native or pyridylethylated) were incubated for 30 min at 37 °C and then loaded onto the column and eluted in the same buffer. Elution was followed at 280 nm.

Reconstitution of the Extrinsic Tenase Complex

The TF-FVIIa complex was reconstituted by incubating 10 pM FVIIa with 70 pM recombinant human TF (Innovin) in Buffer A (20 mM HEPES, 150 mM NaCl, 10 mM CaCl₂, and 1% bovine serum albumin (pH 7.4)) for 10 min at 37 °C. FX was added to the mixture to obtain a final concentration of 30 nM. The activation was stopped by the addition 50 μ l of stop buffer (20 mM HEPES, 150 mM NaCl, 50 mM EDTA, and 1% bovine serum albumin (pH 7.4)) to 50- μ l aliquots of the reaction mixture after 15 min of incubation. FXa formed was measured by the hydrolysis of 1 mM S-2222 in Buffer A in a microtiter plate reader at 405

nm. The inhibitory effect on extrinsic tenase activity was determined by adding the individual proteins or the anticoagulant complex 15 min prior to FX addition.

Serine Protease Specificity

The selectivity profile of anticoagulant proteins and their complex was examined against 12 serine proteases: procoagulant serine proteases (FIXa, FXa, FXIa, FXIIa, plasma kallikrein, and thrombin), anticoagulant serine protease activated protein C, fibrinolytic serine proteases (urokinase, tissue plasminogen activator, and plasmin), and classical serine proteases (trypsin and chymotrypsin). Various concentrations of the purified individual proteins or the reconstituted anticoagulant complex were preincubated with each of the enzymes for 5 min at 37 °C, followed by the addition of the appropriate chromogenic substrate.

In a total volume of 200 μ l in the individual wells of the microtiter plate, the final concentrations were as follows: FVIIa (300 nM)/S-2288, sTF-FVIIa (30 nM)/S-2288, FXa (0.75 nM)/S-2765, α -thrombin (0.66 nM)/S-2238, plasmin (2 nM)/S-2251, FIXa (3 μ M)/Spectrozyme® FIXa, FXIa (0.34 nM)/S-2366, FXIIa (0.4 nM)/S-2302, recombinant tissue plasminogen activator (80 nM)/S-2288, activated protein C (0.34 nM)/S-2366, urokinase/S-2444, plasma kallikrein (0.4 nM)/S-2302, trypsin (2.17 nM)/S-2222, and chymotrypsin (0.4 nM)/S-2586. The kinetic rate of substrate hydrolysis (mOD/min) was measured over 5 min.

Kinetics of Inhibition

All studies were performed in 50 mM Tris-HCl buffer (pH 7.4) containing 150 mM NaCl, 10 mM CaCl₂, and 1% bovine serum albumin at 37 °C. The kinetics of hydrolysis of the chromogenic substrate S-2288 by sTF-FVIIa was measured prior to examining the inhibitory effects of the individual proteins and the reconstituted anticoagulant complex. Reactions were initiated by the addition of S-2288 (0–5 mM) to the individual wells of a 96-well plate containing FVIIa (30 nM) in complex with sTF (100 nM) in a final volume of 180 μ l. Initial reaction velocities were measured as a linear increase in the absorbance at 405 nm over 5 min with a SpectraMax Plus® temperature-controlled microplate spectrophotometer (Molecular Devices Corp., Sunnyvale, CA).

The inhibitory potency of the anticoagulant complex was measured over a range of substrate concentrations. Reactions were initiated by the addition of S-2288 to premixed cofactor-enzyme and inhibitor in the wells of a microtiter plate. Reactions with sTF-FVIIa contained 0.025–0.1 μ M inhibitor complex and 0–3 mM S-2288. The initial velocities were measured over 5 min under steady-state conditions and were fit by reiterative nonlinear regression to Equation 1, describing a classical noncompetitive inhibitor, to derive the *K_i* value.

$$1/V = K_m/V_{\max}(1 + [I]/K_i)1/[S] + 1/V_{\max}(1 + [I]/K_i) \quad (\text{Eq. 1})$$

Isothermal Titration Calorimetry (ITC)

The interaction of the reconstituted anticoagulant complex with FVIIa was monitored with a VP-ITC titration calorimetric system (MicroCal, LLC, Northampton, MA). The instrument was calibrated using the built-in electrical calibration check. FVIIa (10 μ M) in 50 mM Tris-HCl buffer and 10 mM CaCl₂ (pH 7.4) in the calorimetric cell was titrated with the reconstituted anticoagulant complex (0.4 mM) dissolved in the same buffer in a 250- μ l injection syringe with continual stirring at 300 rpm at 37 °C. All protein solutions were filtered and degassed prior to titration. The first injections presented defects in the

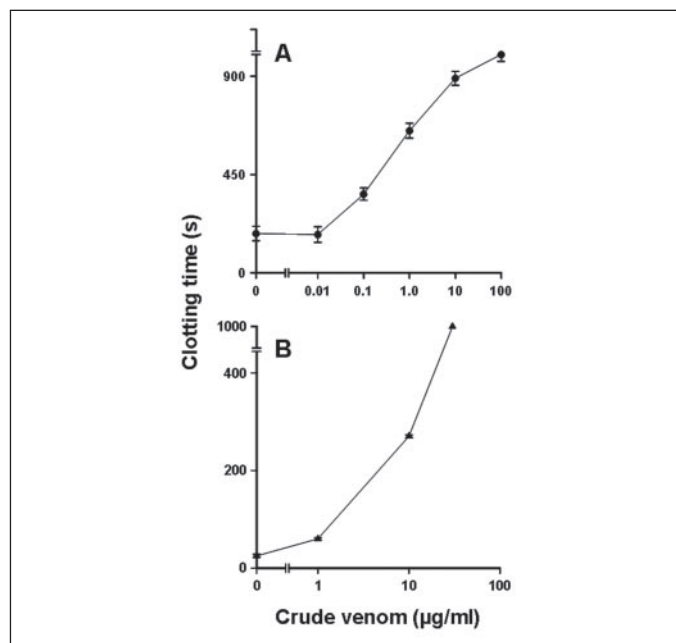


FIGURE 1. **Anticoagulant activity of the crude venom.** Shown are the effects of the crude venom on recalcification time (A) and prothrombin time (B). Note that the venom exhibited potent anticoagulant activity in both assays. Each data point represents the mean \pm S.D.

base line, and these data were not included in the fitting process. The calorimetric data were processed and fitted to the *single set of identical sites* model using MicroCal Origin (Version 7.0) data analysis software supplied with the instrument. The total heat content (Q) of the solution (determined relative to zero for the unliganded species) contained in the active cell volume (V_0) was calculated according to Equation 2,

$$Q = \frac{nM_t\Delta HV_0}{2} \left(1 + \frac{X_t}{nM_t} + \frac{1}{nK_uM_t} - \sqrt{\left(1 + \frac{X_t}{nM_t} + \frac{1}{nK_uM_t} \right)^2 - \frac{4X_t}{nM_t}} \right) \quad (\text{Eq. 2})$$

where K is the binding affinity constant; n is the number of sites; ΔH is the enthalpy of ligand binding; and M_t and X_t are the bulk concentrations of macromolecule and ligand, respectively, for the binding $X + M \leftrightarrow XM$. The change in heat (ΔH) measured between the completions of two consecutive injections is corrected for dilution of the protein and ligand in the cell according to standard Marquardt methods. The free energy change (ΔG) during the interaction was calculated using the relationship $\Delta G = \Delta H - T\Delta S = -RT \ln K_a$, where T is the absolute temperature and R is the universal gas constant.

RESULTS

Purification of the Anticoagulant Protein—Crude venom of *H. haemachatus* exhibited potent anticoagulant activity in both recalcification and prothrombin time assays (Fig. 1, A and B). To purify the anticoagulant protein, the crude venom was size-fractionated by gel-filtration chromatography (Fig. 2A). Fractions corresponding to peaks 2 and 3 contained anticoagulant proteins as determined by prothrombin time assays. Peak 2 corresponded to proteins mostly containing phospholipase A_2 that have been characterized previously (33). However, this peak had milder anticoagulant activity compared with peak 3 (Fig. 2A, inset), so we focused on isolating the anticoagulant protein from

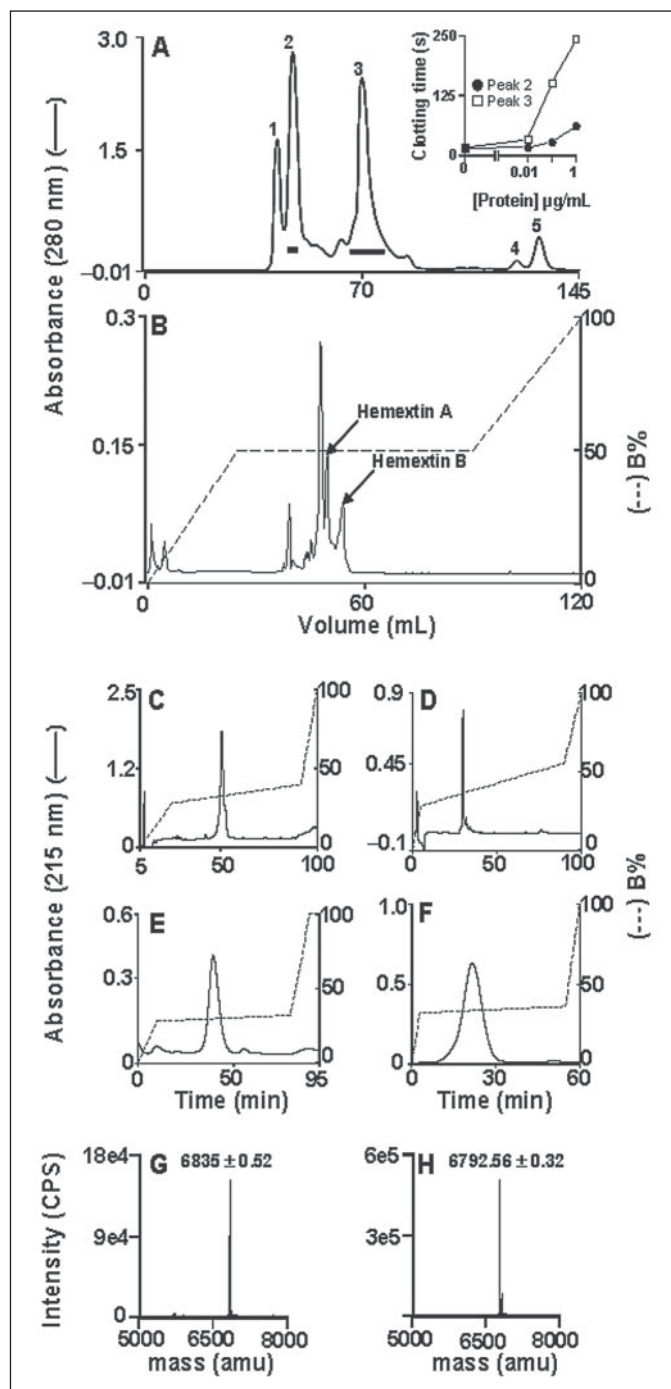


FIGURE 2. **Purification of hemexstins A and B.** A, size-exclusion chromatography of *H. haemachatus* crude venom using a Superdex 30 column. Inset, anticoagulant activity of peaks 2 and 3. B, cation-exchange chromatography of peak 3 using a UNO S6 column. C and D, reverse-phase HPLC profiles of fractions containing hemexstins A and B, respectively, using a Jupiter C_{18} semipreparative column. E and F, capillary liquid chromatography profiles of hemexstins A and B, respectively. The homogeneity and mass of hemexstins A and B were determined by electrospray ionization mass spectrometry. G and H, reconstructed mass spectra of hemexstins A and B, respectively. CPS, counts/s; amu, atomic mass units.

peak 3, which was fractionated further by cation-exchange chromatography on a UNO S6 column (Fig. 2B). Only peak A (labeled *Hemexstin A*) exhibited mild anticoagulant activity. During our preliminary studies, we found that the anticoagulant activity of peak A was potentiated by peak B (labeled *Hemexstin B*; see below). Because this anticoagulant complex specifically inhibited the extrinsic tenase complex (described

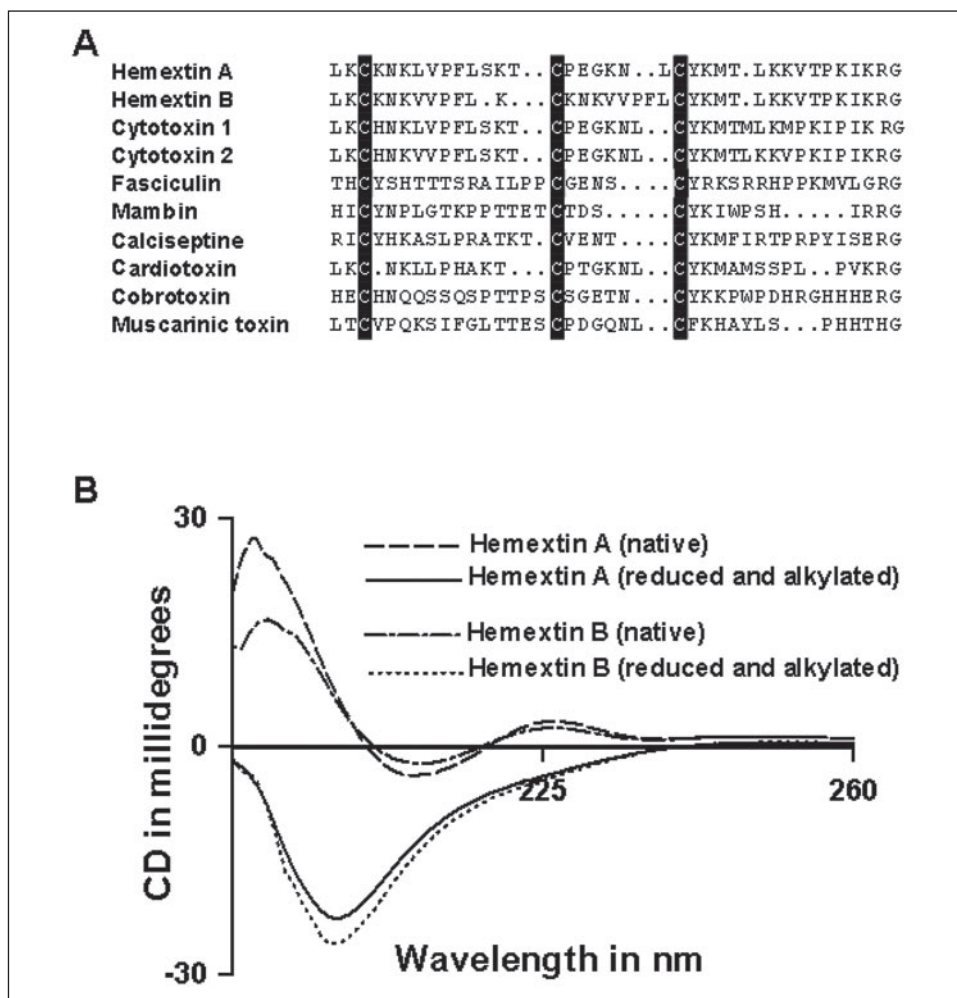


FIGURE 3. **N-terminal sequences of hemexstins A and B.** *A*, the first 25 N-terminal residues of hemexstins A and B were determined by Edman degradation. Conserved cysteine residues in the three-finger toxin family are indicated. *B*, shown are the CD spectra of native and *S*-pyridylethylated hemexstins A and B.

below), we named it the hemexstin AB complex (*Hemachatus* extrinsic tenase inhibitor) and the individual proteins hemexstins A and B, respectively. Fractions corresponding to both hemexstins A and B were pooled separately and purified by reverse-phase HPLC (Fig. 2, *C* and *D*) and capillary liquid chromatography (Fig. 2, *E* and *F*). The homogeneity and mass of the individual proteins were determined by electrospray ionization mass spectrometry. The mass spectra of hemexstins A and B showed three peaks with mass/charge ratios ranging from 3 to 6 charges (data not shown) and their calculated molecular masses as 6835.00 ± 0.52 and 6792.56 ± 0.32 Da, respectively (Fig. 2, *G* and *H*).

N-terminal Sequence Determination—We determined the sequence of the first 25 amino acid residues of hemexstins A and B by Edman degradation (Fig. 3*A*). The locations of the cysteine residues in the proteins were confirmed by sequencing the pyridylethylated proteins. Both proteins show similarity to cardiotoxins, postsynaptic neurotoxins, fasciculin, and other members of the three-finger toxin family (Fig. 3*A*), but not to serine protease inhibitors isolated from snake venoms (34, 35). Thus, hemexstins A and B belong to three-finger toxin family.

CD Spectroscopy—Both hemexstins A and B exhibited negative minima at 215 nm and positive maxima at 194 nm. Thus, similar to other three-finger toxins, both hemexstins A and B exhibited a predominantly β -sheet structure (Fig. 3*B*). However, the *S*-pyridylethylated forms of hemexstins A and B displayed negative minima at 195 nm, *i.e.* a predominantly random-coil structure (Fig. 3*B*). Thus, reduction and pyridylethylation result in the loss of folding and three-dimensional structure in hemexstins A and B.

Anticoagulant Activity of Hemexstins—The anticoagulant activity of hemexstins A and B was determined by the prothrombin time assay (Fig. 4*A*). Hemexstin A prolonged the clotting time and exhibited mild anticoagulant activity, whereas hemexstin B did not show any significant effect on the clotting time even at higher concentrations. Interestingly, an equimolar mixture of hemexstins A and B exhibited more potent anticoagulant activity, indicating synergism between these proteins (Fig. 4*A*). Such an increase in the anticoagulant effect could be due either to the inhibition of two separate steps in the coagulation cascade or to the formation of a complex between them. Because hemexstin B by itself has no significant effect on prothrombin time, it does not inhibit a separate step; instead, it is likely that hemexstins A and B form a complex. *S*-Pyridylethylated hemexstins did not exhibit any anticoagulant activity. An equimolar mixture of *S*-pyridylethylated hemexstins A and B also failed to display any anticoagulant effect (Fig. 4*A*, *inset*). Thus, proper folding is important for the interaction between hemexstins A and B and their anticoagulant activity.

Complex Formation between Hemexstins A and B—To investigate the formation of a complex between the two proteins, we employed a titration experiment in the prothrombin time assay. In this experiment, the concentration of hemexstin A was kept constant at $4.4 \mu\text{M}$, and its anticoagulant activity was monitored with increasing hemexstin B concentrations (Fig. 4*B*). The anticoagulant activity increased with increasing concentrations of hemexstin B until the ratio reached 1:1. Further addition did not increase the anticoagulant effect. The results indicate that

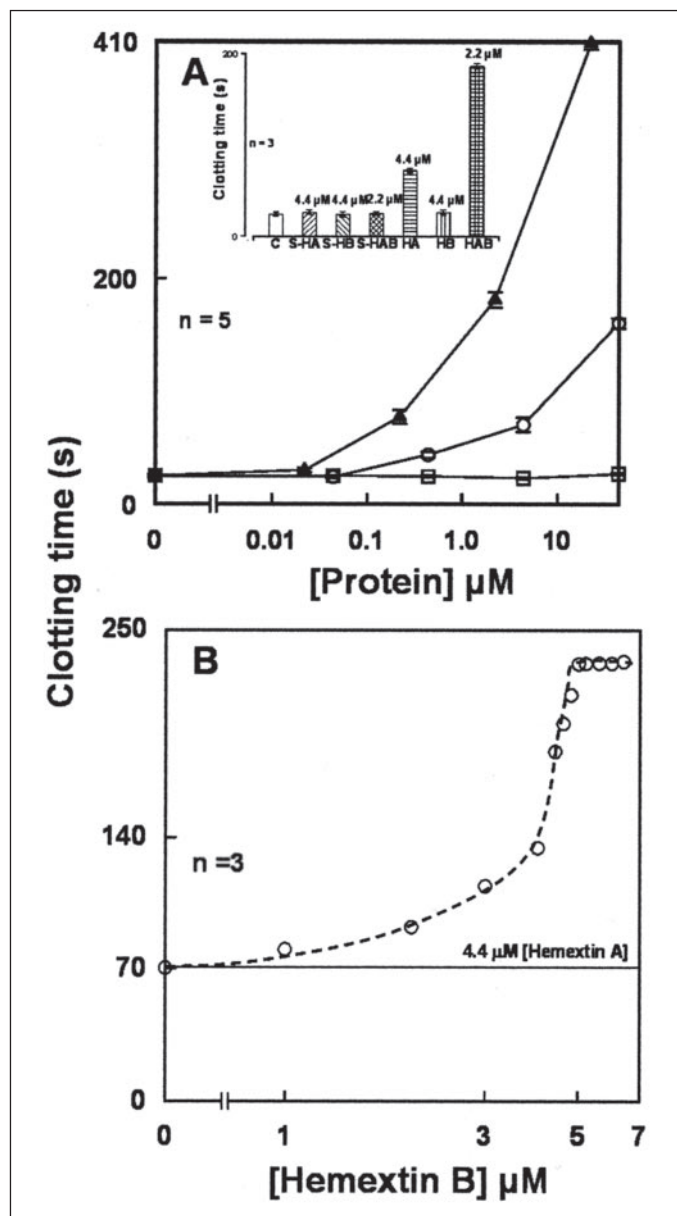


FIGURE 4. Effects of hemexstins A and B on prothrombin time. A, shown are the effects of hemexstins A (○), hemexstins B (□), and the probable hemexstins AB complex (▲) on prothrombin time. Note that the anticoagulant potency of hemexstins A increased in the presence of hemexstins B. Each data point represents the mean \pm S.D. *Inset*, comparison of the anticoagulant activities of the control (C), S-pyridylethylated hemexstins A (S-HA), S-pyridylethylated hemexstins B (S-HB), a mixture of S-pyridylethylated hemexstins A and B (S-HAB), hemexstins A (HA), hemexstins B (HB), and the hemexstins AB complex (HAB). B, complex formation between hemexstins A and B is illustrated by their effect on prothrombin time.

hemexstins A and B form a 1:1 complex and that complex formation is crucial for potent anticoagulant activity.

Complex formation between hemexstins A and B was further confirmed by gel-filtration chromatography. As shown in Fig. 5, the retention time of individual hemexstins A and B was ~ 70 min. However, the reconstituted complex eluted as a major peak with a retention time of ~ 40 min and as a minor peak with a retention time of ~ 70 min. The appearance of the major peak with a reduced retention time corresponding to ~ 27 kDa is consistent with the formation of a tetrameric complex with two molecules each of hemexstins A and B. We also reconstituted the hemexstins AB complex with S-pyridylethylated forms of the native proteins. However, no change in the retention time of the mix-

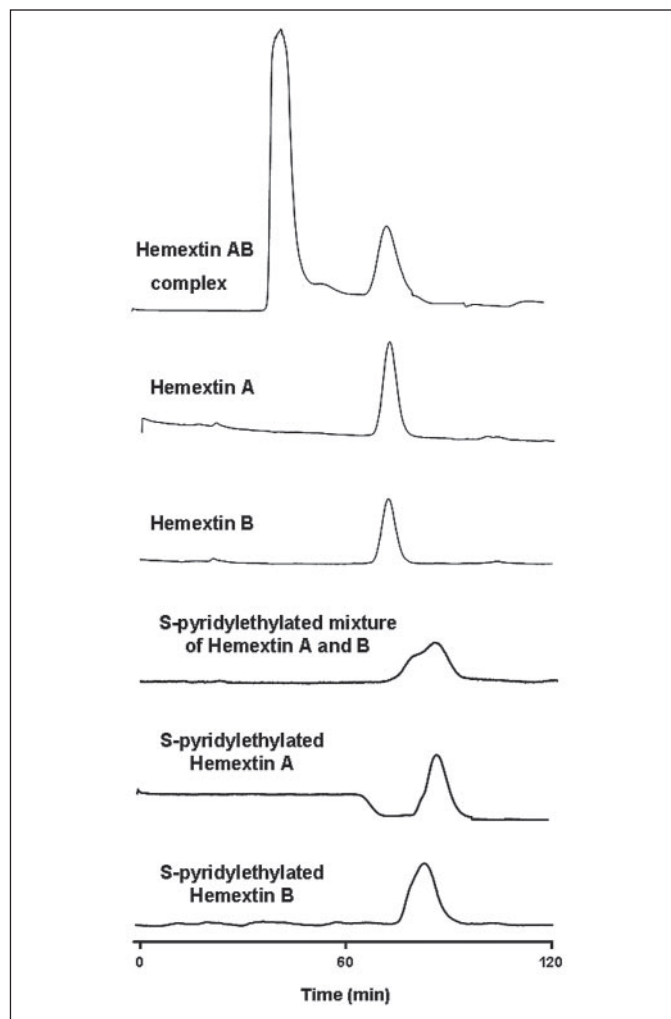


FIGURE 5. Gel-filtration studies on the formation of the hemexstins AB complex. Note that the elution time of the hemexstins AB complex was reduced to ~ 40 min compared with that of the individual hemexstins (~ 70 min). Also note that the mixture of S-pyridylethylated hemexstins A and B was unable to form a complex.

ture was observed compared with those of the individual S-pyridylethylated proteins (Fig. 5). These results indicate that proper folding is essential for the formation of the hemexstins AB complex.

It is important to note that hemexstins A and B do not exist as a complex in the crude venom. Complex formation is probably hindered by the presence of high concentrations of citrate and other salts in the venom. The reconstituted hemexstins AB complex could be easily separated into individual components on a cation-exchange column (data not shown).

Site of Anticoagulant Activity—As shown above, hemexstins A and its complex with hemexstins B prolonged prothrombin time (Fig. 4A). To identify the specific stage in the extrinsic coagulation pathway, we used a simple “dissection approach” (36, 37). We employed three commonly used clotting time assays, *viz.* prothrombin time, Stypven time, and thrombin time. This approach is based on the principle that initiating the cascade “upstream” from the inhibited step will result in elevated clotting times, whereas initiating the cascade “downstream” from the inhibited step will not affect clotting times. Thus, the anticoagulant action of the individual proteins and the complex can be localized to certain activation step(s) in the cascade (for details, see Refs. 32 and 33). Hemexstins A exhibited mild anticoagulant activity by prolonging the clotting time in the prothrombin time assay, but did not prolong

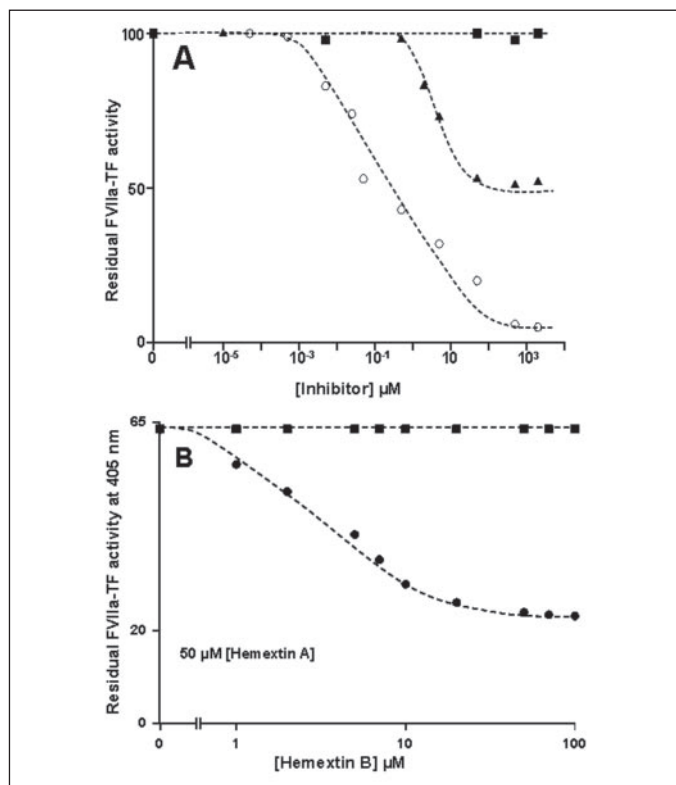


FIGURE 6. **Inhibition of TF-FVIIa activity.** *A*, shown is the hemexin A (▲), hemexin B (●), and hemexin AB complex (■) inhibitory potency on TF-FVIIa activity. *B*, the formation of the hemexin AB complex (●) between hemexin A (■) and hemexin B is illustrated by their effect on TF-FVIIa enzymatic activity. To determine the stoichiometry of complex formation, the concentration of hemexin A was kept low so that 100% TF-FVIIa activity was not inhibited upon complex formation.

Stypven time and thrombin time (data not shown). As expected, hemexin B did not prolong clotting times in the prothrombin time, Stypven time, and thrombin time assays. The hemexin AB complex exhibited potent anticoagulant activity by prolonging the clotting time in the prothrombin time assay. However, the clotting times in the other two assays were not affected (data not shown). These results indicate that hemexin A and the hemexin AB complex affect only the extrinsic tenase complex, but not the prothrombinase complex or conversion of fibrinogen to fibrin clots.

To confirm the site of inhibition, we examined the effects of hemexins A and B and their complex on the reconstituted TF-FVIIa complex (Fig. 6A). Hemexin A exhibited mild inhibitory activity at higher concentrations. On the other hand, hemexin B did not mediate any inhibitory activity on the enzymatic action of the extrinsic tenase complex. However, the hemexin AB complex completely inhibited extrinsic tenase activity (Fig. 6A) with an IC₅₀ (concentration of the inhibitor that inhibits 50% of the activity) of 200 nM. Neither the individual proteins nor the complex mediated any inhibitory effect on FXa amidolytic activity (described below). The effects of the individual hemexins and the hemexin AB complex on the intrinsic pathway were also assessed using recalcification time assays. No anticoagulant activity on the intrinsic pathway was observed (data not shown). Furthermore, the effects of other three-finger toxins, particularly cardiotoxins/cytotoxins, which are structurally similar to hemexins A and B, on TF-FVIIa proteolytic activity were also monitored. CM-14, CM-17, and CM-18 from *N. naja atra* did not inhibit FXa formation by the TF-FVIIa complex (data not shown). To determine the importance of hemexin AB complex formation for the inhibition of the TF-FVIIa complex, we performed a similar

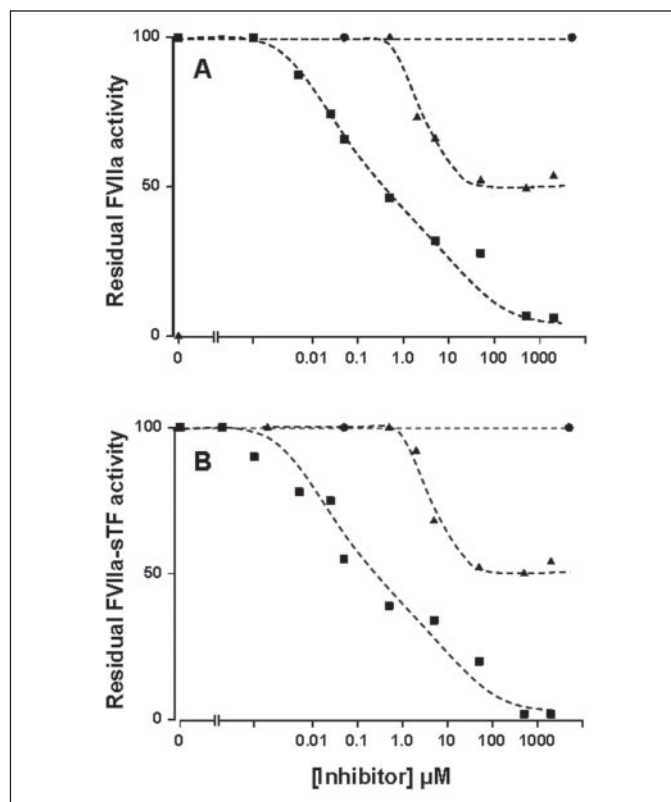


FIGURE 7. **Effect of phospholipids on the inhibitory activity of hemexins A and B and the hemexin AB complex.** Shown is the hemexin A (●), hemexin B (▲), and hemexin AB complex (■) inhibitory potency on FVIIa (*A*) and sTF-FVIIa (*B*) amidolytic activity. Note that the absence of phospholipids did not affect the inhibitory potency of the protein(s) and the reconstituted complex.

titration experiment. The inhibitory activity of hemexin A at 50 μM (the concentration at which the hemexin AB complex inhibited only ~70% of the TF-FVIIa activity) was examined in the presence of increasing concentrations of hemexin B. As shown in Fig. 6B, the inhibitory activity of hemexin A increased with increasing concentrations of hemexin B until the ratio reached 1:1. Further addition did not increase the inhibition. The results indicate that hemexins A and B form a 1:1 complex and that complex formation is crucial for potent anticoagulant activity. These observations further confirm the importance of complex formation between hemexins A and B.

To understand the effect of phospholipids, the inhibitory activity of hemexin A and the hemexin AB complex on FVIIa amidolytic activity was monitored in the presence or absence of sTF. In both the cases, we observed potent inhibitory activity in a dose-dependent manner (Fig. 7, *A* and *B*).

Specificity of Inhibition—To determine the specificity of inhibition, hemexins A and B and their complex were screened against 12 serine proteases. No inhibitory activity was observed against any of the serine proteases with the exception of FVIIa and plasma kallikrein. As with FVIIa, hemexin A and the hemexin AB complex inhibited plasma kallikrein in a dose-dependent manner (Fig. 8). Hemexin B did not inhibit the protease activity of kallikrein. However, the inhibitory potency for FVIIa (in the absence or presence of sTF) was at least 50 times higher than for plasma kallikrein.

Kinetics of Inhibition—To determine the mechanism of inhibition, we examined the kinetics of hemexin AB complex inhibition of the amidolytic activity of the sTF-FVIIa complex in the presence of S-2288. Kinetic studies revealed that hemexin inhibited sTF-FVIIa activity non-competitively. Lineweaver-Burk plots showed that K_m values remained

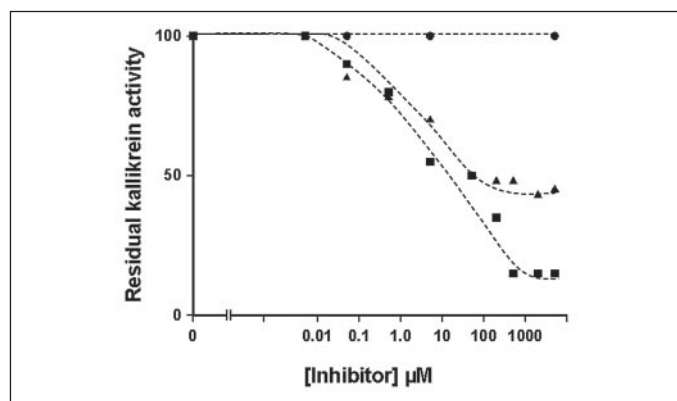


FIGURE 8. Inhibition of plasma kallikrein amidolytic activity. Shown is the hemexin A (\blacktriangle), hemexin B (\bullet), and hemexin AB complex (\blacksquare) inhibitory potency on plasma kallikrein amidolytic activity. Note that the IC_{50} for inhibition was $\sim 10 \mu M$.

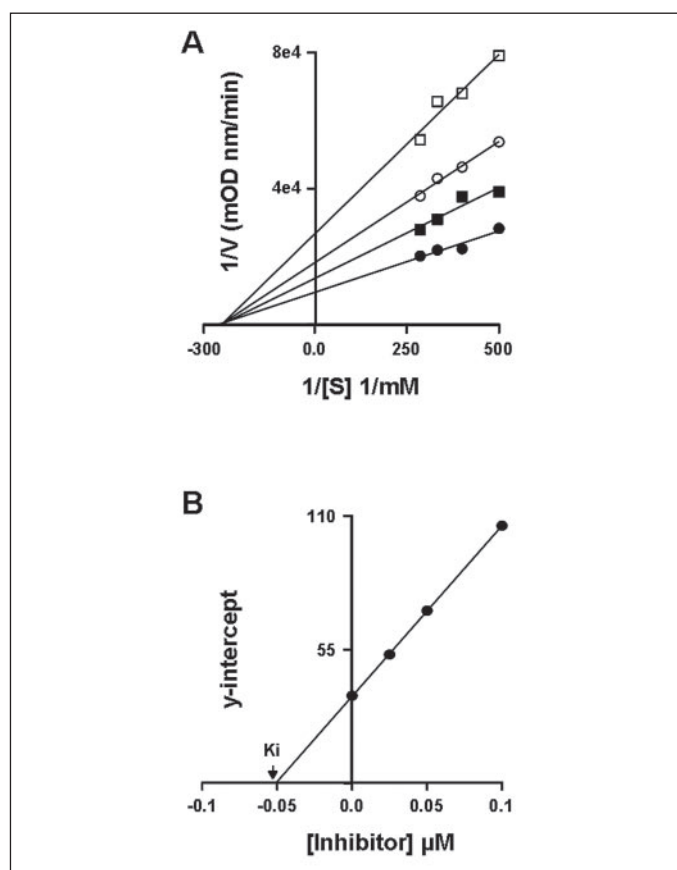


FIGURE 9. Nature of inhibition. A, double-reciprocal (Lineweaver-Burk) plots for the kinetic activity of sTF-FVIIa in the presence of 100 nM (\square ; $2K_i$), 50 nM (\circ ; K_i), and 25 nM (\blacksquare ; $1/2K_i$) reconstituted hemexin AB complex. Also shown is the kinetic activity of sTF-FVIIa in the absence of the hemexin AB complex (\bullet). Note that the V_{max} decreased with increasing inhibitor concentrations, whereas the K_m remained unchanged, a classical phenomenon observed in noncompetitive inhibitors. B, corresponding secondary plot depicting the K_i for inhibition. *mOD*, milli-optical density.

unaltered, whereas V_{max} values decreased with increasing concentrations of the inhibitor (Fig. 9A), a characteristic of a noncompetitive inhibitor. The K_i for inhibition was determined to be 50 nM (Fig. 9B). We also calculated the turnover number (K_{cat} ; moles of substrate converted to product/mol/enzyme/min) at different concentrations of the inhibitor. As observed in the case of classical noncompetitive inhibitors, the K_{cat} decreased with increasing concentrations of the hemexin AB complex (data not shown). Because the amidolytic activity of FVIIa alone is

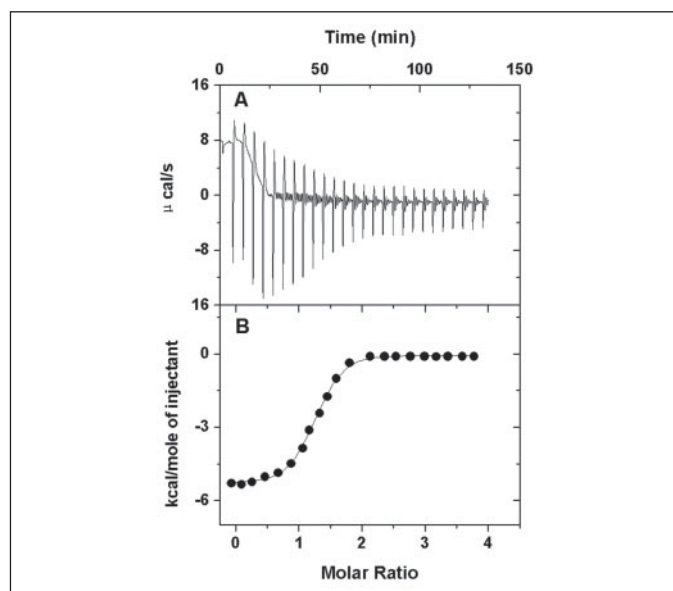


FIGURE 10. ITC studies on the formation of a complex between the hemexin AB complex and FVIIa. A, raw data in microcalories/s versus time showing heat release upon injections of 0.4 mM reconstituted hemexin AB complex into a 1.4-ml cell containing $10 \mu M$ FVIIa; B, integration of the raw data yielding the heat/mol versus molar ratio. The best values of the fitting parameters were $1.62 \times 10^5 M^{-1}$ for K , $-5.445 kcal \cdot M^{-1}$ for ΔH , and $-4.274 cal \cdot M^{-1}$ for ΔS .

very weak (38), we did not study the kinetics of the inhibition of FVIIa amidolytic activity by the hemexin AB complex.

Binding of the Hemexin AB Complex to FVIIa—We studied the interaction between the hemexin AB complex and FVIIa by ITC. We monitored the thermodynamic changes associated with the binding of the hemexin AB complex to FVIIa (Fig. 10). The binding was exothermic, with $\Delta H = -5.445 kcal \cdot M^{-1}$, $\Delta G = -4.121 kcal \cdot M^{-1}$, and $\Delta S = -4.274 cal \cdot M^{-1}$. The calculated K for the binding was $1.62 \times 10^5 M^{-1}$.

DISCUSSION

Initiation of blood coagulation during injury or trauma is essential for the survival of the organism. However, the formation of unwanted clots has detrimental or debilitating effects and hence the need for anticoagulant therapies. The current anticoagulants used for treating these disorders are nonspecific and have a narrow therapeutic range, necessitating careful laboratory monitoring to achieve optimal efficacy and to minimize bleeding. This is further complicated by other factors such as dietary intake (39). Therefore, novel anticoagulant and antiplatelet agents are being sought. Because FVIIa is the key initiator of blood coagulation and is present in the plasma milieu at very low concentrations, it is an attractive drug target for the design and development of anticoagulants.

So far, only two proteins that specifically inhibit the TF-FVIIa complex have been well characterized, *viz.* tissue factor pathway inhibitor (TFPI) and nematode anticoagulant peptide c2 (NAPc2). TFPI is an endogenous inhibitor of this complex (40), whereas NAPc2 is an exogenous inhibitor isolated from canine hookworm (*Ancylostoma caninum*) (41). TFPI is a 42-kDa plasma glycoprotein consisting of three tandem Kunitz-type domains. The first and second units inhibit TF-FVIIa and FXa, respectively. The third Kunitz domain and the C-terminal basic region of the molecule have heparin-binding sites (42). The anticoagulant action of TFPI is a two-stage process. The second Kunitz domain binds first to a molecule of FXa and deactivates it. The first domain then rapidly binds to an adjacent TF-FVIIa complex, preventing further activation of FX (43–45). On the other hand, NAPc2 is an 8-kDa

short polypeptide. Its mechanism of action requires prerequisite binding to FXa or zymogen FX to form a binary complex prior to its interaction and inhibition of membrane-bound TF·FVIIa (41). Therefore, despite the structural differences, both inhibitors form a quaternary complex with TF·FVIIa·FXa. However, in both complexes, the active site of FVIIa is occupied by the respective inhibitors and is not accessible.

Because of the lack of natural inhibitors that specifically interfere with FVIIa activity, a number of artificial inhibitors have been designed and developed. They include proteins that block the association of TF and FVIIa, such as antibodies against TF and FVIIa, TFAA (a TF mutant with reduced cofactor function for FX), FFR-VIIa (inactivated form of FVIIa with 5-fold higher affinity for TF compared with native FVIIa), and peptides derived from TF and FVIIa (47–54). In addition, two series of peptide exosite inhibitors were selected from phage display libraries for their ability to bind to the TF·FVIIa complex (47, 48). They bind to two distinct exosites on the serine protease domain of FVIIa and exhibit steric and allosteric inhibition (50). Although both peptide classes are potent and selective inhibitors of the TF·FVIIa complex, they fail to inhibit 100% activity even at saturating concentrations. This is overcome either by the fusion of the two peptides (51) or by using a protease switch with substrate phage (49). A number of synthetic compounds have also been designed as active-site inhibitors of FVIIa as well as the TF·FVIIa complex (52, 55–58). A number of naphthylamidines have recently been reported to have FVIIa inhibitory activity (59). They were synthesized by the coupling of amidinobenzaldehyde analogs to a polystyrene resin. However, apart from inhibiting FVIIa activity, these synthetic compounds nonspecifically inhibit the activity of other blood coagulation serine proteases (59).

Hemexin AB Complex Is a Novel Anticoagulant—We have reported here the isolation and characterization of two proteins, hemexins A and B, from the venom of *H. haemachatus* that synergistically induce potent anticoagulant activity. Individually, only hemexin A exhibited mild anticoagulant activity, whereas hemexin B had no anticoagulant activity (Fig. 4A). The increase in the anticoagulant potency of hemexin A in the presence of hemexin B (Fig. 4A) indicated probable complex formation between the two proteins. We have shown that 1:1 complex formation is important for potent anticoagulant activity using the prothrombin time assay (Fig. 4B). Complex formation was further confirmed by gel-filtration chromatography (Fig. 5).

Both hemexins A and B belong to the three-finger family of snake venom proteins (Fig. 3A) and not to the family of snake venom serine protease inhibitors. Proteins belonging to this group exhibit a characteristic β -sheet structure (60), also observed in the CD studies (Fig. 3B). It is a well known fact that disulfide bonds associated with cysteine residues are essential structural units in proteins (61). To evaluate the importance of the three-finger fold in both complex formation and anticoagulant activity, we used reduced and subsequently pyridylethylated hemexins A and B. Upon pyridylethylation, they lost their native three-finger fold, as observed in the CD studies (Fig. 3B). The S-pyridylethylated hemexins were functionally inactive (Fig. 4A, inset) and were unable to bind to each other to form the complex, as evident from the gel-filtration studies (Fig. 5). This shows that proper folding of the proteins is important not only for function, but also for complex formation.

Using the dissection approach (36, 37), we identified the site of anticoagulant action of hemexin A and its synergistic complex. Both hemexin A and the hemexin AB complex inhibited the extrinsic tenase complex, but not other steps in the extrinsic pathway. These results were further confirmed by studying the effect of hemexin A and its complex on the reconstituted TF·FVIIa complex. Both hemexin A and

the hemexin AB complex inhibited FXa formation by the reconstituted extrinsic tenase complex (Fig. 6A). Furthermore, hemexin A and the hemexin AB complex inhibited the amidolytic activity of FVIIa in both the presence and absence of sTF (Fig. 7, A and B). The hemexin AB complex inhibited with IC_{50} values of ~ 200 and ~ 210 nM, respectively. Similar IC_{50} values may be indicative of the fact that hemexin A and the hemexin AB complex do not bind to the cofactor-binding site of FVIIa. The inhibitory activity of hemexin A and the hemexin AB complex may not be due to nonspecific interaction of hemexin A or its complex with the phospholipids in the extrinsic tenase complex, as indicated by their inability to prolong Stypven time, because they failed to inhibit the prothrombinase complex, which is also formed on the phospholipid surfaces. This was further confirmed by determining the inhibitory activity of hemexin A and the hemexin AB complex on the amidolytic activity of the reconstituted extrinsic tenase complex using sTF and FVIIa (Fig. 7B). Furthermore, hemexin A and the hemexin AB complex inhibited the amidolytic activity of FVIIa (Fig. 7A). However, hemexin B did not exhibit any inhibitory activity in the absence of hemexin A. To further characterize the inhibitory properties and to determine the specificity of inhibition, we screened hemexins A and B and the hemexin AB complex against 12 serine proteases. In addition to FVIIa and its complexes, hemexin A and the hemexin AB complex inhibited the amidolytic activity of only kallikrein in a dose-dependent manner (Fig. 8). However, the IC_{50} for the inhibition of kallikrein was ~ 10 μ M, in contrast to that of FVIIa/TF·FVIIa/sTF·FVIIa, which was ~ 200 nM. Kinetic studies revealed that the hemexin AB complex is a noncompetitive inhibitor of the sTF·FVIIa complex, with a K_i of 50 nM. Using ITC studies, we have shown that the hemexin AB complex directly interacts with FVIIa (Fig. 10). The binding interaction between FVIIa and the hemexin AB complex is associated with a negative change in free energy, indicating that this complex formation is favored. The negative change in entropy observed upon binding indicates the formation of a tightly folded complex between the two moieties (62). Thus, these data strongly indicate that the hemexin AB complex is a highly specific inhibitor of FVIIa. To our knowledge, this is the first natural inhibitor of FVIIa.

Some other anticoagulants from snake venoms also inhibit the extrinsic tenase complex. However, they are not as specific. For example, CM-IV, a strongly anticoagulant phospholipase A_2 from *Naja nigricollis* venom, prolongs coagulation by inhibiting two successive steps in the coagulation cascade. It inhibits the TF·FVIIa complex by both enzymatic and nonenzymatic mechanisms (63), whereas it inhibits the prothrombinase complex by only a nonenzymatic mechanism (64, 65). Hemexin A and its synergistic complex are the first reported specific inhibitors of FVIIa isolated from snake venom.

The similar dose-dependent inhibition of the TF·FVIIa complex and FVIIa indicates that the hemexin AB complex neither requires TF for its inhibitory activity nor interferes in the binding of TF to FVIIa. Unlike TFPI and NAPc2, it also does not use FXa as a scaffold to bind to FVIIa and thus does not require FX or FXa to inhibit FVIIa. Furthermore, TFPI and NAPc2 bind to the active site of FVIIa. In contrast, as shown by the kinetic studies (Fig. 9), the hemexin AB complex is a noncompetitive inhibitor, unlike competitive inhibitors that bind to the active site. Thus, the hemexin AB complex does not appear to bind to the active site of FVIIa. Therefore, hemexin A and the hemexin AB complex are novel inhibitors of FVIIa and the TF·FVIIa complex.

Hemexin AB Complex Is a Unique Protein Complex—Synergism among snake venom toxins is fairly well characterized, particularly among presynaptic neurotoxins. For example, crotoxin isolated from *Crotalus durissus terrificus* venom contains two subunits; the basic sub-

unit is a phospholipase A₂ enzyme, whereas the acidic subunit is catalytically inactive (although it is derived from a phospholipase A₂-like protein) (66). Individually, only the basic subunit is slightly toxic, whereas the complex exhibits potent toxicity. The acidic subunit appears to act as a chaperone and enhances the specific binding of the basic subunit to the presynaptic site. Similarly, other presynaptic neurotoxins, such as taipoxin from *Oxyuranus scutellatus* (67) and textilotoxin from *Pseudonaja textilis* (68) venoms, contain three and four subunits, respectively. All the subunits are structurally similar to phospholipase A₂ enzymes. The noncovalent interactions between the subunits of these toxins are important for their potent toxicity. Thus, a number of snake venom presynaptic toxins are protein complexes with phospholipase A₂ as an integral part. Taicatoxin, another protein complex isolated from *O. scutellatus* venom, blocks calcium channels and has phospholipase A₂, proteinase inhibitor, and neurotoxin (a three-finger toxin) subunits (69). There are only a few noncovalent protein complexes in snake venoms that do not contain phospholipase A₂ as an integral part. For example, rhodocetin, an antiplatelet protein complex from *Calloselasma rhodostoma* venom, contains two subunits showing structural similarity to C-type lectins (70). Group C prothrombin activators from Australian snakes are procoagulant protein complexes that are structurally and functionally similar to mammalian blood coagulation FXa·FVa complexes (46, 71, 72). The hemexin AB complex is a unique snake venom protein complex formed by the interaction between two three-finger toxins, in which the anticoagulant activity of hemexin A is potentiated by its synergistic interaction with hemexin B. It should be noted that crude snake venom does not contain the hemexin AB complex. It is not clear when and how this complex is formed.

In summary, we have described a unique anticoagulant protein complex from snake venom that specifically and noncompetitively inhibits FVIIa activity. Our results strongly indicate that the interaction between hemexins A and B is essential for potent anticoagulant activity. This new anticoagulant may help us develop different strategies and therapeutic agents to inhibit the initiation step in blood coagulation.

Acknowledgments—We thank Dr. Prakash Kumar (Department of Biological Sciences, National University of Singapore) for reviewing the manuscript and Dr. Rajamani Lakshminarayanan (Department of Chemistry, National University of Singapore) for helpful discussions. We thank all members of the Factor VII Group of KAKETSUKEN (Kazuhiro Tomokiyo, Yasushi Nakatomi, Teruhisa Nakashima, and Soutatou Gokudan) for providing plasma-derived FVII, FVIIa, FX, and FXa. We also thank Hiroshi Kaetsu, Shinji Nakahira, and Takayoshi Hamamoto for providing plasma-derived thrombin, activated protein C, and FIXa, respectively, and Dr. Toshiyuki Miyata for providing recombinant human sTF. We also thank Kumiko Arita (KAKETSUKEN) for help in kinetic studies.

REFERENCES

- Davie, E. W., Fujikawa, K., and Kisiel, W. (1991) *Biochemistry* **30**, 10363–10370
- Davie, E. W. (1995) *Thromb. Haemostasis* **74**, 1–6
- Mann, K. G., Butenas, S., and Brummel, K. (2003) *Arterioscler. Thromb. Vasc. Biol.* **23**, 17–25
- Rapaport, S. L., and Rao, L. V. (1995) *Thromb. Haemostasis* **74**, 7–17
- Morrissey, J. H., Macik, B. G., Neuenschwander, P. F., and Comp, P. C. (1993) *Blood* **81**, 734–744
- Nemerson, Y. (1988) *Blood* **71**, 1–8
- Gustafsson, D., Bylund, R., Antonsson, T., Nilsson, I., Nystrom, J. E., Eriksson, U., Bredberg, U., and Teger-Nilsson, A. C. (2004) *Nat. Rev. Drug Discov.* **3**, 649–659
- Hirsh, J. (1991) *N. Engl. J. Med.* **324**, 1565–1574
- Hirsh, J. (1991) *N. Engl. J. Med.* **324**, 1865–1875
- Hirsh, J., and Weitz, J. I. (1999) *Lancet* **353**, 1431–1436
- Moll, S., and Roberts, H. R. (2002) *Semin. Hematol.* **39**, 145–157
- Hirsh, J. (2001) *Am. Heart J.* **142**, S3–S8

- Morrissey, J. H. (2001) *Thromb. Haemostasis* **86**, 66–74
- Markland, F. S. (1998) *Toxicol.* **36**, 1749–1800
- Higuchi, S., Murayama, N., Saguchi, K., Ohi, H., Fujita, Y., Camargo, A. C., Ogawa, T., Deshimaru, M., and Ohno, M. (1999) *Immunopharmacology* **44**, 129–135
- O'Shea, J. C., and Tchong, J. E. (2002) *Expert Opin. Pharmacother.* **3**, 1199–1210
- Marcinkiewicz, C. (2005) *Curr. Pharm. Des.* **11**, 815–827
- Huang, F., and Hong, E. (2004) *Curr. Med. Chem. Cardiovasc. Hematol. Agents* **2**, 187–196
- Plosker, G. L., and Ibbotson, T. (2003) *Pharmacoeconomics* **21**, 885–912
- Kondo, K., and Umemura, K. (2002) *Clin. Pharmacokinet.* **41**, 187–195
- McClellan, K. J., and Goa, K. L. (1998) *Drugs* **56**, 1067–1080
- Sherman, D. G. (2002) *Curr. Med. Res. Opin.* **18**, Suppl. 2, s48–s52
- Nakagaki, T., Foster, D. C., Berkner, K. L., and Kisiel, W. (1991) *Biochemistry* **30**, 10819–10824
- Wildgoose, P., and Kisiel, W. (1989) *Blood* **73**, 1888–1895
- Stone, M. J., Ruf, W., Miles, D. J., Edgington, T. S., and Wright, P. E. (1995) *Biochem. J.* **310**, 605–614
- Kaetsu, H., Mizuguchi, J., Hamamoto, T., Kamimura, K., Yoshida, Y., Nakagaki, T., Ogata, Y., Miyamoto, S., and Funatsu, A. (1998) *Thromb. Res.* **90**, 101–109
- Okajima, K., Koga, S., Kaji, M., Inoue, M., Nakagaki, T., Funatsu, A., Okabe, H., Takatsuki, K., and Aoki, N. (1990) *Thromb. Haemostasis* **63**, 48–53
- Joseph, J. S., Chung, M. C., Jeyaseelan, K., and Kini, R. M. (1999) *Blood* **94**, 621–631
- Langdell, R. D., Wagner, R. H., and Brinkhous, K. M. (1953) *J. Lab. Clin. Med.* **41**, 637–647
- Quick, A. J. (1935) *J. Biol. Chem.* **109**, 73–74
- Hougie, C. (1956) *Proc. Soc. Exp. Biol. Med.* **98**, 570–573
- Jim, R. (1957) *J. Lab. Clin. Med.* **50**, 45–60
- Condra, E., Fletcher, J. E., Rapuano, B. E., Yang, C. C., and Rosenberg, P. (1981) *Toxicol.* **19**, 61–71
- Chen, C., Hsu, C. H., Su, N. Y., Lin, Y. C., Chiou, S. H., and Wu, S. H. (2001) *J. Biol. Chem.* **276**, 45079–45087
- Hokama, Y., Iwanaga, S., Tatsuki, T., and Suzuki, T. (1976) *J. Biochem. (Tokyo)* **79**, 559–578
- Kini, R. M., and Banerjee, Y. (2005) *J. Thromb. Haemostasis* **3**, 170–171
- Stefansson, S., Kini, R. M., and Evans, H. J. (1989) *Thromb. Res.* **55**, 481–491
- Maun, H. R., Eigenbrot, C., Raab, H., Arnott, D., Phu, L., Bullens, S., and Lazarus, R. A. (2005) *Protein Sci.* **14**, 1171–1180
- Goolsby, M. J. (2002) *J. Am. Acad. Nurse Pract.* **14**, 16–18
- Lindhout, T., Franssen, J., and Willems, G. (1995) *Thromb. Haemostasis* **74**, 910–915
- Lee, A. Y., and Vlasuk, G. P. (2003) *J. Intern. Med.* **254**, 313–321
- Kato, H. (2002) *Arterioscler. Thromb. Vasc. Biol.* **22**, 539–548
- Baugh, R. J., Broze, G. J., Jr., and Krishnaswamy, S. (1998) *J. Biol. Chem.* **273**, 4378–4386
- Broze, G. J., Jr., and Miletich, J. P. (1987) *Blood* **69**, 150–155
- Sanders, N. L., Bajaj, S. P., Zivelin, A., and Rapaport, S. I. (1985) *Blood* **66**, 204–212
- Rao, V. S., Swarup, S., and Kini, R. M. (2004) *Thromb. Haemostasis* **92**, 509–521
- Dennis, M. S., Eigenbrot, C., Skelton, N. J., Ultsch, M. H., Santell, L., Dwyer, M. A., O'Connell, M. P., and Lazarus, R. A. (2000) *Nature* **404**, 465–470
- Dennis, M. S., Roberge, M., Quan, C., and Lazarus, R. A. (2001) *Biochemistry* **40**, 9513–9521
- Maun, H. R., Eigenbrot, C., and Lazarus, R. A. (2003) *J. Biol. Chem.* **278**, 21823–21830
- Roberge, M., Santell, L., Dennis, M. S., Eigenbrot, C., Dwyer, M. A., and Lazarus, R. A. (2001) *Biochemistry* **40**, 9522–9531
- Roberge, M., Peek, M., Kirchhofer, D., Dennis, M. S., and Lazarus, R. A. (2002) *Biochem. J.* **363**, 387–393
- Sorensen, B. B., Persson, E., Freskgard, P. O., Kjalke, M., Ezban, M., Williams, T., and Rao, L. V. (1997) *J. Biol. Chem.* **272**, 11863–11868
- Hirsh, J., O'Donnell, M., and Weitz, J. I. (2005) *Blood* **105**, 453–463
- Johnson, K., and Hung, D. (1998) *Coron. Artery Dis.* **9**, 83–87
- Uchiba, M., Okajima, K., Abe, H., Okabe, H., and Takatsuki, K. (1994) *Thromb. Res.* **74**, 155–161
- Uchiba, M., Okajima, K., Murakami, K., Okabe, H., and Takatsuki, K. (1995) *Thromb. Res.* **77**, 381–382
- Lazarus, R. A., Olivero, A. G., Eigenbrot, C., and Kirchhofer, D. (2004) *Curr. Med. Chem.* **11**, 2275–2290
- Olivero, A. G., Eigenbrot, C., Goldsmith, R., Roberge, K., Artis, D. R., Flygare, J., Rawson, T., Sutherlin, D. P., Kadkhodayan, S., Beresini, M., Elliott, L. O., Deguzman, G. G., Banner, D. W., Ultsch, M., Marzec, U., Hanson, S. R., Refino, C., Bunting, S., and Kirchhofer, D. (2005) *J. Biol. Chem.* **280**, 9160–9169
- Buckman, B. O., Chou, Y. L., McCarrick, M., Liang, A., Lentz, D., Mohan, R., Morrissey, M. M., Shaw, K. J., Trinh, L., and Light, D. R. (2005) *Bioorg. Med. Chem. Lett.* **15**, 2249–2252
- Kini, R. M. (2002) *Clin. Exp. Pharmacol. Physiol.* **29**, 815–822
- Debarbieux, L., and Beckwith, J. (1999) *Cell* **99**, 117–119
- Barry, J. (1976) *Curr. Top. Mol. Endocrinol.* **3**, 451–473

63. Kini, R. M., and Evans, H. J. (1995) *Toxicon* **33**, 1585–1590
64. Stefansson, S., Kini, R. M., and Evans, H. J. (1990) *Biochemistry* **29**, 7742–7746
65. Kerns, R. T., Kini, R. M., Stefansson, S., and Evans, H. J. (1999) *Arch. Biochem. Biophys.* **369**, 107–113
66. Habermann, E., and Breithaupt, H. (1978) *Toxicon* **16**, 19–30
67. Doorty, K. B., Bevan, S., Wadsworth, J. D., and Strong, P. N. (1997) *J. Biol. Chem.* **272**, 19925–19930
68. Su, M. J., Coulter, A. R., Sutherland, S. K., and Chang, C. C. (1983) *Toxicon* **21**, 143–151
69. Possani, L. D., Martin, B. M., Yatani, A., Mochca-Morales, J., Zamudio, F. Z., Gurrola, G. B., and Brown, A. M. (1992) *Toxicon* **30**, 1343–1364
70. Wang, R., Kini, R. M., and Chung, M. C. (1999) *Biochemistry* **38**, 7584–7593
71. Rao, V. S., and Kini, R. M. (2002) *Thromb. Haemostasis* **88**, 611–619
72. Rao, V. S., Swarup, S., and Kini, R. M. (2003) *Blood* **102**, 1347–1354



"This un-edited manuscript has been accepted for publication in *Biophysical Journal* and is freely available on BioFast at <http://www.biophysj.org>. The final copyedited version of the paper may be found at <http://www.biophysj.org>."

Biophysical Characterization of Anticoagulant Hemextin AB Complex from the Venom of Snake *Hemachatus haemachatus*

Yajnavalka Banerjee^{‡*}, Rajamani Lakshminarayanan^{§||}, Subramanian Vivekanandan^{‡†} Ganesh Srinivasan Anand[‡], Suresh Valiyaveetil[§] and R. Manjunatha Kini^{‡*}

From the [‡] Department of Biological Sciences, Faculty of Science, National University of Singapore, Singapore 117543, [§]Department of Chemistry, National University of Singapore, 3 Science Drive 3, Singapore 117543 and ^{*}Department of Biochemistry, VCU Medical Center, Medical College of Virginia, Virginia Commonwealth University, Richmond, VA 23298, USA

Present addresses:

♠ Department of Molecular and Experimental Medicine, The Scripps Research Institute, 10550 North Torrey Pines Road, La Jolla CA 92037, || School of Dentistry, 2250 Alcazar Street, Centre for Craniofacial and Molecular Biology, University of Southern California, Los Angeles CA 90033, †Division of Structural and Computational Biology, School of Biological Sciences, Nanyang Technological University, Singapore - 637 511

E-Mail: dbskinim@nus.edu.sg

Running Title: Anticoagulant complex from snake venom

Address all correspondence to: R. Manjunatha Kini, Protein Science Laboratory, Department of Biological Sciences, Faculty of Science, National University of Singapore, Singapore 117 543; E-Mail: dbskinim@nus.edu.sg

ABSTRACT

Hemextin AB complex from the venom of *Hemachatus haemachatus* is the first known natural anticoagulant that specifically inhibits the enzymatic activity of blood coagulation factor VIIa in the absence of factor Xa. It is also the only known heterotetrameric complex of two three-finger toxins (Banerjee, Y., Mizuguchi, J., Iwanaga, S., and Kini, R. M. (2005) *J Biol.Chem* 280, 42601-42611). Individually only hemextin A has mild anticoagulant activity, whereas hemextin B is inactive. However, hemextin B synergistically enhances the anticoagulant activity of hemextin A and their complex exhibits potent anticoagulant activity. In this study we characterized the nature of molecular interactions leading to the complex formation. Circular

dichroism studies indicate the stabilization of β -sheet in the complex. Hemextin AB complex has an increased apparent molecular diameter in both gas and liquid phase techniques. The complex formation is enthalpically favorable and entropically unfavorable with a negative change in the heat capacity. Thus, the anticoagulant complex shows reduced structural flexibility than individual subunits. Both electrostatic and hydrophobic interactions are important for the complexation; the former driving the process and the latter helping in the stabilization of the tetramer. The tetramer dissociates into dimers and monomers with the increase in the ionic strength of the solution and also with increase in the glycerol concentration in the buffer. The two dimers formed under each of these conditions display distinct differences in their apparent molecular diameters and anticoagulant properties. Based on these results, we have proposed a model for this unique anticoagulant complex.

Keywords: Protein-protein interaction, snake venom, anticoagulant, isothermal titration calorimetry, GEMMA, circular dichroism.

INTRODUCTION

Blood coagulation is a physiological response to vascular injury that results in the formation of hemostatic plug which prevents blood loss (Davie et al., 1991;Davie, 1995). The process is initiated by tissue factor (TF), a cellular receptor for the activated coagulation factor VIIa (FVIIa), which is exposed after vascular injury (Nemerson, 1988). FVIIa bound to TF activates factor X (FX) and factor IX. Activated factor X (FXa) converts small amounts of prothrombin to thrombin (Yegneswaran et al., 2003). Thrombin in turn amplifies the coagulation cascade by activating the platelets (Kumar et al., 1995) and factors V (Myles et al., 2001) and VIII (Saenko et al., 1998;Curtis et al., 1994). Coagulation is propagated when factor IXa binds to factor VIIIa to form intrinsic tenase, a complex that efficiently activates FX. FXa then binds to factor Va to form prothrombinase, thereby increasing the rate of FXa-mediated conversion of prothrombin to thrombin by >300,000-fold (Mann et al., 2003). The resultant burst of thrombin rapidly converts fibrinogen to fibrin. Fibrin monomers polymerize to form the fibrin mesh that is stabilized and cross-linked by transglutaminase factor XIIIa (Higgins et al., 1983;Lewis et al., 1987). Thus the initial formation of TF-FVIIa complex is crucial for the clot initiation and is considered an ideal target for the treatment of thromboembolic disorders. Drugs that target this complex are potent inhibitors of coagulation and thus are highly sought after. Though, naturally occurring inhibitors of FVIIa have been identified, they are not specific. For example, dysinosin A isolated from the sponge family Dysideidae inhibits FVIIa with a K_i of 108 nM. However it also an inhibitor of thrombin (Hanessian et al., 2002;Carroll et al., 2002). Until recently only two natural anticoagulants targeting specifically the TF-FVIIa complex has been identified. They are tissue factor pathway inhibitor (TFPI) (Lindhout et al., 1995;Salemink et al., 1999) and nematode anticoagulant peptide (NAPc2) (Moons et al., 2003;Lee and Vlasuk, 2003). TFPI is a 42-kDa plasma glycoprotein consisting of three tandem Kunitz-type domains. The first and second domains inhibit TF-FVIIa and FXa, respectively. The third Kunitz domain and the C-terminal basic region of the molecule have heparin-binding sites. The anticoagulant action of TFPI is a two-stage process. The second Kunitz domain binds first to a molecule of FXa and deactivates it. The first domain then rapidly binds to an adjacent TF-FVIIa complex, preventing further

activation of FX (Baugh et al., 1998; Broze, Jr. and Miletich, 1987; Sanders et al., 1985). On the other hand, NAPc2 is an 8-kDa short polypeptide. It first binds to FXa or zymogen FX to form a binary complex prior to its interaction and inhibition of membrane-bound TF-FVIIa (Buddai et al., 2002). Therefore, despite the structural differences, both inhibitors form a quaternary complex with TF-FVIIa-FXa. Further, in both the complexes the active site of FVIIa is occupied by the respective inhibitors and is not accessible.

Snake venoms are veritable gold mines of anticoagulant proteins (Kini, 2006). Recently, we isolated and characterized a novel anticoagulant protein complex (hemextin AB complex) from the venom of elapid snake *Hemachatus haemachatus* (African ringhals cobra) (Banerjee et al., 2005a; Banerjee et al., 2005b). Hemextin AB complex specifically and non-competitively inhibits the TF-FVIIa complex with a K_i of 25 nM. Further, it inhibits FVIIa in the absence of TF and FX. Thus, unlike TFPI and NAPc2, this unique complex neither requires FX scaffold nor does it bind to the active site of FVIIa (Banerjee et al., 2005a).

Structurally, hemextin AB complex consists of two proteins – hemextin A and hemextin B both of which belong to the three-finger toxin family of snake venom proteins. Individually, only hemextin A exhibits a mild anticoagulant activity, whereas hemextin B is inactive. However, hemextin B synergistically enhances the anticoagulant activity of hemextin A and their complex has potent anticoagulant activity. Thus, the formation of this unique synergistic complex of three-finger toxins is important for its ability to inhibit clot initiation (Banerjee et al., 2005a). There are only a few non-covalent protein complexes in snake venoms that do not contain phospholipase A₂ as an integral part, such as rhodocetin (Wang et al., 1999; Paaventhana et al., 2005) and pseutarin C (Rao and Kini, 2002). Hemextin AB complex is the only known snake venom protein complex formed by the interaction between two three-finger toxins and is the only known heterotetrameric complex of three-finger toxins.

Since hemextin AB complex is both structurally and functionally unique, we have investigated the molecular interactions involved in the formation of this novel complex. In particular we have examined the role of electrostatic and hydrophobic interactions in the formation of tetrameric anticoagulant complex. Hemextin AB complex has identical molecular diameter in both gas and solution phases. Isothermal titration calorimetry (ITC) studies reveal that the complex formation is entropically unfavored, which indicates the reduced structural flexibility of the complex. Hemextin AB assembly is an enthalpically driven process with some conformational changes accompanying the complexation. The tetrameric complex behaves differently in buffers of higher ionic strength. It is also sensitive to the presence of glycerol in the buffer solution. Thus, a complex interplay of electrostatic and hydrophobic interactions drives the formation and stabilization of this novel anticoagulant protein complex. Based on our observations, we propose a model for the assembly of hemextin AB complex.

MATERIALS AND METHODS

Purification of hemextins A and B – Hemextin A and hemextin B were purified using the methods described earlier (Banerjee et al., 2005a). Briefly, *H. haemachatus* crude venom (100 mg in 1 ml distilled water) was applied to a Superdex 30 gel filtration column (1.6 × 60 cm) equilibrated with 50 mM Tris-HCl buffer (pH 7.4) and eluted using the same buffer, using an ÄKTA Purifier system (Amersham Biosciences, Uppsala, Sweden). Fractions containing potent anticoagulant activity were pooled and sub-fractionated on a Uno S-6 (Bio-Rad, Hercules, CA, USA; column volume, 6 ml) cation-exchange column. The peaks containing hemextin A and

hemexin B were further purified using RP-HPLC on a Jupiter C18 (1× 25 cm) column. Both proteins were found to be homogeneous with molecular masses of 6835.00 ± 0.52 and 6792.56 ± 0.32 Daltons respectively, as determined by electrospray ionization mass spectrometry (ESI-MS) (Banerjee et al., 2005a).

Circular dichroism (CD) spectroscopic studies – Far UV CD spectra (260-190 nm) were recorded using a Jasco J-810 spectropolarimeter (Jasco Corporation, Tokyo, Japan). All measurements were carried out at room temperature (25 °C) using 0.1 cm pathlength stoppered cuvettes. The instrument optics was flushed with 30 l/min of nitrogen gas. The spectra were recorded using a scan speed of 50 nm/min, resolution 0.2 nm, and band width 2 nm. For each spectrum, a total of six scans were recorded, averaged and baseline subtracted. The conformation of hemexin A and hemexin B at different concentrations were monitored in 50 mM Tris-HCl buffer (pH 7.4). To study the complex formation, titration experiments were carried out by keeping the concentration of hemexin A constant at 0.5 mM, and varying the concentration of hemexin B.

Determination of molecular diameters – The apparent molecular diameters of the hemexin AB complex and the individual hemexins were determined in both the gas and solution phases using Gas Phase Electrophoretic Mobility Macromolecule Analyzer (GEMMA) and dynamic light scattering (DLS) respectively.

(A) GEMMA – The molecular diameters in the gas phase were determined with GEMMA (Kaufman, 1995;Knutson and Whitby, 1975) using a nano-differential mobility analyzer, model 3980 with a standard condensation particle counter type 3025 (TSI, St Paul, MN, USA). The instrument was operated in the ‘cone jet’ mode with an operating voltage between 2.5 and 3.0 kV, resulting in currents from 200 to 300 nA. Filtered ambient air at 2 l/min and a concentric sheath gas flow of filtered CO₂ at 0.1 l/min was used to stabilize the electrospray against corona discharge. Sample solutions of hemexin A (4 ng/ml) and hemexin B (4 ng/ml) were prepared in 20 mM ammonium acetate (pH 7.4) immediately prior to the experiment. Hemexin AB complex (4.5 ng/ml) was reconstituted in the above buffer and was incubated at 37 °C for 10 min. Another three-finger protein, toxin C isolated and purified from the same venom was used as a control in the GEMMA experiments. The samples were infused into the electrospray chamber with an inlet flow rate of 100 nl/min. Twenty scans over the whole electrophoretic mobility (EM) diameter range (0 to 25 nm) were recorded and averaged to obtain a GEMMA spectrum. Data presentation was done without the application of any smoothing algorithm.

(B) DLS – The complex formation studies with DLS were carried out at 25 °C using a BI200SM instrument (Brookhaven Instruments Corporation, Holstville, NY, USA). A vertically polarized argon ion laser (514.2 nm, 75 mW; NEC model GLG-3112) was used as the light source. Sample solutions of hemexin A (4 mM), hemexin B (4.1 mM) and hemexin AB complex (4.6 mM) in 50 mM Tris-HCl buffer (pH 7.4) were prepared immediately prior to the experiment. The hydrodynamic diameter for the hemexin AB complex and the individual hemexins were recorded at 25 °C in solutions of different ionic strengths and at different glycerol concentrations. The ionic strengths were varied by the addition of NaCl. From the measured translational diffusion coefficient (D_T), the hydrodynamic radius (R_H) can be calculated using the Stokes-Einstein relation:

$$D_T = k_B T / 6\pi\eta R_H \dots \dots \dots (Eq. 1),$$

where, k_B is the Boltzmann constant, T is the temperature in Kelvin and η is the viscosity of the solvent. The intensity-intensity time correlation functions were obtained with a BI-9000 digital correlator. The particle size and size distribution were obtained by analyzing the field correlation function $|g^{(1)}(\tau)|$ using constrained regularized CONTIN method (Provencher, 1976).

Thermodynamics of hemextin AB complex formation – ITC experiments were performed using a Microcal VP-ITC calorimeter (Microcal LLC, Northampton, MA) to study the thermodynamics of the formation of hemextin AB complex. Unless otherwise noted, all experiments were performed in 50 mM Tris-HCl buffer (pH 7.4). Both the proteins were dissolved in the same buffers, filtered and degassed prior to titration. Hemextin A (0.1 mM) was kept in the sample cell and hemextin B (1 mM) was loaded into the syringe. The syringe stirring speed was set to 300 rpm. Data were collected in high feedback mode, with a filter period of 3 s. For each experiment, a control titration was performed by injecting hemextin B into the appropriate buffer. Finally, the control data were subtracted from the raw data to obtain an isotherm corrected for heats of dilution. The first injections presented defects in the baseline and these data points were not included in the fitting process. The calorimetric data were processed and fitted to the single set of identical sites model using Microcal Origin (Version 7.0) data analysis software supplied with the instrument. The expression for the heat released per injection, $\Delta Q_{(i)}$, is given by

$$\Delta Q_{(i)} = Q_{(i)} + dV_i / 2V_0 [Q(i) + Q(i-1)] - Q(i-1) \dots \dots \dots (Eq. 2)$$

where $Q_{(i)}$ is the total heat content, dV_i is the volume injected at the i th injection, and V_0 is the cell volume. The total heat content Q of the solution (determined relative to zero for the unliganded species) contained in the active cell volume, V_0 , was calculated according to Equation 3, where K_A is the binding affinity constant, n is the number of sites, ΔH is the enthalpy of ligand binding, M_t and X_t is the bulk concentration of macromolecule and ligand, respectively, for the binding $X + M \leftrightarrow XM$

$$Q = \frac{nM_t \Delta H V_0}{2} \left[1 + \frac{X_t}{nM_t} + \frac{1}{nK_A M_t} - \sqrt{\left(1 + \frac{X_t}{nM_t} + \frac{1}{nK_A M_t} \right)^2 - \frac{4X_t}{nM_t}} \right] \dots \dots \dots (Eq. 3)$$

The change in heat (ΔQ) measured between the completions of two consecutive injections is corrected for dilution of the protein and ligand in the cell according to standard Marquardt method (Levenberg, 1944; Marquardt, 1963). The free energy change (ΔG) during the interaction was calculated using the relationship: ($\Delta G = \Delta H - T\Delta S = -RT \ln K_a$). All the experiments were performed at 37 °C unless otherwise indicated.

The role of *electrostatic interactions* in the complex formation was evaluated by performing ITC experiments in 50 mM Tris-HCl buffer of various ionic strengths. The ionic strengths of the buffers were altered by adding sodium chloride (NaCl) (35 mM to 150 mM). To study the role of *hydrophobic interactions* in the complex formation, experiments were performed in 50 mM Tris-HCl buffer (pH 7.4) containing various concentrations of glycerol (125 mM to 250 mM).

Size-exclusion chromatography (SEC) studies – All SEC experiments were carried out at room temperature on a pre-packed Superdex 75 gel filtration column (1.6 × 60 cm) using a ÄKTA Purifier system (Amersham Biosciences, Uppsala, Sweden). The column was eluted with 50 mM

Tris-HCl buffer (pH 7.4) or the specified elution buffer, at a flow rate of 1 ml/min. The sample volume applied to the column was 4 ml. The column was calibrated using ovomucoid (28 kDa) ribonuclease (15.6 kDa), cytochrome C (12 kDa), apoprotinin (7 kDa) and pelovaterin (4 kDa) (Lakshminarayanan et al., 2005) as molecular weight markers. The void volume was determined by running Blue Dextran. The column was equilibrated with at least two bed volumes of the elution buffer prior to each run. *Electrostatic contributions* in the hemextin AB complex formation were studied by monitoring its elution in 50 mM Tris-HCl buffer (pH 7.4) with different concentrations of NaCl (75 mM and 150 mM). *Hydrophobic contributions* for the complex formation were determined by recording the elution of hemextin AB complex in 50 mM Tris-HCl buffer (pH 7.4) with different concentrations of glycerol (125 mM and 250 mM). In both the studies, the column was first equilibrated with the desired buffer prior to the application of the reconstituted hemextin AB complex in the respective buffer to the column. The protein elution was monitored by recording absorbance at 280 nm.

Anticoagulant activity – The anticoagulant activity of individual hemextins and hemextin AB complex were determined using prothrombin time clotting assay (Quick AJ., 1935). The anticoagulant activity of a specific concentration of hemextin A (4.4 μ M), hemextin B (4.4 μ M) and hemextin AB complex (0.22 μ M) was monitored in 50 mM Tris-HCl (pH 7.4) containing different concentrations of NaCl (35 mM to 150 mM for studying the role of *electrostatic interactions*) and glycerol (125 mM to 250 mM for studying the role of *hydrophobic interactions*). The concentrations of hemextin A and hemextin AB complex were chosen in a way such that in the absence of salt/glycerol the recorded clotting times are similar. Control experiments were performed without the addition of the anticoagulant proteins to evaluate the effect of salt and glycerol on clotting.

1D-NMR spectroscopy – One-dimensional proton NMR experiments were carried out using Bruker 700 MHz spectrometer, equipped with a modern cryo-probe, and electronic variable temperature unit. The spectra were acquired using Topspin software (Bruker) interfaced to the spectrometer. Hemextin A (0.5 mM) and hemextin B (0.5 mM) were prepared in 50 mM Tris-HCl buffer (pH 7) and transferred to a 5 mm diameter Willmad NMR tube. All deuterated solvents were purchased from Aldrich Laboratories with 99.9% isotopic purity. The spectral width was set to 11,202 Hz for all NMR experiments. The huge resonance due to the water protons was suppressed by the WATERGATE pulse sequence (Piotto et al., 1992). Typically, 512 scans were averaged for each FID before apodization and then performing the Fourier transformation. ^1H chemical shifts were referenced to a sodium 2,2-dimethyl-2-silapentane-5-sulfonate solution (DSS).

RESULTS AND DISCUSSION

Conformational changes during the complex formation – It has been shown previously that hemextin A and hemextin B interact with each other and form a 1:1 heterotetrameric complex and this complex formation is important for its ability to inhibit FVIIa and clot initiation (Banerjee et al., 2005a). To study the conformational changes associated with the hemextin AB complex formation we used far UV-CD. First, we recorded the CD spectra of individual hemextins A and B (Figure 1, A and B). Their CD spectra display negative minima at 217 nm and positive maxima at 196 nm, which are due to the n to π^* transition and the π to π^* transition

of the amide chromophore, respectively, typical of a β -sheet structure (Figure 1, A and B). Next, a titration CD experiment was performed in order to study the complex formation between the two proteins. In this experiment, the concentration of hemextin A was kept constant at 0.5 mM and the conformational changes in hemextin A in the presence of various concentrations of hemextin B were recorded. The shape of the CD spectrum upon addition of hemextin B to hemextin A did not change significantly (Figure 1C). However, the CD intensity at 217 nm increases with the incremental addition of hemextin B and reaches maximum at the 1:1 molar ratio suggesting increase in β -sheet content and stoichiometric binding of hemextin B to hemextin A respectively (See supporting information- Figure S1A). The difference spectrum obtained by subtracting the CD spectrum of 1:1 complex from the sum of the CD spectra of hemextin A and hemextin B indicates the conservation of β -sheet structure in the complex, suggesting possible folding upon complex formation. (See supporting information- Figure S1B).

Changes in molecular diameters during the complex formation – The diameter of the individual hemextins and hemextin AB complex were determined in both gas and solution phases. In the gas phase analyses using GEMMA, hemextin A and hemextin B showed the apparent molecular diameters of 10.20 ± 0.38 nm and 8.82 ± 0.42 nm, respectively (Figure 2). Hemextin AB complex exhibited a larger diameter of 16.30 ± 0.43 nm. To further confirm on the GEMMA results, we examined the effect of toxin C, another three-finger toxin isolated from the venom of *H. haemachatus*, on the molecular diameters of hemextins A and B, to determine the specificity of interaction. Toxin C did not affect the anticoagulant activity of hemextin A in prothrombin time clotting assay (data not shown) and did not form a complex with hemextin A. At equimolar concentration of toxin C, the molecular diameter of hemextin A or hemextin B remains unaffected (Figure 2). The solution phase studies with DLS also confirmed the increase in molecular diameter associated with the complex formation. Single scattering populations (unimodal distribution) for hemextin A, hemextin B and hemextin AB complex were observed in DLS suggesting the homogeneity of the sample preparations with hydrodynamic diameters of 10.3 nm, 9.9 nm and 16.8 nm, respectively (Figure 3A). The narrow size distribution of a single monodisperse species for 1:1 mixture of hemextin A and hemextin B suggests the formation of a well-defined complex. It is important to note that the tetrameric hemextin AB complex and individual hemextins exhibited comparable molecular diameters in both gas and solution phases. The apparent molecular dimensions are significantly larger than the theoretical diameter estimated for a native protein and much smaller than the estimated length of the proteins in completely “extended conformation” (Wilkins et al., 1999; Lu et al., 1998). Such an anomaly could be due to the non-globular conformation of the proteins (Longhi et al., 2003). The molecular diameter of hemextin AB complex is, however, much smaller compared to the estimated size of a tetramer indicating that the four monomers are compactly packed.

Thermodynamics of the hemextin AB complex formation — ITC permits the study of macromolecular interactions in solution and is the only technique that can resolve the enthalpic and entropic components of binding affinity (Perozzo et al., 2004; Velazquez-Campoy et al., 2004; Weber and Salemme, 2003). It was used to study the thermodynamics of hemextin AB complex formation. Each injection gave rise to negative (exothermic) heat of reaction (Figure 4). The binding isotherm fits to a single set of binding sites model, suggesting an equimolar binding between hemextin A and hemextin B. The interaction between them is thermodynamically

allowed (as indicated by negative ΔG) (Table 1). A favorable negative ΔH but unfavorable negative ΔS changes indicate that the complex formation is enthalpically driven and, van der Waals interactions and hydrogen bonds may play an important role in the complex formation (Katragadda et al., 2004). Also, the formation of a less dynamic complex is entropically disfavored, as has been observed in the studies pertaining to the dimerization of insulin (Tidor and Karplus, 1994). Thus the recorded negative entropic change (ΔS) indicates the formation of a less flexible or less disordered hemextin AB complex. The binding constant (K_A) for the formation of hemextin AB complex was $2.23 \times 10^6 \text{ M}^{-1}$ and it falls within the K_A values for protein-protein interactions in biologically relevant processes that range from 10^4 to 10^{16} M^{-1} (Stites, 1997).

The effect of temperature on the hemextin AB complex formation — To further understand energetics of the complex formation, complete temperature profile of the thermodynamic parameters associated with the binding of hemextin A to hemextin B was studied over the temperature range of 25-45 °C. The temperature dependence of ΔH is shown in Figure 5A and Table 1. The temperature dependence of ΔH over a narrow temperature range is given by the equation:

$$\Delta H = \Delta H_0 + \Delta C_p(T-T_0) \dots \dots \dots (Eq. 4)$$

where, ΔH_0 is the binding enthalpy at an arbitrary reference temperature and ΔC_p is the heat capacity change of binding. The ΔC_p obtained from the slope ($\Delta C_p = \delta \Delta H / \delta T$) (Figure 5A), is $-163 \text{ cal/K}^{-1}\text{mol}^{-1}$. Negative ΔC_p indicates a reduction in the nonpolar solvent-accessible surface area, as explained by the following equation (Murphy and Freire, 1992),

$$\Delta C_p = 0.45(\Delta ASA_{nonpol}) - 0.26 (\Delta ASA_{pol}) \text{ cal /molK} \dots \dots \dots (Eq. 5)$$

where, ΔASA_{pol} and ΔASA_{nonpol} are the change in the polar- and non-polar-accessible surface areas, respectively. Thus, hemextin AB complex formation is associated with the burial of hydrophobic surface area.

Figure 5B shows the plot of ΔG and ΔH as a function of $T\Delta S$. It is clear that the ΔG of binding remained temperature independent and is a result of linear dependence of ΔH on $T\Delta S$. This strongly suggests the enthalpy-entropy compensation for the binding of hemextin A to hemextin B. This phenomenon is a universal feature for protein-peptide interactions, where weak molecular interactions undergo constant rearrangements to realize a lower free energy of binding (Cooper, 1999; Dunitz, 1995; Katragadda et al., 2004; Lumry, 2003). The co-relation between entropy and enthalpy for a range of interacting protein-protein systems was determined ($r^2 = 0.956$). The data for hemextin AB complex falls well along this correlation line (See supporting information- Figure S2).

The negative ΔC_p indicates the net thermodynamic driving force for the association to shift from entropic to enthalpic with increasing temperature. At the intersection point of both lines $\Delta G = \Delta H = -8.4 \text{ kcal.mol}^{-1}$ (Figure 5B), which corresponds to a temperature T_s (Temperature at which the contribution from entropy is zero (Spolar and Record, Jr., 1994; von Hippel, 1994). At T_s the contribution from entropy changes from favorable to unfavorable. From Figure 5A, $\Delta H = -8.4 \text{ kcal.mol}^{-1}$ is connected with a T_s of 16 °C (289 °K).

The negative ΔC_p for the hemextin AB complex formation further suggests that the observed entropy change upon binding must include significant contribution from the hydrophobic effect in the physiological temperature range. Therefore, for protein-protein/ligand interaction(s) the net entropy of association is given by the equation:

$$\Delta S_{assoc} = \Delta S_{HE} + \Delta S_{rt} + \Delta S_{other} \dots\dots\dots (Eq. 6)$$

where, ΔS_{HE} , ΔS_{rt} , and ΔS_{other} are the entropy changes due to hydrophobic effect, reduction of rotational and translational degree of freedom, and from other sources, respectively.

At T_s , the overall entropy of association is zero and the above equation becomes:

$$\Delta S_{assoc} = \Delta S_{HE}(T_s) + \Delta S_{rt} + \Delta S_{other} = 0 \dots\dots\dots (Eq. 7)$$

In the absence of crystallographic data, the $\Delta S_{HE}(T_s)$ was estimated from the equation,

$$\Delta S_{HE}(T_s) = 1.35 \Delta C_p \ln(T_s/386) \dots\dots\dots (Eq. 8)$$

and found to be $64 \text{ cal deg}^{-1} \text{ mol}^{-1}$. It has been shown that protein-protein interaction ΔS_{rt} is nearly equal to $-50 \text{ cal deg}^{-1} \text{ mol}^{-1}$ (Finkelstein and Janin, 1989; Janin and Chothia, 1978). Thus the ΔS_{other} is calculated to be $-14 \text{ cal deg}^{-1} \text{ mol}^{-1}$. Because of experimental uncertainties in the heat capacity change and the entropy of complex formation, as well as in the value of the rotational-translational entropy term, the analysis of coupled folding is typically not suitable for distinguishing small extents of folding from the rigid body case. However, from the non-zero value of ΔS_{other} it can be concluded that there is no evidence for large-scale coupled folding, during the formation of hemextin AB complex. Again, $\Psi = \Delta S_{other} / -5.6 \text{ cal deg}^{-1} \text{ mol}^{-1}$, where Ψ designates the number amino acid residues involved in the folding transition (Hilpert et al., 2003). Therefore, approximately three residues are involved in the folding transition. Also, From Figure 5B the enthalpic counterpart of T_s , namely T_H , the temperature at which the enthalpic contribution to the Gibbs free energy of binding changes from favorable to unfavorable is calculated to be $244 \text{ }^\circ\text{K}$. Therefore, below $-29 \text{ }^\circ\text{C}$ the binding process is entropically driven and only in the interval between T_s and T_H (i.e., between $-29 \text{ }^\circ\text{C}$ and $16 \text{ }^\circ\text{C}$), both the entropic and enthalpic part of the Gibbs free energy of binding are favorable.

Oligomerization states of the anticoagulant complex and individual hemextins – Hemextin AB complex exists as a tetramer and the complex formation is pivotal for its potent anticoagulant activity. Also as determined in prothrombin time and kinetic assays the stoichiometry of complex formation is 1:1 (Banerjee et al., 2005a). We evaluated the role of both electrostatic and hydrophobic interactions in complex formation.

(A) *Electrostatic interactions in hemextin AB complex formation* – Firstly, the binding constant for hemextin AB complex formation was determined by ITC in buffers of increasing ionic strength. The $\log K_A$ values for the complex formation decreased linearly with the increasing NaCl concentration (Figure 6A, Table 1), illustrating the participation of electrostatic interactions in complex formation. Secondly, the effect of buffer ionic strength on the assembly of hemextin AB complex was examined with the help of SEC. In the absence of salt, the

complex eluted as a tetramer and the individual hemextins as monomers (Figure 7A). In the presence of 75 mM NaCl the tetramer started dissociating into dimer (Figure 7B). With further increase in ionic strength of the buffer (NaCl 150 mM) the complex eluted mostly as a dimer and monomer(s). ESI-MS and HPLC analyses of the dimer peak indicated that it contains both hemextins A and B (data not shown). This observation again reconfirms the importance of electrostatic interactions in hemextin AB assembly. Interestingly, an additional protein peak eluted slower than the monomers indicating hemextin A and/or hemextin B was undergoing a conformational change in buffers of high ionic strength. Therefore, we monitored the elution profiles of individual hemextins in buffers of high ionic strength. Hemextin A at 75 mM NaCl concentration showed two peaks; a second protein peak eluted slower than the monomer (Figure 7B). With further increase in the ionic strength (NaCl 150 mM) hemextin A eluted mostly in the second peak. ESI-MS and HPLC analyses of this second peak show that it is structurally intact hemextin A (data not shown). Thus, the change in the elution profile of hemextin A in buffers of higher ionic strength hinted a conformational change in the protein, which was further confirmed by 1D NMR studies (see below). Increased ionic strength of buffer did not have any effect on the elution of hemextin B (Figure 7A and B).

We also determined the hydrodynamic diameters of hemextin AB complex and individual hemextins in buffer solutions of high ionic strength using DLS (Figure 3B). (As GEMMA works on the principle of nano-ESI, we did not determine the molecular diameters in buffers containing high salt using this technique.). At high salt concentrations, the hemextin AB complex exhibits a high polydispersity indicating the presence of different species. At 75 mM NaCl, there are three different populations. In addition to the monomer(s) and the tetramer, there is an additional population with an apparent molecular diameter of 12.4 nm. Based on our SEC results (Figure 7B), we suggest that the 12.4 nm species could be the dimeric hemextin AB complex. As expected, the population of 12.4 nm species increases when the concentration of NaCl is increased to 150 mM (Figure 3B). Thus DLS data also suggests the dissociation of the tetrameric complex to a dimer. As expected, polydispersity was also observed with hemextin A in buffers of high ionic strength (Figure 3B). An additional population of 11.57 nm sized particle, in addition to its native size of 10.4 nm is observed. Based on the SEC (Figure 7B) and 1D-NMR (see below), we suggest that the 11.57 nm species represents the conformationally altered form of hemextin A. No change in the hydrodynamic diameter of hemextin B was observed with the increase in buffer ionic strength (Figure 3B).

To understand the implications of the change in conformation of hemextin A and the breakdown of tetrameric complex, we monitored the anticoagulant activity of the complex and individual hemextins in buffers of high ionic strengths. Higher concentration of NaCl did not affect the anticoagulant activity of hemextin A (Figure 8A). Thus despite the change(s) in conformation (see below), hemextin A retains its anticoagulant activity. The anticoagulant activity of hemextin AB complex, in contrast, decreased with the increase in ionic strength up to 100 mM NaCl (Figure 8A). However, further increase in the salt concentration did not significantly affect the anticoagulant activity. At 150 mM NaCl the complex exists as a mixture of a dimer, monomer(s) and conformationally altered hemextin A as is evident from the SEC experiments (Figure 7B). Therefore, the remaining anticoagulant activity observed at 150 mM or higher NaCl concentration is due to the presence of monomeric hemextin A and not due to dimeric hemextin AB complex. Hence, it can be concluded that the dimer formed at high salt concentrations does not have any significant anticoagulant activity.

Thus, these studies in buffers of high ionic strength strongly suggest that electrostatic interactions play crucial role in the assembly of hemextin AB complex. As hemextin A undergoes conformational change(s) in the presence of salt (see below), the dissociation of tetramer in a buffer of high ionic strength may not only be due to the disruption electrostatic interaction but also due to conformational change(s) in hemextin A. Further, high salt concentration leads to the formation of a dimer which is functionally inert (in terms of lack of synergic increase in anticoagulant activity). Based on the obtained results, we hypothesize that the dimer assembled at 150 mM NaCl concentration is probably formed by the interplay of predominantly hydrophobic interactions. Therefore, successive experiments were carried out to evaluate the importance of hydrophobic interactions in the complex formation.

(B) Hydrophobic interactions in the hemextin AB complex formation – We carried out ITC experiments in buffers containing increasing concentrations of glycerol. Adsorption of glycerol to hydrophobic patches on the surface of proteins interferes in the hydrophobic interactions (Liu et al., 2004). A decrease in the association constant was observed with the increase in glycerol concentration (Figure 6B and Table 1), showing the importance of hydrophobic interactions in the complex formation. We monitored the elution of hemextin AB complex in buffers containing glycerol on a Superdex 75 column (Figure 7C). In buffers containing high glycerol concentration the tetramer dissociates into dimer and monomers. ESI-MS and HPLC analyses of the dimer peak indicate that it contains both hemextins A and B (data not shown). However, no additional peak corresponding to altered conformation of hemextin A was observed. The elution of individual hemextins remained unaltered in the presence of glycerol (Figure 7C). The breakdown of hemextin AB complex in the presence of glycerol was also observed in the DLS studies (Figure 3C). At 125 mM glycerol concentration, an additional population of 12.8 nm-sized species was observed in addition to the monomers and the tetrameric complex. Based on SEC studies, we propose that the 12.8 nm species is a dimer. The 12.8 nm species increases with the increase in glycerol concentration (Figure 3C). It is important to note that the apparent molecular diameter of this dimer is different from the dimer formed in buffers of high ionic strength (12.8 nm versus 12.4 nm; Figure 3B and 3C). (As GEMMA works on the principle of nano-ESI, we did not determine the molecular diameters in buffers containing glycerol using this technique.). No polydispersity was observed in the case of individual hemextins in the presence of glycerol (Figure 3C).

To further understand the implication of the breakdown of hemextin AB complex in glycerol, we monitored its anticoagulant activity and that of the individual hemextins in buffers containing different concentrations of glycerol. The anticoagulant activity of hemextin AB complex decreased with the increase in glycerol concentration (Figure 8B). At 125 mM glycerol concentration there is no decrease in the anticoagulant activity. However, at 250 mM glycerol concentration (at which hemextin AB complex exists as a mixture of dimer and monomers; Figure 7C) there is a decrease in the anticoagulant activity. But this activity is higher than that of the anticoagulant effect of hemextin A alone. Therefore, we conclude that the dimer observed at 250 mM glycerol concentration exhibits the anticoagulant activity higher than hemextin A alone but lower than that of the tetramer. In other words, dimer formed in the presence of glycerol is different from the dimer formed in salt; the former dimer exhibiting an increased anticoagulant activity compared to hemextin A alone, whereas the latter not doing so. Glycerol, however, did not affect the anticoagulant activity of individual hemextins (Figure 8B).

The dissociation of the tetramer into dimer and monomers in the presence of glycerol indicates the importance of hydrophobic interactions in the tetrameric complex formation. This role of hydrophobic interaction is further supported by the negative ΔC_p change observed during the formation of hemextin AB complex.

Our data strongly suggests that both electrostatic and hydrophobic interactions are important for the formation of tetrameric hemextin AB complex. To confirm that decrease in binding affinity between the monomers observed in salt and glycerol is not a solute osmotic effect, the K_A recorded in salt and glycerol was plotted against osmotic pressure (See supporting information-Figure S3). At similar osmolality of salt and glycerol decrease in binding affinity was more pronounced in salt than glycerol. This indicates that fall binding affinity is due to disruption of either electrostatic (for salt) or hydrophobic (for glycerol) interactions.

The effect of buffer conditions on the conformation of hemextins – Earlier studies using SEC (Figure 7B) and DLS (Figure 3) indicated that hemextin A undergoes conformational changes in the presence of salt. We conducted 1D-NMR analysis to study the conformation of hemextins A and B under different buffer conditions (Figure 9). In the presence of NaCl, there is a decrease in the number of H α resonance peaks between 4.8 ppm and 6 ppm in the case of hemextin A (Figure 9A). These chemical shifts contribute to the inter-residue NOE cross peaks between H α of different amino acid residues forming anti-parallel β -sheet structure typically observed in all three-finger toxins (Kini, 2002). Thus a decrease in the β -sheet content of hemextin A is observed in the presence of NaCl. In addition, there are several changes in the chemical shifts of side chains. A notable change is a highly shielded methyl peak which appears at the negative chemical shift value (-0.38 ppm) in the presence of salt. These observations strongly support conformational changes in hemextin A in the presence of NaCl. The overall dispersion of 1D proton NMR spectra of hemextin A in the presence of glycerol (deuterated) remains the same with the subtle changes in the amide region (Figure 9A). Thus, hemextin A did not undergo any significant conformational change upon the addition of glycerol. Similar studies with hemextin B show that it did not undergo any significant conformational changes in the presence of NaCl or glycerol (Figure 9B) since there is almost one to one match for the spectral frequencies.

Model for hemextin AB complex – Based on our studies we propose a model for the assembly of hemextin AB complex (Figure 10). Two molecules each of hemextin A and B form the tetrameric complex in Tris-HCl buffer (Figure 10A). The formation of this compact, synergistic complex is important for its anticoagulant activity. As illustrated earlier, hemextin AB dimer in high salt is different from the dimer formed in the presence of glycerol (Figure 10C). The former dimer has an apparent molecular diameter of 12.4 nm and lacks anticoagulant activity, whereas the latter has an apparent molecular diameter of 12.8 nm and exhibits slightly higher anticoagulant effects (Figure 10C). Thus, the breakdown of tetramer to dimer probably occurs in two different interfaces of interaction between hemextin A and B. One interface is sensitive to the ionic strength of its surroundings while the other is sensitive to glycerol (Figure 10C). Further, in the presence of salt, hemextin A undergoes conformational changes (Figure 10B) which may interfere in the tetramer formation. The dimer formed under high ionic conditions lacks the complete synergistic anticoagulant site (marked by a dotted semicircle in Figure 10C) and hence the resultant dimer is as active as hemextin A alone. (Figure 8). In contrast, hydrophobic interactions are predominant in the second interface. Therefore, glycerol dissociates

the tetramer into dimers. However, in this case only minor changes occur in the synergistic anticoagulant site of the complex (as shown in Figure 10C) and hence the resultant dimer is active (Figure 8). We propose that the tetramer formation most likely stabilizes the anticoagulant site of hemextin A. The binding between hemextin AB complex/ hemextin A and FVIIa has been characterized to validate the proposed model ².

CONCLUSION

Hemextin AB complex is the first synergistic anticoagulant complex isolated from snake venom comprising solely of two three-finger toxins – hemextin A and hemextin B (Banerjee et al., 2005a). The tetrameric complex formation is a pre-requisite for the synergistic inhibition of FVIIa. This complex formation is an enthalpically driven process. The complex exhibits identical apparent molecular diameters in gas and solution phases. Thermodynamics of hemextin AB complex formation indicates the absence of large scale coupled folding. Both electrostatic and hydrophobic interactions are important for the assembly of the tetramer. Based on our results we propose that the tetramer formation takes place by the participation of two interfaces. One of the interfaces is predominantly sensitive to the buffer ionic strength, indicating that electrostatic interactions are predominantly active in that interface. The other being sensitive to glycerol concentration of the solution indicates the participation of mostly hydrophobic interactions. The proposed model may help in a better understanding of the structure-function relationship of this novel anticoagulant complex.

ACKNOWLEDGEMENT

We thank Dr. Jörg Rösger (University of Texas Medical Branch) and Dr. Nina Sidorova and Dr. Donald Rau (NIH/NICHD/LPSB) for kindly providing us the osmolality conversion tables and also for helpful discussions, Dr. Prakash Kumar (Department of Biological Sciences, National University of Singapore) for his constructive comments and for making the manuscript more succinct and concise, Dr Peter Kuhn, Dr Jeremiah Joseph, Dr Subramanian Yegneswaran (The Scripps Research Institute) and Dr Thomas Record Jr. (University of Wisconsin-Madison) for the helpful discussion. We also thank Mrs. Gayathri Subramanian (Department of Chemistry, National University of Singapore) for her help in the DLS studies. YB thanks the National University of Singapore for his research scholarship.

REFERENCES

1. Banerjee, Y., J. Mizuguchi, S. Iwanaga, and R. M. Kini. 2005a. Hemextin AB complex, a unique anticoagulant protein complex from *Hemachatus haemachatus* (African Ringhals cobra) venom that inhibits clot initiation and factor VIIa activity. *J Biol. Chem* 280:42601-42611.
2. Banerjee, Y., J. Mizuguchi, S. Iwanaga, and R. M. Kini. 2005b. Hemextin AB complex--a snake venom anticoagulant protein complex that inhibits factor VIIa activity. *Pathophysiol. Haemost. Thromb.* 34:184-187.
3. Baugh, R. J., G. J. Broze, Jr., and S. Krishnaswamy. 1998. Regulation of extrinsic pathway factor Xa formation by tissue factor pathway inhibitor. *J. Biol. Chem.* 273:4378-4386.
4. Broze, G. J., Jr. and J. P. Miletich. 1987. Characterization of the inhibition of tissue factor in serum. *Blood* 69:150-155.
5. Buddai, S. K., L. Touloukhonova, P. W. Bergum, G. P. Vlasuk, and S. Krishnaswamy. 2002. Nematode anticoagulant protein c2 reveals a site on factor Xa that is important for macromolecular substrate binding to human prothrombinase. *J Biol. Chem* 277:26689-26698.
6. Carroll, A. R., G. K. Pierens, G. Fechner, L. P. De Almeida, A. Ngo, M. Simpson, E. Hyde, J. N. Hooper, S. L. Bostrom, D. Musil, and R. J. Quinn. 2002. Dysinosin A: a novel inhibitor of Factor VIIa and thrombin from a new genus and species of Australian sponge of the family Dysideidae. *J Am. Chem Soc.* 124:13340-13341.
7. Cooper, A. 1999. Thermodynamic analysis of biomolecular interactions. *Curr. Opin. Chem Biol.* 3:557-563.
8. Curtis, J. E., S. L. Helgerson, E. T. Parker, and P. Lollar. 1994. Isolation and characterization of thrombin-activated human factor VIII. *J Biol. Chem* 269:6246-6251.
9. Davie, E. W. 1995. Biochemical and molecular aspects of the coagulation cascade. *Thromb. Haemost.* 74:1-6.
10. Davie, E. W., K. Fujikawa, and W. Kisiel. 1991. The coagulation cascade: initiation, maintenance, and regulation. *Biochemistry* 30:10363-10370.
11. Dunitz, J. D. 1995. Win some, lose some: enthalpy-entropy compensation in weak intermolecular interactions. *Chem Biol.* 2:709-712.
12. Finkelstein, A. V. and J. Janin. 1989. The price of lost freedom: entropy of bimolecular complex formation. *Protein Eng* 3:1-3.

13. Hanessian,S., R.Margarita, A.Hall, S.Johnstone, M.Tremblay, and L.Parlanti. 2002. Total synthesis and structural confirmation of the marine natural product Dysinosin A: a novel inhibitor of thrombin and Factor VIIa. *J Am. Chem Soc.* 124:13342-13343.
14. Higgins,D.L., S.D.Lewis, and J.A.Shafer. 1983. Steady state kinetic parameters for the thrombin-catalyzed conversion of human fibrinogen to fibrin. *J Biol. Chem* 258:9276-9282.
15. Hilpert,K., H.Wessner, J.Schneider-Mergener, K.Welfle, R.Misselwitz, H.Welfle, A.C.Hocke, S.Hippenstiel, and W.Hohne. 2003. Design and characterization of a hybrid miniprotein that specifically inhibits porcine pancreatic elastase. *J Biol. Chem* 278:24986-24993.
16. Janin,J. and C.Chothia. 1978. Role of hydrophobicity in the binding of coenzymes. Appendix. Translational and rotational contribution to the free energy of dissociation. *Biochemistry* 17:2943-2948.
17. Katragadda,M., D.Morikis, and J.D.Lambris. 2004. Thermodynamic studies on the interaction of the third complement component and its inhibitor, compstatin. *J Biol. Chem* 279:54987-54995.
18. Kaufman,S.L. 1995. Analysis of Biomolecules using Electrospray and Nanoparticle Methods:The Gas-Phase Electrophoretic Mobility Molecular Analyzer (GEMMA). *J. Aerosol Sci.* 29:537-552.
19. Kini,R.M. 2002. Molecular moulds with multiple missions: functional sites in three-finger toxins. *Clin Exp Pharmacol. Physiol* 29:815-822.
20. Kini,R.M. 2006. Anticoagulant proteins from snake venoms: structure, function and mechanism. *Biochem. J* 397:377-387.
21. Knutson,E.O. and K.T.Whitby. 1975. Aerosol classification by electric mobility: apparatus, theory, and applications. *J. Aerosol Sci.* 6:451.
22. Kumar,R., S.Beguín, and H.C.Hemker. 1995. The effect of fibrin clots and clot-bound thrombin on the development of platelet procoagulant activity. *Thromb. Haemost.* 74:962-968.
23. Lakshminarayanan,R., E.O.Chi-Jin, X.J.Loh, R.M.Kini, and S.Valiyaveetil. 2005. Purification and characterization of a vaterite-inducing peptide, pelovaterin, from the eggshells of *Pelodiscus sinensis* (Chinese soft-shelled turtle). *Biomacromolecules.* 6:1429-1437.
24. Lee,A.Y. and G.P.Vlasuk. 2003. Recombinant nematode anticoagulant protein c2 and other inhibitors targeting blood coagulation factor VIIa/tissue factor. *J Intern. Med.* 254:313-321.
25. Levenberg,K. 1944. A Method for the Solution of Certain Problems in Least Squares. *Quart. Appl. Math.* 2:164-168.

26. Lewis,S.D., L.Lorand, J.W.Fenton, and J.A.Shafer. 1987. Catalytic competence of human alpha- and gamma-thrombin in the activation of fibrinogen and factor XIII. *Biochemistry* 26:7597-7603.
27. Lindhout,T., J.Franssen, and G.Willems. 1995. Kinetics of the inhibition of tissue factor-factor VIIa by tissue factor pathway inhibitor. *Thromb. Haemost.* 74:910-915.
28. Liu,W., D.Bratko, J.M.Prausnitz, and H.W.Blanch. 2004. Effect of alcohols on aqueous lysozyme-lysozyme interactions from static light-scattering measurements. *Biophys. Chem* 107:289-298.
29. Longhi,S., V.Receveur-Brechot, D.Karlin, K.Johansson, H.Darbon, D.Bhella, R.Yeo, S.Finet, and B.Canard. 2003. The C-terminal domain of the measles virus nucleoprotein is intrinsically disordered and folds upon binding to the C-terminal moiety of the phosphoprotein. *J Biol. Chem* 278:18638-18648.
30. Lu,H., B.Isralewitz, A.Krammer, V.Vogel, and K.Schulten. 1998. Unfolding of titin immunoglobulin domains by steered molecular dynamics simulation. *Biophys. J* 75:662-671.
31. Lumry,R. 2003. Uses of enthalpy-entropy compensation in protein research. *Biophys. Chem* 105:545-557.
32. Mann,K.G., S.Butenas, and K.Brummel. 2003. The dynamics of thrombin formation. *Arterioscler. Thromb. Vasc. Biol.* 23:17-25.
33. Marquardt,D. 1963. An Algorithm for Least-Squares Estimation of Nonlinear Parameters. *SIAM J. Appl. Math.* 11:431-441.
34. McNemar,C., M.E.Snow, W.T.Windsor, A.Prongay, P.Mui, R.Zhang, J.Durkin, H.V.Le, and P.C.Weber. 1997. Thermodynamic and structural analysis of phosphotyrosine polypeptide binding to Grb2-SH2. *Biochemistry* 36:10006-10014.
35. Moons,A.H., R.J.Peters, N.R.Bijsterveld, J.J.Piek, M.H.Prins, G.P.Vlasuk, W.E.Rote, and H.R.Buller. 2003. Recombinant nematode anticoagulant protein c2, an inhibitor of the tissue factor/factor VIIa complex, in patients undergoing elective coronary angioplasty. *J Am. Coll. Cardiol.* 41:2147-2153.
36. Murphy,K.P. and E.Freire. 1992. Thermodynamics of structural stability and cooperative folding behavior in proteins. *Adv. Protein Chem* 43:313-361.
37. Myles,T., T.H.Yun, S.W.Hall, and L.L.Leung. 2001. An extensive interaction interface between thrombin and factor V is required for factor V activation. *J Biol. Chem* 276:25143-25149.
38. Nemerson,Y. 1988. Tissue factor and hemostasis. *Blood* 71:1-8.

39. Paaventhana, P., C. Kong, J.S. Joseph, M.C. Chung, and P.R. Kolatkar. 2005. Structure of rhodocetin reveals noncovalently bound heterodimer interface. *Protein Sci* 14:169-175.
40. Perozzo, R., G. Folkers, and L. Scapozza. 2004. Thermodynamics of protein-ligand interactions: history, presence, and future aspects. *J Recept. Signal. Transduct. Res.* 24:1-52.
41. Piotto, M., V. Saudek, and V. Sklenar. 1992. Gradient-tailored excitation for single-quantum NMR spectroscopy of aqueous solutions. *J Biomol. NMR* 2:661-665.
42. Provencher, S.W. 1976. A Fourier method for the analysis of exponential decay curves. *Biophys. J* 16:27-41.
43. Quick A.J. 1935. The prothrombin time in haemophilia and in obstructive jaundice. *J. Biol. Chem.* 109:73-74.
44. Rao, V.S. and R.M. Kini. 2002. Pseutarin C, a prothrombin activator from *Pseudonaja textilis* venom: its structural and functional similarity to mammalian coagulation factor Xa-Va complex. *Thromb. Haemost.* 88:611-619.
45. Saenko, E.L., D. Scandella, A.V. Yakhyayev, and N.J. Greco. 1998. Activation of factor VIII by thrombin increases its affinity for binding to synthetic phospholipid membranes and activated platelets. *J Biol. Chem* 273:27918-27926.
46. Salemink, I., J. Franssen, G.M. Willems, H.C. Hemker, and T. Lindhout. 1999. Inhibition of tissue factor-factor VIIa-catalyzed factor X activation by factor Xa-tissue factor pathway inhibitor. A rotating disc study on the effect of phospholipid membrane composition. *J Biol. Chem* 274:28225-28232.
47. Sanders, N.L., S.P. Bajaj, A. Zivelin, and S.I. Rapaport. 1985. Inhibition of tissue factor/factor VIIa activity in plasma requires factor X and an additional plasma component. *Blood* 66:204-212.
48. Spolar, R.S. and M.T. Record, Jr. 1994. Coupling of local folding to site-specific binding of proteins to DNA. *Science* 263:777-784.
49. Stites, W.E. 1997. Protein-protein interactions: Interface Structure, Binding Thermodynamics, and Mutational Analysis. *Chem Rev* 97:1233-1250.
50. Tidor, B. and M. Karplus. 1994. The contribution of vibrational entropy to molecular association. The dimerization of insulin. *J Mol. Biol.* 238:405-414.
51. Velazquez-Campoy, A., S.A. Leavitt, and E. Freire. 2004. Characterization of protein-protein interactions by isothermal titration calorimetry. *Methods Mol. Biol.* 261:35-54.
52. von Hippel, P.H. 1994. Protein-DNA recognition: new perspectives and underlying themes. *Science* 263:769-770.

53. Wang,R., R.M.Kini, and M.C.Chung. 1999. Rhodocetin, a novel platelet aggregation inhibitor from the venom of *Calloselasma rhodostoma* (Malayan pit viper): synergistic and noncovalent interaction between its subunits. *Biochemistry* 38:7584-7593.
54. Weber,P.C. and F.R.Salemme. 2003. Applications of calorimetric methods to drug discovery and the study of protein interactions. *Curr. Opin. Struct. Biol.* 13:115-121.
55. Wilkins,D.K., S.B.Grimshaw, V.Receveur, C.M.Dobson, J.A.Jones, and L.J.Smith. 1999. Hydrodynamic radii of native and denatured proteins measured by pulse field gradient NMR techniques. *Biochemistry* 38:16424-16431.
56. Ye,H. and H.Wu. 2000. Thermodynamic characterization of the interaction between TRAF2 and tumor necrosis factor receptor peptides by isothermal titration calorimetry. *Proc. Natl. Acad. Sci U. S. A* 97:8961-8966.
57. Yegneswaran,S., R.M.Mesters, and J.H.Griffin. 2003. Identification of distinct sequences in human blood coagulation factor Xa and prothrombin essential for substrate and cofactor recognition in the prothrombinase complex. *J Biol. Chem* 278:33312-33318.

FOOTNOTE

1. This work was supported in part by the Biomedical Research Council, Agency for Science and Technology, Singapore. The costs of publication of this article were defrayed in part by the payment of page charges. This article must therefore be hereby marked "advertisement" in accordance with 18 U.S.C. Section 1734 solely to indicate this fact.
2. Yajnavalka Banerjee, Jun Mizuguchi, Egon Person, Robin Doley, Sadaaki Iwanaga and R. Manjunatha Kini manuscript under preparation.

Table 1.***Thermodynamic analysis of hemextin A-hemextin B interaction***

ITC experiments	$K_A \times 10^6 (M^{-1})$	ΔH (kcal/mole)	ΔS (cal/deg.mole)	ΔG (kcal/mole)
At different temperatures (°C)				
25	2.07	-9.92	-4.43	-8.6
37	2.23	-11.7	-8.645	-9
45	1.97	-13.12	-12.49	-9.15
At different salt concentrations				
35 mM NaCl	0.63	-10.5	-7.2	-8.2
75 mM NaCl	0.33	-9.32	-4.8	-7.8
100 mM NaCl	0.02	-7.31	-3.82	-6.12
150 mM NaCl	0.002	-5.01	-1.2	-4.6
At different glycerol concentrations				
125 mM glycerol	0.32	-10.8	-11.01	-7.6
175 mM glycerol	0.2	-10.5	-10.6	-7.2
250 mM glycerol	0.05	-9.4	-10	-6.4

Note: All ITC experiments in salt and glycerol were carried out at 37°C

FIGURE CAPTIONS

Figure 1: Conformational changes associated with the formation of hemextin complex. CD spectra of (A) hemextin A (0.5 mM) and (B) hemextin B (0.5 mM). (C) Conformational changes in hemextin A with increasing concentrations of hemextin B: — hemextin A 0.5 mM; — hemextin A 0.5 mM *plus* hemextin B 0.25 mM; — hemextin A 0.5 mM *plus* hemextin B 0.4 mM; — hemextin A 0.5 mM *plus* hemextin B 0.5 mM; — hemextin A 0.5 mM *plus* hemextin B 0.9 mM; *inset*, the observed change in the CD spectra around the 217 nm region.

Figure 2. Measurement of molecular diameter during the hemextin AB complex formation using GEMMA. The molecular diameters of the individual hemextins and the hemextin AB complex are calculated based on their electrophoretic mobility. The formation of hemextin AB complex leads to an increase in the molecular diameter. Addition of equimolar toxin C does not show any significant increase in the molecular diameters of hemextin A and hemextin B validating the obtained data.

Figure 3. Determination of hydrodynamic diameter using DLS. A. CONTIN analysis hemextin A, hemextin B and hemextin AB complex in 50 mM Tris-HCl buffer. Effect various concentrations of NaCl (B) and glycerol (C) on hemextin AB complex. The calculated hydrodynamic diameters for each molecular species are shown. (Note the dimer formed in glycerol has a different diameter than the one formed in salt)

Figure 4. Interaction studies between hemextin A and B using ITC. (A) Raw ITC data showing heat release upon injections of 1 M hemextin B into a 1.4-ml cell containing 0.1 mM of hemextin A; (B) Integration of the raw ITC data yields the heat/mol *versus* molar ratio. The best values of the fitting parameters are 1.04 for N , $2.23 \times 10^6 \text{ M}^{-1}$ for K_A and $-11.68 \text{ kcal.M}^{-1}$ for ΔH (Table 1).

Figure 5. Thermodynamics of hemextin A-hemextin B interaction. (A) Effect of temperature on the energetics of hemextin A-hemextin B interaction: enthalpy change (ΔH), change in entropy term ($T\Delta S$) and free energy change (ΔG). (B) Enthalpy-entropy compensation in complex formation. (Note: Point of intersection of lines corresponding to ΔH and ΔG corresponds to T_s)

Figure 6. Hemextin AB complex formation under different buffer conditions. (A) Dependence of K_A on the ionic strength of the buffer. The binding affinity decreases with the increase in buffer ionic strength indicating the importance of electrostatic interactions. (B) Dependence of K_A on the glycerol concentration. The binding affinity decreases with the increase in glycerol concentration indicating the importance of hydrophobic interactions.

Figure 7. SEC studies of Hemextin AB complex in different buffer conditions. A. Elution profiles of hemextin AB complex in Tris-HCl buffer. Effect various concentrations of NaCl (B) and glycerol (C) on hemextin AB complex. The tetrameric complex (peak denoted by 4) dissociates into dimer and monomer (peaks denoted by 2 and 1, respectively) with the increase in salt or glycerol. *Asterisk* denotes the peak containing conformationally altered hemextin A. (D) Calibration of the column using the following proteins as molecular weight markers – ovomucoid (28 kDa), ribonuclease (15.6 kDa), cytochrome C (12 kDa), apoprotinin (7 kDa) and

pelovaterin (4 kDa). The molecular weights of the tetramer, dimer and monomers were calculated from the calibration curve.

Figure 8. : Effect of buffer conditions on anticoagulant activity. Effect various concentrations of NaCl (A) and glycerol (B) on the anticoagulant activity of hemextin A (O), hemextin B (M), hemextin AB complex (▲). The anticoagulant activity of hemextin AB complex decreases with the increase in concentrations of NaCl and glycerol. The arrows indicate the concentrations of (A) NaCl and (B) glycerol where the anticoagulant complex exists mostly as a mixture of dimer and monomers (see text for details). (■) denotes the anticoagulant activity recorded in the absence of the proteins.

Figure 9: One-dimensional ^1H NMR studies. Spectrum of (A) hemextin A and hemextin B under different buffer conditions. *Note*, in the presence of salt hemextin A undergoes a conformational change. Also, the peaks are sharp through out the spectrum. In addition, all 1D ^1H NMR spectra also exhibited a wide range of chemical shift dispersions (amide region 7 to 10 ppm, $\text{H}\alpha$ region 3.8 to 6 ppm and methyl region -0.4 to 1.5 ppm) which is a characteristics of well folded proteins. Therefore, the observed structural change is not due to resonance broadening or aggregation (as no aggregation state was observed as mentioned) but it is only due to addition of NaCl to hemextin A.

Figure 10: A proposed model of hemextin AB complex. A. Schematic diagram depicting the formation of hemextin AB complex. Hemextins A and B, two structurally similar three-finger toxins, form a compact and rigid tetrameric complex with 1:1 stoichiometry (Banerjee et al., 2005a). B. Schematic diagram showing the effect of salt and glycerol on conformations of hemextins A and B. Hemextin A undergoes a conformational change in the presence of salt. C. Dissociation of the tetrameric hemextin AB complex in the presence of salt and glycerol. The dissociation probably occurs in two different planes. Thus the hemextin AB dimer in high salt is different from the dimer formed in the presence of glycerol. Two putative anticoagulant sites are shown with dotted semicircles (See text for details).

FIGURES

Figure 1

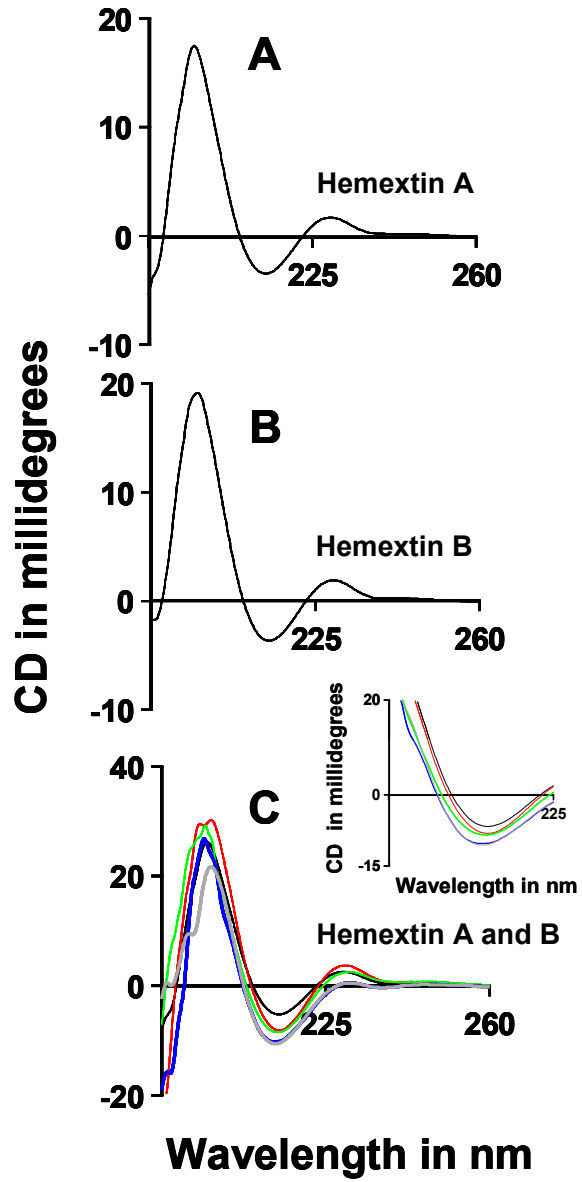


Figure 2

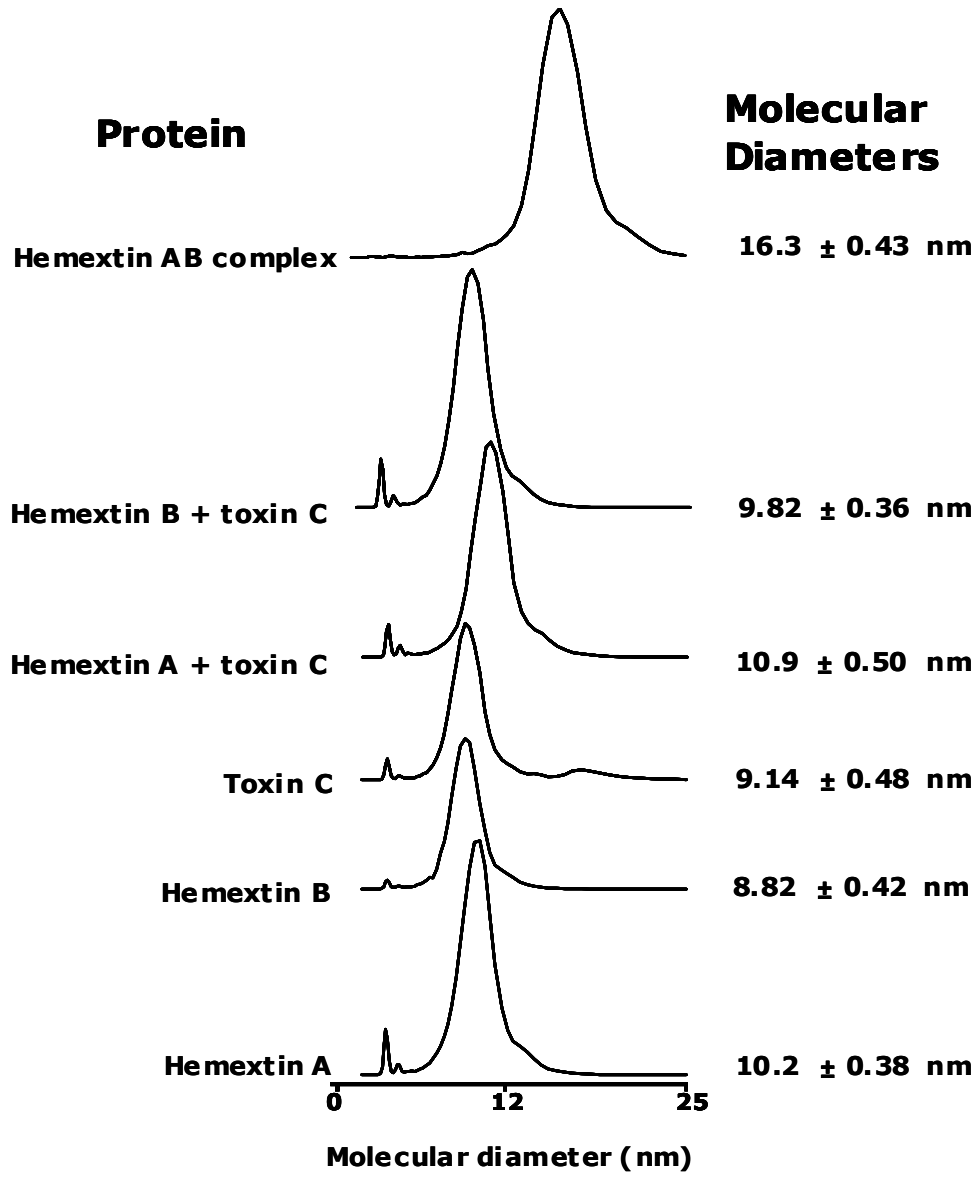


Figure 3

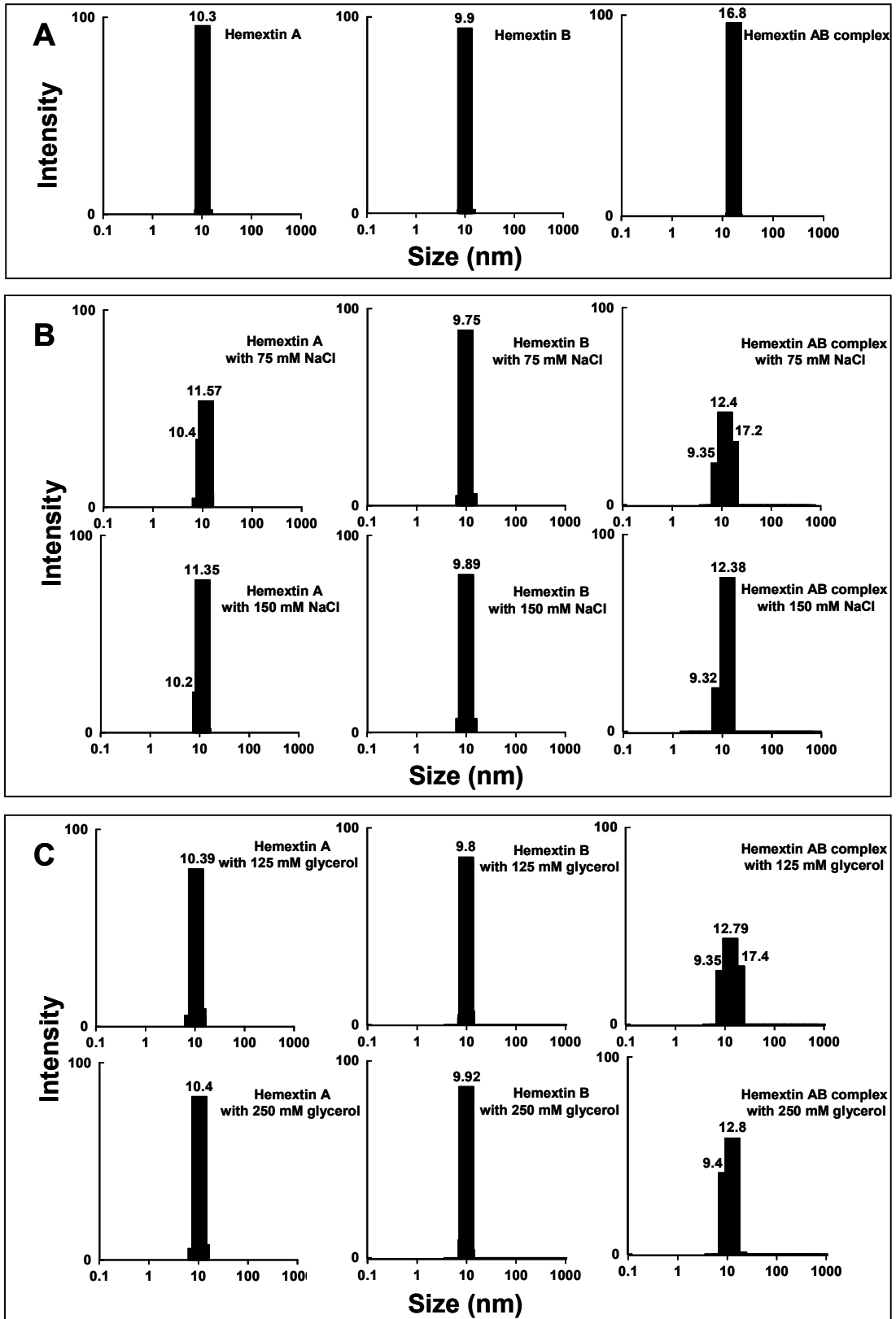


Figure 4

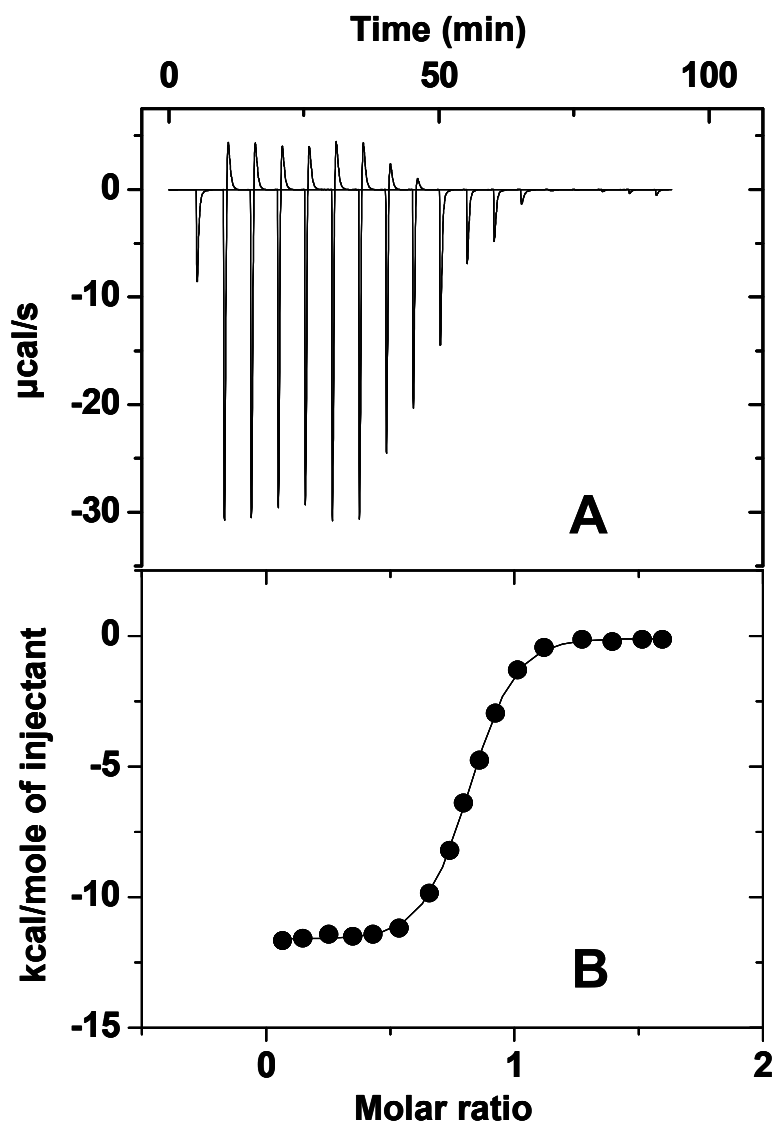


Figure 5

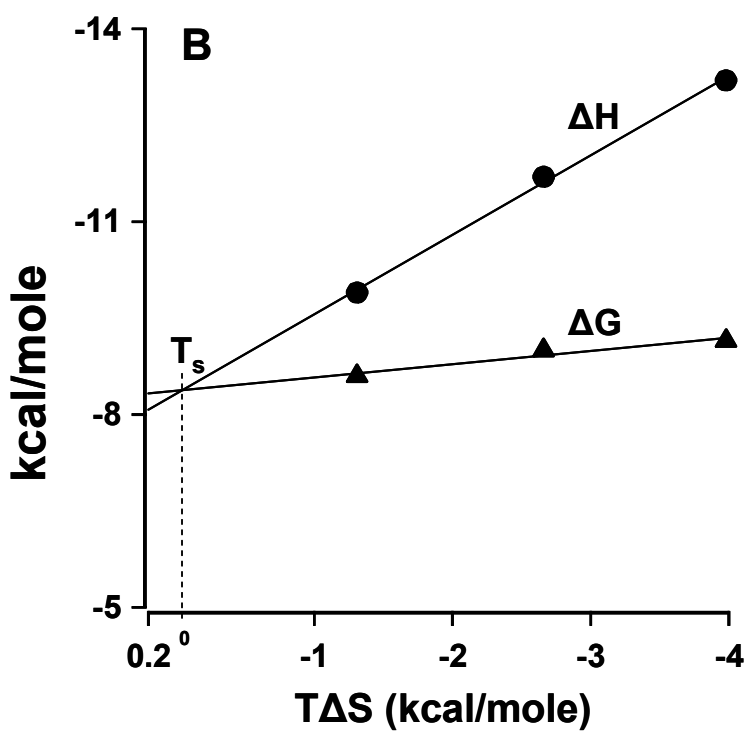
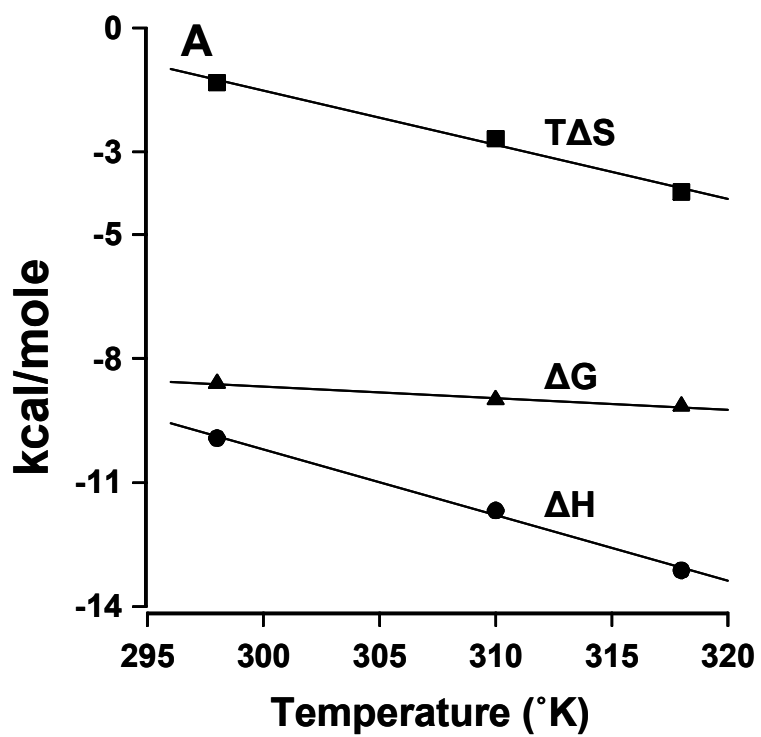


Figure 6

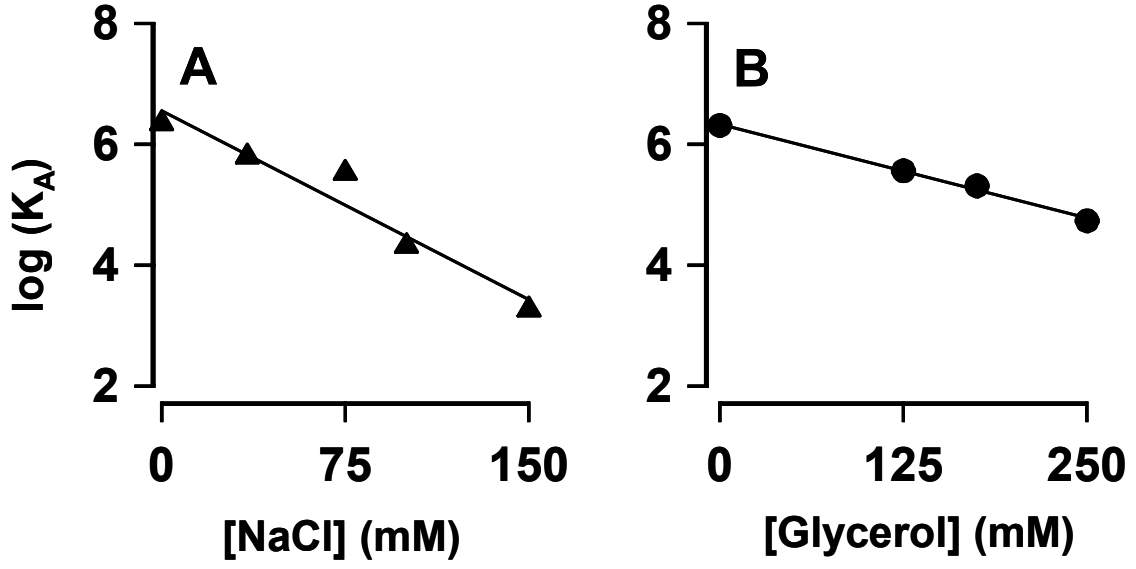


Figure 7

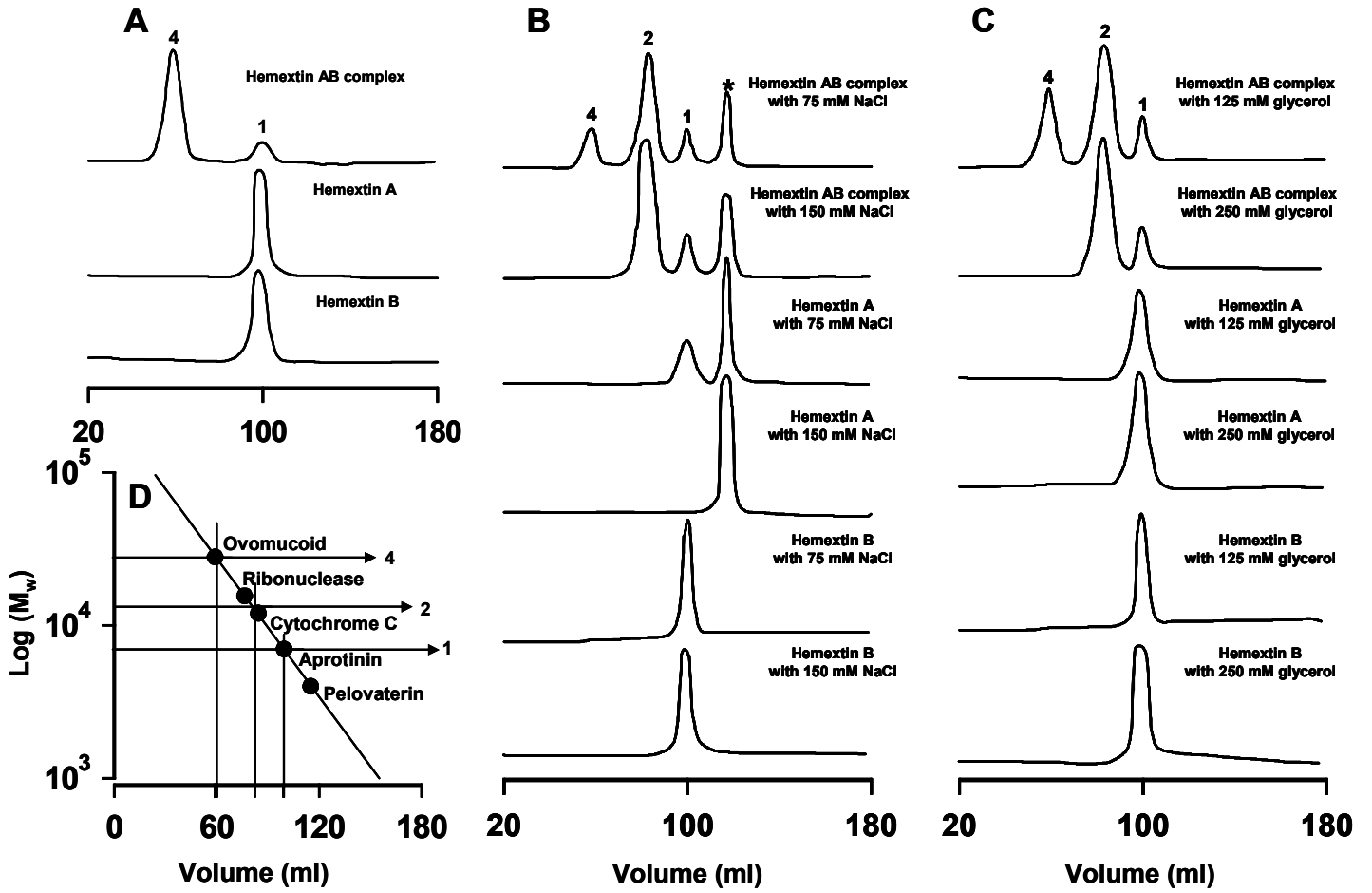


Figure 8

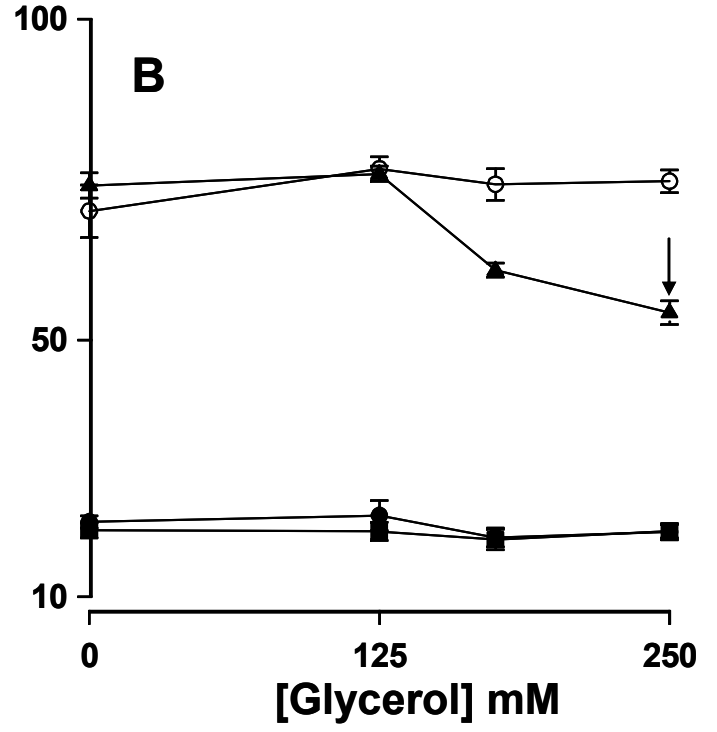
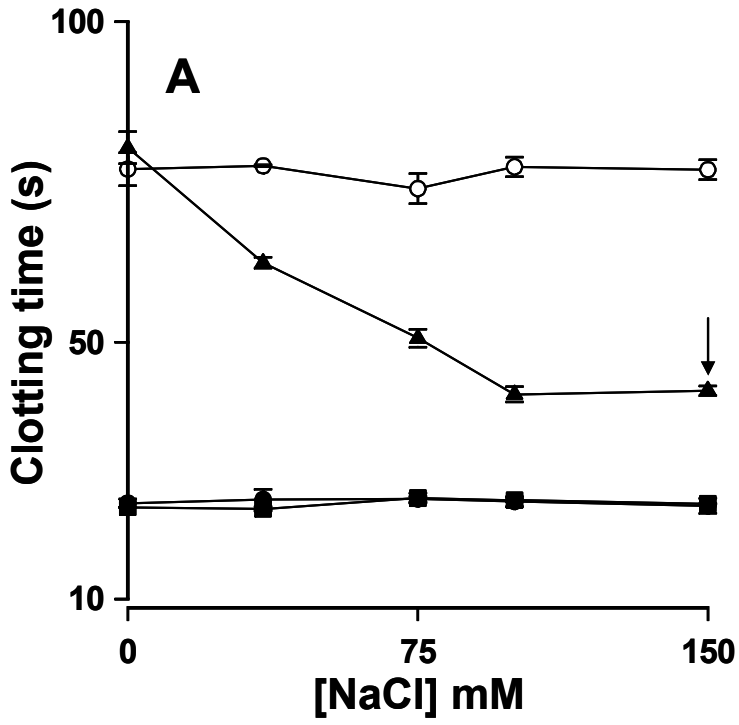


Figure 9

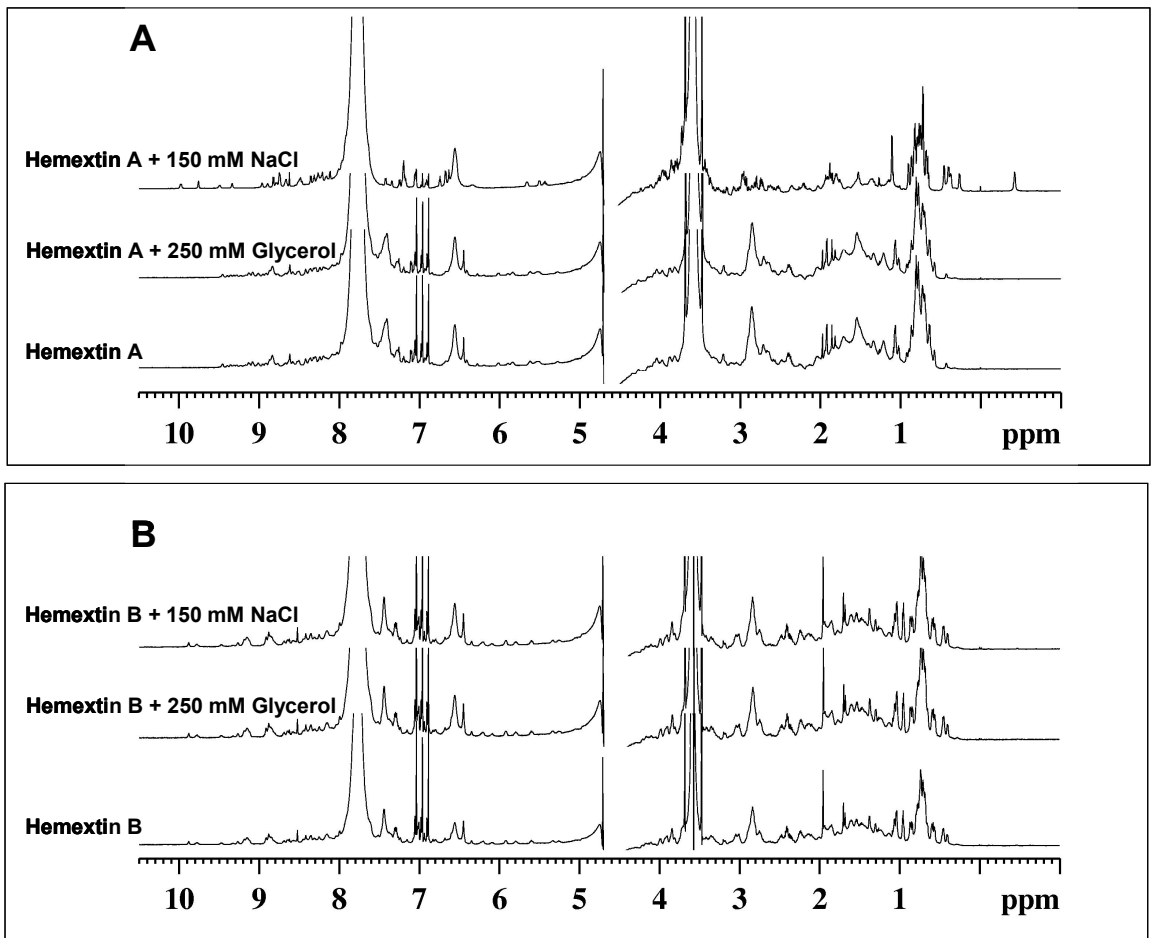
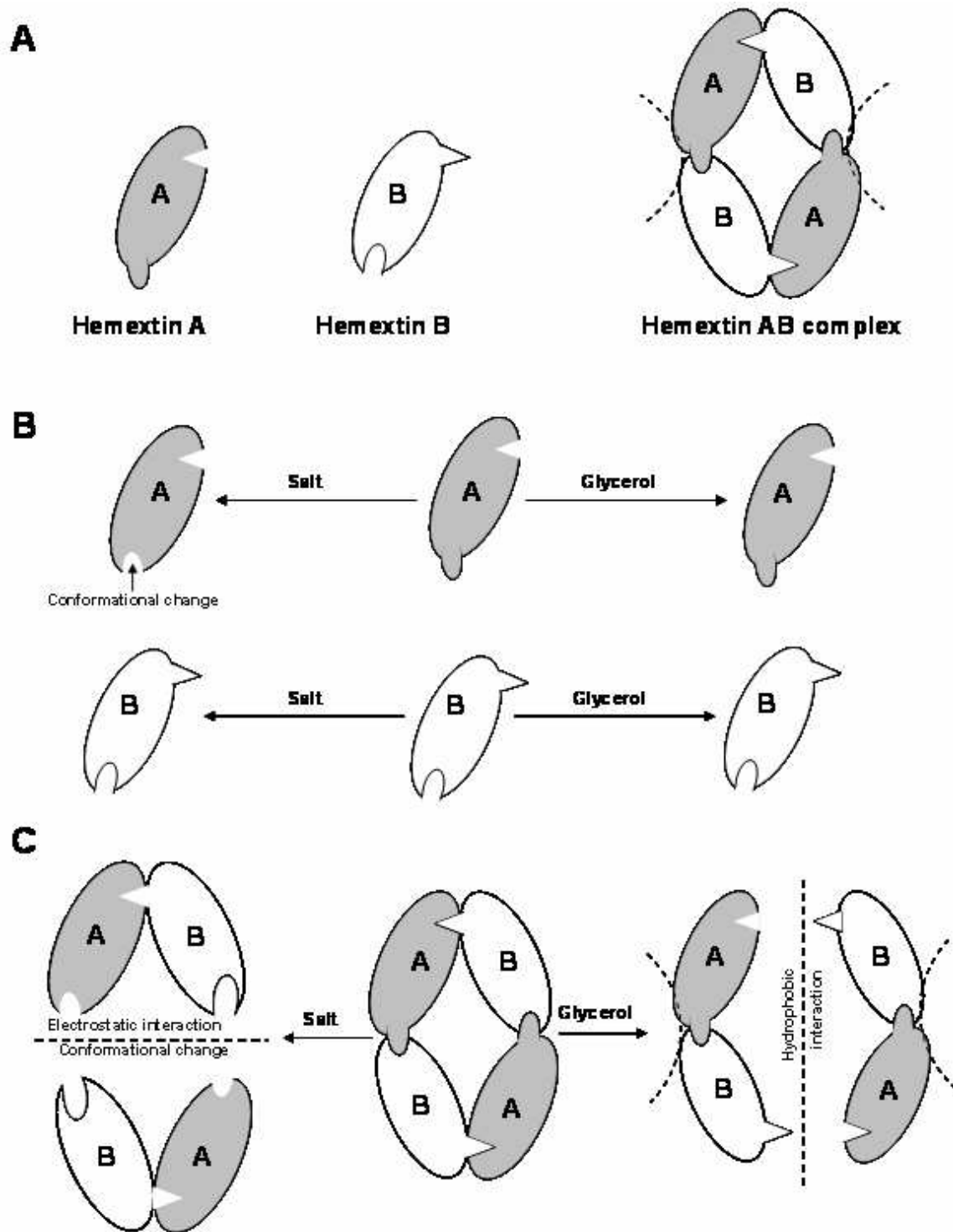


Figure 10



Yajnavalka Banerjee,^a
Sundramurthy Kumar,^a Chacko
Jobichen^a and R. Manjunatha
Kini^{a,b,*}

^aDepartment of Biological Sciences, Faculty of Science, National University of Singapore, 14 Science Drive 4, Singapore 117543, Singapore, and ^bDepartment of Biochemistry, Medical College of Virginia, Virginia Commonwealth University, Richmond, VA 23298-0614, USA

Correspondence e-mail: dbskinim@nus.edu.sg

Received 4 July 2007
Accepted 13 July 2007

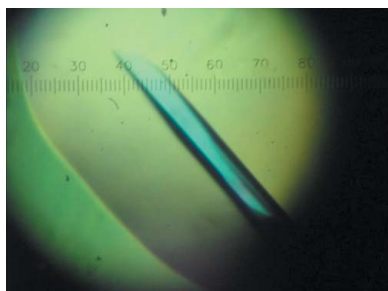
Crystallization and preliminary X-ray diffraction analysis of hemextin A: a unique anticoagulant protein from *Hemachatus haemachatus* venom

Hemextin A was isolated and purified from African Ringhals cobra (*Hemachatus haemachatus*). It is a three-finger toxin that specifically inhibits blood coagulation factor VIIa and clot formation and that also interacts with hemextin B to form a unique anticoagulant complex. Hemextin A was crystallized by the hanging-drop vapour-diffusion method by equilibration against 0.2 M ammonium acetate, 0.1 M sodium acetate trihydrate pH 4.6 and 30% PEG 4000 as the precipitating agent. The crystals belong to space group $P2_12_12_1$, with unit-cell parameters $a = 49.27$, $b = 49.51$, $c = 57.87$ Å and two molecules in the asymmetric unit. They diffracted to 1.5 Å resolution at beamline X25 at BNL.

1. Introduction

Snake venoms are veritable gold mines of pharmacologically active polypeptides and proteins (Kini, 2003; Koh *et al.*, 2006; Marsh & Williams, 2005). The venom from a single species of snake may contain several hundred different proteins, which may however be classified into a small number of superfamilies. The three-finger family, a toxin superfamily, contains proteins with molecular weights in the approximate range 6000–8000 Da and encompasses non-enzymatic polypeptides containing 60–74 amino-acid residues that confer lethality to *Elapidae* and *Hydrophidae* venoms (Kini, 2002). Proteins belonging to this family contain four or five disulfide bridges, of which four are conserved in all members. All proteins belonging to this family show a similar pattern of protein folding; they adopt a leaf-like shape comprising of three adjacent loops ('fingers') forming a large and flat β -pleated sheet that emerges from a small globular core confined by four conserved disulfide bridges, hence their name. Despite their similarity in structure, these proteins differ from each other in their biological activities. Members of this family include nicotinic and muscarinic toxins with selectivity towards distinct types of nicotinic and muscarinic acetylcholine receptors, fasciculins that inhibit acetylcholinesterase (Marchot, 1999; Taylor *et al.*, 1995), calciseptins that block the L-type calcium channels (Joseph *et al.*, 2004), cardiotoxins (cytotoxins) that exert their toxicity by forming pores in cell membranes (Kumar *et al.*, 1996; Menez *et al.*, 1990) and dendroaspins, which are antagonists of various cell-adhesion processes (Williams *et al.*, 1993).

Recently, we isolated and characterized a novel anticoagulant protein complex (hemextin A and B) from the venom of the elapid snake *Hemachatus haemachatus* (African Ringhals cobra; Banerjee *et al.*, 2005a,b). Hemextins A and B belong to the three-finger toxin family of snake-venom proteins. Individually, hemextin A exhibits mild anticoagulant activity, whereas hemextin B is inactive. However, hemextin B synergistically enhances the anticoagulant activity of hemextin A and their complex has potent anticoagulant activity. Thus, the formation of this unique synergistic complex of three-finger toxins is important for its ability to inhibit clot initiation. There are only a few noncovalent protein complexes in snake venoms that do not contain phospholipase A₂ as an integral part, such as rhodocetin (Wang *et al.*, 1999) and pseutarin C (Rao *et al.*, 2003). The hemextin AB complex is the only known snake-venom protein complex formed



© 2007 International Union of Crystallography
All rights reserved

by the interaction between two three-finger toxins and is the only known heterotetrameric complex of three-finger toxins. Here, we report the crystallization and preliminary diffraction studies of hemexin A, a unique anticoagulant protein, with the aim of understanding its structure and the function of this three-finger toxin in the anticoagulant process.

2. Methods and results

2.1. Purification of hemexin A

Hemexin A was purified using previously described methods (Banerjee *et al.*, 2005b). Briefly, crude *H. haemachatus* venom (100 mg in 1 ml distilled water) was applied onto a Superdex 30 gel-filtration column (1.6 × 60 cm) equilibrated with 50 mM Tris-HCl buffer pH 7.4 and eluted with the same buffer using an ÄKTA Purifier system (Amersham Biosciences, Uppsala, Sweden). Fractions containing potent anticoagulant activity were pooled and sub-fractionated on a Uno S-6 (Bio-Rad, Hercules, CA, USA; 6 ml column volume) cation-exchange column. The peaks containing hemexin A were further purified using RP-HPLC on a Jupiter C18 (1 × 25 cm) column (Fig. 1a). The protein was found to be homogeneous, with a molecular weight of 6835.00 ± 0.52 Da as determined by electrospray ionization mass spectrometry (ESI-MS; Fig. 1c).

The presence of hemexin A was confirmed using size-exclusion chromatography (SEC). All SEC experiments were carried out at room temperature on a pre-packed Superdex 75 gel-filtration column (1.6 × 60 cm) using the same ÄKTA Purifier system. The column was eluted with 50 mM Tris-HCl buffer pH 7.4 at a flow rate of 1 ml min^{-1} . The sample volume applied onto the column was 4 ml.

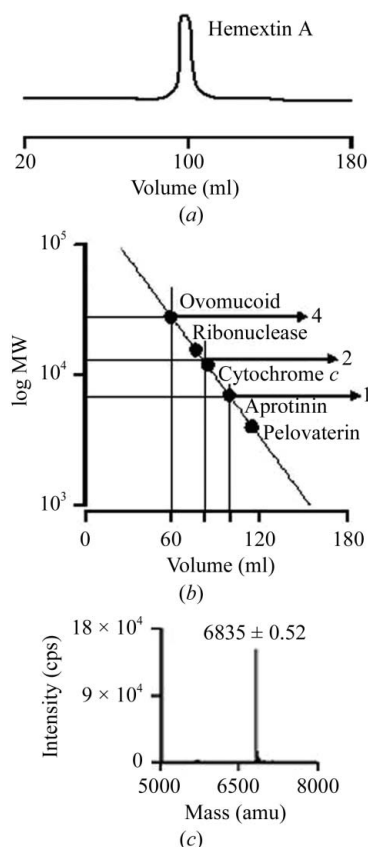


Figure 1
(a) Size-exclusion chromatography elution profile of hemexin A. (b) Molecular-weight standards. (c) Mass spectrum of hemexin A.

The column was calibrated using ovomucoid (28 kDa), ribonuclease (15.6 kDa), cytochrome *c* (12 kDa), apoprotinin (7 kDa) and pelovaterin (4 kDa) as molecular-weight markers (Fig. 1b). The void volume was determined by running Blue Dextran. The column was equilibrated with at least two bed volumes of elution buffer prior to each run.

2.2. Crystallization

Crystallization trials for hemexin A were conducted using the hanging-drop vapour-diffusion method and a wide range of conditions were tested using Hampton Research Crystal Screens I and II. The protein concentration was kept at approximately 30 mg ml^{-1} and the drops were prepared by mixing equal volumes ($1 \mu\text{l}$) of protein solution in 50 mM Tris buffer pH 7.4 and crystallization solution. The screens were set up at 295 K using VDX plates from Hampton Research. $500 \mu\text{l}$ reservoir solution was placed in each well. The initial screen identified a PEG-based crystallization condition. By systematic optimization around the preliminary condition, we obtained diffraction-quality crystals of hemexin A. The best crystals were from a condition consisting of 0.2 M ammonium acetate, 0.1 M sodium acetate trihydrate, 30% (w/v) PEG 4000 pH 4.6. The rod-shaped crystals appeared after 12–15 d (Fig. 2).

2.3. Data collection

We have collected a complete native data set for hemexin A. Prior to data collection, crystals of hemexin A were briefly soaked in a cryoprotectant solution consisting of reservoir solution supplemented with 25% (w/v) glycerol, picked up with a nylon cryo-loop and frozen at 100 K in a nitrogen-gas cold stream (Cryostream cooler; Oxford Cryosystems, Oxford, England). Synchrotron data were collected at beamline X25, NSLS, Brookhaven National Laboratory. Data sets were collected using a Quantum 4 CCD detector and were processed using *HKL-2000* (Otwinowski & Minor, 1997; Table 1). The crystals diffract to 1.5 \AA resolution. The space group was $P2_12_12_1$, with unit-cell parameters $a = 49.27$, $b = 49.51$, $c = 57.87 \text{ \AA}$. The Matthews coefficient V_M of $2.92 \text{ \AA}^3 \text{ Da}^{-1}$ (Matthews, 1968) is within the expected range for two monomers in the asymmetric unit and corresponds to a solvent content of 57.89%.

3. Discussion

Hemexin A, a three-finger toxin, was successfully purified from crude *H. haemachatus* venom. As shown in Fig. 1(a), hemexin A exists as a monomer in solution. Hemexin A was crystallized using

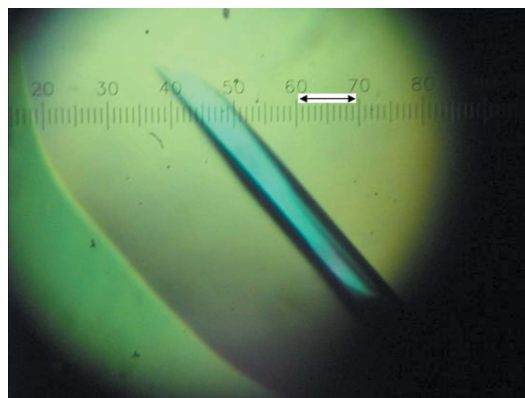


Figure 2
Crystal of hemexin A. Ten divisions of the scale is equivalent to 0.17 mm.

Table 1

Data-collection statistics for hemextin A.

Values in parentheses are for the highest resolution shell.

Beamline	X25, NSLS, BNL
Wavelength (Å)	0.97950
Oscillation range (°)	1
Space group	$P2_12_12_1$
Unit-cell parameters	
<i>a</i> (Å)	49.27
<i>b</i> (Å)	49.51
<i>c</i> (Å)	57.87
Resolution limits (Å)	50–1.5 (1.55–1.50)
No. of molecules in ASU	2
Observed <i>hkl</i>	287505
Unique <i>hkl</i>	23374
Redundancy	12.3
Completeness (%)	100 (100)
Overall $I/\sigma(I)$	10.5
R_{sym}^\dagger (%)	0.071 (0.26)

$^\dagger R_{\text{sym}} = \sum |I_i - \langle I \rangle| / \sum I_i$, where I_i is the intensity of the i th measurement and $\langle I \rangle$ is the mean intensity of the reflection.

the hanging-drop vapour-diffusion method. The X-ray diffraction data showed that the crystal belongs to the orthorhombic system, space group $P2_12_12_1$, with two molecules in the asymmetric unit. Using a three-finger toxin homology structure (PDB code 1ug4) as a search model, the rotation function gave two clear solutions corresponding to two molecules in the asymmetric unit. The translation function calculated in the resolution range 8–4 Å using the program *AMoRe* (Navaza, 1994) had two peaks that were significantly above the background and were of nearly equal height. The translation function confirmed that each of these peaks corresponded to an orientation of one of the two molecules in the asymmetric unit. Rigid-body refinement performed with *AMoRe* after combining the two solutions gave a correlation coefficient of 0.62 and an *R* factor of 0.40. We are now in the process of building the model and refining the

structure. The structure of hemextin A will help in detailed understanding of its anticoagulant activity.

The authors would like to acknowledge beamline X25, NSLS, Brookhaven National Laboratory for data collection and to thank Dr Anand Saxena for help during data collection. We thank Dr J. Sivaraman, Department of Biological Sciences, National University of Singapore for his guidance throughout this project. This work was performed with funding support from the Biomedical Research Council (BMRC – A*STAR).

References

- Banerjee, Y., Mizuguchi, J., Iwanaga, S. & Kini, R. M. (2005a). *Pathophysiol. Haemost. Thromb.* **34**, 184–187.
- Banerjee, Y., Mizuguchi, J., Iwanaga, S. & Kini, R. M. (2005b). *J. Biol. Chem.* **280**, 42601–42611.
- Joseph, R., Pahari, S., Hodgson, W. C. & Kini, R. M. (2004). *Curr. Drug Targets Cardiovasc. Haematol. Disord.* **4**, 437–459.
- Kini, R. M. (2002). *Clin. Exp. Pharmacol. Physiol.* **29**, 815–822.
- Kini, R. M. (2003). *Toxicon*, **42**, 827–840.
- Koh, D. C., Armugam, A. & Jeyaseelan, K. (2006). *Cell. Mol. Life Sci.* **63**, 3030–3041.
- Kumar, T. K., Lee, C. S. & Yu, C. (1996). *Adv. Exp. Med. Biol.* **391**, 115–129.
- Marchot, P. (1999). *J. Soc. Biol.* **193**, 505–508.
- Marsh, N. & Williams, V. (2005). *Toxicon*, **45**, 1171–1181.
- Matthews, B. W. (1968). *J. Mol. Biol.* **33**, 491–497.
- Menez, A., Gatineau, E., Roumestand, C., Harvey, A. L., Mouawad, L., Gilquin, B. & Toma, F. (1990). *Biochimie*, **72**, 575–588.
- Navaza, J. (1994). *Acta Cryst. A* **50**, 157–163.
- Otwinowski, Z. & Minor, W. (1997). *Methods Enzymol.* **276**, 307–326.
- Rao, V. S., Swarup, S. & Kini, R. M. (2003). *Blood*, **102**, 1347–1354.
- Taylor, P., Radic, Z., Hosea, N. A., Camp, S., Marchot, P. & Berman, H. A. (1995). *Toxicol. Lett.* **82–83**, 453–458.
- Wang, R., Kini, R. M. & Chung, M. C. (1999). *Biochemistry*, **38**, 7584–7593.
- Williams, J. A., Lu, X., Rahman, S., Keating, C. & Kakkar, V. (1993). *Biochem. Soc. Trans.* **21**, 73S.

**Characterization of the Binding of Anticoagulant Hemextin AB Complex
from *Hemachatus haemachatus* (African Ringhals Cobra) venom with
Blood Coagulation Factor VIIa**

Journal:	<i>Biochemistry</i>
Manuscript ID:	bi-2007-01766r
Manuscript Type:	Article
Date Submitted by the Author:	29-Aug-2007
Complete List of Authors:	Banerjee, Yajnavalka; Protein Science Laboratory, Faculty of Science, Department of Biological Sciences Persson, Egon; Novo Nordisk A/S Lakshminarayanan, Rajamani; Department of Chemistry, Faculty of Science Mizuguchi, Jun; The Chemo-Sero-Therapeutic Research Institute, Blood Products Research Department Doley, Robin; Protein Science Laboratory, Faculty of Science, Department of Biological Sciences Iwanaga, Sadaaki; The Chemo-Sero-Therapeutic Research Institute, Blood Products Research Department Kini, Manjunatha; National University of Singapore, Biological Sciences



1
2
3
4
5
6
7
8
9
10
11
12
13
14
15
16
17
18
19
20

**Characterization of the Binding of Anticoagulant Hemexin AB Complex from
Hemachatus haemachatus (African Ringhals Cobra) venom with Blood Coagulation
Factor VIIa**

Yajnavalka Banerjee^{††}, Egon Persson[€], Rajamani Lakshminarayanan^{¶¶}, Jun Mizuguchi[§], Robin Doley[‡], Sadaaki Iwanaga[§] and R. Manjunatha Kini^{‡*}

‡Protein Science Laboratory, Department of Biological Sciences[¶], Faculty of Science, National University of Singapore, Singapore 117543; ¶ Department of Chemistry, National University of Singapore, 3 Science Drive 3, Singapore 117543 €Novo Nordisk A/S, Novo Nordisk Park, DK-2760 Måløv, Denmark; §Blood Products Research Department, The Chemo-Sero-Therapeutic Research Institute, Kumamoto 869-1298, Japan; *Department of Biochemistry, Medical College of Virginia, Virginia Commonwealth University, Richmond, VA 23298, USA

21
22
23
24
25
26
27
28
29
30
31
32
33
34

Address all correspondence to: R. Manjunatha Kini, Protein Science Laboratory, Department of Biological Sciences, Faculty of Science, National University of Singapore, Singapore 117 543; E-Mail: dbskinim@nus.edu.sg

Present Addresses:

†Department of Molecular and Experimental Medicine, The Scripps Research Institute, 10550 North Torrey Pines Road, La Jolla CA 92037

¶School of Dentistry, 2250 Alcazar Street, Centre for Craniofacial and Molecular Biology, University of Southern California, Los Angeles CA 90033

35
36
37
38
39
40
41
42
43
44
45
46
47
48
49
50
51
52
53
54
55
56
57
58
59
60

Footnote

This work was supported in part by the Biomedical Research Council, Agency for Science and Technology, Singapore. The costs of publication of this article were defrayed in part by the payment of page charges. This article must therefore be hereby marked "advertisement" in accordance with 18 U.S.C. Section 1734 solely to indicate this fact.

Abstract

Hemextin AB complex from *Hemachatus haemachatus* venom is the only known natural anticoagulant that specifically inhibits factor VIIa (FVIIa) enzymatic activity in the absence of factor Xa (Banerjee, Y., Mizuguchi, J., Iwanaga, S., and Kini, R. M. (2005) J Biol.Chem 280, 42601-42611). It is also the only known hetero-tetrameric complex of two three-finger proteins. Recently, we elucidated the molecular interactions involved in hemextin AB complex formation, proposing a model for its assembly. Here, we biophysically characterize the binding of hemextin AB complex and hemextin A with FVIIa, and localize their binding site in the enzyme. Binding of the anticoagulants with FVIIa was studied using isothermal titration calorimetry (ITC) and size-exclusion chromatography (SEC), in buffers of high ionic strength and that containing glycerol. Hemextin AB complex binds to FVIIa under both conditions with variable affinities. The results from these studies also validated our earlier proposed model of hemextin AB complex assembly. Conformational changes associated with the binding of anticoagulant complex with FVIIa were studied using circular dichroism spectroscopy. The hemextin AB-FVIIa complex exhibited a slight increase in θ_{222} indicating an increase in 3_{10} -helix structure upon complex formation. Binding studies using ITC and SEC indicate that both hemextin A and hemextin AB complex bind to FVIIa in the presence of soluble tissue factor, suggesting that their binding site in FVIIa is distinct from the cofactor binding site. The anticoagulant proteins also exhibited binding with active site blocked FVIIa, confirming their non-competitive nature of inhibition. Further binding studies with the anticoagulant proteins were conducted using separated light and heavy chains of FVIIa. Both hemextin A and hemextin AB complex bind to FVIIa heavy chain with high affinity, but not to light chain indicating the binding site is localized in this chain.

Introduction

Blood coagulation following vascular injury is initiated by exposure of factor VII (FVII) and factor VIIa (FVIIa) to the membrane bound cofactor, tissue factor (TF), resulting in production of Factor FXa (FXa) and more FVIIa (1-4). The process is propagated upon production of factor IXa (FIXa) (5) and more FXa (6) that, upon binding to their respective cofactors FVIIIa and FVa, form platelet bound complexes, ultimately resulting in the formation of thrombin. Thrombin cleaves fibrinogen to fibrin and the polymerized fibrin is cross-linked by transglutaminase FXIIIa (7) to form the fibrin clot staunching the flow of blood thereby preventing blood loss. The initiation and subsequent regulation of coagulation is understandably complex since maintenance of hemostasis is crucial for survival. Abnormal/unwanted blood clot formation, also known as thrombosis, can lead to death and debilitation due to myocardial infarction, acute coronary syndrome, acute ischemic stroke, and pulmonary embolism. Thus, anticoagulants are central for the treatment and prevention of thrombosis (8). Coumarin and heparin are the classical anticoagulants (9;10). However, due to the non-specific mode of action of these anticoagulants, they have a very narrow therapeutic window (11). This limitation has provided the impetus for the design/development of novel anticoagulants targeting specific coagulation enzymes or steps in the coagulation pathway.

There is increasing enthusiasm in the inhibition of FVIIa as a target to achieve therapeutic anticoagulation because of its 'central' and 'upstream' position in the coagulation process and also because of its minute concentrations in the plasma milieu. Snake venoms are veritable goldmines of anticoagulant proteins (12), a number of which have inspired the design and development of therapeutic agents or lead molecules for cardiovascular diseases (13-16). Previously, we reported the purification and characterization of a three-finger toxin, hemextin A,

1
2
3 from the venom of an elapid snake *Hemachatus haemachatus* (African Ringhals cobra) that
4 mediates anticoagulant activity (17;18). Although, individually it has mild anticoagulant activity,
5
6 its 1:1 complex with a second three-finger toxin, hemextin B, enhances its anticoagulant potency.
7
8 Hemextin A and its synergistic complex – hemextin AB complex, specifically inhibit the
9
10 enzymatic activity of FVIIa with a K_i of 25 nM. Further, it inhibits FVIIa in the absence of TF
11
12 and FX. Thus, it is the first and only known natural inhibitor of FVIIa which does not use FXa
13
14 scaffold (17). Two molecules each of hemextin A and B form the tetrameric complex in Tris-
15
16 HCl buffer (Figure 1A) (19). Complex formation leads to the stabilization of β -sheet structure.
17
18 The formation of this compact, synergistic complex is enthalpically driven and is important for
19
20 its anticoagulant activity. The tetramer dissociates into dimer in the presence of salt as well as
21
22 glycerol. Dimer formed in the presence of salt appears to be different from that formed in
23
24 glycerol; hemextin AB dimer in high salt has an apparent molecular diameter of 12.4 nm and
25
26 shows anticoagulant activity of hemextin A alone, whereas the dimer formed in the presence of
27
28 glycerol has an apparent molecular diameter of 12.8 nm and exhibits higher anticoagulant effects
29
30 than hemextin A alone (Figure 1C). Thus, the breakdown of tetramer to dimers probably occurs
31
32 at two different interfaces between hemextin A and B. One interface is sensitive to the ionic
33
34 strength of its surroundings while the other is sensitive to glycerol (Figure 1C). The dissociation
35
36 of the complex in the presence of salt is probably due to the conformational change in hemextin
37
38 A as well as electrostatic interactions (Figure 1B). The dimer formed under high ionic conditions
39
40 lacks the complete synergistic anticoagulant site (marked by a dotted semicircle in Figure 1C).
41
42 This could explain its anticoagulant activity similar to that of hemextin A alone. In contrast,
43
44 hydrophobic interactions are predominant in the second interface. Therefore, glycerol dissociates
45
46 the tetramer into dimers. However, in this case only minor changes occur in the synergistic
47
48
49
50
51
52
53
54
55
56
57
58
59
60

1
2
3 anticoagulant site of the complex (as shown in Figure 1C) and the resultant dimer is active.
4
5 Based on these observations we proposed a model for hemextin AB complex (Figure 1) (19), and
6
7 the tetramer formation most likely stabilizes the anticoagulant site of hemextin AB complex.
8
9

10
11 In this study, we have attempted to understand the interactions between hemextin AB
12
13 complex/hemextin A and FVIIa and to identify the anticoagulant binding site in the enzyme.
14
15 Binding between hemextinA/hemextin AB complex and FVIIa was studied using isothermal
16
17 titration calorimetry (ITC) and size-exclusion chromatography (SEC) in buffers of different ionic
18
19 strengths and containing different concentrations of glycerol. The results of these studies
20
21 validated our previously proposed model (19). Further, interactions of the anticoagulant protein
22
23 and its complex with FVIIa were investigated in the presence of soluble tissue factor (sTF) and
24
25 active site inhibitor D-Phe-L-Phe-L-Arg chloromethyl ketone (FFRck). The results indicate that
26
27 the anticoagulant binding site is probably different from the cofactor binding site and the active
28
29 site. We also examined the binding of individual heavy and light chains of FVIIa to the
30
31 anticoagulant proteins. The results indicated that the binding site of hemextin AB complex and
32
33 hemextin A is localized in the heavy chain of FVIIa. Based on the obtained results we propose a
34
35 model depicting the mechanism of hemextin AB complex activity.
36
37
38
39
40
41

42 **Experimental Procedures**

43
44
45 *Materials* – Lyophilized *H. haemachatus* venom was obtained from African Reptiles and
46
47 Venoms, Gauteng, South Africa. The chromogenic substrate H-D-Ile-Pro-Arg-p-nitroanilide
48
49 (pNA) dihydrochloride (2HCl), (S-2288) was from Chromogenix AB, Stockholm, Sweden and
50
51 was reconstituted in deionized water prior to experiment. FFRck was purchased from Bachem
52
53 (King of Prussia, PA, USA). All other chemicals and reagents used were of highest purity
54
55 available.
56
57
58
59
60

1
2
3
4
5
6
7
8
9
10
11
12
13
14
15
16
17
18
19
20
21
22
23
24
25
26
27
28
29
30
31
32
33
34
35
36
37
38
39
40
41
42
43
44
45
46
47
48
49
50
51
52
53
54
55
56
57
58
59
60

Proteins – Hemextin A and hemextin B was purified using the methods described earlier (17;18). Briefly, *H. haemachatus* crude venom (100 mg in 1 ml distilled water) was applied to a Superdex 30 gel filtration column (1.6 × 60 cm) equilibrated with 50 mM Tris-HCl buffer (pH 7.4) and eluted using the same buffer, using an ÄKTA Purifier system (Amersham Biosciences, Uppsala, Sweden). Fractions containing potent anticoagulant activity were pooled and sub-fractionated on a Uno S-6 (Bio-Rad, Hercules, CA, USA; column volume, 6 ml) cation-exchange column. The peaks containing hemextin A and hemextin B were further purified using RP-HPLC on a Jupiter C18 (1× 25 cm) column. Both proteins were found to be homogeneous with molecular masses of 6835.00 ± 0.52 and 6792.56 ± 0.32 Daltons respectively, as determined by electro spray ionization mass spectrometry (ESI-MS) (17).

Human plasma-derived FVIIa was kindly provided by Factor VII Group (Kazuhiko Tomokiyo, Yasushi Nakatomi, Teruhisa Nakashima, and Soutatou Gokudan) of KAKETSUKEN and were purified as described (20). Recombinant human soluble TF (sTF; residues 1–218) was a gift from Dr. Toshiyuki Miyata (National Cardiovascular Center, Suita, Japan), and it was prepared as described (21).

Reconstitution of the anticoagulant complex – We reconstituted hemextin AB complex for various *in vitro* experiments immediately prior to the experiment by incubating equimolar concentration of hemextin A with hemextin B at 37° C for a period of 5 min in 50 mM Tris-buffer (pH 7.4).

Reconstitution of the sTF-FVIIa complex – sTF-FVIIa complex was reconstituted by incubating 30 nM FVIIa with 100 nM of sTF in 50 mM Tris-HCl buffer (pH 7.4), containing 10 mM CaCl₂, and 1% BSA for 10 min at 37° C. The kinetics of hydrolysis of the chromogenic substrate S-2288 by sTF-FVIIa was measured prior to the studies.

1
2
3 *Preparation of active site inhibited FVIIa* – Active site inhibitor FFR-ck was used for the study.
4
5 For the preparation, FVIIa was treated with and 2-fold molar excess of FFR-ck. Unreacted FFR-
6
7 ck was separated from active site blocked FVIIa by size-exclusion on Superdex 200 gel filtration
8
9 column (1.0 × 30 cm) chromatography using the same ÄKTA Purifier system. The residual
10
11 FVIIa activity of active site inhibited FVIIa was measured in an FVIIa-specific amidolytic assay
12
13 using S-2288 as the substrate.
14
15

16
17
18 *FVIIa-specific amidolytic assay* – The assay was performed in assay buffer containing 50 mM
19
20 Tris-HCl, pH 7.4, containing 10 mM CaCl₂, and 1% BSA at 37 °C. In a total volume of 200 µl in
21
22 the individual wells of the microtiter plate, final concentrations of FVIIa/active site inhibited
23
24 FVIIa was 300 nM. Reactions were initiated by the addition of S-2288 (1 mM). Initial reaction
25
26 velocities were measured as a linear increase in the absorbance at 405 nm over 5 min, with a
27
28 SPECTRAMax plus® temperature-controlled microplate spectrophotometer (Molecular Devices,
29
30 Sunnyvale, CA, USA). FFRck-FVIIa had <5% residual activity (Figure 9A, *inset*) as measured in
31
32 the assay.
33
34
35

36
37
38 *Separation of light and heavy chains of FVIIa* – Human FVIIa (3.5 mg) was incubated with 0.5
39
40 M 2-mercaptoethanol in 1.1 ml of tris-buffered saline (100 mM Tris-HCl, pH 7.5 + 0.9% NaCl)
41
42 (TBS) at 20 °C for 30 min. The mixture was applied to a column (6 ml) of DEAE-Sepharose CL-
43
44 6B equilibrated with TBS containing 0.5 M 2-mercaptoethanol. After washing the column with
45
46 20 ml of the equilibration buffer, the heavy chain of FVIIa was eluted with 35 ml of TBS
47
48 containing 6.0 M urea and 0.5 M 2-mercaptoethanol. Then the column was washed with 20 ml of
49
50 TBS and the light chain of FVIIa was eluted using a linear gradient from 0.1 to 0.6 M NaCl in 50
51
52 mM Tris-HCl, pH 8.0. Both the chains were treated with 10 mM iodoacetamide for 20 min in ice
53
54
55
56
57
58
59
60

1
2
3 water, in the dark. Homogeneity and molecular weight of the chains were determined on SDS-
4
5 PAGE.
6

7
8
9 *Preparation of light chain of FVIIa under non-reduced conditions* – The FVIIa light chain
10
11 (residues 1-144 plus 248-266) was isolated as described in (22).
12

13
14 *Circular dichroism (CD) spectroscopy* – Conformational changes in FVIIa, associated with
15
16 binding to hemextin AB complex were monitored using CD. Far UV CD spectra (260-190 nm)
17
18 were recorded using a Jasco J-810 spectropolarimeter (Jasco Corporation, Tokyo, Japan). All
19
20 measurements were carried out at room temperature using 0.1 cm pathlength stoppered cuvettes.
21
22 The instrument optics was flushed with 40 l/min of nitrogen gas. The spectra were recorded
23
24 using a scan speed of 50 nm /min, resolution 0.2 nm, and band width 2 nm. For each spectrum, a
25
26 total of 4 scans were recorded, averaged and baseline subtracted.
27
28

29
30
31 *Isothermal Titration Calorimetric (ITC) studies* – The thermodynamics of binding of individual
32
33 hemextins and the reconstituted anticoagulant complex with FVIIa and its derivatives was
34
35 monitored using a VP-ITC titration calorimetric system (MicroCal, LLC, Northampton, MA).
36
37 The instrument was calibrated using the built-in electrical calibration check. FVIIa or its
38
39 derivatives was taken in 50 mM Tris-HCl buffer (pH 7.4) in the calorimetric cell and was titrated
40
41 with individual hemextins or the reconstituted anticoagulant complex dissolved in the same
42
43 buffer in a 250- μ l injection syringe with continual stirring at 300 rpm at 37 °C. All protein
44
45 solutions were filtered and degassed prior to titration. The first injections presented defects in the
46
47 base line, and these data were not included in the fitting process. Additional experiments were
48
49 performed with FVIIa in 50 mM Tris-HCl buffer (pH 7.4) containing 150 mM NaCl or 250 mM
50
51 glycerol at 37 °C.
52
53
54
55
56
57
58
59
60

The calorimetric data were processed and fitted to the *single set of identical sites* model using MicroCal Origin (Version 7.0) data analysis software supplied with the instrument. The expression for the heat released per injection, $\Delta Q_{(i)}$, is given by

$$\Delta Q_{(i)} = Q_{(i)} + dV_i / 2V_0 [Q_{(i)} + Q_{(i-1)}] - Q_{(i-1)} \dots \dots \dots (Eq. 1)$$

where, $Q_{(i)}$ is the total heat content, dV_i is the volume injected at the i^{th} injection, and V_0 is the cell volume. The total heat content Q of the solution (determined relative to zero for the unliganded species) contained in the active cell volume, V_o , was calculated according to equation 2.

$$Q = \frac{nM_t \Delta H V_0}{2} \left[1 + \frac{X_t}{nM_t} + \frac{1}{nK_a M_t} - \sqrt{\left(1 + \frac{X_t}{nM_t} + \frac{1}{nK_a M_t} \right)^2 - \frac{4X_t}{nM_t}} \right] \dots \dots \dots (Eq. 2)$$

where, K_a is the binding affinity constant, n is the number of sites, ΔH is the enthalpy of ligand binding, M_t and X_t is the bulk concentration of macromolecule and ligand, respectively, for the binding $X + M \leftrightarrow XM$.

The change in heat (ΔQ) measured between the completions of two consecutive injections is corrected for dilution of the protein and ligand in the cell according to standard Marquardt method (23;24). The free energy change (ΔG) during the interaction was calculated using the relationship: ($\Delta G = \Delta H - T\Delta S = -RT \ln K_a$). All the experiments were performed at 37 °C unless otherwise indicated.

Size-exclusion chromatographic (SEC) studies – Binding studies with FVIIa and its derivatives were also carried out using SEC. All SEC experiments were carried out at room temperature on a pre-packed Superdex 200 gel filtration column (1.0 × 30 cm) using the ÄKTA Purifier system. The column was equilibrated with 50 mM Tris-HCl buffer (pH 7.4) or the specified elution

1
2
3
4
5
6
7
8
9
10
11
12
13
14
15
16
17
18
19
20
21
22
23
24
25
26
27
28
29
30
31
32
33
34
35
36
37
38
39
40
41
42
43
44
45
46
47
48
49
50
51
52
53
54
55
56
57
58
59
60

buffer, at a flow rate of 0.5 ml/min. The sample volume applied to the column was 0.4 ml. The column was calibrated using catalase (232-kDa), lactate dehydrogenase (140-kDa), bovine serum albumin (67-kDa), ovalbumin (43-kDa), chymotrypsinogen A (25-kDa) and ribonuclease A (13.7-kDa) as molecular weight markers. The void volume was determined using Blue Dextran. The column was equilibrated with at least three bed volumes of the elution buffer prior to each run. Protein elution was monitored by recording absorbance at 280 nm.

Results and Discussion

Binding of FVIIa to hemextin AB complex – The binding between hemextin AB complex and FVIIa was studied in Tris buffer (pH 7.4) using ITC (Figure 2A, Table 1); under these conditions the complex exists as a heterotetramer (19). Interestingly, two kinetic phases were associated with each injection. Immediately following injection, an initial exothermic phase (negative numbers) which was followed by a smaller and slower endothermic phase (positive numbers), suggesting that a slow conformational rearrangement may take place upon binding. A similar thermogram has also been observed in the binding of FXa with human secretory phospholipase A₂, where a conformational rearrangement takes place on binding (25). The binding is enthalpically driven with 1:1 stoichiometry (Table 1). SEC studies show that the estimated molecular weight of the tetrameric hemextin AB complex-FVIIa complex is ~88,000 Da (Figure 2B). In the proposed model for hemextin AB complex assembly (Figure 1), the tetramer possesses two identical anticoagulant sites and therefore could bind two molecules of FVIIa. However, both ITC and SEC studies show that hemextin AB complex binds to only one molecule of FVIIa (Figure 2). This could be due to either steric hindrance or negative cooperativity. The two FVIIa binding sites on the tetramer juxtaposed very closely, as a result the binding of the first FVIIa molecule precludes the binding of the second FVIIa molecule. Such

‘steric interference’ in protein-protein interactions is well documented (26;27). Alternatively, the binding of the first FVIIa rapidly induces structural changes destroying the adjacent binding site resulting in ‘negative cooperativity’ (28). The larger size of FVIIa and fairly stable conformation of hemextin AB complex supports the steric hindrance.

The effect of temperature on hemextin AB-FVIIa complex formation – Since, hemextin AB complex is a specific inhibitor of FVIIa, the energetics of complex formation between FVIIa and the anticoagulant complex was investigated in detail. Complete temperature profile of the thermodynamic parameters associated with the binding of hemextin AB complex to FVIIa was studied over the temperature range of 25-45 °C (298-318 K). The temperature dependence of ΔH is shown in Figure 3A and Table 2. The temperature dependence of ΔH over a narrow temperature range is given by the equation:

$$\Delta H = \Delta H_0 + \Delta C_p(T-T_0) \dots \dots \dots (Eq. 3)$$

where, ΔH_0 is the binding enthalpy at an arbitrary reference temperature and ΔC_p is the heat capacity change of binding. The ΔC_p obtained from the slope ($\Delta C_p = \delta\Delta H / \delta T$) (Figure 3A), was found to be $-121.43 \text{ cal K}^{-1}\text{mol}^{-1}$. Such negative ΔC_p indicates a reduction in the nonpolar solvent-accessible surface area, as explained by the following equation (29),

$$\Delta C_p = 0.45(\Delta ASA_{nonpol}) - 0.26 (\Delta ASA_{pol}) \text{ cal /molK} \dots \dots \dots (Eq. 4)$$

where, ΔASA_{pol} and ΔASA_{nonpol} are the change in the accessible polar and nonpolar surface areas, respectively.

Figure 3B shows the plot of ΔG and ΔH as a function of $T\Delta S$. It is clear that the ΔG of binding remained temperature-independent and is a result of linear dependence of ΔH on $T\Delta S$. This strongly suggests the enthalpy-entropy compensation for the binding of hemextin A to hemextin

B. This phenomenon is a universal feature for protein-peptide interactions, where weak molecular interactions undergo constant rearrangements to realize a lower free energy of binding.

The negative ΔC_p also indicates the net thermodynamic driving force for the association to shift from entropic to enthalpic with increasing temperature. At the intersection point of both lines $\Delta G = \Delta H = -7.5 \text{ kCal.mol}^{-1}$ (Figure 3B), which corresponds to a temperature T_s (temperature at which the contribution from entropy is zero). At T_s the contribution from entropy changes from favorable to unfavorable. From Figure 3A, $\Delta H = -7.5 \text{ kCal.mol}^{-1}$ is connected with a T_s of 33.3 °C (306.3 K). A positive entropy change observed at 25 °C (298 K), which is below T_s , further confirms this finding.

The negative ΔC_p for the hemextin AB-FVIIa complex formation further suggests that the observed entropy change upon binding must include significant contribution from the hydrophobic effect in the physiological temperature range. Therefore, for protein-protein/ligand interaction(s) the net entropy of association is given by the equation:

$$\Delta S_{assoc} = \Delta S_{HE} + \Delta S_{rt} + \Delta S_{other} \dots\dots\dots(Eq. 5)$$

where, ΔS_{HE} , ΔS_{rt} , and ΔS_{other} are the entropy changes due to hydrophobic effect, reduction of rotational and translational degree of freedom, and from other sources, respectively.

At T_s , the overall entropy of association is zero and the above equation becomes:

$$\Delta S_{assoc} = \Delta S_{HE}(T_s) + \Delta S_{rt} + \Delta S_{other} = 0 \dots\dots\dots(Eq. 6)$$

In the absence of crystallographic data, the $\Delta S_{HE}(T_s)$ was estimated from the equation,

$$\Delta S_{HE}(T_s) = 1.35 \Delta C_p \ln(T_s/386) \dots\dots\dots(Eq. 7)$$

and found to be $37.86 \text{ cal deg}^{-1} \text{ mol}^{-1}$. It has been shown that for protein-protein interactions ΔS_{rt} is nearly equal to $-50 \text{ cal deg}^{-1} \text{ mol}^{-1}$ (30;31). Thus the ΔS_{other} is calculated to be $-12.14 \text{ cal deg}^{-1} \text{ mol}^{-1}$. Because of experimental uncertainties in the heat capacity change and the entropy of

1
2
3 complex formation, as well as in the value of the rotational-translational entropy term, the
4 analysis of coupled folding is typically not suitable for distinguishing small extents of folding
5 from the rigid body case. However, from the non-zero value of ΔS_{other} can be concluded that that
6 there is no evidence for large-scale coupled folding, during the formation of hemextin AB-FVIIa
7 complex.
8
9

10
11
12
13
14
15 *Conformational changes associated with hemextin AB-FVIIa complex formation* – The above
16 analysis of the thermodynamic parameters indicated a plausible conformational change
17 associated with complex formation between FVIIa and hemextin AB complex. Figure 4A, shows
18 the CD spectra of hemextin AB complex, FVIIa, and hemextin AB-FVIIa complex. The CD
19 spectrum of hemextin AB complex exhibits dominant presence of β -sheet structure. The CD
20 spectrum of FVII exhibits a strong double minimum at 207 nm and 222 nm, and a weak positive
21 maximum around 195 nm indicating the presence of a right-handed helical structure. However,
22 the ratio of $[\theta_{222}]/[\theta_{207}]$ is 0.7 indicates the interconverting populations of both 3_{10} - and α -helical
23 structure (32). The hemextin AB-FVIIa complex exhibited a slight increase in θ_{222} indicating an
24 increase in 3_{10} -helix structure upon complex formation. The results suggest considerable
25 unfolding upon complex formation. Since CD was recorded at room temperature (far below T_s)
26 the complex formation is driven by favorable entropy changes. Thus, CD studies support the
27 thermodynamic data obtained from ITC.
28
29
30
31
32
33
34
35
36
37
38
39
40
41
42
43
44

45
46 *Binding of FVIIa to hemextin A* – For comparison, the binding between hemextin A and FVIIa
47 was also investigated. ITC studies revealed that the binding is predominantly exothermic with
48 1:1 stoichiometry (Figure 5A). Unlike the thermogram of hemextin AB-FVIIa complex
49 formation (Figure 2A), which has two kinetic phases, hemextin A-FVIIa complex had only one
50 kinetic phase. The binding affinity (80 μ M) was also lower than that observed for the binding
51
52
53
54
55
56
57
58
59
60

1
2
3 between tetrameric hemexin AB complex and FVIIa (Table 1), explaining the lower
4 anticoagulant potency of hemexin A as observed earlier (17). The estimated molecular weight of
5
6 anticoagulant potency of hemexin A as observed earlier (17). The estimated molecular weight of
7
8 the hemexin A- FVIIa complex from SEC studies was ~57000 Da (Figure 5B) validating 1:1
9
10 stoichiometry of complex formation. Since hemexin AB complex induces a conformational
11
12 change in the FVIIa molecule on binding, a similar study was conducted with hemexin A
13
14 (Figure 4B). CD studies with hemexin A and FVIIa showed that hemexin A-FVIIa complex has
15
16 a predominantly β -sheeted structure (Figure 4B).
17

18
19
20 *Binding of hemexin AB complex dimers to FVIIa* – Hemexin AB complex predominantly exists
21
22 as a tetramer in Tris buffer at pH 7.5. However, in the presence of glycerol (250 mM) and NaCl
23
24 (150 mM), it dissociates and predominantly exists as two distinct dimers (19). We studied the
25
26 binding between hemexin AB complex dimers (formed in both salt and glycerol) and FVIIa
27
28 using ITC and SEC and compared it to the binding between FVIIa and hemexin A.
29

30
31 ITC experiments show that the interaction of dimeric hemexin AB complex formed in glycerol
32
33 with FVIIa is predominantly exothermic with 1:1 stoichiometry (Figure 6A). This was further
34
35 confirmed using SEC, where the estimated molecular weight of the complex between dimeric
36
37 hemexin AB complex and FVIIa complex was ~64000 Da (Figure 6C). The binding affinity for
38
39 FVIIa was lower than that of the tetrameric hemexin AB complex but higher than that of
40
41 hemexin A alone (Table 1). Binding between hemexin A and FVIIa in the presence of glycerol
42
43 was predominantly exothermic (Figure 6B). The estimated molecular weight of hemexin A–
44
45 FVIIa complex in glycerol was ~57000 Da (Figure 6C). No, significant difference in the binding
46
47 affinity of hemexin A for FVIIa was observed in the presence or absence of glycerol (Table 1).
48
49 The binding affinity of hemexin A for FVIIa was lower than that of the tetrameric hemexin AB
50
51 complex and hemexin AB complex dimer (formed in glycerol) (Table 1).
52
53
54
55
56
57
58
59
60

1
2
3 Hemextin AB complex predominantly exists as a dimer in the presence of 150 mM NaCl. The
4
5 dimer in salt has lower anticoagulant potency than that formed in glycerol (19). However, its
6
7 anticoagulant potency is identical to that of hemextin A. To determine if the dimer in salt binds
8
9 to FVIIa, ITC studies were conducted in 150 mM NaCl. Figure 7A and Table 1 show that the
10
11 binding is predominantly exothermic with 1:1 stoichiometry. The estimated molecular weight of
12
13 the dimeric hemextin AB-FVIIa complex from the SEC experiments was ~57000 Da (Figure
14
15 7C). Interestingly, the binding affinity of the dimer in salt for FVIIa was lower than that of the
16
17 tetramer and the dimer in glycerol, but was almost identical that observed for hemextin A alone
18
19 (Table 1). We also studied the binding of hemextin A to FVIIa in the presence of salt. At high
20
21 salt concentrations hemextin A complexes with FVIIa with a 1:1 stoichiometry (Figure 7B) and
22
23 the binding was predominantly exothermic. The estimated molecular weight of the hemextin A-
24
25 FVIIa complex was ~57000 Da (Figure 7C), confirming the stoichiometry of complex formation.
26
27 The binding affinity of hemextin A for FVIIa in the presence of salt was almost identical to that
28
29 observed in the absence of salt (Table 1). Earlier we have shown that hemextin A undergoes a
30
31 conformational change in the presence of salt (19). As shown here the conformational changes
32
33 occurring in hemextin A in the presence of salt, however, does not alter its affinity for FVIIa.
34
35 The observed binding affinity of hemextin A for FVIIa was lower than that observed for
36
37 tetrameric hemextin AB complex and dimeric hemextin AB complex (formed in glycerol), but
38
39 same as that of dimeric hemextin AB complex (formed in the presence of salt) (Table 1).
40
41 From these observations it can be concluded that the dimer formed in glycerol is different from
42
43 the dimer formed in salt and dissociation of the tetramer into a dimer can take place in two
44
45 different planes depending on buffer conditions (which validates the proposed model). The dimer
46
47 formed in glycerol retains the anticoagulant site and hence exhibits higher anticoagulant potency.
48
49
50
51
52
53
54
55
56
57
58
59
60

1
2
3 However, the lower anticoagulant potency of this dimer compared to that of the tetramer may be
4 due to lower rigidity of the dimer which destabilizes the anticoagulant site. Thus, despite the
5 same stoichiometry, the binding affinity for FVIIa is diminished. In contrast, the dimer in salt has
6 similar binding affinity as hemextin A in the presence of salt (Table 1). Under these conditions
7 only hemextin A forms a complex with FVIIa and the molecular weight is ~57000 Da. These
8 observations corroborate with the proposed model (Figure 1) (19).
9

10
11
12
13
14
15
16
17 *Effect of sTF on the binding of anticoagulant proteins to FVIIa* – Previous studies have shown
18 that hemextin AB complex exhibits similar IC₅₀ values (~100 nM) for inhibition of both FVIIa
19 and sTF-FVIIa (17;18). Therefore, we investigated the binding of the anticoagulant protein and
20 its synergistic complex with sTF-FVIIa, and compared it to the binding to FVIIa alone.
21 Hemextin A binds to sTF-FVIIa (Figure 8A) with 1:1 stoichiometry (Figure 8B). The estimated
22 molecular weight of the sTF-FVIIa-hemextin A complex was ~84000 Da (Figure 8A). Hemextin
23 AB complex also binds to sTF-FVIIa (Figure 8A) in 1:1 stoichiometry, although its binding
24 affinity towards the procoagulant complex is higher than hemextin A alone (Figure 8C) (Table
25 3). The molecular weight of the FVIIa-sTF-hemextin AB complex was estimated to be ~116,000
26 Da (Figure 8A). Interestingly, no significant difference was observed in the binding affinity
27 between FVIIa and the anticoagulant proteins, in the presence of sTF (Table 3). Thus, the regions
28 of FVIIa participating in complex formation with sTF are not involved in binding with the
29 anticoagulant protein or its complex. X-ray crystallographic structure of sTF-FVIIa at 2.0 Å
30 resolution (PDB code 1DAN) (33) shows that the two fibronectin domains of sTF have extensive
31 contact with the γ -carboxyglutamic acid (Gla) and the first epidermal growth factor-like (EGF1)
32 domains of FVIIa. This observation is also supported by mutation studies (34;35). However,
33 minor contact regions do exist between sTF and the second EGF-like and protease domains of
34
35
36
37
38
39
40
41
42
43
44
45
46
47
48
49
50
51
52
53
54
55
56
57
58
59
60

1
2
3 FVIIa. Thus it is most-likely that the light chain of FVIIa is not involved in the interaction with
4
5 hemextin A/ Hemextin AB complex.
6

7
8 *Interaction of anticoagulant proteins with active site inhibited FVIIa* – Previous studies show
9
10 that hemextin AB complex is a non-competitive inhibitor of sTF-FVIIa ($K_i = 25$ nM) and hence
11
12 it does not bind to the active site of FVIIa (17;18). Therefore, we investigated the complex
13
14 formation of active-site blocked FFRck-FVIIa (Figure 9) with hemextin A and hemextin AB
15
16 complex. SEC studies showed that FFRck-FVIIa binds to hemextin A and hemextin AB complex
17
18 (Figure 9A). The estimated molecular weight of FFRck-FVIIa-hemextin A complex and FFRck-
19
20 FVIIa-hemextin AB complex was 57,000 Da and 88,000 Da, respectively. No significant change
21
22 in the molecular weight was observed over that of the corresponding complexes of the
23
24 anticoagulant proteins with FVIIa (Figure 9A) as the molecular weight of FFRck is negligible.
25
26 The binding is exothermic with 1:1 stoichiometry (Figure 9B and C). However, their binding
27
28 affinities are lower towards FFRck-FVIIa than FVIIa (Table 3). This may be because of the
29
30 conformational changes in FVIIa induced by FFRck (36). This observation again highlights the
31
32 binding site of the anticoagulant protein and its complex to be localized in the heavy chain of
33
34 FVIIa, but away from the active site.
35
36
37
38
39

40
41 *Interaction of anticoagulant proteins with individual FVIIa chains* – FVIIa consists of an NH₂-
42
43 terminal light chain (relative molecular mass, 20,000) consisting of 152 amino acid residues and
44
45 a COOH-terminal heavy chain (relative molecular mass, 30,000) consisting of 254 amino acid
46
47 residues linked via a single disulfide bond (Cys135 to Cys262). The light chain contains the
48
49 membrane-binding Gla domain and two EGF-like domains (EGF1 and EGF2), while the heavy
50
51 chain contains the catalytic serine protease domain (37). To further understand the interactions,
52
53
54
55
56
57
58
59
60

1
2
3 we studied the interaction of the individual separated chains of FVIIa (Figure 10A) with
4
5 hemexin A and hemexin AB complex.
6
7

8 The light chain of FVIIa showed no binding to either hemexin A or hemexin AB complex
9
10 (Supplementary Figure 1). This is not due to the conformational change(s) in the light chain
11
12 isolated under reducing conditions since light chain produced under non-reducing conditions did
13
14 not exhibit any binding either (data not shown). This observation ruled out the EGF2 domain of
15
16 FVIIa as a binding site for the anticoagulant protein and its complex. The isolated heavy chain of
17
18 FVIIa exhibited binding to both hemexin A and hemexin AB complex (Figure 10).
19
20 Interestingly, the binding affinity of the anticoagulant protein and its complex for the heavy
21
22 chain was slightly higher than that recorded for FVIIa (Table 3). This may be due to better
23
24 exposure of the anticoagulant binding site or the possibility of hemexin A/AB to interact more
25
26 optimally in the absence of the light chain. Thus, the binding site of hemexin A and hemexin
27
28 AB complex is localized in the heavy chain of FVIIa.
29
30
31
32

33 34 **Conclusion** 35

36 Hemexin A and hemexin AB complex bind to the heavy chain of FVIIa. Binding to these
37
38 anticoagulants is independent of sTF and active site blockers. Thus, there interaction site is
39
40 different from TF-binding sites and the active site. Based on these observations we propose a
41
42 model, for the mechanism of action of hemexin AB complex (Figure 11). FVIIa in the presence
43
44 of TF and phospholipids converts FX to FXa, with the concomitant release of activation peptide
45
46 (AP) (Figure 11A). Hemexin AB complex binds to the heavy chain of FVIIa, at a site distinct
47
48 from the TF binding site and active site as evident from the ITC and SEC studies (see above)
49
50 leading to the formation of the inhibited complex (Figure 11B). This binding of the anticoagulant
51
52 complex to FVIIa induces a conformational change in the enzyme which leads to the change in
53
54
55
56
57
58
59
60

1
2
3 the active site geometry (indicated by the red arrow) resulting in the inhibition of FXa formation
4
5 (Figure 11C) and clot formation. The change in the active site geometry is supported by non
6
7 competitive inhibition of FVIIa by hemextin AB complex FVIIa (17;18). Further studies are
8
9 required to identify the specific region of FVIIa heavy chain that participates in the binding to
10
11 the anticoagulant proteins. Thus, the present data enhances our understanding of the inhibitory
12
13 mechanism of FVIIa by hemextin A and hemextin AB complex that will help in devising novel
14
15 anticoagulation strategies/peptides specifically targeting the heavy chain of FVIIa.
16
17
18
19

20 **Acknowledgements**

21
22 We thank Dr James H. Morrissey (Department of Biochemistry, University of Illinois College of
23
24 Medicine, Urbana-Champaign), Dr Thomas Record Jr. (University of Wisconsin-Madison), Dr
25
26 John H Griffin and Dr Subramanian Yegneswaran (The Scripps Research Institute, La Jolla) for
27
28 helpful discussions. YB thanks the National University of Singapore for his research scholarship.
29
30
31
32
33

34 **References**

- 35
36
37
38 1. Davie, E. W. (2003) A brief historical review of the waterfall/cascade of blood coagulation,
39 *J. Biol. Chem.* 278, 50819-50832.
40
41 2. Mann, K. G. (1999) Biochemistry and physiology of blood coagulation, *Thromb. Haemost.*
42 82, 165-174.
43
44 3. Nakagaki, T., Foster, D. C., Berkner, K. L., and Kisiel, W. (1991) Initiation of the extrinsic
45 pathway of blood coagulation: evidence for the tissue factor dependent autoactivation of
46 human coagulation factor VII, *Biochemistry* 30, 10819-10824.
47
48 4. Davie, E. W., Fujikawa, K., and Kisiel, W. (1991) The coagulation cascade: initiation,
49 maintenance, and regulation, *Biochemistry* 30, 10363-10370.
50
51 5. Lawson, J. H. and Mann, K. G. (1991) Cooperative activation of human factor IX by the
52 human extrinsic pathway of blood coagulation, *J. Biol. Chem.* 266, 11317-11327.
53
54 6. Butenas, S., Orfeo, T., Gissel, M. T., Brummel, K. E., and Mann, K. G. (2004) The
55 significance of circulating factor IXa in blood, *J. Biol. Chem.* 279, 22875-22882.
56
57 7. Ichinose, A., Bottenus, R. E., and Davie, E. W. (1990) Structure of transglutaminases, *J.*
58 *Biol. Chem.* 265, 13411-13414.
59
60

8. Gustafsson, D., Bylund, R., Antonsson, T., Nilsson, I., Nystrom, J. E., Eriksson, U., Bredberg, U., and Teger-Nilsson, A. C. (2004) A new oral anticoagulant: the 50-year challenge, *Nat. Rev. Drug Discov.* 3, 649-659.
9. Hirsh, J. (1991) Heparin, *N. Engl. J. Med.* 324, 1565-1574.
10. Hirsh, J. (1991) Oral anticoagulant drugs, *N. Engl. J. Med.* 324, 1865-1875.
11. Hirsh, J. and Weitz, J. I. (1999) New antithrombotic agents, *Lancet* 353, 1431-1436.
12. Kini, R. M. (2006) Anticoagulant proteins from snake venoms: structure, function and mechanism, *Biochem. J.* 397, 377-387.
13. Markland, F. S. (1998) Snake venoms and the hemostatic system, *Toxicon* 36, 1749-1800.
14. Higuchi, S., Murayama, N., Saguchi, K., Ohi, H., Fujita, Y., Camargo, A. C., Ogawa, T., Deshimaru, M., and Ohno, M. (1999) Bradykinin-potentiating peptides and C-type natriuretic peptides from snake venom, *Immunopharmacology* 44, 129-135.
15. O'Shea, J. C. and Tchong, J. E. (2002) Eptifibatid: a potent inhibitor of the platelet receptor integrin glycoprotein IIb/IIIa, *Expert. Opin. Pharmacother.* 3, 1199-1210.
16. McClellan, K. J. and Goa, K. L. (1998) Tirofiban. A review of its use in acute coronary syndromes, *Drugs* 56, 1067-1080.
17. Banerjee, Y., Mizuguchi, J., Iwanaga, S., and Kini, R. M. (2005) Hemextin AB complex, a unique anticoagulant protein complex from *Hemachatus haemachatus* (African Ringhals cobra) venom that inhibits clot initiation and factor VIIa activity, *J. Biol. Chem.* 280, 42601-42611.
18. Banerjee, Y., Mizuguchi, J., Iwanaga, S., and Kini, R. M. (2005) Hemextin AB complex--a snake venom anticoagulant protein complex that inhibits factor VIIa activity, *Pathophysiol. Haemost. Thromb.* 34, 184-187.
19. Banerjee, Y., Lakshminarayanan, R., Vivekanandan, S., Anand, G. S., Valiyaveetil, S., and Kini, R. M. (2007) Biophysical Characterization of Anticoagulant Hemextin AB Complex from the Venom of *Hemachatus haemachatus* Snake, *Biophys. J.*
20. Nakagaki, T., Foster, D. C., Berkner, K. L., and Kisiel, W. (1991) Initiation of the extrinsic pathway of blood coagulation: evidence for the tissue factor dependent autoactivation of human coagulation factor VII, *Biochemistry* 30, 10819-10824.
21. Stone, M. J., Ruf, W., Miles, D. J., Edgington, T. S., and Wright, P. E. (1995) Recombinant soluble human tissue factor secreted by *Saccharomyces cerevisiae* and refolded from *Escherichia coli* inclusion bodies: glycosylation of mutants, activity and physical characterization, *Biochem. J.* 310 (Pt 2), 605-614.
22. Persson, E. and Petersen, L. C. (1995) Structurally and functionally distinct Ca²⁺ binding sites in the gamma-carboxyglutamic acid-containing domain of factor VIIa, *Eur. J. Biochem.* 234, 293-300.
23. Levenberg, K. (1944) A Method for the Solution of Certain Problems in Least Squares, *Quart. Appl. Math.* 2, 164-168.

- 1
 - 2
 - 3
 - 4
 - 5
 - 6
 - 7
 - 8
 - 9
 - 10
 - 11
 - 12
 - 13
 - 14
 - 15
 - 16
 - 17
 - 18
 - 19
 - 20
 - 21
 - 22
 - 23
 - 24
 - 25
 - 26
 - 27
 - 28
 - 29
 - 30
 - 31
 - 32
 - 33
 - 34
 - 35
 - 36
 - 37
 - 38
 - 39
 - 40
 - 41
 - 42
 - 43
 - 44
 - 45
 - 46
 - 47
 - 48
 - 49
 - 50
 - 51
 - 52
 - 53
 - 54
 - 55
 - 56
 - 57
 - 58
 - 59
 - 60
24. Marquardt, D. (1963) An Algorithm for Least-Squares Estimation of Nonlinear Parameters., *SIAM J. Appl. Math.* *11*, 431-441.
25. Mounier, C. M., Hackeng, T. M., Schaeffer, F., Faure, G., Bon, C., and Griffin, J. H. (1998) Inhibition of prothrombinase by human secretory phospholipase A2 involves binding to factor Xa, *J. Biol. Chem.* *273*, 23764-23772.
26. Lewicki, D. N. and Gallagher, T. M. (2002) Quaternary structure of coronavirus spikes in complex with carcinoembryonic antigen-related cell adhesion molecule cellular receptors, *J. Biol. Chem.* *277*, 19727-19734.
27. Pflieger, K. D. and Eidne, K. A. (2006) Illuminating insights into protein-protein interactions using bioluminescence resonance energy transfer (BRET), *Nat. Methods* *3*, 165-174.
28. Kim, M., Chen, B., Hussey, R. E., Chishti, Y., Montefiori, D., Hoxie, J. A., Byron, O., Campbell, G., Harrison, S. C., and Reinherz, E. L. (2001) The stoichiometry of trimeric SIV glycoprotein interaction with CD4 differs from that of anti-envelope antibody Fab fragments, *J. Biol. Chem.* *276*, 42667-42676.
29. Murphy, K. P. and Freire, E. (1992) Thermodynamics of structural stability and cooperative folding behavior in proteins, *Adv. Protein Chem* *43*, 313-361.
30. Finkelstein, A. V. and Janin, J. (1989) The price of lost freedom: entropy of bimolecular complex formation, *Protein Eng* *3*, 1-3.
31. Janin, J. and Chothia, C. (1978) Role of hydrophobicity in the binding of coenzymes. Appendix. Translational and rotational contribution to the free energy of dissociation, *Biochemistry* *17*, 2943-2948.
32. Millhauser, G. L. (1995) Views of helical peptides: a proposal for the position of 3(10)-helix along the thermodynamic folding pathway, *Biochemistry* *34*, 3873-3877.
33. Banner, D. W., D'Arcy, A., Chene, C., Winkler, F. K., Guha, A., Konigsberg, W. H., Nemerson, Y., and Kirchhofer, D. (1996) The crystal structure of the complex of blood coagulation factor VIIa with soluble tissue factor, *Nature* *380*, 41-46.
34. Higashi, S., Matsumoto, N., and Iwanaga, S. (1996) Molecular mechanism of tissue factor-mediated acceleration of factor VIIa activity, *J. Biol. Chem.* *271*, 26569-26574.
35. Dickinson, C. D., Shobe, J., and Ruf, W. (1998) Influence of cofactor binding and active site occupancy on the conformation of the macromolecular substrate exosite of factor VIIa, *J. Mol. Biol.* *277*, 959-971.
36. Kemball-Cook, G., Johnson, D. J., Tuddenham, E. G., and Harlos, K. (1999) Crystal structure of active site-inhibited human coagulation factor VIIa (des-Gla), *J. Struct. Biol.* *127*, 213-223.
37. Kranjc, A., Kikelj, D., and Peterlin-Masic, L. (2005) Recent advances in the discovery of tissue factor/factor VIIa inhibitors and dual inhibitors of factor VIIa/factor Xa, *Curr. Pharm. Des* *11*, 4207-4227.

Tables

Table 1.

Thermodynamics of binding of hemextin AB complex/hemextin A to FVIIa in different buffer solutions

Binding to FVIIa	$K_A \times 10^5$ (M^{-1})	ΔH (kcal/mole)	ΔS (cal/deg.mole)	ΔG (kcal/mole)	Number of Binding Sites (N)
<i>Hemextin AB complex</i>					
Tetramer in Tris-HCl Buffer	4.11	-7.931	-1.112	-7.586	1.01
Dimer in glycerol	1.77	-3.933	-1.1	-3.62	1.05
Dimer in salt	0.119	-2.994	-1.66	-2.54	0.89
<i>Hemextin A</i>					
In Tris-HCl buffer	0.125	-3.005	-1.7	-2.5	1.00
In glycerol	0.118	-2.821	-1.74	-2.3	0.97
In salt	0.121	-3.042	-1.56	-2.6	1.03

Note: All experiments were carried at 37 °C

Table 2.

Thermodynamic analysis of FVIIa binding to hemextin AB complex at different temperatures

Binding to FVIIa	$K_A \times 10^5$ (M ⁻¹)	ΔH (kcal/mole)	ΔS (cal/deg.mole)	ΔG (kcal/mole)	Number of binding sites (N)
At different temperatures (°C)					
25	3.84	-6.56	3.322	-7.61	0.97
37	4.11	-7.931	-1.112	-7.586	1.01
45	1.55	-9.0010	-4.55	-7.548	1.08

Table 3.

Thermodynamic analysis of binding to FVIIa and its derivatives to hemextin AB complex/hemextin A

Binding to FVIIa and its derivatives	$K_A \times 10^5$ (M ⁻¹)	ΔH (kcal/mole)	ΔS (cal/deg.mole)	ΔG (kcal/mole)	Number of binding site (N)
<i>Hemextin AB complex</i>					
FVIIa	4.11	-7.931	-1.112	-7.586	1.01
sTF-FVIIa	4.06	-7.84	-1.13	-7.49	1.16
FVIIa-Heavy chain	5.2	-7.82	-0.5	-7.67	0.921
FFRck-FVIIa	0.33	-5.01	-3.7	-4.74	1.08
<i>Hemextin A</i>					
FVIIa	0.125	-3.005	-1.7	-2.5	1.00
sTF-FVIIa	0.127	-3.1	-1.5	-2.69	1.07
FVIIa-Heavy chain	0.798	-4.1	-1.2	-3.7	0.96
FFRck-FVIIa	0.065	-2.3	-1.2	-1.3	0.94

Note : All experiments were carried at 37 °C

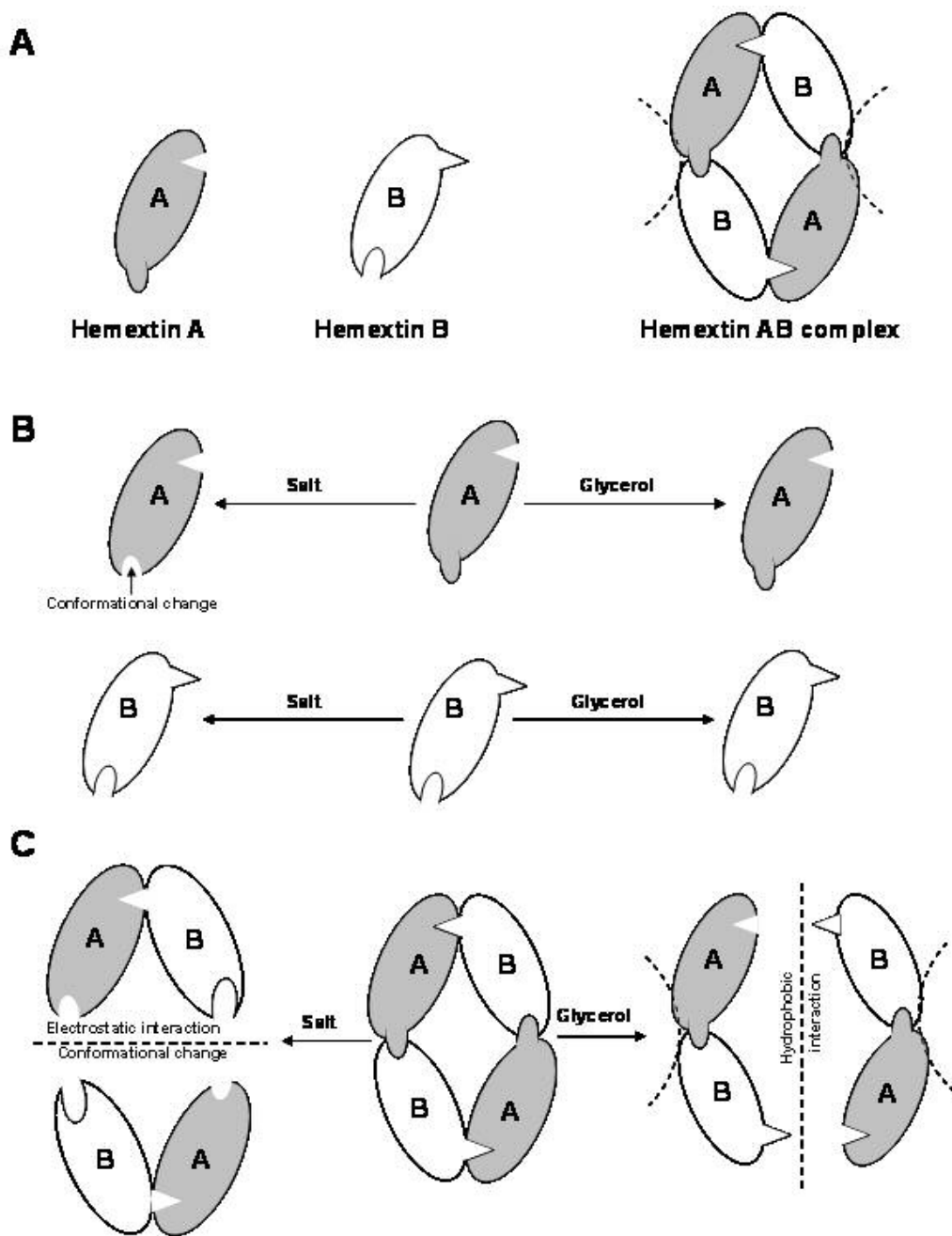
Figures**Figure 1.**

Figure 2.

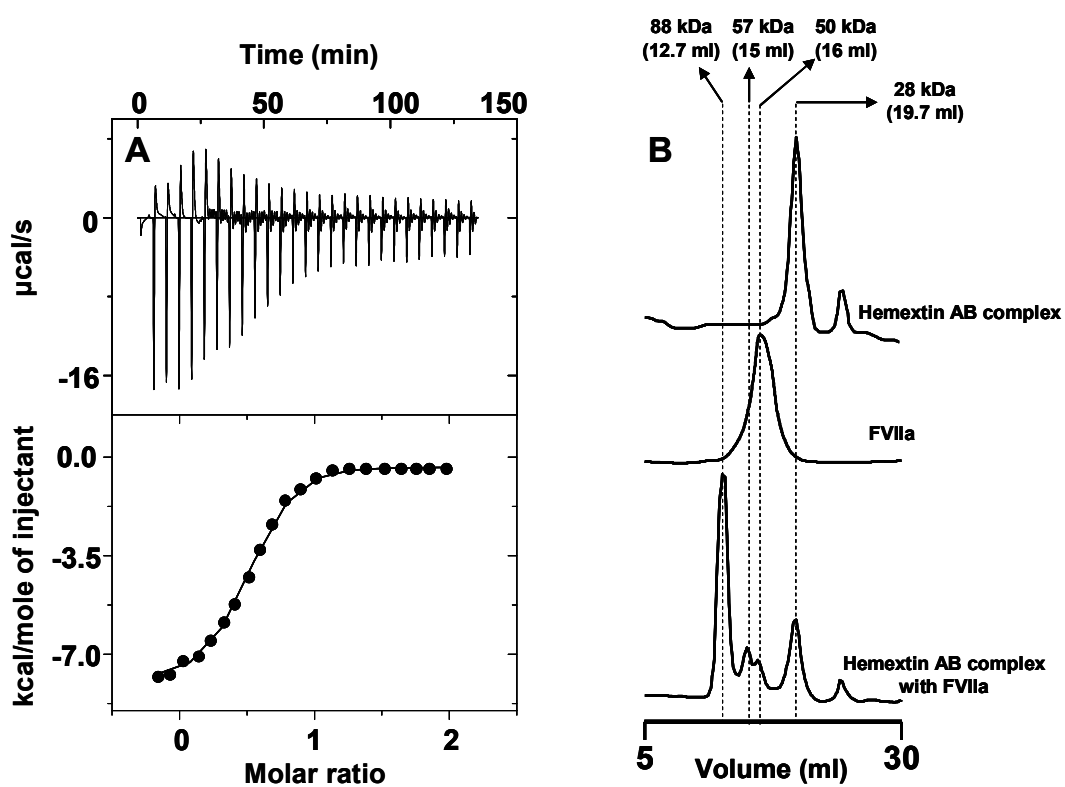


Figure 3.

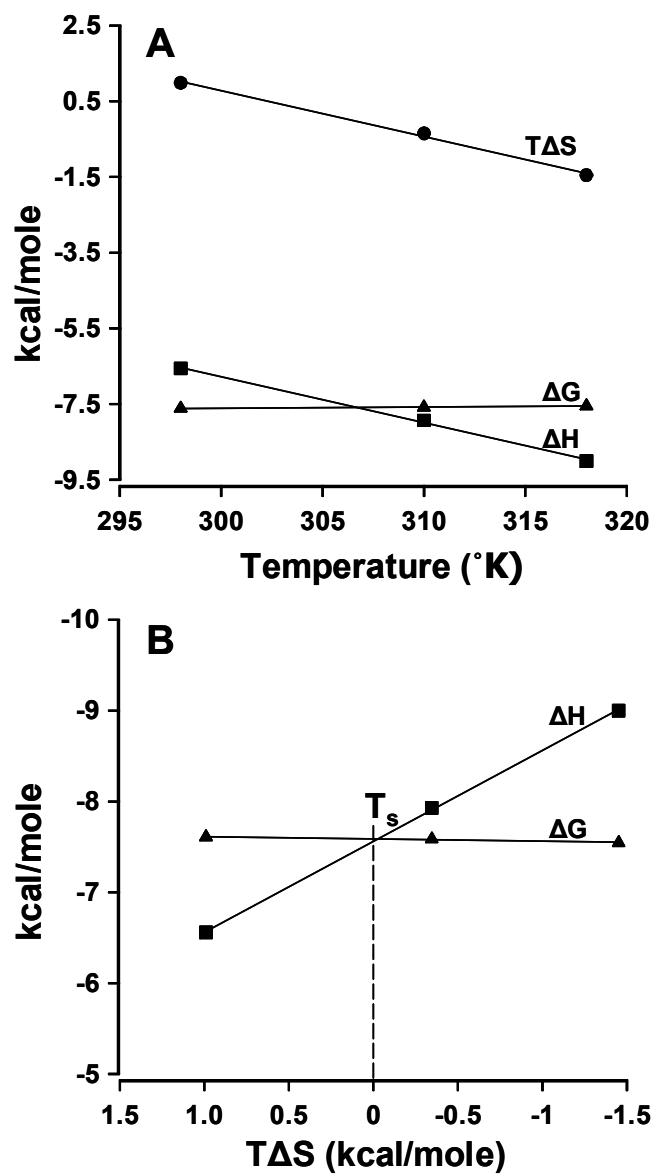


Figure 4.

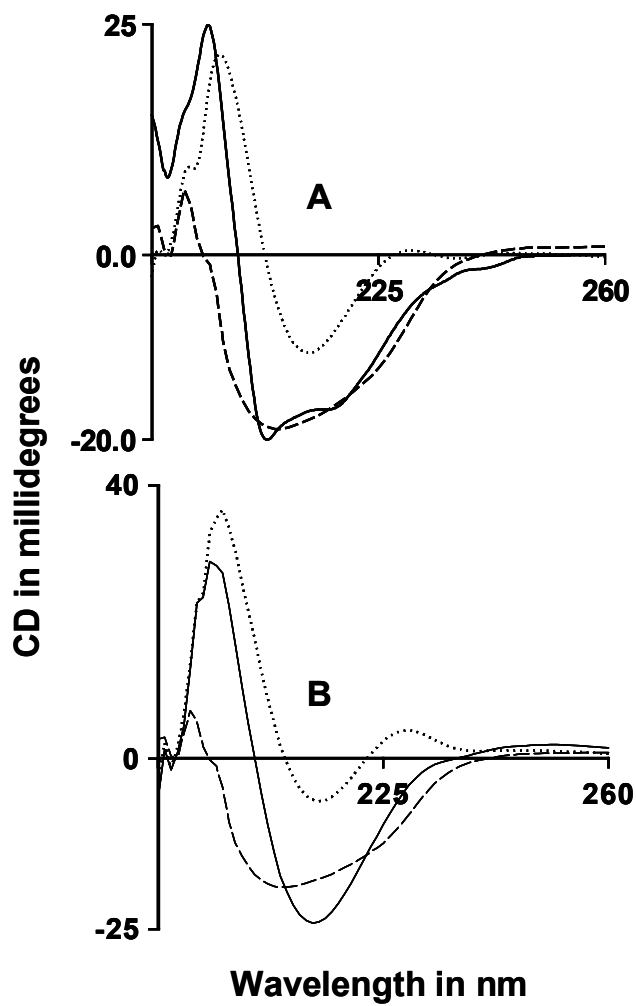


Figure 5.

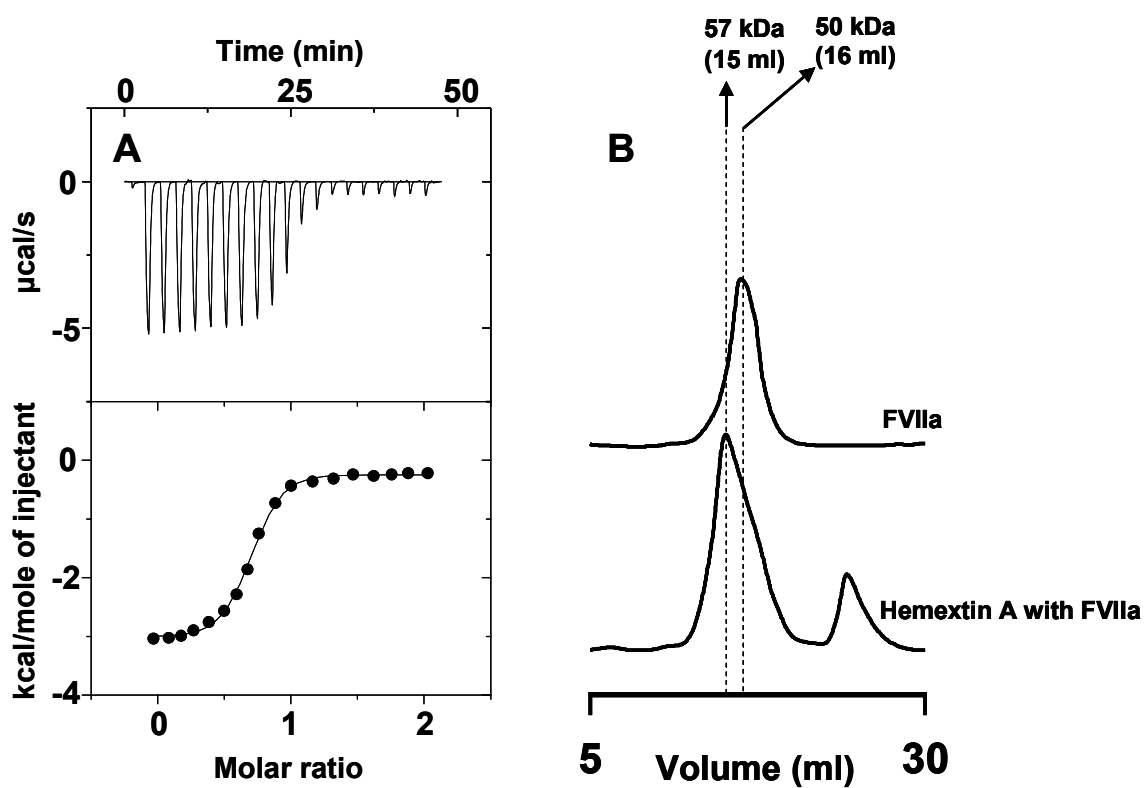


Figure 6.

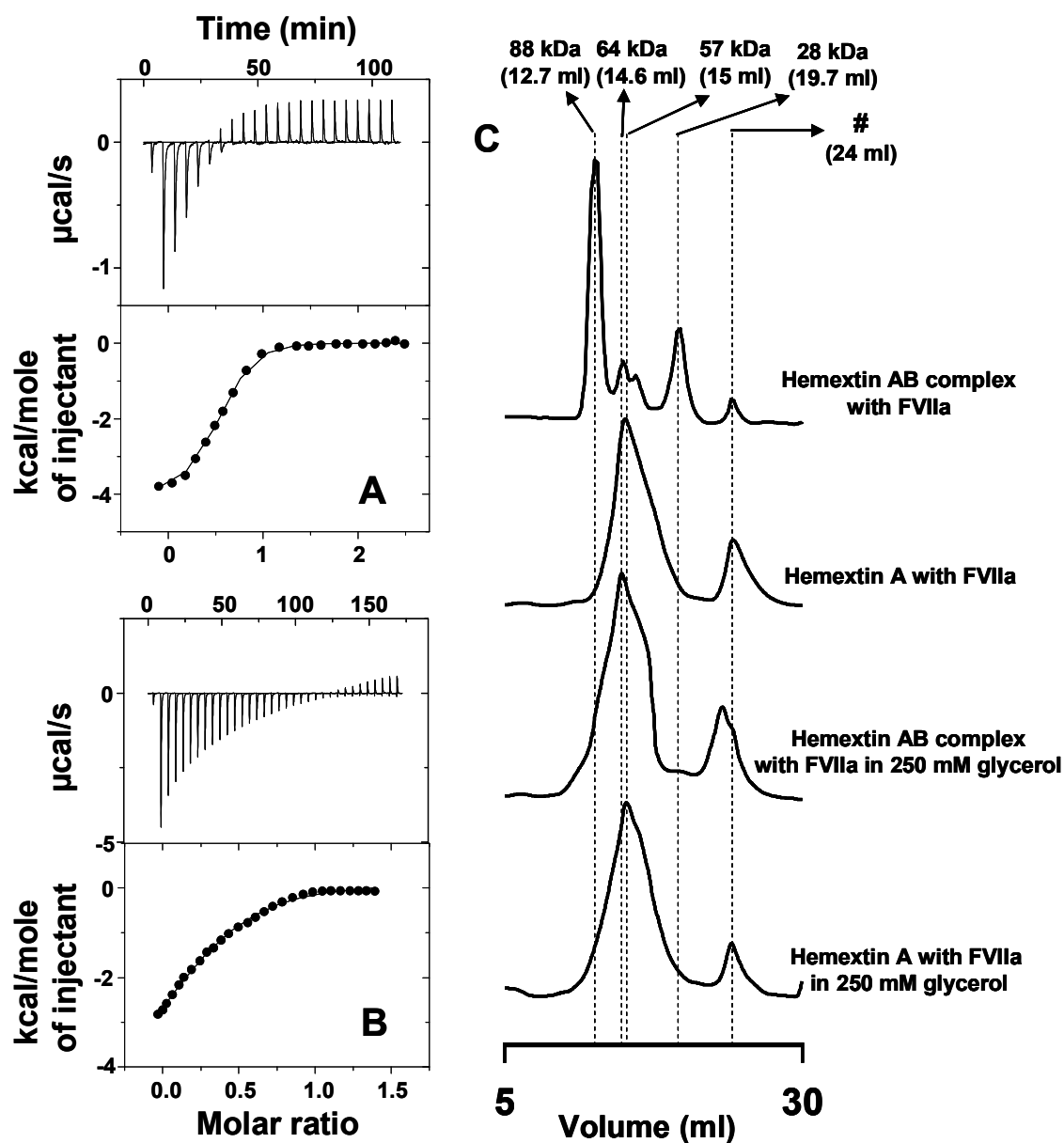


Figure 7.

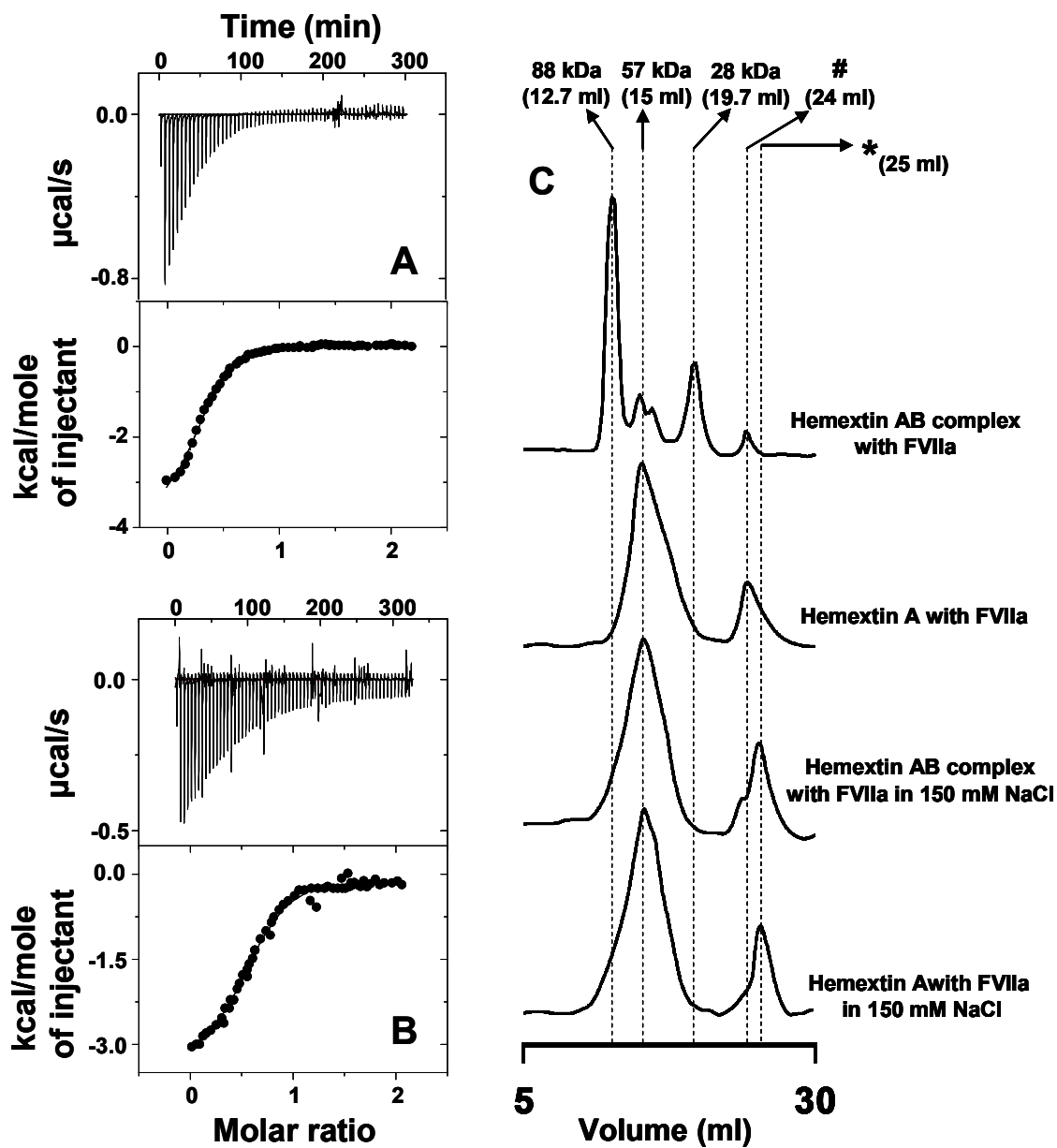


Figure 8.

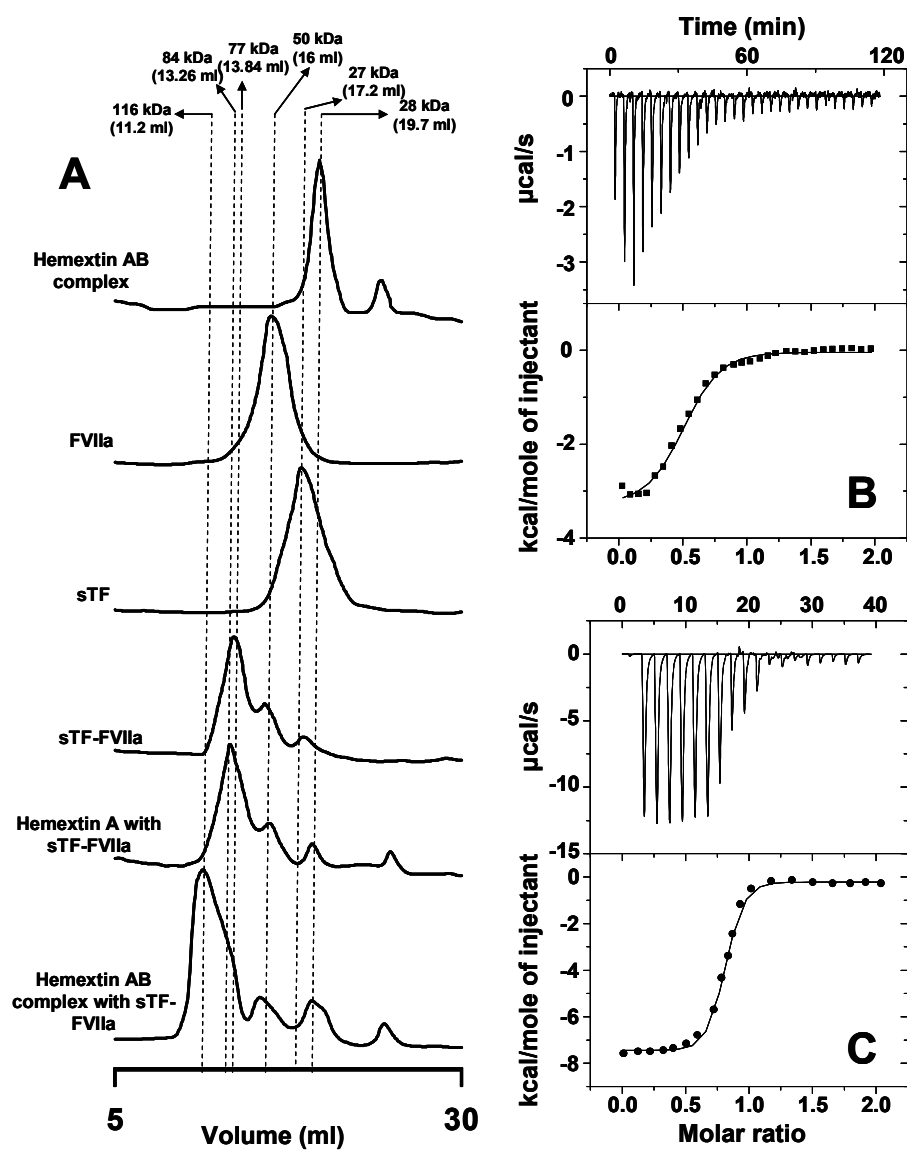


Figure 9

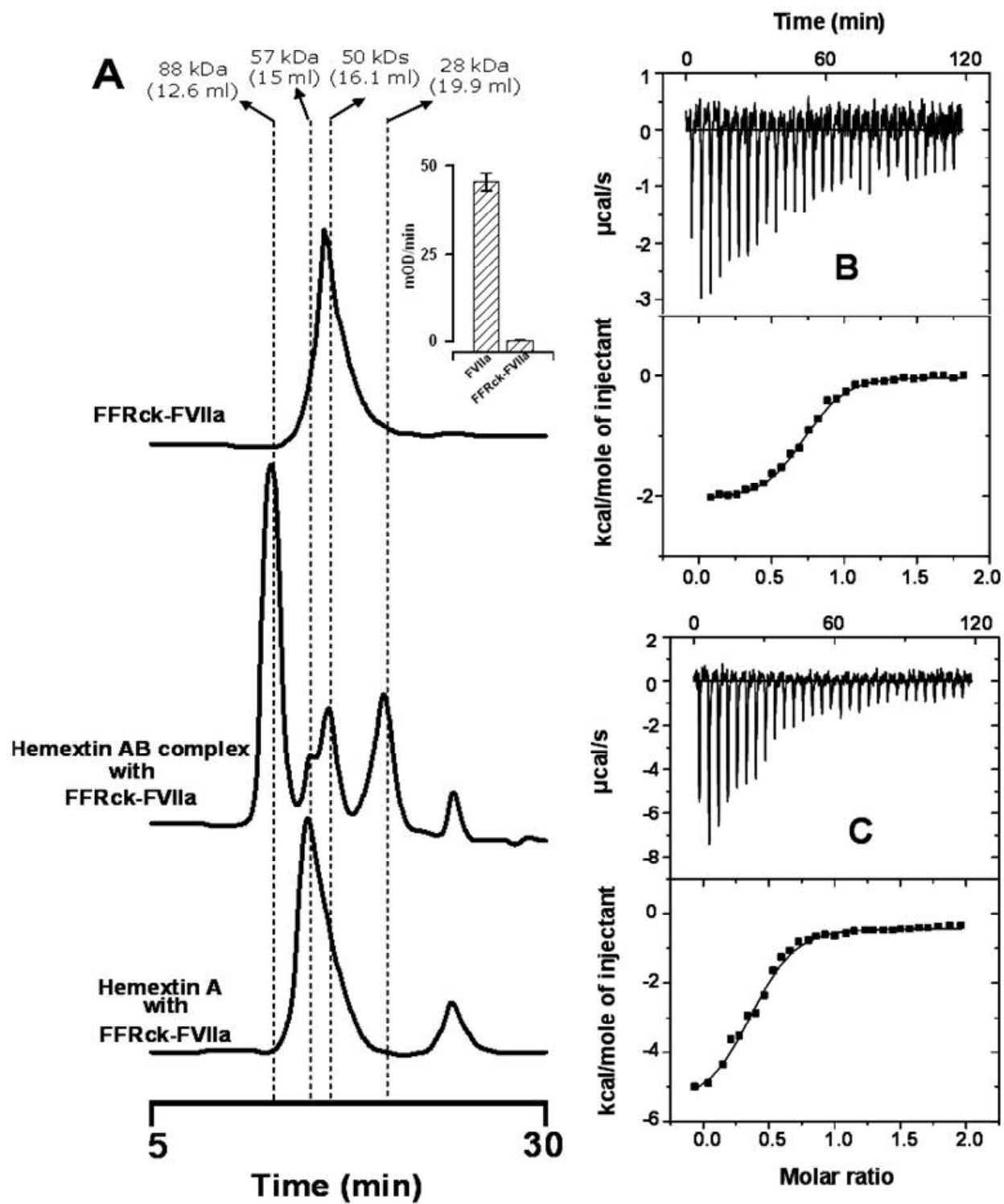


Figure 10

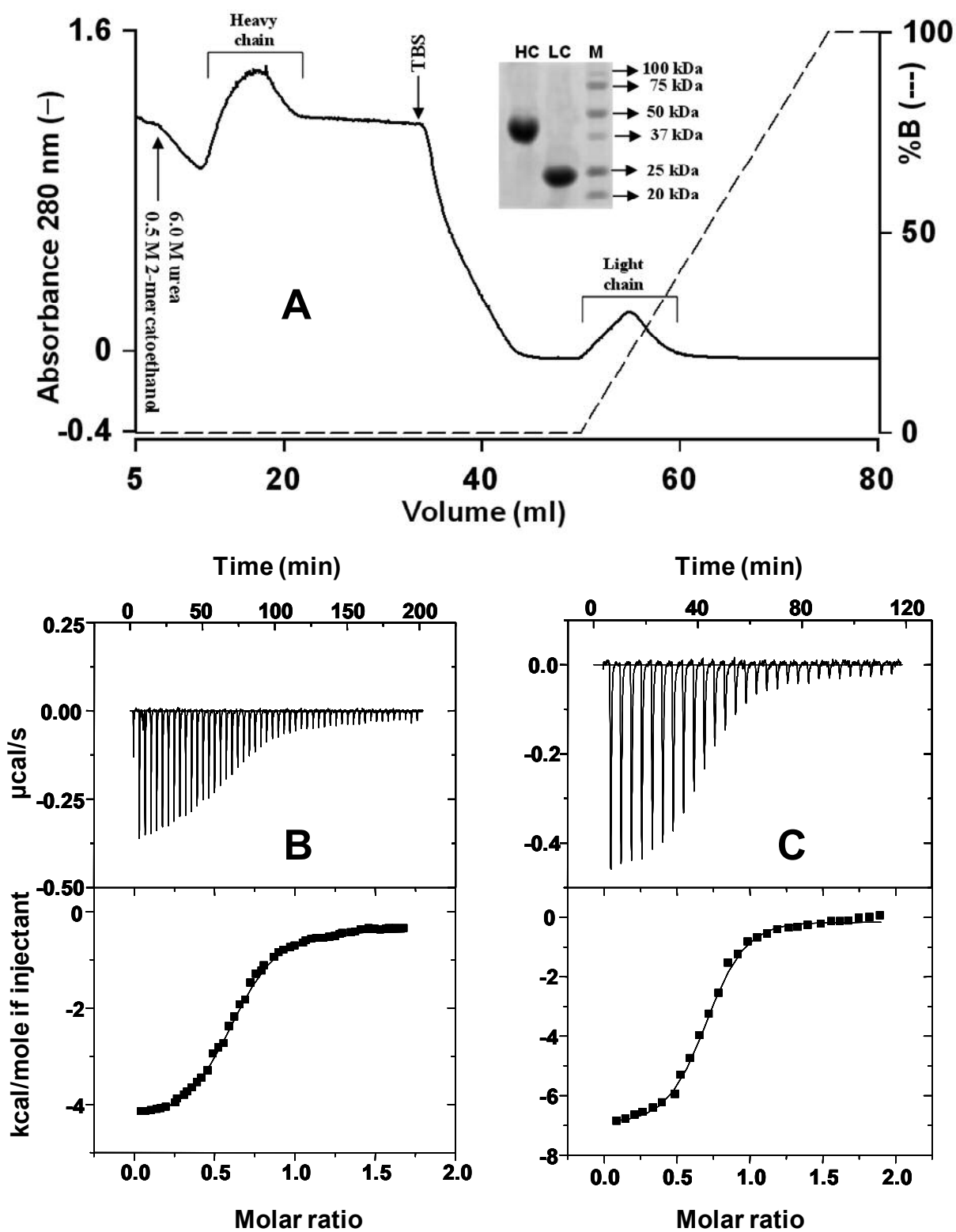


Figure 11

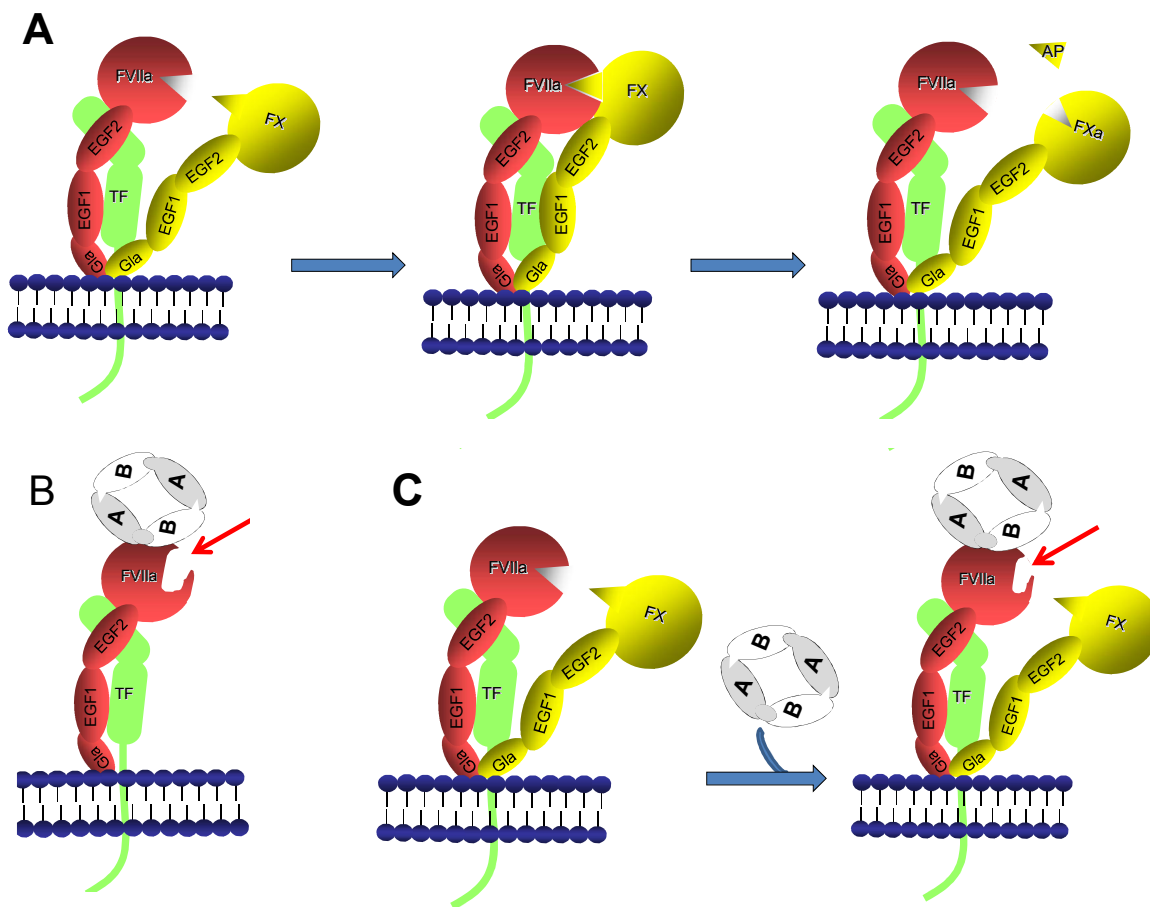


Figure legends

Figure 1: Proposed model of hemextin AB complex. A. Schematic diagram depicting the formation of hemextin AB complex. Hemextins A and B, two structurally similar three-finger toxins, form a compact and rigid tetrameric complex with 1:1 stoichiometry. B. Schematic diagram showing the effect of salt and glycerol on the conformations of hemextins A and B. Hemextin A undergoes a conformational change in the presence of salt. C. Dissociation of the tetrameric hemextin AB complex in the presence of salt and glycerol. The dissociation probably occurs in two different planes. Thus the hemextin AB dimer in high salt is different from the dimer formed in the presence of glycerol. Two putative anticoagulant sites are shown with dotted semicircles (See text for details).

Figure 2. Binding of hemextin AB complex to FVIIa. (A) ITC studies. Thermogram with the corresponding binding isotherm for the binding of hemextin AB complex to FVIIa in 50 mM Tris buffer (pH 7.4). (B) SEC studies. Elution profiles of the complex of FVIIa with hemextin AB complex in 50 mM Tris buffer (pH 7.4). *Note:* Upon complex formation there is a reduction in retention time.

Figure 3. Thermodynamics of FVIIa-hemextin AB complex formation. (A) Effect of temperature on the energetics of FVIIa-hemextin AB complex interaction: enthalpy change (ΔH), change in entropy term ($T\Delta S$) and free energy change (ΔG). (B) Enthalpy-entropy compensation in complex formation. (*Note:* Point of intersection of lines corresponding to ΔH and ΔG corresponds to T_s)

Figure 4. Conformational changes associated with the formation of hemextin AB-FVIIa and hemextin A-FVIIa complexes. (A) Spectra for hemextin AB-FVIIa complex (—), individual spectra of hemextin AB complex (-----) FVIIa (---) are also shown for comparison. (B) Spectra for hemextin A-FVIIa complex (→), individual spectra of hemextin A (-----) FVIIa (---) are also shown for comparison.

Figure 5. Binding of hemextin A to FVIIa. (A) ITC studies. Thermogram with the corresponding binding isotherm for the binding of hemextin A complex to FVIIa in 50 mM Tris buffer (pH 7.4).; *Note* the presence of only one kinetic phase, unlike two as observed in the case of hemextin AB-FVIIa formation (B) SEC studies. Elution profiles of the complex of FVIIa with hemextin AB complex in 50 mM Tris buffer (pH 7.4); *Note* on complex formation there is a reduction in retention time.

Figure 6. Binding of hemextin AB complex or hemextin A to FVIIa in 50 mM Tris buffer (pH 7.4) containing 250 mM glycerol. Thermograms with the corresponding binding isotherms for the binding of (A) hemextin AB complex or (B) hemextin A to FVIIa in Tris buffer

1
2
3 containing 250 mM glycerol. (C) Elution profiles of hemexin AB complex or hemexin A with
4 FVIIa in Tris-HCl buffer containing 250 mM glycerol.
5
6
7

8 **Figure 7. Binding of hemexin AB complex or hemexin A to FVIIa in 50 mM Tris buffer**
9 **(pH 7.4) containing 150 mM salt.** Thermograms with the corresponding binding isotherms for
10 the binding of (A) hemexin AB complex or (B) hemexin A to FVIIa in Tris buffer containing
11 150 mM NaCl. (C) Elution profiles of hemexin AB complex or hemexin A with FVIIa in Tris-
12 HCl buffer containing 150 mM NaCl.
13
14
15

16 **Figure 8. Binding of hemexin A/hemexin AB complex to sTF-FVIIa.** (A) Elution profiles of
17 the complex of sTF-FVIIa with hemexin AB complex/hemexin A. Thermograms with the
18 corresponding binding isotherms for the binding of (B) hemexin A and (C) hemexin AB
19 complex to sTF-FVIIa. (*Note: the presence of sTF does not affect the binding between FVIIa and*
20 *the anticoagulant protein or its complex.*)
21
22
23

24 **Figure 9. Binding of hemexin A/hemexin AB complex to active site blocked FVIIa**
25 **(FFRck-FVIIa).** (A) Elution profiles of the complex of FFRck-FVIIa with hemexin AB
26 complex/hemexin A (*inset*, the pooled fractions corresponding to FFRck-FVIIa had <5%
27 residual activity. Thermograms with the corresponding binding isotherms for the binding of (B)
28 hemexin A and (C) hemexin AB complex to FFRck-FVIIa.
29
30
31

32 **Figure 10. Binding of hemexin A/hemexin AB complex to the heavy chain of FVIIa.** (A)
33 Separation of light and heavy chains derived from FVIIa. Human FVIIa (3.5 mg) was incubated
34 with 0.5 M 2-mercaptoethanol in 1.1 ml of TBS at 20 °C for 30 min. The sample was applied to a
35 column (6 ml) of DEAE-Sepharose CL-6B equilibrated with TBS containing 0.5 M 2-
36 mercaptoethanol. The flow rate was 2 ml/min. After washing the column with 20 ml of the
37 equilibration buffer, the heavy chain of FVIIa was eluted with 35 ml of TBS containing 6.0 M
38 urea and 0.5 M 2-mercaptoethanol. Then the column was washed with 20 ml of TBS and a linear
39 gradient from 0.1 to 0.6 M NaCl in 50 mM Tris-HCl, pH 8.0 was performed to elute the light
40 chain of FVIIa. The patterns of the isolated light and heavy chains on SDS-PAGE are shown in
41 the *inset*: HC, heavy chain of FVIIa; LC light chain of FVIIa; M, molecular mass of standard
42 proteins used. Thermograms with the corresponding binding isotherms for the binding of (A)
43 hemexin A and (B) hemexin AB complex to the heavy chain of FVIIa.
44
45
46

47 **Figure 11. Model showing the binding of hemexin AB complex to FVIIa.** (A) Conversion of
48 FX to FXa by FVIIa in the presence of TF and phospholipids in the absence of hemexin AB
49 complex. (B) Formation of inhibitor complex (*Note the binding of the inhibitor induces a*
50 *conformational change in active site*) (C) Inhibition of FXa formation, since the conformational
51 change inhibits the binding of FX.
52
53
54
55
56
57
58
59
60